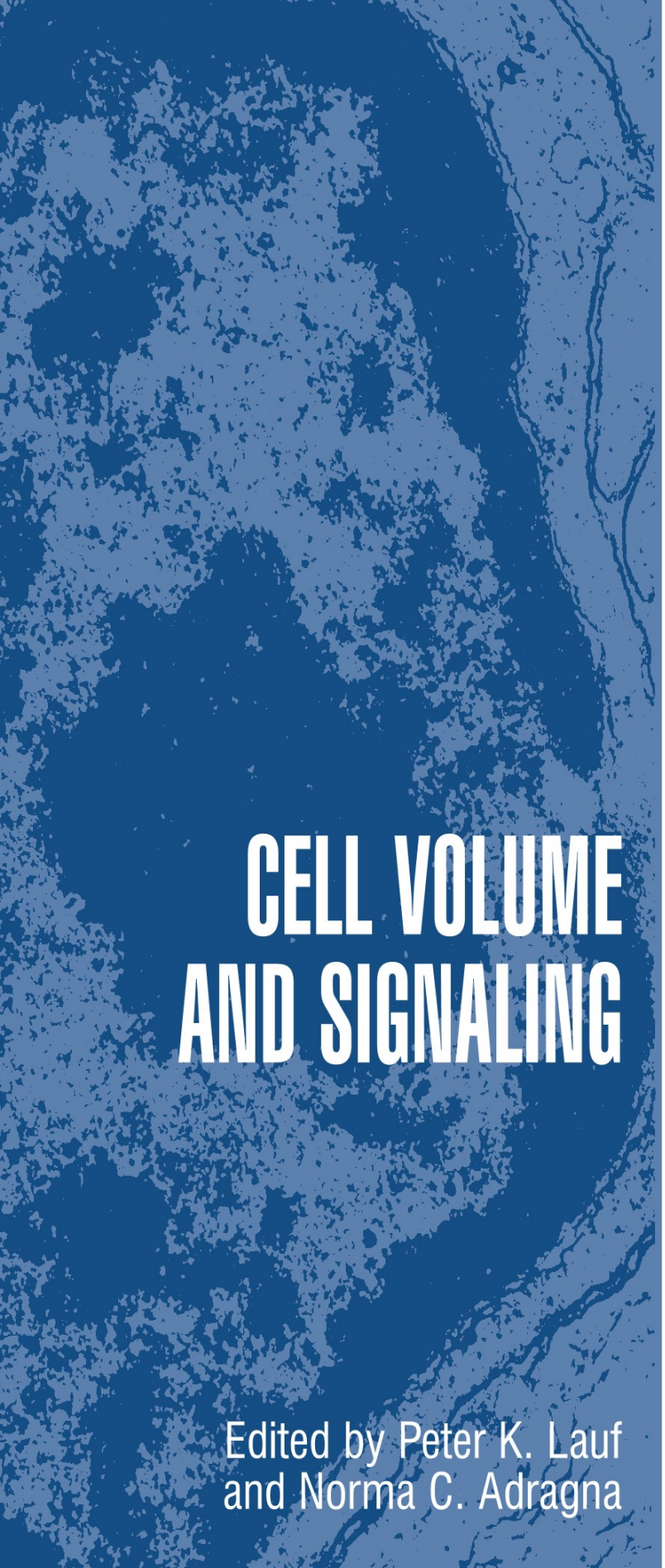

ADVANCES IN EXPERIMENTAL MEDICINE AND BIOLOGY

Volume 559

CELL VOLUME AND SIGNALING

Edited by Peter K. Lauf and Norma C. Adragna

Cell Volume and Signaling

ADVANCES IN EXPERIMENTAL MEDICINE AND BIOLOGY

Recent Volumes in this Series

Volume 551
POST GENOMIC PERSPECTIVES IN MODELING AND CONTROL OF BREATHING
Edited by Jean Champagnat, Monique Denavit-Saubie, Gilles Fortin, Arthur S. Foutz, and Muriel Thoby-Brisson

Volume 552
TYPE I DIABETES: Biomedical Science and Technology
Edited by George Eisenbarth

Volume 553
BIOMATERIALS: From Molecules to Engineered Tissues
Edited by Nesrin Hasırcı and Vasıf Hasırcı

Volume 554
PROTECTING INFANTS THROUGH HUMAN MILK: Advancing the Scientific Evidence
Edited by Larry K. Pickering, Ardythe L. Morrow, Guillermo M. Ruiz-Palacios, and Richard J. Schanler

Volume 555
BREAST FEEEDING: Early Influences on Later Health
Edited by Gail Goldberg, Andrew Prentice, Ann Prentice, Suzanne Filteau, and Elsie Widdowson

Volume 556
IMMUNOINFORMATICS: Opportunities and Challenges of Bridging Immunology with Computer and Information Sciences
Edited by Christian Schoenbach, V. Brusic, and Akihiko Konagaya

Volume 557
BRAIN REPAIR
Edited by M. Bähr

Volume 558
DEFECTS OF SECRETION IN CYSTIC FIBROSIS
Edited by Carsten Schultz

Volume 559
CELL VOLUME AND SIGNALING
Edited by Peter K. Lauf and Norma C. Adragna

Cell Volume and Signaling

Edited by

Peter K. Lauf
Wright State University
Dayton, Ohio

and

Norma C. Adragna
Wright State University
Dayton, Ohio

Springer

A C.I.P. Catalogue record for this book is available from the Library of Congress.

ISSN: 0065 2598
ISBN: 0-387-23299-0

Proceedings of the 2003 Dayton International Symposium on Cell Volume Regulation and Signaling

Printed in the United States of America.

9 8 7 6 5 4 3 2

springeronline.com

FOREWORD

In front of you is the finished product of your work, the text of your contributions to the 2003 Dayton International Symposium on Cell Volume and Signal Transduction. As we all recall, this symposium brought together the Doyens of Cellular and Molecular Physiology as well as aspiring young investigators and students in this field. It became a memorable event in an illustrious series of International Symposia on Cell Volume and Signaling. This series, started by Professors Vladimir Strbák, Florian Lang and Monte Greer in Smolenice, Slovakia in 1997 and continued by Professors Rolf Kinne, Florian Lang and Frank Wehner in Berlin in 2000, is projected for 2005 in Copenhagen to be hosted by our colleague, Professor Else Hoffmann and her team.

We dearly miss Monte Greer to whom this symposium was dedicated and addressed so eloquently by Vladimir Strbák in his Dedication to Monte. Monte and I became friends in Smolenice and had begun to discuss the 2003 meeting only a few days before his tragic accident in 2002. There are others who were not with us, and we missed them, too.

We would not have been able to succeed in this event without the unflagging support of our higher administration at Wright State University, the NIDDKD of the National Institute of Health, and the Fuji Medical System (see Acknowledgments).

The special touch of our Symposium Coordinator / Editorial Assistant Donna Maas was reflected in the management and organization of the symposium details, generation of program highlights, and finally, as you all know from the many e-mails, in the hard work thereafter to edit all our chapters readying them for final publication. We all owe her a big thanks and round of applause.

In the final layout of this volume and the listing of its chapters, we adhered to the original program which divided the symposium into four major topics at the cutting edge of research in cell volume and signal transduction. There is an Abstract appendix containing those abstracts that were expanded by some of the poster presenters.

At the concluding dinner of the Dayton International Symposium at the Dayton Art Institute, our dear colleague and friend Hector Rasgados-Flores, physiologist and composer, dedicated a Sarabanda for Cello and Piano which he together with our cellist son Adrian Lauf performed. This fine piece of music is published herein for the first time and interwoven between the chapters and abstracts.

Our special thanks to every member on the Editorial/Advisory Committee for reviewing and editing each page of this book. On behalf of the members of this committee and Wright State University, we would like to thank all who helped and our colleagues and friends who came from near and far to make the 2003 Dayton International Symposium on Cell Volume and Signal Transduction such a resounding success.

For the Editorial/Advisory Committee,

Peter K. Lauf,
University Professor

Norma C. Adragna
Professor of Pharmacology & Toxicology

DEDICATION

Monte Arnold Greer
(1922-2002)

This Symposium is dedicated to the memory of Monte Arnold Greer, pioneer in the field of cell swelling-induced secretion, exceptional scientist and rare friend, who died on March 24, 2002 in an auto accident in Oregon.

It was in the early eighties when Monte noticed that an improperly prepared perfusion solution was surprisingly effective in the stimulation of pituitary hormone secretion. Interestingly enough, secretion returned to basal values and responded again to different stimuli. It looked like a joke and that was enough to attract Monte's attention. He was unaware of any similar observations. Now, we know that some other people noticed a similar behavior for one particular hormone, but it was Monte who was thunderstruck by finding that it was a broad, universal phenomenon. And so this highly reputed neuroendocrinologist spent the rest of his carrier studying and admiring cell swelling-induced hormone secretion. Illustrative is the title of his paper: Greer MA, Greer SE, Opsahl Z, McCafferty L, Maruta S: *Hyposmolar stimulation of in vitro pituitary secretion of luteinizing hormone: a potent clue to the secretory process*, Endocrinology 113: 1531-1533,1983. Over the following years, Monte published many elegant papers in prestigious scientific journals; however, he did not evoke an expected interest among orthodox endocrinologists. In the years 1994-1998, we worked on a joint project *Isosmotic Ethanol-induced Neural Cell Swelling and Thyroliberin Release* supported by the US-Slovak Science and Technology Cooperation Program. During one of my visits in Portland, Monte suggested contacting relevant people in various fields to organize a symposium on cell swelling. We were impressed by the number of top scientists who worked on cell volume regulation and were pleased that many of them attended our first International Symposium on **Primary Role of Cell Volume Changes in Controlling Cell Function,** in Smolenice Castle in Slovakia, June 23-27, 1997. As the main organizers, Monte, Florian Lang and I served as chairpersons of the meeting. That was the beginning of this series. It was followed by the International Conference on **Cell Volume: Signalling and Regulation**, Max Plank Institute, Berlin, October 25-28, 2000, and now, by the present International Symposium on **Cell Volume & Signaling,** September 20-24, 2003, at Wright State University in Dayton, Ohio.

Monte Arnold Greer was born in Portland, Oregon; he received his A.B. in Biology (1944) and M.D. (1947) at Stanford University. After working in Bethesda, Boston and San Francisco, he accepted an offer as head of the Division of Endocrinology, Department of Medicine, Oregon Health Sciences University, in Portland, Oregon, in

1956. Under his leadership (1956-1990), first as Associate Professor of Medicine (1956) and then Professor of Medicine and Physiology (1962), the Endocrinology Division in Portland developed into an eminent clinical and research institution.

Monte Greer was an excellent clinician and gifted researcher who pioneered work in several fields. Most acknowledged has been the field of hypothalamic regulation of pituitary hormone secretion. He was the first to publish proof of the role of the hypothalamus in thyroid regulation – a lesion of the hypothalamus prevented goiter development in experimental rats. Twenty-five years later, A. Shally and R. Guilemin shared the Nobel Prize for the isolation of the thyrotropin-releasing hormone from the hypothalamus. Naturally, Monte was included in the prestigious publication: Pioneers in Neuroendocrinology (M. A. Greer: Why I am still waiting for the free trip to Stockholm, chapter 13, *Plenum Publishing Corporation,* 1978).

Among the awards Monte Greer received were the Oppenheimer Award of the Endocrine Society and Honorary memberships in the Japanese and Czechoslovak Endocrine Societies. Monte's achievements were also recognized by his appropriate roles in professional societies:

American Thyroid Association	President
Endocrine Society	Vice President
Western Society for Clinical Research	President
American Society for Clinical research	Chair, Subsection on Endocrinology

In addition, he served as a member of the editorial boards of *Endocrinology, Neuroendocrinology* and *Endocrinologia Experimentalis.*

Monte's charming personality, esprit, rare sense of humor and friendliness made him popular with friends all over the world. His personality is best reflected in his statement: "Nobody is as bad as his publications!" The sad message of his death deeply touched his former research fellows and coworkers and their families in USA, Japan, Switzerland, France, Germany, Slovakia, China and possibly other countries. We are all very pleased to devote this exciting meeting to the memory of our friend Monte Arnold Greer.

Vladimir Strbak

ACKNOWLEDGMENTS

We want to express our gratitude for the unflagging support—moral and financial—we received from **Wright State University**, in particular:

Dr. Perry Moore, Executive Vice President

Dr. David Hopkins, Provost

Dr. Joseph Thomas, Associate Provost

Dr. Howard Part, Dean, School of Medicine

Mr. John Bale, Associate Dean, School of Medicine

Dr. Robert Fyffe, Associate Dean for Research Affairs, School of Medicine

Dr. Michele Wheatly, Dean, College of Science and Mathematics

Dr. Gerald Alter, Biomedical Sciences Ph.D. Program

Dr. Arthur Pickoff, Department of Pediatrics, Children's Medical Center

This symposium was supported by a grant from the **National Institute of Diabetes, Digestive and Kidney Diseases** of the **National Institutes of Health (1R13DK064886-01)**. We would like to thank Program Director **Dr. David Badman**,for helping us achieve the goals of this meeting.

In addition, our thanks go to **Mr. Bob Coyne** of **Fuji Medical Systems** for his generous support of the 2003 Dayton International Symposium on Cell Volume Regulation and Signaling.

CONTENTS

FOREWORD v

DEDICATION vii

ACKNOWLEDGMENTS ix

1. THE BALANCING ACT OF THE NAKED CELL: A BRIEF HISTORY OF MEMBRANE REGULATION OF ANIMAL CELL VOLUME BEFORE 1978 1
John S. Willis (Pre-Symposium Lecturer)

ELECTRONEUTRAL COTRANSPORTERS

2. TWENTY-FIVE YEARS OF K-Cl COTRANSPORT: FROM STIMULATION BY A THIOL REACTION TO CLONING OF THE FULL-LENGTH KCCs 11
Peter K. Lauf and Norma C. Adragna

3. MOLECULAR PHYSIOLOGY OF MAMMALIAN K^+-CL^- COTRANSPORTERS 29
Adriana Mercado, Gerardo Gamba, and David B. Mount

4. STE20 KINASES AND CATION-CHLORIDE COTRANSPORTERS: A MINI REVIEW 43
Eric Delpire

5. MOLECULAR PHYSIOLOGY OF THE RENAL Na^+:Cl^- AND Na^+:K^+:2Cl^- COTRANSPORTERS 55
Gerardo Gamba and Norma A. Bobadilla

6. THE ROLE OF THE BLOOD-BRAIN BARRIER Na-K-Cl COTRANSPORTER IN STROKE: A Minireview 67
Martha E. O'Donnell, Tina I. Lam, Lien Tran and Steven E. Anderson

7. REGULATION OF Na-K-2Cl COTRANSPORT IN RED CELLS 77
Peter Flatman

8. A NOVEL NHE1 FROM RED BLOOD CELLS OF THE WINTER FLOUNDER: REGULATION BY MULTIPLE SIGNALING PATHWAYS 89
Stine F. Pedersen

ION CHANNELS AND EXCHANGERS

9. PROBING OF THE ICln CHANNEL PORE BY CYSTEINE MUTAGENESIS AND CADMIUM-BLOCK 99
M. Jakab, M. L. Garavaglia, J. Fürst, S. Rodighiero, F. Guizzardi, G. Meyer, M. Ritter, and M. Paulmichl

10. VOLUME–DEPENDENT AND -INDEPENDENT ACTIVATED ANION CONDUCTANCES AND THEIR INTERACTION IN THE RENAL INNER MEDULLARY COLLECTING DUCT (IMCD) 109
Stefan H. Boese, Mike A. Gray, and Nick L. Simmons

11. SECRETORY CONTROL OF BASOLATERAL MEMBRANE POTASSIUM AND CHLORIDE CHANNELS IN COLONIC CRYPT CELLS 119
Dan R. Halm

12. EFFECTS OF AMMONIUM ON ION CHANNELS AND TRANSPORTERS IN COLONIC SECRETORY CELLS 131
Roger T. Worrell and Jeffrey B. Matthews

13. THE VOLUME-ACTIVATED CHLORIDE CURRENT DEPENDS ON PHOSPHOLIPASE C ACTIVATION AND INTRACELLULAR CALCIUM MOBILIZATION 141
D. Varela, F. Simon, A. Riveros, F. Jørgensen and A. Stutzin

14. NITRIC OXIDE (NO) MODULATION OF CL-DEPENDENT TRANSPORTERS IN THE KIDNEY 147
Pablo A. Ortiz and Jeffrey L. Garvin

15. VOLUME ACTIVATED ON CHANNEL AND ASTROCYTIC CELLULAR DEMA IN TRAUMATIC BRAIN INJURY AND STROKE 157
Harold K. Kimelberg (Keynote Speaker)

CELL VOLUME, CYTOSKELETON AND APOPTOSIS

16. EFFECTORS AND SIGNALING EVENTS ACTIVATED BY CELL SHRINKAGE IN EHRLICH ASCITES TUMOR CELLS: IMPLICATIONS FOR CELL PROLIFERATION AND PROGRAMMED CELL DEATH 169
Else K. Hoffmann and Stine Falsig Pedersen

17. WATER MOVEMENT DURING APOPTOSIS: A ROLE FOR AQUAPORINS IN THE AVD 179
Elizabeth Jablonski, Ashley Webb and Francis M. Hughes, Jr.

18. APOPTOSIS AND CELL VOLUME REGULATION: The importance of ions and ion channels 189
Gerd Heimlich, Carl D. Bortner and John A. Cidlowski

19. ANION CHANNEL INVOLVED IN INDUCTION OF APOPTOSIS AND NECROSIS 205
Yasunobu Okada, Emi Maeno, and Shin-ichiro Mori

20. ERYTHROCYTE ION CHANNELS IN REGULATION OF APOPTOSIS 211
Florian Lang, Christina Birka, Svetlana Myssina, Karl S. Lang, Philipp A. Lang, Valerie Tanneur, Christophe Duranton, Thomas Wieder, and Stephan M. Huber

21. APOPTOSIS *VS.* ONCOSIS: ROLE OF CELL VOLUME AND INTRACELLULAR MONOVALENT CATIONS 219
Sergei N. Orlov and Pavel Hamet

22. POLYCYSTIN-2 AS A SIGNAL TRANSDUCER 235
H. F. Cantiello, N. Montalbetti, G. A. Timpanaro, and S. González-Perrett

23. FURTHER CHARACTERIZATION OF THE NEMATODE ICLNN2 PROTEIN RECONSTITUTED IN LIPID BILAYERS 245
M. Ritter, C. Bertocchi, M. Jakab, J. Fürst, M. Paulmichl

24. HYPERTONICITY-INDUCED CATION CHANNELS IN RAT HEPATOCYTES AND THEIR INTRACELLULAR REGULATION 253
Frank Wehner and Heidrun Olsen

25. CELL VOLUME SENSING AND REGULATION IN SKELETAL MUSCLE CELLS: Lessons from an Invertebrate 263
Hector Rasgado-Flores, Jillian Theobald, Susan Markowitz, Darryl Zlatnick, Pei-Ang Yee, Pei-Ping Yee, Lauren Trais, Kathy Gohar, David Hergan, Robert Buechler, Robert Lajvardi and Cecilia Pena-Rasgado

26. Q-VD-OPh, NEXT GENERATION CASPASE INHIBITOR 293
Thomas L. Brown

OSMOLYTE TRANSPORTERS AND SIGNALING

27. ARE MEMBRANE TYROSINE KINASE RECEPTORS INVOLVED IN OSMOTRANSDUCTION? 301
H. Pasantes-Morales, R. Lezama and R. Franco

28. GLIAL-NEURONAL SIGNALING AND ASTROGLIAL SWELLING IN PHYSIOLOGY AND PATHOLOGY 313
Elisabeth Hansson and Lars Rönnbäck

29. CELL SWELLING-INDUCED PEPTIDE HORMONE SECRETION 325
Vladimir Strbák, Julius Benicky, Susan E. Greer, Zuzana Bacova, Miroslava Najvirtova, and Monte A.Greer

30. VOLUME REGULATION OF THE HIPPOCAMPUS 331
James E. Olson and Norman R. Kreisman

31. CELL VOLUME REGULATION IN INTESTINAL EPITHELIAL CELLS 339
Sebastian F.B.Tomassen, Hugo R. de Jonge and Ben C. Tilly

32. REGULATION OF EPITHELIAL ELECTROLYTE TRANSPORTERS THROUGH PROTEIN-PROTEIN INTERACTIONS 349
Carole M. Liedtke

33. THE ROLE OF THE PHOSPHOINOSITIDE PATHWAY IN HORMONAL REGULATION OF THE EPITHELIAL SODIUM CHANNEL 359
Bonnie L. Blazer-Yost and Charity Nofziger

34. MODULATION OF VOLUME-SENSITIVE TAURINE RELEASE FROM NIH3T3 MOUSE FIBROBLASTS BY REACTIVE OXYGEN SPECIES 369
Ian H. Lambert

35. HYPERTENSION IN K-CL COTRANSPORTER-3 KNOCKOUT MICE 379
Norma C. Adragna, Yanfang Chen, Eric Delpire, Peter K. Lauf and Mariana Morris

ABSTRACTS

36. PHYSIOLOGY AND PATHOPHYSIOLOGY OF THE ERYTHROCYTE GARDOS CHANNEL IN HEMATOLOGICAL DISEASES 387
Carlo Brugnara, Lucia De Franceschi, and Alicia Rivera

37. SWELLING-ACTIVATED CALCIUM-DEPENDENT POTASSIUM CHANNELS IN AIRWAY EPITHELIAL CELLS 388
José M. Fernández-Fernández, Esther Vázquez, Maite Arniges, Muriel Nobles, Aoife Currid and Miguel A. Valverde

38. KCNQ CHANNELS ARE SENSORS OF CELL VOLUME..... 389
Morten Grunnet, Thomas Jespersen, Nanna K. Jørgensen, Nanna MacAulay, Nicole Schmitt, Olaf Pongs, Henrik S. Jensen, Søren-Peter Olesen and Dan A. Klaerke

39. MEMBRANE LOCALIZATION OF THE NEURONAL K-CL COTRANSPORTER (K-Cl COT, KCC2) IN RAT CEREBELLUM 390
Kenneth B.E. Gagnon, Peter K. Lauf, and Robert E.W. Fyffe

40. K-Cl COTRANSPORT (K-Cl COT, KCC) ACTIVATION BY *N*-ETHYLMALEIMIDE IN C6 GLIOMA CELLS 391
Kenneth B.E. Gagnon, Norma C. Adragna, Robert E.W. Fyffe, and Peter K. Lauf

41. EXPRESSION OF PLASMA MEMBRANE CA^{2+} ATPASE IN CRAYFISH DURING MOLTING 393
Y.P. Gao, M. Nade and M.G. Wheatly

42. SALINITY AFFECTS CRAYFISH PMCA AND NCX EXPRESSION……..…….... 396
Y.P. Gao and M.G. Wheatly

43. CRAYFISH EPITHELIAL CA^{2+} CHANNEL-LIKE GENE (*ECAC*) ……..……. 398
Y.P. Gao and M.G. Wheatly

44. MODULATION OF KCNQ4 CHANNELS BY CHANGES IN CELL VOLUME …… 401
Charlotte Hougaard, Dan A. Klaerke, Søren-Peter Olesen, Else K. Hoffmann, and Nanna K. Jorgensen

45. PKA PHOSPHORYLATION OF SGK MODULATES ADH-STIMULATED Na^+ TRANSPORT IN A6 MODEL RENAL CELLS …….. 403
Nathan Kast, Nicola Perrotti and Bonnie L. Blazer-Yost

46. CELL VOLUME MODIFIES AN ATP-SENSITIVE ANION CONDUCTANCE IN CULTURED HIPPOCAMPAL ASTROCYTES ……. 405
Guangze Li and James E. Olson

47. ADH-STIMULATED Na^+ TRANSPORT: INTERACTION BETWEEN THE cAMP/PKA AND PHOSPHOINOSITIDE SIGNALING PATHWAYS …….. 407
Charity Nofziger and Bonnie L. Blazer-Yost

48. EFFECT OF ALDOSTERONE ON Na^+ TRANSPORT IN A MODEL RENAL EPITHELIAL CELL LINE A proteomic approach …… 409
Puneet Souda, Frank Witzmann and Bonnie L. Blazer-Yost

49. UPREGULATION OF NCX PROTEIN IN HEPATOPANCREAS AND ANTENNAL GLAND OF FRESHWATER CRAYFISH ASSOCIATED WITH ELEVATED CA^{2+} FLUX……. 411
La'Tonia M. Stiner, Yongping Gao and Michele Wheatly

SPECIAL MUSICAL CONTRIBUTION (SARABANDA) FOR PETER LAUF, MD 415
Hector Rasgado-Flores

INDEX…….....…….. 427

CONTRIBUTORS

Norma C. Adragna (Co-Chair, Organizing Committee)
Department of Pharmacology and Toxicology
Wright State University
012 Mathematics and Microbiology
3640 Colonel Glenn Highway
Dayton, OH 45435
937-775-2104
937-775-2759
norma.adragna@wright.edu

Maite Arniges
Dept de Ciencia Experimentales y de la Salud
Universitat Pompeu Fabra
c/o Dr. Aiguader, 80
08003 Barcelona,
Spain
93-542-28-84
93-542-28-02
maite.arniges@cexs.upf.es

Julius Benicky
Institute of Experimental Endocrinology
Slovak Academy of Sciences
Vlarska 3
SK-88306 Bratislava,
Slovakia
421-2-5477-3800
421-2-5477-4247
julius.benicky@savba.sk

Bonnie L Blazer-Yost
Biology Department
Indiana U-Purdue Univ Indianapolis
723 W Michigan Street
Indianapolis, IN 46202-5132
317-278-1145
317-274 2846
bblazer@iupui.edu

Stefan H. Boese
Institut für Biochemie & Biologie Zoophysiologie
Universität Potsdam
Villa Liegnitz
Lennéstrasse. 7a
D-14471 Potsdam,
Germany
phone:#49-(0)331-977 4850
fax: #49-(0)331-977 4861
sboese@rz.uni-potsdam.de

Carl D. Bortner
National Institute of Environmental Health Science
111 Alexander Drive MD F3-07
Research Triangle Park, NC 27709
919-541-7535
919-541-1367
bortner@niehs.nih.gov

Thomas L. Brown
Anatomy and Physiology
Wright State University
042 Biological Sciences Bldg
3640 Colonel Glenn Highway
Dayton, OH 45435
937-775-3809
937-775-3769
thomas.l.brown@wright.edu

Carlo Brugnara
Children's Hospital Bader, 760
300 Longwood Ave.
Boston, MA 02115
1-617-355-6610
1-617-355-6081
brugnara@tch.harvard.edu

Horacio F. Cantiello
Renal Unit
Massachusetts General Hospital East
149 13th St.
Charleston, MA 02129
1-617-726-5640
1-617-726-5669
cantiell@helix.mgh.harvard.edu

John A Cidlowski
Lab Signal Tranduction NIEHS
NIH Bldg 10 RM 1A01
PO BOX 12233
MDE2-02, 111 Alexander Drt
Research Triangle Park, NC 27709
919-541 1564
919-541 1367
cidlows1@niehs.nih.gov

Eric Delpire
Dept. Anesthesiology
Vanderbilit Univ. Med. Ctr.
1161 21st Ave. S., T-4202, MCN
Nashville, TN 37232-2520
1-615-343-7409
1-615-343-3916
eric.delpire@mcmail.Vanderbilt.edu

Jose M. Fernandez-Fernandez
Dept de Ciencia Experimentales y de la Salud
Universitat Pompeu Fabra
c/o Dr. Aiguader, 80
08003 Barcelona,
Spain
93 542 28 89
93 542 28 02
jmanuel.fernandez@cexs.upf.es

Peter W Flatman
Membrane Biology Group
Biomedical and Clinical Laboratory Sciences
The University of Edinburgh
Hugh Robson Building
George Square
Edinburgh, EH8 9XD,
Scotland, UK
44-0-131-650-3254
44-0-131-650-6527
peter.flatman@ed.ac.uk

Robert E. Fyffe (Member, Organizing Committee)
Associate Dean
SOM Research Affairs
Wright State University
3640 Colonel Glenn Highway
Dayton, OH 45435
937-775-3018
937-775-3009
robert.fyffe@wright.edu

Kenneth Gagnon
Vanderbilit University
T-4202, Medical Center North
1161 21st Avenue South
Nashville, TN 37232-2520
1-615-343-5347
1-615-343-3916
ken.gagnon@vanderbilt.edu

Gerardo Gamba
Inst. National Nutric, Salvador Zubrian Inst.
Invest. Biomed., UNAM
Vasco Quiroga 15
Tlalpan, 14000
Mexico City,
Mexico
1-525-513-3868
1-525-655-0382
gamba@biomedicas.unam.mx

Yongping Gao
c/o Michele Wheatly, Dean
College of Science and Mathematics
Wright State University
3640 Colonel Glenn Highway
Dayton, OH 45435
937-775-2611
937-775-3068
ping.gao@wright.edu or
michele.wheatly@wright.edu

Dan Halm (Member, Organizing Committee)
Anatomy and Physiology Dept
Wright State University
063 Medical Sciences Bldg
3640 Colonel Glenn Highway
Dayton, OH 45435
937-775-2742
937-775-3769
dan.halm@wright.edu

Elisabeth Hansson,
Institute of Clinical Neuroscience
Göteborg University
Medicinaregatan 5
SE 405 30
Göteborg,
Sweden
+46-31-773-3363
+46-31-773-3330
elisabeth.hansson@anatcell.gu.se
hanssone@mailer.mednet.gu.se

Else K. Hoffmann
Reader in Biochemistry
August Krogh Institute, Univ. of Copenhagen
13, Universitetsparken
2100 Copenhagen, ø
Denmark
45-3532-1695
45-35321567
ekHoffmann@aki.ku.dk

Charlotte Hougaard
Biochemical Dept.
August Krogh Institute
13, Universitetsparken
DK-2100 Copenhagen,
Denmark
45-35-32-17-17
45-35-32-15-67
chougaard@aki.ku.dk

Francis "Monty" Hughes, Jr.
Dept of Biology
University of North Carolina at Charlotte
9201 University City Blvd.
Charlotte, NC 28223
704-687-2934
704-687-3128
mhughes@email.uncc.edu

Nathan Kast c/o Bonnie Blazer-Yost
Biology Department
Indiana U-Purdue Univ Indianapolis
723 W Michigan Street
Indianapolis, IN 46202-5132
317-278-1145
317-274 2846
nkast@iupui.edu

Harold K Kimelberg
Neural and Vascular Biology Theme
Associate Director, Ordway Research Institute
150 New Scotland Avenue
Albany, NY 12208
518-262-6097
518-262-6178
hkimelberg@ordwayresearch.org

Daniel Klaerke
University of Copenhagen
The Planum Institute
Blegdamsvej 3
DK-2200 Copenhagen N,
Denmark
45-35-327569
45-35-327526
klaerke@mfi.ku.dk

Ian Henry Lambert
The August Krogh Institute
Biochemical Department
Universitetsparken 13
2100 Copenhagen 0,
Denmark
45-35321697
45-35321567
ihlambert@aki.ku.dk

Florian Lang
Physiologisches Institut
Eberhard-Karls-Universität Tübingen
Gmelinstr. 5
72076 Tübingen,
Germany
49-7071-2972194
49-7071-295618
florian.lang@uni-tuebingen.de

Peter Lauf (Chair, Organizing Committee)
Laboratory of Cell Biophysics
Wright State University
014 Mathematics and Microbiology
3640 Colonel Glenn Highway
Dayton, OH 45435
937-775-3024
937-775-2759
peter.lauf@wright.edu

Guagnze Li
Emergency Medicine
052B Cox Institute
Wright State University
3640 Colonel Glenn Highway
Dayton, OH 45435
937-395-8839
937-775-8387
guangze.li@wright.edu

Carole M Liedtke
Pediatric Pulmonology
Case Western Reserve University BRB 824
2109 Adelbert Road
Biomed Res Bldg
Cleveland, OH 44106-4948
216-368-4629
216-368 4223
carole.liedtke@case.edu

Jeffrey Matthews
University of Cincinnati College of Medicine
231 Albert Sabin Way
Cincinnati, OH 45267-0558
(513) 558-5333
(513) 558-2585
jeffrey.mathews@uc.edu

Adriana Mercado
Brigham and Women's Hospital - Harvard
Medical School
Room 542-, Harvard Institutes of Medicine
77 Avenue Louis Pasteur
Boston, MA 02115
617-525-5888
617-525-5830
amercado@rics.bwh.harvard.edu

David B. Mount, M.D.
West Roxbury Veterans Administration Medical Center
1400 VFW Parkway,
West Roxbury, MA 02132
617-525-5876
617-525-5830
dmount@rics.bwh.harvard.edu

Minal Nade
Biology Department
Wright State University
215 Biological Sciences
Dayton, OH 45435
937-775-2083
937-775-3200
nade.2@wright.edu

Charity Nofziger c/o Bonnie Blazer-Yost
Biology Department
Indiana U-Purdue Univ Indianapolis
723 W Michigan Street
Indianapolis, IN 46202-5132
317-278-1145
317-274 2846
c_stripes@yahoo.com

Martha Eaton O'Donnell
Dept Human Physiology
U Cal-Davis Sch Med
One Shields Avenue
Davis, CA 95616-8644
530-752-7626
530-752-5423
meodonnell@ucdavis.edu

Yasunobu Okada
Department of Cell Physiology
National Institute for Physiological Sciences
Myodaiji-cho
Okazaki, 444-8585
Japan
81-564-55-7731 or 7734
81-564-55-7735 or 52-7913
okada@nips.ac.jp

James E. Olson (Member, Organizing Committee)
Research Laboratory - Emergency Medicine
Cox Institute
Wright State University
3640 Colonel Glenn Highway
Dayton, OH 45435
937-395-8839
james.olson@wright.edu

Sergei Nicholai Orlov
Dept Molec Med Ctr Research
Univ of Montreal
3850 Street Urabin
Montreal, Quebec,
Canada
514-843 2925
514-843 2911
sergei.n.orlov@umontreal.ca

Pablo Ortiz
Henry Ford Hospital
2799 West Grand Blvd
Detroit, MI 48202
313-916-8501
313-916-1479
PORTIZI@hfhs.org

Herminia Pasantes-Morales
Instituto de Fisiologia Celular
Universidad Nacional Antónoma de México
Ciudad Universitaria
Apdo. Postal 70-253
C.P. 04510 Mexico, D.F.,
Mexico
525-622-5588
525-622-5607
hpasante@ifisiol.unam.mx
hpasante@ifc.unam.mx

Markus Paulmichl
Institut für Physiologie
Universität Innsbrück
Fritz-Pregl-Str. 3
A-6020 Innsbrück,
Austria
43-512-507-3756
43-512-507-7656
markus.paulmichl@uibk.ac.at

Stine Falsig Pedersen
Department of Biochemistry
August Krogh Institute
University of Copenhagen
3, Universitetsparken
DK-2100 Copenhagen ø
Denmark
+45-35321546
+45-353215671
shpedersen@aki.ku.dk

Cecilia Pena-Rasgado-Flores
Dept Physiology and Biophysics
Finch Univ Health Sci/Chicago Medical School
333 Greem Nau Rpad
N.Chicago, IL 60064-3037
847-578-3425
847-578-3265
floresh@finchcms.edu

Hector Rasgado Rasgado-Flores
Department Physiology and Biophysics
Chicago Medical School
Rosalind Franklin University
333 Green Bay Road
N.Chicago, IL 60064-3037
847-578 3425
847-578 3265
hector.rasgado@rosalindfrannklin.edu

Markus Ritter
Institut für Physiologie
Universität Innsbrück
Fritz-Pregl-Str. 3
A-6020
Innsbruck,
Austria
43-512-507-3766
43-512-507-2853
markus.ritter@uibk.ac.at

Alicia Rivera
Children's Hospital Boston
300 Longwood Avenue Bader 7
Boston, MA 02115
6173557413
6177134347
alicia.rivera@tch.harvard.edu

Puneet Souda c/o Bonnie Blazer-Yost
Biology Department
Indiana U-Purdue Univ Indianapolis
723 W Michigan Street
Indianapolis, IN 46202-5132
317-278-1145
317-274 2846
psouda@iupui.edu

La'Tonia Stiner
Biology Department
Wright State University
215 Biological Sciences
3640 Colonel Glenn Highway
Dayton, OH 45435
937-775-2083
937-775-3200
Lstiner788@aol.com

Vladimir Strbák
Institute of Experimental Endocrinology
Slovak Academy of Sciences
Vlárska 3
Bratislava 83306,
Slovakia
421-7-54774101
421-7-54774908
vladimir.strbak@savba.sk

Andres Stutzin
ICBM Facultad de Medicine
Universidad de Chile
Independencia 1027
Santiago,
Chile
56-2-678-6494
56-2-737-6240
astutzin@bitmed.med.uchile.cl

Ben C. Tilly
Dept. of Biochemistry
Erasmus University Medical Center
P.O. Box 1738
3000 DR Rotterdam,
The Netherlands
31-0-10-4087323
31-0-10-408-9472
b.tilly@erasmusmc.nl

Diego Varela
Universidad de Chile
Independencia 1027
6530499 Santiago
Chile
56-2-678-6494
562-737-6240
dvarela@bitmed.med.uchile.cl

Esther Vazquez
Cell Signalling Unit
Universitat Pompeu Fabra
Dpto. De Ciencies Experimentals
08003 Barcelona,
Spain
34-93-542-2884
34-93-542-2802
esther.vazquez@cexs.upf.es

Frank Wehner
Max-Planck-Institut für molekulare Physiologie
Abteilung Epithelphysiologie
Postfach 50 02 47
44202 Dortmund,
Germany
49-231-1332225
49-231-1332699
frank.wehner@mpi-dortmund.mpg.de

Michele G. Wheatly
College of Science and Mathematics
Wright State University
3640 Colonel Glenn Highway
Dayton, OH 45435
937-775-2611
937-775-3068
michele.wheatly@wright.edu

John S. Willis
Department of Cellular Biology
Medical College of Georgia
Athens, GA 30602
706-542-3323
706-542-4271
jswillis@cellmate.cb.uga.edu
iswillis@isp.com

Roger T. Worrell
The Vontz Center for Molecular Studies
Epithelial Pathobiology Group
Department of Surgery
University of Cincinnati
3125 Eden Avenue
Cincinnati, OH 45219-0581
513-558-6489
roger.worrell@uc.edu

1

THE BALANCING ACT OF THE NAKED CELL

A brief history of membrane regulation of animal cell volume before 1978

John S. Willis*

1. INTRODUCTION

Asked to discuss the history of cell volume regulation, my first reaction was one of panic. This was alleviated by my realization that the first task of a would-be "historian" is to choose his dates. Accordingly, I have limited myself in this review to a few of the central issues that were of concern prior to 1978. Twenty-five years ago is a convenient date from which to mark the beginnings of the modern era of this subject, and so I shall discuss the foundation upon which it is based, in other words, its "prehistory." Two excellent reviews appeared in 1977[1, 2] that obviate a further detailed accounting; therefore, my role here diminishes mainly to a ceremonial one of invoking the names of heroes and the memory of their key accomplishments.

Consensus regarding cell volume regulation prior to 1978 was based on three main propositions that traced their origins back more than 50 years: (1) The plasma cell membrane is incapable of resisting significant tension; (2) Accordingly, cells of animals are generally isosmotic with the internal environment that surrounds them and (3) This osmotic balance is achieved by managing the cells' selective permeability to ions and by extruding excess sodium ions. By 1978, cracks had begun to appear in this simplified picture, leading to the modern expansion of the subject.

* John S. Willis, Department of Cellular Biology, University of Georgia, Athens, GA 30602 USA

2. FRAGILE MEMBRANES

The concept that the membrane of naked animal cells is too fragile to resist tension or to stretch was initially based on experiments of E. Newton Harvey[3,4] in the early 1930's that showed the force required to break eggs of sea urchins and other marine invertebrates viewed in a centrifugal field under a centrifuge microscope[5] was very small, corre-sponding to 1 dyne/cm or less.

In 1937, Eric Ponder[6] found that after rabbit red cells were made spherical by treatment with lecithin, their surface area was reduced by 23 per cent below that of the normally discoid cells. When these sphericized cells were then exposed to media with lower osmolarities, their surface area expanded with swelling, and they lysed when their surface area returned to its original value in the discoid cells. The conclusion from these two studies was that the membrane of animal cells is too fragile to withstand osmotic pressure differences. This conclusion was reexamined over the ensuing 40 years with greater sophistication of methods and analysis,[7] but without any basic revision.

3. ISOTONICIY OF CYTOPLASM

The notion that animal cells – or at least mammalian cells – were isotonic with their medium was for a long time conventional wisdom, weakly supported, if at all, by evidence. In 1923, van Slyke[8] and his colleagues assumed isotonicity entirely on the basis of the discoid shape of red cells, since they were capable of swelling and changing shape in hypotonic media. John P. Peters was a strong spokesperson for the dogma of isosmolarity from as early as 1935. In a 1944 review, he proclaimed, "Despite the extreme differences in composition of the contents of its various compartments, a uniform osmotic pressure prevails throughout the fluids of the body."[9] This assertion was seriously challenged by several investigators during the 1950's, most notably by James R. Robinson, then of the Pathology Department at Cambridge, and later Professor of Physiology at the University of Dunedin in New Zealand. Robinson wrote several reviews between 1950 and 1960, but my favorite is his 1954 SEB Symposium paper[10] in which he defended the unlikely proposition of active transport of water from the cell as being a beneficial intellectual exercise as recommended by "Carroll, 1872." The Carroll reference was to Lewis Carroll's *Through the Looking Glass: And What Alice Found There*!

Robinson's argument[10] was based in part on the contractile vacuoles of fresh water protozoa (as they were then called in the mistaken belief that they were animals). These organelles appeared to secrete water and to be responsible for the metabolically dependent osmotic balance of protista such as ciliates and amoebae, as inferred from numerous microscopic observations such as those of Kitching.[11] Robinson's other arguments were that certain epithelial cells must face on one surface a hypotonic medium, so cannot be in equilibrium on both faces, that cryoscopic measurements for half a century before had often indicated that tissues were hypertonic to their environment and that metabolically compromised cells swelled in putatively isosmotic medium and were only prevented from swelling in hypertonic medium. Swelling in some of these cases, he said, could not be ascribed to inhibition of Na pumps because similar results were obtained in Na-free balanced media.[10]

The possibility that tissue cells such as kidney, liver and heart were hypertonic to their environment was laid to rest largely through the detailed cryoscopic measurements of Maffly and Leaf[12] and of Appelboom *et al.*[13] Both these studies involved elaborate precautions against autolysis causing a spurious rise in solute concentration before freezing was initiated and by using melting rather than freezing point as the measure of total osmotic concentration. In the case of Maffly and Leaf,[12] tissue taken from living anesthetized animals was quick-frozen in liquid nitrogen, pulverized and suspended in silicone. The deeply frozen samples were allowed to warm with stirring to prevent thermal gradients and the curve of melting time (converted to per cent water melted) *vs.* rising temperature was compared with samples of serum and found to be the same. The approach of Appelboom *et al.*[13] involved dropping snippets of freshly collected tissue into boiling water to kill autolytic enzymes, then determining total solute content of the known volume of the mixture by melting point depression. Robinson[14] professed himself satisfied with the conclusion from these results that at least these tissues were isotonic.

4. THE DOUBLE DONNAN CONCEPT

The reason the presumption of isotonicity had become so wide-spread without prior rigorous testing was that it fit well with the equally ingrained belief in the Double-Donnan system as a basis for explanation of ion distributions across the cell membrane and stability of cell volume. The explicit first proposal of a Double Donnan hypothesis appears to have been that of Hsien Wu[15] (Union Medical College, Beijing) in a brief note in the Journal of Biological Chemistry in 1926 in reference to work he had carried out earlier in collaboration with Van Slyke's group.[8] Wu stated that the concentration gradients of animal cells could be explained by a Donnan equilibrium determined by the fixed position of impermeant organic anions in the cytoplasm and of crystalloids, e.g., Na ion, in the cell's environment. Later extension of the hypothesis predicted that in muscle, nerve and other nucleated cells, the membrane can be freely permeable to K ion and that cells will swell if Na is replaced in the medium by K, provided Cl is also free to move. That cell swelling does indeed occur in frog muscle fibers incubated with elevated K concentration was, according to Kleinzeller,[16] first observed by Loeb in 1898 and studied in more detail by Overton in 1902 in connection with inactivation of excitability by extracellular K.

In my generation, the foundation of the idea that cells are in a Double Donnan equilibrium was laid by the classic paper of Boyle and Conway[17] published in 1941, beginning on page 1 of volume 100 of the Journal of Physiology. That study hinged on the issue of K permeability, and indeed, this 62 page paper began with the sentence, "We are concerned here chiefly with an account of the mechanism underlying the accumulation of potassium in the excised sartorius of the frog." They showed, among many things, that gain of K as a function of K in the medium was linear and fit with expectations from calculations based on a Donnan Equilibrium. Their evidence for impermeability of the membrane to Na was weak and was based mainly on the lack of gain of Na when swelling was occurring under conditions of elevated K. They also cited some early, apparently crude, experiments with radioactive Na that suggested the isotope only equilibrated into the extracellular space of the muscle.

There ought to be a corollary of Parkinson's Law stating that once a paradigm is firmly established, the seeds of its demise are already sprouting. That at least was the case for the concept that animal cells are in an osmotic equilibrium based on absolute impermeability to Na. Even at the time of publication of Boyle and Conway, evidence was emerging that the membrane was not impermeable to Na: frog muscle, after all, gained Na when it was electrically stimulated and when it was stored in the cold or in K-free medium. It was such observations by H. Burr Steinbach[18] on frog muscle in low K medium that lead Robert Dean[19] at Rochester University to propose in 1941 that the gradient for Na must occur through metabolically dependent extrusion of Na by means of some kind of "pump" in the cell membrane.

Once it was accepted that animal cells live in a dynamic steady state (now called a Double Donnan system, as distinct from an equilibrium), it became necessary to explain the swelling of cells under metabolic inhibition that was being used as an argument for their hypertonicity. This issue was explored by several investigators in the early 1950's, most notably by Mudge in rabbit kidney slices.[20] These early studies showed that when cells swelled under metabolic inhibition, there was a gain of Na and Cl along with the water taken up by swelling. A quantitative accounting for the solute causing the uptake was obscured by use of fresh tissue weight or water content as a mass base and by the apparent complementarity of K loss with Na gain. In 1956, Alexander Leaf[21] published a particularly clear and quantitative demonstration that the fluid which accumulated in metabolically inhibited guinea pig kidney slices was isotonic. In other words, the net increase of chloride and excess Na (beyond that balanced by K loss) computed on the basis of dry weight of tissue was isotonic with the medium when divided by the water uptake, also computed on a dry weight basis. Thus, the swelling was explained by the collapse of the Na and Cl gradients and the fluid being taken up was not hypotonic, as would have been required by the hypertonicity-water pump hypothesis. These results and conclusions were confirmed in studies of rat diaphragm by Rixon and Stevenson.[22]

5. THE PUMP-LEAK HYPOTHESIS

Based on his results both on directly measured tonicity of tissues and on the ion movements in metabolically inhibited cells, Leaf,[23] in 1959, propounded the model of a metabolically dependent Na-K pump balancing a passive leak. Inhibition of this pump would then lead to collapse of the gradients and movement toward a single Donnan, swollen state.

During the 1950’s, center stage was thus largely occupied by net movements occurring in rather sloppy, tissue slice preparations. The apotheosis of the "pump-leak" model, however, came with the publication in 1960 of a paper by Tosteson and Hoffman[24] from the NIH in which isotopically measured *unidirectional* fluxes of Na and K in red blood cells were used to validate a mathematically rigorous version of the model. In their mathematical model, cell volume and ion concentrations could be predicted by three transport parameters − the ratio of rate coefficients of passive leak of Na and of passive leak of K, the ratio for K pump flux to K leak flux, and the coupling ratio of the Na-K pump. The validating measurements to test the mathematical model were carried out in

HK and LK sheep red cells in which vastly different natural rates of pump activity could be compared with leak fluxes and cell ion concentrations.

6. BEYOND PUMP AND LEAK

Once again, however, the complacency that any of us might have felt at having arrived at a satisfactory stopping place was short-lived. By 1960, ouabain and other cardiac glycosides had been shown to be powerful and specific inhibitors of the Na-K pump. Therefore, numerous tests of the pump-leak model hinged upon the success or failure of ouabain-treated cells to behave according to that expectation.

In the sloppy slice arena, trouble began with the findings of Kleinzeller and Knotkova[25] in 1964 that in Na-loaded rabbit kidney slices reincubated under favorable metabolic conditions, a considerable portion of Na extrusion and reversal of swelling occurred in the presence of ouabain. Ouabain also failed to cause swelling in fresh slices. In the ensuing two years, Whittembury[26] and I[27] independently observed that there was a corresponding component of Na extrusion from Na-loaded kidney slices that was independent of K in the medium.

In 1968, I reported that if one combined these two treatments − K-free incubation and presence of ouabain − then Na extrusion from Na-loaded kidney slices, measured after one hour of reincubation, was fully blocked.[28] So, I suggested that the failure of either ouabain or K-free incubation to block Na extrusion fully in the earlier studies was due to the possibly restricted localization of pumps to inaccessible lateral intercellular spaces, coupled with local loss of K interfering with ouabain inhibition. This was in keeping with the finding of Kleinzeller and Knotkova[25] that liver slices, where accessibility of pumps would have been less of an issue, did not show the failures of ouabain they saw in kidney slices. So it seemed that “pump-leak” might be rescued. However, in the volume of BBA published just prior to the one containing my own paper was a paper by ADC MacKnight[29] that I had overlooked. This paper described results in which K-free incubation with ouabain present did fail to block a component of Na extrusion at early times, e.g., less than 15 minutes, of reincubation. Reuptake of Na occurred by one hour that would have accounted for my observations, and this secondary reuptake he attributed to other, non-pump related processes.

This puzzling state of affairs in kidney slices persisted, e.g., Whittembury and Proverbio[30] and to my knowledge was never satisfactorily resolved. Shortly after this time, interest turned away from volume regulation in sloppy slices with their cellular heterogeneity and structural complexity to better defined preparations such as renal tubules, cell cultures, and other models that lent themselves to isotopic flux measurements.

In the same period, red blood cells were the king of simple, homogenous cell models, ideal for isotopic flux measurements. These also began to exhibit unexplained departures from the minimal pump-leak hypothesis. First, there were the observations by Kregenow and Hoffman[31] of an ouabain-insensitive, ethacrynic acid-sensitive, so-called "pump II" in human red cells. Then, there were the high-Na red cells of dogs that John Parker[32] found maintained volume regulation without any Na-K pump at all but had volume-sensitive passive movements of Na and K. Parker later found that maintenance of cell volume depended upon Ca in the medium and that dog red cells, unlike red cells of other

mammals outside the order of Carnivora, also possessed a Na-Ca exchanger. Thus, he could establish a hypothesis[32] by which an ATP-dependent Ca pump could maintain a stable concentration of cytoplasmic Na, albeit a very high one.

Finally, there was the emergence of studies based on responses of cells to anisotonic medium, especially hypotonic media, in which it was shown that cells have rapid-response membrane transport systems, insensitive to ouabain, that return cell volume to its normal value following swelling or shrinking. Notable among these early findings were those of Floyd Kregenow[33] with duck red cells. He postulated rapid alterations of membrane passive permeability, especially to K during swelling (similar to that seen in the dog red cells) and was confirmed in this by numerous studies in other cell models.

So, three assumptions upon which the Tosteson-Hoffman model had been based were now seen not to hold in exceptional cases: The Na-K pump need not be the only metaboli-cally dependent mechanism involved in cell volume regulation, and under challenging conditions, the rate of K leak to K pumping need not be a constant nor the ratio of Na leak to K leak.

The stage was then set for the modern era of discovery of ever more diverse membrane transport mechanisms involved with maintenance of constant volume in naked animal cells. What was classically seen as a balancing act has now, in modern times, become a juggling act. In this act, the basic pump and “leak” are supplemented by the downhill or secondary uphill movements of diverse solutes that can be traded or coupled to ensure the appropriate net movement of water.

7. ORPHANED QUESTIONS

Four questions linger from the classical period that have been largely ignored or forgotten, "orphaned" as it were, or at best kept alive by a "single parent." These are: (1) Where does the membrane come from that allows cells to swell? (2) Is there a common "leak" pathway in animal cells in the sense envisioned in the "pump-leak" hypothesis? (3) What happened to explaining contractile vacuoles, and are they relevant to mammalian cells? (4) How does temperature impinge on cell volume regulation?

7.1 Source of Membrane for Swelling?

Many of us are accustomed to thinking in terms of the biconcave mammalian red cell becoming spherical and swelling without stretching its membrane. Other cells may benefit from some similar geometric trick. For, example, microvilli were shown to disappear with swelling in Lettré cells.[34] But not all cells have odd shapes or surface wrinkles to contribute. Even the red cells in Ponder's experiments were sphericized before they swelled, and Ponder[6] had the grace to wonder where the membrane "had gone" and where it "came back from." He postulated subcellular vesicles as membrane reserves. Cell biology has since taught us much about membrane dynamics and exchanges with vesicles, but seldom, if ever, in the context of cell swelling.

7.2 A Common Leak?

In the classical discussions, leakiness was viewed as a common and possibly essential feature of animal cells. Since then, we have been faced with the discovery of a plethora of passive transport systems for electrolytes, exchangers, cotransporters and channels of various kinds: ligand-gated, voltage-gated, volume-sensitive, stretch-sensitive, and so on. Yet, the complement of these is cell-specific and usually operative only under special circumstances. So, when things are quiet, is there still a common leak? If so, what is it? In red cells it has been suggested that the linearly diffusive influx of K is a proton-cation exchanger.[35] Genomics has permitted the identification of putatively generic leak chan-nels in *C. elegans*. Are these present in mammalian cells?

7.3 Contractile Vacuoles?

The classical view of contractile vacuoles (CV) was that in free-living cells they secreted water or at least a solution hypotonic to the cytoplasm. Some cryoscopic observations have indeed indicated that the CV contents may be hypotonic. Since the 50's, it has been found that a network of membrane-limited spaces, the "spongiome," connect to a contractile vacuole,[36] raising the possibility of primary transport of solute followed by water to fill the system, followed in turn by secondary modification to remove solute from the final excreted fluid.[37] However, recent studies indicate an actually hypertonic solution of KCl in the CV of Paramecium[38] and an accumulation of phosphate compounds in trypanosomes.[39] In their 1977 review, MacKnight and Leaf[1] recognized the possibility that vesicular exocytoplasmic space could play an important role in cell volume regula-tion. Beginning in 1977 and continuing to the present, studies by George van Rossum and his colleagues at Temple have demonstrated there does indeed appear to be such a role – vesicular systems in liver and other tissue cells that fill with fluid during swelling and empty during recovery – and that, like contractile vacuole systems, possess V-ATPase in the membrane along with ion exchangers.[40, 41] These could easily account for ouabain-insensitive isotonic NaCl extrusion of Na-loaded cells. Thus, as in canine red cells, a different ATPase could be a backup to the Na-K ATPase as a primary governor of Na content and cell volume.

7.4 Effect of and Response to Temperature Change?

In the original sloppy slice studies, the most common method of reversibly Na-loading cells was to place them at temperatures close to 0°C, supposedly inhibiting energy metabolism. Since then, numerous but scattered studies have indicated that cooling cells does not necessarily lower ATP content. In my laboratory at Illinois, Marina Marjanovic demonstrated in human and guinea pig red cells that inhibition of Na-K pump at reduced temperature was not due to decline of ATP but rather was caused by a loss of affinity of the pump for ATP.[42] The remaining question is how do cells manage in the face of more moderately varying temperatures? In the classical pump leak model, the Na-K pump could have compensated for varying Na load by the direct stimulation of cytoplasmic Na on the ATPase. Now, with the plethora of diverse leak pathways, the likelihood that Na leak maintains a constant relationship to K leak with varying temperature is unlikely.

Indeed, we have found that increase in temperature *inhibits* Na-K-Cl cotransport and Na-H exchange in red blood cells while greatly stimulating K-Cl cotransport.[43, 44] The mechanisms that balance the multiplicity of these leaks with pump activity are yet to be discovered.

Thus, in addition to being a high-wire juggler, the naked animal cell may also be like a magician, pulling membrane out of a hat, hiding fluid and pumps in deep pockets, and escaping the effects of heat and cold.

8. REFERENCES

1. A.D.C. MacKnight, and A. Leaf, Regulation of cellular volume, *Physiol. Rev.* **57**, 510-572 (1977).
2. E.K. Hoffmann, Control of cell volume, in: *Transport of Ions and Water*, edited by B. Gupta, J. Oschmann, and B. Wall, (Academic Press, New York) pp.285-332 (1977).
3. E.N. Harvey, A determination of the tension of the surface of the eggs of the annelid, *Chaetopterus, Biol. Bull.* **60**, 67-71 (1931).
4. E.N. Harvey, The tension at the surface of marine eggs, especially those of the sea urchin, *Arbacia*, *Biol. Bull.* **61**, 273-279 (1931).
5. E.N. Harvey, A microscope-centrifuge, *Science*, **72**, 42-44 (1930).
6. E. Ponder, The spherical form of the mammalian erythrocyte III. Changes in surface area in disks and spheres, *J. Exp. Biol.* **14**, 267-277 (1937).
7. E.A. Evans, and R.M. Hochmuth, Membrane viscoelasticity, *Biophys. J.* **16**, 1-11 (1976).
8. D.D. van Slyke, H. Wu, and F.C. McLean, Studies of gas and electrolyte equilibria in the blood. V. Factors controlling the electrolyte and water distribution in the blood, *J. Biol. Chem.* **56**, 765-849 (1923).
9. J.P. Peters, Water exchange, *Physiol. Rev.* **24**, 491-531 (1944).
10. J.R. Robinson, Secretion and transport of water, *SEB Symp*. **8**, 42-62 (1954).
11. J.A. Kitching, Osmoregulation and ionic regulation in animals without kidneys, *SEB Symp.* **8**, 63-75 (1954).
12. R.H. Maffly and A. Leaf, The potential of water in mammalian tissues, *J. Gen. Physiol.* **47**, 1257-1275 (1959).
13. J.W.T. Appelboom, W. A. Brodsky, W. S. Tuttle, and I. Diamond, The freezing point depression of mammalian tissues after sudden heating in boiling distilled water, *J. Gen. Physiol*. **41**, 1153-1169 (1958).
14. J.R. Robinson, Metabolism of intracellular water, *Physiol. Rev.* **40**, 112-149 (1960).
15. H. Wu, Note on Donnan equilibrium and osmotic pressure relationship between the cells and the serum, *J. Biol Chem.* **70**, 203-205 (1926).
16. A. Kleinzeller, Charles Ernest Overton's concept of a cell membrane, *Curr. Topics in Membranes* **48**, 1-22 (1999).
17. P.J. Boyle, and E. J. Conway, Potassium accumulation in muscle and associated changes, *J. Physiol. Lond.* **100**, 1-63 (1941).
18. H B. Steinbach, Sodium and potassium in frog muscle, *J. Biol. Chem.* **133**, 695-701 (1940).
19. R. Dean, Theories of electrolyte equilibrium in muscle, *Biol. Symposia* **3**, 331-348 (1941).
20. G. Mudge, Electrolyte and water metabolism of rabbit kidney slices: Effect of metabolic inhibitors, *Am. J. Physiol.* **167**, 206-223 (1951).
21. A. Leaf, On the mechanism of fluid exchange of tissues *in vitro*, *Biochem. J.* **62**, 241-248 (1956).
22. R H. Rixon, and J.A.F. Stevenson, Movements of sodium, potassium and water in rat diaphragm i*n vitro*, *Am. J. Physiol.* **194**, 363-368 (1958).
23. A. Leaf, Maintenance of concentration gradients and regulation of cell volume, *Ann., N. Y. Acad. Sci.* **72**, 396-404 (1959).
24. D.C. Tosteson, and J.F. Hoffman, Regulation of cell volume by active cation transport in high and low potassium sheep red cells, *J. Gen. Physiol.* **44**, 169-194 (1960).

25. A. Kleinzeller, and A. Knotkova, The effect of ouabain on the electrolyte and water transport in kidney cortex and liver slices, *J. Physiol. Lond.***175**, 172-192 (1964).
26. G. Whittembury, Sodium extrusion and potassium uptake in guinea pig kidney cortex slices, *J. Gen. Physiol.* **48**, 699-717 (1965).
27. J.S. Willis, Characteristics of ion transport in kidney cortex of mammalian hibernators, *J. Gen. Physiol.* **49**, 1221-1299 (1966).
28. J.S. Willis, The interaction of K^+, ouabain and Na^+ on the cation transport and respiration of renal cortical slices of hamsters and ground squirrels, *Biochim. Biophys. Acta* **163**, 516-530 (1968).
29. A.D.C. MacKnight, Water and electrolyte contents of rat renal cortical slices incubated in potassium-free media and media containing ouabain, *Biochim. Biophys. Acta* **150**, 263-270 (1968).
30. G. Whittembury and F. Proverbio, Two modes of Na extrusion in cells from guinea pig kidney cortex slices, *Pflug. Archiv.* **316**, 1-25 (1970).
31. J. Hoffman and F. Kregenow, The characterization of new energy dependent cation transport processes in red blood cells, *Ann. N. Y. Acad. Sci.* **137**, 566-576 (1966).
32. J.C. Parker, Solute and water transport in dog and cat red blood cells, in: *Membrane Transport in Red Blood Cells,* edited by J. C. Ellory and V. L. Lew (Academic Press, London) pp. 427-465 (1977).
33. F.M. Kregenow, *Transport in avian red cells, in: Membrane Transport in Red Blood Cells*, edited by J.C. Ellory and V.L. Lew (Academic Press, London) pp. 383-465 (1977).
34. S.D. Knutton, D. Jackson, J.M. Graham, K.J. Micklem, and C.A. Pasternak, Microvilli and cell swelling, *Nature* **262**, 52-54 (1976).
35. S. Richter, J. Hamann, and I. Bernhardt, The monovalent cation "leak" transport in human erythrocytes: An electroneutral exchange process, *Biophys. J.* **73**, 733-745 (1997).
36. R. Allen, The contractile vacuole and its membrane dynamics, *BioEssays* **22**, 1035-1042 (2000).
37. J. Heuser, Q. Zhu, and M. Clarke, Proton pumps populate the contractile vacuoles of Dictyostelium amoebae, *J. Cell Biol.* **121**, 1311-1327 (1993).
38. C. Stock, H.K. Gronlien, R.D. Allen, and Y. Naitoh, Osmoregulation in *Paramecium: in situ* ion gradients permit water to cascade through the cytosol to the contractile vacuole, *J. Cell Sci.* **115**, 2339-2348 (2002).
39. R. Docampo, and C.N.J. Moreno, The acidocalcisome, *Molec. Biochem. Parasit.* **33**, 151-159 (2001).
40. G.D.V. van Rossum, M.A. Russo, and J.C. Schisselbauer, Role of cytoplasmic vesicles in volume maintenance, *Curr. Topics in Membranes and Transport* **30**, 45-74 (1987).
41. G.D.V. van Rossum and J. Wadsworth, Role of intracellular organelles in the control of cell pH and volume, *Acta Medica Romana* **39**, 221-237 (2001).
42. M. Marjanovic and J.S. Willis, ATP dependence of Na^+-K^+- pump of cold-sensitive and cold-tolerant mammalian red blood cells, *J. Physiol. Lond.* **456**, 575-590 (1991).
43. J.S. Willis, On thermal stability of cation gradients in mammalian cells, *Advances in Molecular and Cell Biology*, **19**, 193-222 (1997).
44. J. . Willis and G.L. Anderson, Activation of K-Cl cotransport by mild warming in guinea pig red cells, *J. Membrane Biol.* **163**, 193-203 (1998).

2

TWENTY-FIVE YEARS OF K-Cl COTRANSPORT: FROM STIMULATION BY A THIOL REACTION TO CLONING OF THE FULL-LENGTH KCCs

Peter K. Lauf[†] and Norma C. Adragna*

1. INTRODUCTION

This chapter combines a review of research on a chemical intervention that, over a period of 15 years, preceded the molecular identification of the mechanism of K-Cl cotransport (potassium chloride cotransporter, KCC) and new data that reveals the caveats of an approach successfully used to unravel kinetic, thermodynamic and regulatory properties of this transporter. A recent comprehensive review from our laboratory on K-Cl cotransport, function, pathology and molecular properties[1] as well as several excellent earlier reviews[2-5] should be consulted for further details.

2. THIOL-MODIFICATION ACTIVATES K-Cl COTRANSPORT

Twenty-five years ago, we observed that N-ethylmaleimide (NEM) treatment of sheep red blood cells (RBCs) with genetically low (L) internal potassium (K) levels unexpectedly enhanced their passive, ouabain-insensitive K-permeability four- to eight-fold without changing their Na-permeability.[6] This effect, unusual since thiol-alkylation by NEM was expected to alter cation permeability *non-selectively*,[7] was repeated in LK goat RBCs but was barely in evidence in genetically high K (HK) sheep or goat RBCs. Simultaneously, one of us was studying the effect of chaotropic anions on the osmotic behavior of RBCs of *Opsanus Tau*, the ugly beauty of oyster toad fish, in the brackish waters around Pivers Island at Duke's Marine-Biological Station in Beaufort, North Carolina. It was noted that the nucleated RBCs of this species, upon swelling in hyposmotic media, showed regulatory volume decrease (RVD) in Cl but not in non-Cl media with NO_3 or SCN as replacement anions, with a net loss of K and Cl, i.e., they possessed a swelling-activated Cl-dependent K transport system inhibited by DIDS (4,4'-

* P. K. Lauf, Cell Biophysics Laboratory, Dept of Pathology and N. C. Adragna, Cell Biophysics Laboratory, Dept. of Pharmacology and Toxicology, Wright State University School of Medicine, Dayton, OH

diisothiocyanatostilbene-2,2'-disulfonic acid).[8] This effect resembled a behavior described in nucleated RBCs from *Amphiuma* possessing a K/H exchanger thermodynamically coupled to a DIDS-sensitive Cl/HCO_3 exchanger.[9] However, the fact that furosemide also inhibited RVD in *Opsanus Tau* RBCs pointed in another direction—that of loop diuretic-inhibited electroneutral Na-K-2Cl cotransporters seen in Ehrlich ascites cells[10] and in the thick ascending limb of Henle's loop.[11] Comparison of data in both sheep and fish species and studies on the cation-dependency of ouabain-insensitive K or Rb influx suggested a Na-independent, furosemide- (and DIDS-) sensitive, Cl-dependent K transport pathway. Results of these data together with work from Cambridge[12] on swollen LK sheep RBCs were later coined K-Cl cotransport. Such ouabain-insensitive, Na-independent K fluxes were actually first seen ten years earlier in human RBCs suspended in Mg media.[13]

Figure 1 with controls compares the remarkable effect of NEM on the zero-trans K efflux rate constants (left panel) in LK sheep RBCs. As shown on the right, there was a pronounced dose-dependence of the NEM-effect on K efflux rate constants abating at higher concentrations, whereas NEM did not affect Na efflux rate constants.

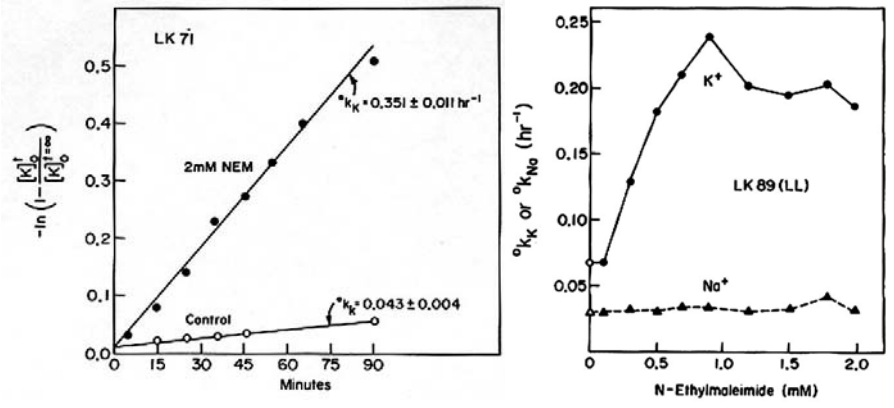

Figure 1. Left panel: N-ethylmaleimide (2 mM) stimulates the zero-trans K efflux rate more than eight-fold as compared to controls. Right panel: The effect of NEM on K efflux rate constants is sharply dose-dependent, whereas Na efflux rate constants in choline were not affected (with permission of the publisher[6]).

The argument that NEM targets not only thiols within a narrow, slightly alkaline pH range but also amino groups was soon laid to rest by our finding that a highly specific thiol alkyl reagent, methylmethanethiolsulfonate (MMTS), selectively activated K-Cl cotransport.[14] Furthermore, as shown in Figure 2 (left panel), hetero- or homo-functional dithiol formation by the membrane-permeable thiol oxidant diamide revealed for the first time an inverse relationship between cellular glutathione levels and K-Cl cotransport activity, suggesting the redox-dependence of this transporter in erythrocytes from a variety of species.[15-17] This diamide-induced oxidation is fully reversible, an advantage unnoticed in much of the work published later in this field. Upon subsequent incubation of LK SRBCs in glucose-containing media in the absence of diamide (Figure 2, right panel) or after treatment with 3 mmol dithiothreitol (DTT)/liter of cells (about twice the

cellular GSH concentration, Figure 3), GSH was fully restored and the previously stimulated ouabain-resistant K flux again inactivated. Although in ruminant RBCs, diamide activated K-Cl cotransport with little effect on diffusional fluxes, in human RBCs, it exerts a major effect on the latter through cytoskeletal modifications.[18] Whether diamide oxidation only involves the redox system governing a regulatory signal transduction pathway or directly affects sulfhydryls in the transporter remains to be seen.

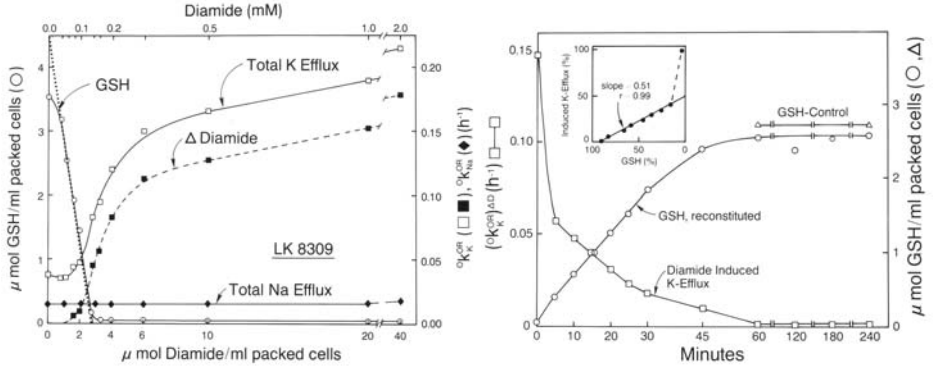

Figure 2. Apparent redox-dependence of K-Cl cotransport in LK sheep red blood cells. Left panel: Cellular GSH (left ordinate) and rate constants for K or Na effluxes (right ordinate) as function of diamide concentration in the medium (upper abscissa) or per liter of cells (lower abscissa). With an expected cellular molar ratio of close to 0.5 diamide/GSH, ouabain-resistant K, but not Na, efflux is stimulated as GSH levels fall below 50%. Right panel: Previously stimulated ouabain-resistant K efflux (left ordinate) decreases with restoration of cellular GSH (right ordinate) by incubation in glucose- and phosphate-containing media. Insert: the slope between changes in K efflux and GSH level is 0.5, indicating the close association of K-Cl cotransport activation with the oxidized GSH (GSSG) levels and cellular redox status (with permission of the publisher[15]).

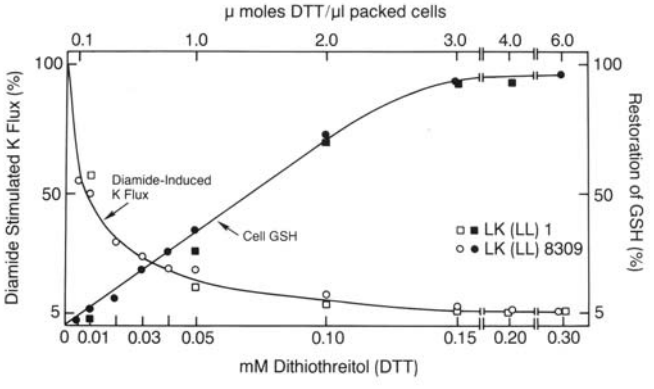

Figure 3. Dithiothreitol (DTT, abscissa), with a roughly two-fold stoichiometric ratio, restores cellular GSH (right ordinate) and abolishes the activation of the diamide-stimulated K flux (left ordinate) attributed to K-Cl cotransport in two samples of LK SRBCs (with permission of the publisher[15]).

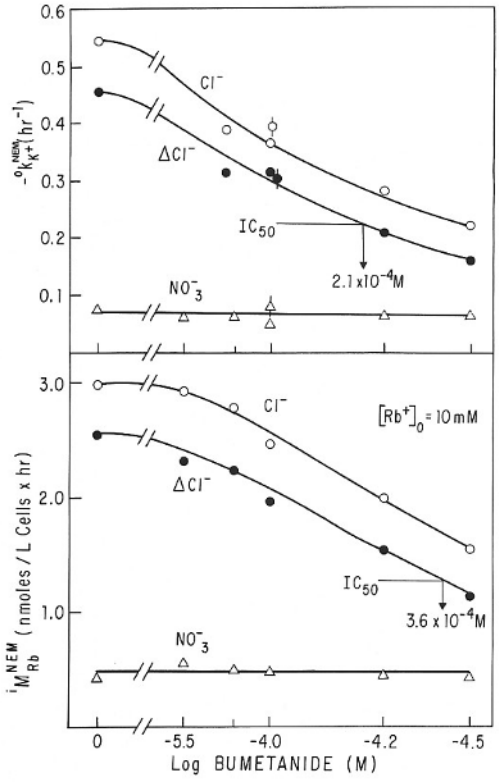

Figure 4. Bumetanide inhibition of NEM-stimulated zero-trans K efflux and Rb influx in LK SRBCs in Cl and NO_3. LK SRBCs were treated with 1 mM NEM for 15 min and preincubated for 30 min in the presence and absence of the bumetanide concentrations indicated on the abscissa, both at 37°C, prior to measuring K loss and Rb uptake. K efflux and Rb influx (ordinate) were calculated from the extracellular K and intracellular Rb, respectively, sampled under initial velocity at 5 time points within one hour after addition of Rb at zero-trans K.

Although initially HK sheep RBCs appeared to be unaffected by NEM, we later established there was also a very small activation of K-Cl cotransport in these cells, indicating a quantitative rather than qualitative difference in K-Cl cotransport activity. This result means the NEM effect on K efflux may be found in any erythrocyte and differences in K-Cl cotransport may be at the regulatory level. NEM has been shown to stimulate K-Cl cotransport in RBCs from man, rabbit, rat, mouse, and lamprey.[19-24] In hindsight, it is not surprising that, as in the fish erythrocyte, K-Cl cotransport in LK sheep RBCs is inhibited by furosemide[25] and DIDS[26] with K_d values of 300μM and 3μM, respectively. Since we showed earlier there was no functional evidence for Na-K-2Cl cotransport in sheep RBCs,[27-28] bumetanide, its classical inhibitor, was tested on K-Cl cotransport in LK SRBCs. In a heretofore unpublished experiment, Figure 4 shows where 210μM and 360μM bumetanide reduced NEM-activated K efflux and K influx by 50% (IC_{50}), respectively. This information is useful for ongoing work in other systems where bumetanide may suppress K-Cl cotransport at too high concentrations. Whereas the inhibition by furosemide and bumetanide fits into our understanding of action of loop

diuretics on electroneutral cotransporters, inhibition by DIDS, especially its augmentation by external K as also shown in other expression systems,[29] remains unresolved. Whether protein-protein interactions occur directly between the K-Cl cotransporter and the DIDS-inhibited anion exchanger (AE1) or indirectly involving the cytoskeleton is unknown.

Sheep RBCs remain a viable model for functional proteomics studies on K-Cl cotransport, currently under investigation in our laboratory, for another reason. There are two surface antigens present that are functionally associated with the Na/K pump (the L_p antigen) and K-Cl cotransport (the L_l antigen). Whereas the L_p antigen is a functional repressor of the pump, the L_l antigen appears to activate K-Cl cotransport. Antibodies against L_p activate Na/K pump flux and against L_l, inhibit K-Cl cotransport [30].

3. MEMBRANE AND REGULATORY MODELS

By the mid-eighties, three key observations led to an early membrane model of the K-Cl cotransport mechanism in RBCs based on the following findings. First, K-Cl cotransport activation by NEM occurred through low pK_a thiols, suggesting nearby imidazolium (histidine) residues.[31, 32] Figure 5 shows the pH-dependence of NEM action on the ouabain-insensitive K efflux rate constants. Since the effect is entirely Cl-dependent, it is K-Cl cotransport that is stimulated by NEM in LK SRBCs (and barely in HK SRBCs, sqares) at low pH and inhibited at high pH, near the normal pK_a of cysteine.

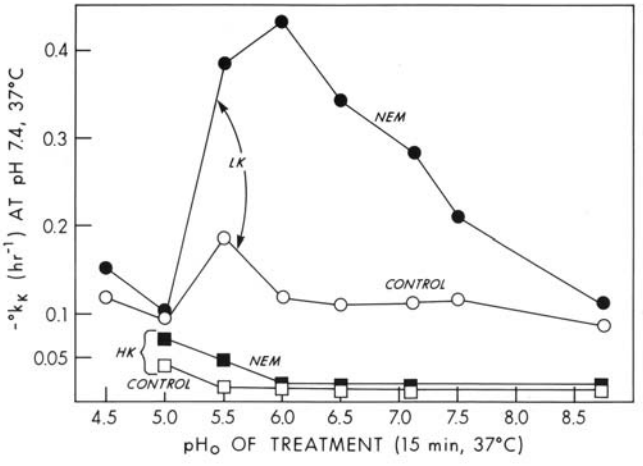

Figure 5. Effect of treatment pH (abscissa) on stimulation of the rate constant of ouabain-insensitive K efflux (ordinate) by 2 mM NEM in LK (circles) and HK (squares) SRBCs. Controls without NEM. (Data modified from[31] with permission of publisher.)

Second, ATP is required for thiol-stimulation of K-Cl cotransport, a finding as yet unexplained. Figure 6A shows the time course of ATP depletion in human RBCs by the deoxy-D-glucose method (left ordinate) is followed with about a one hour delay by inactivation of the NEM-stimulated ouabain-resistant Rb influx (K-Cl cotransport, right

ordinate).[33] Also seen in LK sheep RBCs,[34] this effect is fully reversible before NEM treatment, suggesting that ATP with an apparent affinity of 290μM is required to uphold the thiol modification, hence K-Cl cotransport stimulation (Figure 6, right panel).

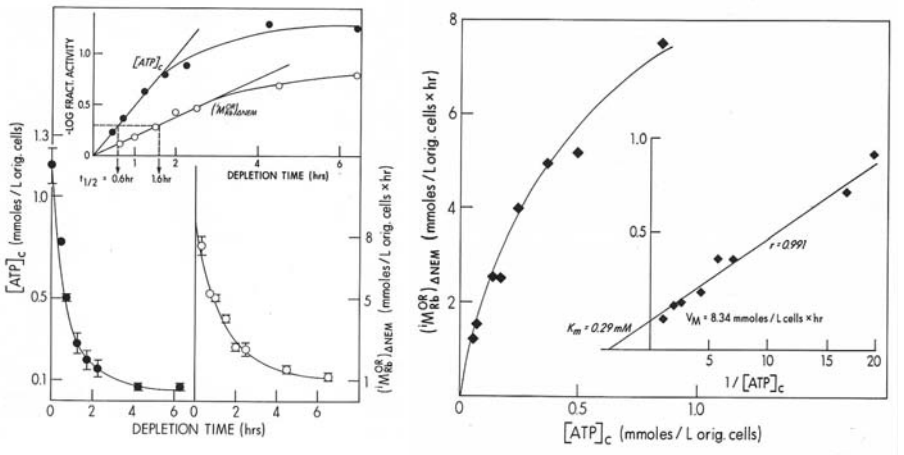

Figure 6. ATP-dependence of the NEM 'effect.' Left panel: Cellular ATP (left ordinate) and NEM-stimulated ouabain-resistant Rb influx (right ordinate) after 0-6 hours incubation in 2-deoxy-D-glucose depleting ATP. Insert: semilog plot of activity levels versus time; changes in ATP preceded those in the flux by ~1 h. (From ref.[33] with permission of publisher). Right panel: ATP-dependence of the NEM-supported K-Cl cotransport activity. The NEM-stimulated ouabain-resistant Rb influx is plotted as function of cellular ATP. Insert: double reciprocal plot of the same data yielding a K_m of 0.29mM.

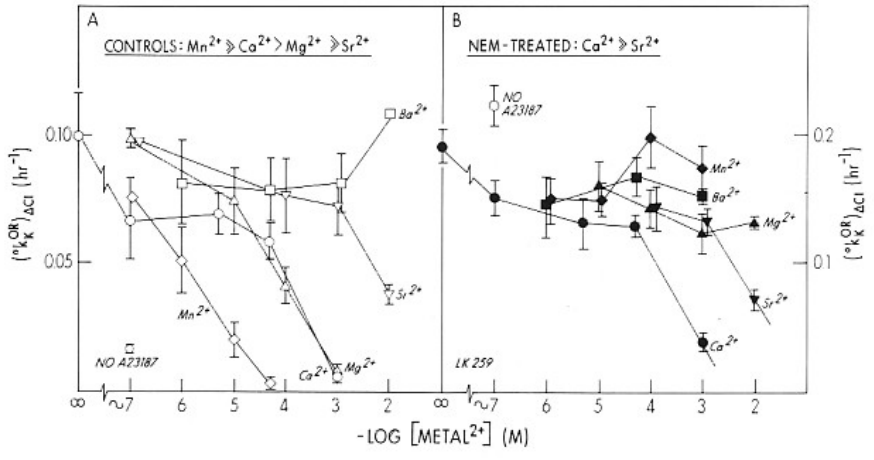

Figure 7. Modulation of K-Cl cotransport by divalent metal ions introduced in LK SRBCs by A23187. Panel A: K-Cl cotransport in controls (left ordinate) is inhibited by divalents in the order of Mn>Mg =Ca>Sr with the A23187-impermeable Ba ineffective. Panel B: Failure of Mn and Mg, but not of Ca or Sr, to inhibit NEM-stimulated K-Cl cotransport (right ordinate). From ref [35] with permission of the publisher.

Third, when introduced into RBCs by A23187, at least four divalent metal ions (Mn, Mg, Ca, and Sr) inhibit basal K-Cl cotransport in a dose-dependent manner. Figure 7A shows the usual inhibition of the basal cotransport efflux rate constants (left ordinate) by Mn and Mg is abolished by NEM treatment (figure 7B), suggesting thiol-sensitive Mn and Mg binding sites. The inhibition by Ca and Sr was unaffected.[35] The effects of Mg and MgATP are complex and have been studied in detail.[36-38]

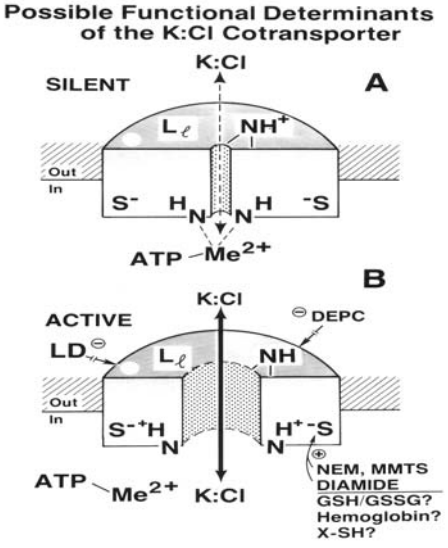

Figure 8: The early « membrane model » of K-Cl cotransport in erythrocytes. MeATP (presumably MgATP) binds via imidazolium moieties influencing the pK_a of neighboring thiols of the closed-state transporter, providing access for thiol reagents low pK_a thiols. Upon thiol modification by NEM, diamide and others, MeATP leaves its site shifting the transporter into the open state. This process is blocked by diethyl-pyrocarbonate (DEPC), probably at the external face of the transporter, and by anti-L_l, the antibody against the L antigen associated with K-Cl cotransport in LK SRBCs. (From ref.[41] with permission of publisher)

Coined "membrane model" and depicted in Figure 8, this model emerged naturally from our understanding of active monovalent cation transport. Previously, the protection of catalytic sites by ATP and protein conformational aspects[39] dominated the field of membrane transport more than signal transduction. In the model, the closed or resting state of the K-Cl cotransporter (A), MeATP (presumably MgATP) binds via imidazolium moieties that influence the pK_a of neighboring thiols, allowing thiol reagents such as NEM access to low pK_a thiols. Upon thiol modification by NEM, diamide and other thiol alkylants or oxidants, Me-ATP leaves its site and the transporter shifts into the open state. The V_{max} effect after chemical modification of low pK_a thiols (imidazolium-thiolates) was explained in terms of recruiting "silent" sites into the active state by Mg-ATP-dependent conformational changes within the transporter itself. This process is blocked by diethyl-pyrocarbonate (DEPC) probably acting at the external face of the transporter and by anti-L_l, the inhibitory antibody against the L antigen associated with K-Cl cotransport in LK SRBCs.[30, 40]

Thus, our membrane model combined a closed state of the transporter with reduced thiols and bound MgATP and an open state with oxidized thiols without ATP.[41] In effect, this model is compatible principally with the subsequent regulatory model of Jennings[43] in which the closed or resting state is phosphorylated by a volume and/or NEM-sensitive kinase and the open or active state dephosphorylated by either protein phosphatases 1 and 2A.[42] The two-state model is shown in the center of Figure 9. While the rate analysis of the activation (slow) and inactivation (fast) of K-Cl cotransport is commensurate with a simple phosphorylation equilibrium,[20, 43] combinatorial studies with inhibitors other than calyculin A (a PP1 inhibitor) such as the kinase inhibitors staurosporine, tyrphostin B46 and genistein led to the conclusion that the regulation may indeed be complex.[44-48] Thus, Figure 9 is expanded by including modifications based on the potential actions of thiol reagents on kinases of a regulatory cascade in control of the phosphatase PP1/PP2A.[44-48]

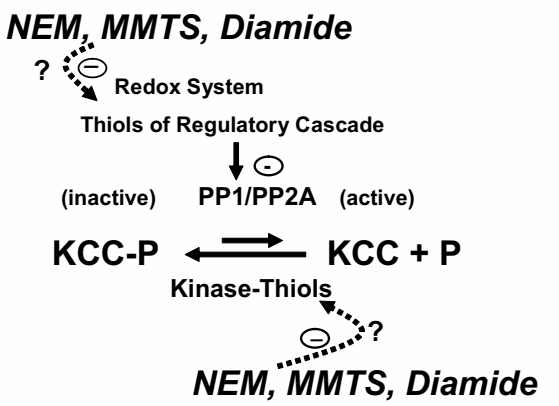

Figure 9. Regulatory Model of K-Cl Cotransport (KCC). At the heart of the model is the phosphorylation/ dephosphorylation mechanism of KCC maintained by a kinase/PP1 and PP2A equilibrium proposed by Jennings.[20, 43] The long solid arrow for the phosphorylation reaction and the shorter arrow for the dephosphorylation reaction are commensurate with the fast inactivation by shrinking and slow activation of the transporter by swelling. In this model, NEM, MMTS and diamide as well as Mg(ATP) depletion inhibit a kinase that directly phosphorylates KCC. Our data, as well as those of others, place the action of thiol compounds at the redox level removing the control of phosphatases (vertical arrow and negative sign in the circle).

4. FROM MODELS TO MOLECULAR REALITIES

Between 1978 and 1996, this laboratory was identifying the characteristics of K-Cl cotransport while the molecular nature remained elusive. K-Cl cotransport was reported to play an important role in the hydration status of human HbS (sickle) cells, an issue addressed by Carlo Brugnara[49] and in this symposium. Shortly after we presented preliminary data (1995 Membrane Biophysics Symposium, Beaufort, NC) on a swelling-activated K-Cl cotransport expression from a trout liver library in *Xenopus Laevi* oocytes,[50] the first two KCC isoforms, KCC1 and KCC2 were cloned and expressed.[51, 52] The open reading frame of the two cDNAs were 1086 and 1150 amino acids. KCC1, occurring in every cell and tissue analyzed, is considered the 'house-keeping' isoform; KCC2 only occurs in neuronal tissue.[52] Soon thereafter, at least three more isoforms were discovered: KCC3a,b[53-55] and KCC4, with distributions throughout many organs including muscle,

heart, vascular smooth muscle,[56-57] brain and kidney.[33] The KCC1-4 isoforms are now well-established members of a superfamily of solute cotransporters (SLC) to which the Na-Cl and Na-K-2Cl cotransporters and their isoforms also belong.[1, 2-4] In the studies showing molecular expression of these KCCs, activation through thiol groups by NEM was a convenient experimental tool to demonstrate successful transfection with KCC isoforms of human embryonic kidney (HEK293) cell lines,[51, 52, 58] NIH3T3 cells,[58, 59] and to correlate molecular expression with functional activity in vascular smooth muscle cells,[60] C6 glioma cells[61] and human lens epithelial B3 cells.[62] Even *Xenopus laevi* oocytes expressing KCC4 respond to NEM.[29]

At this point, we refrain from further review of well-established 'molecular realities,' since a wealth of information on the molecular properties of the KCC isoforms and their regulation will be presented in this Symposium Volume by David Mount, Eric Delpire, Gerardo Gamba and Martha O'Donnell. The consequences of the absence of the KCC2, 3 and 4 isoforms[63] are distinct pathologies of the central and peripheral nervous system, the auditory system, the vascular smooth muscle cells and the kidneys (see review[1]). In these proceedings, Norma Adragna will present evidence for hypertension in mice with KCC3 deficiency.[64] Without doubt, more abnormalities will be discovered with time.

5. POST-STIMULATORY NEM-INACTIVATION OF K-Cl COTRANSPORT

During the first decade of clarifying details of the NEM-stimulated K-Cl cotransport, little attention was paid to the fact that higher NEM concentrations actually inhibited the « NEM effect ». In a systematic study, we looked at this *post-stimulatory* inactivation by NEM in LK sheep RBCs[65] and found that, independently of the mode through which K-Cl cotransport was stimulated (NEM and other thiol reagents, swelling, Mg-depletion, and hydroxylamine), application of NEM concentrations higher than 0.5 mM at 37°C caused subsequent complete inhibition of K-Cl cotransport. We explained this phenomenon in terms of deocclusion of inhibitory thiols within the activated K-Cl cotransport complex, not reversible by mercaptoethanol.[65] The affinity of these inhibitory thiols for NEM is lower (about 2 mM) as opposed to the stimulatory thiols (0.2 mM). However, important for studies on tissue culture expression of KCC cDNAs where the stimulatory effect of NEM can easily be missed due to excessively high concentrations of the chemical or to overexposure time, the nature of this effect, possibly at the level of the transporter, is still largely unexplored.

In this section, we shall present this secondary effect of NEM in a human embryonic kidney cell line (HEK293) before and after stable transfection with rbKCC1 cDNA[58] and in primary rat aortic vascular smooth muscle cells.[66] Indication for occurrence of the effect in a third cell line, the C6 glioma cell, is presented as an abstract elsewhere in this symposium. For reference, Figure 10 shows the time dependence of the NEM effect on Na-independent ouabain-, bumetanide- and gadolinium-insensitive Rb uptake in HEK293 cells stably transfected with full length (fl) rabbit (rb) KCC1 cDNA. With a distinct lag phase, Rb uptake in Cl was maximally stimulated after 10 min but was statistically unchanged in sulfamate (SFM). Since, by definition, the Cl-dependent difference between Rb uptake in Cl and SFM is K-Cl cotransport, we conclude that 10 min exposure to 0.05 mM NEM suffices for maximum stimulation. The transient nature of the NEM effect is shown in the right panel of Figure 10. First, there was no significant change in basal K-Cl

cotransport with or without the reducing agent dithiothreitol (DTT). At zero time, i.e., immediately after NEM (0.05 mM) treatment for 10 min, Rb flux in Cl was stimulated three-fold over the basal flux. However, pre-flux incubation up to 50 min gradually abolished the NEM stimulation of K-Cl cotransport and this effect was not prevented by DTT, suggesting that the inhibitory NEM action was irreversible.

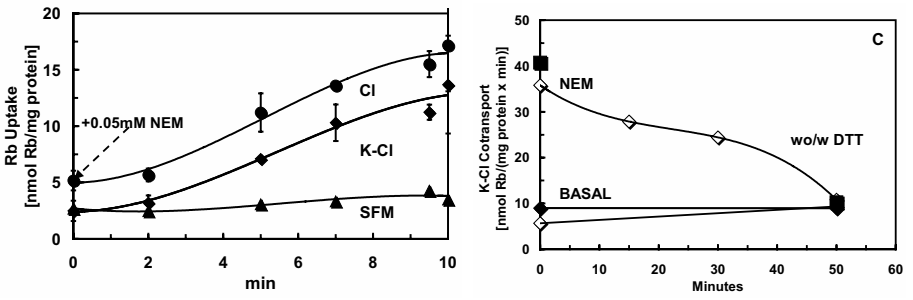

Figure 10. Post-stimulatory inactivation of K-Cl cotransport in human embryonic kidney (HEK293) cells stably transfected with rbKCC1 cDNA (kindly provided by Dr. Chris Gillen, Kenyon College, OH). Cells grown to 80% confluence in 12-well plates were washed in a temperature-equilibrated balanced NaCl solution (BSS), pH 7.4, then in BSS with bovine serum albumin and either Cl or sulfamate (SFM), and Na replaced by N-methyl-D-glucamine. Left panel: Media were removed and replaced with 37°C equilibrated flux solutions with 0.05 mM NEM in BSS-Cl or SFM and 10mM Rb in presence of (mM) 0.1 ouabain, 0.01 $GdCl_3$ and 0.01 bumetanide to inhibit Na/K pump, stretch-activated ion channels and Na-K-2Cl cotransport. After 0,2,5,7,9 and 10 min, cells were washed in isotonic $MgCl_2$, Tris/Cl buffered at 7.4. Protein was measured by Lowry method and Rb content by Atomic Absorption Spectrometry. Statistics on triplicate or quadruplicate wells of individual plates with n ± SD. K-Cl is the calculated difference of Rb influx in Cl and sulfamate (SFM). Right panel: Effect of pre-flux incubation on K-Cl cotransport in controls (squares) or with 0.05 mM NEM (rhomboids) in presence (filled symbols) or absence (open symbols) of 2 mM dithiothreitol (DTT, open symbols).

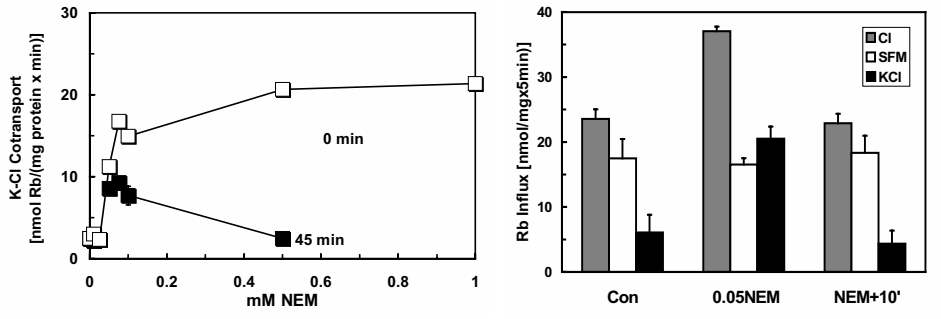

Figure 11. Transient nature of K-Cl cotransport stimulation in two different cell lines. Left: NEM-dose response of K-Cl cotransport stimulation in rbKCC1 cDNA stable-transfected HEK293 cells either immediately (0 min, open squares) or 45 min (filled squares) after 10 min exposure to the thiol reagent. K-Cl cotransport was measured as in Figure 9. Data points for n=3 with bars for SD. Right: Loss of NEM stimulation of Rb influx in rat aortic vascular smooth muscle cells (primary cultures, passage 6). After treatment with 0.05 mM NEM, Rb uptake (5 min) in Cl (striped columns) and in sulfamate (open columns) in presence of 1 mM ouabain and 30 μM bumetanide commenced immediately (0.05 NEM) or 10 min later (NEM+10'). Black columns: calculated K-Cl cotransport.

Figure 11 reveals the transient nature of NEM stimulation in two cell lines. The left panel shows K-Cl cotransport in HEK293 cells transfected with fl-rbKCC1 cDNA, either 0 (open squares) or 45 min (filled squares) after exposure to 0-1 mM NEM. After 45 min, the maximum stimulation of K-Cl cotransport was significantly reduced at 0.05 and 0.1 mM NEM and completely at 0.5 mM. In the right panel, post-stimulatory inhibition by NEM is shown for primary cultures of rat aortic smooth muscle cells. Whereas 0.05 mM NEM stimulated K-Cl cotransport three-fold above controls as calculated from Rb influx in Cl and sulfamate right after exposure to the thiol reagent,[67] the effect was lost after an additional 10 min incubation placed between treatment and flux periods.

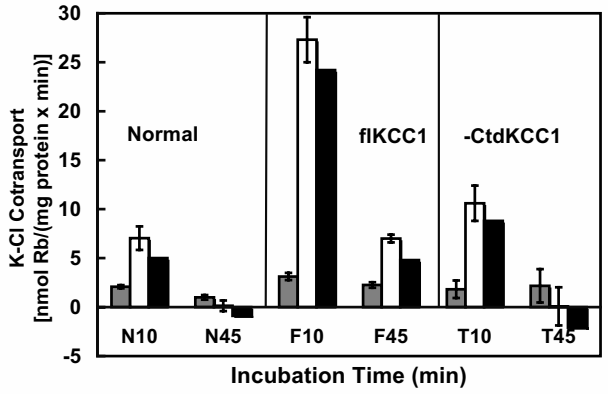

Figure 12. Post-treatment incubation-induced loss of NEM stimulation of K-Cl cotransport in normal (left) and experimental HEK293 cells transfected with either fl-rbKCC1 (center) or its C-terminal domain-truncated version, -CtdKCC1 (right). The basal K-Cl cotransport was highest in fl-rbKCC1 cDNA-transfected cells (compare striped columns in F10 and T10 with N10) and largely unaffected by length of post-treatment incubation (N,F,T10 vs N,F,T45, striped columns). NEM treatment 10 min prior to flux stimulated K-Cl cotransport in normals cells >3-fold and in flKCC1-transfected cells >4-fold (empty columns), an effect sharply reduced (center panel) or abolished (left or right panels) when the flux was measured 35 min later (NEM-specific components, N,F,T45, filled columns). Error bars for n=4 ± SD.

Since RBCs inhibited by NEM primarily affected the stimulated K-Cl cotransporter, we compared K-Cl cotransport in HEK293 cells before (normal) and after transfection with fl- or Ctd- (C-terminal domain) truncated rbKCC1 cDNAs, respectively, under the experimental regimen shown in Figure 9. In Figure 12, control and transfected HEK293 cells were exposed to 0.05 mM NEM for 10 min at 37°C followed by commencement of Rb uptake, immediately or 45 min later. The ordinate plots calculated K-Cl cotransport as defined above. In the left panel, 0.05 mM NEM stimulated K-Cl cotransport by three-fold (white columns) right after NEM exposure (N10). Removing NEM and incubating the cells for another 45 min followed by Rb uptake reduced the basal flux and eliminated the NEM effect so that the NEM-stimulated flux component (black columns) dropped from 5 to 0 nmol/(mg proteinxmin) (N45). In fl-rbKCC1 cDNA-transfected cells (center panel), the basal K-Cl cotransport was elevated as compared to controls, and NEM-stimulated flux measured immediately after treatment was five-fold above the value in normal cells (F10). Yet, measuring Rb influx 45 min later collapsed the NEM stimulation to values seen immediately after NEM-treatment (compare N10 with F45). Most likely, this is

residual transport activity through the transfection-expressed system, i.e., a kinetic effect, as borne out in cells transfected with the truncated mutant (-CTD KCC1, right panel). Here, NEM applied directly prior to Rb influx does not stimulate K-Cl cotransport significantly above the control (T10 vs N10), consistent with earlier reports for requirement of the C-terminal domain in the signal transduction process.[58, 68] When Rb influx commenced 45 min later, the residual NEM stimulation was completely obliterated (T45).

To counter the argument that when applied to the tissue culture, the decay rate of NEM, unstable at alkaline pH, was accelerated, we applied a second NEM treatment prior to the flux assay. Figure 13 compares normal (non-transfected, open columns) with fl-rbKCC1-transfected HEK293 cells (filled columns). The impressive stimulation by NEM in both normal and trans-fected cells at the end of the preincubation period (45-/10+) over the control (55-/-) was lost when NEM treatment was followed by further incubation (10+/45) and remained so upon a second NEM treatment (10+/35/10+).

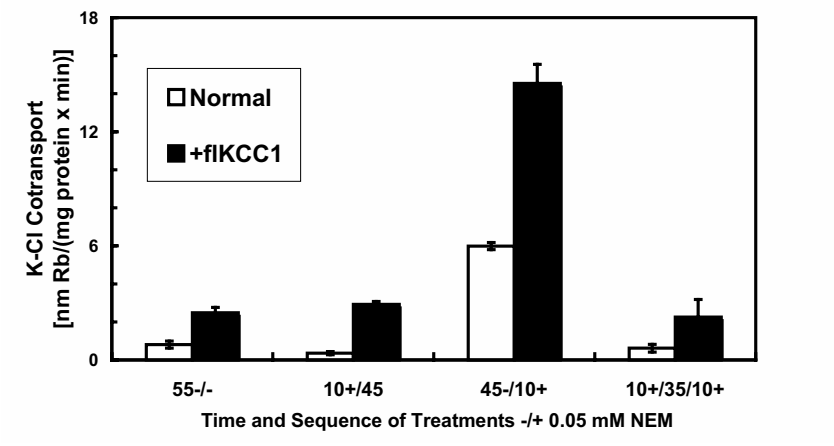

Figure 13. Irreversible loss of NEM-stimulated K-Cl cotransport in normal (open columns) and flKCC1-transfected (filled columns) HEK293 cells. Total incubation time was 55 min. In the absence of 0.5mM NEM (-/-), K-Cl cotransport in flKCC1 transfected cells was 3-fold above normal cells. When cells were first NEM-treated for 10 min and then kept for 45 min (10+/45), K-Cl cotransport in normal cells was obliterated and unchanged in flKCC1-transfected cells. An inverse procedure, i.e., first incubation for 45 min in the absence of NEM then 10 min prior to flux (54-/10+), led to the characteristic stimulation in both normal and flKCC1-transfected cells. Finally, after expoure to NEM at the beginning and end of the incubation separated by an NEM-free period of 35 min, no further stimulation of K-Cl cotransport occurred in normal and flKCC1 transfected cells (10+/35/10+).

As discussed, for erythrocytes, K-Cl cotransport stimulation by NEM requires cellular ATP and is inversely correlated with cellular GSH levels.[14-17, 33, 34] Figure 14 shows striking differences between ATP (left panel) and GSH (right panel) levels measured over 50 min following 10 min treatment with buffered media (open symbols) or with 0.1 mM NEM (closed symbols) in normal HEK293 cells in Cl (circles) or sulfamate (SFM, triangles). ATP decreased approximately 15% in sulfamate as compared to Cl in both controls and NEM-treated cultures, whereas cellular GSH was reduced by about 90% in both Cl and sulfamate following NEM treatment.

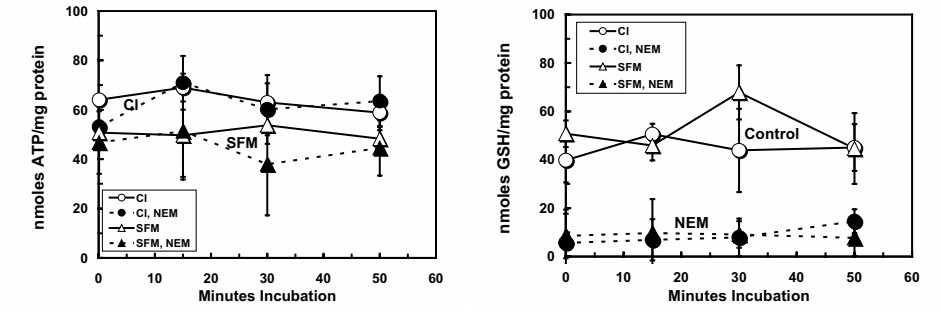

Figure 14. Effect of post-NEM (0.1 mM) treatment incubation on cellular ATP and GSH levels of non-transfected HEK293 cells. ATP was assayed by luciferin-luciferase and GSH by reduction of 5,5'-dithiobis(2-nitrobenzoic acid) at 412 nm. Left: ATP levels were resilient to NEM treatment (filled symbols) and slightly lower in cells incubated in sulfamate (SFM, triangles) than in chloride (Cl, circles). Right: GSH levels of controls (open symbols) in Cl and SFM were not different, ranging between 40-70 nmol/mg protein. However, independent of post-NEM treatment time, the GSH levels were reduced to about 1/10 of the untreated control values in either anionic medium (filled symbols). N = 3 ± SD.

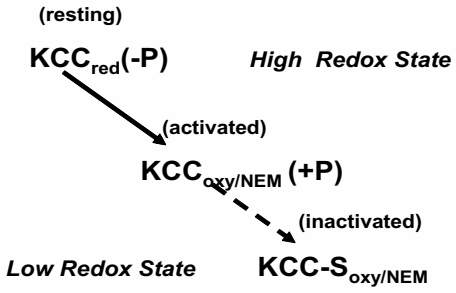

Figure 15. Redox control of phosphorylated and reduced K-Cl cotransporter ($KCC_{red}(-P)$), its transition to the activated mechanism ($KCC_{oxy/NEM}$ (+P)) under mild oxidizing conditions and subsequent irreversible inactivation at low redox state ($KCC\text{-}S_{oxy/NEM}$) at which "inhibitory" thiols have reacted.

In erythrocytes, we ascribed the phenomenon of post-stimulatory inactivation of K-Cl cotransport by NEM to the deocclusion of thiols by conformational changes brought about by various stimuli (NEM, staurosporine, hydroxylamine, Mg-depletion, and cell swelling)[64] and proposed the RAI (Resting, Activated, Inhibited) model.[46] Commensurate with this earlier model, we envision (Figure 15) that during moderate thiol modification/treatment, the normally high redox state is lowered and a kinase reversibly inhibited depending on the nature of the thiol modifying chemical (NEM versus diamide) causing the transition of the resting phosphorylated KCC ($KCC_{red}(-P)$) to the activated dephosphorylated KCC plus released phosphate ($KCC_{oxy/NEM}$ + P). Dephosphorylation then may expose/deocclude specific thiols within the K-Cl cotransporters through which NEM irreversibly inhibits K-Cl cotransporter function, perhaps by collapsing the putative transmembrane domains responsible for K binding and translocation (TMD 2). Possibly, the inhibitory thiols may constitute oxidized thiyls resulting from free radicals originating uncontrolled within the low redox state cell.[69]

Recently, we cloned and expressed sheep KCC1cDNA (Gene bank AF515770) translating about 20 cysteine residues in its 1086 amino acids.[70] Any of these cysteines may be targets for thiol modification, including four relatively unique cysteines (#160-163) within TMD 2. Whatever their location, the "inhibitory" cysteines appear to have pK_a values probably characteristic of 'normal' cysteine thiols since our earlier work established an alkaline pH optimum for NEM inhibition of K-Cl cotransport.[31, 32]

Does the model of the inhibitory action of NEM proposed for erythrocytes (c.f. Figure 15) explain the findings presented with HEK293 cells in this study? The answer is that a simple extrapolation from the erythrocyte to the nucleated cell is not feasible for the following reasons. First, a nucleated cell offers vast thiol-containing targets of functionally interdependent signalling pathways. In contrast, an enucleate RBC possesses mainly the glycolytic pathway and signaling systems in rudimentary form, probably not required in its final journey to the spleen. If there are indeed functional equivalents in both RBCs and nucleated cells, their regulation could be different. Corroborating other reports,[47] a case in point is staurosporine-stimulated K-Cl cotransport in RBCs[44] but not in control and fl-rbKCC1 cDNA-transfected HEK293 cells,[58] in C6 glia cells,[61] or in human lens epithelial cells.[62] Whereas calyculin A inhibition of K-Cl cotransport activetion by NEM, swelling, staurosporine and Mg depletion can easily be shown in RBCs, an effect by this protein phosphatase-1 inhibitor is more difficult to prove in C6 glia cells[61] and human lens epithelial B3 cells.[63] This fact may be due to different phosphorylation mechanisms prevailing in nucleated over enucleate cells, i.e., different kinases, absence of phosphatases, commensurate with a recent report that tumor virus-immortalized cell lines lack phosphatases.[71] A clearer answer may be forthcoming as kinases phosphorylating the KCCs and NKCCs and their phosphorylated domains are defined.[72] Second, KCCs may interact with the structural cytoskeletal components of the cell that, dynamically different in enucleate and nucleated cells, may also exhibit different susceptibilities to thiol modification. At the NEM concentrations and exposure times used, the erythrocyte shows little morphological change, whereas the nucleated cell may undergo morphological alterations associated with loss of cellular material where thiol modification-sensitive proteins could participate. Third, the absence of hemoglobin as a major buffer for thiol oxidation as well as interactive partner for membrane transport regulation (band 3[73]) may explain the relatively high sensitivity of HEK293, C6 glia and vascular smooth muscle cells to the inactivating NEM effects. Finally, there may be differences in tissues (vascular vs epithelial) and species (human vs rat or sheep).

6. CONCLUSIONS

In the discovery of the K-Cl cotransport system, N-ethylmaleimide, like cell swelling[8,12], Mg depletion[37,38] and staurosporine[44,47], was instrumental in preparing the grounds for the molecular realization of the KCCs. In this process, activation of the K-Cl cotransporter by thiol modification enabled many investigators to approach kinetic, thermodynamic and regulatory aspects of the system, first and foremost in erythrocytes, and subsequently to demonstrate the expression of the various KCC isoforms before and after transfection in mammalian nucleated cells as well in *Xenopus laevi* oocytes. Two temporally sequential models were reviewed: a membrane and a regulatory model. Although the evidence for the regulatory model seems to be overwhelming, a membrane

model may explain the irreversible inactivation by NEM of K-Cl cotransport, once activated by sulfhydryl reagents, swelling, kinase inhibitors, and oxidants in erythrocytes and nucleated cells. The data published for the first time here on the irreversible loss of NEM-activated K-Cl cotransport are relevant for any work involving approaches to demonstrate K-Cl cotransport with thiol reagents in nucleated cells. In considering the exact molecular mechanism by which this NEM "anti-effect" occurs in nucleated cells, we would like to draw attention to an early observation made in isolated hepatocytes.[74] Alteration of the redox state of these cells by t-butyl hydroperoxide, interesting a stimulant of K-Cl cotransport,[75] lowered GSH and mitochondrial as well as extramitochondrial Ca, causing plasma membrane surface blebbing. This "old" finding suggests the possibility of activation of K-Cl cotransport in nucleated cells by membrane stretch due to blebbing and inactivation due to disconnection from the cell's signaling cascade.

7. ACKNOWLEDGMENTS

This work was done with support by grants from the NIH/NIDDK (R01 DK36170 and R21DK064140 to PKL), and the American Heart Association (AHA0060451N to NCA). We owe special thanks to the NIH/NIDDK (R13 DK064886 to NCA and PKL) and Wright State University who supported this International Symposium. We thank Dr. Jin J. Zhang transfecting HEK293 cells with full length and cytoplasmic C-terminal domain truncated rbKCC1 cDNA, and Ms Kathy Rainey for the measurements of the functional expression of K-Cl cotransport. Ms Donna Maas proof-edited the manuscript.

8. REFERENCES

1. N.C. Adragna, M. Di Fulvio and P.K. Lauf, Regulation of K-Cl cotransport: From function to genes, *J. Memb. Bio.* (2004), in press.
2. E. Delpire, Cation-chloride cotransporters in neuronal communication, *News Physiol. Sc.* **15,** 309-312 (2000).
3. P.K. Lauf, N.C. Adragna, K-Cl Cotransport: Properties and Molecular Mechanism, *Cell Physiol. Biochem.* **10,** 341-354 (2000)**.**
4. D.B. Mount, E. Delpire, G. Gamba, A.E. Hall, E. Poch, R.S. Hoover, and S.C. Hebert, The electroneutral cation-chloride cotransporters, *J. Exp. Biol*. **201**, 2091-2102 (1998).
5. P.B. Dunham and R. Blostein, L antigens of sheep red cell membranes and modulation of ion transport. *Am. J. Physiol.* **272**, C357-C368 (1997).
6. P.K. Lauf and B.E. Theg, A chloride-dependent K^+ flux induced by N-ethylmaleimide in genetically low K^+ sheep and goat erythrocytes, *Biochem. Biophys. Res. Commun*. **92**, 1422 (1980).
7. A. Roths*tein,* Sulfhydryl groups in membrane structure and function, in *Current Topics in Membrane Transport*, edited by F. Bronner and A. Kleinzeller, Vol. 1, Acad. Press, New York, 135-176 (1970).
8. P.K. Lauf, Evidence for chloride-dependent potassium and water transport induced by hyposmotic stress in erythrocytes of the marine teleost Opsanus Tau, *J. Comp. Physiol*. **146,** 9 (1982).
9. P.M. Cala, Volume Regulation by Amphiuma Red Blood Cells, *J. Gen. Physiol*. **76**. 683 (1980).
10. P. Geck, C. Pietrzyk, B.C. Burckhardt, B. Pfeiffer and E. Heinz, Electrically silent cotransport of Na^+,K^+ and Cl^- in Ehrlich cells, *Biochim. Biophys. Acta* **600**, 432 (1980).
11. E. Schlatter, R. Greger and C. Weidtke, Effect of « high ceiling » diuretics on active salt transport in the cortical thick ascending limb of Henle's loop of rabbit kidney, *Pflüger's Arc.* **396**, 210 (1983).
12. P.B. Dunham and J.C. Ellory, Passive potassium transport in low potassium sheep red cells: dependence upon cell volume and chloride, *J Physiol. (London)* **318**, 511-530 (1981).
13. L.A. Beauge and N.C. Adragna, The kinetics of ouabain inhibition and partition of rubidium influx in human red blood cells, *J. Gen. Physiol*. **57**, 576-592 (1971).

14. P. K. Lauf, Kinetic Comparison of ouabain-resistant K:Cl fluxes (K:Cl [CO]-transport) stimulated in sheep erythrocytes by membrane thiol oxidation and alkylation, *Mol Cell Biochem* **82,** 97-106 (1988).
15. P.K. Lauf, Thiol-dependent K:Cl transport in sheep red cells: VIII. Activation through metabolically and chemically reversible oxidation by diamide, *J. Memb. Bio.,* **101,** 179-188 (1988).
16. N.C. Adragna and P.K. Lauf, Oxidative stimulation of K-Cl cotransport in red cells of different species including human with abnormal hemoglobins, *J. Memb. Biol*. **155,** 207-217 (1997).
17. H. Fujise, K. Higa, T. Kanemaru, M. Fukuda, N.C. Adragna, and P.K. Lauf, Effect of GSH depletion of K-Cl cotransport and regulatory volume decrease in high K/high GSH dog red blood cells, *Am. J. Physiol*. **281,** C2003-C2009 (2001).
18. C.W.M. Haest, D. Kamp, G. Plasa and B. Deuticke, Intra- and intermolecular cross-linking of membrane proteins in intact erythrocytes and ghosts by SH-oxidizing agents, *Biochim. Biophys. Acta* **469,** 226-230 (1977).
19. P.K. Lauf, N.C. Adragna, and R.P. Garay, Activation by N-ethylmaleimide of a latent K^+Cl^- flux in human erythrocytes, *Am. J. Physiol.* **246**, C385-390, 1984.
20. M.L. Jennings and N. Al-Rohil, Kinetics of activation and inactivation of swelling-stimulated K+Cl-cotransport. The volume-sensitive parameter is the rate constant for inactivation, *J. Gen. Physiol*. **95,** 1021-1040 (1990).
22. W. Su, B.F. Shmukler, M.N. Chernova, A.K. Stuart-Tilley, L. De Franceschi, C. Brugnara and S.L. Alper, Mouse K-Cl cotransporter KCC1: cloning, mapping, pathological expression and functional regulation, *Am. J. Physiol*. **277**, C860-867 (1999).
23. K. Kirk, The effect of N-ethylmaleimide on K^+ and Cl^- transport pathways in the lamprey erythrocyte membrane: activation of K^+/Cl^- cotransport, *J. Exp. Biol*. **159,** 325-334 (1991).
24. W.C. O'Neill, Cl-dependent K transport in a pure population of volume-regulating human erythrocytes, *Am. J. Physiol*. **256,** C858-C864 (1989).
25. P.K. Lauf, Thiol dependent, passive K/Cl transport in sheep erythrocytes. IV. Furosemide inhibition and the role of external Rb^+, Na^+ and Cl^-, *J. Memb. Biol.* **77,** 57-62 (1984).
26. E. Delpire and P.K. Lauf, Kinetics of DIDS inhibition of swelling-activated K-Cl cotransport in low K sheep erythrocytes, *J. Memb. Biol*. **126**, 89-96 (1992).
27. P.K. Lauf, Thiol stimulated passive K/Cl transport in sheep red cells. I. Dependence on chloride and external K^+ (Rb^+) ions, *J. Memb. Biol.* **73**, 237-246 (1983).
28. P.K. Lauf, Thiol dependent passive K/Cl transport in sheep red cells. II. Loss of Cl^- and N-ethylmaleimide sensitivity in maturing high K^+ cells, *J. Memb. Biol.* **73**, 247-256, (1983).
29. A. Mercado, L. Song, N. Vasquez, D.B. Mount and G. Gamba, Functional comparison of the K^+-Cl^- cotransporters KCC1 and KCC4, *J. Biol. Chem*. **275**, 30326-30334 (2000).
30. P.K. Lauf, Active and passive monovalent ion transport association with membrane antigens in sheep red blood cells: a molecular riddle, In: *Red Cell Membrane Transport in Health and Disease*, J. C. Ellory and I. Bernhardt (Eds.), Springer-Verlag, 691-720 (2003).
31. J. Bauer and P.K .Lauf, Thiol dependent passive K/Cl transport in sheep erythrocytes. III. Differential reactivity of membrane SH groups with N-ethylmaleimide and iodoacetamide, *J. Memb. Biol.* **73**, 257-261, (1983).
32. K.H. Ryu and P.K. Lauf, Evidence for inhibitory SH groups in the thiol-activated K:Cl cotransporter of low K sheep red blood cells, *Molec. Cell. Biochem.* **97,** 145-150 (1990).
33. P.K. Lauf, C.M. Perkins, and N.C. Adragna, Metabolic and volume effects of N-ethylmaleimide-activated K^+Cl^- flux in human red cells, *Am. J. Physiol.* **249,** C126-C128 (1985).
34. P.K. Lauf, Thiol dependent, passive K/Cl transport in sheep erythrocytes. V. Stimulation by N-ethylmaleimide requires cellular ATP, *Am. J. Physiol.* **245**, C14. 44-48 (1983).
35. P.K. Lauf, K^+ Cl Cotransport: Sulfhydryls, divalent cations and the mechanism of volume activation in a red cell, *J. Memb. Biol.* **88,** 1-13 (1985).
36. O.E. Ortiz-Carranza, N.C. Adragna and P.K. Lauf, Modulation of K-Cl cotransport in volume clamped LK sheep erythrocytes by pH, magnesium and ATP, *Am. J. Physiol.* **271,** C1049-C1058 (1996).
37. P.B. Dunham, J. Klimczak and P.J. Logue. Swelling-activation of K-Cl cotransport in LK sheep erythrocytes: a three state process, *J. Gen Physiol.,* **101**, 733-765 (1993).
38. E. Delpire and P.K. Lauf, Magnesium and ATP dependence of K:Cl Cotransport in low K sheep red blood cells. *J. Physiol. (LondoN)* **441,** 219-231 (1991).
39. W.M. Hart, Jr., and E.O. Titus, Isolation of a protein component of sodium-potassium transport adenosine triphosphatase containing ligand-protected sulfhydryl groups, *J. Biol. Chem.* **248**, 1365-1371 (1973).
40. P. K. Lauf, Thiol-dependent passive K:Cl transport in sheep red blood cells: X. A hydroxylamine-oxidation induced K:Cl flux blocked by diethylpyrocarbonate. *J. Memb. Biol.* **118,** 153-160 (1990).
41. P.K. Lauf, K:Cl Cotransport: Emerging molecular aspects of a ouabain-resistant, volume-responsive transport system in red blood cells, *Renal Physiol.* **3-5**, 248-259 (1988).

42. I. Bize, B. Güvenec, G. Buchbinder and C. Brugnara, Stimulation of human erythrocyte K-Cl cotransport and protein phosphatase type 2A by N-ethylmaleimide: role of intracellular Mg^{++}, *J. Memb. Biol.* **177,** 159-168 (2000).
43. M.L. Jennings, Volume-sensitive K^+Cl^- cotransport in rabbit erythrocytes. Analysis of the rate-limiting activation and inactivation events, *J. Gen. Physiol.* **114**, 743-758 (1999).
44. P. Flatman, N.C. Adragna and P.K. Lauf, The role of protein kinases in regulating sheep erythrocyte K-Cl cotransport, *Am. J. Physiol.* **271,** C255-C263 (1996).
45. P.K. Lauf, N.C. Adragna, and N. Agar, Glutathione removal reveals kinases as common targets for K-Cl cotransport stimulation in sheep erythrocytes, *Am. J. Physiol.* **269,** C234-241 (1995).
46. P.K. Lauf, A. Erdmann and N.C. Adragna, Response of K-Cl cotransport pH, and role of Mg in volume-clamped low K sheep erythrocytes: Three equilibrium states, *Am. J. Physiol.* **266,** C95-C103 (1994).
47. I. Bize and P.B. Dunham, Staurosporine, a protein kinase inhibitor activates K-Cl cotransport in LK sheep erythrocytes, *Am. J. Physiol.* **266,** C759-C770 (1994).
48. I. Bize, B. Güvenc, A. Robb, G. Buchbinder, C. Brugnara, Serine/threonine protein phosphatases and regulation of K-Cl cotransport in human erythrocytes, *Am. J. Physiol*. **277**, C926-C936 (1999).
49. C. Brugnara, Membrane transport of Na and K and cell dehydration in sickle erythrocytes, *Experientia* **49**, 100-109 (1993).
50. N.C. Adragna L. Lu and P.K. Lauf, Functional expression of K-Cl cotransport in Xenopus Oocytes. In: *Fifth Biennial Conference of the Membrane Biophysics Subgroup,* October 14-17 (1995).
51. C.M. Gillen, S. Brill, J.A. Payne and B. Forbush III, Molecular cloning and functional expression of the K-Cl cotransporter from rabbit, rat and human, *J. Biol. Chem*. **271**, 16237-16244 (1996).
52. J.A. Payne, T.J. Stevenson and L.F. Donaldson, Molecular characterization of a putative K-Cl cotransporter in rat brain, *J. Biol. Chem.* **271**, 16245-16252 (1996).
53. K. Hiki, R.J.D'Andrea, J. Furze, J. Crawford, E. Woollatt, G.R. Sutherland, M.A. Vadas, and J.R. Gamble, Cloning, characterization, and chromosomal location of a novel human K^+-Cl^- cotransporter, *J. Biol. Chem.* **274**:10661-10667 (1999).
54. J.E. Race, F.N. Makhlouf, P.J. Logue, F.H. Wilson, P.B. Dunham, and E.J. Holtzman. Molecular cloning and functional characterization of KCCC3, a new K-Cl cotransporter, *Am. J. Physiol*. **277,** C1210-C1219 (1999).
55. D.B. Mount, A. Mercado, L. Song, J. Xu, A.L. George, Jr., E. Delpire, and G. Gamba, Cloning and expression of KCC3 and KCC4, new members of the cation-chloride cotransporter gene family, *J. Biol. Chem.* **274**, 16355-16362 (1999).
56. M. Di Fulvio, T.M. Lincoln, P.K. Lauf, and N.C. Adragna, Protein kinase G regulates the potassium-chloride cotransporter-3 (KCC3) expression in primary cultures of rat vascular smooth muscle cells, *J. Biol. Chem.* **276**, 21046-21052 (2001).
57. M. Di Fulvio, P.K. Lauf, and N.C. Adragna, Nitric oxide signaling pathway regulates the potassium-chloride cotransporter-1 mRNA expression in vascular smooth muscle cells, *J. Biol. Chem.* **276**, 44534-44540 (2001).
58. P.K.Lauf, J.J. Zhang, E. Delpire, R.E.W. Fyffe, and N.C. Adragna, K-Cl Cotransport: Immunohistochemical and ion flux studies in human embryonic kidney (HEK293) cells transfected with full-length and C-terminal-domain-truncated KCC1 cDNAs, *Cell Physiol Biochem.* **11**, 143-160 (2001).
59. M.R. Shen, C.H. Chou, and J.C. Ellory, Volume-sensitive KCl cotransport associated with human cervical carcinogenesis. *Pflüger's Arch.* **440,** 751-760 (2000).
60. J. Zhang, P.K. Lauf and N.C. Adragna, Platelet-derived growth factor regulates K-Cl cotransport in vascular smooth muscle cells, *Am. J. Physiol.,* **284,** C674-C680 (2003).
61. K. Gagnon, N.C. Adragna, R.E.W. Fyffe and P.K. Lauf, Functional and immunochemical evidence for K-Cl cotransport KCC1 in C6 Glia cells, *Glia,* submitted for publication (2004).
62. P.K. Lauf, S.Misri, R.Warwar, T.L. Brown and N.C. Adragna, Functional and molecular evidence for K-Cl cotransport and KCC1,3a,b and 4 isoforms in human lens epithelial cells and in human lens tissue, *Exp. Eye Research* (2004) submitted.
63. T. Boettger, C.A. Huebner, H. Maler, M.B. Rust, F.X. Beck and T.J. Jentsch, Deafness and renal tubular acidosis in mice lacking the K-Cl cotransporter KCC4, *Nature* **416,** 874-878 (2002).
64. Y. Chen, M. Morris, E. Delpire, P.K. Lauf and N.C. Adragna, Hypertension in K-Cl cotransporter-3 knockout mice, *FASEB J* **17**, A 858 (2003).
65. P.K. Lauf and N.C. Adragna, Temperature-induced functional deocclusion of thiols inhibitory for sheep erythrocyte K-Cl cotransport, *Am. J. Physiol.* **269,** C1167-C1175 (1995).
66. P.K. Lauf, Jin Zhang, Jing Zhang, and N.C. Adragna, Transient nature of the stimulatory "NEM Effect" on K-Cl cotransport in KCCl-transfected HEK 293 and primary rat aortic smooth muscle cells, *J. Gen. Physiol.* **116**:20a (2000).
67. N.C. Adragna, J. Zhang, M. Di Fulvio, T.M. Lincoln, and P.K. Lauf , K-Cl cotransport regulation and protein kinase G in cultured vascular smooth muscle cells, *J. Memb. Biol*. **187**, 157-165 (2002).

68. S. Casula, B.E. Shmukler, S. Wilhelm, A.K. Stuart-Tilley, W. Su, M.N. Chernova, C. Brugnara and S. Alpers, A dominant negative mutant of the KCC1 K-Cl cotransporter, *J. Biol. Chem.* **276**, 41870-41878 (2001).
69. M.J. Davies and C.L Hawkins, EPR spin trapping of protein radicals. Free Radical Biol. Med. 36, 1072-1086 (2004)**.**
70. J.J. Zhang, S. Misri, N.C. Adragna, K.E.B. Gagnon, R.E.W. Fyffe and P.K. Lauf, Cloning and expression of sheep K-Cl cotransporter KCC1, *Cell Physiol Biochem*., submitted (2004).
71. C.J. Oliver and S. Shenolikar, Physiologic importance of protein phosphatase inhibitors, in *Frontiers in Biosciences* **3**, 961-972 (1998).
72. K. Piechotta, J. Lu, and E. Delpire, Cation chloride cotransporters interact with the stress-related kinases Ste20-related proline-alanine-rich kinase (SPAK) and oxidative stress response I (OSR1), *J. Biol. Chem*. **277,** 50812-50819 (2002).
73. R.E. Weber, W. Voelter, A. Fago, H. Echner, E. Campanella, and P.S. Low, Modulation of red cell glycolysis: Interaction between vertebrate hemoglobins and cytoplasmic domains of band 3 red cell membrane proteins, *Am. J. Physiol.* (2004) in press.
74. S.A. Jewell, G. Bellomo, H. Thor, S. Orrenius and M.T. Smith, Bleb formation in hepatocytes during drug metabolism is caused by disturbances in thiol and calcium ion homeostasis *Science,* **217**, 1257-1258 (1982).
75. H.E. Sheerin, L.M Snyder and G. Fairbanks, Cation transport in oxidant-stressed erythrocytes: heightened N-ethylmaleimide activation of passive K+ influx after mild peroxidation, *Biochim. Biophys. Acta* **983**, 65-76 (1989).

3

MOLECULAR PHYSIOLOGY OF MAMMALIAN K^+-CL^- COTRANSPORTERS

Adriana Mercado, Gerardo Gamba, and David B. Mount*

1. INTRODUCTION

Potassium-chloride (K^+-Cl^-) cotransport is a major pathway for the coupled, electroneutral exit of K^+ and Cl^- from perhaps all mammalian cells. This transport activity is mediated by KCC proteins encoded by four genes in the SLC12 family of electroneutral cation-chloride cotransporters.[1] Almost a quarter of a century has passed since the initial papers describing K^+-Cl^- cotransport;[2, 3] a symposium honoring one of the most prolific investigators in the field seems a fitting opportunity to review progress in the molecular physiology of these important transporters. This serves as an update to prior comprehensive reviews on K^+-Cl^- cotransport in general[4] and its role in specific tissues.[5, 6]

2. RED CELL K^+-CL^- COTRANSPORT

The extensive literature on red cell K^+-Cl^- cotransport has provided an extremely important conceptual framework for the molecular physiology of the four KCCs and bears review in this context. The K^+-Cl^- cotransporters were first described as a K^+ efflux pathway in red cells, activated by both cell swelling[2] and the sulfhydryl-alkylating reagent N-ethylmaleimide (NEM).[3] Red cell K^+-Cl^- cotransport is strongly activated by cell swelling and functions in regulatory volume decrease (RVD).[7, 8] In human erythrocytes, K^+-Cl^- cotransport is most robust in a reticulocyte-rich low-density fraction, and transport activity decreases as the cells age and decrease in size.[9,10] Excessive activity of both K^+-Cl^- cotransport and the Gardos Ca^{2+}-activated K^+ channel (SK4 or KCNN4) have been implicated in the pathogenesis of sickle cell anemia; however, their relative roles in the genesis of red cell dehydration are still not entirely clear.[11, 12]

* Adriana Mercado and David B. Mount, Renal Divisions, West Roxbury VA Medical Center and Brigham and Women's Hospital, Harvard Medical School, Boston, MA, Gerardo Gamba, Molecular Physiology Unit, Instituto de Investigaciones Biomédicas, Universidad Nacional Autónoma de México and Instituto Nacional de Ciencias Médicas y Nutrición Salvador Zubirán, Tlalpan 14000, Mexico City, Mexico

The cotransport of K^+ and Cl^- in red cells is interdependent, with a 1:1 stoichiometry and low affinity constants for both ions[13]. Ion substitution experiments indicate that Br^- can substitute for Cl^- in human and sheep red cells.[2, 14, 15] In sheep red cells, an anion series of $Br^->Cl^->>I^->SCN^->NO3^-$ has thus been reported for K^+-Cl^- cotransport.[14] In contrast, Na^+-K^+-$2Cl^-$ cotransport (NKCC1) is inhibited up to 50% by bromide substitution.[16] Red cell K^+-Cl^- cotransport is sensitive to the loop diuretics bumetanide and furosemide, with much lower affinities than that of Na^+-K^+-$2Cl^-$ cotransport.[7] There are few, if any, inhibitors that reliably discriminate between K^+-Cl^- cotransport, Na^+-K^+-$2Cl^-$ cotransport, and/or other anion transport pathways. For example, millimolar furosemide and bumetanide also inhibit the anion exchangers SLC26A4 (pendrin)[17] and SLC26A3 (DRA).[18] However, the bumetanide derivative H74[19] and the alkaloid DIOA[20-24] have been reported to inhibit K^+-Cl^- cotransport selectively. DIOA also inhibits cloned KCCs;[25, 26] although, activity against other anion transporters has not been rigorously defined. Less-specific transport inhibitors with reported activity include DIDS[27] and the ion channel blockers quinine and quinidine.[28]

The main physiological activators of red cell K^+-Cl^- cotransport appear to include cell swelling, low pH, high PO_2, and urea.[7, 29-31] Pharmacological activation of red cell K^+-Cl^- cotransport can also be achieved with the thiol-alkylating agent NEM (N-ethyl maleimide) and by oxidizing agents such as H_20_2[32] and peroxynitrite.[33] These reagents are considered to act on thiol groups present in upstream regulatory proteins (kinases, phosphatases, etc.);[4] however, direct interaction with KCC proteins has not been ruled out. Indeed, careful studies by Lauf et al. yielded evidence for temperature-dependent *inhibition* of the KCCs by NEM and other thiol-reactive compounds,[4] perhaps due to direct interaction with transporter cysteine residues that are "deoccluded"[34] after activation. Regardless, activation of K^+-Cl^- cotransport by cell swelling or NEM is blocked by protein phosphatase inhibitors, specifically calyculin-A and okadaic acid.[4] More recent data suggest the involvement of membrane-bound protein phosphatase-1 (PP1) and PP2A red cells.[35, 36] These serine-threonine phosphatases are under tonic negative control by upstream kinases in that the potent kinase inhibitor staurosporine is capable of activating K^+-Cl^- cotransport under isotonic conditions.[37] Data from double knockout mice suggest the Src tyrosine kinases *Fgr* and *Hck* are the relevant staurosporine-sensitive kinases.[38]

It is likely there are further levels of complexity in the regulation of red cell K^+-Cl^- cotransport,[8, 39-41] e.g., tyrosine kinases inhibitors inhibit activation by staurosporine and NEM and also decrease resting K^+-Cl^- cotransport.[40] Of note, all four of the cloned KCC proteins are predicted substrates for tyrosine kinases, and at least KCC2 appears to be phosphorylated on tyrosine *in vivo*[42] with subsequent activation.[43] Thus, tyrosine kinases may have two opposing roles in the regulation of K^+-Cl^- cotransport: activating via direct phosphorylation of the transporter protein and inhibiting by negative effects on PP-1.[38]

3. PHYSIOLOGICAL CHARACTERIZATION OF THE KCCS

The functional characteristics of K^+-Cl^- cotransport are similar in many respects to Na^+-K^+-$2Cl^-$ cotransport: a mutual dependence on the presence of all the transported ions, shared sensitivity to loop diuretics, and reciprocal regulation by protein phosphorylation/dephosphorylation (NKCC1 is activated by phosphatase inhibition and inhibited by staurosporine,[44] i.e. the opposite of K^+-Cl^- cotransport). These similarities ultimately led

to the molecular identification of the first KCCs in 1996 via their homology to the cation-chloride cotransporters NKCC1, NKCC2, and NCC.[45, 46] Progress since that time has been gratifying, with the subsequent cloning of KCC3[47, 48] and KCC4,[48] functional comparison of the four KCCs, generation of several KCC-null mouse strains,[49-52] and the demonstration that KCC3 is involved in a Mendelian disease.[51]

3.1. KCC1

KCC1 was cloned by identification of expressed sequence tags (ESTs) homologous to the other cation-chloride cotransporters; full-length cDNAs have been reported for rat,[45] rabbit,[45] human,[45] pig,[53] mouse[25] and dog.[54] The 3'-UTR is less than 200 bp upstream of the gene for lecithin:cholesterol acyltransferase (LCAT) on chromosome 16q22.1.[55] KCC1 is ubiquitously expressed by Northern blot analysis, suggestive of a housekeeping role in cell volume regulation. Transcription of human KCC1 is driven off of a TATA-less promoter, with a downstream promoter element.[56] Very little tissue localization data has been published and in the absence of a knockout mouse, nothing is known about the global physiological role of this cotransporter. In adult rat brain, there is widespread, low-level expression of KCC1,[57] with particularly abundant transcript in choroid plexus, olfactory bulb, and cerebellum.[58] The available KCC1-specific antibodies are not ideal. However, it appears that KCC1 is unique among the three renal KCCs in targeting the apical membrane of the distal nephron (DBM et al., unpublished results). This is of particular significance in view of the evidence that luminal K^+-Cl^- cotransport plays a role in distal K^+ secretion.[59-61]

The predicted KCC1 protein is 1085 amino acids long, with 75% identity to KCC3. Although not formally evaluated, KCC1 and the other KCCs are thought to have a total of 12 hydrophobic transmembrane (TM) domains. A major departure is the prediction of a glycosylated extracellular loop between TM5 and TM6, versus TM7-8 in the Na^+-linked cotransporters. Expression of KCC1 in *Xenopus* oocytes[25, 26, 48] and HEK293 cells[45, 53, 62] reveals the functional characteristics expected of a K^+-Cl^- cotransporter. Thus, transport is not detected under isotonic conditions and swelling-induced activation is blocked by phosphatase inhibition.[25, 26, 62] Of interest, baseline Na^+-K^+-$2Cl^-$ cotransport activity is elevated and intracellular [Cl^-] reduced in KCC1-HEK293 cells compared to the parental cell line.[62] NKCC1 is thought to be activated by decreases in intracellular [Cl^-] via phosphorylation by an as yet unidentified Cl^--sensitive kinase,[63] such that Cl^- efflux mediated by the KCCs may activate NKCC1. KCC1 and KCC3 share several otherwise divergent residues within TM2, a region implicated in cation affinity of Na^+-K^+-$2Cl^-$ cotransport.[64, 65] The functional correlate of this similarity is that the cation affinities of these two KCCs are lower than those of KCC2 and KCC4.[26, 66-68] Thus, the K_m's of KCC1 for K^+ and Cl^- are 25.5 and 17.5 mM, respectively, with an anion preference of $Cl^- > SCN^- = Br^- >> PO_4$.[3-26] As discussed elsewhere,[26] these characteristics differ from red cell K^+-Cl^- cotransport which has a much lower K^+ affinity and seems to prefer Br^- over Cl^-.[14] Therefore, although KCC1 is evidently expressed in red cells from several species,[25,69] it seems unlikely this is the sole erythroid KCC.

3.2 KCC2

The KCC2 protein is expressed at the cell membrane of both neuronal stomata and dendrites[85, 86] and is co-localized at inhibitory synapses with subunits of the $GABA_A$

receptors[85] and associated proteins.[49] Robust expression of KCC2 is already detectable at embryonic day 12.5 in the ventral horns of the developing spinal cord.[49, 87] Spinal motoneurons at embryonic day E18.5 respond to GABA and glycine with a depolarizing and excitatory response absent in KCC2-null mice[49]. The phenotypic correlates in KCC2-null mice include a spastic posture and immediate postnatal death from apnea, the latter attributed to a defect in the regulation of respiratory motoneurons.[49]

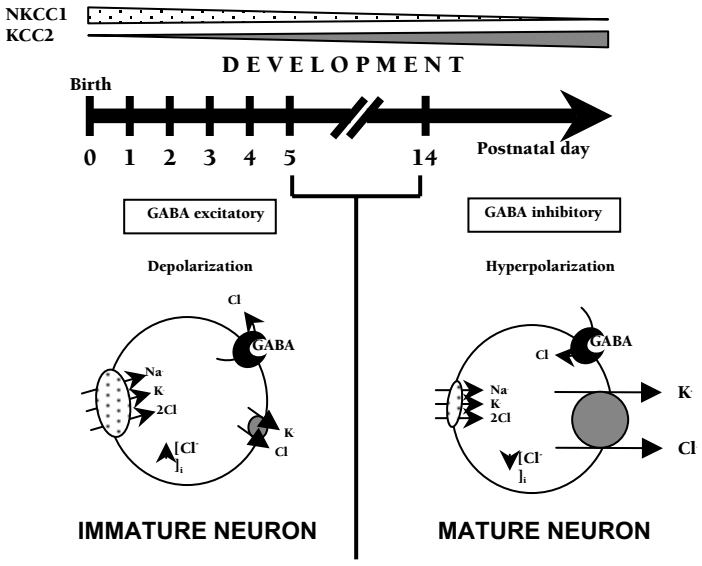

Figure 1. The role of chloride entry (NKCC1; SLC12A1) and exit (KCC2; SLC12A5) in the neuronal response to the neurotransmitter GABA (γ-aminobutyric acid). Modified from[126] with permission. The expression levels of NKCC1 and KCC2 are reciprocally regulated during the early postnatal development of most neurons, with a predominance of NKCC1 during early development and of KCC2 in adult neurons. Consequently, there is a decrease in neuronal $[Cl^-_i]$ during the first week of life and a switch in the neuronal response to GABA, from depolarizing and excitatory to hyperpolarizing and inhibitory.

The developmental pattern of KCC2 expression appears to correlate with neuronal maturation in several regions of the CNS.[87, 88] GABA was recently shown to induce expression of the KCC2 protein, thus limiting its brief window of neurotrophic effect.[77] Of note, however, two other studies directly[89] and indirectly[90] contradict this finding that KCC2 induction is GABA-dependent. Brain-derived neurotrophic factor (BDNF) and neurotrophin-4 dramatically *decrease* KCC2 expression, with the potential to significantly amplify neuronal excitability after epileptic seizures which induce expression of these neurotrophic factors.[91] BDNF appears to play a crucial role in a dramatic downregulation of KCC2 expression in hippocampal slices in which sustained neuronal hyperactivity is induced by low magnesium or by the proconvulsant drug AP4.[92] Neuronal activity in this preparation releases endogenous BDNF which reduces membrane expression of KCC2 via activation of the TrkB tyrosine kinase and downstream signaling pathways.[92] Paradoxically, transgenic overexpression of BDNF early in neuronal development results in increased expression of KCC2, likely via the induction of GABAergic neurons.[93] This

illustrates the difficulty in separating direct effects on KCC2 expression from more general effects on neuronal maturation.

In keeping with its crucial role in neuronal function, the predicted KCC2 protein is the most highly conserved of the four KCCs, with >99% identity between the human, mouse and rat orthologs.[46, 68] Unique to KCC2 is an expanded domain of ~100 amino acids near the end of the cytoplasmic C-terminus.[46, 68] Rich in prolines, serines, and acidic residues, this expansion contains two predicted PEST motifs;[94] none of the other KCCs contain PEST motifs in this region. PEST motifs are thought to serve as signals for rapid proteolytic degradation via the 26S proteasome or through calpain-mediated degradation.[94] PEST-directed calpain cleavage of KCC2 may thus be an activating event given the effects of proteolysis of ion channels[95] and signaling proteins.[96] Functional expression in HEK293 cells and *Xenopus* oocytes reveals KCC2 is unique in mediating isotonic K^+-Cl^- cotransport.[67, 68, 97] KCC2-KCC4 chimeras have recently localized this characteristic to the C-terminal KCC2-unique expansion.[98] Note that although the increase in activity induced by cell swelling is blocked by phosphatase inhibition, the isotonic activity of KCC2 and KCC4-KCC2 C-terminal chimeras is not affected, suggesting a distinct mechanism for the constitutive activity of KCC2.[68, 98] Mutagenesis studies suggest a C-terminal tyrosine predicted to be a substrate for tyrosine kinases is required for activity of rat KCC2 in *Xenopus* oocytes.[97] Although tyrosine kinase inhibitors do not affect KCC2 in oocytes, the same reagents inhibit K^+-Cl^- cotransport in primary neuronal culture,[43] suggesting KCC2 is directly phosphorylated by tyrosine kinases in neurons. This was recently confirmed with phosphotyrosine-specific antibodies;[42] however, it is yet unknown whether the predicted C-terminal tyrosine (Y1097) is the relevant phosphotyrosine.

Kinetic characterization of rat and human KCC2 indicates a much higher cation affinity than the other three KCCs, with K_ms of ~5.2 and 9.2 mM, respectively.[67, 68] There is a significant discrepancy in the reported Cl^- affinity of human KCC2 and rat KCC2, with K_ms of >50 mM and 6.8 mM, respectively. The lower K_m is closer to the intracellular [Cl^-] activity of mature neurons that express KCC2.[68] Physiological relevance assumes, however, that the intracellular affinity for Cl^- efflux is similar to that of influx. The high ion affinities of KCC2 befit a buffer of external K^+ and internal Cl^- as first noted by Payne.[67] As extracellular K^+ increases to 10-12 mM during neuronal activity, the range wherein KCC2 is highly active, the driving force for net K^+-Cl^- cotransport will switch from efflux to influx. In this regard, reversibility of K^+-Cl^- cotransport mediated by neuronal KCCs has been verified experimentally.[81-83] Bi-directional transport via neuronal KCCs may explain activity-dependent disinhibition,[67] whereby repetitive activation of GABA receptors results in increased extracellular [K^+], an increase in neuronal [Cl^-] due to K^+-Cl^- influx and a reduction in the inhibitory GABA effect.[99]

The role of KCC2 in GABA-mediated neuronal inhibition and activity-dependent disinhibition suggests a role in human epilepsy. Indeed, KCC2 knockout mice with modest residual KCC2 expression have a severe seizure disorder and exhibit early postnatal mortality.[100] The human *SLC12A5* gene on chromosome 20q13 is not linked to Mendelian forms of human epilepsy.[68] However, a complex and polymorphic dinucleotide repeat is found within the first intron of *SLC12A5* near a conserved binding site for neuronal restrictive silencing factor[68] which appears to silence activity of this gene in non-neuronal tissues.[101] It is thus conceivable that genetic variation here and elsewhere in human *SLC12A5* might affect epilepsy and the neuronal response to injury, particularly since GABA has been shown to have excitatory effects after neuronal trauma.[102] In addition, genetic variation in the negative transcriptional response of KCC2 to neurotrophins may

have a role in sustained epileptic activity.[91] Reduced expression of KCC2 has also been reported in a model of neuropathic pain.[103] Thus, pharmacological activation of KCC2 is an attractive goal, since such drugs are likely to have significant impact on disorders in which reduced expression of KCC2 has been implicated.

3.3. KCC3

KCC3 has an expression pattern intermediate between that of KCC1 (ubiquitous) and KCC2 (tissue-specific) with abundant transcript in muscle, brain, spinal cord, kidney, heart, pancreas, and placenta.[47, 48, 104] KCC3 is unique in that the *SLC12A6* gene encoding this transporter has two separate first coding exons.[51] This results in the expression of two separate KCC3 isoforms with different N-terminal ends; we have denoted these isoforms KCC3a[48] and KCC3b.[47] KCC3a expression is more widespread than that of KCC3b which is particularly abundant in kidney.[105] The predicted KCC3a protein is longer by 50 amino acids[48] and contains several potential phosphorylation sites for protein kinase C that are not present in the KCC3b-unique N-terminus.[47]The functional or regulatory consequences of this variation are as yet unclear.

Expression of KCC3 in the brain and spinal cord was of particular interest[105] in light of the genetic linkage between the region encompassing the *SLC12A6* gene on chromosome 15q14 and several neurological syndromes.[48] Genomic characterization of *SLC12A6* was pursued by this group, revealing a 26-exon gene spanning ~160 kb. Whereas patients with epilepsy syndromes linked to 15q14 were not found to carry coding sequence mutations,[106] four loss-of-function mutations in *SLC12A6* were recently characterized in kindreds with "peripheral neuropathy with or without agenesis of the corpus callosum" (ACCPN).[51] This syndrome is particularly common in the Saguenay-St. Lawrence region of Quebec, Canada, due to a founder effect. The complete syndrome encompasses several peripheral neuropathy, agenesis of the corpus callosum, mental retardation, psychosis and a progressive course suggestive of a neurodegenerative process. The Quebec founder effect mutation is a single base deletion at the end of coding exon 18 resulting in a mRNA splicing error and a premature stop codon. The predicted protein is missing the C-terminal 338 residues and is non-functional when expressed in *Xenopus* oocytes.[51] Of note, in comparison to loss-of-function mutations in NCC[107] and other transport proteins, deletion of the C-terminus of KCC3 does not affect glycosylation, homodimerization or expression at the surface of *Xenopus* oocytes.

Despite clear genetic and functional evidence implicating KCC3 in ACCPN, the pathophysiology of this neurological deficit remains unclear. Although there is heavy oligodendrocytic expression of the KCC3 protein in CNS white matter tracts, including the corpus callosum,[105] the two reported strains of KCC3 knockout mice have intact corpora callosa.[51, 52] Interestingly, however, agenesis/dysgenesis of the corpus callosum is a partially penetrant phenotype in ACCPN even within single affected families.[108] Expression of KCC3 in large neurons[105] and the human NT2-N neuronal cell line[68] has also been reported, compatible perhaps with the neuropsychiatric manifestations of ACCPN. In one knockout mouse[52] but not the other[51], degeneration of neurons in the CNS has been reported. At the cellular level, KCC3 has been implicated in the cells' response to both vascular endothelial growth factor[47] and insulin-like growth factor-1;[109] loss of KCC3 may thus affect the proliferation and/or survival of neurons and oligodendrocytes. Regulatory volume decrease (RVD) is also impaired in hippocampal neurons of the

KCC3-deficent mice described by Boettger et al.[52] This loss of RVD may lead to progressive neurodegeneration in KCC3 deficiency. A major paradox is the severe peripheral neurop-athy associated with loss of KCC3 in mouse[51,52] and man,[51] despite the minimal expres-sion in peripheral nervous tissue.[105] Future studies using neuronal-specific deletion of KCC3 will hopefully resolve this issue.

Unlike KCC4 expressed at the basolateral membrane of multiple renal tubular segments, KCC3 expression is unique to the proximal tubule (PT).[52, 110, 111] Physiological and functional evidence also suggests the existence of basolateral K^+-Cl^- cotransport in the proximal tubule.[5] Thus a 1 mM concentration of furosemide sufficient to inhibit the red cell K^+-Cl^- cotransporter does not inhibit this cotransport activity under baseline condi-tions.[112] Earlier studies also failed to detect an effect of 1 mM furosemide on the trans-epithelial potential difference. Only 10% of baseline K^+ efflux in the proximal tubule is through a furosemide-sensitive pathway[113] which is likely quiescent in the absence of cell swelling. However, activation of apical Na^+-glucose transport in PT cells strongly activates a Ba^{2+}-resistant K^+ efflux pathway that is 75% inhibited by 1 mM furose-mide,[114] pharmacology consistent with a K^+-Cl^- cotransporter. Therefore, cell swelling in the proximal nephron in response to apical Na^+ absorption was postulated to activate a volume-sensitive basolateral K^+-Cl^- cotransporter.[5] Data from KCC3 knockout mice is consistent with this hypothesis in that proximal transepithelial fluid transport in these mice is reduced by ~50%. In addition, RVD in Ba^{2+}-blocked proximal tubules swollen by hypotonic conditions is blocked by 1 mM furosemide.[115] Recent data from other KCC3 knockout mice reveal a crucial role for basolateral K^+-Cl^- cotransport in proximal tubular RVD.[52] Therefore, it is increasingly apparent that K^+-Cl^- cotransport plays a sig-nificant role in the physiology of this nephron segment. Of note, it is conceivable that severe motor and sensory neuropathy in human ACCPN[51] and KCC3-deficient mice[51,52] is accompanied by reduced renal innervation. It is well-documented that acute renal denervation reduces proximal reabsorption of both Na^+-Cl^- and bicarbonate[116,117] such that the renal phenotype of KCC3 -/- mice may be a downstream effect of their severe peripheral neuropathy. Therefore, these studies will need to be confirmed in mice with KCC3 deletion limited to the renal proximal tubule.

Finally, several lines of evidence suggest KCC3 and other KCCs play an important role in vascular physiology. First, KCC3b was initially cloned as a transcript upregulated by the vascular survival factor VEGF.[47] Second, a series of studies by Adragna et al. has revealed K^+-Cl^- cotransport is activated by nitric oxide and related vasodilators in vascular smooth muscle cells;[118] both KCC3 and KCC1 seem to be involved.[119] A vascular mechanism may underlie the reported hypertension in KCC3-deficient mice,[52, 120] particularly given the *hypotension* and reduced vascular tone in NKCC1-deficient mice.[121]

3.4 KCC4

Much like KCC1, KCC4 is widely expressed; a differentiating feature is that KCC4 expression within specific tissues is more discrete than that of KCC1. Although transcript is undetectable in human or mouse brain by Northern analysis, there is localized expression of KCC4 within specific CNS neurons.[87, 122] KCC4 protein is localized at the apical membrane of choroids plexus[122] versus the basolateral distribution of KCC3 in these cells.[105] Expression is particularly robust in kidney, where the KCC4 protein has been localized at the basolateral membrane of proximal tubule, thick ascending limb, macula densa, distal convoluted tubule, and type A intercalated cells.[50, 110, 111] Swelling-activated

Cl^- exit mediated by KCC4 and KCC3 is thought to play a role in transepithelial transport of Na^+-Cl^- and other solutes by the proximal tubule.[5] However, RVD in the proximal tubule is more impaired in KCC3-deficient mice than in KCC4-deficiency.[52] Mice deficient in KCC4 manifest a renal tubular acidosis attributed to defects in acid secretion by intercalated cells.[50] Other possibilities include reduced countercurrent multiplication of NH_4^+ due to reduced basolateral NH_4^+-Cl^- cotransport in the thick ascending limb.[110, 111, 123] Like some forms of human hereditary distal renal tubular acidosis, the KCC4 -/- mice are also profoundly deaf. Careful histological analysis reveals degeneration of outer hair cells, presumably due to impaired K^+ uptake by supporting Deiter's cells.[50]

Functional characterization in *Xenopus* oocytes reveals K_ms for K^+ and Cl^- of 17.5 mM and 16.2 mM.[26] However, unlike KCC2 which is ~75% identical, KCC4 does not mediate K^+-Cl^- cotransport under isotonic con-ditions in *Xenopus* oocytes and mediates higher swelling-activated cotransport.[26, 68]

4. PERSPECTIVE

Thus far, progress on the molecular physiology of the KCCs has been largely descriptive, outlining their expression patterns, basic physiological roles and functional characteristics. Clarification of several important mechanistic issues remains. First, what protein domains and/or phosphorylation sites confer volume sensitivity? Chimeric cDNAs have localized the protein domain responsible for isotonic transport in KCC2.[98] Alternative approaches will be required to delineate the domain(s) responsible for swelling-activation, a feature common to all four KCCs. Second, does phosphorylation of KCCs vary in a volume-sensitive fashion? If so, what acceptor sites are phosphorylated and by which kinases? Third, what is the role of direct modification of cysteine residues in KCCs by NEM and related compounds as opposed to modulation of upstream signaling events?[4] KCCs are rich in cysteine residues, e.g., KCC4 contains a total of 23. In contrast, the anion exchanger AE1 (SLC4A1) contains only six. Surprisingly, only a handful of the absolutely conserved cysteine residues found in the KCCs are singly required for K^+-Cl^- cotransport activity.[124] Thus, identification of the NEM-activating and NEM-inhibiting cysteines will soon be forthcoming. Finally, there are clear therapeutic indications for both KCC3/KCC1-specific inhibitors in sickle cell anemia[12] and KCC2-specific activators in epilepsy,[91, 92, 100] neuronal injury,[102] and neuropathic pain;[103] at least one company is actively pursuing these goals. It is likely that understanding the mechanisms of such pharmacological agents, once they emerge, will yield important mechanistic insight.[125, 126]

5. ACKNOWLEDGMENTS

This work was supported by a Career Development Award from the VA to DBM, NIH RO1 DK57708 (DBM), and research grants 36124-M from the Mexican Council of Science and Technology (CONACYT) and No. 75197-553601 from Howard Hughes Medical Institute to GG.

6. REFERENCES

1. S.C. Hebert, D.B. Mount and G. Gamba, Molecular physiology of cation-coupled Cl-cotransport: the SLC12 family, *Pflugers Arch* **447**, 580-93 (2004).
2. P.B. Dunham, G.W. Stewart and J.C. Ellory, Chloride-activated passive potassium transport in human erythrocytes, *Proc Natl Acad Sci U S A* **77**, 1711-5 (1980).
3. P.K. Lauf and B.E. Theg, A chloride dependent K^+ flux induced by N-ethylmaleimide in genetically low K^+ sheep and goat erythrocytes, *Biochem Biophys Res Commun* **92**, 1422-8 (1980).
4. P.K. Lauf, and N.C. Adragna, K-Cl cotransport: properties and molecular mechanism, *Cell Physiol Biochem* **10**, 341-54 (2000).
5. D.B. Mount and G. Gamba, Renal K-Cl cotransporters, *Curr Opin Nephrol Hypertens* **10**, 685-692 (2001).
6. J.A. Payne, C. Rivera, J. Voipio and K. Kaila, Cation-chloride co-transporters in neuronal communication, development and trauma, *Trends Neurosci* **26**, 199-206 (2003).
7. P.K. Lauf, J. Bauer, N.C. Adragna, H. Fujise, A.M. Zade-Oppen, K.H. Ryu and E. Delpire, Erythrocyte K-Cl cotransport: properties and regulation, *Am J Physiol* **263**, C917-32 (1992).
8. A.R. Cossins and J.S. Gibson, Volume-sensitive transport systems and volume homeostasis in vertebrate red blood cells, *Journal of Experimental Biology* **200**, 343-52 (1997).
9. A.C. Hall and J.C. Ellory, Evidence for the presence of volume-sensitive KCl transport in 'young' human red cells, *Biochim Biophys Acta* **858**, 317-20 (1986).
10. C. Brugnara and D.C. Tosteson, Cell volume, K transport, and cell density in human erythrocytes, *Am J Physiol* **252**, C269-76 (1987).
11. C. Brugnara, H.F. Bunn and D.C. Tosteson, Regulation of erythrocyte cation and water content in sickle cell anemia, *Science* **232**, 388-90 (1986).
12. C. Brugnara, Sickle cell disease: from membrane pathophysiology to novel therapies for prevention of erythrocyte dehydration, *J Pediatr Hematol Oncol* **25**, 927-33 (2003).
13. P.K. Lauf, Kinetic comparison of ouabain-resistant K-Cl fluxes (K-Cl [Co]- transport) stimulated in sheep erythrocytes by membrane thiol oxidation and alkylation, *Mol Cell Biochem* **82**, 97-106 (1988).
14. P.K. Lauf, Volume and anion dependency of ouabain-resistant K-Rb fluxes in sheep red blood cells, *Am J Physiol* **255**, C331-9 (1988).
15. D. Kaji, Volume-sensitive K transport in human erythrocytes, *J Gen Physiol* **88**, 719-38 (1986).
16. P. Geck, C. Pietrzyk, B.C. Burckhardt, B. Pfeiffer and E. Heinz, Electrically silent cotransport on Na+, K+ and Cl- in Ehrlich cells, *Biochim Biophys Acta* **600**, 432-47 (1980).
17. R.H. Moseley, Downregulated in adenoma gene encodes a chloride transporter defective in congenital chloride diarrhea, *Am J Physiol* **276**, G185-92 (1999).
18. D.A. Scott, R. Wang, T.M. Kreman, V.C. Sheffield and L.P. Karniski, The Pendred syndrome gene encodes a chloride-iodide transport protein, *Nat Genet* **21**, 440-3 (1999).
19. J.C. Ellory, A.C. Hall, S.O. Ody, H.C. Englert, D. Mania, and H.J. Lang, Selective inhibitors of KCl cotransport in human red cells, *FEBS Lett* **262**, 215-8 (1990).
20. R.P. Garay, C. Nazaret, P.A. Hannaert and E.J. Cragoe, Jr., Demonstration of a [K^+Cl^-]-cotransport system in human red cells by its sensitivity to [(dihydroindenyl)oxy]alkanoic acids: regulation of cell swelling and distinction from the bumetanide-sensitive [$Na^+K^+Cl^-$]-cotransport system, *Mol Pharmacol* **33**, 696-701 (1988).
21. D. Vitoux, O. Olivieri, R.P. Garay, E.J. Cragoe, Jr., F. Galacteros, and Y. Beuzard, Inhibition of K^+ efflux and dehydration of sickle cells by [(dihydroindenyl)oxy]alkanoic acid: an inhibitor of the K^+Cl^- cotransport system, *Proc Natl Acad Sci U S A* **86**, 4273-6 (1989).
22. M. Saitta, S. Cavalier, R. Garay, E. Cragoe, Jr. and P. Hannaert, Evidence for a DIOA-sensitive [K^+Cl^-]-cotransport system in cultured vascular smooth muscle cells, *Am J Hypertens* **3**, 939-42 (1990).
23. C.C. Armsby, C. Brugnara and S.L. Alper, Cation transport in mouse erythrocytes: role of K^+-Cl^- cotransport in regulatory volume decrease, *Am J Physiol* **268**, C894-902 (1995).
24. S.M. Linton and M.J. O'Donnell, Contributions of K^+-Cl^- cotransport and Na^+/K^+-ATPase to basolateral ion transport in Malpighian tubules of Drosophila melanogaster, *J Exp Biol* **202**, 1561-1570 (1999).
25. W. Su, B.E. Shmukler, M.N. Chernova, A.K. Stuart-Tilley, L. de Franceschi, C. Brugnara, and S.L. Alper, Mouse K-Cl cotransporter KCC1: cloning, mapping, pathological expression, and functional regulation, *Am J Physiol* **277**, C899-C912 (1999).
26. A. Mercado, L. Song, N. Vazquez, D.B. Mount and G. Gamba, Functional Comparison of the K^+-Cl^- Cotransporters KCC1 and KCC4, *J Biol Chem* **275**, 30326-30334 (2000).
27. E. Delpire and P.K. Lauf, Kinetics of DIDS inhibition of swelling-activated K-Cl cotransport in low K sheep erythrocytes, *J Membr Biol* **126**, 89-96 (1992).

28. N.C. Adragna and P.K. Lauf, Quinine and quinidine inhibit and reveal heterogeneity of K-Cl cotransport in low K sheep erythrocytes, *J Membr Biol* **142**, 195-207 (1994).
29. C.C. Armsby, A.K. Stuart-Tilley, S.L. Alper and C. Brugnara, Resistance to osmotic lysis in BXD-31 mouse erythrocytes: association with upregulated K-Cl cotransport, *Am J Physiol* **270**, C866-77 (1996).
30. D.M. Kaji and C. Gasson, Urea activation of K-Cl transport in human erythrocytes, *Am J Physiol* **268**, C1018-25 (1995).
31. P.K. Lauf, K^+-Cl^- cotransport: 'to be or not to be' oxygen sensitive, *J Physiol (Lond)* **511**, 1 (1998).
32. I. Bize and P.B. Dunham, H_2O_2 activates red blood cell K-Cl cotransport via stimulation of a phosphatase. *Am J Physiol* **269**, C849-55 (1995).
33. A. Grzelak, J. Mazur and G. Bartosz, Peroxynitrite activates K^+-Cl^- cotransport in human erythrocytes, *Cell Biol Int* **25**, 1163-5 (2001).
34. P.K. Lauf and N.C. Adragna, Temperature-induced functional deocclusion of thiols inhibitory for sheep erythrocyte K-Cl cotransport, *Am J Physiol* **269**, C1167-75 (1995).
35. I. Bize, B. Guvenc, G. Buchbinder and C. Brugnara, Stimulation of human erythrocyte K-Cl cotransport and protein phosphatase type 2A by n-ethylmaleimide: role of intracellular Mg^{++}, *J Membr Biol* **177**, 159-68. (2000).
36. I. Bize, B. Guvenc, A. Robb, A., G. Buchbinder and C. Brugnara, Serine/threonine protein phosphatases and regulation of K-Cl cotransport in human erythrocytes, *Am J Physiol* **277**, C926-36. (1999).
37. I. Bize and P.B. Dunham, Staurosporine, a protein kinase inhibitor, activates K-Cl cotransport in LK sheep erythrocytes, *Am J Physiol* **266**, C759-70 (1994).
38. L. de Franceschi, L. Fumagalli, O. Olivieri, R. Corrocher, C.A. Lowell and G. Berton, Deficiency of Src family kinases Fgr and Hck results in activation of erythrocyte K/Cl cotransport, *Journal of Clinical Investigation* **99**, 220-7 (1997).
39. A.R. Cossins, Y.R. Weaver, G. Lykkeboe and O.B. Nielsen, Role of protein phosphorylation in control of K flux pathways of trout red blood cells, *Am J Physiol* **267**, C1641-50 (1994).
40. P.W. Flatman, N.C. Adragna and P.K. Lauf, Role of protein kinases in regulating sheep erythrocyte K-Cl cotransport, *Am J Physiol* **271**, C255-C263 (1996).
41. J.R. Sachs, Soluble polycations and cationic amphiphiles inhibit volume-sensitive K-Cl cotransport in human red cell ghosts, *Am J Physiol* **266**, C997-1005 (1994).
42. V. Stein, I. Hermans-Borgmeyer, T.J. Jentsch and C.A. Hubner, Expression of the KCl cotransporter KCC2 parallels neuronal maturation and the emergence of low intracellular chloride, *J Comp Neurol* **468**, 57-64 (2004).
43. W. Kelsch, S. Hormuzdi, E. Straube, A. Lewen, H. Monyer and U. Misgeld, Insulin-like growth factor 1 and a cytosolic tyrosine kinase activate chloride outward transport during maturation of hippocampal neurons, *J Neurosci* **21**, 8339-47 (2001).
44. C. Lytle, A volume-sensitive protein kinase regulates the Na-K-2Cl cotransporter in duck red blood cells, *Am J Physiol* **274**, C1002-10. (1998).
45. C.M. Gillen, S. Brill, J.A. Payne and B. Forbush, III, Molecular cloning and functional expression of the K-Cl cotransporter from rabbit, rat, and human. A new member of the cation-chloride cotransporter family, *J Biol Chem* **271**, 16237-44 (1996).
46. J.A. Payne, T.J. Stevenson and L.F. Donaldson, Molecular characterization of a putative K-Cl cotransporter in rat brain. A neuronal-specific isoform, *J Biol Chem* **271**, 16245-52 (1996).
47. K. Hiki, R.J. D'Andrea, J. Furze, J. Crawford, E. Woollatt, G.R. Sutherland, M.A. Vadas and J.R. Gamble, Cloning, characterization, and chromosomal location of a novel human K+-Cl- cotransporter, *J Biol Chem* **274**, 10661-7 (1999).
48. D.B. Mount, A. Mercado, L. Song, J. Xu, A.L. George, Jr., E. Delpire, and G. Gamba, Cloning and characterization of KCC3 and KCC4, new members of the cation-chloride cotransporter gene family, *J Biol Chem* **274**, 16355-16362 (1999).
49. C.A Hubner, V. Stein, I. Hermans-Borgmeyer, T. Meyer, K. Ballanyi and T.J. Jentsch, Disruption of KCC2 reveals an essential role of K-Cl cotransport already in early synaptic inhibition, *Neuron* **30**, 515-24. (2001).
50. T. Boettger, C. Hubner, H. Maier, M. Rust, F. Beck and T. Jentsch, Deafness and renal tubular acidosis in mice lacking the K-Cl cotransporter KCC4, *Nature* **416**, 874-878 (2002).
51. H.C. Howard, D.B. Mount, D. Rochefort, N. Byun, N. Dupre, J. Lu, X. Fan, L. Song, J.B. Riviere, C. Prevost, J. Horst, A. Simonati, B. Lemcke, R. Welch, R. England, F.Q. Zhan, A. Mercado, W.B. Siesser A.L. George, M.P. McDonald, J.P. Bouchard, J. Mathieu, E. Delpire and G.A. Rouleau, The K-Cl cotransporter KCC3 is mutant in a severe peripheral neuropathy associated with agenesis of the corpus callosum, *Nat Genet* **32**, 384-392 (2002).
52. T. Boettger, M.B. Rust, H. Maier, T. Seidenbecher, M. Schweizer, D.J. Keating, J. Faulhaber, H. Ehmke, C. Pfeffer, O. Scheel, B. Lemcke, J. Horst, R. Leuwer, H.C. Pape, H. Volkl, C.A. Hubner and T.J. Jentsch,

Loss of K-Cl co-transporter KCC3 causes deafness, neurodegeneration and reduced seizure threshold, *Embo J* **22**, 5422-34 (2003).
53. E.J. Holtzman, S. Kumar, C.A. Faaland, F. Warner, P.J. Logue, S.J. Erickson, G. Ricken, J. Waldman and P.B. Dunham, Cloning, characterization, and gene organization of K-Cl cotransporter from pig and human kidney and C. elegans, *Am J Physiol* **275**, F550-64 (1998).
54. H. Ochiai, K. Higa and H. Fujise, Molecular identification of K-CL cotransporter in dog erythroid progenitor cells, *J Biochem (Tokyo)* **135**, 365-74 (2004).
55. F. Larsen, J. Solheim, T. Kristensen, A.B. Kolsto and H. Prydz, A tight cluster of five unrelated human genes on chromosome 16q22.1, *Hum Mol Genet* **2**, 1589-95 (1993).
56. G.P. Zhou, C. Wong, R. Su, S.C. Crable, K.P. Anderson and P.G. Gallagher, Human potassium chloride cotransporter 1 (SLC12A4) promoter is regulated by AP-2 and contains a functional downstream promoter element, *Blood* **103**, 4302-9 (2004).
57. G.H. Clayton, G.C. Owens, J.S. Wolff and R.L. Smith, Ontogeny of cation-Cl- cotransporter expression in rat neocortex, *Brain Res Dev Brain Res* **109**, 281-92 (1998).
58. C. Kanaka, K. Ohno, A. Okabe, K. Kuriyama, T. Itoh, A. Fukuda and K. Sato, The differential expression patterns of messenger RNAs encoding K-Cl cotransporters (KCC1,2) and Na-K-2Cl cotransporter (NKCC1) in the rat nervous system. *Neuroscience* **104**, 933-46 (2001).
59. D.H. Ellison, H. Velazquez and F.S. Wright, Stimulation of distal potassium secretion by low lumen chloride in the presence of barium, *Am J Physiol* **248**, F638-49 (1985).
60. D.H. Ellison, H. Velazquez and F.S. Wright, Unidirectional potassium fluxes in renal distal tubule: effects of chloride and barium, *Am J Physiol* **250**, F885-94 (1986).
61. J.B. Amorim, M.A. Bailey, R. Musa-Aziz, G. Giebisch and G. Malnic, Role of luminal anion and pH in distal tubule potassium secretion, *Am J Physiol Renal Physiol* **284**, F381-8 (2003).
62. C.M. Gillen and B. Forbush, III, Functional interaction of the K-Cl cotransporter (KCC1) with the Na-K-Cl cotransporter in HEK-293 cells, *Am J Physiol* **276**, C328-36. (1999).
63. M. Haas and B. Forbush, III, The Na-K-Cl cotransporter of secretory epithelia. *Annu Rev Physiol* **62**, 515-34 (2000).
64. C. Plata, P. Meade, N. Vazquez, S.C. Hebert and G. Gamba, Functional properties of the apical Na^+-K^+-2Cl- cotransporter isoforms, *J Biol Chem* **277**, 11004-12 (2002).
65. P. Isenring, S.C. Jacoby, J. Chang and B. Forbush, Mutagenic mapping of the Na-K-Cl cotransporter for domains involved in ion transport and bumetanide binding, *J Gen Physiol* **112**, 549-58 (1998).
66. A. Mercado, D.B. A., Mount, N. Vazquez, L. Song and G. Gamba, Functional characteristics of the renal KCCs, *Faseb J* **14**, A341 (2000).
67. J.A. Payne, Functional characterization of the neuronal-specific K-Cl cotransporter: implications for $[K^+]o$ regulation, *Am J Physiol* **273**, C1516-C1525 (1997).
68. L. Song, et.al., Molecular, functional, and genomic characterization of human KCC2, the neuronal K-Cl cotransporter, *Molecular Brain Research* **103**, 91-105 (2002).
69. P.K. Lauf, J. Zhang, E. Delpire, R.E.W. Fyffe, D.B. Mount and N.C. Adragna, Erythrocyte K-Cl cotransport: immunocytochemical and functional evidence for more than one KCC isoform in HK and LK sheep red blood cells, *Comp Biochem Physiol* **130**, 499-509 (2002).
70. N. Vardi, L.L. Zhang, J.A. Payne and P. Sterling, Evidence that different cation chloride cotransporters in retinal neurons allow opposite responses to GABA. *J Neurosci* **20**, 7657-63 (2000).
71. T.Q. Vu, J.A. Payne and D.R. Copenhagen, Localization and developmental expression patterns of the neuronal K-Cl cotransporter (KCC2) in the rat retina, *J Neurosci* **20**, 1414-23 (2000).
72. R. Miles, Neurobiology. A homeostatic switch, *Nature* **397**, 215-6 (1999).
73. J. Yamada, A. Okabe, H. Toyoda, W. Kilb, H.J. Luhmann and A. Fukuda, Cl- uptake promoting depolarizing GABA actions in immature rat neocortical neurones is mediated by NKCC1, *J Physiol* **557**, 829-41 (2004).
74. A. Fukuda, K. Muramatsu, A. Okabe, Y. Shimano, H. Hida, I. Fujimoto and H. Nishino, Changes in intracellular Ca^{2+} induced by $GABA_A$ receptor activation and reduction in Cl^- gradient in neonatal rat neocortex, *J Neurophysiol* **79**, 439-46. (1998).
75. X. Leinekugel, I. Medina, I. Khalilov, Y. Ben-Ari and R. Khazipov, Ca^{2+} oscillations mediated by the synergistic excitatory actions of GABA(A) and NMDA receptors in the neonatal hippocampus, *Neuron* **18**, 243-55. (1997).
76. S. Marty, B. Berninger, P.Carroll and H. Thoenen, GABAergic stimulation regulates the phenotype of hippocampal interneurons through the regulation of brain-derived neurotrophic factor, *Neuron* **16**, 565-70. (1996).
77. K. Ganguly, A.F. Schinder, S.T. Wong and M. Poo, Gaba itself promotes the developmental switch of neuronal gabaergic responses from excitation to inhibition, *Cell* **105**, 521-32. (2001).

78. J. Kirsch and H. Betz, Glycine-receptor activation is required for receptor clustering in spinal neurons, *Nature* **392**, 717-20. (1998).
79. C. Rivera, J. Voipio, J.A. Payne, E. Ruusuvuori, H. Lahtinen, K. Lamsa, U. Pirvola, M. Saarma andL/ Kaila, The K^+-Cl^- cotransporter KCC2 renders GABA hyperpolarizing during neuronal maturation, *Nature* **397**, 251-255 (1999).
80. J. Lu, M. Karadsheh and E. Delpire, Developmental regulation of the neuronal-specific isoform of the K-Cl cotransporter, KCC2, in postnatal rat brains, *J Neurobiology* **39**, 558-568 (1999).
81. W. Jarolimek, A. Lewen and U. Misgeld, A furosemide-sensitive K^+-Cl^- cotransporter counteracts intracellular Cl^- accumulation and depletion in cultured rat midbrain neurons, *J Neurosci* **19**, 4695-704 (1999).
82. Y. Kakazu, S. Uchida, T. Nakagawa, N. Akaikeand and J. Nabekura, Reversibility and cation selectivity of the K^+-Cl^- cotransport in rat central neurons, *J Neurophysiol* **84**, 281-8. (2000).
83. R.A. DeFazio, S. Keros, S., M.W. Quick and J.J. Hablitz, Potassium-coupled chloride cotransport controls intracellular chloride in rat neocortical pyramidal neurons, *J Neurosci* **20**, 8069-76 (2000).
84. K. Haug, M. Warnstedt, A.K. Alekov, T. Sander, A. Ramirez, B. Poser, S. Maljevic, S. Hebeisen, C. Kubisch, J. Rebstock, S. Horvath, K. Hallmann, J.S. Dullinger, B. Rau, F. Haverkamp, S. Beyenburg, H. Schulz, D. Janz, B. Giese, G. Muller-Newen, P. Propping, C.E. Elger, C. Fahlke, H. Lerche and A. Heils, Mutations in CLCN2 encoding a voltage-gated chloride channel are associated with idiopathic generalized epilepsies, *Nat Genet* **33**, 527-32 (2003).
85. J.R. Williams, J.W. Sharp, V.G. Kumari, M. Wilson and J.A. Payne, The neuron-specific K-Cl cotransporter, KCC2. Antibody development and initial characterization of the protein, *J Biol Chem* **274**, 12656-12664 (1999).
86. A.I. Gulyas, A. Sik, J.A. Payne, K. Kaila and T.F. Freund, The KCl cotransporter, KCC2, is highly expressed in the vicinity of excitatory synapses in the rat hippocampus, *Eur J Neurosci* **13**, 2205-17. (2001).
87. H. Li, J. Tornberg, K. Kaila, M.S. Airaksinen and C. Rivera, Patterns of cation-chloride cotransporter expression during embryonic rodent CNS development, *Eur J Neurosci* **16**, 2358-70 (2002).
88. S. Mikawa, C. Wang, F. Shu, T. Wang, A. Fukuda and K. Sato, Developmental changes in KCC1, KCC2 and NKCC1 mRNAs in the rat cerebellum, *Brain Res Dev Brain Res* **136**, 93-100 (2002).
89. A. Ludwig, H. Li, M. Saarma, K. Kaila and C. Rivera, Developmental up-regulation of KCC2 in the absence of GABAergic and glutamatergic transmission, *Eur J Neurosci* **18**, 3199-206 (2003).
90. S. Titz, M. Hans, W. Kelsch, A. Lewen, D. Swandulla and U. Misgeld, Hyperpolarizing inhibition develops without trophic support by GABA in cultured rat midbrain neurons, *J Physiol* **550**, 719-30 (2003).
91. C. Rivera, H. Li, J. Thomas-Crusells, H. Lahtinen, T. Viitanen, A. Nanobashvili, Z. Kokaia, M.S. Airaksinen, J. Voipio, K. Kaila and M. Saarma, BDNF-induced TrkB activation down-regulates the K+-Cl- cotransporter KCC2 and impairs neuronal Cl- extrusion, *J Cell Biol* **159**, 747-52 (2002).
92. C. Rivera, J. Voipio, J. Thomas-Crusells, H. Li, Z. Emri, S. Sipila, J.A. Payne, L. Minichiello, M. Saarma, and K. Kaila, Mechanism of activity-dependent downregulation of the neuron-specific K-Cl cotransporter KCC2, *J Neurosci* **24**, 4683-91 (2004).
93. F. Aguado, M.A. Carmona, E. Pozas, A. Aguilo, F.J. Martinez-Guijarro, S. Alcantara, V. Borrell, R. Yuste, C.F. and E. Soriano, BDNF regulates spontaneous correlated activity at early developmental stages by increasing synaptogenesis and expression of the K^+Cl^- co-transporter KCC2, *Development* **130**, 1267-80 (2003).
94. M. Rechsteiner and S.W. Rogers, PEST sequences and regulation by proteolysis, *Trends Biochem Sci* **21**, 267-71 (1996).
95. V. Vallet, A. Chraibi, H.P. Gaeggeler, J.D. Horisberger and B.C. Rossier, An epithelial serine protease activates the amiloride-sensitive sodium channel, *Nature* **389**, 607-10 (1997).
96. M. Gu and P.W. Majerus, The properties of the protein tyrosine phosphatase PTPMEG, *J Biol Chem* **271**, 27751-9 (1996).
97. K. Strange, T.D. Singer, R. Morrison and E. Delpire, Dependence of KCC2 K-Cl cotransporter activity on a conserved carboxy terminus tyrosine residue, *Am J Physiol Cell Physiol* **279**, C860-7. (2000).
98. A. Mercado, A.H. Enck, K. Zandi-Nejad, G. Gamba and D.B. Mount, Role of the C-terminus of K-Cl cotransporter proteins in volume sensitivity, *J Am Soc Nephrol* **14**, 546A (2003).
99. S.M. Thompson and B.H. Gahwiler, Activity-dependent disinhibition. II. Effects of extracellular potassium, furosemide, and membrane potential on ECl- in hippocampal CA3 neurons, *J Neurophysiol* **61**, 512-23. (1989).
100. N.S. Woo, J. Lu, R. England, R. McClellan, S. Dufour, D.B. Mount, A.Y. Deutch, D.M. Lovinger and E. Delpire, Hyperexcitability and epilepsy associated with disruption of the mouse neuronal-specific K-Cl cotransporter gene, *Hippocampus* **12**, 258-68 (2002).
101. M.F. Karadsheh and E. Delpire, Neuronal restrictive silencing element is found in the kcc2 gene: molecular basis for kcc2-specific expression in neurons, *J Neurophysiol* **85**, 995-7. (2001).

102. A.N. van den Pol, K. Obrietan and G. Chen, Excitatory actions of GABA after neuronal trauma, *J Neurosci* **16**, 4283-92 (1996).
103. J.A. Coull, D. Boudreau, K. Bachand, S.A. Prescott, F. Nault, A. Sik, P. De Koninck and Y. De Koninck, Trans-synaptic shift in anion gradient in spinal lamina I neurons as a mechanism of neuropathic pain, *Nature* **424**, 938-42 (2003).
104. J.E. Race, F.N. Makhlouf, P.J. Logue, F.H. Wilson, P.B. Dunham and E.J. Holtzman, Molecular cloning and functional characterization of KCC3, a new K-Cl cotransporter, *Am J Physiol* **277**, C1210-9 (1999).
105. M.M. Pearson, J. Lu, D.B. Mount and E. Delpire, Localization of the K^+-Cl^- cotransporter, KCC3, in the central and peripheral nervous systems: expression in the choroid plexus, large neurons and white matter tracts, *Neuroscience* **103**, 481-491. (2001).
106. O.K. Steinlein, B. Neubauer, T. Sander, L. Song, J. Stoodt and D.B. Mount, Mutation analysis of the potassium-chloride cotransporter KCC3 (SLC12A6) in rolandic and idiopathic generalized epilepsy, *Epilepsy Research* **44**, 191-5 (2001).
107. S. Kunchaparty, M. Palcso, J. Berkman, H. Velazquez, G.V. Desir, P. Bernstein, R.F. Reilly and D.H. Ellison, Defective processing and expression of thiazide-sensitive Na-Cl cotransporter as a cause of Gitelman's syndrome, *Am J Physiol* **277**, F643-9 (1999).
108. N. Dupre, H.C. Howard, J. Mathieu, G. Karpati, M. Vanasse, J.P. Bouchard, S. Carpenter and G.A. Rouleau, Hereditary motor and sensory neuropathy with agenesis of the corpus callosum, *Ann Neurol* **54**, 9-18 (2003).
109. M.R. Shen, C.Y. Chou, K.F. Hsu, H.S. Liu, P.B. Dunham, E.J. Holtzman and J.C. Ellory, KCl cotransporter isoform KCC3 can play an important role in cell growth regulation, *Proc Natl Acad Sci U S A* **98**, 14714-9. (2001).
110. L. Song, E. Delpire, G. Gamba and D.B. Mount, Localization of the K-Cl cotransporters KCC3 and KCC4 in mouse kidney, *FASEB Journal*, A341 (2000).
111. D.B. Mount, L. Song, A. Mercado, A., G. Gamba and E. Delpire, Basolateral localization of renal tubular K-Cl cotransporters, *J. Am. Soc. Nephrol.* **11**, 35A (2000).
112. K. Ishibashi, F.C. Rector, Jr. and C.A. Berry, Chloride transport across the basolateral membrane of rabbit proximal convoluted tubules, *Am J Physiol* **258**, F1569-78 (1990).
113. B.C. Kone, H.R. Brady and S.R. Gullans, Coordinated regulation of intracellular K^+ in the proximal tubule: Ba^{2+} blockade down-regulates the Na^+,$^{K+}$-ATPase and up-regulates two K^+ permeability pathways, *Proc Natl Acad Sci U S A* **86**, 6431-5 (1989).
114. M.J. Avison, S.R. Gullans, T. Ogino and G. Giebisch, Na^+ and K^+ fluxes stimulated by Na^+-coupled glucose transport: evidence for a Ba^{2+}-insensitive K^+ efflux pathway in rabbit proximal tubules, *J Membr Biol* **105**, 197-205 (1988).
115. P.A. Welling and M.A. Linshaw, Importance of anion in hypotonic volume regulation of rabbit proximal straight tubule, *Am J Physiol* **255**, F853-60 (1988).
116. M.G. Cogan, Neurogenic regulation of proximal bicarbonate and chloride reabsorption, *Am J Physiol* **250**, F22-6 (1986).
117. A. Quan and M. Baum, The renal nerve is required for regulation of proximal tubule transport by intraluminally produced ANG II, *Am J Physiol Renal Physiol* **280**, F524-9 (2001).
118. N.C. Adragna, R.E. White, S.N. Orlov and P.K. Lauf, K-Cl cotransport in vascular smooth muscle and erythrocytes: possible implication in vasodilation, *Am J Physiol* **278**, C381-390 (2000).
119. M. Di Fulvio, P.K. Lauf, S. Shah and N.C. Adragna, NONOates regulate KCl cotransporter-1 and -3 mRNA expression in vascular smooth muscle cells, *Am J Physiol Heart Circ Physiol* **284**, H1686-92 (2003).
120. Y. Chen, M. Morris, E. Delpire, P.K. Lauf and N.C. Adragna, Hypertension in K-Cl cotransporter-3 knockout mice, *Faseb J* **17**, A462 (2003).
121. J.W. Meyer, M. Flagella, R.L. Sutliff, J.N. Lorenz, M.L. Nieman, C.S. Weber, R.J. Paul and G.E. Shull, Decreased blood pressure and vascular smooth muscle tone in mice lacking basolateral Na^+-K^+-$2Cl^-$ cotransporter, *Am J Physiol Heart Circ Physiol* **283**, H1846-55 (2002).
122. M.F. Karadsheh, N. Byun, D.B. Mount and E. Delpire, Localization of the KCC4 potassium-chloride cotransporter in the nervous system, *Neuroscience* **123**, 381-91 (2004).
123. H. Amlal, M. Paillard and M. Bichara, Cl^--dependent NH_4^+ transport mechanisms in medullary thick ascending limb cells, *American Journal of Physiology* **267**, C1607-15 (1994).
124. A. Mercado, A.H. Enck, K. Zandi-Nejad and D.B. Mount, Functional roles of conserved and variant cysteine residues in the KCC4 K-Cl cotransporter, *J Am Soc Nephrol* **14**(2003).
125. R. Estevez, B.C. Schroeder, A. Accardi, T.J. Jentsch and M. Pusch, Conservation of chloride channel structure revealed by an inhibitor binding site in ClC-1, *Neuron* **38**, 47-59 (2003).
126. E. Delpire, Cation-chloride cotransporters in neuronal communication, *News Physiol Sci* **15**, 309-312 (2000).

4

STE20 KINASES AND CATION-CHLORIDE COTRANSPORTERS

Eric Delpire and Kerstin Piechotta*

1. INTRODUCTION

In yeast, STE20p is a protein kinase that transmits pheromone signals from G proteins ,γ to downstream components of the signaling pathway.[1] Ste20p can be regarded as a MAP4K because it activates a signaling cascade by direct phosphorylation of a MAP3K. Over thirty Ste20-related protein kinases have been identified in mammalian cells. Most of these kinases serve as upstream activators of MAP kinase cascades.[2] The group of Ste20 kinases was subdivided into 10 subfamilies in mammals, based on their phylogenetic relationships.[2] Ste20-related kinases are characterized by a large regulatory domain fused to the kinase domain. In two subfamilies, in which the prototype member is PAK1, the regulatory domain is located upstream from the kinase domain (N-terminal regulatory domain). In contrast, the eight additional mammalian Ste20 kinase subfamilies have regulatory domains which are located downstream from the kinase domain (C-terminal regulatory domain). The prototype member of these eight subfamilies is the germinal center kinase, or GCK. SPAK[3] (or PASK[4]) and OSR1[5] belong to the GCK subfamily VI, which also comprises Fray,[6] a Drosophila homologue, and Y59A8B.23, a *C. elegans* homologue.[2]

2. SPAK/OSR1 AND CATION-CHLORIDE COTRANSPORTERS

Using a yeast two-hybrid screen, we identified the **S**te20-related **P**roline **A**lanine-rich **K**inase (SPAK[3]) as a candidate protein interacting with the N-terminal tail of KCC3a.[7] Interaction between KCC3 and mouse OSR1 (a related kinase that shares an overall 67% identity with mouse SPAK) was also demonstrated in yeast. The original cloning papers of SPAK and OSR1 were submitted independently for publication in 1998. As a consequence, OSR1 (oxidative stress response-1) was named based on 20% homology to SOK-1, a Ste20 kinase stimulated by oxidative stress.[8] In contrast to the mouse EST (expressed sequence tags) database, which contains a large number of clones for both SPAK and OSR1, the amphibian EST database only contains sequences for OSR1. This observation suggests that Fray and the *C. elegans* clone are likely homologues of OSR1 and that SPAK evolved from post-amphibian gene duplication.

*Eric Delpire and Kerstin Piechotta, Department of Anesthesiology, Vanderbilt University Medical Center, Nashville, TN, 37232-2520

2.1. Interacting Sites

Using deletion mutants, we determined that the binding of SPAK involved nine residues located in the N-terminal tail of KCC3a.[7] Despite the overall low degree of conservation within the N-termini of cation-chloride cotransporters, we found some conservation within the SPAK binding domain: a phenylalanine residue that is often preceded by an arginine residue and followed by a valine residue two positions later. The motifs from all cation-chloride cotransporters were then tested by yeast two-hybrid. Functional binding sites for SPAK were observed in KCC3a, KCC3b, NKCC1 and

Table 1. Mutation analysis of SPAK binding site

KCC3a			**NKCC2**		
R F M V T P T K I	w.t.	+	R F Q V H V I N E	w.t.	+
A F M V T P T K I	mutant	-	E N I V H V Q F R	reversed	-
R **A** M V T P T K I	mutant	-	**A** F Q V H V I N E	mutant	-
R F **A** V T P T K I	mutant	+	**K** F Q V H V I N E	mutant	+
R F M **A** T P T K I	mutant	+	**H** F Q V H V I N E	mutant	-
R F M V **A** P T K I	mutant	+	**E** F Q V H V I N E	mutant	-
R F M V T **A** T K I	mutant	+/-	R **A** Q V H V I N E	mutant	-
R F M V T P **A** K I	mutant	+	R **Y** Q V H V I N E	mutant	-
R F M V T P T **A** I	mutant	+/-	R **V** Q V H V I N E	mutant	-
R F M V T P T K **A**	mutant	+/-	R F **A** V H V I N E	mutant	+
R F M V T P T **A** **A**	mutant	-	R F **E** V H V I N E	mutant	+
R F M V **A** **A** **A** K I	mutant	-	R F Q **A** H V I N E	mutant	-
			R F Q **W** H V I N E	mutant	+
KCC4			R F Q **L** H V I N E	mutant	-
N F T V V P V E A	w.t.	-	R F Q V **A** V I N E	mutant	+
R F T V V P V E A	mutant	+	R F Q V H **A** I N E	mutant	+
			R F Q V H V **A** N E	mutant	+/-
NKCC1			R F Q V H V I **A** E	mutant	+
R F Q V D P V S E	w.t. (1)	+	R F Q V H V I N **A**	mutant	+/-
R F R V N F V D P	w.t. (2)	+			

Sequences from several cation-chloride cotransporters were tested for interaction with SPAK using yeast two-hybrid. The sequence is either wild-type or mutated. w.t.: wild-type sequence, mutant: one or several residues were mutated, positive signs indicate strong SPAK interaction, negative signs indicate absence of SPAK interaction, and plus/minus signs indicate weakened SPAK interaction. For NKCC1, two SPAK binding motifs were identified within the N-terminus.[9] They are indicated by the number (1) and the number (2), respectively.

NKCC2, whereas corresponding motifs within KCC1, KCC4 and NCC lacked interaction. Mutation analysis of the SPAK binding site in KCC3, NKCC1 and NKCC2 (Table I) allowed us to propose a consensus binding motif for the kinase with the conserved residues (R/K)F*X*(V/I), followed by five essential residues to which no consensus was found. As indicated in the table, we were able to render the sequence of KCC4 active in interacting with SPAK by replacing the asparagine residue at position 1 by an arginine residue. A genome-wide search of proteins comprising the 4 letter motif (R/K)F*X*(V/I) revealed that apart from the cation-chloride cotransporters, mammalian kinases and cytoskeletal proteins showed the largest frequency of putative SPAK/OSR1 binding sites. This observation is compatible with yeast two-hybrid data obtained with SPAK as a bait[9] (see below).

Using a set of SPAK deletion mutants, we determined that the last 97 residues of the SPAK protein constitute the domain of the kinase interacting with cation-chloride cotransporters. As shown in Figure 1, deletion of a few residues at the 5' or 3' end of the 97 residue segment obliterated interaction. It is worth noting that the SPAK interacting domain starts precisely at a place in the carboxyl-terminus that resumes high homology with the related kinase OSR1 (See Figure 1).

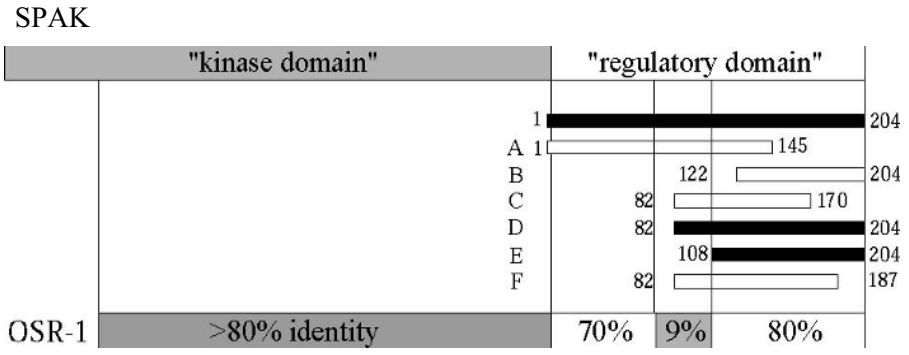

Figure 1. Schematic representation of SPAK and OSR1 kinases with the high homology upstream kinase domain (>80% identity) and the downstream regulatory domain. Alignment of the regulatory domains of SPAK and OSR1 identifies three regions: a 5' region of high homology (70% identity), a medial region of low homology, and a 3' region of very high homology (80% identity). Filled bars represent positive yeast two-hybrid interaction (with KCC3a N-terminal bait), open bars represent negative interaction. Note that the segment interacting with the cotransporter starts where the homology in the regulatory domain between SPAK and OSR1 is the highest.

2.2. SPAK/OSR1 as Regulators of Cotransporter Activity

In a recent study, Dowd and Forbush examined the effect of overexpressing wild-type rat PASK (SPAK) and dominant-negative PASK in HEK-293 cells that expressed either human or shark NKCC1.[10] The effect of the kinase on NKCC1 cotransport activity was measured under low Cl^- conditions. In control cells, reducing internal Cl^- from 150 mM to 0 mM increased NKCC1 activity significantly with a $[Cl]_i$ giving half-maximal activation at 20 mM for human NKCC1 and 40 mM for shark NKCC1. Overexpression of the kinase shifted the Cl^- effect from 20 to 30 mM for cells expressing human NKCC1 and from 40 to 80 mM in cells expressing the shark cotransporter. They reported a complete absence of NKCC1 activation in cells overexpressing the inactive kinase. These data suggest that the kinase is involved in NKCC1 activation. However, a detailed time course analysis of NKCC1 activation under different stimuli, including low internal Cl^-, showed that only the kinetics of activation were affected by the kinase; the cotransporter was fully activated after 15 minutes of different treatments. Overexpression of the dominant negative kinase only reduced the rate of activation. Using an anti-phospho-NKCC1 antibody that recognizes two threonines controlling NKCC1 activity,[11] Dowd and Forbush showed a • 25% increase in NKCC1 phosphorylation in cells expressing wild-type SPAK, and a • 75% reduction in NKCC1 phosphorylation in cells

overexpressing the dominant negative kinase. Altogether, these data indicate that SPAK is involved in phosphorylating NKCC1 at residues Thr^{184}/Thr^{189} (shark sequence) and in modulating the rate of NKCC1 activation.

2.3. SPAK Binding and Cotransporter Function

Analysis of the NKCC1 amino acid sequence revealed the presence of two putative SPAK/OSR1 binding sites within the N-terminus of the cotransporter. Using yeast two-hybrid, we demonstrated that these two sites are functional binding domains for the kinase. Indeed, mutation of both SPAK/OSR1 binding domains is required for complete abolishment of interaction.[9] Interestingly, one of the SPAK/OSR1 binding sites overlaps with a binding motif for protein phosphatase-1 (PP1). Whether the kinase and the phosphatase can simultaneously bind to the cotransporter or the binding of one protein prevents interaction with the other protein remains to be determined. Existence of overlapping SPAK and PP1 binding motifs suggests reciprocal action between the kinase and the phosphatase. Of interest is the observation that SPAK/OSR1 binding domains are not located in the vicinity of the two threonine residues identified by Darman and Forbush.[11] For the mouse NKCC1, the SPAK/OSR1 binding domains are respectively located 120-128 and 64-72 residues upstream of the first threonine residue (Thr^{206}). However, binding sites and phosphorylation sites may not necessarily coincide as proteins have complex quaternary structures.

Mutations of the two SPAK/OSR1 binding domains, resulting in the abolishment of kinase-cotransporter interaction, was shown to be without consequence on cotransporter function, as measured by baseline- or activated ^{86}Rb uptakes in *Xenopus laevis* oocytes.[9] Differences between our data and those of Forbush's group might be explained by the time of the influx: our oocyte uptakes were measured over a one hour period and no kinetic analysis of NKCC1 activation was measured in the oocytes. Alternatively, SPAK-dependent phosphorylation and activation of NKCC1 might be processes that are completely independent from SPAK binding.

2.4. Is the Binding of SPAK Regulated?

As previously demonstrated by Ushiro[4] and Tsutsumi,[12] and shown in Figure 2, SPAK is found in the cell in a soluble or cytosolic form as well as closely associated with membranes. A sizable fraction of the protein is resistant to Triton X-100 treatment, indicating a tight association with the membrane-bound cytoskeleton. We have previously shown that SPAK is in close association with NKCC1 on the apical membrane of choroid plexus and on the basolateral membrane of salivary gland epithelial cells.[7] The kinase is highly expressed in dorsal root ganglion neurons,[13] sensory cells that abundantly express NKCC1.[14] More recently, we also reported co-localization of SPAK and NKCC1 in sciatic nerve's node of Ranvier.[9] These results indicate that in subdomains of tissues where NKCC1 is highly expressed, the kinase is found associated with the cotransporter. This view is strengthened by the observation that in the NKCC1 knockout mouse, SPAK staining in choroid plexus is cytosolic rather than associated with the apical membrane.[7] Taken together, these observations demonstrate that cation-chloride cotransporters are significant anchors of the kinase in tissues. This, however, does not exclude the kinase interaction with other membrane transport proteins, ion channels, or other proteins.

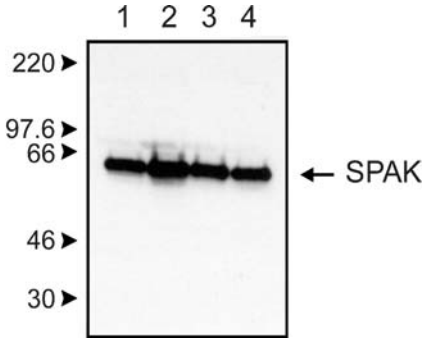

Figure 2. Western blot analysis of brain proteins with anti-SPAK antibody (30 μg/lane). The brain of one adult C57BL6 mouse was homogenized in 10 ml of a buffer containing 0.32M sucrose, 5 mM Tris-HCl, pH 7.5, 2 mM EDTA. Homogenate was divided into two 5 ml aliquots. Triton X-100 was added to one aliquot to a final concentration of 1% and incubated on ice for 30 min prior to centrifugation at 1,000 g, 10,000 g, and 100,000 g. Lanes: 1, microsomal proteins with Triton X-100; 2, microsomal proteins; 3, soluble proteins with Triton X-100; 4, soluble proteins.

To determine whether the binding of SPAK is regulated during cellular stress, we examined the apical surface expression of the kinase in choroid plexus using tissue exposed to several stimuli. Choroid plexi from lateral ventricles were dissected from adult mouse brains, placed in 6-well plates containing artificial cerebrospinal fluid (aCSF) equilibrated with 5%CO_2/95%O_2. The tissues were incubated for 30 min in aCSF, aCSF + 1 mM arsenite, aCSF + 100 mM sucrose, aCSF-low Na^+ (½ NaCl concentration), aCSF + 0.1% DMSO (vehicle for bumetanide), aCSF + 100 μM bumetanide/0.1% DMSO. The aCSF contains in mM: NaCl, 150; KCl, 5; $CaCl_2$, 0.5; $MgCl_2$, 1; glucose, 10; sucrose, 17; HEPES, 10; pH 7.4. The tissue was then fixed for 2 hours in 4% paraformaldehyde, cryoprotected in 30% sucrose, frozen and sectioned. Sections (10 μm) were stained with anti-SPAK antibody. No differences in SPAK location and SPAK intensity were observed under the different treatments (data not shown). In all cases, the kinase was abundantly localized to the apical membrane of the epithelial cells, as shown in our previous publications.[7, 9] Using Western blot analysis, Tsutsumi and colleagues observed, however, a significant translocation of SPAK from Triton X-100 soluble to insoluble fractions in NIH 3T3 and PC12 cells treated with hyperosmolarity, hydrogen peroxide and heat shock,[12] The authors suggested translocation from the cytosol to the cytoskeleton in response to cellular stresses. Whether the Triton X-100 soluble fraction originates solely from the cytosol, as they indicate, or originates also from membrane-bound proteins remains to be determined. In the latter case, translocation could occur from membrane transporters to membrane associated cytoskeleton with no observable change in immunofluorescence localization.

3. INTERACTORS OF SPAK/OSR1

As mentioned above, a systematic search of Genebank has identified a large number of proteins comprising (R/K)F*X*(V/I) motifs. Interestingly, these motifs are abundantly found in kinases, cytoskeletal proteins, and various membrane transporters and channels.

Whether or not these motifs constitute functional SPAK/OSR1 binding sites remains to be determined. Based on their locations within proteins, some of these motifs might likely be inaccessible for protein-protein interactions. Because SPAK/OSR1 interaction requires 9 residues, the nature of the five residues following the basic motif might also determine the faith of the interaction. In an attempt to identify novel SPAK interactors, we screened a mouse brain cDNA library with the binding domain of SPAK as a bait. Intriguingly, all proteins identified are involved in trafficking or response to cellular stress.[9]

3.1. WNK4

WNK4 belongs to a novel subfamily of protein kinases and can be distinguished from other kinases by the absence of a conserved lysine residue (**w**ith **n**o **K**=lysine) in the catalytic domain. Four of these kinases have been described in the mammalian genome: WNK1-4.[15] Of interest is the fact that the catalytic domain of WNK1 has closest homology to human PAK2, a Ste20 kinase. WNK4 was isolated twice from the brain yeast two-hybrid library while screening for interactions with SPAK. We identified one SPAK binding motif (RFQVTSSKE) in the C-terminal tail of WNK4. The kinase is involved in monogenic[16] (pseudohypoaldosteronism type-2) as well as polygenic[17] hypertension through a deficient regulation in the trafficking of the distal convoluted tubule thiazide-sensitive Na-Cl tubule

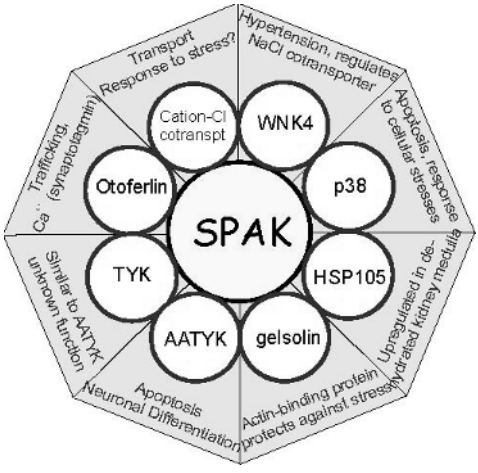

Figure 3. Drawing representing several proteins that were shown to interact with SPAK. With the exception of p38, in which interaction with SPAK was identified functionally[3] and by co-immunoprecipitation;[7] all other interactions were identified using yeast two-hybrid.[9]

thiazide-sensitive Na-Cl cotransporter. Indeed, wild-type WNK4 acts as a negative regulator of Na-Cl cotransporter trafficking. Mutations in WNK4 results in a significant increase in the expression of functional Na-Cl cotransporters on the apical membrane of distal convoluted tubule cells, leading to an increased reabsorption of Na^+. This increase in Na^+ reabsorption is similar to the one observed in pseudohypoaldosteronism type-1, where mutations in the Nedd4 binding domains of the epithelial Na^+ channel result in an

increase in cell surface expression of the channel.[18]

3.2. Apoptosis Associated Tyrosine Kinase (AATYK)

Two of the proteins isolated from mouse brain cDNA libraries while screening for SPAK interactors were tyrosine kinases. The first kinase, termed apoptosis-associated tyrosine kinase, or AATYK, is up-regulated during differentiation and apoptosis of myeloid precursor cells[19] and neurons.[20] In neurons from cerebrum and cerebellum, AATYK expression is up-regulated during postnatal development (from P2 to P21) and remains high through adulthood. When overexpressed in cultured cerebellar granular cells, AATYK induces neurite outgrowth. Whether or not these processes involve the Ste20 kinases SPAK and OSR1 is unknown. The second protein kinase identified as a SPAK interacting protein is novel and shares an overall 30% identity at the amino acid level with AATYK. The identity increases to 62% within the tyrosine kinase domain. As shown in Table 2, four sequences in the carboxyl-terminal regulatory tail of AATYK and one sequence in the novel protein (AATYK2) resembling the SPAK binding motifs were identified. The four sequences of AATYK were tested for interaction with SPAK. Only the sites located at the extreme C-terminus which were in agreement with our consensus sequence (R/K)F*X*(V/I) demonstrated interaction with SPAK.

Table 2. SPAK binding sites in AATYK

AATYK (1-1317)			**AATYK2 (1-1307)**		
R F E W D G D F P	1240 - 1248	-	**R F** S **V** S P A L E	1234 - 1242	N.d.
D **F** P L V P G K A	1246 - 1254	-			
R F T **V** S P T P A	1279 - 1287	+			
R F S **I** T H I S D	1289 - 1297	+			

Sequences of the putative SPAK binding motifs (9 residues) are given with their position within the protein. Underlined are those that conform with the SPAK consensus binding motif (R/K)F*X*(V/I). N.d. not determined.

3.3. HSP105

Heat shock protein-105 or HSP105 was originally cloned as a protein markedly up-regulated in the renal medulla upon dehydration or hypertonicity.[21] Follow-up studies showed that the heat shock protein is expressed at exceptionally high levels in the brain as compared with other tissues and is overexpressed in a variety of human tumors,[22] in multiple sclerosis lesions,[23] and in brains exposed to morphine.[24] The protein plays an antiapoptotic role in mature cells but has pro-apoptotic properties in immature cells. Indeed, studies in embryonic cell lines indicate that HSP105α may play a role in organogenesis during embryonic development by enhancing apoptosis. Among other factors, this process involves the activation of p38 MAPK. A recent yeast two-hybrid study has shown that HSP105 also tightly associates with α-tubulin.[25]

3.4 Otoferlin

Otoferlin, a member of a mammalian gene family related to *C. elegans* fer-1, was identified in a search for genes involved in human deafness.[26] Otoferlin transcripts are found in a variety of tissues including inner ear (sensory hair cells), heart, placenta, liver,

pancreas, skeletal muscle, kidney, and brain.[27] Otoferlin contains six predicted C2 domains which are known to interact with phospholipids as well as proteins. C2 domains have been shown to participate, in a calcium-dependent fashion, in the docking of synaptic vesicles to plasma membranes. Other proteins that contain C2 domains and are involved in vesicle-membrane fusion include synaptotagmins and rabphilin 3A.

3.5. Gelsolin

Gelsolin is a protein involved in dynamic changes in the actin cytoskeleton during a variety of cellular processes. Under appropriate conditions, gelsolin severs and caps assembled actin filaments. This actin binding protein plays an important role in cell motility, the regulation of ion channel function, lipid signaling, apoptosis, and in the cell's response to stress (For review, see[28]).

3.6. p38 MAPK

In contrast to the other proteins, p38 MAPK was not identified in our yeast two-hybrid screen designed to uncover novel binding partners of SPAK. Examining the stress-response pathways activated by the Ste20 kinase, Johnston and colleagues observed that p38 MAPK was activated by SPAK overexpression, whereas the ERK and JNK pathways were unaffected.[3] We subsequently demonstrated that p38 MAPK can be co-immunoprecipitated with NKCC1,[7] and this can be reversed by cell stress conditions.[9] The p38 MAP kinase pathway is involved in cell proliferation, differentiation and apoptosis and is activated by a variety of factors including growth hormones, cytokines and cellular stresses. Hyperosmotic stress, for instance, significantly activates p38 MAPK in a variety of cells. The activation of the kinase is required for cell volume regulation, as regulatory volume increase (RVI) is impaired by p38 MAPK inhibitors. The stress kinase is thought to contribute to increased RVI efficacy by altering F-actin depolymerization/polymerization.[29] There is accumulating evidence that p38 MAPK signaling pathways also modulate the activity of membrane transport processes.[30-32] As far as cation-chloride cotransporters are concerned, in skeletal muscle, the activation of p38 MAP kinase by insulin inhibits ERK-dependent NKCC1 activity.[33] In the same cells, as well as others, p38 MAPK does not seem to be involved in the hypertonically induced activation of NKCC1. This absence of p38 MAPK involvement is slightly peculiar in light of the relationship between NKCC1 and F-actin.[34]

4. MEMBRANE TRANSPORT AND SIGNALING

From the extensive work of the last three decades, it is clear that membrane carriers (channels and transporters) are regulated by a variety of signaling events. The idea that membrane transporters themselves can initiate signaling cascades is, however, only an emerging concept. In cortical thick ascending limb of Henle (cTALH), lowering the external Cl^- concentration or adding bumetanide results in a significant activation of p38 MAPK.[35] This activation leads to the up-regulation of cyclooxygenase-2 and, through transcriptional effects, to the increased production of renin. Because bumetanide specifically inhibits the absorptive Na-K-2Cl cotransporter in these cells, it can be

concluded that reducing the activity of NKCC2 or changing the conformation of the cotransporter leads to the activation of p38. A direct link between the activity of the Na^+-dependent glucose cotransporter, SGLT1, and p38 activity was also demonstrated in Caco-2 cells.[36] The concept that plasma membrane transporters, through protein-protein interactions, can trigger signaling cascades was also proposed to occur in cardiac myocytes. In these cells, the addition of small amounts of ouabain results in activation of src kinase, a process that likely involves conformational change of the Na^+/K^+ pump and interaction with anchored proteins.[37] Taken together, these studies indicate that changes in substrate binding, conformation, and/or activity of membrane transport proteins such as cotransporters and pumps might lead, through protein-protein interactions, to the initiation of signaling cascades. These signals may be important for cell proliferation, differentiation, and cell death or survival.

5. CONCLUSIONS

The conserved short C-terminal regions of SPAK and OSR1 are now known to bind to proteins containing (R/K)F*X*(V/I)*XXXXX* motifs.[7, 9] Together with a variety of membrane transporters and channels, cation-chloride cotransporters constitute anchors for SPAK and OSR1. The functional significance of the interaction between SPAK/OSR1 and the cotransporters is not fully understood. The two Ste-20 kinases seem to serve multiple roles: they may modulate the activity of the cotransporters, may recruit additional stress proteins in the vicinity of the cotransporters, and may transmit signals about the cotransporters' activity or conformation to downstream signaling pathways.

6. ACKNOWLEDGMENTS

This work was supported by a National American Heart Association grant-in-aid. We thank Jianming Lu and Roger England for their technical expertise.

7. REFERENCES

1. E. Leberer, D. Dignard, D. Harcus, D. Y. Thomas and M. Whiteway, The protein kinase homologue Ste20p is required to link the yeast pheromone response G-protein beta gamma subunits to downstream signaling components, *EMBO J.* **11**, 4815 (1992).
2. I. Dan, N. M. Watanabe and A. Kusumi, The Ste20 group kinases as regulators of MAP kinase cascades, *Trends Cell. Biol.* **11**, 220 (2001).
3. A. M. Johnston, G. Naselli, L. J. Gonez, R. M. Martin, L. C. Harrison and H. J. Deaizpurua, SPAK, a Ste20/SPS1-related kinase that activates the p38 pathway *Oncogene* **19**, 4290 (2000).
4. H. Ushiro, T. Tsutsumi, K. Suzuki, T. Kayahara and K. Nakano, Molecular Cloning and Characterization of a novel Ste20-related protein kinase enriched in neurons and transporting epithelia, *Arch. Biochem. Biophys.* **355**, 233 (1998).
5. M. Tamari, Y. Daigo and Y. Nakamura, Isolation and characterization of a novel serine threonine kinase gene on chromosome 3p22-21.3, *J. Hum. Genet.* **44**, 116 (1999).
6. W. M. Leiserson, E. W. Harkins and H. Keshishian, Fray, a drosophila serine/threonine kinase homologous to mammalian PASK, is required for axonal ensheatment, *Neuron* **28**, 793 (2000).
7. K. Piechotta, J. Lu and E. Delpire, Cation-chloride cotransporters interact with the stress-related kinases SPAK and OSR1, *J. Biol. Chem.* **277**, 50812 (2002).

8. C. M. Pombo, J. V. Bonventre, A. Molnar, J. Kyriakis and T. Force, Activation of a human Ste-20-like kinase by oxidant stress defines a novel stress response pathway, *EMBO J.* **15**, 5437 (1996).
9. K. Piechotta, N. J. Garbarini, R. England and E. Delpire, Characterization of the interaction of the stress kinase SPAK with the Na^+-K^+-$2Cl^-$ cotransporter in the nervous system: Evidence for a scaffolding role of the kinase, *J. Biol. Chem.***278**, 52848 (2003).
10. B. F. Dowd and B. Forbush, PASK (Proline-Alanine-rich STE20-related Kinase), a Regulatory Kinase of the Na-K-Cl Cotransporter (NKCC1)*, J. Biol. Chem.* **278**, 27347 (2003).
11. R. B. Darman and B. Forbush, A regulatory locus of phosphorylation in the N terminus of the Na-K-Cl cotransporter, NKCC1, *J. Biol. Chem.* **277**, 37542-37550 (2002).
12. T. Tsutsumi, H. Ushiro, T. Kosaka, T. Kayahara and K. Nakano, Proline- and alanine-rich Ste20-related kinase associates with F-actin and translocates from the cytosol to cytoskeleton upon cellular stresses, *J. Biol. Chem.* **275**, 9157-9162 (2002).
13. N. Miao, B. Fung, R. Sanchez, J. Lydon, D. Barker and K. Pang, Isolation and expression of PASK, a serine/threonine kinase during rat embryonic development, with special emphasis on the pancreas, *J. Histochem. Cytochem.* **48**, 1391-1400 (2000).
14. M. D. Plotkin, M. R. Kaplan, L. N. Peterson, S. R. Gullans, S. C. Hebert and E. Delpire, Expression of the Na^+-K^+-$2Cl^-$cotransporter BSC2 in the nervous system, *Am. J. Physiol. (Cell Physiol.).* **272**, C173C183 (1997).
15. F. Verissimo and P. Jordan, WNK kinases, a novel protein kinase subfamily in multi-cellular organisms*, Oncogene* **20**, 5562 (2001).
16. F. H. Wilson, et al. Human hypertension caused by mutations in WNK kinases, *Science* **293**, 1107 (2001).
17. J. Monti, H. Zimdahl, H. Schulz, R. Plehm, D. Ganten and N. Hubner, The role of Wnk4 in polygenic hypertension: a candidate gene analysis on rat chromosome 10, *Hypertension* **41**, 938 (2003).
18. O. Staub, I. Gautschi, T. Ishikawa, K. Breitschopf, A. Ciechanover, L. Schild and D. Rotin, Regulation of stability and function of the epithelial Na^+ channel (ENaC) by ubiquitination, *EMBO J.* **16**, 6325 (1997).
19. C. Friend, W. Scher, J. G. Holland and T. Sato, Hemoglobin synthesis in murine virus-induced leukemic cells in vitro: stimulation of erythroid differentiation by dimethyl sulfoxide, *Proc. Natl. Acad. Sci. USA.* **68**, 378 (1971).
20. M. Tomomura, Y. Hasegawa, T. Hashikawa, A. Tomomura, M. Yuzaki, T. Furuichi and R. Yano, Differential expression and function of apoptosis-associated tyrosine kinase (AATYK) in the developing mouse brain, *Brain Res. Mol. Brain Res.* **112**, 103 (2003).
21. R. Kojima, J. Randall, B. M. Brenner and S. R. Gullans, Osmotic stress protein 94 (Osp94). A new member of the Hsp110/SSE gene subfamily, *J. Biol. Chem.* **271**, 12327 (1996).
22. M. Kai, T. Nakatsura, H. Egami, S. Senju, Y. Nishimura and M. Ogawa, Heat shock protein 105 is overexpressed in a variety of human tumors, *Oncol. Rep.* **10**, 1777 (2003).
23. M. Minohara, Heat shock protein 105 in multiple sclerosis, *Nippon Rinsho.* **61**, 1317 (2003).
24. S. Ammon, P. Mayer, U. Riechert, H. Tischmeyer and V. Hollt, Microarray analysis of genes expressed in the frontal cortex of rats chronically treated with morphine and after naloxone precipitated withdrawal, *Brain Res. Mol. Brain Res.* **112**, 113 (2003).
25. Y. Saito, N. Yamagishi, K. Ishihara and T. Hatayama, Identification of alpha-tubulin as an hsp105alpha binding protein by the yeast two-hybrid system, *Exp. Cell Res.* **286**, 233 (2003).
26. S. Yasunaga, M. Grati, M. Cohen-Salmon, A. El-Amraoui, M. Mustapha, N. Salem, E. El-Zir, J. Loiselet and C. Petit, A mutation in OTOF, encoding otoferlin, a FER-1-like protein, causes DFNB9, a nonsyndromic form of deafness, *Nature Genet.* **21**, 363-369 (1999).
27. S. Yasunaga, M. Grati, S. Chardenoux, T. N. Smith, T. B. Friedman, A. K. Lalwani, E. R. Wilcox and C. Petit, OTOF encodes multiple long and short isoforms: genetic evidence that the long ones underlie recessive deafness DFNB9, *Am. J. Hum. Genet.* **67**, 591-600 (2000).
28. D.J. Kwiatkowski, Functions of gelsolin: motility, signaling, apoptosis, cancer, *Curr. Opin. Cell Biol.* **11**: 103-108 (1999)
29. M. Bustamante, F. Roger, M. L. Bochaton-Piallat, G. Gabbiani, P. Y. Martin and E. Feraille, Regulatory volume increase is associated with p38 kinase-dependent actin cytoskeleton remodeling in rat kidney MTAL, *Am. J. Physiol. Renal Physiol.* **285**, F336-F347 (2003).
30. K. Lemieux, D. Konrad, A. Klip and A. Marette, The AMP-activated protein kinase activator AICAR does not induce GLUT4 translocation to transverse tubules but stimulates glucose uptake and p38 mitogen-activated protein kinases alpha and beta in skeletal muscle, *FASEB J.* **17**, 1658-1665 (2003).
31. M. R. Shen, C. Y. Chou, K. F. Hsu and J. C. Ellory, Osmotic shrinkage of human cervical cancer cells induces an extracellular Cl^--dependent nonselective cation channel, which requires p38 MAPK, *J. Biol. Chem.* **277**, 45776-45784 (2002).
32. S. Apparsundaram, U. Sung, R. D. Price and R. D. Blakely, Trafficking-dependent and -independent

pathways of neurotransmitter transporter regulation differentially involving p38 mitogen-activated protein kinase revealed in studies of insulin modulation of norepinephrine transport in SK-N-SH cells, *J. Pharmacol. Exp. Ther.* **299**, 666-677 (2001).

33. A. R. Gosmanov, E. G. Schneider and D. B. Thomason, NKCC activity restores muscle water during hyperosmotic challenge independent of insulin, ERK, and p38 MAPK, *Am. J. Physiol. Regul. Integr. Comp. Physiol.* **284**, R655-R665 (2002).
34. J. B. Matthews, J. A. Smith, K. J. Tally, C. S. Awtrey, H. Nguyen, J. Rich and J. L. Madara, Na-K-2Cl cotransport in intestinal epithelial cells. Influence of chloride efflux and F-actin on regulation of cotransporter activity and bumetanide binding, *J. Biol. Chem.* **269**, 15703-15709 (1994).
35. H. F. Cheng, J. L. Wang, M. Z. Zhang, J. A. McKanna and R. C. Harris, Role of p38 in the regulation of renal cortical cyclooxygenase-2 expression by extracellular chloride, *J. Clin. Invest.* **106**, 681-688 (2000).
36. J. R. Turner and E. D. Black, NHE3-dependent cytoplasmic alkalinization is triggered by Na^+-glucose cotransport in intestinal epithelia, *Am. J. Physiol. Cell Physiol.* **281**, (2001).
37. Z. Xie, Molecular mechanisms of Na/K-ATPase-mediated signal transduction, *Ann. N. Y. Acad. Sci.* **986**, 497-503 (2003).

5

MOLECULAR PHYSIOLOGY OF THE RENAL Na^+-Cl^- AND Na^+-K^+-$2Cl^-$ COTRANSPORTERS

Gerardo Gamba and Norma A. Bobadilla*

1. INTRODUCTION

In absorptive and secretory epithelia, ion transport depends on specific plasma membrane proteins for mediating ion entry and exit from the cell. Sodium exit occurs through Na^+-K^+-ATPase and chloride exit occurs predominantly through anion-selective channels, while Na^+, K^+ and Cl^- entry is often mediated by an electroneutral process in which chloride movement is coupled to a cation that can be sodium and/or potassium. Transporters performing this coupling are known as electroneutral cation Cl^- coupled cotransporters (CCC).

In epithelial cells, CCCs are implicated in ion absorption and secretion. In non-epithelial cells, they play a key role in maintenance and regulation of cell volume. In addition, electroneutral cotransporters regulate the intraneuronal Cl^- concentration, thus modulating neurotransmission.[1]

Based on the cation that is coupled to chloride, the stoichiometry of transport process and the sensitivity to inhibitors, four groups of electroneutral cotransporter systems have been identified: 1) thiazide-sensitive Na^+-Cl^- cotransporters (TSC); 2) bumetanide-sensitive Na^+-K^+-$2Cl^-$ cotransporters (BSC/NKCC); 3) bumetanide-sensitive Na^+-Cl^- symporters, and 4) DIOA-sensitive K^+-Cl^- cotransporters (KCC).

Major advances have been made in the past decade in the molecular identification of the CCCs which began with the isolation of cDNA from fish.[2, 3] Then, homology-based approaches were used to isolate cDNA encoding CCCs from mammalian sources, forming the solute carrier family 12 (SLC12)[1] from which nine genes have now been identified (Table 1): two encoding isoforms of the Na^+-K^+-$2Cl^-$ cotransporter (one of which is BSC1/NKCC2 that is exclusively expressed in thick ascending limb of Henle), one encoding the "renal" TSC, present only in the apical membrane of the distal

* Gerardo Gamba and Norma A. Bobadilla. Molecular Physiology Unit. Instituto Nacional de Ciencias Médicas y Nutrición Salvador Zubirán and Instituto de Investigaciones Biomédicas, UNAM. Vasco de Quiroga No. 15, Tlalpan 14000, Mexico City, Mexico

convoluted tubule (DCT), four encoding isoforms of the K^+-Cl^- cotransporter and two orphan genes.[4-7] Molecular diversity of the family is increased by the existence of alternatively spliced isoforms within several members including at least TSC, BSC1/NKCC2, BSC2/NKCC1, and KCC3.[8]

Table 1. Identified genes of the SLC12 family of solute carriers

Gene	cDNA name	Tissue	Chromosome
SLC12A1	BSC1/NKCC2	Kidney	15
SLC12A2	BSC2/NKCC1	Ubiquitous	5
SLC12A3	TSC	Kidney	16
SLC12A4	KCC1	Ubiquitous	16
SLC12A5	KCC2	Central Nervous System	20
SLC12A6	KCC3	Several	15
SLC12A7	KCC4	Several	5
SLC12A8	CCC9	Several	7
SLC12A9	CIP	Several	3

Hydropathy analysis indicates that CCCs share a similar general structure. Most CCCs are proteins of around 1000-1200 amino acid residues with molecular masses between 110-130 kDa. Proposed topology features a central hydrophobic domain of about 500 amino acid residues that is flanked by a short hydrophilic amino-terminal domain (130-278 amino acid residues) and a long carboxyl terminal hydrophilic loop (~500 residues). The amino and carboxyl terminal domains are presumably located within the cell and contain several putative protein kinase A (PKA) and protein kinase C (PKC) phosphorylation sites. In the central hydrophobic domain, there are twelve putative transmembrane-spanning segments (TM 1-12) with a hydrophilic loop exhibiting at least two putative N-linked glycosylation sites. This loop resides between TMs 5 and 6 in the KCCs and TMs 7 and 8 in the Na-coupled cotransporters (TSC and BSC/NKCC). This 12 TM topology scheme was experimentally confirmed for BSC2/NKCC1,[9] and biochemical evidence indicates that BSC1/NKCC2 and TSC form homodimers.[10, 11]

In this chapter, we present a review of major advances during the last few years in molecular physiology of renal diuretic sensitive Na^+-Cl^- and Na^+-K^+-$2Cl^-$ cotransporters.

2. BSC1/NKCC2 AND TSC IN RENAL PHYSIOLOGY, PHARMACOLOGY AND PATHOPHYSIOLOGY

In the mammalian kidney, BSC1/NKCC2 is present only in the apical membrane of the TALH cells responsible for reabsorbing 10-20% of the salt filtrated at the glomerulus which are implicated in the generation and maintenance of renal medullary hypertonicity. TSC has been specifically localized at the apical membrane of the distal DCT, a nephron region that mediates the reabsorption of 5-10% of the glomerular filtrate. Thus, the combined function of BSC1/NKCC2 and TSC is responsible for 20-30% of the reabsorbed salt. These transporters are also involved in calcium, potassium and acid-base metabolism.[5, 6]

BSC1/NKCC2 and TSC play a key role in renal and cardiovascular pharmacology since they serve as the target for loop diuretics (BSC1/NKCC2) and thiazide-type diuretics (TSC). Loop diuretics such as furosemide and bumetanide are the most potent diuretics available in clinical medicine, and their major indications are the treatment of edematous states, e.g., chronic cardiac failure, chronic renal failure, chronic liver failure, nephrotic syndrome, as well as in severe derangements of calcium metabolism such as life threatening hypercalcemia. Thiazide-type diuretics such as hydrochlorothiazide and chlortalidone are considered as the first line therapy of arterial hypertension and are also indicated for the prevention of renal stone disease and osteoporosis. Therefore, the blockade of renal electroneutral cation-chloride cotransporters is often used in the management of clinical conditions that are among the greatest health care burden of the current century.

The fundamental role of BSC1/NKCC2 and TSC in salt balance, divalent cation and acid-base metabolism has been firmly established by demonstrating that inactivation of mutations in *SLC12A1* and *SLC12A3* is the cause of inherited hypokalemic metabolic alkalosis syndromes known as Bartter and Gitelman diseases, respectively.[12] A phenotype resembling Bartter or Gitelman disease was obtained in mice by targeted disruption of BSC1/NKCC2 or TSC genes, respectively.[13] TSC also seems to be implicated in the development of a salt-dependent form of human arterial hypertension known as pseudohypoaldosteronism type II (PHAII), an autosomal-dominant hypertension with hyperkalemia that can be reversed by thiazides.[14] PHAII is produced by mutations in the kinases WNK1 and WNK4[15] that are expressed in the DCT and collecting duct. It has been shown recently that WNK4 down-regulates TSC activity,[16, 17] suggesting that loss of the WNK4-induced negative effect upon TSC function is associated with development of arterial hypertension. Therefore, participation of BSC1/NKCC2 and TSC in monogenic diseases featuring high or low blood pressure suggests these genes could be involved in complex polygenic diseases such as arterial hypertension.

3. FUNCTIONAL PROPERTIES OF THE RENAL APICAL TSC

Having established an excellent method for expression of TSC from different species in *X. laevis* oocytes,[4, 18-20] and in order to take advantage of structural differences between mammalian and fish TSC, we recently determined and compared the functional, pharmacological and regulatory properties of rat, mouse and flounder TSC[19, 20] by assessing $^{22}Na^+$ uptake in *X. laevis* oocytes microinjected with cRNA *in vitro* transcribed from each of these orthologues. As shown in Table 2, a number of interesting differences were observed between species. The analysis of ion transport kinetic properties revealed that the apparent Km values for Na^+ and Cl^- in mammalian TSC proteins, either rTSC or mTSC, are significantly lower than those observed in flTSC teleost protein. Thus, the affinity for cotransported ions is higher in mammalian TSC. Interestingly, in rTSC or mTSC, the affinity for both ions was similar, whereas in flTSC, the affinity for extracellular Cl^- was higher than for Na^+.

The following was also observed regarding the affinity for thiazide-type diuretics. The inhibitory profile polythiazide > metolazone > bendroflumethiazide = trichloromethiazide > hydrochlorothiazide = chlorthalidone was similar between teleost and mammalian TSC. However, flTSC exhibited a lower affinity for every thiazide diuretic tested. The

case of polythiazide is shown in Table 2. In fact, at 10^{-4} M concentration, less potent thiazides such as trichloromethiazide and chlortalidone reduced the function of flTSC by only 68% and 46%, respectively,[20] whereas in rTSC or mTSC, the same thiazide concentration inhibited cotransporter function by more than 95%.[19] Therefore, the higher affinity for ions in mammalian TSC goes together with the higher affinity for thiazides. In this regard, we also observed differences in the interactions between thiazide diuretics and cotransported ions. When the extracellular Na^+ or Cl^- concentration was reduced to a value below the apparent Km, the rTSC affinity for metolazone increased, i.e., the curve is shifted to the left in the presence of low Cl^- [2 mM] or low Na^+ [2 mM]. Whereas in flTSC, metolazone affinity was not affected, suggesting that mammalian and teleost TSC exhibit a different type of interaction between Na^+ and Cl^-, in presence of thiazide diuretics. As shown in Table 2, in addition to kinetic and pharmacological differences, mammalian and teleost TSC are regulated differently by cell volume. rTSC and mTSC are inhibited by cell swelling and are not affected by cell shrinkage, whereas flTSC activity is decreased by cell shrinkage and is not affected by cell swelling. Thus, there are significant physiological, pharmacological and regulatory differences between mammalian and teleost TSC.

Table 2. Functional properties of rat (rTSC), mouse (mTSC), and flounder TSC (flTSC)

	rTSC	mTSC	flTSC
Na^+ Km (mM)	7.6 ± 1.6	7.2 ± 0.4	58.2 ± 7.1
Cl^- Km (mM)	6.3 ± 1.1	5.6 ± 0.6	22.1 ± 4.2
Polythiazide IC_{50} (μM)	0.3	0.4	7.0
Effect of swelling	Inhibition	Inhibition	No effect
Effect of shrinkage	No effect	No effect	Inhibition

4. STRUCTURE-FUNCTION RELATIONSHIPS IN TSC

Little is currently known about the structure-function relationships in TSC since few studies addressing this issue have been reported. Hoover et al.[21] analyzed the role of two N-glycosylation sites present in the long extracellular loop of rat TSC located between TM 7 and 8, following a site-directed mutagenesis strategy in which each or both sites were eliminated by changing asparagine residues 404 and 424 to glutamine, generating the single mutants N404Q and N424Q and the double mutant N404,424Q. Functional analysis revealed that elimination of either site alone or both sites together was associated with 50% and 95% reduction in TSC activity, respectively. Functional and confocal analysis of wild type and mutant TSC proteins previously tagged with the enhanced green fluorescent protein (EGFP-TSC) showed that a reduction in surface expression of TSC underlies the reduction in TSC activity. Interestingly, as shown in Figure 1, elimination of glycosylation sites was associated with an increased affinity for thiazides since the metolazone IC_{50} was shifted to the left in mutant cotransporters. The shift was greater in the double mutant; therefore, it is likely that TSC affinity for thiazide diuretics is related to the glycosylation extent of the cotransporter. It should be noted that flTSC exhibits

lower affinity for thiazides and contains 3 putative glycosylation sites in the extracellular loop.

More recently, an analysis of functional consequences of a single nucleotide polymorphism (SNP) in the human *SLC12A3* gene revealed that a glycine at position 264, located within transmembrane domain 4 and conserved among all CCC members, affects the ion translocation rate of the cotransporter as well as the affinities for Cl^- and thiazides.[22] The G264A SNP results in a cotransporter that exhibits a 50-60% reduction in transport rate with an increase in affinity for extracellular Cl^- and metolazone. The affinity for extracellular sodium was not affected by the G264A polymorphism. Finally, functional analysis of some of Gitleman disease mutations has revealed that substitution of certain key amino acid residues results in TSC proteins that are not properly glycosylated and processed, whereas other mutations produce TSC proteins that can be glycosylated and processed but exhibit a reduced rate of TSC insertion into the plasma membrane.[23-25]

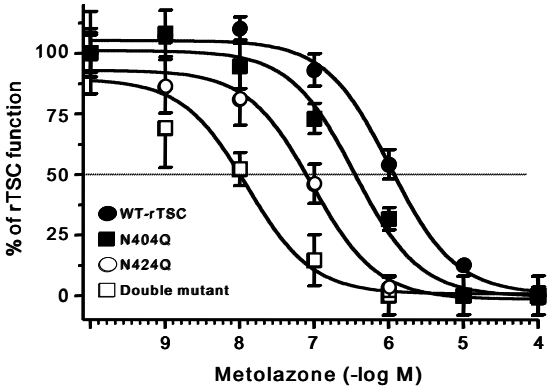

Figure 1. Dose response to metolazone in wild type TSC and glycosylation mutants.[21]

5. THE RENAL APICAL BSC1/NKCC2 SPLICED ISOFORMS

5.1. Functional Properties As Na^+-Cl^- or Na^+-K^+-$2Cl^-$ Cotransporter

Three isoforms, due to alternative splicing of BSC1/NKCC2 have, been shown to be expressed in mammalian kidney. These isoforms are due to the existence of three mutually exclusive cassette exons of 96 bp that encode 31 amino acid residues that are part of TM2 and the interconnecting segment between TM2 and TM3.[26] Studies with *in situ* hybdridization[27] and single nephron PCR[28] revealed that these isoforms exhibit axial distribution along the thick ascending limb of Henle (TALH). Isoform A is present all along the TALH, whereas isoform F is only present in the inner stripe of the outer medulla, i.e., at the beginning of medullary TALH, and isoform B is only expressed in the cortical TALH, i.e., in the last portion of TALH. Recent studies have shown that these variants exhibit clear differences in functional properties. The affinity profile for the three cotransported ions is B > A > F and transport capacity is A > B = F.[29, 30] Thus, the lower

affinity transporter F is located at the beginning of the TALH where ions are highly concentrated, and the higher affinity isoform B is located in the cortical TALH where tubular fluid has been diluted. This splicing mechanism seems to be the reason for TALH dilution power.

In addition to the alternative splicing of the three mutually exclusive cassette exons A, B, and F, there is another splicing mechanism that occurs in murine BSC1/NKCC2 which utilizes a poly-adenylation site in the intron between coding exons 16 and 17, predicting a protein with a shorter carboxyl-terminal domain.[31] The longer isoform that we have named BSC1-L (long) exhibits a carboxyl-terminus of 457 amino acid residues from which the last 383 are not present in the shorter isoform, named as BSC1-S (short). In contrast, the truncated isoform exhibits a carboxyl-terminus of 129 residues from which the last 55 are not present in BSC1-L.[31]Immunohistochemical analysis demonstrated that BSC1-L and BSC1-S are expressed toward the apical membrane of the TALH. Because the two splicing mechanisms can be combined, six isoforms are expressed in the mouse kidney: BSC1-L(A, B or F) and BSC1-S(A, B or F), respectively.

As shown above, studies using *X. laevis* oocytes as a heterologous expression system have shown that the longer isoforms BSC1-L A, B and F encode the Na^+-K^+-$2Cl^-$ cotransporter[18, 32] with distinct kinetic properties.[29] In contrast, the shorter isoform BSC1-S encodes a furosemide and bumetanide-sensitive, K^+-independent, Na^+-Cl^- cotransporter.[33] This transport pathway is not functional in regular isotonic media but is activated when oocytes are exposed to hypotonicity. In addition, activity of BSC1-S is inhibited by cAMP. The existence in the mouse kidney of a long isoform encoding Na^+-K^+-$2Cl^-$ and a short isoform performing as a Na^+-Cl^- cotransporter is relevant since it has been shown that two distinct Na-coupled Cl^- cotransporter systems are functional in the mouse TALH.[34] In this place, vasopressin modulates the NaCl transport pathway. In the absence of this hormone, NaCl is transported through a K^+-independent, furosemide-sensitive Na^+-Cl^- cotransporer, whereas its presence (increase in cAMP) switches the NaCl transport mode to a fuorsemide-sensitive Na^+-K^+-$2Cl^-$ cotransporter.[34] Supporting these observations, Haas et al.[35] identified in mouse kidney two different bumetanide-binding sites corresponding to proteins of 75 and 150 kDa that could correspond to BSC1-S and BSC1-L, respectively. A similar regulatory mechanism that exhibits a furosemide-sensitive Na^+-Cl^- cotransporter switched to a Na^+-K^+-$2Cl^-$ class by hypertonicity also occurs in rabbit TALH.[36]

Based on previous observations, we have suggested that, depending on the prevalent stimuli, there are two models of operation of the TALH.[33] As shown in Figure 2, one model operates during water conservation, a situation in which renal medulla osmolarity is high and vasopressin is present (high cAMP). In these conditions, salt enters the TALH through the Na^+-K^+-$2Cl^-$ cotransporter encoded by BSC1-L. Since the apical membrane of the TALH is impermeable to water, intense reabsorption of salt dilutes the tubular fluid and concentrates the medullary interstitium. In contrast, during maximal water diuresis, wherein medullary tonicity washout provides a relatively hypotonic environment and the vasopressin secretion rate is low (low cAMP), the Na^+ transport pathway of the apical membrane would be by the Na^+-Cl^- cotransporter encoded by BSC1-S. In this regard, cells take up water due to their high content of osmotically active substances when interstitial solute concentration decreases in renal medulla.[37, 38] Thus, it is possible that under these circumstances, TALH cells swell and the salt transport pathway in the apical membranes operates as a Na^+-Cl^- rather than a Na^+-K^+-$2Cl^-$ cotransporter. This switching in the transport mode, together with the known activation of the K^+-Cl^-

cotransporter and K^+ or Cl^- conductances in the basolateral membrane,[39] allows regulation of cell volume in TALH cells without completely halting salt reabsorption.

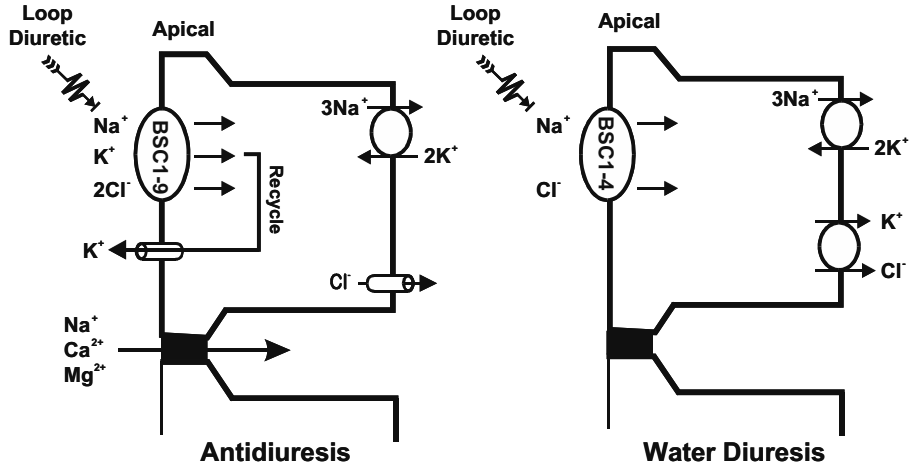

Figure 2. Proposed model for murine TALH function.[33]

5.2. Regulatory Properties of BSC1-S Isoform

Increasing net NaCl reabsorption in the TALH by hormones that generate cAMP, e.g., cathecolamines, calcitonin, parathyroid hormone and vasopressin, is an essential mechanism that regulates salt transport in this nephron segment.[40] Studies by Molony et al.[41] suggested that vasopressin directly activates the apical Na^+-K^+-$2Cl^-$ cotransporter in mouse TALH. The mechanism, however, has not been elucidated. In this regard, an emerging field of regulation of several membrane transporters appears to involve the generation of alternative splicing variants possessing regulatory properties.[8] These mechanisms seem to be implicated in the regulation of renal Na^+-K^+-$2Cl^-$ cotransporter by cAMP.

In our initial experiments about regulation of BSC1-L, we observed that activation of PKA with cAMP/IBMX had no effect upon the $^{22}Na^+$ uptake in BSC1-L cRNA injected oocytes, suggesting other factors could be required to reconstitute the observed cAMP activation of apical Na^+-K^+-$2Cl^-$ cotransport in murine TALH.[32] We observed that the truncated isoform BSC1-S exerts a clearly dominant-negative effect upon the BSC1-L Na^+-K^+-$2Cl^-$ cotransporter activity. Competition for translation in BSC1-L + BSC1-S co-injected *X. laevis* oocytes did not account for reduced Na^+-K^+-$2Cl^-$ cotransporter activity, because co-injecting BSC1-L with unrelated cRNAs did not significantly reduce the uptake.[32]

Interestingly, the negative effect of BSC1-S upon Na^+-K^+-$2Cl^-$ cotransporter activity can be abrogated by PKA activation with cAMP/IBMX.[33] Thus, it is possible that BSC1-L and BSC1-S interaction is critical for activation of the Na^+-K^+-$2Cl^-$ cotransporter

by cAMP. For this reason, in order to understand the interaction between BSC1-S and BSC1-L of the murine *SLC12A1* gene, we assessed the surface expression of BSC1-L in *X. laevis* oocytes alone or in the presence of BSC1-S, using a construct in which BSC1-L was tagged with EGFP into the amino-terminal domain.[42] As shown in Figure 3, the fluorescence intensity on the EGFP-BSC1-L construct in the oocyte plasma membrane was assessed by using a laser scanning confocal microscope. Results revealed that surface expression of the EGFP-BSC1-L isoform did not change in the presence of cAMP/IBMX. In contrast, when co-injected, the BSC1-S isoform induced a significant reduction in the surface expression of the BSC1-L cotransporter (EGFP-BSC1-L vs. EGFP-BSC1-L+BSC1-S in Figure 3). Reduction of EGFP-BSC1-L surface expression induced by co-injection with BSC1-S was abrogated after PKA activation by cAMP/IBMX in the extracellular medium (EGFP-BSC1-L+BSC1-S+cAMP/IBMX in Figure 3) and was associated with an increased activity of the cotransporter.[42] In addition, the cAMP/IBMX positive effect in surface and functional expression was prevented by the inhibitor of the exocytosis machinery, colchicine. Thus, it is likely that the presence of the BSC1-S isoform precludes the BSC1-L complex migration to the plasma membrane. This BSC1-S negative effect is inhibited by cAMP and because colchicine prevented the cAMP effect, a submembrane vesicle exocytosis is probably involved. Interestingly, expression of BSC1-S in TALH is axially distributed, because cortical TALH express less BSC1-S than outer medullary segments.[31] This heterogeneity in BSC1-S expression along the TALH may underlie the observation in mouse that vasopressin increased the salt reabsorption in medullary rather than cortical TALH.[43]

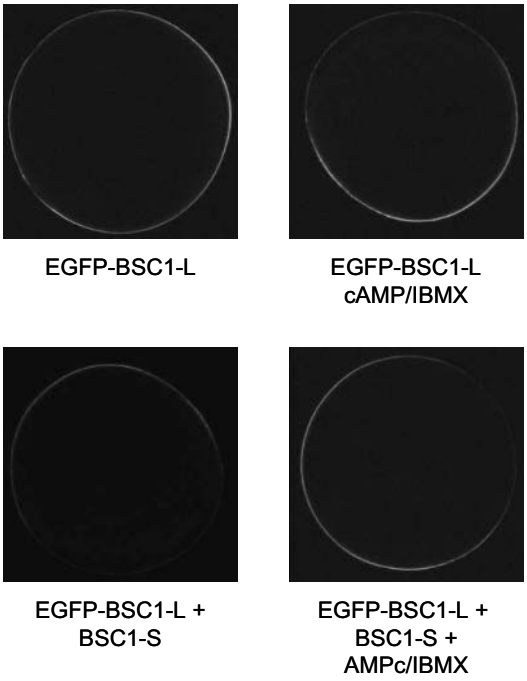

Figure 3. Confocal image analysis depicting plasma membrane fluorescence in *X. laevis* oocytes injected with EGFP-BSC1-L cRNA, alone or together with BSC1-S cRNA, and the effect of cAMP/IBMX (as stated).

A recent study has addressed the mechanisms underling the vasopressin-induced activation of the BSC1/NKCC2 cotransporter in mouse kidney *in vivo*.[44] After treatment of the animals with a single dose of the vasopressin analogue dAVP, renal proteins were studied with a panel of anti-BSC1/NKCC2 specific antibodies. Two monoclonal antibodies (T9 and T4) were used that recognize BSC1/NKCC2 with or without phosphorylation and a phosphospecific antibody (R5) that recognizes BSC1/NKCC2 when phosphorylated in a particular region of the amino-terminal domain. The results revealed that dAVP in mouse stimulated BSC1/NKCC2 phosphorylation. Immunohistochemical and electron microscopy analysis showed that non-phosphorylated BSC1/NKCC2 protein (immunostained with T9 antibody) was abundant in the cytoplasm, while the phosphorylated cotransporter (immunostained with R5 antibody) mainly appeared as a sharp line in the apical membrane of TALH cells. These observations suggest that phosphorylation of Na^+-K^+-$2Cl^-$ via vasopressin-cAMP increases cotransporter traffic to the cell membrane and support our conclusions in EGFP-BSC1-L and BSC1-S co-injected oocytes.

6. ACKNOWLEDGMENTS

We thank the support of the Mexican Council of Science and Technology (CONACYT) grants No.36124 and G34511M, the NIH grant No. DK36803 and The Wellcome Trust grant No. GR070159MA to GG.

7. REFERENCES

1. S.C. Hebert, D.B. Mount, & G. Gamba, Molecular physiology of cation-coupled Cl(-) cotransport: the SLC12 family, *Pflugers Arch.* **447**, 580-593 (2004).
2. G Gamba, S.N. Saltzberg, M Lombardi, A. Miyanoshita, J Lytton, M.A. Hediger, B.M. Brenner and S.C. Hebert, Primary structure and functional expression of a cDNA encoding the thiazide-sensitive, electroneutral sodium-chloride cotransporter, *Proc. Natl. Acad. Sci. USA* **90**, 2749-2753 (1993).
3. J.C. Xu, C. Lytle, T.T. Zhu, J.A. Payne, Jr. E. Benz and B. Forbush, Molecular cloning and functional expression of the bumetanide-sensitive Na-K-Cl cotransporter, *Proc. Natl. Acad. Sci. USA* **91**, 2201-2205 (1994).
4. P. K. Lauf, Thiol-dependent passive K/Cl transport in sheep red cells: IV. Furosemide inhibition as a function of external Rb+, Na+, and Cl-, *J Membr. Biol.* **77**, 57-62 (1984).
5. Gamba, G, Electroneutral chloride-coupled co-transporters, *Curr. Opin. Nephrol. Hypertens.* **9**, 535-540 (2000).
6. G. Gamba, Molecular biology of distal nephron sodium transport mechanisms, *Kidney Int.* 56, 1606-1622 (1999).
7. D.B. Mount and G. Gamba, Renal potassium-chloride cotransporters, *Curr. Opin. Nephrol. Hypertens.* **10**, 685-691 (2001).
8. G. Gamba, Alternative splicing and diversity of renal transporters, *Am J Physiol Renal Physiol* **281**, F781-F794 (2001).
9. T. Gerelsaikhan and R.J. Turner, Transmembrane topology of the secretory Na^+-K^+-$2Cl^-$ cotransporter (NKCC1) studied by in vitro translation, *J Biol. Chem.* **275**, 40471-40477 (2000).
10. P.G. Starremans, F.F. Kersten, L.P. van den Heuvel, N.V. Knoers, and R.J. Bindels, Dimeric architecture of the human bumetanide-sensitive Na-K-Cl Co-transporter, *J. Am. Soc. Nephrol.* **14**, 3039-3046 (2003).
11. J.C. De Jong, P.H. Willems, F.J. Mooren, L.P. van den Heuvel, N.V. Knoers, and R.J. Bindels, The structural unit of the thiazide-sensitive NaCl cotransporter is a homodimer, *J. Biol. Chem.* **278**, 24302-24307 (2003).
12. I. Kurtz, Molecular pathogenesis of Bartter's and Gitelman's syndromes, *Kidney Int.* **54**, 1396-1410 (1998).

13. E. Delpire, and D.B Mount Human and murine phenotypes associated with defects in cation-chloride cotransport, *Annu. Rev. Physiol* **64**, 803-843 (2002).
14. H. Mayan, I. Vered, M. Mouallem, M. Tzadok-Witkon, R. Pauzner, and Z. Farfel, Pseudohypoaldosteronism type II: marked sensitivity to thiazides, hypercalciuria, normomagnesemia, and low bone mineral density, *J. Clin. Endocrinol. Metab* **87**, 3248-3254 (2002).
15. F.H. Wilson, S. Disse-Nicodeme, K.A. Choate, K. Ishikawa, C. Nelson-Williams, I. Desitter, M. Gunel, D.V. Milford, G.W. Lipkin, J.M. Achard, Human hypertension caused by mutations in WNK kinases, *Science* **293**, 1107-1112 (2001).
16. F.H. Wilson, K.T. Kahle, E. Sabath, M.D. Lalioti, A.K. Rapson, R.S. Hoover, S.C. Hebert, G. Gamba, and R.P. Lifton, Molecular pathogenesis of inherited hypertension with hyperkalemia: The Na-Cl cotransporter is inhibited by wild-type but not mutant WNK4, *Proc. Natl. Acad. Sci. U. S. A* **100**, 680-684 (2003).
17. C.L. Yang, J. Angell, R. Mitchell, and D.H. Ellison, WNK kinases regulate thiazide-sensitive Na-Cl cotransport, *J. Clin. Invest* **111**, 1039-1045 (2003).
18. G. Gamba, A. Miyanoshita, M. Lombardi, J. Lytton, W.S. Lee, M.A. Hediger and S.C. Hebert, Molecular cloning, primary structure and characterization of two members of the mammalian electroneutral sodium-(potassium)-chloride cotransporter family expressed in kidney, *J. Biol. Chem.* **269**, 17713-17722 (1994).
19. A. Monroy, C. Plata, S.C. Hebert, and G. Gamba, Characterization of the thiazide-sensitive Na^+-Cl^- cotransporter: a new model for ions and diuretics interaction, *Am. J. Physiol. Renal Physiol.* **279**, F161-F169 (2000).
20. N. Vazquez, A. Monroy, E. Dorantes, R.A. Munoz-Clares, and Gamba, G, Functional differences between flounder and rat thiazide-sensitive Na- Cl cotransporter, *Am. J. Physiol. Renal Physiol.* **282**, F599-F607 (2002).
21. R.S. Hoover, E. Poch, A. Monroy, N. Vazquez, T. Nishio, G. Gamba and S.C. Hebert, N-Glycosylation at Two Sites Critically Alters Thiazide Binding and Activity of the Rat Thiazide-sensitive Na^+-Cl^- Cotransporter, *J. Am. Soc. Nephrol.* **14**, 271-282 (2003).
22. E. Moreno, C. Tovar-Palacio, P. De los Heros, B. Guzman, N.A. Bobadilla, N. Vazquez, D. Riccardi, E. Poch and G. Gamba, A single nucleotide polymorphism alters the activity of the renal Na+-Cl- cotransporter and reveals a role for transmembrane segment 4 in chloride and thiazide affinity, *J. Biol. Chem.* **279** 16553-16560 (2004).
23. S. Kunchaparty, M. Palcso, J. Berkman, H Vazquez, G.V. Desir, P. Bernstein, R.F. Reilly and D.H. Ellison, Defective processing and expression of thiazide-sensitive Na-Cl cotransporter as a cause of Gitelman's syndrome, *Am. J. Physiol.* **277**, F643-F649 (1999).
24. J. C. De Jong, W. A. Van Der Vliet, L. P. van den Heuvel, P. H. Willems, N. V. Knoers, and R.J. Bindels, Functional Expression of Mutations in the Human NaCl Cotransporter: Evidence for Impaired Routing Mechanisms in Gitelman's Syndrome, *J Am Soc. Nephrol.* **13**, 1442-1448 (2002).
25. S. Sabath, P. Meade, J. Berkman, P. de los Heros, E. Moreno, N. A. Bobadilla, N. Vazquez, D.H. Ellison and G. Gamba, Pathophysiology of Functional Mutations of the Thiazide-sensitive Na-Cl Cotransporter in Gitelman Disease. Journal of the American Society of Nephrology. Characterization of functional mutations in Gitelman's disease, *Am. J. Physiol. (Renal Physiol.)* (April 6, 2004). 10.1152/ajprenal.00044.2004.
26. J.A. Payne and B. Forbush Alternatively spliced isoforms of the putative renal Na-K-Cl cotransporter are differentially distributed within the rabbit kidney, *Proc. Natl. Acad. Sci. USA* **91**, 4544-4548 (1994).
27. P. Igarashi, G.B. Vanden Heuver, J.A. Payne and B. Forbush, Cloning, embryonic expression, and alternative splicing of a murine kidney-specific Na-K-Cl cotransporter, *Am. J. Physiol. (Renal Fluid Electrolyte Physiol.)* **269**, F406-F418 (1995).
28. T. Yang, Y.G. Huang, I. Singh, J. Schnermann and J.P. Briggs, Localization of bumetanide- and thiazide-sensitive Na-K-Cl cotransporters along the rat nephron, *Am. J. Physiol. (Renal Fluid Electrolyte Physiol.)* **271**, F931-F939 (1996).
29. C. Plata, P. Meade, N. Vazquez, S.C. Hebert and G. Gamba, Functional properties of the apical Na+-K+-2Cl- cotransporter isoforms, *J Biol. Chem.* **277**, 11004-11012 (2002).
30. I. Gimenez, P. Isenring and B. Forbush, Spatially distributed alternative splice variants of the renal Na-K-Cl cotransporter exhibit dramatically different affinities for the transported ions, *J Biol. Chem.* **277**, 8767-8770 (2002).

31. D.B. Mount A. Baekgard, A.E. Hall, C. Plata, J. Xu, D.R. Beier, G. Gamba and S.C. Hebert, Isoforms of the Na-K-2Cl transporter in murine TAL I. Molecular characterization and intrarenal localization, *Am. J. Physiol. Renal Physiol.* **276**, F347-F358 (1999).
32. C. Plata, D.B. Mount, V. Rubio, S.C. Hebert and G. Gamba, Isoforms of the Na-K-2Cl cotransporter in murine TAL. II. Functional characterization and activation by cAMP, *Am. J. Physiol.(Renal Physiol.)* **276**, F359-F366 (1999).
33. C. Plata, P. Meade, A.E. Hall, R.C. Welch, N. Vazquez, S.C. Hebert, and Gamba, Alternatively spliced isoform of the apical Na-K-Cl cotransporter gene encodes a furosemide sensitive Na-Cl cotransporter, *Am. J. Physiol. (Renal Physiol.)* **280**, F574-F582 (2001).
34. A. Sun, E.B. Grossman, M. Lombardi and S.C. Hebert, Vasopressin alters the mechanism of apical Cl^- entry from Na^+-Cl^- to Na^+-K^+-2Cl^- cotransport in mouse medullary thick ascending limb, *J. Membrane Biol.* **120**, 83-94 (1991).
35. M. Haas, P.B. Dunham and B. Forbush, [^{3}H]Bumetanide binding to mouse kidney membranes: Identification of corresponding membrane proteins, *Am. J. Physiol (Cell Physiol)* **260**, C791-C804 (1991).
36. J. Eveloff and J. Calamia, Effect of osmolarity on cation fluxes in medullary thick ascending limb cells, *Am. J. Physiol.(Renal Physiol.)* **250**, F176-F180 (1986).
37. F. Beck, A. Dörge , R. Rick and K Thurau, Osmoregulation of renal papillary cells, *Pflugers Arch.* **405**, S28-S32 (1985).
38. F.X. Beck, W.G. Guder and M. Schmolke, Cellular osmoregulation in kidney medulla, in *Cell Volume Regulation*, ed. Lang F (Karger, Basel), pp. 169-184 (1998).
39. A. Di Stefano, R. Greger, E. Desfleurs, C. de Rouffignac and M. Wittner, A Ba^{2+}-insensitive K^+ conductance in the basolateral membrane of rabbit cortical thick ascending limb cells, *Cell Physiol. Biochem.* **8**, 89-105 (1998).
40. S.C. Hebert, R.M. Culpepper and T.E. Andreoli, NaCl transport in mouse medullary thick ascending limbs. II. ADH enhancement of transcellular NaCl cotrasport; origin of transepithelial volatge, *Am. J. Physiol. (Renal Fluid Electrolyte Physiol.)* **241**, F432-F442 (1981).
41. D.A. Molony, W.B. Reeves, S.C. Hebert and T. Andreoli, ADH increases apical Na^+,K^+,2Cl^- entry in mouse medullary thick ascending limbs of Henle, *Am. J. Physiol. (Renal Physiol.)* **252**, F177-F187 (1987).
42. P. Meade, R. Hoover, C. Plata, N. Vazquez, N.A. Bobadilla, G. Gamba, and S.C. Hebert, cAMP-dependent activation of the renal-specific Na+-K+-2Cl- cotransporter is mediated by regulation of cotransporter trafficking, *Am. J. Physiol (Renal Physiol.)* **284**, F1145-F1154 (2003).
43. S.C. Hebert, R.M. Culpepper and T.E. Andreoli, NaCl transport in mouse medullary thick ascending limbs. I. Functional nephron heterogeneity and ADH-stimulated NaCl cotransport, *Am. J. Physiol. (Renal Physiol.)* **241**, F412-F431 (1981).
44. I. Gimenez and B Forbush, Short-term stimulation of the renal Na-K-Cl cotransporter (NKCC2) by vasopressin involves phosphorylation and membrane translocation of the protein, *J. Biol. Chem.* **278**, 26946-26951 (2003).

6

THE ROLE OF THE BLOOD-BRAIN BARRIER Na-K-2Cl COTRANSPORTER IN STROKE

Martha E. O'Donnell, Tina I. Lam, Lien Tran and Steven E. Anderson*

1. INTRODUCTION

The blood-brain barrier (BBB), which is formed by endothelial cells of brain microvessels, is highly restrictive to passage of solutes and water between the blood and brain interstitium.[1] Electrolytes, nutrients and other solutes must cross the BBB via specific transporters. Among the many BBB functions critical to maintaining an appropriate neural environment is the regulation of brain interstitial fluid volume and composition. The BBB transports K from brain to blood when necessary to guard against elevation of brain extracellular [K]. The BBB is also known to secrete Na and Cl into the brain, producing up to 30% of brain interstitial fluid; the remainder is produced by the choroid plexus.[2, 3] As yet unknown, the ion transport mechanisms responsible are thought to involve luminal Na and Cl transporters coupled with the abluminally located Na/K ATPase.[1, 4] In ischemic stroke, this secretion of NaCl is significantly increased and associated with formation of cerebral edema, a major cause of brain damage in stroke.[5, 6] It has been shown that the BBB does not break down until four to six hours after the onset of ischemic stroke. Thus, the ischemia-induced hypersecretion of NaCl and edema formation occurs in the presence of an intact BBB.[5, 6] The BBB transporters that participate in this process have not yet been identified; although, previous studies suggest that a luminally located Na transporter is involved.[5-8] We have hypothesized that a Na-K-2Cl cotransporter in the luminal BBB membrane participates in secretion of brain interstitial fluid by working in conjunction with the abluminal Na/K ATPase and an abluminal Cl efflux pathway, e.g., a Cl channel. We have further hypothesized that during stroke, increased activity of the Na-K-2Cl cotransporter contributes to edema formation. These scenarios are depicted in Figure 1. During cerebral ischemia, astrocytes swell as they take up Na, Cl and water (cytotoxic edema). At the same time, as the BBB increases secretion of NaCl and water into the brain, it essentially facilitates or becomes permissive to the

* M.E. O'Donnell, T.I. Lam, L. Tran and S.E. Anderson, Department of Physiology and Membrane Biology, University of California, One Shields Ave., Davis, CA 95616

astrocyte swelling. In our model, factors present during cerebral ischemia, including hypoxia and vasopressin, stimulate activity of the BBB Na-K-2Cl cotransporter during early stages of stroke, promoting edema formation across the intact barrier. The following sections describe previous studies that led to this hypothesis and recent studies suggesting these events may indeed occur.

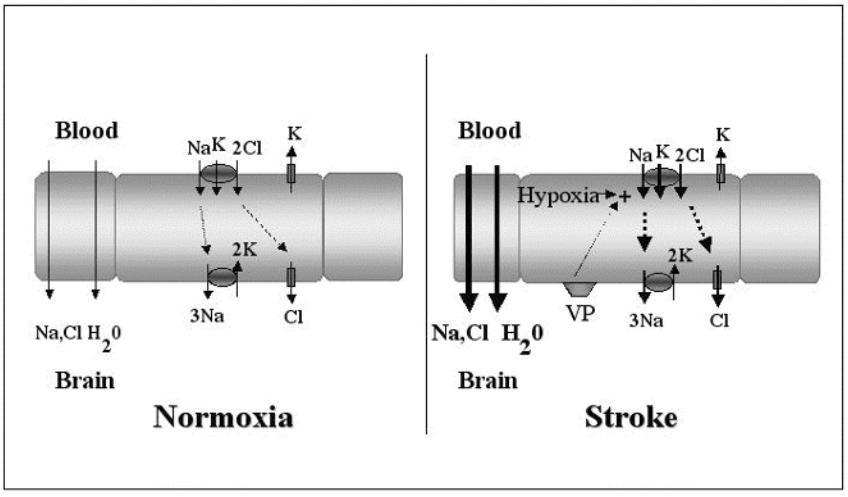

Figure 1. Hypothesized role of Na-K-2Cl cotransport in blood-brain barrier endothelial cells. The blood-brain barrier (BBB) secretes up to 30% of brain interstitial fluid under normoxic conditions via luminal and abluminal Na and Cl transporters. Our experimental findings suggest that a luminal Na-K-2Cl cotransporter may contribute to this process. During the early hours of ischemic stroke, secretion of brain interstitial fluid across an intact BBB is greatly increased. We have hypothesized that conditions present during cerebral ischemia cause stimulation of luminal Na-K-2Cl cotransport to increase transport of Na, Cl and water into the brain, contributing to edema formation.

2. Na-K-2Cl COTRANSPORT OF BLOOD-BRAIN BARRIER ENDOTHELIAL CELLS: STIMULATION BY FACTORS PRESENT DURING ISCHEMIA

Using cultured bovine cerebral microvascular endothelial cells, early studies in this laboratory demonstrated the presence of prominent Na-K-2Cl cotransporter activity, assessed as a Na- and Cl-dependent bumetanide-sensitive K influx (using ^{86}Rb as a tracer for K).[9, 10] In these studies, we also found that both Na-K-2Cl cotransporter activity and cotransporter protein are increased by exposure of the endothelial cells to either astrocyte conditioned medium (CM), C6 glial cell CM or to co-culture with C6 glial cell CM,[9-11] as shown in Table 1. This suggests that as in tight junctions, i.e., Na/K ATPase and other components upregulated by astrocytes, the Na-K-2Cl cotransporter is important in BBB function.

Our studies also revealed that the cotransporter is sensitive to regulation by a number of peptides.[9] Table 2 shows that vasopressin stimulates activity of the cotransporter, while atrial natriuretic peptide inhibits the cotransporter. The ionophore A23187 elevates intracellular [Ca] in these cells and also stimulates the cotransporter, while elevation of

cyclic AMP inhibits cotransport activity, consistent with vasopressin acting via a V_1 rather than a V_2 VP receptor. In addition, elevation of intracellular cyclic GMP inhibits the cotransporter, consistent with the known ANP-induced increase in cellular cyclic GMP.

Previous studies have shown that VP receptors are present on cerebral microvessels and that an increased release of VP occurs in the vicinity of the microvessels during ischemic stroke.[12-14] Ischemia-induced cerebral edema can be attenuated by VP antagonists in rats subjected to experimental ischemic stroke, while VP-deficient Brattelboro rats exhibit less cerebral edema during stroke.[15-17] Together, these findings suggest that edema formation involves VP actions at the BBB. They also support our hypothesis that during ischemia, VP stimulates BBB Na-K-2Cl cotransporter activity, thereby promoting edema formation. We and others have found evidence that the BBB Na-K-2Cl cotransporter is also stimulated by hypoxia which develops rapidly during cerebral ischemia. Oligomycin, which induces a form of chemical hypoxia and reduces cellular ATP levels, stimulates brain microvascular endothelial cell cotransporter activity within 30 minutes of exposure.[18-20] In addition, exposure of these cells to true hypoxia in an O_2-controlled glove box also rapidly stimulates the cotransporter.[21] These findings are consistent with previous reports that deoxygenation stimulates Na-K-2Cl cotransport activity of erythrocytes.[22-24] Finally, in other studies, the peptide endothelin-1, which is also increased during hypoxia, has been found to stimulate activity of the brain microvascular Na-K-2Cl cotransporter.[25] Collectively, these findings support our hypothesis that during ischemic stroke, hypoxia also acts to stimulate the BBB Na-K-2Cl cotransporter and promote cerebral edema formation.

Table 1. Astrocyte-induced increase in cerebral microvascular endothelial cell Na-K-2Cl cotransporter activity and protein

Condition	NKCC activity (% control K influx)[a]	NKCC protein (% control densitometry units)[a]
Control	100	100
C6 glial cell CM	161.24 ± 8.93	149.24 ± 10.05
Astrocyte CM	143.87 ± 13.54	153.28 ± 11.87
C6 Co-culture	184.67± 23.99	154.55 ± 1.39

[a] Values shown are means ± SE. NKCC, Na-K-2Cl cotransport. CM - conditioned medium. Cotransport activity was assessed as bumetanide-sensitive K influx. Control K influx in these experiments was 10.19 ± 0.78 μmol/gm protein · min. Na-K-2Cl cotransport protein levels were determined by Western blot analysis.

Table 2. Regulation of cerebral microvascular endothelial cell Na-K-2Cl cotransporter activity

Condition	Bumetanide-sensitive K influx[a] (% control flux)
Control	100
Vasopressin (100 nM)	190.42 ± 13.66
ANP (100 nM)	82.45 ± 5.12
A23187 (1 μM)	152.86 ± 12.68
8-Br-cAMP (10 μM)	60.81 ± 7.21
8-Br-cGMP (10 μM)	62.05 ± 4.89

[a] Values shown are means ± SE. Na-K-2Cl cotransport activity assessed as bumetanide-sensitive K influx. Control cotransport activity was 10.54 ± 0.32 μmol/gm protein · min.

3. CELLULAR LOCATION OF THE BLOOD-BRAIN BARRIER Na-K-2Cl COTRANSPORTER

Previous studies from this laboratory examined brain microvascular endothelial cells cultured on permeable filters for specific binding of ^{3}H-bumetanide, an index of the amount of cotransporter present. The studies revealed that approximately 90% of the binding was at the apical surface, suggesting that the BBB cotransporter may be asymmetrically distributed, residing predominantly at the luminal surface.[10] In recent studies,

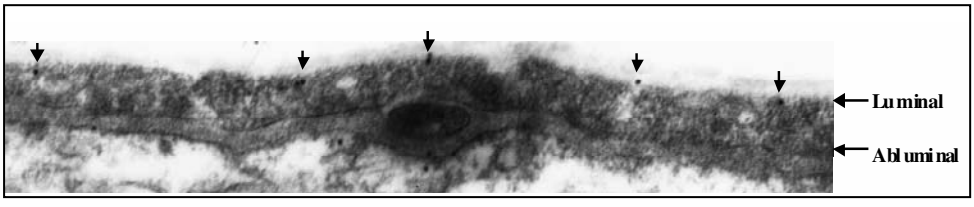

Figure 2. *In situ* distribution of blood-brain barrier (BBB) Na-K-2Cl cotransporter. Perfusion-fixed rat brains were thin-sectioned, then labeled with primary antibody that recognizes the Na-K-2Cl cotransporter protein (T4 monoclonal shown in this image) followed by 15 nm gold-particle-conjugated secondary antibody. Immuno-electron micrographs of the labeled images were then analyzed for distribution of gold particles between luminal and abluminal BBB endothelial membranes. In this micrograph, some gold particles can also be seen in astrocyte perivascular end feet lying below the basal lamina (gray homogenous band immediately below the BBB abluminal membrane).

we have employed immunoelectron microscopy and perfusion-fixed rat brains to examine the *in situ* cellular location of the BBB Na-K-2Cl cotransporter.[26] These studies used two different antibodies that specifically recognize the Na-K-2Cl cotransporter protein: T4, a monoclonal antibody, and T84, a polyclonal antibody, coupled with secondary antibodies conjugated to gold particles. A representative immunoelectron micrograph is shown in Figure 2. The majority of gold particles are seen at the luminal membrane of the BBB endothelial cells. In this image, the basal lamina appears as a homogenous band below the BBB and gold particles present in the astrocyte end feet cell membrane can also be seen. In these, we examined gold particle distribution between luminal and abluminal BBB membranes using a range of primary antibody dilutions as shown in Table 3. For both the T4 and the T84 antibodies, approximately 80% of the gold particles were found at the luminal membrane. Thus, the Na-K-2Cl cotransporter does indeed appear to reside predominantly in the luminal membrane of BBB endothelial cells.

Table 3. Relative luminal versus abluminal distribution of Na-K-2Cl cotransporter at the blood-brain barrier

Gold particle distribution Luminal/(Luminal + Abluminal) x 100[a]			
T4 antibody		T84 antibody	
Dilution		Dilution	
1:1000	82.63 ± 3.50	1:100	86.85 ± 6.67
1:2500	76.85 ± 8.31	1:5000	83.27 ± 3.21
1:7500	77.4 ± 5.73	1:7500	79.86 ± 8.08

[a] Values shown are means ± SE and were obtained by analyzing gold particle distribution between luminal and abluminal BBB membranes using micrographs from 6 or more micro-vessels for each dilution.

4. BUMETANIDE ATTENUATION OF ISCHEMIA-INDUCED CEREBRAL EDEMA AND BRAIN INFARCT

In recent studies, we have employed the rat middle cerebral artery occlusion (MCAO) model of stroke and magnetic resonance diffusion weighted imaging (DWI) to evaluate the effects of Na-K-2Cl cotransport inhibition on cerebral edema formation *in vivo*.[26] From these data, we calculated apparent diffusion coefficients (ADC). A drop in ADC values has been shown to provide a good index of edema formation in ischemic stroke. In these studies, we determined ADC values for different regions in both cortex and striatum and determined the ratios of ipsilateral (occluded) to contralateral (control non-occluded) ADC values for each animal. Figure 3 shows ADC ratios obtained for a region in the upper frontoparietal cortex of rats subjected to MCAO or Sham surgery. In

MCAO rats, the ipsilateral/contralateral ADC ratio falls below 1.0 indicating the presence of edema. However, in rats administered intravenous bumetanide (30 mg/kg) 20 minutes prior to MCAO, the drop in ADC ratio was significantly attenuated, indicating reduction of edema formation. This effect of bumetanide was sustained throughout the three-hour occlusion. At the end of these experiments, the rats were killed and the brains sectioned into 2-mm slices which were then evaluated for infarct by TTC staining (2,3,5-triphenyltetrazolium chloride from Sigma Aldrich Corp., St. Louis, MO). Figure 4 shows that in rats subjected to MCAO, a large infarct (seen as the pale region in the left hemisphere) is present. However, in rats subjected to MCAO and also intravenous bumetanide, the infarct is substantially reduced. The brain slices shown in this figure are 4, 6 and 8 mm from the frontal pole. In these studies, we quantitatively analyzed the total infarct volume in rats subjected to MCAO and either vehicle or three different doses of bumetanide. By our estimation, the lowest dose, 7.6 mg/kg, is equivalent to a blood concentration of 100 μM bumetanide. We found all three intravenous doses of bumetanide significantly reduced the total infarct volume induced by 180 minutes of MCAO. It should be noted that bumetanide and the chemically similar loop diuretics furosemide and torasemide distribute only in the extracellular fluid and do not readily cross plasma membranes.[27, 28] Also, a study of chemical properties determining the ability of various drugs to cross the BBB demonstrated that furosemide does not cross the barrier.[29] Thus, in our experimental setting, although bumetanide should readily distribute in extracellular fluid outside the brain, it should not penetrate into the brain in the presence of an intact BBB. Together, these findings suggest that in rats subjected to up to three hours of permanent MCAO during which time the BBB remains intact, intravenous bumetanide inhibits the luminal BBB Na-K-2Cl cotransporter with a resulting decrease in ischemia-induced cerebral edema and infarct volume.

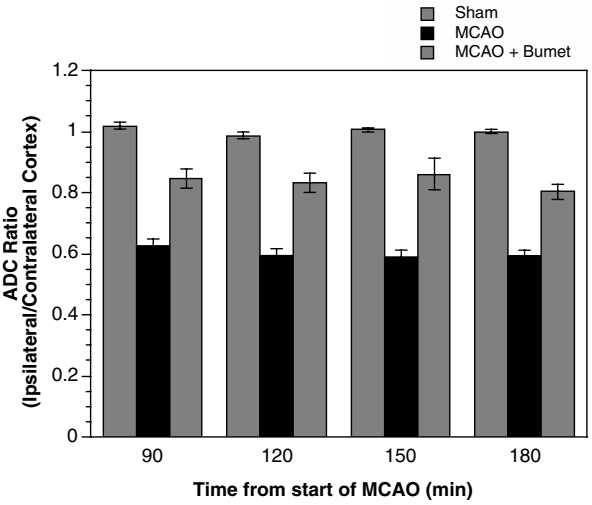

Figure 3. Bumetanide attenuation of cerebral edema formation in permanent middle cerebral artery occlusion (MCAO). ADC values were determined for the occluded (ipsilateral) and control, non-occluded (contralateral) cortex following induction of MCAO. Rats were given an intravenous injection of bumetanide (30 mg/kg) or vehicle 20 min prior to MCAO. Data shown are from the upper frontoparietal cortex and represent 4-9 animals for the three conditions.

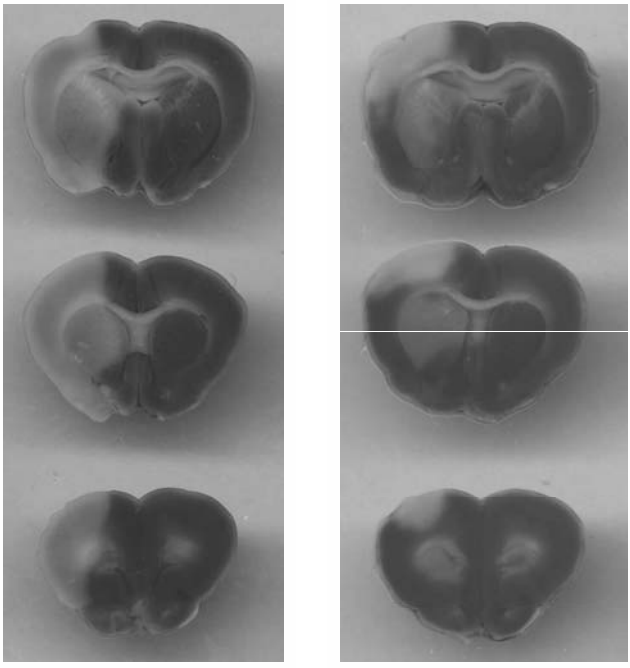

Figure 4. Bumetanide reduction of MCAO-induced brain infarct. Rats were treated with intravenous bumetanide (30 mg/kg) or vehicle for 20 minutes then subjected to 180 minutes of permanent middle cerebral artery occlusion. Brain slices (2 mm) were then stained with 2.3.5-triphenyltetrazolium chloride (TTC) to assess infarct size. Slices shown are 4, 6 and 8 mm from the frontal pole (bottom to top).

Table 4. Bumetanide reduction of cerebral infarct volume in rats subjected to MCAO

Bumetanide dose (mg/kg)	Percent total infarct[a]
0	39.36 ± 2.08
7.6	25.12 ± 2.21
15	20.35 ± 2.09
30	17.73 ± 1.36

[a] Values shown are means ± SE. Infarct sizes of TTC-stained brain slices were determined following 180 minutes of middle cerebral artery occlusion in rats treated intravenously with varying doses of bumetanide or vehicle. The total volume of the infarct was then calculated for each brain. Infarct volume is expressed as percent of total hemispheric volume.

5. SUMMARY

Studies from this and other laboratories have shown that the Na-K-2Cl cotransporter is present in BBB endothelial cells is stimulated by factors present during cerebral ischemia. Further, our *in situ* studies have shown that the cotransporter resides predominantly in the luminal BBB membrane. This is consistent with the hypothesis that a luminal cotransporter works with abluminal Na/K ATPase to secrete NaCl into the brain, and during stroke, BBB cotransporter activity is increased such that the barrier hypersecretes NaCl and water into the brain, facilitating cytotoxic edema formation. Our *in vivo* MCAO stroke studies provide further support for a role of the BBB cotransporter in cerebral ede-ma formation. Collectively, these findings suggest that the BBB Na-K-2Cl cotransporter does indeed substantially contribute to cerebral edema formation in stroke.

6. ACKNOWLEDGMENTS

This work was supported by an American Heart Association National Center Grant-in-Aid, National Institutes of Health NINDS NS039953 and an External Research Program Grant from Philip Morris USA, Inc.

7. REFERENCES

1. A. L. Betz and G. W. Goldstein, Specialized properties and solute transport in brain capillaries, *Ann. Rev. Physiol.* **48**, 421-250 (1986).
2. M. W. B. Bradbury, The structure and function of the blood-brain barrier, *Fed. Proc.* **43**,186-190 (1984).
3. H. F. Cserr, M. DePasquale, C. S. Patlak and R. G. L. Pullen, Convection of cerebral interstitial fluid and its role in brain volume regulation, *Ann. N. Y. Acad. Sci.* **481**, 123-134 (1989).
4. A. L. Betz, Sodium transport from blood to brain: Inhibition by furosemide and amiloride, *J. Neurochem.* **41**, 1158-1164 (1983).
5. G. P. Schielke, H. C. Moises and A. L. Betz, Blood to brain sodium transport and interstitial fluid potassium concentration during focal ischemia in the rat, *J. Cereb. Blood Flow Metab.***11**, 466-471 (1991).
6. S. A. Menzies, A. L. Betz and J. T. Hoff, Contributions of ions and albumin to the formation and resolution of ischemic brain edema, *J. Neurosurg.* **78**, 257-266 (1993).
7. A. L. Betz, R. F. Keep, M. E. Beer and X. Ren, Blood-brain barrier permeability and brain concentration of sodium, potassium, and chloride during focal ischemia, *J. Cereb. Blood Flow Metab.* **14**, 29-37 (1994).
8. H. K. Kimelberg, Current concepts of brain edema. Review of laboratory investigations, *J. Neurosurg.* **83**, 1051-1059 (1995).
9. M. E. O'Donnell, A. Martinez and D. Sun, Cerebral microvascular endothelial cell Na-K-Cl cotransport: Regulation by astrocyte-conditioned medium, *Am. J. Physiol Cell Physiol.* **268**, C747-C754 (1995).
10. D. Sun, C. Lytle and M. E. O'Donnell, Astroglial cell-induced expression of Na-K-Cl cotransporter in brain microvascular endothelial cells, *Am. J. Physiol. Cell Physiol.* **269**, C1506-C1512 (1995).
11. D. Sun, C. Lytle and M. E. O'Donnell, Il-6 secreted by astroglial cells regulates Na-K-Cl cotransport in brain microvessel endothelial cells, *Am J. Physiol. Cell Physiol.* **272**, C1829-C1835 (1997).
12. I. Jójárt, F. Joó, L. Siklós and F. A. László, Immunoelectronhistochemical evidence for innervation of brain microvessels by vasopressin-immunoreactive neurons in the rat, *Neurosci. Lett.* **51**, 259-264 (1984).
13. R. Landgraf, Central release of vasopressin: Stimuli, dynamics, consequences, *Prog.Brain Res.* **91**, 29-39 (1992).

14. P. S. Sorensen, A. Gjerris and M. Hammer, Cerebrospinal fluid vasopressin in neurological and psychiatric disorders, *J. Neurol. Neurosurg. Psych.* **48**, 50-57 (1985).
15. L. D. Dickinson and A. L. Betz, Attenuated development of ischemic brain edema in vasopressin-deficient rats, *J. Cereb. Blood Flow Metabl.* **12**, 681-690 (1992).
16. G. A. Rosenberg, E. Estrada and W. T. Kyner, Vasopressin-induced brain edema is mediated by the v1 receptor, *Adv. Neurol.* **52**, 149-154 (1990).
17. A. Shuaib, C. X. Wang, T. Yang and R. Noor, Effects of nonpeptide v1 vasopressin receptor antagonist sr-49059 on infarction volume and recovery of function in a focal embolic stroke model, *Stroke* **33**, 3033-3037 (2002).
18. M. E. O'Donnell, V. Duong and A. Martinez, Brain microvessel endothelial cell Na-K-Cl cotransport: Regulation by conditions of cerebral ischemia. *FASEB J.* **13**, A709 (1999).
19. N. Kawai, R. M. McCarron and M. Spatz, Effect of hypoxia on Na^+-K^+-Cl^- cotransport in cultured brain capillary endothelial cells of the rat, *J. Neurochem.* **66**, 2572-2579 (1996).
20. N. Kawai, R. M. McCarron and M. Spatz, Na^+-K^+-Cl^- cotransport system in brain capillary endothelial cells: Response to endothelin and hypoxia, *Neurochem. Res.* **21**, 1259-1266 (1996).
21. S. Fouroutan and M. E. O'Donnell, Hypoxia elevation of blood-brain barrier Na-K-Cl cotransporter and Na/K pump activities, *FASEB J.* **18**, A88, Late Breaking Abstracts (2004).
22. P. W. Flatman, Deoxygenation stimulates Na^+-K^+-$2Cl^-$ cotransport in ferret erythrocytes, *J. Physiol. (Lond.)* **531**, 122P-123P (2001).
23. P. W. Flatman, Regulation of Na-K-2Cl cotransport by phosphorylation and protein-protein interactions, *Biochim. Biophys. Acta* **1566**, 140-151 (2002).
24. M. C. Muzyamba, A. R. Cossins and J. S. Gibson, Regulation of Na-K-2Cl cotransport in turkey red cells: The role of oxygen tension and protein phosphorylation, *J. Physiol.* **517**, 2:421-429 (1999).
25. M. Spatz, K. N. Merkel, J. Bembry and R. M. McCarron, Functional properties of cultured endothelial cells derived from large microvessels of human brain, *Am. J. Physiol. Cell Physiol.* **272**, C231-C239 (1997).
26. M. O'Donnell, L. Tran, T. I. Lam, X. B. Liu and S. E. Anderson, Bumetanide inhibition of the blood-brain barrier Na-K-Cl cotransporter reduces edema formation in the rat middle cerebral artery occlusion model of stroke, *J. Cereb. Blood Flow Metab.* **24**, in press (2004).
27. B. P. Chen, Loop diuretics: Comparison of torasemide, furosemide, and bumetanide, *Drug information update: Hartford hospital* **60**, 343-354 (1996).
28. H. A. Friedel and M. M. T. Buckley, Torasemide: A review of its pharmacological properties and therapeutic potential, *Drug Eval.* **41**, 81-103 (1991).
29. H. Fischer, R. Gottschlich and A. Seelig, Blood-brain barrier permeation: Molecular parameters governing passive diffusion, *J. Memb. Biol.* **165**, 201-211 (1998).

7

REGULATION OF Na-K-2Cl COTRANSPORT IN RED CELLS

Peter W Flatman*

1. INTRODUCTION

Starting in the late 1950s, studies of K and Na transport in red cells were among the first to indicate that cell membranes contain the transporter we know today as the Na-K-2Cl cotransporter.[1] Since that time, red cells have been an important model system with which to study the properties and regulation of cotransport.[2] In addition to providing general insight into cotransporter function, studies on red cells indicate that the cotransporter can have very specific roles in these cells, enabling them to resolve particular physiological problems and challenges. Several excellent reviews[2-6] discuss the discovery, properties and regulation of the cotransporter. In this chapter, I shall give a brief outline of the behavior of the transporter in red cells and then focus on recent analyses of how changes in cotransporter phosphorylation may affect transport.

2. PROPERTIES OF THE COTRANSPORTER

The Na-K-2Cl cotransporter is member of the cation-chloride-cotransporter (CCC) superfamily.[7] It moves one Na, one K, and two Cl ions in the same direction across the cell membrane in an electroneutral fashion. Operation of the transporter does not, therefore, generate a current nor do changes in transmembrane potential affect cotransporter mediated fluxes.[8,9] The cotransporter can operate in either direction, moving ions into or out of cells depending on the chemical gradients of the participating ions.[10] When the transporter is at equilibrium, the quotient:

$$[Na^+]_o[K^+]_o[Cl^-]_o^2/[Na^+]_i[K^+]_i[Cl^-]_i^2$$

* Peter W Flatman, Membrane Biology Group, College of Medicine and Veterinary Medicine, The University of Edinburgh, Hugh Robson Building, George Square, Edinburgh EH8 9XD Scotland UK

is equal to 1. If the quotient is >1, activation of the transporter results in ions entering the cell, whereas if it is <1, they leave. For epithelia, this quotient is normally >>1, so activation of the cotransporter leads to influx of ions followed by osmotically obliged water and possible cell swelling. As turnover of the transporter is high (>1000 s^{-1}),[6, 11] and four osmotically active particles move in each cycle, the transporter has the potential to rapidly alter cell volume without changing membrane potential. Therefore, it is not surprising that it plays an important part in the regulatory volume increase seen in several cell types following osmotic shrinkage. In red cells, however, the cotransporter is close to equilibrium (Cl is at electrochemical equilibrium across the red cell membrane), and the direction of net transport depends more on the extracellular K concentration.[2]

In many cells types, the cotransporter plays important roles in regulating cell K and Cl concentration but has little effect on cell Na concentration because of the regulatory power of the Na-pump.[3] In red cells, the ability of the cotransporter to influence cell Cl content is also abrogated by the very high levels of the anion exchanger (AE1, Band 3). The red cell cotransporter appears mainly involved in K homeostasis. Experiments with human red cells show a negative correlation between the maximum rate of cotransport and cell K content, suggesting that the red cell transporter may be operating in efflux mode *in vivo.*[12] Recent studies in the rat suggest that the direction of cotransporter operation may change during red cell maturation from inward in young reticulocytes to outward in mature cells.[13] Thus, the transporter may help maintain the low volume of mature red cells. In ferret red cells which have a high rate of cotransport and a low K content, the cotransporter may also play a role in regulating plasma K concentration, the cells acting as a large source or sink for K depending on need. Such a role for the red cell cotransporter has, however, been ruled out in humans.[14]

The rate of cotransport varies widely in red cells from different species. Cotransporter-mediated fluxes are low in human red cells (<1 mmol (l cell h)$^{-1}$), being much smaller than fluxes through the Na-pump, and show little dependence on cell volume.[12, 15, 16] Meta-analysis of 20 studies of cotransport in humans shows that transport rates are lower in red cells from women and people with a family history of essential hypertension.[16] At the other extreme, fluxes through the noradrenaline-stimulated transporter in avian red cells can reach levels greater than 100 mmol (l cell h)$^{-1}$ and are activated by cell shrinkage.[2] In duck red cells, the Na-K-2Cl cotransporter, together with the closely related K-Cl cotransporter, has been shown to play a key role in regulating cell volume.[17] Cotransport rates in ferret red cells are also very high, about 16 mmol (l cell h)$^{-1}$ in resting cells and reaching about 50 mmol (l cell h)$^{-1}$ when maximally stimulated.[18-20] Cotransport is activated by cell shrinkage.[21] As these cells do not have operational Na-pumps, their K content is low (about 7 mM) so that unidirectional K uptake can be used as a measure of transport rate with little interference from K-K exchange that occurs in normal high K cells.[10, 22] Thus, these cells are an excellent model in which to study the mammalian cotransporter.

The cotransporter is characterized by its sensitivity to inhibition by loop diuretics with bumetanide being particularly potent (IC_{50} is about 50 – 100 nM in many red cells). Low doses (10 μM) of bumetanide can be used to selectively inhibit the transporter and define cotransporter-mediated fluxes.[3]

3. COTRANSPORTER REGULATION

In addition to being regulated by the concentration of substrate ions, cotransporter activity is stimulated by hypoxia,[23-25] growth factors,[26] hormones such as noradrenaline[27] and vasopressin,[28, 29] cell shrinkage (a powerful stimulant in epithelial cells and avian, but not human, red cells) and a fall in intracellular Cl concentration. The latter was found in epithelial cells where Cl appears to be acting at a site distinct from the substrate site. The fall in Cl concentration may activate a kinase that phosphorylates the cotransporter and stimulates transport.[30-32] This effect has not been demonstrated in red cells, where, if the pathway exists, it may need to be modified because of the high resting Cl level in these cells.

The ability of the cotransporter to respond to most of these signals is compromised when cells are treated with inhibitors of protein kinases or phosphatases. This suggests that changes in transport result from changes in protein phosphorylation (though the effects of some growth factors may be independent of changes in cotransporter phosphorylation[26]). As many of these signals have been shown to alter phosphorylation of the cotransporter itself, it has been suggested that cotransporter phosphorylation is a major common pathway in transporter regulation.[33-37] However, under certain circumstances, inhibitory signals from the cytoskeleton can prevent cotransporter phosphorylation causing transport stimulation.[4, 5, 38]

4. THE COTRANSPORTER IS PHOSPHORYLATED AT MULTIPLE SITES

During activation by diverse stimuli, the cotransporter is phosphorylated on five or six threonine and serine (but not tyrosine) residues.[33, 39] The phosphopeptide maps generated from the cotransporter stimulated by a variety of factors are very similar. Together with pharmacological data, this has been interpreted as showing the cotransporter is phosphorylated at multiple sites by a single kinase and dephosphorylated by a single phosphatase. Thus, regulation of cotransporter activity would revolve around the regulation of these two enzymes – the cotransporter kinase (CT-kinase, CT-K) and phosphatase (CT-phosphatase, CT-PrP).[4] Fitting in nicely with this idea is the finding that phosphorylation of three threonine residues close together in the N-terminus seems particularly important in regulating transport (Thr^{184}, Thr^{189}, Thr^{202} in the shark cotransporter).[40] Close to these residues is a binding site for protein phosphatase 1 (PrP-1) which appears ideally placed to dephosphorylate the transporter when circumstances demand.[41] Inhibitors of PrP-1 (calyculin A and okadaic acid) are potent activators of transport in a wide variety of cells as expected.[23, 39, 42] Evidence suggests that PrP-1 is a CT-phosphatase. However, the identity of the CT-kinase is uncertain. C-Jun kinase,[43] PASK[44, 45] (or SPAK, proline and alanine rich Ste20 related), and OSR1[44] (oxidative-stress related) kinase have all been suggested; although, compelling proof for any of these is lacking. SGK (serum and glucocorticoid activated kinase) has also been suggested, but this may activate the cotransporter by facilitating its insertion into the membrane.[46] A volume-sensitive kinase that autophosphorylates to enhance its activity may be involved.[2,47] Myosin light chain kinase clearly plays a role in the activation of the cotransporter by hypertonicity[38, 48] but is probably not a CT-kinase.

5. COTRANSPORT AND PHOSPHORYLATION IN FERRET RED CELLS

Our work aims to characterize and ultimately, identify the CT-kinase(s) and CT-phosphatase(s) in ferret red cells. Starting with the premise that the single kinase/single phosphatase model is correct, we predicted it should be possible to maximally activate the transporter by inhibiting the CT-phosphatase and completely inhibit it by inhibiting the CT-kinase.

As with other cells, 20-50 nM calyculin A rapidly and maximally activates the transporter in ferret red cells, consistent with the idea that PrP-1 plays an important role in dephosphorylating the cotransporter here.[20]

Next, it was necessary to establish that inhibition of the CT-kinase abolishes cotransport fluxes. As there are conflicting views on the identity of the CT-kinase, we decided to use a non-specific method for inhibiting kinases – the removal of intracellular Mg. This is based on the standard biochemical practice of adding excess EDTA to a biological extract to chelate Mg and inhibit all kinases therein. One of the benefits of using red cells is that we can achieve this with only a minor modification to the procedure. Intracellular Mg concentration can be reduced to sub-micromolar levels by incubating cells in a medium containing EDTA (usually 1-2 mM for cells suspended at 10% haematocrit) and then adding 5-10 μM A23187, an ionophore that permeabilizes the cell membrane to Mg. Within 5 minutes, virtually all Mg has left the cells, as determined by atomic absorption spectroscopy.[49] The presence of external EDTA alone has little effect on cotransport. However, following the addition of A23187, transport rate falls rapidly but by only about 40%, and this level is well maintained for the next hour.[50] This finding was unexpected. Had there been any residual CT-phosphatase activity, inhibition of all kinases should result in the complete, though possibly slow, inhibition of transport. Unless of course, the phosphatase is also inhibited by Mg-removal.

Then, ferret red cells were used to screen kinase inhibitors for their ability to inhibit transport, an approach limited by the membrane permeability of the inhibitors. Three substances were found to be particularly potent: staurosporine, PP1 (4-amino-5-(4-methylphenyl)-7-(t-butyl)pyrazolo[3,4-d]pyrimidine) and genistein.[20] However, as with Mg-removal, they only inhibited 40% of resting transport. Interestingly, all three of these compounds inhibit tyrosine kinases, yet changes in tyrosine phosphorylation of the cotransporter have not been observed to correlate with changes in transport rate.[33, 39, 51] PP1 is a very selective tyrosine kinase inhibitor (src kinases, c-kit and Bcr-Abl).[52, 53] Genistein also inhibits tyrosine kinases,[54] as does staurosporine which affects many threonine and serine kinases too.[55] In addition, the use of these inhibitors in combination with each other or with Mg-removal was no more effective than any treatment alone. It appears that these compounds act indirectly, and if such an entity exists, a potent inhibitor of the CT-kinase is still to be discovered.

The finding that Mg-removal and three different kinase inhibitors leave the same substantial amount of residual transport (about 60% resting level) suggests: 1) there are either two forms of the cotransporter, one in which transport is stimulated by phosphorylation and another which is constitutively active, or (2) Mg-removal and the different kinase inhibitors all trap the cotransporter in a partially phosphorylated, partially active state. To distinguish between these possibilities, we attempted to measure the extent of threonine phosphorylation of the transporter under different conditions. The cotransporter was immunoprecipitated from ferret red cells, treated with kinase or phosphatase inhibitors using the T4 monoclonal antibody developed to the C-terminus of the

human cotransporter.[56] Proteins in the immunoprecipitate were then separated by gel electrophoresis and probed with antibodies to phosphothreonine.[51]

The ferret red cell cotransporter runs on polyacyrlamide gels as a smear with an apparent molecular weight of 140-160 kDa (sometimes this appears as a clear doublet with bands centred at 140 and 160 kDa), probably corresponding to monomeric forms of the cotransporter. However, a substantial amount of the cotransporter appears in high molecular weight forms (300-320 kDa).[57] This may represent formation of dimers as found in studies of the cotransporter in parotid glands.[58] Some sharp bands are seen at intermediate weights and some very high molecular weight complexes (>400 kDa) are also apparent. All of these high molecular weight forms were seen despite the samples having been heated with SDS and reducing agents. Phosphothreonine is detected in these immunoprecipitates with molecular weights centered at about 150 and 300 kDa.[51] The proportion of cotransporter phosphorylated in the low molecular weight band is similar to the proportion in high molecular weight band for each condition tested, suggesting that phosphorylation of the cotransporter does not affect its propensity to form or dissociate from high molecular weight forms (Flatman & Matskevich, unpublished). It is clear from these experiments that the cotransporter is phosphorylated in both its low and high molecular weight forms in control cells and that treatment of cells with calyculin A almost doubles phosphothreonine in both bands. 1 mM Na arsenite, which stimulates transport to the same extent as calyculin,[59] more than doubles the amount of phosphothreonine in T4 immunoprecipitates. On the other hand, treatment of cells with PP1, genistein or staurosporine, or removal of Mg, all reduce, but do not abolish, the level of phosphothreonine to the same extent. Phosphothreonine levels in the cotransporter under these conditions are about 60% of those seen in control cells, consistent with the observed reduction in transport rate under the same conditions.[51] We did not find any conditions where the cotransporter was completely dephosphorylated. The findings are compatible with the idea that all these treatments trap the cotransporter in a partially phosphorylated, partially active form.

The appearance of the cotransporter in some western blots as a doublet (using the T4 antibody) is intriguing. Initially, we speculated there are two isoforms of the cotransporter in ferret red cells, one band representing a form in which transport is sensitive to phosphorylation and another representing a constitutively active form. These could arise from truncation or alternative splicing[60, 61] of the transporter that affects its ability to bind kinases and phosphatases, thus influencing its phosphorylation state. However, we have not been able to correlate the appearance of the doublet with transport rate or phosphorylation state.

We can learn much about the regulation of cotransport not only by examining the effects of kinase and phosphatase inhibitors on transport and phosphorylation when used alone but also by examining the effects of these agents when used in combination. We have shown that addition of PP1, genistein and staurosporine, or Mg-removal, before calyculin, prevent it from activating transport.[20] On the other hand, when added after calyculin, they cause only a small reduction (30%) in transport. Thus, kinase inhibition whether highly specific (PP1) or non-specific (Mg-removal) prevents but does not reverse stimulation by calyculin. In similar experiments, these same kinase inhibitors prevented but also reversed stimulation caused by arsenite.[59] Clearly, calyculin and arsenite affect different sites in the regulatory process. When used together, calyculin and arsenite give the most robust stimulation of transport, even in cells that have been stored for a few days, which greatly reduces the response to either of these agents alone.[59] Only

Mg-removal completely prevents stimulation by this combination. PP1 is completely ineffective, whereas genistein and staurosporine partially prevent stimulation. Neither Mg-removal nor any of these kinase inhibitors reverse stimulation caused by a combination of calyculin and arsenite.

Generally, transport rate and threonine phosphorylation of the cotransporter correlate well in controls and cells treated with calyculin, PP1, staurosporine, Mg-removal and combinations of these. However, under some conditions arsenite causes additional threonine phosphorylation of the cotransporter that does not correlate well with changes in transport rate.[51] Thus, threonine phosphorylation of the cotransporter does not always imply transport stimulation.

It is possible to explain these data by assuming that regulatory phosphorylation of the cotransporter is carried out by a single kinase and phosphatase.[59] However, construction of such a model puts severe limits on where the inhibitors work. For instance, calyculin cannot inhibit the CT-phosphatase, and PP1, genistein and staurosporine cannot inhibit the CT-kinase. It is necessary to postulate that the CT-phosphatase itself is regulated (inhibited) by phosphorylation and that calyculin inhibits the phosphatase that regulates this process, whereas PP1, staurosporine and genistein inhibit, indirectly, the kinase. The CT-phosphatase needs to be Mg-sensitive. This model explains the results described so far, e.g., the partial inhibition of transport by kinase inhibitors and the effects of combinations of calyculin, arsenite and kinase inhibitors. However, it does not account well for the observation that Mg-removal completely reverses stimulation caused by arsenite.

Further problems for the one kinase/one phosphatase model arise from experiments examining the effects of deoxygenation. Reduction of the oxygen tension in equilibrium with ferret red cell suspensions to 1-3 mm Hg for 30 minutes stimulates cotransport to the same extent as treating them with calyculin or arsenite.[25] The effect is quickly reversible on reoxygenation. Half maximal stimulation is seen with an oxygen tension of about 23 mm Hg. Stimulation by deoxygenation is completely prevented and reversed by kinase inhibitors or Mg-removal. On the surface, the actions of arsenite and deoxygenation appear similar and an attractive explanation for arsenite's effects is that it mimics deoxygenation. However, this is not the case. Stimulation by either arsenite or deoxygenation is reversed by PP1. It follows that if arsenite and deoxygenation affect the same processes, the combined effects of deoxygenation and arsenite should also be reversed by PP1. However, when this hypothesis was tested, it was found that PP1 had little, if any, effect on cotransport stimulated by this combination (Flatman, unpublished).

6. A MULTIPLE KINASE/PHOSPHATASE MODEL

It is difficult to incorporate these findings into the one kinase/one phosphatase model. In order to encompass all these data, it is necessary to abandon this model in favor of one that assumes regulatory phosphorylation of the cotransporter is carried out by several kinases and phosphatases.[36, 40, 62] Multiple kinase/phosphatase models can be complex, and there is a temptation to introduce new kinases and phosphatases to explain every quirk in the data. However, there is good evidence that the cotransporter is dephosphorylated by at least 3 phosphatases in ferret red cells:

- PrP-1 – inhibited by calyculin A (Once we abandon the one kinase/one phosphatase model, it is possible to propose that there is a site on the cotransporter that is dephosphorylated by PrP-1.),
- a phosphatase inhibited by Mg-removal, possibly PrP-2C (This would explain why Mg-removal does not inhibit all cotransport fluxes.), and
- a phosphatase that dephosphorylates the sites on the cotransporter that are phosphorylated when oxygen tension is reduced.

There are probably at least three distinct conjugate kinases involved in phosphorylating these sites.

A model that explains our data can be broken down into four sections that address the four major questions raised by our experiments. It proposes that phosphorylation of at least four sets of residues, not necessarily all threonine, is involved in regulating transport under the conditions described here. Phosphopeptide mapping using ^{32}P suggests that five or six threonine and serine residues become phosphorylated when the transporter is fully active in shark rectal gland and avian red cells.[33, 39] Also, our experiments with anti-phosphothreonine antibodies suggest that up to four threonine residues may be involved, assuming a single threonine residue is phosphorylated under Mg-free conditions (Flatman & Matskevich, unpublished). We find no changes in tyrosine phosphorylation, as determined by a variety of anti-phosphotyrosine antibodies, corresponding to changes in transport rate.[51]

First, it is necessary to explain why Mg-removal, PP1, staurosporine and genistein only partially inhibit cotransport and why residual transport activity is the same under all these conditions. These observations can be explained if there is a threonine residue (COT1 in Figure 1) on the cotransporter that is phosphorylated by a kinase (CT-K1) not inhibited by PP1, staurosporine or genistein. Most importantly, it is dephosphorylated by a Mg-sensitive phosphatase (CT-PrP1). This is probably a member of the protein phosphatase 2C family, PrP-2C[63] (PrP-7 is also Mg-dependent but has only been found in retina[64]) which is characterized by a requirement for millimolar Mg (or Mn) and its insensitivity to NaF, calyculin, okadaic acid and microcystin.[63, 64] Under normal circumstances, COT1 will be fully phosphorylated, and this maintains transport rate at 60% control. As we shall see later, none of the other regulatory sites should be phosphorylated in the presence of the kinase inhibitors or in the absence of Mg. In addition, as long as CT-PrP1 is more sensitive to Mg-removal than CT-K1 (generally PrP-2C requires much higher Mg levels for activity than kinases), COT1 should remain phosphorylated when cell Mg is reduced.

Second, it is necessary to account for the rapid maximal stimulation of transport by calyculin. This can be explained if there is another threonine residue (possibly two or three) on the cotransporter (COT2 in Figure 1) that is phosphorylated by a kinase (CT-K2) which is inhibited, indirectly by PP1, staurosporine and genistein. It is dephosphorylated by a calyculin-sensitive phosphatase (CT-PrP2), probably PrP-1. The very rapid activation of transport by calyculin suggests that the kinase is highly active in control cells and that this activity is revealed when the phosphatase is inhibited. Phosphorylation of COT2 maximally activates the transporter, about 2.5 fold. COT2 may correspond to Thr^{189} (and possibly the neighbouring threonine residues) in the shark cotransporter, the residue that plays a key role in regulating shark cotransporter activity.[40]

Phosphorylation of COT2 may also explain the stimulation of transport by arsenite. The simplest explanation is that arsenite stimulates kinase CT-K2 which would also

explain why the effects of arsenite are prevented and reversed by kinase inhibitors, and importantly, by Mg-removal.

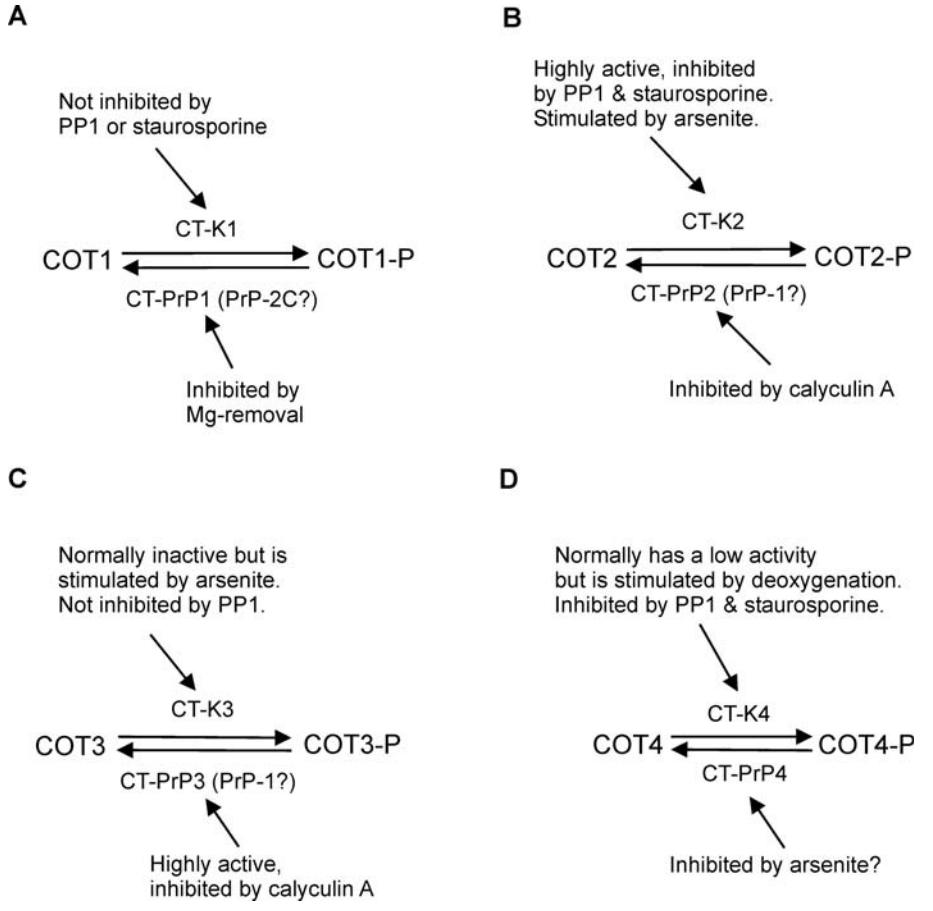

Figure 1. Transport rate is affected by phosphorylation of at least four sets of residues on the cotransporter. In this multiple kinase/phosphatase model of regulatory phosphorylation panel **A** depicts phosphorylation of a threonine residue that maintains transport (20% maximum) in the absence of Mg, panel **B** depicts phosphorylation of threonine residues that accounts for the maximal stimulation of transport by calyculin or arsenite when used alone, and panel **C** represents the PP1-resistant phosphorylation of residues by the combination of calyculin with arsenite that maximally stimulates transport. Panel **D** represents phosphorylation of residues caused by a fall in oxygen tension. This can also maximally stimulate transport.

Third, it is necessary to explain why PP1 does not prevent stimulation of transport by the combined effects of calyculin and arsenite. It is proposed that at least one additional site (COT3 in Figure 1) exists that causes maximal activation of transport when phosphorylated. COT3 is dephosphorylated by a highly active, calyculin-sensitive phosphatase (CT-PrP3, also PrP-1?). Under normal conditions, the conjugate kinase (CT-K3) is either inactive or only slightly active. It is stimulated by arsenite but is not inhibited by PP1. It may be weakly inhibited by staurosporine and genistein.[59] Thus, COT3 is not

normally phosphorylated. Addition of arsenite alone will activate the kinase but not enough to significantly increase phosphorylation because of the highly active phosphatase. Addition of calyculin alone will inhibit the phosphatase, but the very low kinase activity again produces little, if any, phosphorylation. Phosphorylation by this route may explain the small amount of transport stimulation seen when calyculin is added after PP1.[20] However, when both arsenite and calyculin are added, COT3 is quickly phosphorylated and transport is maximally stimulated.

Finally, it is necessary to explain the stimulation of transport by deoxygenation. In order to do this, we propose the existence of a site (COT4 in Figure 1) that is phosphorylated by a kinase (CT-K4) which is activated by deoxygenation. The kinase has a low activity when the oxygen tension is high and is inhibited by PP1, staurosporine and genistein. COT4 is dephosphorylated by a phosphatase (CT-PrP4) that does not require Mg and is not inhibited by calyculin. On the other hand, inhibition of this phosphatase by arsenite would explain why stimulation caused by a combination of arsenite and deoxygenation is not reversed by PP1.

7. CONCLUSION

Different stimuli regulate phosphorylation of the cotransporter by activating or inhibiting distinct sets of cotransporter kinases and phosphatases, resulting in distinct patterns of phosphorylation. Phosphorylation of these sites may have a profound direct effect on transport rate, but this is not always the case. Phosphorylation may also determine how the transporter interacts with other regulatory proteins, perhaps helping the cell to integrate cotransporter activity in response to different, possibly conflicting, stimuli.

8. ACKNOWLEDGMENTS

Thanks to: Drs Jim Creanor and Iuolia Matskevich for their work on the projects, Mrs Catriona Armstrong for editorial assistance and the Wellcome Trust for funds.

9. REFERENCES

1. J. S. Wiley and R. A. Cooper, A furosemide-sensitive cotransport of sodium plus potassium in the human red cell, *J. Clin. Invest.* **53**, 745-755 (1974).
2. C. Lytle, in: *Red Cell Membrane Transport in Health and Disease*, edited by I. Bernhardt and J. C. Ellory (Springer, Berlin, 2003), 173-195.
3. J. M. Russell, Sodium-potassium-chloride cotransport, *Physiol. Rev.* **80**, 211-276 (2000).
4. M. Haas and B. Forbush, III, The Na-K-Cl cotransporter of secretory epithelia, *Annu. Rev. Physiol.* **62**, 515-534 (2000).
5. M. Haas, The Na-K-Cl cotransporters, *Am. J. Physiol.* **267**, C869-C885 (1994).
6. M. Haas, Properties and diversity of (Na-K-Cl) cotransporters, *Annu. Rev. Physiol.* **51**, 443-457 (1989).
7. E. Delpire and D. B. Mount, Human and murine phenotypes associated with defects in cation-chloride cotransport, *Annu. Rev. Physiol.* **64**, 803-843 (2002).
8. P. Geck, C. Pietrzyk, B.-C. Burckhardt, B. Pfeiffer, and E. Heinz, Electrically silent cotransport of Na^+, K^+ and Cl^- in Ehrlich cells, *Biochim. Biophys. Acta* **600**, 432-447 (1980).

9. M. Haas, W. F. Schmidt, III, and T. J. McManus, Catecholamine-stimulated ion transport in duck red cells. Gradient effects in electrically neutral [Na+K+2Cl] co-transport, *J. Gen. Physiol.* **80**, 125-147 (1982).
10. C. Lytle, T. J. McManus, and M. Haas, A model of Na-K-2Cl cotransport based on ordered ion binding and glide symmetry, *Am. J. Physiol.* **274**, C299-C309 (1998).
11. M. Haas and B. Forbush, III, [^{3}H]Bumetanide binding to duck red cells, *J. Biol. Chem.* **261**, 8434-8441 (1986).
12. J. Duhm and B. O. Göbel, Role of the furosemide-sensitive Na^+/K^+ transport system in determining the steady-state Na^+ and K^+ content and volume of human erythrocytes *in vitro* and *in vivo*, *J. Membr. Biol.* **77**, 243-254 (1984).
13. H. Mairbäurl, S. Schulz, and J. F. Hoffman, Cation transport and cell volume changes in maturing rat reticulocytes, *Am. J. Physiol.* **279**, C1621-C1630 (2000).
14. N. Maassen, M. Foerster, and H. Mairbäurl, Red blood cells do not contribute to removal of K^+ released from exhaustively working forearm muscle, *J. Appl. Physiol.* **85**, 326-332 (1998).
15. J. Duhm, Modes of furosemide-sensitive K (Rb) transport in human (and rat) erythrocytes: effects of Na_o, Na_i, K_i, pH, cell volume, and NEM., *Fed. Proc.* **46**, 2383-2385 (1987).
16. T. Tepper, W. J. Sluiter, R. M. Huisman, and D. de Zeeuw, Erythrocyte Na^+/Li^+ countertransport and Na^+/K^+-$2Cl^-$ co-transport measurement in essential hypertension: useful diagnostic tools or failure? A meta-analysis of 17 years of literature, *Clin. Sci.* **95**, 649-657 (1998).
17. C. Lytle and T. McManus, Coordinate modulation of Na-K-2Cl cotransport and K-Cl cotransport by cell volume and chloride, *Am. J. Physiol. Cell. Physiol.* **283**, C1422-C1431 (2002).
18. P. W. Flatman, Sodium and potassium transport in ferret red cells, *J. Physiol. (Lond)* **341**, 545-557 (1983).
19. A. C. Hall and J. C. Ellory, Measurement and stoichiometry of bumetanide-sensitive (2Na:1K:3Cl) cotransport in ferret red cells, *J. Membr. Biol.* **85**, 205-213 (1985).
20. P. W. Flatman and J. Creanor, Regulation of Na^+-K^+-$2Cl^-$ cotransport by protein phosphorylation in ferret erythrocytes, *J. Physiol. (Lond)* **517**, 699-708 (1999).
21. H. Mairbäurl and C. Herth, Na^+-K^+-$2Cl^-$ cotransport, Na^+/H^+ exchange, and cell volume in ferret erythrocytes, *Am. J. Physiol.* **271**, C1603-C1611 (1996).
22. P. W. Flatman and P. L. R. Andrews, Cation and ATP content of ferret red cells, *Comp. Biochem. Physiol.* **74A**, 939-943 (1983).
23. M. C. Muzyamba, A. R. Cossins, and J. S. Gibson, Regulation of Na^+-K^+-$2Cl^-$ cotransport in turkey red cells: the role of oxygen tension and protein phosphorylation, *J. Physiol. (Lond)* **517**, 421-429 (1999).
24. H. Mairbäurl and C. Lytle, Shrinkage and deoxygenation stimulate NKCC independent of Mg_i in ferret red blood cells, *FASEB J.* **13**, A716 (1999).
25. P. W. Flatman, Deoxygenation stimulates Na^+-K^+-$2Cl^-$ cotransport in ferret erythrocytes, *J. Physiol. (Lond)* **531**, 122P-123P (2001).
26. G. Jiang, J. D. Klein, and W. C. O'Neill, Growth factors stimulate the Na-K-2Cl cotransporter NKCC1 through a novel Cl^--dependent mechanism, *Am. J. Physiol. Cell. Physiol.* **281**, C1948-C1953 (2001).
27. W. F. Schmidt, III and T. J. McManus, Ouabain-insensitive salt and water movements in duck red cells. II. Norepinephrine stimulation of sodium plus potassium cotransport, *J. Gen. Physiol.* **70**, 81-97 (1977).
28. I. Giménez and B. Forbush, Short-term stimulation of the renal Na-K-Cl cotransporter (NKCC2) by vasopressin involves phosphorylation and membrane translocation of the protein, *J. Biol. Chem.* **278**, 26946-26951 (2003).
29. M. E. O'Donnell, A. Martinez, and D. Sun, Endothelial Na-K-Cl cotransport regulation by tonicity and hormones: phosphorylation of cotransport protein, *Am. J. Physiol.* **269**, C1513-C1523 (1995).
30. M. Haas, D. McBrayer, and C. Lytle, $[Cl^-]_i$-dependent phosphorylation of the Na-K-Cl cotransport protein of dog tracheal epithelial cells, *J. Biol. Chem.* **270**, 28955-28961 (1995).
31. C. Lytle and B. Forbush, III, Regulatory phosphorylation of the secretory Na-K-Cl cotransporter: modulation by cytoplasmic Cl, *Am. J. Physiol.* **270**, C437-C448 (1996).
32. C. M. Liedtke, R. Papay, and T. S. Cole, Modulation of Na-K-2Cl cotransport by intracellular Cl^- and protein kinase C-δ in Calu-3 cells, *Am. J. Physiol. Lung Cell. Mol. Physiol.* **282**, L1151-L1159 (2002).
33. C. Lytle and B. Forbush, III, The Na-K-Cl cotransport protein of shark rectal gland. II. Regulation by direct phosphorylation, *J. Biol. Chem.* **267**, 25438-25443 (1992).
34. J. Torchia, C. Lytle, D. J. Pon, B. Forbush, III, and A. K. Sen, The Na-K-Cl cotransporter of avian salt gland. Phosphorylation in response to cAMP-dependent and calcium-dependent secretogogues, *J. Biol. Chem.* **267**, 25444-25450 (1992).
35. A. Tanimura, K. Kurihara, S. J. Reshkin, and R. J. Turner, Involvement of direct phosphorylation in the regulation of the rat parotid Na^+-K^+-$2Cl^-$ cotransporter, *J. Biol. Chem.* **270**, 25252-25258 (1995).

36. P. W. Flatman, Regulation of Na-K-2Cl cotransport by phosphorylation and protein-protein interactions, *Biochim. Biophys. Acta* **1566**, 140-151 (2002).
37. A. W. Flemmer, I. Giménez, B. F. X. Dowd, R. B. Darman, and B. Forbush, Activation of the Na-K-Cl cotransporter NKCC1 detected with a phospho-specific antibody, *J. Biol. Chem.* **277**, 37551-37558 (2002).
38. J. D. Klein and W. C. O'Neill, Volume-sensitive myosin phosphorylation in vascular endothelial cells: correlation with Na-K-2Cl cotransport, *Am. J. Physiol.* **269**, C1524-C1531 (1995).
39. C. Lytle, Activation of the avian erythrocyte Na-K-Cl cotransport protein by cell shrinkage, cAMP, fluoride, and calyculin-A involves phosphorylation at common sites, *J. Biol. Chem.* **272**, 15069-15077 (1997).
40. R. B. Darman and B. Forbush, A regulatory locus of phosphorylation in the N terminus of the Na-K-Cl cotransporter, NKCC1, *J. Biol. Chem.* **277**, 37542-37550 (2002).
41. R. B. Darman, A. Flemmer, and B. Forbush, Modulation of ion transport by direct targeting of protein phosphatase type I to the Na-K-Cl cotransporter, *J. Biol. Chem.* **276**, 34359-34362 (2001).
42. H. C. Palfrey and E. B. Pewitt, The ATP and Mg^{2+} dependence of Na^+-K^+-$2Cl^-$ cotransport reflects a requirement for protein phosphorylation: studies using calyculin A, *Pflügers Arch.* **425**, 321-328 (1993).
43. J. D. Klein, S. T. Lamitina, and W. C. O'Neill, JNK is a volume-sensitive kinase that phosphorylates the Na-K-2Cl cotransporter in vitro, *Am. J. Physiol.* **277**, C425-C431 (1999).
44. K. Piechotta, J. Lu, and E. Delpire, Cation chloride cotransporters interact with the stress-related kinases Ste20-related proline-alanine-rich kinase (SPAK) and oxidative stress response 1 (OSR1), *J. Biol. Chem.* **277**, 50812-50819 (2002).
45. B. F. X. Dowd and B. Forbush, PASK (proline-alanine-rich STE20-related kinase), a regulatory kinase of the Na-K-Cl cotransporter (NKCC1), *J. Biol. Chem.* **278**, 27347-27353 (2003).
46. S. Fillon, S. Wärntges, J. Matskevitch et al., Serum- and glucocorticoid-dependent kinase, cell volume, and the regulation of epithelial transport, *Comp. Biochem. Phys. A* **130**, 367-376 (2001).
47. C. Lytle, A volume-sensitive protein kinase regulates the Na-K-2Cl cotransporter in duck red blood cells, *Am. J. Physiol.* **274**, C1002-C1010 (1998).
48. C. Di Ciano-Oliveira, G. Sirokmány, K. Szászi et al., Hyperosmotic stress activates Rho: differential involvement in Rho kinase-dependent MLC phosphorylation and NKCC activation, *Am. J. Physiol. Cell. Physiol.* **285**, C555-C566 (2003).
49. P. W. Flatman and V. L. Lew, Magnesium buffering in intact human red blood cells measured using the ionophore A23187, *J. Physiol. (Lond)* **305**, 13-30 (1980).
50. P. W. Flatman, The effects of magnesium on potassium transport in ferret red cells, *J. Physiol. (Lond)* **397**, 471-487 (1988).
51. I. Matskevich and P. W. Flatman, Regulation of Na^+-K^+-$2Cl^-$ cotransport by threonine phosphorylation in ferret red cells, *J. Physiol. (Lond)* **547.P**, C20 (2003).
52. J. H. Hanke, J. P. Gardner, R. L. Dow et al., Discovery of a novel, potent, and Src family-selective tyrosine kinase inhibitor, *J. Biol. Chem.* **271**, 695-701 (1996).
53. L. Tatton, G. M. Morley, R. Chopra, and A. Khwaja, The Src-selective kinase inhibitor PP1 also inhibits Kit and Bcr-Abl tyrosine kinases, *J. Biol. Chem.* **278**, 4847-4853 (2003).
54. T. Akiyama and H. Ogawara, Use and specificity of genistein as inhibitor of protein-tyrosine kinases, *Methods Enzymol.* **201**, 362-370 (1991).
55. T. Tamaoki, Use and specificity of staurosporine, UCN-01, and calphostin C as protein kinase inhibitors, *Methods Enzymol.* **201**, 340-347 (1991).
56. C. Lytle, J.-C. Xu, D. Biemesderfer, and B. Forbush, III, Distribution and diversity of Na-K-Cl cotransport proteins: a study with monoclonal antibodies, *Am. J. Physiol.* **269**, C1496-C1505 (1995).
57. I. Matskevich, D. K. Apps, and P. W. Flatman, The Na-K-2Cl cotransporter forms high molecular weight complexes in ferret red blood cell membranes, *Pflügers Arch.* **443**, -S186 (2002).
58. M. L. Moore-Hoon and R. J. Turner, The structural unit of the secretory Na^+-K^+-$2Cl^-$ cotransporter (NKCC1) is a homodimer, *Biochemistry* **39**, 3718-3724 (2000).
59. P. W. Flatman and J. Creanor, Stimulation of Na^+-K^+-$2Cl^-$ cotransport by arsenite in ferret erythrocytes, *J. Physiol. (Lond)* **519**, 143-152 (1999).
60. J. Randall, T. Thorne, and E. Delpire, Partial cloning and characterization of *Slc12a2*: the gene encoding the secretory Na^+-K^+-$2Cl^-$ cotransporter, *Am. J. Physiol.* **273**, C1267-C1277 (1997).
61. C. R. T. Vibat, M. J. Holland, J. J. Kang, L. K. Putney, and M. E. O'Donnell, Quantitation of Na^+-K^+-$2Cl^-$ cotransport splice variants in human tissues using kinetic polymerase chain reaction, *Anal. Biochem.* **298**, 218-230 (2001).
62. T. Krarup, L. D. Jakobsen, B. S. Jensen, and E. K. Hoffmann, Na^+-K^+-$2Cl^-$ cotransport in Ehrlich cells: regulation by protein phosphatases and kinases, *Am. J. Physiol.* **275**, C239-C250 (1998).

63. S. Shenolikar and A. C. Nairn, Protein phosphatases: recent progress, *Advances in Second Messenger and Phosphoprotein Research* **23**, 1-121 (1991).
64. P. M. Bryan and L. R. Potter, The atrial natriuretic peptide receptor (NPR-A/GC-A) is dephosphorylated by distinct microcystin-sensitive and magnesium-dependent protein phosphatases, *J. Biol. Chem.* **277**, 16041-16047 (2002).

8

A NOVEL NHE1 FROM RED BLOOD CELLS OF THE WINTER FLOUNDER

Regulation by multiple signaling pathways

Stine Falsig Pedersen*

1. PHYSIOLOGICAL ROLES OF NHE1

The ubiquitously expressed plasma membrane Na^+/H^+ exchanger, NHE1, plays a major role in the regulatory volume increase (RVI) process after cell shrinkage. NHE1 is also activated by acidification, stimulation of receptors for a wide range of hormones and growth factors, and inhibition of Ser/Thr protein phosphatases by DNA tumor viruses or compounds such as okadaic acid and calyculin A.[1-6] Consequently, NHE1 serves important physiological functions not just as a mechanism of pH- and cell volume homeostasis but also as a signal transducer which converts growth hormone signals into pH- and/or cell volume changes away from the steady state set point. In turn, these changes can modulate cell migration,[7] cell cycle control,[8] and programmed cell death.[9] In teleost red blood cells (RBCs), a major physiological function of NHE1 is the modulation of hemoglobin (Hb) O_2 affinity. Exposure of fish to hypoxia or exercise stress elicits release of catecholamines which act on β-adrenergic receptors on the RBCs, resulting in increased cellular cAMP levels, and NHE1 activation. In trout, the receptor involved was recently identified as a novel, isoproterenol-sensitive β_3 isoform.[10] Both the ensuing intracellular alkalinization and cell swelling contribute to increase the O_2 affinity of Hb, the former via the Bohr/Root effects, the latter as a result of the dilution of [Hb].[11] Reflecting this special function, NHE1s from teleost RBCs tend to be robustly activated by cAMP but display little or no activity in response to osmotic shrinkage, especially at physiological P_{O2}.[12, 13]

Given the pleiotropic roles of NHE1, it is perhaps not surprising that excessive NHE1 activity has been found to play a major role in a number of important pathological states. One example is that of hypoxia/ischemia-induced cell damage. During ischemia/ reperfusion in the heart, activation of NHE1 increases $[Na^+]_i$, resulting in reversal of Na^+/Ca^{2+} exchange and Ca^{2+} overload.[14] NHE1 is also activated during brain hypoxia/

* Stine F. Pedersen, Dept. of Biochemistry, August Krogh Institute, 13, Universitetsparken, DK-2100 Copenhagen Ø, Denmark

ischemia, with apparently similar effect.[15,16] Another example is that of many cancer cell types where the growth advantage and invasive properties are dependent on increased NHE1 activity and expression.[17, 18]

These clinically important implications of deranged NHE1 activity underscore the need to elucidate the signaling events controlling NHE1 activity. That protein phosphorylation, directly or indirectly, plays an important role in regulation of NHE1 is well established but exactly how is not fully understood.[3] For instance, NHE1 is directly phosphor-ylated in response to growth factor activation, but there is no clear picture as to the extent this phosphorylation is necessary for the ensuing activation of NHE1.[3] The mammalian NHE1 has been shown to bind directly to a wide range of proteins and other accessory factors which are themselves regulated by phosphorylation-dependent processes includ-ing calmodulin,[19] the band 4/ezrin/radixin/moesin (FERM) proteins[20] and via them, F-actin, the phospholipid phosphatidyl inositol 4,5 bisphosphate ($PtdIns(4,5)P_2$),[21] and car-bonic anhydrase II.[22] Thus, evidence is accumulating that NHE1 is part of a tightly regulated multi-protein complex and stimuli affecting NHE1 activity could act either on NHE1 itself or on an associated protein.

In cells in which NHE1 is activated by osmotic shrinkage, its activity in parallel with the Cl^-/HCO_3^- exchanger (AE) results in RVI by net uptake of NaCl and osmotically obliged water with no or only modest change in pH_i, depending on the coupling ratio between the two transporters. Evidence for this coupling of two electroneutral membrane transporters as a mechanism of RVI came from studies in RBCs of the giant salamander, *Amphiuma tridactylum.*[23] Prior to this, studies in RBCs of the winter flounder, *Pseudopleuronectes amricanus*, had demonstrated a robust RVI which, in the presence of the Na^+,K^+ ATPase inhibitor ouabain, was a consequence of net NaCl uptake with no change in K^+ content.[24] This indicated that the molecular mechanism of RVI in winter flounder RBCs differs, e.g., from that in duck RBCs, where K^+ uptake via a Na^+-K^+-$2Cl^-$ cotransporter (NKCC1) accounts for the majority of the cation gain.[25, 26] The identity of the transporters mediating RVI in flounder RBCs was not established in early studies. The potent shrinkage-induced Na^+ uptake was in contrast to the modest or absent shrinkage-induced NHE activation at physiological O_2 pressure in most teleost RBCs. When preliminary studies further suggested the RVI response was unaffected by NHE1 inhibitors[27] as well as the NKCC1 inhibitor bumetanide, we decided to revisit the flounder RBC system to solve this apparent conundrum (S.F. Pedersen, S.A. King, P.M. Cala, unpublished, postdoc experiments in collaboration with Dr. Cala and lab, including Ph.D. student R.R. Rigor, and postdoctoral fellows S. A. King, and Z. Zhuang).

2. THE PANHE1 PROTEIN: SEQUENCE, TOPOLOGY AND LOCALIZATION

We cloned the paNHE1 protein from RNA from winter flounder RBCs, starting with primers based on conserved regions in the human (h)NHE1, the *Amphiuma tridactylum* RBC (at NHE1) and the trout βNHE.[28] The 3'- and 5'-untranslated regions (UTRs) were obtained by rapid amplification of cDNA-ends (RACE). The open reading frame (ORF) was found to span 2340 base pairs, corresponding to a 779 amino acid protein with a calculated molecular weight of 86.6 kDa. Hydropathy analyses predict a membrane topology similar to that recently suggested for hNHE1,[29] with 12 transmembrane (TM) domains, a re-entrant loop between TM 9 and 10, and a C-terminal entry cytoplasmic tail.[28] paNHE1 runs as a band of about 100 kDa in Western blots of crude membrane

fractions, suggesting that it is glycosylated *in vivo*, similar to other NHE1 homologues studied,[3] and localizes primarily to the marginal band of intact flounder RBCs. Other NHE isoforms than paNHE1 were never detected in the flounder RBCs, neither by PCR using primers specific for NHE1-4 and βNHE, respectively, nor by isoform-specific antibodies[28] (S.F. Pedersen unpublished). Thus, similar to human RBCs,[30] it appears that the flounder RBCs contain only a single NHE isoform. Interestingly, however, we detected the presence of several partially different 3' UTRs, and the ORF exhibited three silent dimorphisms.[28] This suggests the presence of multiple paNHE1 gene copies, a phenomenon recently found to be widespread in fish,[31] although developmental 3' UTR differences could also be involved.[28]

As seen in Table 1, the NHE cloned from winter flounder RBCs is clearly an NHE1 homologue, with 65% identity at the amino acid level to hNHE1 and much lower homology (≤ 46% identity) to the other NHE isoforms, hence the name *Pseudopleuronectes americanus* (pa)NHE1. Notably, although paNHE1 has high homology (74% identity) with the trout βNHE, the homology to other teleost NHE1s is not consistently higher than that of the mammalian or amphibian NHE1s (Table 1).

The cytoplasmic tail of paNHE1 exhibits consensus sites for protein kinase A (PKA), C (PKC), and casein kinase II. The PKA consensus sites are identical to two of four such sites found in βNHE, whereas hNHE1 lacks PKA consensus sites. In contrast, in the region (amino acids 636-656 in hNHE1, 624-644 in paNHE1) identified in hNHE1 as a high-affinity calmodulin-binding region,[19] paNHE1 is more similar to hNHE1 despite its overall greater homology to βNHE.[28] Interestingly, the calmodulin-binding region has been implicated in shrinkage-mediated activation of hNHE1,[19] pointing to the possibility that these sequence differences may underlie the markedly different shrinkage-sensitivity of paNHE1 and βNHE.

Table 1. Amino acid sequence identity/similarity between paNHE1 and other NHE isforms and NHE1 homologs

	Compared to paNHE1	
NHE isoform/homolog	Identity (%)[a,b]	Similarity (%)[c]
Human NHE1	65	71
Human NHE2	46	54
Human NHE3	41	51
Amphiuma tridactylum (giant salamander) NHE1	65	71
Salmo gairdneri (trout) βNHE	74	79
Anguilla anguilla (European eel) NHE1	57	63

a All identity and similarity data were calculated in Genetics Computer Group (GCG) software, using the BLOSUM62 matrix. Sequence information was obtained from the relevant GenBank entries.

b Identity denotes identical amino acids.

c Similarity denotes identical amino acids and amino acids with similar properties.

3. PANHE1 IS A UNIQUE AMILORIDE-, EIPA-, AND HOE 694-INSENSITIVE NHE1

A hallmark of essentially all NHE1 homologues studied is their potent inhibition by amiloride and amiloride-derivatives, e.g., 5´N-ethylisopropylamiloride, EIPA, and by benzoylguanidine-type compounds, e.g., HOE 694, whereas, NHE3 is insensitive to these compounds.[3] Exactly how NHE1 interacts with these inhibitors is controversial and incompletely understood. Mutations of residues in TM4 and TM9 alter the drug sensitivity of rat NHE1.[3, 32, 33] On the other hand, NHE1 from *Amphiuma tridactylum* RBCs (at NHE1) is amiloride- and EIPA-sensitive but HOE 694-insensitive, and analyses of the drug sensitivity of hNHE1-atNHE1 chimeras indicated that both the N-terminal, transmembrane region and the C-terminal tail are involved in determining inhibitor sensitivity.[34] Remarkably, paNHE1 is insensitive to even very high doses of amiloride (up to 1 mM), EIPA and HOE 694 (both up to 100 μM).[28] Analysis of the paNHE1 sequence revealed that in a highly conserved region in TM4, paNHE1 has a motif identical to that in NHE3 (FFFYLLP), which differs in two amino acids from that in all the other NHE1s (FFLFLLP in hNHE1 and atNHE1, FFLCLLP in βNHE). Thus, specific motifs in TM4 and TM9 as well as interactions between the N- and C-terminal domains of NHE1 appear to be involved in inhibitor binding. We are currently testing this hypothesis by a comparative approach, using electron spin resonance to assess conformational changes in the three wild-type proteins (hNHE1, atNHE1, and paNHE1) and relevant mutants upon inhibitor binding.

4. RVI IN WINTER FLOUNDER RBCS IS MEDIATED BY PARALLEL ACTIVITY OF PANHE1 AND A CL^-/HCO_3^- EXCHANGER

Currently, there are no known inhibitors of paNHE1. To circumvent the problem, we took advantage of the fact that pharmacological inhibition of the Cl^-/HCO_3^- exchanger (AE) can be used to distinguish between the involvement of a NKCC and an NHE in RVI. If an NHE1 is operating, HCO_3^- efflux through AE will buffer the NHE-mediated H^+ efflux, i.e., AE will act as a H^+ recycler, and pH_o, measured in poorly buffered media, will be largely unaffected. Inhibition of AE by DIDS will prevent the shrinkage-induced increase in cellular Cl^- content and cause pH_o to decrease. Conversely, if an NKCC is operating, Cl^- will recycle *out* through AE (AE will act as a Cl^- recycler), and pH_o will decrease in the absence of DIDS. In this case, the shrinkage-induced decrease in pH_o is prevented by DIDS, but the increase in Cl^- content is unaffected.

In the winter flounder RBCs, DIDS treatment has no effect on the shrinkage-induced increase in Na^+ content but blocks the increase in Cl^- content. There is no change in pH_o in poorly buffered media during normal RVI, whereas, RVI in DIDS treated cells is associated with a robust decrease in pH_o.[28] Moreover, the cellular content of both Na^+ and Cl^- is increased by about 100 mmol/kg dcs after 1 h of hypertonic shrinkage (twice isotonic osmolarity), while in the presence of ouabain, K^+ content is unaffected or slightly decreased.[24, 28] Finally, the Na^+ uptake was a graded function of the degree of cell shrinkage.[28] It is concluded that paNHE1 is a volume-sensitive, shrinkage-activated transporter and that shrinkage-induced NaCl uptake in winter flounder RBCs is mediated by the parallel operation of paNHE1 and AE. **REGULATION OF PANHE1:**

ACTIVATION BY DIFFERENT PATHWAYS AFTER EXPOSURE TO OSMOTIC SHRINKAGE, -ADRENERGIC AGONISTS, AND SER/THR PROTEIN PHOSPHATASE INHIBITORS

As noted, paNHE1 exhibits consensus sites for phosphorylation by PKA and other Ser/Thr protein kinases. Therefore, we pursued the question of its regulation by phosphorylation-dependent processes. The -adrenergic agonist isoproterenol rapidly activates paNHE1 (Figure 1A). Increasing the cellular cAMP level by direct activation of adenylate cyclase with forskolin has the same effect, indicating that the signal for paNHE1 activation is an increase in the cellular cAMP level.[28] Calyculin A (CLA), an inhibitor of Ser/Thr protein phosphatases PP1 and PP2A, also potently activates paNHE1, indicating that PP1 and/or PP2A play an important role in maintaining NHE1 in a silent state in unstimulated cells (Figure 1A). The isotonic activation of paNHE1 by isoproterenol or CLA elicits substantial NaCl uptake and cell swelling, with no change in cellular K^+ content.[28] Concomitantly, pH_i as calculated from the Cl^- distribution ratio increases from about 7.2 in unstimulated cells to about 7.40-7.45 after 1 h of stimulation by shrinkage, isoproterenol or CLA.[28] This intracellular alkalinization occurs in spite of the rapid Cl^-/HCO_3^- exchange through AE because extracellular HCO_3^--CO_2 conversion is uncatalyzed, therefore inefficient, in the inorganic medium as well as in plasma.[11, 35]

Osmotic shrinkage, isoproterenol, and CLA are only partially additive in their effect on paNHE1, suggesting the signaling pathways involved are not identical[28] (Figure 1A). A quantitative estimate of this is shown in Figure 1B. The magnitudes of the three stimuli are chosen to elicit the maximal possible paNHE1 activation by that stimulus alone. The measured Na^+ content at time 30 min (open bars) is compared to the calculated sum of the values for the corresponding individual stimuli minus one mean baseline value (hatched bars). As seen, activation by isoproterenol appears to be fully additive to activation by either CLA or RVI, suggesting the pathways are separate. On the other hand, CLA, RVI, and all three stimuli together, are only partly additive in their effect on paNHE1, suggesting the involvement of partially similar signaling pathways.

Analysis of the convergent and non-convergent signaling event involved in activation of paNHE1 by osmotic shrinkage, isoproterenol, and CLA is complex but is a potentially valuable tool with which to answer important general questions about the pathways of NHE1 regulation. -adrenergic receptor activation is known to elicit both cAMP-dependent and -independent effects.[36] The cAMP-dependent effects are not limited to activation of PKA but include activation, e.g., of mitogen-activated protein kinases (MAPKs) p42/p44 (ERK1/2).[37] PP1 and PP2A are relatively broad specificity Ser/Thr protein kinases and the kinases themselves,[11] in many cases. Moreover, activity of PP1 and PP2A is highly regulated *in vivo*, often in a phosphorylation-dependent manner. For instance, PKA modulates the activity of PP1 by phosphorylation of inhibitor-1.[38, 39] Relaxation kinetic analyses in RBCs from several species indicate that osmotic shrinkage activates, and conversely, osmotic swelling inhibits protein kinase(s) involved in the control of volume-regulatory membrane transport.[40, 41] Also in some species, the protein phosphatase(s) are volume-sensitive, being inhibited by osmotic shrinkage and activated by osmotic swelling[42] (A. Ortiz-Acevedo, H. Maldonado, R. Rigor, and P.M. Cala, unpublished). Thus, there are multiple possible interactions between the signaling events activated by shrinkage, isoproterenol and CLA.

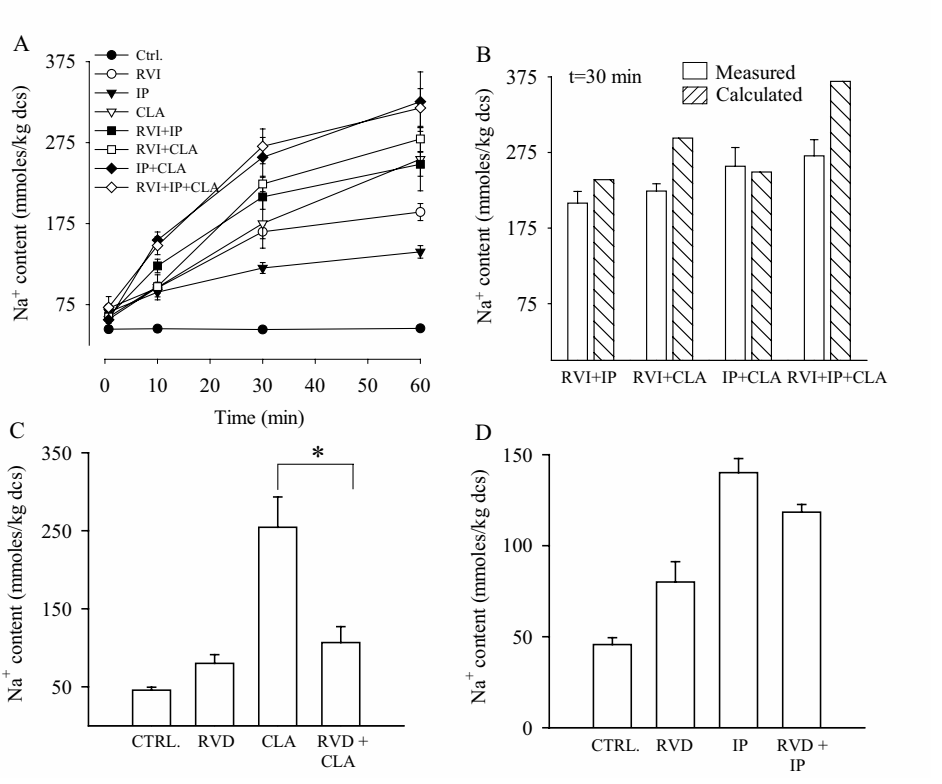

Figure 1. Activation of paNHE1 by osmotic shrinkage, isoproterenol, and calyculin A. Winter flounder RBCs were washed three times in 8-10 volumes of isotonic medium (in mM: 148 NaCl, 3 KCl, 1 $MgCl_2$, 0.75 $CaCl_2$, 30 HEPES, pH 7.65, 360 mOsm), incubated at 10% hematocrit for 2 h, and pretreated with 1 mM ouabain to inhibit the Na^+,K^+ATPase. Cellular content of Na^+, K^+, Cl^-, and water was determined by net flux measurements as previously described.[24, 28] Hypertonic challenge (2.0 RVI) or treatment with isoproterenol (IP, 10 μM) or calyculin A (CLA, 100 nM) were initiated at time zero. Hypo- (RVD) and hypertonic (RVI) media were, respectively, half and twice the osmolarity of the isotonic medium and were made by adjusting NaCl content. *A.* Cellular Na^+ content over time after exposure to hypertonic shrinkage, IP, CLA, or combinations thereof. The magnitudes of the three stimuli are chosen to elicit the maximal possible paNHE1 activation by that stimulus alone. Cellular Cl^- and water content increased in parallel with the increase in Na^+, while K^+ content was unchanged or slightly decreased (not shown). Data are mean ± S.E.M. of 13 (IR), 10 (IP), 7 (CLA), or 3 (all others) experiments. *B.* A quantitative estimate of the additivity of paNHE1 activation by shrinkage, IP and CLA. The mean measured Na^+ content at time 30 min (open bars) is compared to that calculated as the sum of the mean values for the corresponding individual stimuli, minus one mean baseline (isotonic unstimulated) value (hatched bars). The data are calculated from the experiments shown in A. *C-D.* Effect of osmotic shrinkage on paNHE1 activation by CLA (C) or IP (D). Experimental conditions were as in A, data are mean ± S.E.M. of 13 (IR), 4 (RVD), 3 (RVD + IP), or 2 (RVD + CLA) experiments. These data were previously reported at the Experimental Biology meeting 2004.[43]

When cells are osmotically swollen, paNHE1 cannot be activated by CLA treatment, while the isoproterenol-induced paNHE1 activation is not, or only slightly, affected (Figure 1C-D). Thus, the effect of CLA on paNHE1 is impaired by osmotic swelling and augmented by osmotic shrinkage, consistent with the interpretation that PP1 and/or PP2A counteract paNHE1 activation by dephosphorylating a substrate(s) of a kinase which is

essentially silent in osmotically swollen cells, moderately active under isotonic conditions, and highly active in osmotically shrunken cells. In contrast, -adrenergic stimulation of paNHE1 appears insensitive to cell volume status (Figure 1D). -adrenergic stimulation greatly increases the cAMP level in the winter flounder RBCs, while neither CLA nor osmotic shrinkage affect cellular cAMP.[43] Accordingly, NHE1 activation by isoproterenol is partially blocked by the PKA inhibitor H89 (10 μM), while the shrinkage- and CLA-mediated activation is unaffected.[43] Interestingly, osmotic shrinkage significantly delays the isoproterenol-induced increase in cAMP, while CLA has no effect.[43] Inhibitors of PKC, myosin light chain kinase (MLCK), and protein kinase G (PKG) have no effect on activation of paNHE1 by shrinkage, isoproterenol, or CLA, arguing against a role for these Ser/Thr kinases in regulation of paNHE1.[43] Finally, direct Ser phosphorylation of paNHE1 (in the context of positive or neutral amino acids, i.e., consistent with the consensus sequence for PKA and PKC but not MAPKs), was increased after stimulation with isoproterenol and CLA but appeared unaffected by osmotic shrinkage.[43]

6. CONCLUSION: WORKING MODEL FOR REGULATION OF PANHE1

Based on these data, the following working model for regulation of paNHE1 is proposed (Figure 2). Activation of -adrenergic receptors—physiologically by exposure of the fish to hypoxia or exercise stress, here experimentally by isoproterenol treatment—elicits an increase in the cellular cAMP level resulting in activation of PKA. This activates paNHE1 and concomitantly increases direct paNHE1 phosphorylation, consistent with the presence of two PKA consensus sites in the C-terminal tail of paNHE1. The fact that inhibition of PKA only partially blocks NHE1 activation indicates additional involvement of PKA-independent cAMP effectors. A likely candidate is ERK1/2 which are activated by elevated cAMP and which activate NHE1 in mammalian cells.[3, 37]

Inhibition of PP1 and PP2A by CLA appears to increase the direct NHE1 phosphorylation at yet unidentified Ser residues. Given the broad specificity of PP1 and PP2A, the effect of CLA could reflect reduced dephosphorylation of paNHE1 residues phosphorylated by PKA or by other Ser/Thr kinases, and could also involve reduced dephosphorylation at the regulator level, e.g., kinase. Physiologically, the potent effect of CLA is notable because inactivation of protein phosphatases is an integral part of signaling by hormones and growth factors and because many DNA tumor viruses and tumor promoters specifically target PP1 and PP2A.[38, 39] Thus, deranged regulation of PP1 and PP2A could underlie the excessive NHE1 activity in cancer development. In fact, activation of NHE1 by Simian virus 40 (SV40) small t antigen was recently demonstrated.[2]

Cell shrinkage stimulates a volume-sensitive kinase via mechanisms which are still fairly enigmatic in eukaryotic cells. Since activation of paNHE1 by CLA and osmotic shrinkage is only partially additive, it seems likely that shrinkage also inhibits the corresponding Ser/Thr phosphatase. In any event, the net effect of both CLA and shrinkage is an increased kinase/phosphatase activity ratio, resulting in activation of paNHE1 via an unknown mechanism. As the shrinkage-induced activation appears independent of direct paNHE1 phosphorylation, it seems reasonable to suggest that phosphorylation-dependent regulation of the interaction between paNHE1 and associated factor(s) is involved.

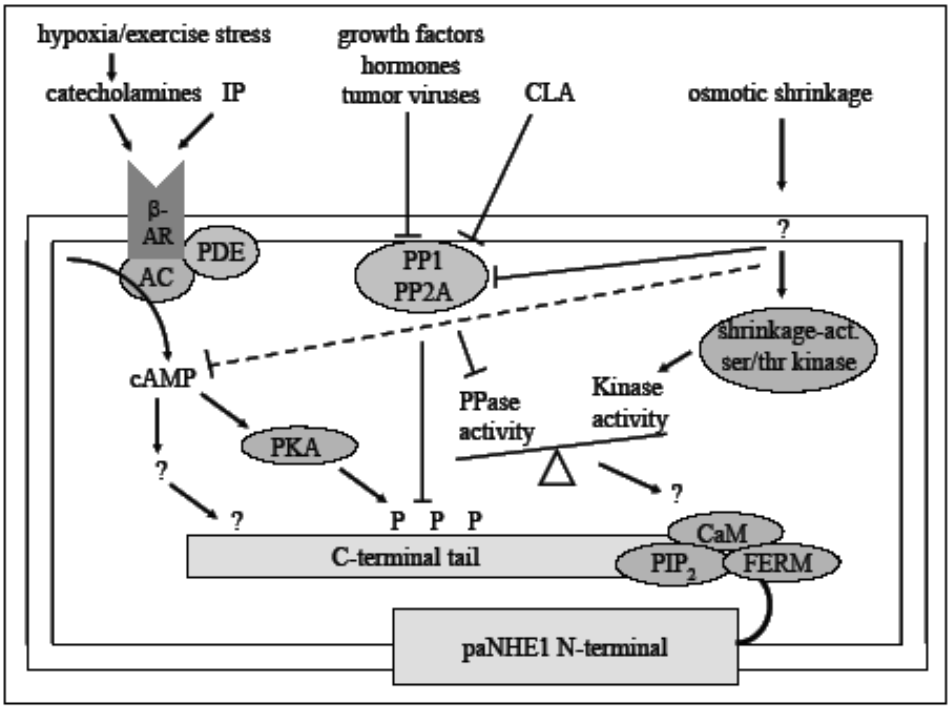

Figure 2. Working model for activation of paNHE1 by osmotic shrinkage, β-adrenergic stimuli, and inhibition of Ser/Thr protein phosphatases. See text for details. Abbreviations are: AC: adenylate cyclase, β-AR: β-adrenergic receptor, CaM: calmodulin, CLA: calyculin A, E: epinephrine, FERM: band 4.1/ezrin/radixin/moesin, IP: isoproterenol, NE: norepinephrine, PDE: phosphodiesterase, PIP_2: phosphatidyl inositol(4,5) bisphosphate, PKA: protein kinase A, PP1/PP2A: Ser/Thr protein phosphatase 1 and -2A.

The interaction of NHE1 with accessory proteins has been studied only in mammalian cells. However, the sequence homology between paNHE1 and the mammalian NHE1s is remarkably high in the proximal part of the C-terminal tail where most of these interactions occur, indicating that at least some of these interactions are also found in the flounder RBCs. Thus, the 56% identity between paNHE1 and hNHE1 for the C-terminal tail overall (290 and 315 amino acids in paNHE1 and hNHE1, respectively), reflects 78% identity between the two species in the proximal 156 amino acids, i.e., to the end of the high affinity calmodulin-binding region, and only 30% identity for the remainder of the C-terminal tail (calculated using Genetics Computer Group (GCG) software and BLOSUM62 scoring matrix). Notably, the fact that β-adrenergic stimulation and inhibition of PP1/PP2A increases paNHE1 phosphorylation does not necessarily mean that this phosphorylation mediates its activation by these stimuli. As mentioned above, this is a point of controversy also in mammalian cells, and it is perhaps relevant in this regard that the distal part of the C-terminal tail, which contains the majority of the residues phosphorylated *in vivo*, is rather poorly conserved.

In conclusion, paNHE1 exhibits high sequence similarity to both human and teleost NHE1s and shares regulatory properties of both but is uniquely insensitive to commonly

used NHE1 inhibitors. These properties make paNHE1 a useful tool for comparative analyses of NHE1 sequence-function relationships and interaction with inhibitors.

7. ACKNOWLEDGMENTS

Drs. P. M. Cala, I. H. Lambert, and C. Hougaard are gratefully acknowledged for stimulating discussions and critical reading of the manuscript.

8. REFERENCES

1. L Bianchini, M Woodside, C Sardet, J Pouyssegur, A Takai and S Grinstein, Okadaic acid, a phosphatase inhibitor, induces activation and phosphorylation of the Na^+/H^+ antiport, *J Biol Chem* **266**, 15406-15413 (1991).
2. AK Howe, S Gaillard, JS Bennett and K Rundell K, Cell cycle progression in monkey cells expressing simian virus 40 small t antigen from adenovirus vectors, *J Virol* **72**, 9637-9644 (1998).
3. J Orlowski and S Grinstein, Diversity of the mammalian sodium/proton exchanger SLC9 gene family, *Pflugers Arch* DOI: **10**.1007/s00424-003-1110-3 (2003).
4. SF Pederson, C Varming, ST Christensen and EK Hoffmann, Mechanisms of activation of NHE by cell shrinkage and by calyculin A in Ehrlich ascites tumor cells, *J Membr Biol* **189**, 67-81 (2002).
5. S Wakabayashi, M Shigekawa and J Pouyssegur, Molecular physiology of vertebrate Na^+/H^+ exchangers, *Physiol Rev* **77**, 51-74 (1997).
6. W Yan, K Nehrke, J Choi and DL Barber, The Nck-interacting kinase (NIK) phosphorylates the Na^+-H^+ exchanger NHE1 and regulates NHE1 activation by platelet-derived growth factor, *J Biol Chem* **276**, 31349-31356 (2001).
7. A Lagana, J Vadnais, PU Le, TN Nguyen, R Laprade, IR Nabi and J Noel, Regulation of the formation of tumor cell pseudopodia by the Na^+/H^+ exchanger NHE1, *J Cell Sci* **113**, 3649-3662 (2000).
8. LK Putney and DL Barber, Na-H exchange-dependent increase in intracellular pH times G2/M entry and transition, *J Biol Chem* **278**, 44645-44649 (2003).
9. F Lang, M Ritter, N Gamper, S Huber, S Fillon, V Tanneur, S Lepple-Wienhues, I Szabo and E Gulbins, Cell volume in the regulation of cell proliferation and apoptotic cell death, *Cell Physiol Biochem* **10**, 417-428 (2000).
10. JG Nickerson, SG Dugan, G Drouin, SF Perry and TW Moon, Activity of the unique beta-adrenergic Na^+/H^+ exchanger in trout erythrocytes is controlled by a novel beta3-AR subtype, *Am J Physiol Regul Integr Comp Physiol* **285**, R526-R535 (2003).
11. M Nikinmaa, Haemoglobin function in vertebrates: evolutionary changes in cellular regulation in hypoxia, *Respir Physiol* **128**, 317-329 (2001).
12. JS Gibson, AR Cossins and JC Ellory, Oxygen-sensitive membrane transporters in vertebrate red cells, *J Exp Biol* **203**, 1395-1407 (2000).
13. M Malapert, H Guizouarn, B Fievet, R Jahns, F Garcia-Romeu, R Motais and F Borgese, Regulation of Na^+/H^+ antiporter in trout red blood cells, *J Exp Biol* **200** (Pt 2), 353-360 (1997).
14. SE Anderson, PM Cala, C Steenbergen, RE London and E Murphy, Effects of hypoxia and acidification on myocardial Na and Ca. Role of Na-H and Na-Ca exchange, *Ann N Y Acad Sci* **639**, 453-455 (1991).
15. NK Jorgensen, SF Petersen, I Damgaard, A Schousboe and EK Hoffmann, Increases in $[Ca^{2+}]_i$ and changes in intracellular pH during chemical anoxia in mouse neocortical neurons in primary culture, *J Neurosci Res* **56**, 358-370 (1999).
16. JJ Vornov, AG Thomas and D Jo. Protective effects of extracellular acidosis and blockade of sodium/hydrogen ion exchange during recovery from metabolic inhibition in neuronal tissue culture, *J Neurochem* **67**, 2379-2389 (1996).
17. LA McLean, J Roscoe, NK Jorgensen, FA Gorin and PM Cala, Malignant gliomas display altered pH regulation by NHE1 compared with nontransformed astrocytes, *Am J Physiol Cell Physiol* **278**, C676-C688 (2000).
18. SJ Reshkin, A Bellizzi, S Caldeira, V Albarani, I Malanchi, M Poignee, M Alunni-Fabbroni, V Casavola and M Tommasino, Na+/H+ exchanger-dependent intracellular alkalinization is an early event in malignant transformation and plays an essential role in the development of subsequent transformation-associated phenotypes, *FASEB J* **14**, 2185-2197 (2000).

19. B Bertrand, S Wakabayashi, T Ikeda, J Pouyssegur and M Shigekawa, The Na^+/H^+ exchanger isoform 1 (NHE1) is a novel member of the calmodulin-binding proteins. Identification and characterization of calmodulin-binding sites, *J Biol Chem* **269**, 13703-13709 (1994).
20. SP Denker, DC Huang, J Orlowski, H Furthmayr and DL Barber, Direct binding of the Na-H exchanger NHE1 to ERM proteins regulates the cortical cytoskeleton and cell shape independently of H^+ translocation, *Mol Cell* **6**, 1425-1436 (2000).
21. O Aharonovitz, HC Zaun, T Balla JD York, J Orlowski and S Grinstein, Intracellular pH regulation by Na^+/H^+ exchange requires phosphatidylinositol 4,5-bisphosphate, *J Cell Biol* **150**, 213-224 (2000).
22. X Li, B Alvarez, JR Casey, RA Reithmeier and L Fliegel, Carbonic anhydrase II binds to and enhances activity of the Na^+/H^+ exchanger, *J Biol Chem* **277**, 36085-36091 (2002).
23. PM Cala, Volume regulation by Amphiuma red blood cells, The membrane potential and its implications regarding the nature of the ion-flux pathways, *J Gen Physiol* **76**, 683-708 (1980).
24. PM Cala, Volume regulation by flounder red blood cells in anisotonic media, *J Gen Physiol* 69, 537-**552 (**1977).
25. FM Kregenow, The response of duck erythrocytes to hypertonic media. Further evidence for a volume-controlling mechanism, *J Gen Physiol* **58**, 396-412 (1971).
26. HC Palfrey and MC Rao, Na/K/Cl co-transport and its regulation, *J Exp Biol* **106**, 43-54 (1983).
27. RR Rigor, Z Zhuang, and PM Cala, Volume regulation by flounder red blood cells: the nature of the ion flux pathways, *Bull.Mt.Desert Island* **40**, 68-70. (2001).
28. SF Pedersen, SA King, RR Rigor, Z Zhuang, JM Warren and PM Cala, Molecular cloning of NHE1 from winter flounder RBCs: activation by osmotic shrinkage, cAMP, and calyculin A, *Am J Physiol Cell Physiol* **284**, C1561-C1576, 2003.
29. S Wakabayashi, T Pang, X Su and M Shigekawa, A novel topology model of the human Na^+/H^+ exchanger isoform 1, *J Biol Chem* **275**, 7942-7949 (2000).
30. R Sarangarajan, N Dhabia, M Soliemani, N Baird and C Joiner, NHE-1 is the sodium-hydrogen exchanger isoform present in erythroid cells, *Biochim Biophys Acta* **1374**, 56-62 (1998).
31. J Wittbrodt, A Meyer and M Schartl, More genes in fish? *Bioessays* **20**, 511-515 (1998).
32. A Khadilkar, P Iannuzzi and J Orlowski, Identification of sites in the second exomembrane loop and ninth transmembrane helix of the mammalian Na^+/H^+ exchanger important for drug recognition and cation translocation, *J Biol Chem* **276**, 43792-43800 (2001).
33. J Orlowski and RA Kandasamy, Delineation of transmembrane domains of the Na^+/H^+ exchanger that confer sensitivity to pharmacological antagonists, *J Biol Chem* **271**, 19922-19927 (1996).
34. LA McLean, S Zia, FA Gorin and PM Cala, Cloning and expression of the Na+/H+ exchanger from Amphiuma RBCs: resemblance to mammalian NHE1, *Am J Physiol* **276**, C1025-C1037 (1999).
35. R Motais, B Fievet, F Garcia-Romeu and S Thomas, Na^+-H^+ exchange and pH regulation in red blood cells: role of uncatalyzed H_2CO_3 dehydration, *Am J Physiol* **256**, C728-C735 (1989).
36. YC Ma and XY Huang, Novel signaling pathway through the beta-adrenergic receptor, *Trends Cardiovasc Med* **12**, 46-49 (2002).
37. N Laroche-Joubert, S Marsy, S Michelet, M Imbert-Teboul and A Doucet, Protein kinase A-independent activation of ERK and H,K-ATPase by cAMP in native kidney cells: role of Epac I, *J Biol Chem* **277**, 18598-18604 (2002).
38. V Janssens and J Goris, Protein phosphatase 2A: a highly regulated family of serine/threonine phosphatases implicated in cell growth and signalling, *Biochem J* **353**, 417-439 (2001).
39. CJ Oliver and S Shenolikar, Physiologic importance of protein phosphatase inhibitors, *Front Biosci* **3**, D961-D972 (1998).
40. ML Jennings and N al Rohil, Kinetics of activation and inactivation of swelling-stimulated K^+/Cl^- transport. The volume-sensitive parameter is the rate constant for inactivation, *J Gen Physiol* **95**, 1021-1040 (1990).
41. JC Parker, GC Colclasure and TJ McManus, Coordinated regulation of shrinkage-induced Na/H exchange and swelling-induced [K-Cl] cotransport in dog red cells, Further evidence from activation kinetics and phosphatase inhibition. *J Gen Physiol* **98**, 869-880 (1991).
42. I Bize, B Guvenc, A Robb, G Buchbinder and C Brugnara, Serine/threonine protein phosphatases and regulation of K-Cl cotransport in human erythrocytes. *Am J Physiol* **277**, C926-C936 (1999).
43. SF Pedersen, ME Holt, SA King, and PM Cala, Activation of paNHE1 by osmotic shrinkage, isoproterenol, and calyculin A: evidence for involvement of distinct signaling pathways, *FASEB J*., abstract submission (2003).

9

PROBING OF THE ICln CHANNEL PORE BY CYSTEINE MUTAGENESIS AND CADMIUM-BLOCK

M. Jakab, M. L. Garavaglia, J. Fürst, S. Rodighiero, F. Guizzardi, G. Meyer, M. Ritter, M. Paulmichl*

1. INTRODUCTION

Reconstitution of purified ICln protein cloned from *M*adine *D*arby *c*anine *k*idney (MDCK) cells in artificial Diph-PC lipid bilayers induces an ion current with biophysical and pharmacological characteristics resembling those of the swelling-dependent regulatory volume decrease channels/currents (RVDC) described in native cells.[1] ICln channels reconstituted in Diph-PC bilayers differ from RVDC insofar as the former are cation selective; whereas, the latter are anion selective.[1-3] Addition of Ca^{2+} to the experimental solution or acidification, however, shifts the permeability of reconstituted ICln toward Cl^{-1}. Only recently, we demonstrated that incorporation of ICln in a 'native' lipid environment, i.e., membranes composed of heart lipid extract, yields a Cl^--selective current phenotype.[3]

ICln is a ubiquitous, highly conserved protein expressed in all species and cell types investigated so far.[4,5] In *Caenorhabditis elegans* two splice variants of ICln are present which display different biophysical properties when reconstituted in artifical bilayers.[4] In the nematode, the ICln gene is embedded in an operon together with two genes coding for proteins, one of which was shown to interact with ICln on a functional level, an approach that seems to be a general gene-finding tool for the identification of parter-proteins.[6] In undifferentiated cells the majority of ICln is diffusely dispersed in the cytosol and only a minor fraction is localized in the membrane compartment. Upon hypotonicity, however, the amount of ICln in the membrane was found to increase[7,8] and recently, Ritter et al.[9] could link this cell swelling-induced translocation of ICln to an altered behavior of native RVDC.

*M. Jakab, M. Ritter, J. Furst and M Paulmichl Department of Physiology, University of Innsbruck, Fritz-Pregl-Str. 3, A-6020 Innsbruck, Austria. M. Paulmichl, M. L. Garavaglia, Rodighiero, F. Guizzardi, and G. Meyer, Department of Biomolecular Science and Biotechnology, Università degli Studi di Milano, Via Celoria 26, I-20133 Milan, Italy. Correspondence to martin.jakab@uibk.ac.at, or markus.paulmichl@uibk.ac.at.

The crucial and probably multifunctional involvement of ICln in cellular homeostasis and cell volume regulation has been demonstrated in numerous studies.[10-20] The role of the protein, whether forming an ion conduction pore itself or being part of it, or functioning as an ion channel regulator, is still a matter of debate.[2,5,21,22]

Analysis of the amino acid hydrophobicity pattern suggests a transmembranal topology of the N-terminal part of ICln consisting of a four-stranded membrane-spanning β-sheet[23] (Figures 2a and b) which is structurally similar to the pore-forming β-hairpins of the water-soluble bacterial toxins α-haemolysin and leukocidin[24]. Recently, the ICln model was confirmed by NMR studies.[25] An ICln homo-dimer can be envisioned as the minimal pore structure required for the passage of ions and osmolytes but also larger multimeres are likely to occur. In order to confirm and refine the model deduced from sequence analysis and NMR studies, site-directed mutagenesis studies were performed.[1] Mutation of negatively charged amino acids in the outer vestibulum of the channel pore (E41C or D48A) abolishes the described Ca^{2+}-sensitivity of reconstituted ICln and thus allowed us to identify E41 and D48 as Ca^{2+} binding sites. Reconstituted ICln channels can be blocked by the guanosine analog acyclovir.[1] Mutation of G49 within the predicted nucleotide binding site at the entrance of the ICln channel pore causes acyclovir-insensitivity. Application of Ni^{2+} shifts the relative permeability of reconstituted ICln toward anions, and mutation of the histidine at position 64 into a glutamate abolishes the Ni^{2+} effect.[1] This confirms that H64 is, as predicted by the model, located within the ion conducting pore.

In a β-barrel, subsequent amino acids forming the ion conducting pore are expected to be alternately orientated toward the hydrophobic membrane phase or to the aqueous phase of the pore lumen. The introduction of cysteine mutations allows us to perform pore probing of ion channels by using cysteine reactive agents like the metal cations Cd^{2+} or Ag^{2+}. Cd^{2+} forms coordinated complexes with the thiol groups of cysteine sidechains[26-28] which influences the gating behavior and/or the channel conductance. Therefore, the substitution of amino acids for cysteines makes possible the study of the functional modification of proteins by metal bridge formation upon addition of Cd^{2+}, an approach used to characterize the gating behavior of inwardly rectifying (Kir)-, voltage-gated (*Shaker* Kv)- and I(Ks) potassium channels[29-31] and to investigate ligand-receptor interactions.[32] In the present study, we performed cysteine mutagenesis of single amino acids in the putative pore region of ICln and reconstituted protein in artificial bilayers. In order to test the accuracy of the ICln channel model obtained by structure analysis or to refine it, the effect of Cd^{2+} application on the current amplitude and single channel open probability was investigated to gain information about the position and accessibility of the mutated amino acids within the conducting pore.

The data presented here further characterize the molecular architecture and functional properties of the ICln protein in its 'ion channel function' when reconstituted in artificial lipid bilayers.

2. EXPERIMENTAL

Mutagenesis and cloning: Site-directed mutagenesis was done by two-stage PCR-directed mutagenesis with megaprimers as described.[33] The mutations were confirmed by restriction enzyme digestions and DNA sequencing. The open reading frames (ORF) of wild-type[23] and mutated MDCK ICln were cloned in frame into the pET3-His vector (kindly provided by T. Hai, Ohio State University[34]) adding a histidine (H)-tag to the N-terminus of the ICln protein for purification of ICln on a Ni-NTA column (Quiagen, Germany). A single protein band of the expected size can be obtained after the expression and purification in *Escherichia coli* [BL21 (DE3)]. The protein was stored at –80°C in the elution buffer (50 mM K_2HPO_4, 200 mM imidazole, pH 8.0) at a concentration of ~0.4 μg/μl.

Bilayer Experiments: **(a)** Macroscopic currents were recorded as described in Fürst, et al.[24] The lipid bilayer [1% (w/v) 1,2-diphytanoyl-*sn*-glycero-3-phosphocholine (Diph-PC, Avanti Polar Lipids, USA) in *n*-decane and butanol] was painted on an aperture of 1 mm diameter in a Teflon diaphragm separating the *cis* and *trans* chamber, each holding 5 ml of experimental solution (10 mM KCl *cis*/150 mM KCl *trans*, 5 mM HEPES, pH 8.0). The selectivity of reconstituted ICln channels was determined as previously described.[1] The permeability ratio of P_{K^+}/P_{Cl^-} was calculated according to the Goldman-Hodgkin-Katz (GHK) equation; the actual Cl^- gradient was measured after each experiment using Cl^--selective electrodes and reversal potentials were determined graphically by interpolation of current-voltage plots. Currents were recorded by a pair of Ag^+/AgCl reference electrodes (Metrohm, Switzerland) connected in series with a voltage source (*cis*) and a current-to-voltage-converter (*trans*) which was made using a Burr Brown operational amplifier (9407/0541F). Signals were filtered at 330 Hz. Purified ICln protein (2-4 μg) was added to the *cis* and *trans* chamber. The signals were recorded with a strip chart recorder (BBC Inc.). All experiments were performed at room temperature (20-25°C).

(b) For the recording of single-channel, currents the 'tip-dip' method was used.[35] Planar lipid bilayers (1% Diph-PC in pentane) were established on patch pipettes. The pipette solution consisted of (mM): KCl 10 (asymmetric conditions) or 100 (symmetric conditions), HEPES 5, pH 8.0, and the bath solution was (mM): KCl 100, HEPES 5, pH 8.0. The protein was added to the bath solution only. Currents were recorded using an EPC-7 patch–clamp amplifier (HEKA, Germany) and data were stored on tape or hard disk. For analysis signals were filtered at 0.2 kHz.

Statistical analysis: All values are given as mean±SEM. Data were tested for differences in the means by Student's *t*-test. Statistically significantly different values were assumed at $p<0.05$ and are marked in graphs as asterisks.

3. RESULTS AND DISCUSSION

In agreement with our previous studies,[1,3] the addition of purified wild-type MDCK ICln to the experimental solutions on the *cis* and *trans* side of the macroscopic bilayer membrane led to spontaneous incorporation of the protein into the membrane without prior incorporation into lipid vesicles. This induced a macroscopic ion current as shown in Figure 1. Under asymmetric KCl conditions (10 mM *cis*, 150 mM *trans*) and in the absence of Ca^{2+}, the current reversed at 22.7±3.8 mV (n=14). Calculation of P_{K^+}/P_{Cl^-} (see

Experimental) gave a value of 12.2±5.0 (n=14). The K^+ selectivity is consistent with the results of our previous work[1,3] and with the findings of Li et al.[2] for rat ICln reconstituted in artificial bilayers.

In order to probe the pore region of ICln and to verify the β-strand structure, we engineered a series of single cysteine mutations in the putative ion conducting pathway of the protein as depicted in Figure 2a. If the β-strand model shown in Figure 2a is correct and a homo-dimeric structure is assumed as the minimal pore forming complex of ICln, the binding of Cd^{2+} to cysteine residues projecting into the pore lumen can be assumed to influence permeation of ions through the pore.

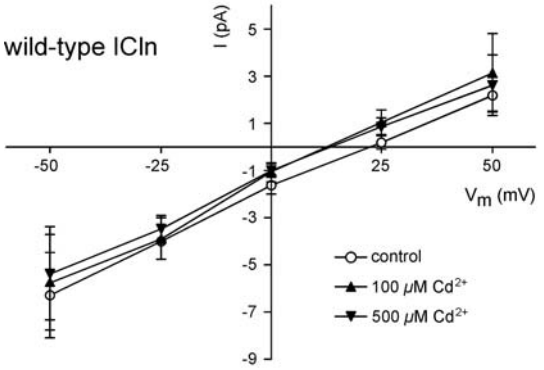

Figure 1. Current-voltage relation of wild-type ICln reconstituted in artificial lipid bilayers composed of Diph-PC before (control) and after addition of 100 or 500 μM Cd^{2+}.

According to Figure 1, wild-type ICln, which possesses two naturally occurring cysteines (C128 and C130),[23] was not responsive to Cd^{2+}. Addition of 100 or 500 μM cadmium (Cd^{2+}) to the *cis* and *trans* side of the bilayer membrane did not significantly change the current amplitude or ion selectivity of wild-type ICln channels. This implies that the cysteines at positions 128 and 130 are not part of the pore-forming region of the protein which is in accordance with the proposed channel model[23] and further shows that in this concentration range, Cd^{2+} does not interfere with the Ca^{2+} binding site of ICln, i.e., E41 or D48 in the vestibulum of the ICln channel pore.[1,3] Remarkably, ICl swell in native cells such as ventricular myocytes and T84 cells is also not Cd^{2+}-sensitive in the same concentration range as used in this study.[36-38]

Figure 2b summarizes the results obtained from macroscopic current measurements of reconstituted ICln proteins in which single amino acids at the positions indicated in Figure 2a were exchanged for cysteines. In the case of ICln-G49C and ICln-S55C, the addition of 100 μM Cd^{2+} led to a significant reduction of the macroscopic current measured at –25 mV to 47.0±8.9 % and to 39.2±10.6 %, respectively, and 500 μM Cd^{2+} further reduced the ICln-S55C current to 12.0±4.3 % of control values (not shown). For ICln-S50C, ICln-G51C and ICln-L52C, the current was not significantly different from wild-type currents. Mutations ICln-G53C and ICln-F54C could not be tested due to the lack of expression of these proteins in the *E. coli* expression system. The results are

consistent with a reduction of the pore diameter upon Cd^{2+} binding and thus imply that G49 and S55 are indeed parts of the pore forming region of ICln. Further, the data confirm the projection of G49 and S55 into the aqueous phase and the orientation of L52 toward the lipid phase, as indicated in Figure 2a. However, G51, which was supposed to face the pore lumen, obviously does not bind Cd^{2+} probably due to its orientation toward the membranous phase, thus its inaccessibility for Cd^{2+}.

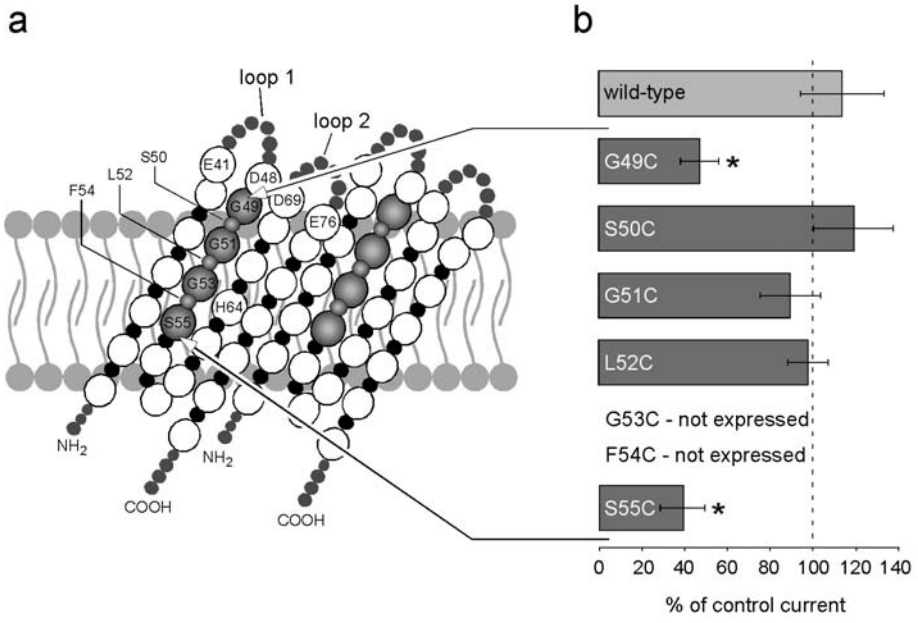

Figure 2. Cysteine mutagenesis in ICln. (a) Proposed transmembrane topology of an ICln homo-dimer. Two monomers comprised of four antiparallel β-stands each, connected by extacellular loops, form a membrane spanning β-barrel. Large spheres and small spheres indicate amino acids orientated toward the aqueous and lipid phase, respectively. The amino acids which were replaced by cysteines are depicted as dark gray spheres. The four negatively charged amino acids at the outer vestibulum of the channel pore, two of which we identified as Ca^{2+} binding sites (E41 and D48), and H64 within the ion conduction pathway are also shown.[1] N- and C-termini are not shown proportionally. (b) Results of macroscopic current measurements given as % of control currents prior to the application of 100 µM $CdCl_2$ at a holding potential of –25 mV.

The current-voltage relationships of ICln-G49C and ICln-S55C under control conditions and after application of 100 or 500 µM Cd^{2+} are shown in Figures 3a and 3b, respectively. In both cases, the currents were significantly reduced at negative voltages and the block was clearly concentration dependent as shown for ICln-S55C. It must be noted that the absoute current of ICln-S55C measured at –25 mV was significantly lower compared to wild-type ICln (wild-type: -4.0±0.7 pA, n=14; ICln-S55C: -1.1±0.2 pA, n=7; $p<0.05$). In contrast to wild-type ICln and the other mutations tested, the shift of the reversal potential toward more negative values upon application of 100 µM Cd^{2+} in the case of ICln-S55C results in a significant shift of the ion selectivity toward Cl^- (control:

3.7±0.8, n=5; 100 μM Cd^{2+}: 0.9±0.1, n=5; $p<0.05$), as shown in the inset of Figure 3b. This indicates a dual effect of Cd^{2+}: the reduction of pore diameter by Cd^{2+} binding leads to a reduced current amplitude, and the introduction of a positive charge in the pore shifts the ion selectivity toward Cl^-.

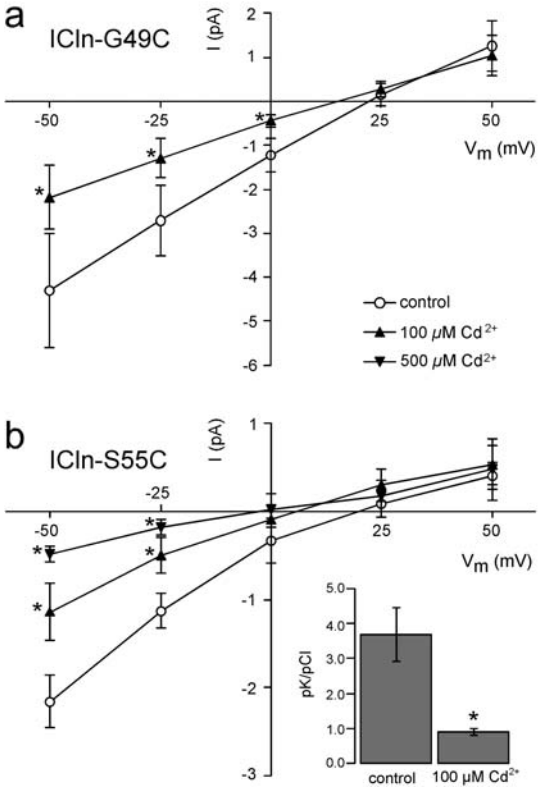

Figure 3. Current-voltage relations of ICln-G49C (a) and ICln-S55C (b) reconstituted in artificial lipid bilayers before (control) and after addition of 100 μM $CdCl_2$ (ICln-G49C), or 100 and 500 μM $CdCl_2$ (ICln-S55C). The inset shows the selectivity-shift of ICln-S55C after application of 100 μM Cd^{2+}. Note different scaling of y-axes in the Figures 1, 3a and 3b.

Measurements using the 'tip-dip' recording technique confirmed the results obtained from macroscopic current experiments on the single-channel level. For tip-dip recordings, artificial lipid bilayer membranes are formed on the tip of patch clamp electrodes;[1, 35] due to the restricted membrane area, this technique allows single channel measurement similar to cell-attached- or cell-free patch clamp recordings. As shown in Figure 4, incorporation of purified ICln-S55C in tip-dip bilayer membranes induced single channel currents which could be inhibited by 500 μM Cd^{2+}. Under symmetric KCl conditions (100 mM in pipette- and bath solution) and prior to the application of Cd^{2+} (control conditions), the current-voltage relation was linear (Figure 5a). In the presence of Cd^{2+},

the channel open probability (Po) was reduced; whereas, the current amplitude was unaffected (Figures 4 and 5). Figure 5b shows the time course of Po calculated from nine individual experiments. 2 and 3 min after the addition of 500 μM Cd^{2+}, the Po was significantly reduced. In the same timeframe, the single channel current amplitude remains unchanged (Figure 5c).

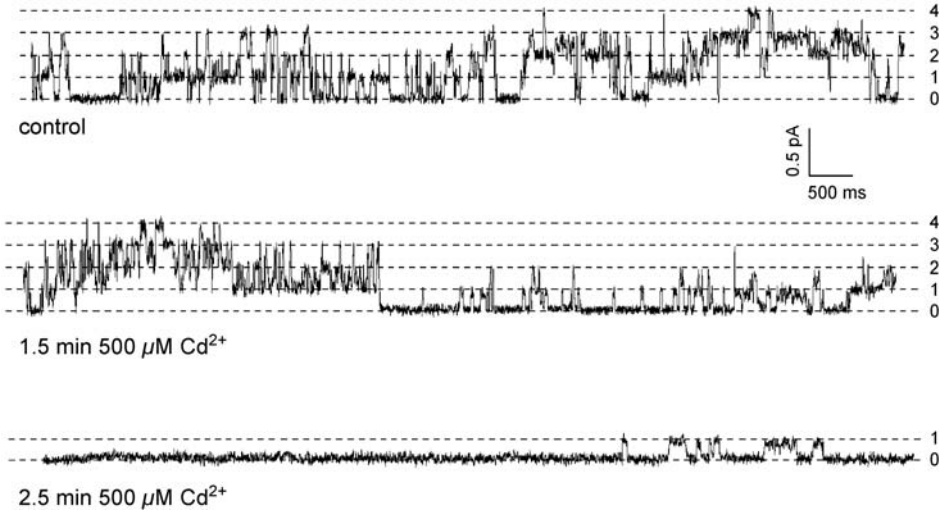

Figure 4. Tracings obtained by reconstitution of ICln-S55C in Diph-PC lipid bilayers prior to the application of $CdCl_2$ (control, upper tracing), 1.5 min (middle trancing) and 2.5 min (lower tracing) after the addition of 500 μM $CdCl_2$ at a membrane potential of +75 mV. Four channels can be identified in this experiment (levels are indicated by dotted lines; 1-4=open states, 0=closed state). The tracings are timeframes of 10 sec taken from 30-sec-recordings which were used for the calculation of the open probability and single-channel current shown in Figure 5.

4. CONCLUSIONS

Purified, water-soluble ICln protein forms ion channels by spontaneously incorporating into artificial lipid bilayers. Site-directed mutation experiments revealed E41 and D49 as the amino acids responsible for the Ca^{2+}-dependence of the channels' ion selectivity and G49 to be part of the putative nucleotide binding site of the protein. H64 could be pinpointed within the ion conducting pathway of ICln. In the present study, cysteine mutagenesis and Cd^{2+} block was used to further investigate the pore structure of the membrane spanning β-barrel formed by ICln, as proposed by the computer model and NMR studies. The results confirm that the amino acids G49 and S55 have access to the pore lumen of reconstituted ICln channels, as predicted by the model, and that S50 and L52 are facing the hydrophobic membraneous phase. According to the lack of Cd^{2+}-block of ICln-G51C channels, the proposed ICln channel model has to be revised insofar as G51 seems not to face the pore lumen or is not accessible to Cd^{2+}.

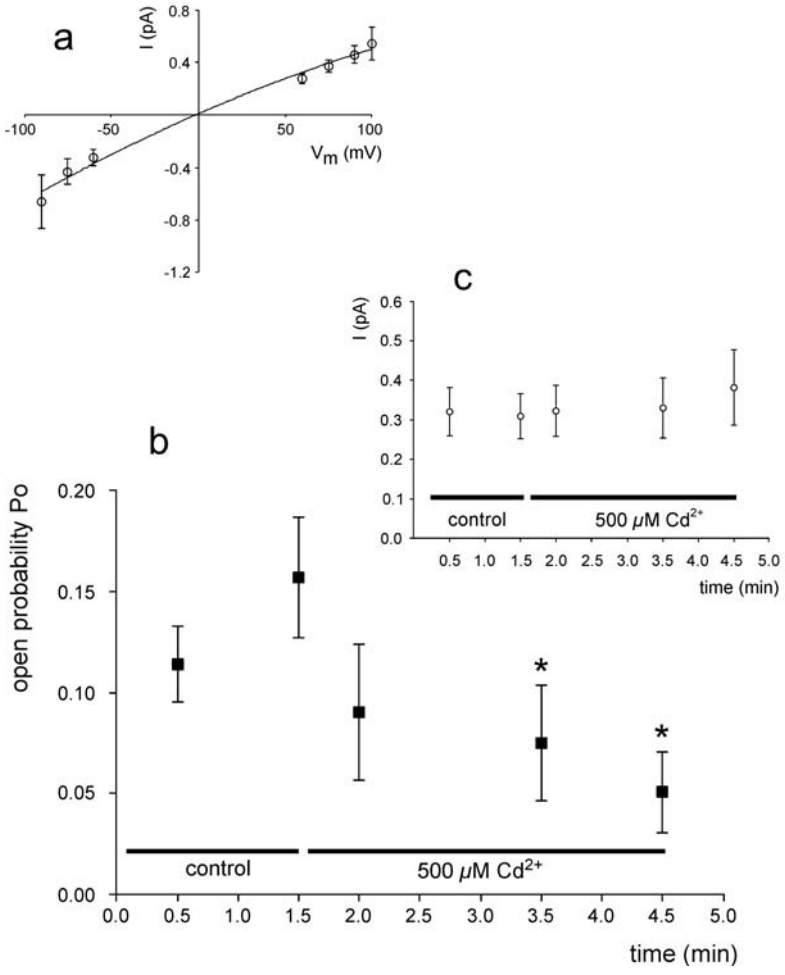

Figure 5. Tip-dip recordings of ICln-S55C incorporated into Diph-PC lipid bilayers. (a) Current-voltage relation of ICln-S55C under symmetric (100 mM in pipette- and bath solution) KCl conditions. (b) The single-channel open probability (Po) of ICln-S55C shows a time-dependent reduction upon addition of 500 μM $CdCl_2$. 2 and 3 min after the application of Cd^{2+}, the Po is significantly reduced; whereas, the single-channel current amplitude remains unchanged (c). Means±SEM of nine individual experiments were calculated from 30-sec-recordings.

5. ACKNOWLEDGMENTS

The help of Robert H. Guy (NIH, Bethesda, USA) with the sequence analysis and the technical assistance of Anna Baumgartner are gratefully acknowledged. This work was supported in part by grants from the Austrian Science Foundation (FWF; grant # P12337, P13041, P12467, P14102-med), the Austrian National Bank (grant # 8444, 6994) and the Gastein Foundation (grant # FP41/FP46) to MR and MP.6.

6. REFERENCES

1. J. Furst, C. Bazzini, M. Jakab, G. Meyer, M. Konig, M. Gschwentner, M. Ritter, A. Schmarda, G. Botta, R. Benz, P. Deetjen, and M. Paulmichl, Functional reconstitution of ICln in lipid bilayers, *Pflugers Arch,* 440(1), 100-15 (2000).
2. C. Li, S. Breton, R. Morrison, C.L. Cannon, F. Emma, R. Sanchez-Olea, C. Bear, and K. Strange, Recombinant pICln forms highly cation-selective channels when reconstituted into artificial and biological membranes, *J Gen Physiol*, 112(6), 27-36 (1998).
3. M. L. Garavaglia, S. Rodighiero, C. Bertocchi, R. Manfredi, J. Furst, M. Gschwentner, M. Ritter, C. Bazzini, G. Botta, M. Jakab, G. Meyer, and M. Paulmichl, ICln channels reconstituted in heart-lipid bilayer are selective to chloride, *Pflugers Arch,* 443(5-6), 748-53 (2002).
4. J. Furst, M. Ritter, J. Rudzki, J. Danzl, M. Gschwentner, E. Scandella, M. Jakab, M. Konig, B. Oehl, F. Lang, P. Deetjen, and M. Paulmichl, ICln ion channel splice variants in Caenorhabditis elegans: voltage dependence and interaction with an operon partner protein, *J Biol Chem,* 277(6), 4435-45 (2002).
5. J. Furst, M. Gschwentner, M. Ritter, G. Botta, M. Jakab, M. Mayer, L. Garavaglia, C. Bazzini, S. Rodighiero, G. Meyer, S. Eichmuller, E. Woll, and M. Paulmichl, Molecular and functional aspects of anionic channels activated during regulatory volume decrease in mammalian cells, *Pflugers Arch*, 444 (1-2), 1-25 (2002).
6. S. Eichmuller, V. Vezzoli, C. Bazzini, M. Ritter, J. Furst, M. Jakab, A. Ravasio, S. Chwatal, S. Dossena, G. Botta, G. Meyer, B. Maier, G. Valenti, F. Lang, and M. Paulmichl, A new gene-finding tool: using the Caenorhabditis elegans operons for identifying functional partner proteins in human cells, *J Biol Chem*, 279(8) 7136-46 (2004).
7. M.W. Musch, C.A. Luer, E.M. Davis-Amaral, and L. Goldstein, Hypotonic stress induces translocation of the osmolyte channel protein pICln in embryonic skate (Raja eglanteria) heart, *J Exp Zool*, 277(6), 460-3 (1997).
8. M.W. Musch, E.M. Davis-Amaral, H.H. Vandenburgh, and L. Goldstein, Hypotonicity stimulates translocation of ICln in neonatal rat cardiac myocytes, *Pflugers Arch*, 436(3), 415-22 (1998).
9. M. Ritter, A. Ravasio, M. Jakab, S. Chwatal, J. Furst, A. Laich, M. Gschwentner, S. Signorelli, C. Burtscher, S. Eichmuller, and M. Paulmichl, Cell swelling stimulates cytosol to membrane transposition of ICln, *J Biol Chem*, 278(50), 50163-74 (2003).
10. F. Emma, R. Sanchez-Olea, and K. Strange, Characterization of pI(Cln) binding proteins: identification of p17 and assessment of the role of acidic domains in mediating protein-protein interactions, *Biochim Biophys Acta,* 1404(3), 321-8 (1998).
11. M. Gschwentner, U.O. Nagl, A. Schmarda, E. Woll, M. Ritter, W. Waitz, P. Deetjen, and M. Paulmichl, Structure-function relation of a cloned epithelial chloride channel, *Ren Physiol Biochem,* 17(3-4), 148-52 (1994).
12. M. Gschwentner, U.O. Nagl, E. Woll, A. Schmarda, M. Ritter, and M. Paulmichl, Antisense oligonucleotides suppress cell-volume-induced activation of chloride channels, *Pflugers Arch,* 430(4), 464-70 (1995).
13. M. Gschwentner, J. Furst, M. Ritter, C. Bazzini, E. Woll, A. Dienstl, M. Jakab, M. Konig, E. Scandella, J. Rudzki, G. Botta, G. Meyer, F. Lang, P. Deetjen, and M. Paulmichl, ICln, an ion channel-forming protein associated with cell volume regulation, *Exp Physiol,* 84(6), 1023-31 (1999).
14. W. T. Pu, K. Wickman, and D.E. Clapham, ICln is essential for cellular and early embryonic viability, *J Biol Chem,* 275(17), 12363-6 (2000).
15. A. Schmarda, F. Fresser, M. Gschwentner, J. Furst, M. Ritter, F. Lang, G. Baier, and M. Paulmichl, Determination of protein-protein interactions of ICIn by the yeast two-hybrid system, *Cell Physiol Biochem,* 11(1), 55-60 (2001).
16. W. T. Pu, G.B. Krapivinsky, L. Krapivinsky, and D.E. Clapham, pICln inhibits snRNP biogenesis by binding core spliceosomal proteins, *Mol Cell Biol*, 19(6) 4113-20 (1999).
17. G. Krapivinsky, W. Pu, K. Wickman, L. Krapivinsky, and D.E. Clapham, pICln binds to a mammalian homolog of a yeast protein involved in regulation of cell morphology, *J Biol Chem*, 273(18), 10811-4 (1998).
18. C. J. Tang and T.K. Tang, The 30-kD domain of protein 4.1 mediates its binding to the carboxyl terminus of pICln, a protein involved in cellular volume regulation, *Blood,* 92(4), 1442-7 (1998).
19. G. Z. Tao and Y. Tashima, A peptide derived from pICln induced a strong hypotonic resistance in Escherichia coli cells, *Peptides,* 21(4), 485-90 (2000).

20. R. S. Schwartz, A.C. Rybicki, and R.L. Nagel, Molecular cloning and expression of a chloride channel-associated protein pICln in human young red blood cells: association with actin, *Biochem J,* 327 (Pt 2), 609-16 (1997).
21. Y. Okada, Volume expansion-sensing outward-rectifier Cl- channel: fresh start to the molecular identity and volume sensor, *Am J Physiol,* 273(3 Pt 1), C755-89 (1997).
22. K. Strange, Molecular identity of the outwardly rectifying, swelling-activated anion channel: time to reevaluate pICln, J Gen Physiol, 111(5), 617-22 (1998).
23. M. Paulmichl, Y. Li, K. Wickman, M. Ackerman, E. Peralta, and D. Clapham, New mammalian chloride channel identified by expression cloning, *Nature*, 356(6366), 38-41 (1992).
24. J. Furst, M. Jakab, M. Konig, M. Ritter, M. Gschwentner, J. Rudzki, J. Danzl, M. Mayer, C.M. Burtscher, J. Schirmer, B. Maier, M. Nairz, S. Chwatal, and M. Paulmichl, Structure and function of the ion channel ICln, *Cell Physiol Biochem*, 10(5-6), 329-34 (2000).
25. A. Schedlbauer, G. Kontaxis, M. Konig, J. Furst, M. Jakab, M. Ritter, L. Garavaglia, G. Botta, G. Meyer, M. Paulmichl, and R. Konrat, Sequence-specific resonance assignments of ICln, an ion channel cloned from epithelial cells, *J Biomol NMR*, 27(4), 399-400 (2003).
26. H. Satofuka, T. Fukui, M. Takagi, H. Atomi, and T. Imanaka, Metal-binding properties of phytochelatin-related peptides, *J Inorg Biochem*, 86(2-3), 595-602 (2001).
27. X. Li, K. Suzuki, K. Kanaori, K. Tajima, A. Kashiwada, H. Hiroaki, D. Kohda, and T. Tanaka, Soft metal ions, Cd(II) and Hg(II), induce triple-stranded alpha-helical assembly and folding of a de novo designed peptide in their trigonal geometries, *Protein Sci*, 9(7), 1327-33 (2000).
28. M. Matzapetakis, B.T. Farrer, T.C. Weng, L. Hemmingsen, J.E. Penner-Hahn, and V.L. Pecoraro, Comparison of the binding of cadmium(II), mercury(II), and arsenic(III) to the de novo designed peptides TRI L12C and TRI L16C, *J Am Chem Soc*, 124(27), 8042-54 (2002).
29. H. Chen, F. Sesti, and S.A. Goldstein, Pore- and State-Dependent Cadmium Block of I(Ks) Channels Formed with MinK-55C and Wild-Type KCNQ1 Subunits, *Biophys J*, 84(6), 3679-89 (2003).
30. J. Xiao, X.G. Zhen, and J. Yang, Localization of PIP2 activation gate in inward rectifier K+ channels, Nat *Neurosci,* 6(8), 811-8 (2003).
31. E. J. Neale, D.J. Elliott, M. Hunter, and A. Sivaprasadarao, Evidence for intersubunit interactions between S4 and S5 transmembrane segments of the Shaker potassium channel, *J Biol Chem,* 278(31), 29079-85 (2003).
32. A. M. Rosati and U. Traversa, Mechanisms of inhibitory effects of zinc and cadmium ions on agonist binding to adenosine A1 receptors in rat brain, *Biochem Pharmacol,* 58(4), 623-32 (1999).
33. A. B. Ekici, O.S. Park, C. Fuchs, and B. Rautenstrauss, One-tube, two-stage PCR-directed *in vitro* mutagenesis using megaprimers, *[Technical Tips].* TTO, 1(14), T01122 (1997).
34. B. P. Chen and T. Hai, Expression vectors for affinity purification and radiolabeling of proteins using Escherichia coli as host, *Gene*, 139(1), 73-5 (1994).
35. B. E. Ehrlich, Planar lipid bilayers on patch pipettes: bilayer formation and ion channel incorporation, *Methods Enzymol,* 207, 463-70 (1992).
36. T. D. Bond, S. Ambikapathy, S. Mohammad, and M.A. Valverde, Osmosensitive C1- currents and their relevance to regulatory volume decrease in human intestinal T84 cells: outwardly vs. inwardly rectifying currents, *J Physiol*, 511 (Pt 1), 45-54 (1998).
37. J. Fritsch and A. Edelman, Osmosensitivity of the hyperpolarization-activated chloride current in human intestinal T84 cells, *Am J Physiol*, 272(3 Pt 1), C778-86 (1997).
38. L. M. Shuba, T. Ogura, and T.F. McDonald, Kinetic evidence distinguishing volume-sensitive chloride current from other types in guinea-pig ventricular myocytes, *J Physiol*, 491 (Pt 1), 69-80 (1996).

10

VOLUME-DEPENDENT AND -INDEPENDENT ACTIVATED ANION CONDUCTANCES AND THEIR INTERACTION IN THE RENAL INNER MEDULLARY COLLECTING DUCT (IMCD)

Stefan H. Boese, Mike A. Gray, and Nick L. Simmons*

1. INTRODUCTION

Cells of the renal medullary collecting duct are normally exposed to large variations in external osmolality.[1] To cope with these changes the cell can activate a variety of transport proteins in the plasma membrane.[2] Swelling-activated anion/organic osmolyte channels or volume-regulated anion conductance (VRAC) play a major part in cell volume recovery after hyposmotic perturbation in the renal inner medullary collecting ducts (IMCD).[3]

Besides VRAC, inner medullary collecting duct cells possess other functionally active anion conductances,[4] namely the Cystic Fibrosis Transmembrane conductance Regulator (CFTR[5]) and a Ca^{2+}-activated Cl^- conductance (CaCC[4]). Studies using primary cultures of rat IMCD cells[6] established cell lines derived from the IMCD.[5, 7-9] Most recently, fluid secretory studies from isolated native rat IMCD[10] have provided strong evidence for these conductances' seeming involvement in transepithelial Cl^- secretion.

In this short review, we give an overview about the operative properties of the anion conductances in the renal IMCD as well as their functional interaction.

2. EXPERIMENTAL

We used short circuit current measurements (I_{sc}) and whole cell patch clamp measurements to investigate anion channels and their interactions in the mouse IMCD. In

* Stefan H. Boese, Zoophysiology, Institute for Biochemistry & Biology, University of Potsdam, Lennéstr. 7a, D-14471, Germany. Mike A. Gray & Nick L. Simmons, School of Cell & Molecular Biosciences, University Medical School, Framlington Place, Newcastle upon Tyne, NE2 4HH, UK

addition, reverse-transcriptase-polymerase chain reaction (RT-PCR) molecular methods were used to search for expression of known members of molecular identified chloride-channel families.

3. THE RENAL INNER MEDULLARY COLLECTING DUCT

The mammalian collecting duct consists of three major segments: the cortical collecting duct, the outer medullary collecting duct (OMCD) and the IMCD. The IMCD is a direct continuation of the OMCD and extends from the boundary between the outer and inner medulla to the tip of the papilla (for review about IMCD structure, see Madsen *et al*[11].).

Functionally, the IMCD plays an important role in urinary concentration and dilution.[12-14] The process of determination of final urinary salt composition is controlled through the regulatory action of natriuretic hormones and paracrines that act on this last segment of the nephron.[14, 15]

4. ANION CHANNELS IN THE IMCD

As mentioned above the IMCD is capable of NaCl transport. Although the nature and regulation of Na^+ transport is clearly established[16, 17] information about the anion exit pathways, their regulation and interactions during net transepithelial Cl^- secretion have only started to emerge during the last couple of years.

During recent years, analysis of the mouse renal IMCD-K2 cell line and primary cultures from the mouse IMCD revealed the following anion conductances are present in this final part of the nephron.

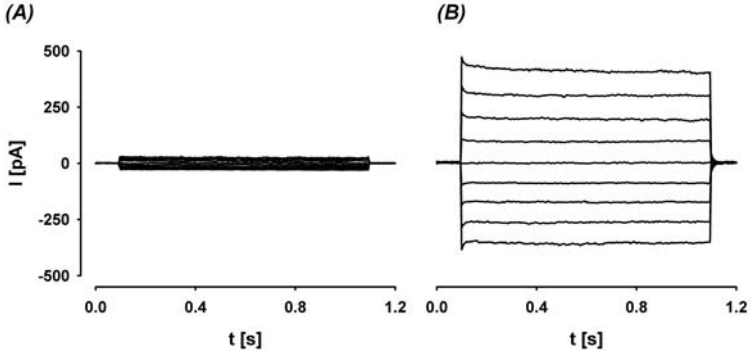

Figure 1. CFTR conductance in m IMCD-K2 cell. (A) representative traces of basal current; (B) representative traces of forskolin-activated (10 μM) current. Cells were held at 0 mV and pulsed between ±80 mV in 20 mV steps. Cationic currents were blocked by NMDG.

4.1 The CFTR

CFTR-like channel activity has been shown to be associated with the apical membrane (and transepithelial Cl^- secretion) in IMCD cell lines.[18]

Forskolin-stimulated whole cell currents were time independent (Figure 1) and the I/V relationship was linear. These results are typical for CFTR and substantiate the observations of Vandorpe et al.[19] who examined 8-(4 chlorophenylthio)-adenosine 3',5' cyclic-monophosphate (CPTcAMP) stimulation of whole cell currents using the fast whole cell patch configuration. The conductance showed an anion selectivity of $Cl^- = Br^- > I^-$.[19]

4.2 The CaCC

Since the renal deficit in cystic fibrosis is not profound compared with pancreas or small intestine (but see Simmons[20] for a discussion of studies of renal deficit in cystic fibrosis patients), alternative mechanisms must exist to compensate for loss of CFTR function.[21] Thus, it is likely that multiple Cl^- channels are expressed in renal epithelial cells. The proposed candidate that could substitute for CFTR is CaCC (for review about function of CaCC in kidney, see Boese et al.[22]).

In IMCD epithelial layers, ATP, bradykinin and ionomycin stimulated an inward I_{sc} dependent upon basal medium Na^+ and Cl^-/HCO_3^- but independent of the presence of apical bathing medium Na^+ and Cl^-/HCO_3^- .[4, 23]

Moreover, extracellular ATP stimulated a transient increase in both whole cell Cl^- conductance (selectivity: $I^- > Br^- > Cl^-$ [4]) and intracellular free Ca^{2+} ($[Ca^{2+}]_i$). In contrast, ionomycin caused a sustained increase in whole cell Cl^- conductance (Figure 2A). Preloading cells with the Ca^{2+} buffer BAPTA abolished the ATP-dependent responses and delayed the onset of the increase observed with ionomycin.[4] Removal of extracellular Ca^{2+} had no major effect on the peak Cl^- conductance or the increase in $[Ca^{2+}]_i$ induced by ATP, suggesting that Ca^{2+} released from intracellular stores directly activates CaCC.

A rectifying, time and voltage-dependent current was observed when $[Ca^{2+}]_i$ was fixed between 100-500 nM via patch pipette. Maximal activation occurred at around 1 μM $[Ca^{2+}]_i$ with currents displaying a linear I/V relationship (Figure 2Bd and References 4, 24). From Ca^{2+}-dose response curves an EC_{50} value of around 650 nM at -80 mV was obtained suggesting that under physiological conditions, the CaCC would be almost fully activated by mucosal nucleotides.[24]

Our data indicates that CaCC in mIMCD-K2 cells is a Cl^- channel whose activity is tightly coupled to changes in $[Ca^{2+}]_i$ over the normal physiological range.[24]

4.3 Chloride Channels and Calcium-Activated Chloride Channels

Besides CFTR, other identified anion channels have been found in the IMCD. They belong to the CLC (9 member, voltage-activated Cl^- channels) and the CLCA (4 member, Ca^{2+}-activated Cl^- channels [Figure 2] families of ion channels) [For review, see Jentsch et al.[25]]. Surprisingly, RT-PCR showed expression of nearly all members of the CLC and the CLCA families in the IMCD (Mike Glanville, personal communication).

Why so many different anion channels are expressed in the IMCD is still unclear, but some members of the CLC family are thought to be endosomal anion channels.[25]

CLC-3 is regarded by some investigators as the molecular identity of VRAC, (see 4.4) but this assumption is still highly controversial, e.g., pro[26] contra.[27]

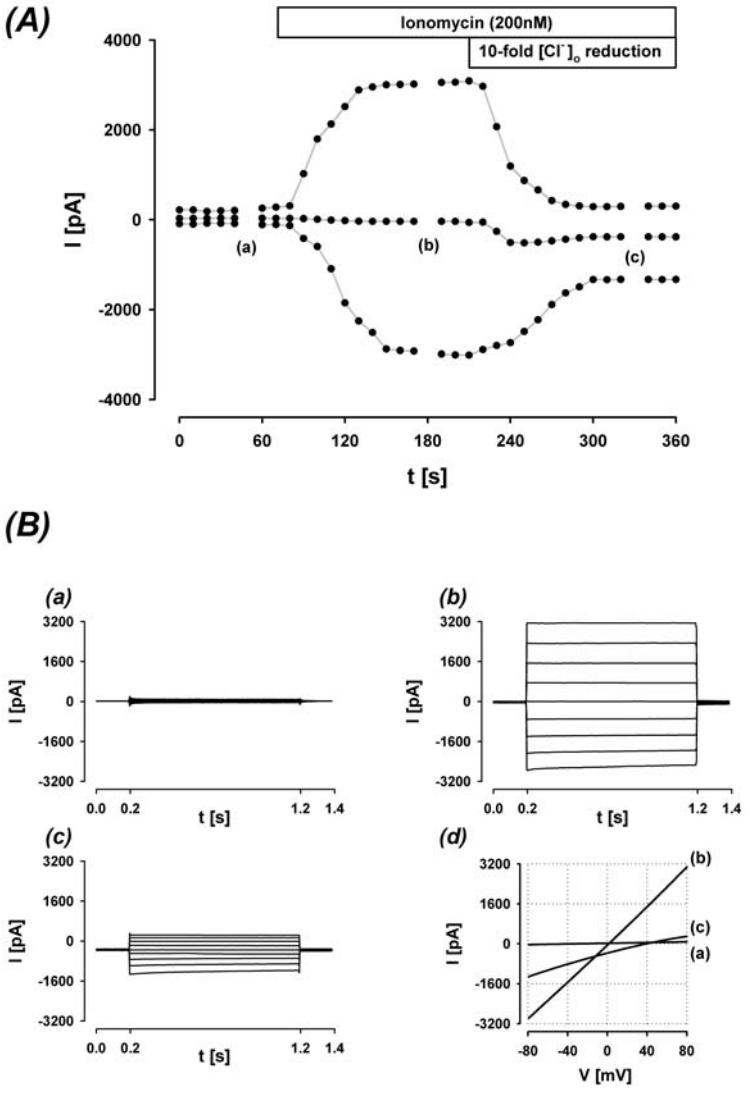

Figure 2. Activation of the CaCC by ionomycin in mIMCD-K2 cells. (A) Example of a typical experiment showing the change in whole cell current measured at +80, 0 and -80 mV evoked by bath application of 200 nM ionomycin. At points labeled a-c, the pulse protocol was interrupted in order to obtain current profiles and I/V relationships (see B below). (*Ba*) Example of a family of basal (control) whole cell currents at voltages between -80 and +80 mV (20 mV increment steps) starting from a holding potential of 0 mV (*Bb*) 120 s after ionomycin application, (*Bc*) whole cell currents after bath chloride was reduced 10-fold, 240 s after ionomycin application. (*Bd*) voltage ramps (-80 mV to 80 mV, 1 s duration) performed under conditions (*a*) to (*c*)

Members of the CLCA family are thought to be Ca^{2+}-activated Cl^- channels,[28] but so far, only whole cell patch clamp measurements with non-physiological $[Ca^{2+}]_i$ have been done (2 mM). Furthermore, at this point, it cannot be excluded that CLCA proteins activate endogenous Cl^- channels rather than being channels themselves.[25]

Recently, yet another family of anion channels has started to emerge: the vitelliform macular dystrophy protein bestrophin.[29] Some of the family members seem to be Ca^{2+}-activated anion channels, e.g., hBest1[29] and xBest2.[30] In contrast to the CLCA family, the Ca^{2+} dependence of the Best proteins lies within the physiological range (EC_{50} ~ 200-250 nM).[30]

Further investigations are needed to identify the molecular correlates of VRAC and CaCC in the renal IMCD.

4.4 The VRAC

A reduction in extracellular osmolality at constant ionic strength increases whole cell conductance in IMCD cells which is reversed upon restoration of standard bath tonicity.[31, 32] Responsible for this increase in whole cell current is a volume-regulated Cl^- conductance (VRAC). Currents activated by exposing the cells to hypotonicity exhibited characteristic outward rectification and time- and voltage-dependent inactivation at positive potentials (Figure 3) and showed an anion selectivity of $I^- > Br^- > Cl^- > Asp^-$. Furthermore, this conductance is permeable for organic osmolytes like taurine.[32] 5-nitro-2-(3-phenylpropylamino) benzoic acid (NPPB) inhibited the current in a voltage independent manner, as did exposure to tamoxifen and niflumic acid (NFA). In contrast, 4,4'-diisothiocyanatostilbene-2,2'-disulfonic acid (DIDS) blocked the current with a characteristic voltage dependency.[31] Single channel conductances of 35 pS at negative holding potentials and 75 pS at positive holding potentials were found.[33]

These properties closely resemble those reported for other cell types, including, glial,[34] intestinal,[35] and primary cultured kidney cells.[32] Variation in these basic properties occur mainly in the response to pharmacological agents and in the exact voltage dependence of VRAC.

These characteristics of VRAC in mIMCD-K2 cells are essentially identical to those of heterologously expressed cardiac CLC-3 (see 4.3). A defining feature of CLC-3 is that activation of protein kinase C (PKC) by phorbol 12,13-dibutyrate (PDBu) inhibits the conductance. In mIMCD-K2 cells, pre-incubation with PDBu prevented the activation of VRAC by hypotonicity. However, PDBu inhibition of VRAC was reversed after PDBu withdrawal, but this was refractory to subsequent PDBu inhibition.[31]

Thus, VRAC in the IMCD is a close relative to VRAC found in many other tissues, and its molecular identity is still in doubt.

5. INTERACTIONS

5.1 CFTR & CaCC

As shown above, the renal IMCD possesses a Ca^{2+}- and a cAMP-dependent anion conductance (4.1 & 4.2). A pharmacological distinction between Ca^{2+}-activated and forskolin-activated Cl^- currents may only be made by using DIDS. Ionomycin-stimulated

whole cell currents were reduced to ~50% of control values, whereas forskolin-stimulated currents were unaffected in the presence of DIDS.[4] All other commonly used anion channel blockers, e.g., NPPB and glibenclimide, inhibited both conductances to nearly the same extent.[36]

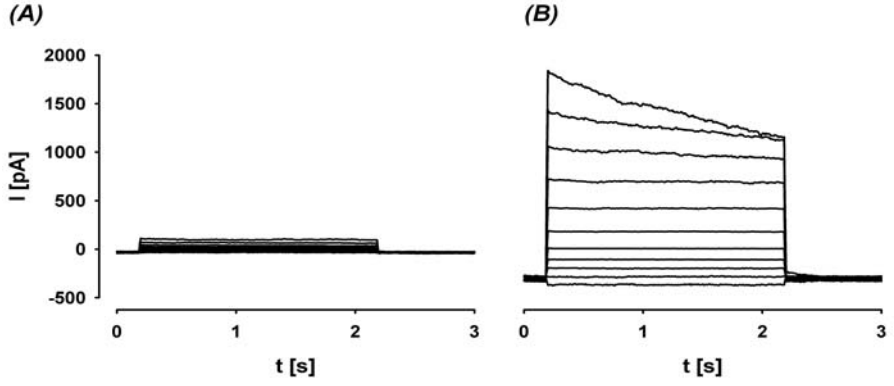

Figure 3. Voltage-dependence of VRAC whole-cell currents. The voltage protocol used was −80 to +120 mV in 20 mV increments starting from a holding potential of −60 mV. (*A*) Isotonic control conditions, (*B*) 10 min after hypotonic shock. Cationic currents were blocked by NMDG.

Furthermore, I_{sc} measurements confirmed that DIDS is a potent drug to distinguish between CFTR- and CaCC-dependent Cl^- secretion in the IMCD. Whereas Ca^{2+}-activated Cl^- secretion was fully blocked after DIDS application, cAMP-dependent Cl^- secretion was unaffected (Figure 4).

Both conductances reside in the apical membrane. In contrast, a basolateral location of the Ca^{2+} activated Cl^- conductance would short circuit secretion stimulated via apical CFTR[18] by enhancing futile cycling across the basolateral membrane.[37] Accordingly, the effect of ionomycin was tested alone and in combination with forskolin. After stimulation with forskolin, ionomycin addition provided a further (peak) stimulation of inward I_{sc}. This suggests that both Ca^{2+}-activated and cAMP-activated Cl^- channels are present at the apical membrane.[4]

Furthermore, a key observation from whole cell recordings was that both Ca^{2+}-activated and forskolin-activated Cl^- conductances coexist in the same cells, since additive activation of whole cell currents are observed by maximal stimulation with forskolin plus ATP.[4] Thus, mIMCD-K2 cells are similar to other secretory cells.[38] In addition, this observation argues against the possibility that an intermediate, e.g., prostaglandin, is involved in the stimulation of CFTR Cl^- currents by ATP.

5.2 VRAC & CaCC

Reducing the osmolality of the bath solution by dilution with distilled water or omission of uncharged sugars activated VRAC (Figure 4.4). However, changing both ionic composition concurrently with bath osmolality had additional effects on cellular conductance. The activation of VRAC was preceded by a brief and transient activation of an

additional Cl^- conductance with characteristics that were distinct and resembled CaCC.[31] Activation of CaCC has always been correlated with an increase in intracellular $Ca^{2+}]_i$. During hypotonic challenge a global increase in $[Ca^{2+}]_i$ could not be detected, suggesting that only a local change in $[Ca^{2+}]_i$ close to the membrane occurs.

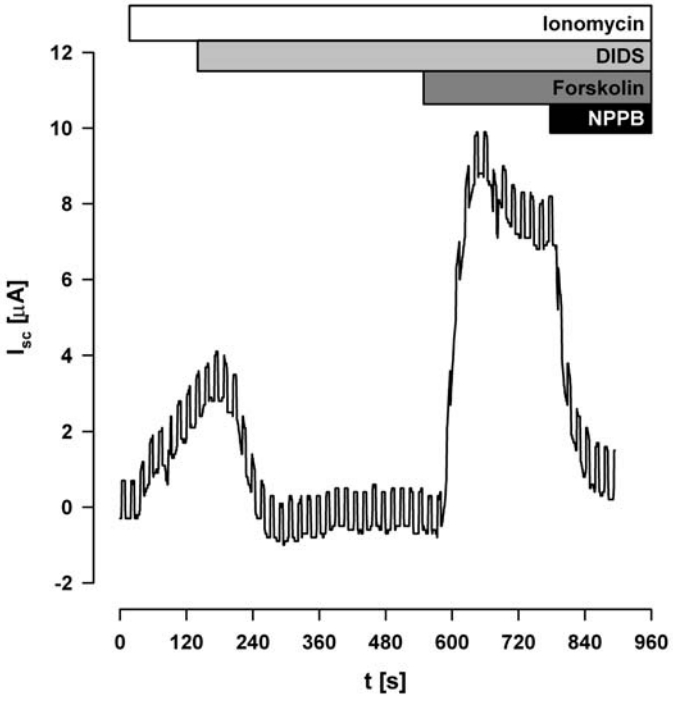

Figure 4. DIDS discriminates between CaCC and CFTR. 100 nM ionomycin gives a progressive stimulation of I_{sc} which is inhibited by 500 µM DIDS. Subsequent addition of 10 µM forskolin to the basal bathing solution results in prompt stimulation of inward I_{sc} which is inhibited by apical NPPB (50 µM). Representative of 4 experiment layers.

Taken together, these results indicate changes in $[Ca^{2+}]_i$ are not required for VRAC activation,[31] but even small changes in extracellular ionic conditions in concert with osmolality changes will activate more than one Cl^- conductive pathway.

5.3 CFTR, CaCC & VRAC

CFTR and CaCC are involved in transepithelial Cl^- secretion and are present at the apical plasma membrane (see 4.1, 4.2, & 5.1). VRAC activation in I_{sc} experiments inhibited CFTR- and CaCC-mediated Cl^- secretion.[31] This can be explained by the localization of VRAC to the basolateral membrane. Activation of VRAC will therefore control transepithelial anion secretion by decreasing the electrochemical driving force for Cl^- across the apical membrane.

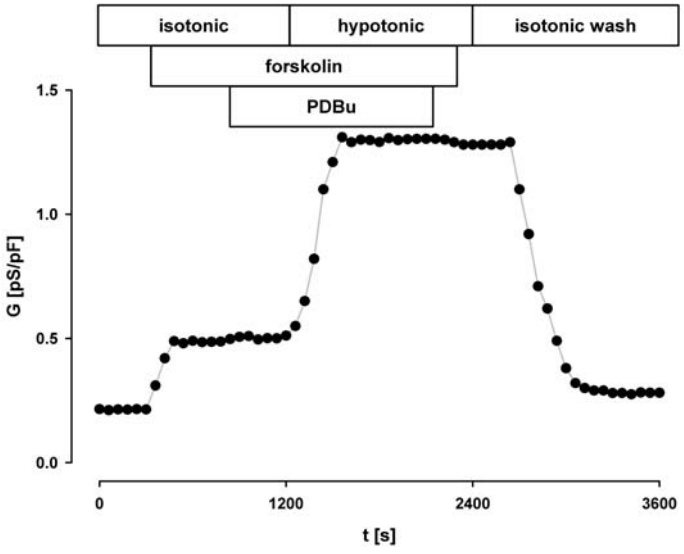

Figure 5. Sequential experimental data where CFTR activation by forskolin (10 μM) abolishes the inhibitory effect of PDBu pre-incubation (100 nM) on the development of VRAC. Inactivation of VRAC occurs upon restoration of medium tonicity.

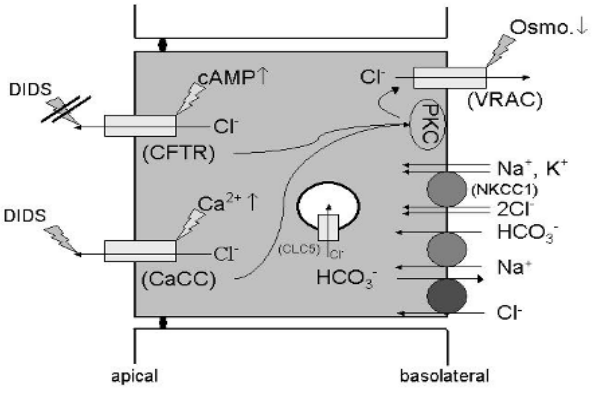

Figure 6. Summary of systems involved in Cl^- transport in renal IMCD. Basolateral located transport systems can accumulate Cl^- above its electrochemical equilibrium.[39] Activated by diverse stimuli apical and basolateral-positioned anion conductive passways can thereafter release Cl^- from the cell. For further information see text.

As mentioned (4.4), VRAC activation could be blocked by PKC activation prior to a hypotonic challenge. On the other hand, PKC activation had no effect on CFTR or CaCC when applied before or after activation of these conductances.[31] Activation of the CFTR or the Ca^{2+}-activated Cl^- conductance, which are coexpressed in mIMCD-K2 cells (5.1)

prior to PDBu treatment, abolished the PDBu inhibition of VRAC (Figure 5). Further effects of an active CaCC or CFTR conductance on VRAC could not be detected.

Control of VRAC by PKC therefore depends on the physiological status of the cell.[31]

6. CONCLUSIONS

In addition to being a major player in cellular volume regulation, VRAC, in concert with CFTR and CaCC, can tightly regulate chloride secretion and thereby, fluid movement in the IMCD (Figure 6).

7. ACKNOWLEDGMENTS

We are grateful to Omar Aziz, Michael Glanville, John A. Sayer, and Gavin S. Stewart for their support and involvement in our research. This work was supported by the Wellcome Trust (UK) & the National Kidney Research Fund (UK).

8. REFERENCES

1. F.X. Beck, A. Dröge, and K. Thurau, Cellular osmoregulation in renal medulla, *Renal Physiol. Biochem.* **11**, 174-186 (1988).
2. F. Wehner, H. Olsen, H. Tinel, E. Kinne-Saffran, and R.K.H. Kinne, Cell volume regulation: osmolytes, osmolyte transport, and signal transduction, *Rev. Physiol. Biochem. Pharmacol.* **148** (1), 1-80 (2003).
3. R.K.H. Kinne, S.H. Boese, E. Kinne-Saffran, B. Ruhfus, H. Tinel, and F. Wehner, Osmoregulation in the Renal Papilla — Membranes, Messengers and Molecules, *Kidney Int.* **49**, 1686-1689 (1996).
4. S.H. Boese, M. Glanville, O. Aziz, M.A. Gray, and N.L. Simmons, Ca^{2+} and cAMP-activated Cl^- conductances mediate Cl^- secretion in a mouse renal inner medullary collecting duct cell line, *J. Physiol. (London)* **523.2**, 325-338 (2000).
5. N.L. Kizer, D. Vandorpe, B. Lewis, B. Bunting, J. Russell, and B.A. Stanton, Vasopressin and cAMP stimulate electrogenic chloride secretion in an IMCD cell line, *Am. J. Physiol. Renal. Physiol.* **268**, F854-F861 (1995).
6. C. Zhang, R.F. Husted, and J.B. Stokes, Effect of cAMP agonists on cell pH and anion transport by cultured rat inner medullary collecting duct cells, *Am. J. Physiol. Renal. Physiol.* **270**, F131-F140 (1996).
7. N.L. Kizer, B.Lewis, and B.A. Stanton, Electrogenic sodium absorption and chloride secretion by an inner medullary collecting duct cell line (mIMCD-K2), *Am. J. Physiol. Renal. Physiol.* **268**, F347-355 (1995).
8. R.F. Husted and J.B. Stokes, Separate regulation of Na^+ and anion transport by IMCD: location, aldosterone, hypertonicity, TGF-β1 and cAMP, *Am. J. Physiol. Renal. Physiol.* **271**, F433-F439 (1996).
9 R.F. Husted, C. Zhang, and J.B. Stokes, Concerted actions of IL-1β inhibit Na+ absorption and stimulate anion secretion by IMCD cells, *Am. J. Physiol. Renal. Physiol.* **275**, F946-F954 (1998).
10. D.P. Wallace, L.A. Rome, L.P. Sullivan, and J.J. Grantham, cAMP-dependent fluid secretion in rat inner medullary collecting ducts, *Am. J. Physiol. Renal. Physiol.* **280**, F1019-F1029 (2001).
11. K.M. Madsen, W.L. Clapp, and J.W. Verlander, Structure and function of the inner medullary collecting duct, *Kidney Int.* **34**, 441-454 (1988).
12. P.S. Chandhoke, G.M. Saidel, and M.A. Knepper, Role of inner medullary collecting duct NaCl transport in urinary concentration, *Am. J. Physiol. Renal. Physiol.* **249**, F688-.F697 (1985).
13. J.P. Kokko, The role of the collecting duct in urinary concentration, *Kidney Int.* **31**, 606-610 (1987).
14. J.J. Grantham and D.P. Wallace, Return of the secretory kidney, *Am. J. Physiol. Renal. Physiol.* **282**, F1-F9 (2002).
15. E.K. Schwiebert, D.P. Wallace, G.M. Braunstein, S.R. King, J. Peti-Peterdi, K. Hanaoka, W.B. Guggino, L.M. Guay-Woodford, P.D. Bell, L.P. Sullivan, J.J. Grantham, and A.L. Taylor, Extracellular nucleotide signalling along the renal epithelium, *Am. J. Physiol. Renal. Physiol.* **282**, F763-F775 (2002).
16. F. Ciampolillo, D.E. McCoy, R.B. Green, K.H. Karlson, A. Dagenais, R.S. Molday, and B.A. Stanton, Cell specific expression of amiloride-sensitive, Na^+-conducting ion channels in the kidney, *Am. J. Physiol. Cell Physiol.* **271**, C1303-1315 (1996).

17. D. H. Vandorpe, F. Ciampolillo, R. B. Green, and B. A. Stanton, Cyclic nucleotide-gated cation channels mediate sodium absorption by IMCD (mIMCD-K2) cells, *Am. J. Physiol. Cell. Physiol.* **272**, C901-C910 (1997).
18. R. F. Husted, K. A. Volk, R. D. Sigmund, and J. B. Stokes, Anion secretion by the inner medullary collecting duct, *J. Clin. Invest.* **95**, 644-650 (1995).
19. D.H. Vandorpe, N.L. Kizer, F. Ciampollilo, B. Moyer, K. Karlson, W.B. Guggino, and B.A. Stanton, CFTR mediates electrogenic secretion in mouse inner medulla collecting duct (mIMCD-K2) cells, *Am. J. Physiol. Cell Physiol.* **269**, C683-C689 (1995).
20. N.L. Simmons, Renal epithelial Cl^- secretion, *Exp. Physiol.* **78**, 117-137 (1993).
21. M.A. Gray, J.P. Winpenny, B. Verdon, C.M. O'Reilly, and B.E. Argent, Properties and role of calcium-activated chloride channels in pancreatic duct cells, *Current Topics in Membr*anes **53**, 231-256 (2002).
22. S.H. Boese, J. Sayer, G. Stewart, M. Glanville, M.A. Gray, and N.L. Simmons, Renal expression of Ca^{2+} -activated Cl^- channels, *Current Topics in Membranes* **53**, 283-307 (2002).
23. H. Kose, S.H. Boese, M. Glanville, M.A. Gray, C.D.A. Brown, and N.L. Simmons, Bradykinin regulation of salt transport across mouse inner medullary duct epithelium involves activation of a Ca^{2+}-dependent Cl^- conductance, *Br. J. Pharmacol.* **131**, 1689-1699 (2000).
24. S.H. Boese, O. Aziz, M.A. Gray, and N.L. Simmons, Intracellular Ca^{2+} directly regulates the Ca^{2+}-activated Cl^- conductance in mouse inner medullary collecting duct cells, *J. Gen. Physiol.* **122**, 87 (2003).
25. T.J. Jentsch, V. Stein, F. Weinreich, and A.A. Zdebik, Molecular Structure and Physiological Function of Chloride Channels, *Physiol. Rev.* **82**, 503-568 (2002).
26. G.-X. Wang, W.J. Hatton, G.L. Wang, J. Zhong, I. Yamboliev, D. Duan, and J.R. Hume, Functional effects of novel anti-ClC-3 antibodies on native volume-sensitive osmolyte and anion channels in cardiac and smooth muscle cells, *Am. J. Physiol. Heart Circ. Physiol.*, **285**(4), H1453-1463 (2003).
27. X. Li, T. Wang, Z. Zhao, and S.A. Weinman, The ClC-3 chloride channel promotes acidification of lysosomes in CHO-K1 and Huh-7 cells, *Am. J. Physiol. Cell. Physiol.* **282**, 1483-1491 (2002).
28. S.A. Cunningham, M.S. Awayda, J.K. Bubien, I.I. Ismailov, M.P. Arrate, B.K. Berdiev, D.J. Benos, and C.M. Fuller, Cloning of an Epithelial Chloride Channel from Bovine Trachea, *J. Biol. Chem.* **270**, 31016-31026 (1995).
29. H. Sun, T. Tsunenari, K.-W. Yau, and J. Nathans, The vitelliform macular dystrophy protein defines a new family of chloride channels, *P.N.A.S. USA* **99**: 4008-4013 (2002).
30. Z. Qu, R.W. Wei, W. Mann, and H.C. Hartzell, Two Bestrophins cloned from *Xenopus laevis* oocytes express Ca-activated Cl- currents, *J. Biol. Chem.* **10.1074**/jbc.M308414200 (2003).
31. S.H. Boese, M. Glanville, M.A. Gray, and N.L. Simmons, The Swelling-Activated Anion Conductance in the Mouse Renal Inner Medullary Collecting Duct Cell Line mIMCD-K2, *J Membrane Biol* **177**, 51–64 (2000).
32. S.H. Boese, F. Wehner, and R.K.H. Kinne, Taurine permeation through swelling-activated anion conductance in rat IMCD cells in primary culture, *Am. J. Physiol. Renal. Physiol.* **271**, F498-F507 (1996).
33. S.H. Boese, R.K.H. Kinne, and F. Wehner, Single-channel properties of swelling-activated anion conductance in rat inner medullary collecting duct cells, *Am. J. Physiol. Renal. Physiol.* **271**, F1224-F1233 (1996).
34. P.S. Jackson and K. Strange, Volume-sensitive anion channels mediate swelling-activated inositol and taurine efflux, *Am. J. Physiol. Cell Physiol.* **5**, C1489-C1500 (1993).
35. M. Kubo and Y. Okada, Volume-regulatory Cl^- channel currents in cultured human epithelial cells, *J Physiol.(London)* **456**, 351-371 (1992).
36. S.H. Boese, M.A. Gray, and N.L. Simmons, Pharmacological inhibition of cAMP and Ca^{2+}-activated Cl^--conductances at the apical membrane of mouse renal inner medullary collecting duct cells (mIMCD-K2), *J. Physiol. (London)* **520**P, 44P (1999).
37. N.L. Simmons, The effect of hypoosmolarity upon transepithelial ion transport in cultured renal epithelial layers (MDCK), *Pflügers Arch. – Eur. J. Physiol.* **419**, 572-579 (1991).
38. M.P. Anderson and M.J. Welsh, Calcium and cAMP activate different chloride channels in the apical membrane of normal and cystic fibrosis epithelia, *P.N.A.S. USA* **88**, 6003-6007 (1991).
39. M. Glanville, S. Kingscote, D.T. Thwaites and N.L. Simmons, Expression and role of sodium, potassium, chloride cotransport (NKCC1) in mouse inner medullary collecting duct (mIMCD-K2) epithelial cells, *Pflügers Arch. – Eur. J. Physiol.* **443**, 123–131 (2001).

11

SECRETORY CONTROL OF BASOLATERAL MEMBRANE POTASSIUM AND CHLORIDE CHANNELS IN COLONIC CRYPT CELLS

Dan R. Halm*

Fluid secretion across epithelia generally is driven by the active secretion of ions and serves to lubricate surfaces and propel macromolecules such as mucus.[1, 2] In the colonic epithelium, secretion of Cl^- and K^+ is activated to drive water movement into the lumen. Several types of signals act to initiate this secretion, including nerve activity and paracrine release from cells in the intestine. Two potent stimulators of this Cl^- and K^+ secretion are cholinergic nerves and prostaglandins released from cells in the intestinal mucosa and muscle. K^+ secretion without concurrent Cl^- secretion also is stimulated through these routes, specifically by epinephrine acting via -adrenergic receptors and by prostaglandin-E_2 acting via prostanoid EP2 receptors.[3, 4]

The cellular mechanism for primary K^+ secretion[3] is similar to the standard model for Cl^- secretion,[1] except that apical membrane Cl^- channels need not open (Figure 1). Functional measures of K^+ and Cl^- secretion[5-7] support the concept that the columnar cells of colonic crypts are capable of both modes of ion secretion, and simply respond to distinct classes of secretagogues by activating different sets of ion transporters. Thus, the dependence of K^+ secretion on operation of Na^+:K^+:2Cl^--cotransporters in the basolateral membrane requires that another transport protein coordinates Cl^- exit back across the basolateral membrane. Together, the requirements for maintaining a stable intracellular Cl^- concentration and membrane electrical potential difference could be satisfied by the presence of basolateral membrane Cl^- channels.

Activation of either Cl^- or K^+ secretion obviously requires increased flow through each one of the transport proteins involved (Figure 1). For these ion secretions, the changes in driving forces are too small to be responsible for the increased flow. Both the ion concentration gradients[5, 6] and membrane electrical potential[7] are largely unchanged during sustained ion secretion in the colonic epithelium, so that the permeability of each transporter must increase either through greater numbers becoming present in the membrane or by higher activity. Apparently, maintaining a fairly constant cellular

* Dan R. Halm, Department of Anatomy and Physiology, Wright State University, Dayton, OH 45435.

environment is a prerequisite for any additional functions that might be performed by these cells. A consequence of operating cellular processes in this manner is that intracellular signaling pathways must coordinate the activity of all components in any particular functional system such that the overall cellular steady-state is maintained.

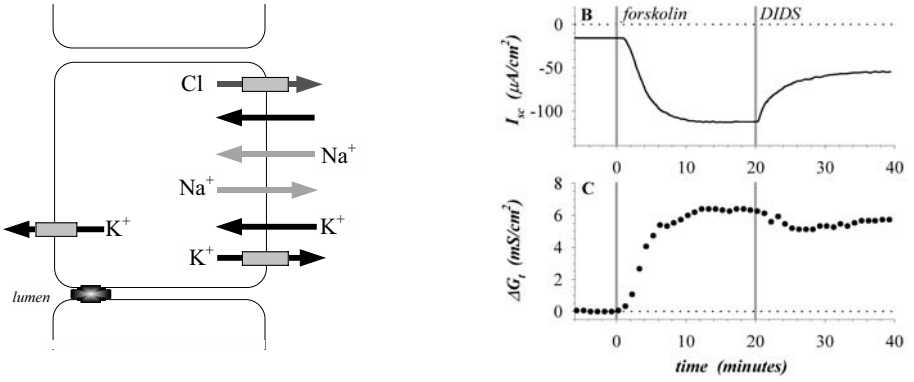

Figure 1. The cellular model for electrogenic K^+ secretion in distal colonic epithelium (A) would make the lumen positive with respect to the interstitium, in contrast to Cl^- secretion. Transepithelial current (I_{sc} ;B) and conductance (G_t ;C) were measured in guinea pig colonic mucosa. Forskolin added to the serosal bath [300 nM] stimulated a response consistent with K^+ secretion; serosal DIDS [100 μM] partially inhibited this response. From reference 8, with permission.

Secretion of Cl^- is activated through cAMP-dependent as well as Ca^{++}-dependent signaling.[1] In the intestinal mucosa, these signaling pathways correspond to initiation via specific receptors such as vasoactive intestine peptide and acetylcholine, respectively. However, other receptors that are thought to act via cAMP, in particular -adrenergic and prostanoid EP2, lead to electrogenic K^+ secretion without any accompanying sustained Cl^- secretion.[3, 4] This conflict in the use of cAMP to activate two distinct modes of ion secretion is not resolved by separate cell types for each, since crypt columnar cells appear capable of both K^+ and Cl^- secretion.[5, 6] The resolution of this problem likely involves other intracellular signaling pathways that add to the cAMP actions in order to coordinate all of the transporters.

The connection of K^+ secretion with activation through cAMP-dependent signaling is supported by the action of forskolin, which activates adenylyl cyclase, to stimulate transepithelial current (I_{sc}) and conductance (G_t) in guinea pig distal colon[8] (Figure 1). At higher concentrations (>1 μM), forskolin also stimulates Cl^- secretion along with the K^+ secretion.[8] Seemingly, cAMP alone would be insufficient to sustain both of these secretory modes. Specifically, K^+ channels in the apical and basolateral membrane guide the K^+ flow and determine the rate of K^+ secretion. Similarly, apical and basolateral Cl^- channels govern the path of Cl^- flow and how much will be secreted into the lumen. Thus, the opening of apical membrane Cl^- channels and basolateral membrane K^+

channels that favors Cl^- secretion must be repressed at low forskolin concentration in order to produce the observed primary K^+ secretion.

Control of basolateral membrane K^+ and Cl^- channels becomes crucial to the determination of ion secretory rates because these conductive pathways not only help direct ion flow but also contribute to setting the membrane electrical potential such that both K^+ and Cl^- will exit through the channels that open. Although activating basolateral K^+ channels hastens Cl^- secretion by hyperpolarizing the membrane potential and thereby increasing the electrochemical gradient for Cl^- exit, increased basolateral K^+ conductance reduces K^+ secretion by leading K^+ back out across the basolateral membrane (Figure 1). Instead, during K^+ secretion, basolateral K^+ conductance needs to be moderated in order to redirect K^+ exit into the lumen. Similarly, basolateral Cl^- conductance aids K^+ secretion by providing an exit path for Cl^- entering via Na^+:K^+:2Cl^--cotransporters, but this Cl^- conductance needs to be minimized during Cl^- secretion in order to favor Cl^- exit into the lumen.

1. ACTIVATION OF BASOLATERAL K^+ CHANNELS

Several types of K^+ channels have been observed in the basolateral membranes of intestinal crypt cells.[9-17] Specifically, large conductance K^+ channels have been seen[9, 10, 13, 15, 16, 18, 19] that may be the Ca^{++}-activated BK channel [KCNMA][20] as well as smaller inwardly rectified and Ca^{++}-activated channels[10, 12, 15, 21] that resemble the IK channel [KCNN4].[20] In addition, a cAMP-activated K^+ conductance occurs in rat colonic crypts that is likely due to KvLQT channels [KCNQ].[11, 22] Guinea pig colonic crypts exhibit an inwardly rectified K^+ channel (Figure 2) that is unlikely to be IK because changes in Ca^{++} activity at the intracellular face of the channel do not alter open probability (P_o).[16] An interesting feature of the rectified behavior of this K^+ channel is that current flow is not rectified when extracellular K^+ is at a low, physiologic, concentration of 5 mM. Apparently, the lower external K^+ concentration reduces inward current flow in proportion to the degree of conductive rectification so that the current-voltage relation of this particular K^+ channel is linear under physiologic conditions, with a single channel conductance (γ) of 9 pS.

Activity of this inwardly rectified K^+ channel in guinea pig crypts ($^{gp}K_{ir}$) is altered by the secretagogues that produce Cl^- and K^+ secretion.[16] Spontaneous activity of $^{gp}K_{ir}$ occurs in two apparent modes with high and low P_o (Figure 2). Stimulation of a Cl^- secretory state with high concentration forskolin activates previously quiescent $^{gp}K_{ir}$ and increases the P_o of those in the low activity mode. The similarity of the forskolin stimulated state with the spontaneous high activity mode suggests that this activity mode may result from basal cAMP activation. Interestingly, K^+ secretagogues such as epinephrine or PGE_2 activate $^{gp}K_{ir}$ with P_o values intermediate to the two spontaneous modes. In addition, any $^{gp}K_{ir}$ activated by forskolin or spontaneously at high P_o are inhibited by these K^+ secretagogues to an intermediate P_o level (Figure 2). Similarly, somatostatin inhibits the P_o of a K_{ir} in crypts from human colon.[15] Activation of $^{gp}K_{ir}$ to the high activity mode would enhance Cl^- secretion by increasing the driving force for apical Cl^- exit, whereas the intermediate activity mode with K^+ secretagogues would allow more K^+ to exit into the lumen.

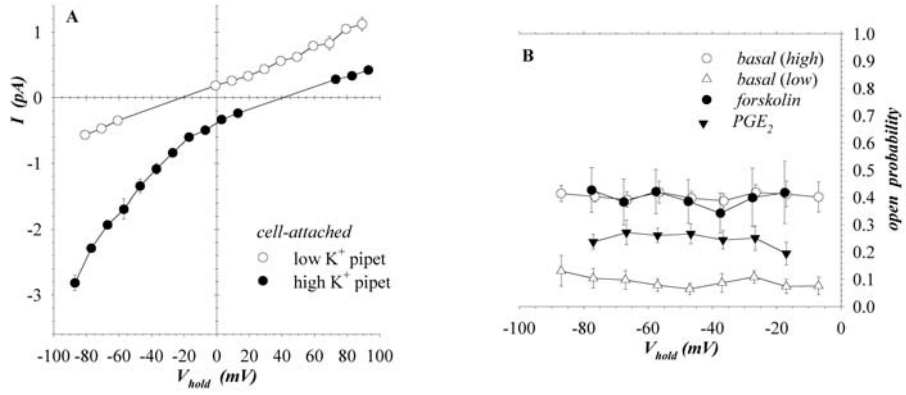

Figure 2. Single channel currents (A) of inwardly rectified K^+ channels were detected during cell-attached recording on the basolateral membrane of colonic crypts from guinea pig distal colon. Pipet solutions (extracellular face of channel) contained either 5 mM K^+ or 140mM K^+. Open probability (B) of these K^+ channels was calculated from the spontaneously observed condition (basal) or after stimulation of Cl^- secretion by forskolin [10 μM] or after stimulation of K^+ secretion by PGE_2 [100 nM]. Spontaneous activity occurred in two modes, either high activity or low activity. From reference 16, with permission.

The three distinct P_o modes that $^{gp}K_{ir}$ exhibits lend support to the concept that multiple intracellular regulators likely act to determine channel open status. Even though β-adrenergic and prostanoid EP2 receptors act to increase intracellular cAMP levels, the difference in response compared with forskolin suggests that another signal must be released by these receptors to produce the intermediate P_o mode. The low P_o mode may represent a transitional state not related to either the Cl^- or K^+ secretory states. Kinetic analysis of the single channel openings and closings further supports that $^{gp}K_{ir}$ activation occurs in several distinguishable modes (Figure 3).

The P_o of each activation mode can be characterized by the distribution of open and closed durations, such that an increased P_o could be accomplished through increasing open durations, decreasing closed durations or a combination of changes to both open and closed durations. The distribution of closed duration indicates the presence of six apparent closed states, similar to the kinetics of other K^+ channels.[16, 23] Forskolin activation of $^{gp}K_{ir}$ occurs almost solely through a decrease in the number of long closed lifetimes, without any change in the distribution of open lifetimes (Figure 3). These long duration closed lifetimes likely represent repressed states of the channel when it is essentially inactivated, such that the key activation event initiated by cAMP would be to limit entry into these repressed states.

Interestingly, even though the spontaneous high P_o mode and the forskolin mode have similar average P_o, the high P_o mode has a shorter mean open lifetime and fewer short duration closed events. These kinetic differences suggest that the high P_o mode is not simply the result of cAMP stimulation. Furthermore, excision of patches with $^{gp}K_{ir}$ in the low P_o or forskolin modes produced kinetics nearly identical to the high P_o mode, suggesting that an easily detached regulator is responsible for keeping $^{gp}K_{ir}$ out of the spontaneous high P_o mode.

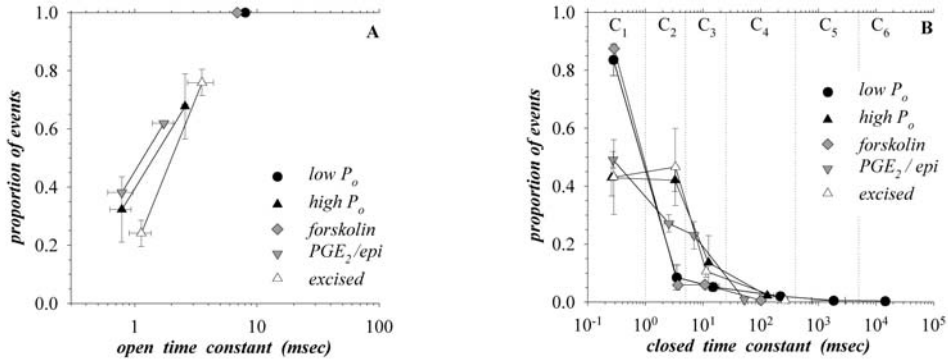

Figure 3. Kinetics of $^{gp}K_{ir}$ were analyzed to obtain the time constants of single channel openings (A) and closings (B), together with the proportion of events occurring with these mean lifetimes. Lines connect the multiple time constants found for specific modes of stimulation. The multiple closed time constants occurred in separable groups (C_n). From reference 16, with permission.

Conversion of $^{gp}K_{ir}$ kinetics into the K^+ secretagogue mode away from either the spontaneous high P_o mode or the forskolin mode occurs primarily through an increase in the proportion of closed duration events with an intermediate length mean lifetime (from C_2 into C_3). Thus, a relatively minor alteration in the distribution of closed lifetimes limits the P_o of $^{gp}K_{ir}$, reduces the basolateral membrane K^+ conductance and thereby favors K^+ secretion.

2. ACTIVATION OF BASOLATERAL Cl^- CHANNELS

Outwardly rectified Cl^- channels have been observed in the basolateral membranes of intestinal crypt cells, together with other types of Cl^- channels.[8, 13, 17, 24] These Cl^- channels may contribute to volume regulation[14, 25] as well as transepithelial transport. In particular, volume-activated Cl^- currents have outwardly rectified current-voltage relations, but the single channel identity of this channel type has not been conclusively resolved.[26] The outwardly rectified Cl^- channel actually may be the splice variant of the CLC3 Cl^- channel that allows that protein to be inserted into the plasma membrane.[27] Guinea pig colonic crypts exhibit two types of Cl^- currents based on current-voltage relations (Figure 4A), outwardly rectified ($^{gp}Cl_{or}$, γ of 29 pS at V_{hold}=0 mV) and linear ($^{gp}Cl_L$, γ subtypes of 21 pS, 13 pS, 8 pS).[8] At negative holding potentials, $^{gp}Cl_{or}$ has a conductance intermediate to $^{gp}Cl_{L21}$ and $^{gp}Cl_{L13}$. Whether these channel behaviors represent distinct proteins or are simply conductance and kinetic modes of a single channel protein cannot be resolved by comparison with known Cl^- channel types, since relatively little single channel characterization has been accomplished.

Further support for the distinct nature of these Cl^- currents is apparent from the voltage dependence of P_o (Figure 4B). Three of the conductance forms, $^{gp}Cl_{or}$, $^{gp}Cl_{L21}$ and $^{gp}Cl_{L13}$ have a voltage dependent P_o that is highest at positive holding potentials, but each has a unique relation. All three are half-activated at voltages depolarized from the resting

cell potential; $^{gp}Cl_{L13}$ has the steepest voltage dependence and the lowest minimum P_o (Table 1). The smallest in conductance of the group ($^{gp}Cl_{L8}$) has voltage independent P_o that occurs in two modes, either low at ~0.2 or higher at ~0.5. Together, these conductance and kinetic features support the presence of 4 separable Cl^- channel behaviors in the basolateral membrane of colonic crypt cells.

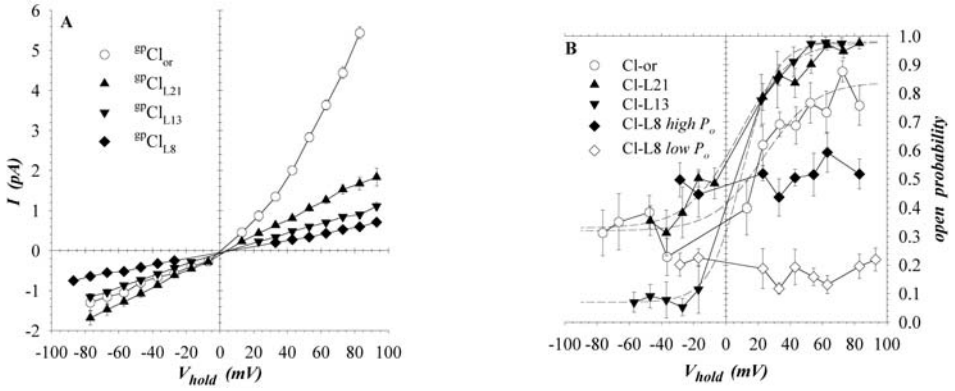

Figure 4. Single channel currents (A) of Cl^- channels were detected during cell-attached recording on the basolateral membrane of colonic crypts from guinea pig distal colon; four channel types were discernable. Open probability (B) of these Cl^- channels were calculated from the records. The voltage dependent relations were fit to Boltzmann distributions (dashed lines). From reference 8, with permission.

Table 1. Properties of $^{gp}Cl_{or}$ and $^{gp}Cl_L$

	γ (pS)	P_o	$V_{1/2}$ (mV)	z_g	action on N
$^{gp}Cl_{or}$	29.0	0.40 (0.20)	−18 (+23)	1.6 (1.0)	increase
$^{gp}Cl_{L21}$	21.4	0.55	−34	1.6	increase
$^{gp}Cl_{L13}$	13.2	0.35 (0.50)	−31	2.5	increase
$^{gp}Cl_{L8}$	8.3	0.19 or 0.54	-	-	increase

Shown are the mean of single-channel conductance (γ) and open probability (P_o) from figure 4 for $^{gp}Cl_{or}$ and $^{gp}Cl_L$ when cell-attached at spontaneous V_{cell} (V_{hold} = 0 mV).[8] Voltages at half-activation for P_o ($V_{1/2}$) and equivalent gating charges (z_g) are from fits to Boltzmann distributions in Figure 4. Values during K^+ secretagogue activation are shown in parentheses. Actions of K^+ secretagogues on channel number (N) are indicated.

Stimulation with K^+ secretagogues, such as epinephrine or low concentration PGE_2 and forskolin, increases the number of active Cl^- channels from each of the 4 groups (Table 1). This K^+ secretory activation also decreases the voltage dependence of $^{gp}Cl_{L13}$ such that the P_o is higher at the resting cell potential.[8] $^{gp}Cl_{or}$ channels activated by

epinephrine have a voltage dependence for P_o shifted to more positive values than for those activated by forskolin,[8] which occurs via several changes to the flickery kinetics of opening and closing (Figure 5). The predominant brief closures and longer open lifetimes of the spontaneous and forskolin modes are replaced by open and closed lifetimes of nearly the same length (~2ms). In addition, the intermediate length closed lifetime is voltage dependent during epinephrine stimulation, unlike the forskolin mode. This distinctive rapid kinetic mode of $^{gp}Cl_{or}$ is not induced by epinephrine addition during forskolin stimulation, suggesting that high cAMP may bar entry into this buzz mode. In other studies of Cl_{or}, a similar buzzing kinetic mode is produced by addition of small steroid-like molecules,[28] which suggests that the epinephrine induced mode may be produced through a signaling molecule with a similar chemical nature. Excision of patches containing $^{gp}Cl_{or}$ leads to a high, voltage-independent P_o. And, when epinephrine-activated $^{gp}Cl_{or}$ are excised, the buzzing kinetics revert to the flickery mode.[8] Apparently, several easily dislodged control molecules are present that contribute to determining the kinetic modes of $^{gp}Cl_{or}$ and thereby the activation status.

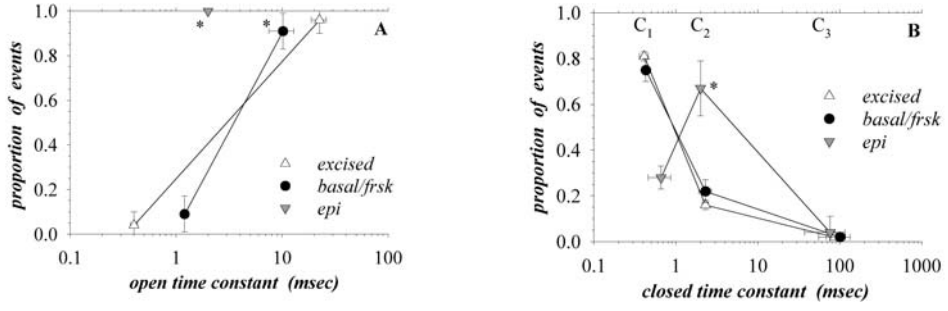

Figure 5. Kinetics of $^{gp}Cl_{or}$ were analyzed to obtain the time constants of single channel openings (A) and closings (B), together with the proportion of events occurring with these mean lifetimes. Lines connect the multiple time constants found for specific modes of activation. Voltage dependent time constants are indicated by an asterisk. The multiple closed time constants occurred in separable groups (C_n). From Reference 8, with permission.

Comparison of these Cl^- channels in the guinea pig distal colon with other recorded Cl^- currents is hampered because most of those findings are whole-cell currents without any single channel information. Using the single channel conductance and P_o, the time-averaged currents for the four channel types can be calculated (Figure 6) to allow direct comparison with whole-cell currents recorded in other cell types. Three of the four have outwardly rectified current voltage relations, $^{gp}Cl_{or}$, $^{gp}Cl_{L21}$ and $^{gp}Cl_{L13}$. The steep voltage dependence of $^{gp}Cl_{L13}$ produces a relation just as rectified as for $^{gp}Cl_{or}$, making these two Cl^- channel forms difficult to distinguish. However, activation with epinephrine or PGE_2 would lead to a nearly linear time-averaged current for $^{gp}Cl_{L13}$, such that activation status would aid in distinguishing $^{gp}Cl_{L13}$ from $^{gp}Cl_{or}$.

The most studied outwardly rectified Cl^- currents are those activated by cell swelling. However, several characteristics of these volume-activated Cl^- currents suggest

that Cl_{or} is not the volume activated Cl^- channel.[26] A more likely candidate protein for Cl_{or} is CLC3B, a splice variant of CLC3 found in epithelia, that is outwardly rectified and has similar kinetics[27]. Both $^{gp}Cl_{L21}$ and $^{gp}Cl_{L13}$ resemble the Cl^- channels of the CLC family.[29, 30] particularly due to the voltage dependence of P_o (Figure 4). The higher P_o at positive holding potentials is consistent with kinetics dominated by the fast gate. Although CLC2 could be considered a possibility because of a generally wide tissue distribution,[29] CLC2 is absent from crypt cells of guinea pig distal colon based on antibodies and *in situ* hybridization,[31] which suggests that another CLC channel protein would have to be involved. The small γ and voltage independent P_o of $^{gp}Cl_{L8}$ (Table 1) resembles the character of the CFTR Cl^- channel,[29] but this is scant information to support such an unusual placement and transport involvement for CFTR. Although definitive identification of the Cl^- channel types in colonic crypt cells cannot be made at present, the observed functional behavior of these channels may result from the combined action of channel and regulatory subunits.

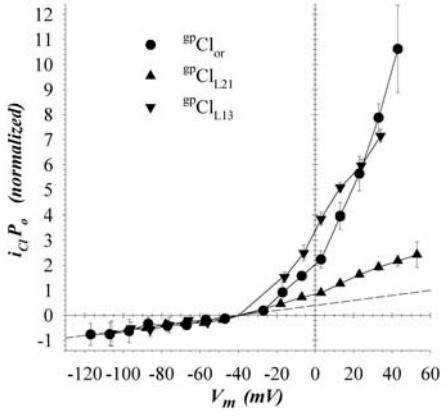

Figure 6. Time averaged Cl^- currents were calculated ($i_{Cl}P_o$) from the single channel current voltage relations and dependence of P_o on voltage (Figure 4). From Reference 8, with permission.

3. ELECTROGENIC K^+ SECRETION

Colonic epithelial cells are capable of secreting both Cl^- and K^+ by a common cellular mechanism involving Cl^- channels, K^+ channels, Na^+:K^+:2Cl^--cotransporters and Na^+/K^+-ATPase (Figure 1A). Although secretagogues initiate these ion secretions by opening apical membrane Cl^- and K^+ channels to provide a pathway for exit into the lumen, appropriate basolateral membrane ion conductance is equally important in order to set the electrochemical driving forces so that ion exit does occur at the apical membrane. During Cl^- secretion, sufficient basolateral K^+ conductance must be activated to ensure that the apical membrane potential is hyperpolarized from the value set by the apical Cl^- concentration gradient.[11, 12, 16] Similarly, sufficient basolateral Cl^- conductance is needed during primary K^+ secretion to assure a large driving force for K^+ exit across

the apical membrane.[8] In addition, during primary K^+ secretion, basolateral K^+ conductance is reduced to accentuate K^+ secretion by redirecting flow to apical K^+ channels.[16] Another consequence of this lower basolateral K^+ conductance is that the membrane electrical potential will be further from the K^+ equilibrium potential, thereby increasing the driving force for K^+ exit. Maximizing secretion thus becomes the role of intracellular signals to produce the balance of conductances that optimizes these driving forces for conductive K^+ and Cl^- exit at the apical and basolateral membranes.

The primary electrogenic K^+ secretion of the colonic epithelium[3,32] shares similarities with K^+ secretion in the thick ascending limb of Henle's loop of the kidney as well as the strial marginal cells in the stria vascularis and vestibular dark cells in the vestibular labyrinth of the inner ear.[33, 34] Each uses a slightly different combination of K^+ channels, Cl^- channels, Na^+:K^+:2Cl^--cotransporters and Na^+/K^+-ATPase to produce electrogenic K^+ secretion. Whereas the colonic epithelial cells respond to K^+ secretagogues by choosing K^+ secretion over Cl^- secretion, the thick ascending limb cells and inner ear cells appear set to perform one primary ion transport task. The thick ascending limb cells differ from the colonic epithelial cells and inner ear cells by having Na^+:K^+:2Cl^--cotransporters in the apical membrane rather than the basolateral membrane; but, both the thick ascending limb and inner ear cells have basolateral membranes conductive primarily to Cl^-, with little if any K^+ conductance. During activation with K^+ secretagogues, the colonic epithelial cells mimic this situation by reducing basolateral K^+ conductance. The variety of K^+ and Cl^- channels available in the genome[20, 29] presumably allows each of these epithelia to choose the specific versions most suited to the particular requirements needed in that cell. For the colonic crypt cells, the basolateral channel types present may suit the demands of coordinating responses to secretagogues with distinct Cl^- and K^+ secretory responses.

4. ACKNOWLEDGMENTS

These studies were supported by a grant from the National Institutes of Health, DK39007.

5. REFERENCES

1. E. Chang and M. Rao, Intestinal water and electrolyte transport: mechanisms of physiological and adaptive responses, in: *Physiology of the Gastrointestinal Tract*, L. Johnson, ed., (Raven Press, New York, 1994) 2027-2081.
2. D. Halm and S. Halm, Secretagogue response of goblet cells and columnar cells in human colonic crypts, *Am. J. Physiol (Cell Physiol.)* **277**, C501-C522, *corrigenda* **278**, C212-C233 (1999).
3. G. Rechkemmer, R. Frizzell and D. Halm, Active K^+ transport across guinea pig distal colon: action of secretagogues, *J. Physiol.* **493**, 485-502 (1996).
4. D. Halm and S. Halm, Prostanoids stimulate K^+ and Cl^- secretion in guinea pig distal colon via distinct pathways, *Am. J. Physiol., Gastrointest. Liver Physiol.* **281**, G984-G996 (2001).

5. D. Halm, K. Kirk and K. Sathiakumar, Stimulation of Cl^- permeability in colonic crypts of Lieberkühn measured with a fluorescent indicator, *Am. J. Physiol., Gastrointest. Liver Physiol.* **265**, G423-G431 (1993).
6. D. Halm and R. Rick, Secretion of K^+ and Cl^- across colonic epithelium: cellular localization using electron microprobe analysis, *Am. J. Physiol., Cell Physiol.* **262**, C1392-C1402 (1992).
7. E. Lohrmann and R. Greger, The effect of secretagogues on ion conductance of in vitro perfused, isolated rabbit colonic crypts, *Pflügers Arch.* **427**, 494-502 (1995).
8. Y. Li, S. Halm and D. Halm, Secretory activation of basolateral membrane Cl^- channels in guinea pig distal colonic crypts, *Am. J. Physiol., Cell Physiol.* **284**, C918-C933 (2003).
9. D. Loo and J. Kaunitz, Calcium and cAMP activate K^+ channels in the basolateral membrane of crypt cells isolated from rabbit distal colon, *J. Memb. Biol.* **110**, 19-28 (1989).
10. C. McNicholas, G. Fraser and G. Sandle, Properties and regulation of basolateral K^+ channels in rat duodenal crypts, *J. Physiol.* **477**, 381-392 (1994).
11. R. Warth, N. Riedemann, M. Bleich, W. Van Driessche, A. Busch and R. Greger, The cAMP-regulated and 293B-inhibited K^+ conductance of rat colonic crypt base cells, *Pflügers Arch.* **432**, 81-88 (1996).
12. M. Nielsen, R. Warth, M. Bleich, B. Weyand and R. Greger, The basolateral calcium-dependent K^+ channel in rat colonic crypt cells, *Pflügers Arch.* **435**, 267-272 (1998).
13. A. Butt and K. Hamilton, Ion channels in isolated mouse jejunal crypts, *Pflügers Arch.* **435**, 528-538 (1998).
14. G. Schultheiss and M. Diener, Potassium and chloride conductances in the distal colon of the rat, *Gen. Pharmacol.* **31**, 337-342 (1998).
15. G. Sandle, G. Warhurst, I. Butterfield, N. Higgs and R. Lomax, Somatostatin peptides inhibit basolateral K^+ channels in human colonic crypts, *Am. J. Physiol., Gastrintest. Liver Physiol.* **277**, G967-G975 (1999).
16. Y. Li and D. Halm, Secretory modulation of basolateral membrane inwardly rectified K^+ channel in guinea pig distal colonic crypts, *Am. J. Physiol., Cell Physiol.* **282**, C719-C735 (2002).
17. M. Bleich, N. Riedemann, R. Warth, D. Kerstan, J. Leipziger, M. Hör, W. Van Driessche and R. Greger, Calcium regulated K^+ and non-selective cation channels in the basolateral membrane of rat colonic crypt base cells, *Pflügers Arch.* **432**, 1011-1022 (1996).
18. D. Klærke, H. Wiener, T. Zeuthen and P. Jørgensen, Calcium activation and pH dependence of a maxi K^+ channel from rabbit distal colon epithelium, *J. Memb. Biol.* **136**, 9-21 (1993).
19. K. Turnheim, H. Plass and W. Wyskovsky, Basolateral potassium channels of rabbit colon epithelium: role in sodium absorption and chloride secretion, *Biochim. Biophys. Acta.* **1560**, 51-66 (2002).
20. W. Coetzee, Y. Amarillo, J. Chiu, A. Chow, D. Lau, T. McCormack, H. Moreno, M. Nadal, A. Ozaita, D. Pountney, M. Saganich, E. De Miera and B. Rudy, Molecular diversity of K^+ channels, *Annals N. Y. Acad. Sci.* **868**, 233-285 (1999).
21. R. Warth, K. Hamm, M. Bleich, K. Kunzelmann, T. von Hahn, R. Schreiber, E. Ullrich, M. Mengel, N. Trautmann, P. Kindle, A. Schwab and R. Greger, Molecular and functional characterization of the small calcium-regulated K^+ channel (rSK4) of colonic crypts, *Pflügers Arch.* **438**, 437-444 (1999).
22. R. Kunzelmann, M. Hübner, R. Schreiber, R. Levy-Holzman, H. Garty , M. Bleich , R. Warth , M. Slavik , T. von Hahn and R. Greger, Cloning and function of the rat colonic epithelial K^+ channel KvLQT1, *J. Memb. Biol.* **179**, 155-164 (2001).
23. B. Hille, Gating mechanisms: kinetic thinking, *Ion Channels of Excitable Membranes, 3rd edition*, (Sinauer Associates, Sunderland, MA, 2001) pp.575-602.
24. O. Mignen, S. Egee, M. Liberge and B. Harvey, Basolateral outward rectifier Cl^- channel in isolated crypts of mouse colon, *Am. J. Physiol., Gastrointest. Liver Physiol.* **279**, G277-G287 (2000).
25. M. Diener, M. Nobles and W. Rummel, Activation of basolateral Cl^- channels in the rat colonic epithelium during regulatory volume decrease, *Pflügers Arch.* **421**, 530-538 (1992).
26. Y. Okada, Volume expansion-sensing outward-rectifier Cl^- channel: fresh start to the molecular identity and volume sensor, *Am. J. Physiol., Cell Physiol.* **273**, C755-C789 (1997).
27. T. Ogura, T. Furukawa, T. Toyozaki, K. Yamada, Y. Zheng, Y. Katayama, H. Nakaya and N. Inagaki, CLC-3B, a novel CLC-3 splicing variant that interacts with EBP50 and facilitates expression of CFTR-regulated ORCC, *FASEB J.* **16**, 863-865 (2002).
28. A. Rabe and E. Frömter, Micromolar concentrations of steroids and of aldosterone antagonists inhibit the outwardly rectifying Cl^- channels with different kinetics, *Pflügers Arch.* **439**, 559-566 (2000).
29. T. Jentsch, V. Stein, F. Weinreich and A. Zdebik, Molecular structure and physiological function of Cl^- channels, *Physiol. Rev.* **82**, 503-568 (2002).
30. N. Wills and P. Fong, CLC Cl^- channels in epithelia: recent progress and remaining puzzles, *News Physiol. Sci.* **16**, 161-166 (2001).
31. M. Catalán, I. Cornejo, C. Figueroa, M. Niemeyer, F. Sep⁂lveda and L. Cid, CLC-2 in guinea pig colon: mRNA, immunolabeling, and functional evidence for surface epithelium localization, *Am. J. Physiol., Gastrointest. Liver Physiol.* **283**, G1004-G1013 (2002).

32. D. Halm and R. Frizzell, Active K^+ transport across rabbit distal colon: relation to Na^+ absorption and Cl^- secretion, *Am. J. Physiol., Cell Physiol.* **251**, C252-C267 (1986).
33. W. Reeves, C. Winters and T. Andreoli, Chloride channels in the loop of Henle, *Annu. Rev. Physiol.* **63**, 631-645 (2001).
34. P. Wangemann, K^+ cycling and the endocochlear potential, *Hearing Res.* **165**, 1-9 (2002).

12

EFFECTS OF AMMONIUM ON ION CHANNELS AND TRANSPORTERS IN COLONIC SECRETORY CELLS

Roger T. Worrell and Jeffrey B. Matthews*

1. INTRODUCTION

Ammonia and ammonium ions exist in an equilibrium determined by the relation of Equation 1. Ammonia (NH_3) is a weak base with a pKa=9.2 and, with some notable exceptions,[1, 2] can diffuse across the plasma membrane. However, at physiological pH, approximately 98% of NH_3 exists in the ionized form NH_4^+ (ammonium) which is not freely permeable across the plasma membrane. This distinction is often blurred in the literature where both species have often been referred to as ammonia. As with other ions, cell permeability to ammonium requires channels, co-transporters, or pumps within the membrane. Ammonium is of similar molecular size to K^+ and has been found to substitute for K^+ on a number of ion channels, co-transporters, and pumps.

$$NH_3 + H^+ \leftrightarrow NH_4^+ \quad (1)$$

Ammonium is produced within the body through the deaminization of protein and amino compounds within the gut, metabolism of urea and glutamine by the colonocytes, and hydrolysis of glutamine in the kidneys. Ammonium ions (NH_4^+) are toxic to most cells within the body; therefore, systemic levels must be kept low. The liver serves to detoxify NH_4^+ by conversion to glutamine and urea. However, some cells within the kidney and colon are exposed to high levels of ammonium on a continual basis. Ammonium concentrations of 9-23 mM in rat inner medulla have been reported.[3, 4] Colonic lumen NH_4^+ concentration can range from 15 to 100 mM in human[5] with a normal range being 3-44 mM in human fecal dialysates[6] and 20-70 mM in rat colon.[7] Normal arterial plasma levels of NH_4^+ are relatively low at 45 μM.[5, 8] Net absorption across the colonic epithelium is indicated by the fact that portal vein NH_4^+ levels are elevated (~350 μM) with respect to arterial plasma.[5] Although the NH_4^+ concentration at or near the base of the colonic epithelium, e.g., basolateral membrane, is unknown, it is likely significantly higher (in the 3-10 mM range) than that in portal vein due to an approximate tenfold dilution of

* Roger T. Worrell (Corresponding Author: Roger.Worrell@uc.edu) and Jeffrey B. Matthews, Departments of Surgery and of Molecular & Cellular Physiology, University of Cincinnati, Cincinnati, OH 45219.

the 'colonic' blood by the time it reaches the portal vein.[9] This estimation also predicts that ammonium does not freely distribute across the colonic epithelium.

Excess in systemic NH_4^+ levels can lead to hyperammonemia associated encephalopathy which can be life threatening. Although the kidney is attributed to carry out the bulk of body NH_4^+ homeostasis, it is likely that some level of body NH_4^+ control can be accomplished via changes in colonic function and/or in the level of ammonium production within the lumen of the colon. In particular, treatment regimes for hyperammonemia, principally caused by liver failure, have generally been directed at reducing ammonium production within the colon[10] or in extreme cases removal of the colon. Despite this, relatively little is known regarding the way ammonium is handled by colonocytes and how these cells are affected by ammonium.

2. AMMONIA AND AMMONIUM EFFECTS ON INTRACELLULAR pH

The NH_3/NH_4^+ pre-pulse method has been used extensively as a means of altering intracellular pH (pH_i). Given Equation 1, by this method, NH_3^+ entry into the cell on application of external ammonium will cause intracellular alkalization. Subsequent removal of external ammonium with NH_3 exit will lead to intracellular acidification. If on the other hand, NH_4^+ entry occurs with external ammonium application, intracellular acidification will occur. Likewise, with external ammonium removal and NH_4^+ exit intracellular alkalization will occur. Thus, not only can pH_i be affected by ammonium, but by measuring changes in pH_i, one can determine the net uptake or exit of NH_3 and NH_4^+. Although some reports have shown that the apical membrane of colonic crypts is relatively impermeable to NH_3 and NH_4^+,[2, 11] this does not appear to be the case using cultured cells. In T84 cells, ammonium application on either the apical or basolateral side leads to intracellular alkalization consistent with net NH_3 entry. However, with basolateral application, cell acidification quickly follows, indicative of subsequent net NH_4^+ entry.[12] 1999). In HT29-Cl cells, apical or basolateral ammonium also produced an intracellular alkalization, although the subsequent acidification with basolateral ammonium application was not observed.[13] As demonstrated by Ramirez, *et al.*, rat colonic crypts display acidification with exposure to basolateral ammonium.[14] These observations raise interesting questions regarding ammonium effects on the colon. If indeed, the apical or luminal membrane of crypt cells is impermeable to ammonia and ammonium, there should be no net uptake of ammonium in the colon unless that uptake occurs at the surface epithelia. Such an apical entry pathway for NH_4^+ in surface cells of rat colon has been demonstrated by Lohrmann and Feldman[15] and is supported by the observation that the acid load following urinary intestinal diversion is due to NH_4^+, not NH_3 absorption.[16] Secondly, an ammonium entry pathway appears to exist in the basolateral membrane of at least one crypt cell type, rat crypts, and most likely is present to varying degrees in all secretory cell types as discussed below.

3. AMMONIUM EFFECT ON Cl^- SECRETION

Previous studies in rat and human colon demonstrated that luminal ammonium can inhibit both Na^+ and Cl^- absorption, an effect which involves ammonium interaction with an apical Na^+/H^+-exchanger.[17, 18] Luminal ammonium inhibition of forsokolin-activated short circuit current has been reported in rat and human colon by Mayol, *et al.*, but little effect was observed with basolateral ammonium.[19] However, it was unclear in this study

to what extent K^+ secretion may have contributed to the measured current. In contrast, Cermak, *et al*., found little effect of luminal ammonium on Cl^- secretion in rat colon using Cl^- flux measurements.[17]

Using the T84 secretory colonic cell line, it was shown that NH_4^+ can inhibit cAMP- and cGMP-dependent Cl^- secretion but not carbachol-induced (Ca^{++}) secretion.[20] Ammonium was of mixed impact on Ca^{++}-dependent Cl^- secretion. Although ammonium did not inhibit the secretory response to carbachol or thapsigargin, pre-treatment with ammonium was found to blunt the secretory response of T84 cells to Ca^{++}-ionophore mediated secretion. Post-treatment with ammonium did not affect the Ca^{++}-ionophore mediated secretion.[20]

In T84 cells, K^+ secretion is virtually absent, presumably due to the lack of an appropriate apical K^+ channel. In these cells, stimulated secretion in the absence of bicarbonate can be attributed almost entirely to Cl^- secretion. Under bicarbonate free conditions, there was a sidedness to the ammonium inhibition on cAMP-stimulated Cl^- secretion in these cells, with application to the basolateral side having a K_i=5 mM and apical application a K_i=50 mM.[21] This suggested the ammonium effect on Cl^- secretory rate occurred by affecting the basolateral membrane transport processes. In addition, ammonium was found not to alter the apical Cl^- conductance (CFTR) but did affect the basolateral K^+ conductance.[12] Comparision of pHi changes with half maximal inhibition of current with apical or basolateral ammonium determined that the changes in pH_i did not correlate with those in Cl^- secretion.[12] Furthermore, it was demonstrated by Worrell, *et al.,* (2003) that the basolateral ammonium inhibition of current in the absence of K^+ was not as significant as in the presence of K^+, with maximal inhibition observed at a mole fraction ratio of 0.25 K^+/NH_4^+.

The minimalist model for electrogenic Cl^--secretion in T84 cells includes an apical Cl-conductance in series with basolateral Na^+/K^+-ATPase, Na^+-K^+-$2Cl^-$ cotransporter, and K^+ conductance.[22-24] Since NH_4^+ is similar in size to K^+, it is likely that NH_4^+ interacts with one or more of these basolateral components to inhibit Cl^- secretion.

4. AMMONIUM EFFECT ON Na^+-K^+-ATPase

Na^+-K^+-ATPase has been shown in a number of tissues to act as a Na^+-NH_4^+-ATPase. Indeed, early studies of Na^+-K^+-ATPase activity demonstrated an enhanced activity with NH_4^+.[25, 26] NH_4^+ substitution for K^+ on Na^+-K^+-ATPase with equal affinity has been shown in crab gill membrane vesicles,[27] rat,[28] and rabbit[29] proximal tubules. Furthermore, Wall, *et.al*., determined that NH_4^+ uptake by Na^+-K^+-ATPase was necessary for acid secretion in the inner medullary collecting duct.[30] In T84 cells, NH_4^+ uptake also occurs via Na^+-K^+-ATPase with equal or slightly better affinity than K^+ and shows no anomalous mole fraction behavior.[9] As has been shown in the kidney, where [NH_4^+] approaches or exceeds that of [K^+] at the basolateral membrane, it is reasonable that a significant amount of NH_4^+ would be pumped into the crypt secretory cell by Na^+-K^+-ATPase when basolateral NH_4^+ levels are high relative to K^+.

5. AMMONIUM EFFECT ON Na^+-K^+-$2Cl^-$ COTRANSPORTER

NH_4^+ has been shown to be transported on the K^+ site of NKCC-1 in kidney,[31] in rat parotid acini[32] and NKCC-2 in kidney.[33] As previously stated, one means of accessing NH_4^+ entry is to observe the pH_i changes with the addition of NH_4^+. The observation that

intracellular alkalization upon addition of NH_4^+ is bumetanide sensitive in T84 cells suggested that NH_4^+ can be transported by NKCC-1 in these cells.[9] Experiments using ^{86}Rb-uptake in T84 cells indicated that K^+ and NH_4^+ acted in a similar manner to inhibit apparent NKCC activity, likely by competition with ^{86}Rb, thereby reducing ^{86}Rbuptake.[9] This finding is supported by a study involving NKCC-2 from rabbit kidney TAL in which bumetanide-sensitive ^{86}Rb uptake was inhibited by NH_4^+, whereas ^{22}Na uptake was not.[33] Although no anomalous mole fraction behavior was observed for NH_4^+ on bumetanide-sensitve ^{86}Rb uptake as measured by flux, NH_4^+ did produce anomalous mole fraction behavior when bumetanide-sensitive $^{36}Cl^-$ uptake was used to assess NKCC activity.[9] Interestingly, uptake in 10 mM NH_4^+ was higher than in equal molar K^+, thus, as with Na^+-K^+-ATPase, T84 cells are poised to take up NH_4^+ when basolateral NH_4^+ levels are elevated with respect to K^+.

The difference in ^{86}Rb and ^{36}Cl uptake is also somewhat interesting. NKCC-1 is known to exhibit K^+/K^+ exchange activity under which no Cl^- flux occurs,[34] thus one possibility is that NH_4^+/K^+ interaction might favor the exchange mode of NKCC-1. Alternatively, the anomalous behavior may be a reflection of the anomalous behavior associated with NH_4^+ inhibition of Cl^- secretion, i.e., a change in intracellular Cl^- and/or K^+ at or near the cytoplasmic side of NKCC-1. Increases in intracellular Cl^- or extracellular K^+ will reduce NKCC-1 activity.[35] In addition, Gillen and Forbush have shown a steep relation between $[Cl^-]_i$ and NKCC-1 activity within the physiological range of $[Cl^-]_i$.[36]

6. AMMONIUM EFFECT ON K^+ CHANNELS

A number of K^+ channels have been shown to conduct NH_4^+.[37-40] Several basolateral K^+ channels have been reported to occur in colonic crypts[41-43] and in T84 cells.[44-46] Although the most widely accepted cAMP-activated channel is KNQ1(K_vLQT1)/ KCNE3, the presence of other cAMP-responsive K^+ channels may indicate a less simplistic model for basolateral K^+ exit.

Previous data have indicated that NH_4^+ inhibition of Cl^- secretion in T84 is due in part to NH_4^+ block of the cAMP-stimulated basolateral K^+ channel.[12, 9] Indeed, Worrell, *et al.,* showed that the anomalous mole fraction behavior seen with transepithelial current measurements was mimicked by the anomalous mole fraction behavior seen with basolateral K^+ conductance measurements.[9]

Anomalous mole fraction behavior has been demonstrated for a number of ion channel types and is most often attributed to an ion channel with multiple ion binding sites and single file flow.[38] Yang and Sigworth have reported a permeability sequence for KCNQ1[47] but did not include NH_4^+ or mole fraction experiments in their study. To our knowledge, possible anomalous mole fraction effects of NH_4^+ and K^+ in KCNQ1 or other K^+ channels identified in the T84 secretory cells or colonocytes have not been reported.

7. AMMONIUM EFFECT ON TRANSEPITHELIAL RESISTANCE

Longterm exposure of T84 cells to NH_4^+ leads to an increase in transepithelial resistance.[9] Interestingly, on removal of external ammonium, transepithelial resistance further increases. The increase in monolayer resistance is not associated with an increase in either the apical or basolateral membrane resistive elements, thus by default, must involve an increase in the paracellular resistance. Interestingly, pH_i acidifies with longterm

NH_4^+ as well as on wash out of NH_4^+. Thus, the increase in transepithelial resistance might involve pHi changes.[9]

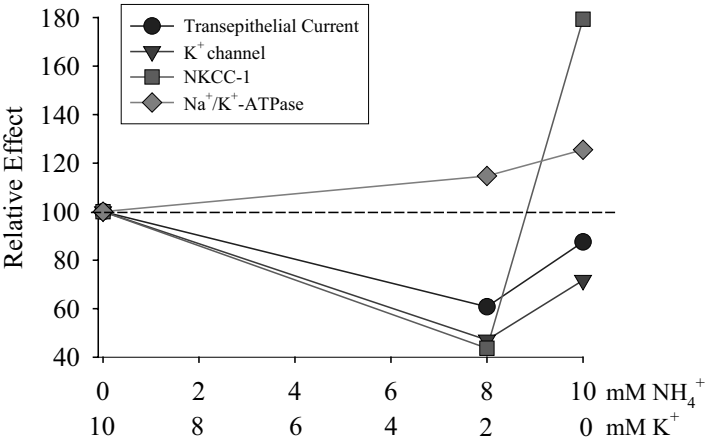

Figure 1. Relative effects of ammonium on Cl^- secretion and on each basolateral component of secretion. Adapted from Worrell, *et.al*.[9]

This is supported by a number of observations. The increase in resistance does not show anomalous mole fraction behavior but rather follows the ammonium concentration. Other monovalent cations which inhibit current (Cs^+, $NMDG^+$, Tl^+) do not significantly increase resistance. In addition, Turner, *et al.*, using intestinal Caco-2 cells, have proposed that cytoplasmic alkalization leads to a decreased transepithelial resistance.[48] This implies that acidification could lead to an increased transepithelial resistance.

8. IMPLICATIONS OF HIGH AMMONIUM ON COLONIC CRYPT CELLS

NH_4^+ effects on both K^+ conductance and NKCC-1 show anomalous mole fraction behavior, but no such behavior is observed on Na^+/K^+-ATPase activity. Figure 1 provides a qualitative summary of these effects relative to 10 mM basolateral K^+ for comparison. NH_4^+ inhibition of transepithelial current is most closely correlated with the effects of NH_4^+ on the basolateral K^+ conductance. In the mix of K^+ with NH_4^+, inhibition of NKCC-1 activity correlates well with the inhibition of Cl^- secretion. However, under conditions of pure NH_4^+, NKCC-1 activity is elevated, whereas total transepithelial current is slightly inhibited. Na^+/K^+-ATPase activity is also elevated relative to that seen with 10 mM basolateral K^+. It is noteworthy that the maximal inhibition relative to 10 mM basolateral K^+ seen on any one component of Cl^- secretion is 44%. Thus, Cl^- secretion can be supported by basolateral NH_4^+, i.e., NKCC-1 can function in a Na^+-NH_4^+-$2Cl^-$ mode and Na^+/K^+-ATPase in a Na^+/NH_4^+-ATPase mode in the T84 cells. Indeed, data indicate that under conditions of nominally free basolateral K^+ with NH_4^+, both NKCC-1 and Na^+/K^+-ATPase activities are elevated which would further support uptake of NH_4^+. Additionally, under mixed K^+/NH_4^+ conditions, the K^+/K^+ exchange mode of NKCC-1 appears favored which would support K^+/NH_4^+ secretion over Cl^- secretion. Given an apical exit pathway

for NH_4^+, it is reasonable to hypothesize that NH_4^+ secretion is likely to occur in colonic crypts (Figure 2). The notion that NH_4^+ secretion can be driven by NKCC and Na^+/K^+-ATPase with an opposing exit pathway is supported by work involving renal cells.[33, 31] In fact, Kinne, *et.al*., estimated that it is energetically possible for NKCC and Na^+/K^+-ATPase under physiogical conditions to generate a $[NH_4^+]_i/[NH_4^+]_o$ ratio of approximately 2000.[33]

Under conditions where cAMP is only slightly elevated, K^+ secretion occurs and predominates in colonic crypts. This is due to the preferential activation of apical versus basolateral K^+ channels[42] and basolateral versus apical Cl^- channels.[49] Although the apical K^+ channel(s) responsible for K^+ secretion is not clearly defined, candidates include inward rectifiers of the ROMK family. It is intriguing that both ROMK2[39] and $K_{ir}2.1$[50, 40] conduct NH_4^+ at physiological membrane potentials. In a preliminary report, $K_{ir}2.1$ was identified by immunostaining in the apical membrane of T84 cells;[51] although there is no evidence to date that this channel is functional in these cells. Regardless, most K^+ channels studied to date do show NH_4^+ conductivity. Partial inhibition of the basolateral K conductance in T84 cells[12, 9] by NH_4^+ would tend to support K^+ or NH_4^+ secretion under conditions where an apical conductance to K^+ or NH_4^+ was functional.

The fact that cellular pH acidifies (net NH_3 exit) on removal of basolateral NH_4^+ indicates NH_4^+ exit across the basolateral membrane is limited. Interestingly, Singh, *et al*. and Hasselblatt, *et al.,* have reported that colonic crypts (not cAMP-stimulated) have a low permeability to apically applied NH_3/NH_4^+.[2, 11] A low apical NH_3 permeability would be an expected criteria to effectively secrete NH_4^+ given the equilibrium between NH_3 and NH_4^+. The longterm effect of NH_4^+ on TER could also contribute to crypt NH_4^+ secretion by limiting NH_3/NH_4^+ backflux. Thus, were NH_4^+ present, limited basolateral NH_4^+ exit with driven NH_4^+ uptake in combination with limited apical NH_3 entry would support NH_4^+ secretion.

This hypothesis raises the interesting point that the net NH_4^+ absorption known to occur in the colon may derive from the same general phenomena of fluid balance, i.e., a balance between an absorptive process and a secretory process. In this case, one might assume that the bulk of NH_4^+ absorption in the colon occurs at the level of the surface cells as is thought to be the case for NaCl absorption.

The anomalous mole fraction effect in a K^+, NH_4^+ mix suggests a relevance of physiologic importance not merely a biophysical phenomena, since a K^+/NH_4^+ mixture is invariably present *in vivo*. Thus, the colon may be self-regulating in regard to net NH_4^+ absorption based on the $[K^+]_o$ to $[NH_4^+]_o$ ratio at the basolateral membrane of the crypt cells. These findings support the hypothesis that cells of the colonic crypt are sensitive not only to the basolateral level NH_4^+ but also to the ratio of NH_4^+ to K^+.

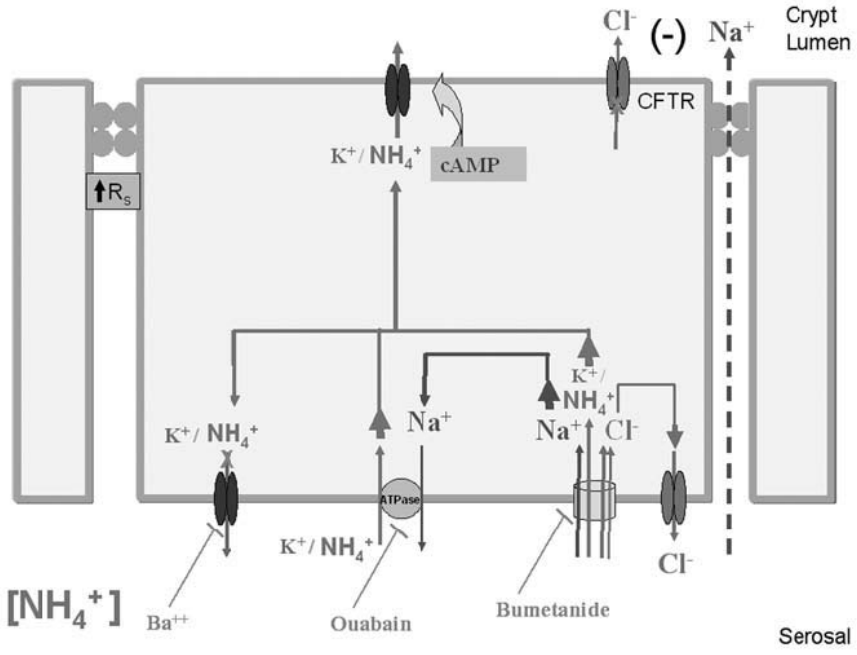

Figure 2. Proposed model for crypt colocyte ammonium secretion.

9. SUMMARY

Basolateral ammonium produces an inhibition of Cl^- secretion the magnitude of which is dependent on the NH_4^+ to K^+ concentration ratio. Inhibition is maximal at a mole fraction ratio of 0.25 K^+ to NH_4^+. This anomalous mole fraction effect is due to effects on the basolateral K^+ channel as well as Na^+-K^+-$2Cl^-$ cotransporter. However, only Cl^- loading, not K^+ loading, appears affected in an anomalous mole fraction manner. Trans-epithelial current is only slightly inhibited relative to equilmolar K^+ by NH_4^+. As in other systems, both Na^+-K^+-ATPase and Na^+-K^+-$2Cl^-$ can act in Na^+-NH_4^+-ATPase and Na^+-NH_4^+-$2Cl^-$ transport modes. NH_4^+ conducts through most K^+ channels and thus likely through the apical K^+ channel present in native crypt cells. This suggests that, similar to the kidney, colonic secretory cells have the capacity to secrete NH_4^+ when in a K^+-secreting mode with elevated basolateral NH_4^+ levels.

10. REFERENCES

1. D. Kikeri, A. Sun, M.L. Zeidel, and S.C. Hebert, Cell membranes impermeable to NH_3, *Nature* **339,** 478-480 (1989).
2. S.K. Singh, H.J. Binder, J.P. Geibel, and W.F. Boron, An apical permeability barrier to NH_3/NH_4^+ in isolated, perfused colonic crypts, *PNAS* **92,** 11573-11577 (1995).
3. J. Buerkert, D. Martin, and D. Trigg, Ammonium handling by superficial and juxtamedullary nephrons in the rat: evidence for an ammonia shunt between the loop of Henle and the collecting duct, *J. Clin*. Invest. **70,** 1-12 (1982).

4. L. Stern, K.A. Backman, and J.P. Hayslett, Effect of cortical-medullary gradient for ammonia on urinary excretion of ammonia, *Kidney Int.* **27,** 652-661 (1985).
5. W. Silen, H.A. Harper, D.L. Mawdsley, and W.L. Weirich, Effect of antibacterial agents on ammonia production within the intestine, *Proc. Soc. Exp. Bio. and Med.* **88,** 138-140 (1955).
6. O.M. Wrong, A. Metcalfe-Gibson, R.B.T. Morrison, and A.V. Howard, *In vivo* dialyses of faeces as a method of stool analysis. Techniques and results in normal subjects, *Clin. Sci*. **28,** 357-375 (1965).
7. H.C. Lin and W.J. Visek, Large intestinal pH and ammonia in rats: dietary fat and protein interactions, *J. Nutr.* **121,** 832-843 (1991).
8. J.O. Clemmesen, J. Kondrup, and P. Ott, Splanchnic and leg exchange of amino acids and ammonia in acute liver failure, *Gastroenterology* **118,** 1131-1139 (2000).
9. R.T. Worrell, J. Oghene, and J.B. Matthews, Ammonium effects on colonic Cl- secretion: anomalous mole fraction behavior, *Am J Physiol Gastrointest Liver Physiol* (August 28, 2003).**10**, 1152/ajpgi.00196.
10. A.T.Blei, Diagnosis and treatment of hepatic encephalopathy, *Baillieres Best Pract Res Clin Gastroenterol* **14,** 959-974 (2000).
11. P. Hasselblatt, R. Warth, A. Schulz-Blades, R. Greger, and M. Bleich, pH regulation in isolated in vitro perfused rat colonic crypts, *Pflugers Arch* **441,** 118-124 (2000).
12. B.J. Hrnjez, J.C. Song, M. Prasad, J.M. Mayol, and J.B. Matthews, Ammonia blockade of intestinal epithelial K^+ conductance, *Am. J. Physiol*. **277,** G521-G532 (1999).
13. D. Maouyo, S. Chu, and M.H. Montrose, pH heterogeneity at intracellular and extracellular plasma membrane sites in HT29-C1 cell monolayers, *Am. J. Physiol* . **278,** C973-C981 (2000).
14. M.R. Ramirez, R. Fernaddez, and G. Malnic, Permeation of NH_3/NH_4^+ and cell pH in colonic crypts of the rat, *Pflugers Arch*. **438,** 508-515 (1999).
15. W.E. Lohrmann and G.M. Feldman, NH_3 and NH_4^+ permeance of the colonocyte apical membrane, *Contrib Nephrol*. **110,** 120-126 (1994).
16. M.C. Hall, M.O. Koch, and W.S. McDougal, Mechanism of ammonium transport by intestinal segments following urinary diversion: Evidence for ionized NH_4^+ transport via K^+-pathways, *J. Urol*. **148**, 453-457 (1992).
17. R. Cermak, C. Lawnitzak, and E. Scharrer, Influence of ammonia on sodium absorption in rat proximal colon, *Pflugers Arch* **440,** 619-626 (2000).
18. R. Cermak, K. Minck, C. Lawnitzak, and E. Scharrer, Ammonia inhibits sodium and chloride absorption in rat distal colon, *Exp. Physiol*. **87**, 311-319 (2002).
19. J.M. Mayol, P. Alarma-Estrany, T.C. O'Brien, J.C. Song, M. Prasad, Y. Adame-Navarrete, J.A. Fernandez-Represa, E.D. Mun, and J.B. Matthews, Electrogenic ion transport in mammalian colon involves an ammonium-sensitive apical membrane K^+ conductance, *Dig. Dis. and Sci*. **48,** 116-125 (2003).
20. J.M. Mayol, B.J. Hrnjez, H.I. Akbarali, J.C. Song, J.A. Smith, and J.B. Matthews, Ammonia effect on calcium-activated chloride secretion in T84 intestinal epithelial monolayers, *Am. J. Physiol*. **273,** C634-C642 (1997).
21. M. Prasad, J.A. Smith, A. Resnick, C.S. Awtrey, B.J. Hrnjez, and J.B. Matthews, Ammonia inhibits cAMP-regulated intestinal Cl^- transport, *J. Clin. Invest*. **96,** 2142-2151 (1995).
22. P. Silva, J. Stoff, M. Field, L. Fine, J.N. Forrest and F.H. Epstein, Mechanism of active chloride secretion by shark rectal gland: Role of Na-K-ATPase in chloride transport, *Am. J. Physiol*. **233,** F298-F306 (1977).
23. M.J. Welsh, P.L. Smith, and R.A. Frizzell, Chloride secretion by canine tracheal epithelium: II. The cellular electrical potential profile, *J. Membr. Biol*. **70,** 227-238 (1982).
24. M.J. Welsh, P.L. Smith, and R.A. Frizzell, Chloride secretion by canine tracheal epithelium: III. Membrane resistances and electromotive forces, *J. Membr. Biol*. **71,** 209-218 (1983).
25. J.C. Skou, Preparation from mammalian brain and kidney of the enzyme system involved in active transport of Na^+ and K^+, *Biochim. Biophys. Acta* **58,** 314-325 (1962).
26. J.D. Robinson, J.D., Interactions between monovalent cations and Na^+-K^+-ATPase, *Arch Biochem. Biophys*. **139,** 17-27 (1970).
27. D.W. Towle and T. Hølleland, Ammonium ion substitutes for K^+ in ATP-dependent Na^+ transport by basolateral membrane vesicles, *Am. J. Physiol*. **252,** R479-R489 (1987).
28. I. Kurtz and R.S. Balaban, Ammonium as a substrate for Na^+-K^+-ATPase in rabbit proximal tubules, *Am. J. Physiol.* **250**, F497-F502 (1986).
29. J.L. Garvin, M.B. Burg, and M.A. Knepper, Ammonium replaces potassium in supporting sodium

transport by the Na-K-ATPase of renal proximal straight tubules, *Am. J. Physiol*. **249,** F785-F788 (1985).
30. S.M. Wall, B.S. Davis, K.A. Hassell, P. Mehta, and S.J. Park, In rat tIMCD, NH_4^+ uptake by Na^+-K^+-ATPase is critical to net acid secretion during chronic hypokalemia, *Am. J. Physiol*. **277**, F866-F874 (1999).
31. S.M. Wall, H.N. Trinh, and K. E. Woodward, Heterogeneity of NH_4^+ transport in mouse medullary collecting duct cells, *Am. J. Physiol*. **269,** F536-F544 (1995).
32. R.L. Evans, R.L. and R.J. Turner, Evidence for a physiological role of NH_4^+ transport on the secretory Na^+-K^+2Cl^- cotransporter, *BBRC* **245,** 301-306 (1998).
33. R. Kinne, E. Kinne-Saffran, H. Schülz, and B. Scholermann, Ammonium transport in medullary thick ascending limb of rabbit kidney: Involvement of the Na^+, K^+, Cl^+-cotransporter, *J. Membr. Biol*. **94,** 279-284 (1986).
34. C. Lytle, T.J. McManus, and M. Haas, A model of Na-K-2Cl cotransport based on ordered ion binding and glide symmetry, *Am. J. Physiol*. **274,** C299-C309 (1998).
35. C. Lytle and B. Forbush 3rd, Regulatory phosphorylation of the secretory Na-K-Cl cotransporter: modulation by cytoplasmic Cl, *Am. J. Physiol*. **270**, C437-C448 (1996).
36. C.M. Gillen, and B. Forbush III, Functional interaction of the K-Cl cotransporter (KCC1) with the Na-K-Cl cotransporter in HEK-293 cells, *Am. J. Physiol*. **276,** C328-C336 (1999).
37. W. Zeiske and W. Van Driessche, The interaction of "K^+-like" cations with the apical K^+ channel in frog skin, *J. Membr. Biol*. **76,** 57-72 (1983).
38. G. R. Eisenman, R. Latorre, and C. Miller, Multi-ion conduction and selectivity in the high-conductance Ca^{++}-activated K^+ channel from skeletal muscle, *Biophys. J.* **50,** 1025-1034 (1986).
39. H Choe, H. Sackin, and L.G. Palmer, Gating properties of inward-rectifier potassium channels: Effects of permeant ions, *J. Membr. Biol*. **184,** 81-89 (2001).
40. H.K. Chang and R.C. Shieh, Conformation changes in $K_{ir}2.1$ channels during NH_4^+-induced inactivation, *J. Biol. Chem*. **278,** 908-918 (2003).
41. K. Kunzelmann, M. Hübner, R. Schreiber, R. Levy-Holzmann, H. Garty, M. Bleich, R. Warth, M. Slavik, T. von Hahn, and R. Greger, Cloning and function of the rat colonic epithelial K^+ channel K_VLQT1, *J. Membr. Biol*. **179,** 155-164 (2001).
42. Y. Li and D.R. Halm, Secretory modulation of basolateral membrane inwardly rectified K^+ channel in guinea pig distal colonic crypts, *Am. J. Physiol*. **282,** C719-C735 (2002).
43. K. Turnheim, H. Plass, and W. Wyskovsky, Basolateral potassium channels of rabbit colon epithelium: role in sodium absorption and chloride secretion, *Biochimica et Biophysica Acta* **1560,** 51-66 (2002).
44. D.C. Devor and R.A. Frizzell, Modulation of K^+ channels by arachidonic acid in T84 cells. I. Inhibition of the Ca^{2+}-dependent K^+ channel, *Am. J. Physiol*. **274,** C138-C148 (1998a).
45. D.C. Devor and R.A. Frizzell, Modulation of K^+ channels by arachidonic acid in T84 cells. II. Activation of a Ca^{2+}-independent K^+ channel, *Am. J. Physiol*. **274,** C149-C160 (1998b).
46. L.T. Izu, S.L. McCulle, M.T. Ferreri-Jacobia, D.C. Devor, and M.E. Duffey, Vasoactive intestinal peptide-stimulated Cl^- secretion: Activation of cAMP-dependent K^+ channels, *J. Membr. Biol*. **186,** 145-157 (2002).
47. Y. Yang and F.J. Sigworth, Single-channel properties of I_{ks} potassium channels, *J. Gen. Physiol.* **12,** 665-678 (1998).
48. J.R.Turner, E.D. Black, J. Ward, C.-M. Tse, F.A. Uchwat, H.A. Alli, M. Donowitz, J.L. Madara, and J.M. Angle, Transepithelial resistance can be regulated by the intestinal brush-border Na^+/H^+ exchanger NHE3, *Am. J. Physiol.* **279,** C1918-C1924 (2000).
49. Y. Li, S.T. Halm, and D.R. Halm, Secretory activation of basolateral membrane Cl^- channels in guinea pig distal colonic crypts, *Am. J. Physiol*. **284,** C918-C933 (2003).
50. R.C. Shieh and Y.L. Lee, Ammonium ions induce inactivation of $K_{ir}2.1$ potassium channels expressed in Xenopus oocytes, *J. Physiol* **535,** 359-370 (2001).
51. J. Cuppoletti, D.H. Malinowska, K.P. Tewari, R.T. Worrell, and J.B. Matthews, Biophysical, regulatory, and pharmacological properties of $K_{ir}2.1$: a K^+ channel of the intestinal epithelia, *DDW* (2002).

13

THE VOLUME-ACTIVATED CHLORIDE CURRENT DEPENDS ON PHOSPHOLIPASE C ACTIVATION AND INTRACELLULAR CALCIUM MOBILIZATION

D. Varela, F. Simon, A. Riveros, F. Jørgensen and A. Stutzin*

1. INTRODUCTION

Mammalian cells are constantly exposed to changes in cell volume and recovery of cell volume after cell swelling requires the activation of K^+ and Cl^- channels and organic osmolyte permeability pathways with subsequent water efflux. This process, termed regulatory volume decrease (RVD),[1-3] prevents against irreversible swelling which leads to cell death.[4, 5] Despite the vast amount of experimental data gathered so far, the mechanisms that couple cell swelling and volume-dependent gating of Cl^- channels remain largely undefined.

Here, we discuss some of our recent findings on the activation of the volume-activated Cl^- current ($I_{Cl,vol}$) in HTC cells. It has been previously reported that in HTC cells exposed to hypotonicity, PLCγ becomes activated with consequent intracellular Ca^{2+} mobilization,[6] indicating this signaling pathway could be playing a significant role in cell volume recovery. Thus, we explored the possibility that intracellular Ca^{2+} mobilization evoked by cell-swelling activates $I_{Cl,vol}$.

2. EXPERIMENTAL

HTC cells were cultured as previously described[7] and currents were recorded using the nystatin-perforated whole-cell patch-clamp technique.[8] Briefly, cells were mounted on a microchamber installed on an inverted microscope. Solution changes were effected by a local perfusion system. The bath solution contained (mM): 100 NaCl, 2 $CaCl_2$, 1

* D. Varela, F. Simon, A Riveros and A. Stutzin, Centro de Estudios Moleculares de la Célula & Instituto de Ciencias Biomédicas, Facultad de Medicina Universidad de Chile, Santiago-6530499, Santiago-Chile. F. Jørgensen, IMB, Physiology and Pharmacology, Southern Danish University, Odense, Denmark.

$MgCl_2$, 100 sorbitol, and 10 Hepes, pH 7.4 adjusted with Tris (300 ± 5 mosmol l^{-1}). The pipette solution contained (mM): 5 NaCl, 133 CsCl, 1 $MgCl_2$, and 10 Hepes, pH 7.2 adjusted with Tris (295 ± 5 mosmol l^{-1}). Hypotonic solution (200 ± 5 mosmol l^{-1}) was obtained by omitting sorbitol. To allow the formation of the giga-seal, the pipette tip was filled with nystatin-free solution, whereas the pipette bulk was backfilled with the nystatin-containing solution. Usually after ~10 min from seal formation, a stable access was achieved (R_a ~15 MΩ). All reagents were of analytical grade. Asterisks in the figures indicate significance ($p < 0.01$).

3. RESULTS AND DISCUSSION

Upon exposure to hypotonicity, HTC cells activate an outwardly rectifying Cl^- current, as depicted in Figure 1.

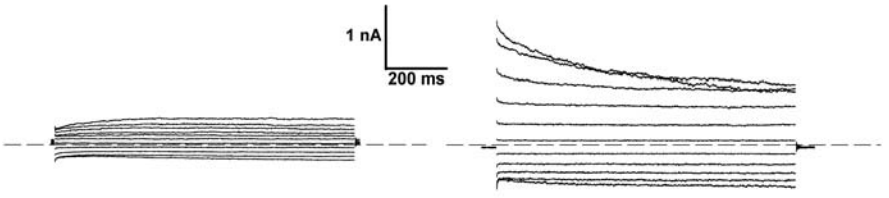

Figure 1. A representative family of hypotonicity (30%) induced outwardly-rectifying Cl^- currents in HTC cells. Right panel shows the current in isotonicity; left panel depicts the currents after 5 min in hypotonicity. Holding potential was -10 mV; voltages ranged from -100 to 100 mV in steps of 20 mV.

This current displays deactivation at high positive potentials which has been correlated to the permeant anion.[9,10] Figure 2 shows the time course of this current in HTC cells in response to hypotonicity and after changing to an isotonic extracellular solution.

Swelling-mediated Ca^{2+} mobilization has been reported in many different cell types,[11,12] and in HTC cells, PLCγ has been shown to be responsible for this process.[6] Figure 3 shows the effect of the generic PLC inhibitor U73122 on the activation of $I_{Cl,vol}$. It can be seen that PLC blockade completely prevents activation of $I_{Cl,\ vol}$, whereas the inactive analogue has no effect. This result clearly indicates that $I_{Cl,vol}$ activation is critically dependent on PLC activity.

The results shown in Figure 3 suggest that intracellular Ca^{2+} mobilization upon cell swelling may be dependent on the activation of IP_3 receptors.[6] To test this, HTC cells were exposed to the IP_3 receptor blocker 2-APB (2-aminoethoxydiphenyl borate). As shown in Figure 4, 2-APB inhibited $I_{Cl,vol}$ by almost 70%, indicating IP_3-mediated Ca^{2+} release is necessary for activation of the current. In order to study further the role of Ca^{2+}, we tested the effect of extracellular Ca^{2+} removal.

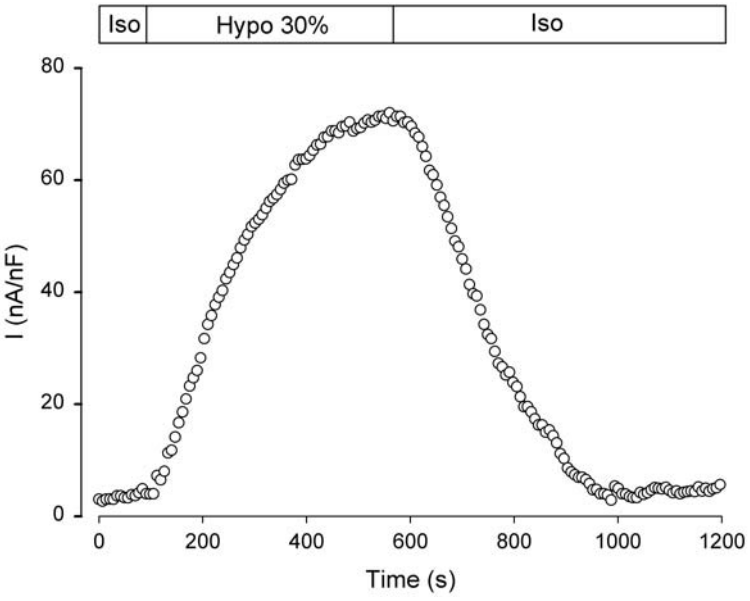

Figure 2. Time course of $I_{Cl,\ vol}$ activation by hypotonicity (Hypo 30%) and deactivation by isotonicity (Iso). Each current point was obtained at 80 mV.

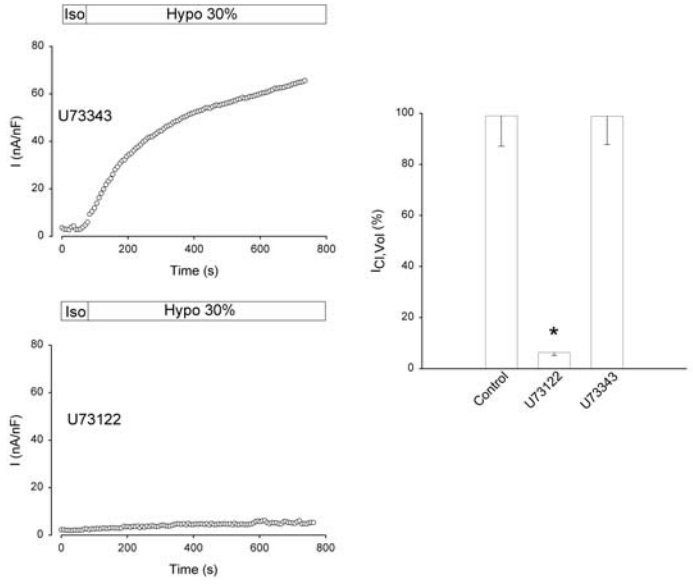

Figure 3. Effect of PLC inhibition on the development of $I_{Cl,vol}$. The time course of $I_{Cl,vol}$ development in the presence of the PLC inhibitor (U73122, 10 μM) and its inactive analogue (U73343, 10 μM) is depicted on the left panel. The right panel shows the percentage of current inhibition.

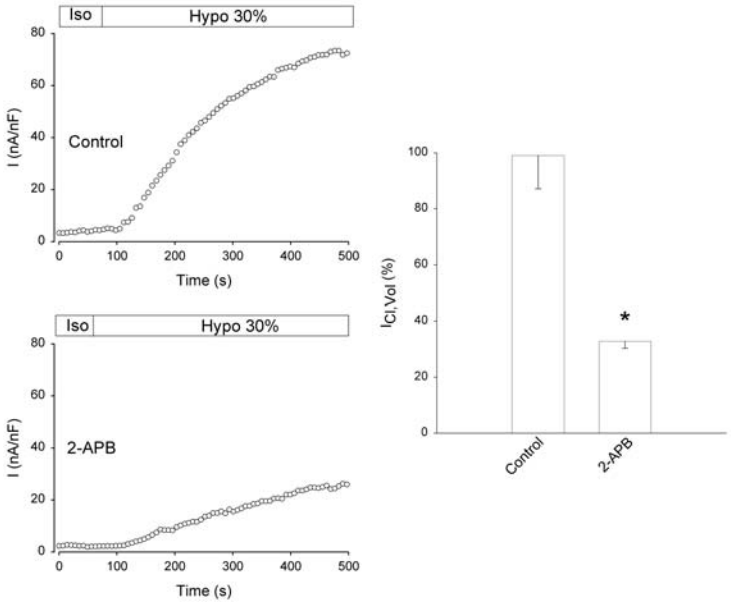

Figure 4. Effect of IP_3 receptor inhibition on the development of $I_{Cl,vol}$. The time course of $I_{Cl,vol}$ development in the presence of 2-APB (50 μM). The right panel shows the percentage of current inhibition

As shown in Figure 5, removal of extracellular Ca^{2+} significantly delayed the onset of the current, indicating that extracellular Ca^{2+} has a potentiating effect on $I_{Cl,vol}$ activetion. This finding is in agreement with other studies in different cells types, suggesting that extracellular Ca^{2+} is not critical for $I_{Cl,vol}$ activation[13,14] but is necessary for modulating this conductance.

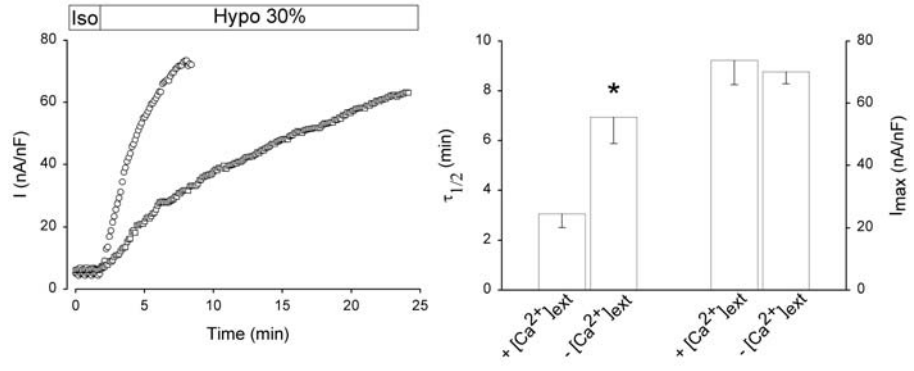

Figure 5. $I_{Cl,vol}$ activation in the presence (○) or absence (□) of extracellular Ca^{2+} is depicted on the left panel. The right panel shows the half-maximal time constant for current onset and the maximal current achieved at steady-state in both conditions.

4. CONCLUSIONS

We have shown that in HTC cells, $I_{Cl,vol}$ is critically dependent on PLC activation. Moreover, mobilization of Ca^{2+} from IP_3-sensitive intracellular stores plays a fundamental role in the development of this current. On the other hand, extracellular Ca^{2+} removal slowed the half-maximal activation time constant without affecting the maximal current achieved at steady-state, indicating that intracellular Ca^{2+} mobilization is sufficient to trigger $I_{Cl,vol}$ activation and that extracellular Ca^{2+} potentiates current activation.

5. ACKNOWLEDGMENTS

This work was supported by FONDECYT 1010994 and FONDAP 1501006.

6. REFERENCES

1. E.K. Hoffmann and P.B. Dunham**,** Membrane mechanisms and intracellular signalling in cell volume regulation. *Int. Rev Cytol.* **161**, 173 (1995)**.**
2. K. Strange, F. Emma and P.S. Jackson, Cellular and molecular physiology of volume-sensitive anion channels. *Am. J. Physiol.* **270**, C711 (1996).
3. U. Banderali and G.J. Roy, Activation of K^+ and Cl^- channels in MDCK cells during volume regulation in hypotonic media. *J. Membrane Biol.* **126**, 219 (1992).
4. C.D. Bortner and J.A. Cidlowski, A necessary role for cell shrinkage in apoptosis. *Biochem. Pharmacol.* **56**, 1549 (1998).
5. Y. Okada, E. Maeno, T. Shimizu, K.Dezaki, J. Wang and S. Morishima, Receptor-mediated control of regulatory volume decrease (RVD) and apoptotic volume decrease (AVD)**.** *J. Physiol.* **532**, 3 (2001).
6. A.L. Moore, M.W.Roe, R.F. Melnick and S.D. Lidofsky, Calcium mobilization evoked by hepatocellular swelling is linked to activation of phospholipase Cγ. *J. Biol.Chem.* **277**, 34030 (2002).
7. M.W. Roe, A.L. Moore and S.D. Lidofsky, Purinergic-independent calcium signaling mediates recovery from hepatocellular swelling: implications for volume regulation. *J. Biol.Chem.* **276**, 30871 (2001).
8. R. Horn and A. Marty, Muscarinic activation of ionic currents measured by a new whole- cell recording method. *J .Gen. Physiol.* **92**, 145 (1988).
9. M. Pusch, U. Ludewig, A. Rehfeldt and T.J. Jentsch, Gating of the voltage-dependent chloride channel ClC-0 by the permeant anion. *Nature* **373**, 527 (1995).
10. A. Stutzin, A.L. Eguiguren, L.P. Cid and Sepúlveda, F.V., Modulation by extracellular Cl^- of volume-activated organic osmolyte and halide permeabilities in HeLa cells. *Am. J. Physiol.* **273**, C999 (1997).
11. J.A. Felix, M.L. Woodruff and E.R. Dirksen, Stretch increases inositol 1,4,5-trisphosphate concentration in airway epithelial cells. *Am. J. Respir. Cell Mol. Biol.* **14**, 296 (1996).
12. K. Shinozuka, N. Tanaka, K. Kawasaki, H. Mizuno, Y. Kubota, K. Nakamura, M. Hashimoto and M.Kunitomo, Participation of ATP in cell volume regulation in the endothelium after hypotonic stress. *Clin. Exp. Pharmacol. Physiol.* **28**, 799 (2001).
13. G. Szücs, G. Buyse, J. Eggermont, G. Droogmans and B. Nilius, Characterization of volume-activated chloride currents in endothelial cells from bovine pulmonary artery. *J. Membrane Biol.* **149**, 994 (1996).
14. M. Díaz and F. V. Sepúlveda, Characterisation of Ca^{2+}-dependent inwardly rectifying K^+ currents in HeLa cells. *Pflügers Arch.* **430**, 168 (1995).

14

NITRIC OXIDE (NO) MODULATION OF CL-DEPENDENT TRANSPORTERS IN THE KIDNEY

Pablo A. Ortiz and Jeffrey L. Garvin*

1. INTRODUCTION

The free radical nitric oxide (NO) was originally described as an endothelium-derived relaxing factor produced in the mammalian cardiovascular system. It is now known to play an important role in various physiological processes such as ion transport regulation,[1] cell growth and differentiation[2] cardiac contractility[3] and neuronal synapses.[4] In the kidney, NO regulates water and electrolyte excretion by modulating the activity of transporters along the nephron. In the proximal tubule, NO decreases the activity of the apical Na/H exchanger which likely inhibits sodium and water absorption. In the thick ascending limb of the loop of Henle, NO inhibits apical Na/K/2Cl cotransport and apical and basolateral Na/H exchange, thereby decreasing net NaCl and bicarbonate absorption. In the macula densa, NO inhibits apical Na/K/2Cl cotransport, while in the collecting duct, NO inhibits sodium and water absorption. Overall, the effect of NO on individual transporters is in agreement with the diuretic and natriuretic role of NO observed *in vivo*. In this review, we will focus on the role of NO in regulating Cl-dependent and Cl-independent sodium transporters in the kidney.

2. NO PRODUCTION IN THE KIDNEY

In mammalian cells NO is produced by conversion of the amino acid L-arginine to L-citrulline. This reaction is catalyzed by an enzyme called NO synthase (NOS).[5] There are three NOS isoforms: neuronal NOS (nNOS), inducible NOS (iNOS) and endothelial NOS (eNOS), all of which are expressed in renal tubules with a distinct pattern of localization along the cells comprising the nephron.

* Pablo A. Ortiz, Henry Ford Hospital, 2799 West Grand Blvd, Detroit, MI 48202, 313-916-8501, 313-916-1479, PORTIZ1@hfhs.org. Jeffrey L. Garvin,

nNOS was originally cloned from brain tissue and is strongly expressed in most neuronal cell types. In the kidney, nNOS is expressed in cells of the macula densa and in the collecting ducts.[6, 7] Little is known about the signaling mechanisms that regulate nNOS activity and expression in these cells.

In most cell types, iNOS is not expressed constitutively, rather its expression is rapidly induced by various inflammatory stimuli such as lipopolysaccharides (LPS), cytokines and other mediators of inflammation. However, in the kidney,l constitutive iNOS expression has been reported in the proximal tubule, thick ascending limbs and inner medullary collecting duct.[8, 9] Induction of iNOS in cultured proximal tubule cells resulted in increased NO production and inhibition of Na/K ATPase activity,[10] suggesting that iNOS regulates transport at least in this nephron segment. However, the role of iNOS in the regulation of other nephron transporters is less clear.

eNOS was originally cloned from vascular endothelial cells where its function has been studied in depth. However, it has also been found in epithelial cells from most tissues such as lung, testis, brain and kidney where it regulates ion transport by different mechanisms.[11] In the kidney, eNOS is present in proximal tubules, thick ascending limbs, and collecting ducts.[1] While its function in proximal tubules and collecting duct is still unknown, we have recently shown that eNOS is essential to regulation of ion transport in the thick ascending limb[12] which will be discussed in depth.

Overall, the three NOS isoforms are present in epithelial cells along the nephron where they regulate ion transport. In this review, we will focus on data regarding the effect of NO on Cl-dependent and Cl-independent transporters along the nephron.

3. REGULATION OF Na/K/2Cl COTRANSPORT BY NO

3.1. Thick Ascending Limb

The thick ascending limb reabsorbs 25 to 30 % of the filtered NaCl load while being water impermeable. The apical Na/K/2Cl cotransporter accounts for most of the NaCl reabsorbed in this segment.[13] The Na/K/2Cl cotransporter present in the thick ascending limb has been cloned and named NKCC2 or BSC-1 (bumetanide-sensitive cotransporter-1).[14,.15] NKCC2 differs from the other Na/K/2Cl cotransporter (NKCC1) in its amino acid sequence (60-70% homology) and its pattern of tissue expression, being expressed only in the thick ascending limb and cells of the macula densa.[16-19] As in most epithelial cells, the driving force for NaCl entry is generated by Na/K-ATPase.[20] The apical membrane of the thick ascending limb has two types of K channels.[21] K recycling across the apical membrane is important for Na/K/2Cl cotransport and generates a positive luminal potential that provides the driving force for paracellular transport of cations such as Ca^{2+} and Mg^{2+}. [22]

In isolated, perfused rat thick ascending limbs, NO produced exogenously by the donor spermine NONOate decreased net Cl absorption (J_{Cl}).[23] Because all Cl in these cells is absorbed via Na/K/2Cl cotransport, the data suggested NO may directly inhibit Na/K/2Cl cotransport. Adding L-arginine, the substrate for NOS, to the bath stimulated endogenous NO production and also reversibly decreased thick ascending limb J_{Cl}.[24] The effect of L-arginine was prevented by blocking NOS with L-NAME, indicating that endogenously-produced NO mediates the effect of L-arginine. Although these data show NO inhibits J_{Cl}, they do not address which transporter is affected by NO.

The inhibitory effect of NO on net NaCl transport could be mediated by blockade of apical transporters or basolateral Na/K ATPase. We measured intracellular ion concentration by fluorescence microscopy and found that NO decreased both intracellular Na and Cl levels by approximately 30%, suggesting that NO decreases NaCl entry via the Na/K/2Cl cotransporter. Using the initial rate of increase in intracellular Na when NaCl is added to the luminal perfusate as a measure of Na/K/2Cl cotransporter activity, we observed that NO decreased Na/K/2Cl cotransport. NO did not appear to decrease luminal K permeability, as determined by changes in membrane potential when the luminal K concentration was increased from 1 to 25 mM.[25] Moreover, Lu, et al., found that NO did not decrease but rather stimulated activity of the luminal 70-pS K channel in the rat thick ascending limb, as measured in cell-attached patch-clamp experiments.[26] The data showing that NO decreases Na/K/2Cl activity do not rule out the possibility that this effect is secondary to inhibition of basolateral Na/K ATPase activity. The effects of NO on pump activity were investigated using measurement of oxygen consumption in the presence of a Na ionophore and varying concentrations of extracellular Na. NO did not affect maximal turnover or the affinity of Na/K ATPase for intracellular Na.[25] Taken together, these data suggest that NO suppresses net NaCl absorption primarily by directly inhibiting the Na/K/2Cl cotransporter, NKCC2.

Despite the importance of NKCC2 in NaCl absorption by the thick ascending limb, little is known about the molecular mechanisms that regulate its activity. In most cells, NO exerts its effects by activating soluble guanylate cyclase (sGC) which in turn increases intracellular cGMP levels. In other cells, cGMP has been shown to directly inhibit Na/K/2Cl cotransport,[27] and in the thick ascending limb, cGMP was shown to inhibit net Cl absorption.[28] We hypothesized that NO could inhibit Na/K/2Cl cotransport via a cGMP-dependent mechanism. To determine whether endogenous NO inhibits thick ascending limb chloride absorption by stimulating sGC, we tested whether LY-83583, a sGC inhibitor, could block the effects of L-arginine on thick ascending limb Cl absorption. We found that in the presence of LY-83583, L-arginine did not decrease Cl absorption. We also studied whether the effects of L-arginine and cGMP were additive and found that in the presence of 50 μmol/L db-cGMP, increasing NO production did not further decrease Cl absorption.[29] Taken together, these data suggest that cGMP mediates all of the effects of NO on thick ascending limb Cl absorption.

cGMP may activate either protein kinase G (PKG) or the cGMP-dependent phosphodiesterases, PDE II or PDE III. Stimulation of PDE II decreases intracellular levels of cAMP which is known to stimulate thick ascending limb Cl transport. To test whether inhibition of PDE II activity could block the effect of NO, we used the PDE II inhibitor EHNA. In the presence of EHNA (50 μmol/L), NO only decreased Cl absorption by 13% instead of the 35% inhibition observed in control tubules. Because activation of PDE II mediates the effects of NO, we next tested whether we could block its effects by treating tubules with a cAMP analogue not hydrolyzed by PDE II (23). We found that in the presence of db-cAMP (10^{-5} M), increasing endogenous NO did not decrease chloride absorption.[29] These results show that preventing the fall in intracellular cAMP blocks NO-induced inhibition of chloride absorption.

Because activation of PKG decreases cAMP in the cortical collecting duct, we questioned whether PKG activation is a necessary step in the NO second messenger cascade. For this purpose we tested the effect of NO in the presence of KT-5823, a PKG inhibitor. We found that KT-5823 (2 μM) did not block the inhibitory effect of NO on Cl

absorption,[29] indicating that PKG does not play a major role in NO-induced inhibition of Na/K/2Cl cotransport.

Together, these results suggest that NO decreases Na/K/2Cl cotransport by increasing cGMP which in turn decreases basal cAMP levels by activating PDE II. However, it is still not clear how a decrease in cAMP could inhibit Na/K/2Cl cotransport. Recent data suggest that stimulation of NKCC2 is likely due to an increase in NKCC2 at the apical membrane of thick ascending limbs.[30] Thus it is possible that NO decreases NKCC2 activity either by inhibiting exocytic insertion of newly formed cotransporters or by inducing its endocytosis and thus decreasing the number of functional units at the membrane. While this is a plausible hypothesis, it has not yet been tested experimentally.

The thick ascending limb expresses all three isoforms of NOS. To determine the contribution of NO produced by the different isoforms on Na/K/2Cl cotransport regulation in the thick ascending limb, we studied the effect of L-arginine on Cl absorption by thick ascending limbs isolated from nNOS, iNOS and eNOS knock-out mice. L-arginine decreased Cl absorption in thick ascending limbs isolated from nNOS and iNOS knock-out mice but failed to inhibit Cl fluxes in eNOS knock-out mice.[31] To make sure eNOS is the NOS isoform that regulates thick ascending limb transport, an *in vivo* gene transfer technique was used to selectively transduce thick ascending limbs from eNOS knock-out mice with eNOS. In thick ascending limbs transduced with eNOS, L-arginine inhibited Cl absorption as it did in wild-type animals; whereas in eNOS knock-out mice transduced with a reporter construct, L-arginine failed to inhibit Cl absorption.[12] These data indicated that NO produced by eNOS is responsible for inhibition of the thick ascending limb Na/K/2Cl cotransporter.

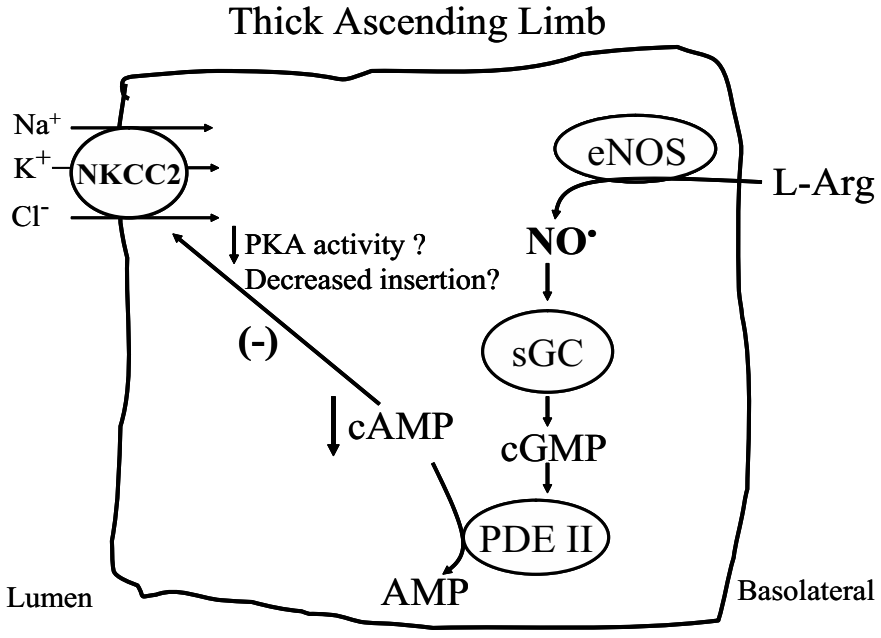

Figure 1. Mechanism by which NO inhibits NKCC2 activity in the thick ascending limb.

3.2. Macula Densa Cells

The Na/K/2Cl cotransporter NKCC2 is also present at the apical membrane of macula densa cells.[18] In these cells, NKCC2 is important not only for transepithelial NaCl absorption, but acts also as a sensor of luminal NaCl concentration, producing the initial signal for the tubulo-glomerular feedback (TGF) response. The TGF response is initiated by a change in luminal NaCl concentration at the lumen of the macula densa which results in a decrease in the diameter of the afferent arteriole.[32] Although the signaling of the TGF response is known to be very complex, it was first shown that apical Na/K/2Cl cotransport was essential for TGF, since the addition of furosemide to the macula densa lumen completely abolished TGF. Thus, regulation of Na/K/2Cl cotransport in the macula densa is important for regulation of afferent arteriolar tone.

The NOS isoform nNOS is expressed in the macula densa and its expression in these cells is higher than in tubular cells, suggesting an important role for this isoform in modulating the function of the macula densa and juxtaglomerular apparatus.[33] In fact, studies using pharmacological inhibitors of NOS have shown that nNOS-derived NO produced in the macula densa blunts TGF responses in rats, rabbits, and mice.[34] However, the precise mechanism by which nNOS-derived NO attenuated the TGF response was unknown. Because it was found that NO decreases the activity of the apical Na/K/2Cl cotransporter in the thick ascending limb,[25] it could be hypothesized that NO acts in an autocrine manner in the macula densa, blunting TGF by tonically inhibiting NaCl entry via the Na/K/2Cl cotransporter. He, et al.,[28] studied the effect of NO on Na/K/2Cl cotransport activity in cultured renal epithelial cells having the properties of macula densa cells (MMDD1). They found that the NO donors sodium nitroprusside (SNP) and S-nitroso-N-acetylpenicillamine (SNAP) inhibited Na/K/2Cl cotransport activity in a dose-dependent manner as measured by a decrease in ouabain-insensitive bumetanide-sensitive Rb uptake. To study if endogenously produced NO inhibits Na/K/2Cl cotransport in these macula densa cells, they studied the effect of 7-NI, a selective nNOS inhibitor, and found that nNOS inhibition stimulated bumetanide-sensitive Rb uptake. Kovacs, et al.,[35] studied the effect of endogenous NO on Na/K/2Cl cotransport in intact macula densa cells from microdissected juxtaglomerular apparatus. In agreement with the results obtained in cultured cells, these investigators observed that inhibition of nNOS with 7-NI stimulated Na/K/2Cl cotransport activity, indicating that endogenous NO tonically inhibits NKCC2 activity in these cells. Thus, most data support the conclusion that NO also inhibits Na/K/2Cl cotransport in macula densa cells.

In contrast to the mechanism observed in the thick ascending limb, He, et al.,[28] found that NO did not stimulate cGMP production or alter cAMP levels in cultured macula densa cells nor did it increase intracellular Ca^{2+} levels or stimulate ERK kinase activity in these cells. However, pre-treatment of macula densa cells with inhibitors of the cytochrome P-450 enzyme abolished the inhibitory effect of NO on Na/K/2Cl cotransporter activity. These data indicate that the mechanisms by which NO inhibits Na/K/2Cl cotransport is cell-type specific. However, it is still not clear how cytochrome P-450 stimulation by NO inhibits Na/K/2Cl cotransporter activity in the macula densa or the thick ascending limb as shown by others.

4. REGULATION OF OTHER Cl-DEPENDENT TRANSPORTERS BY NO

Other Cl-dependent transporters are expressed along the nephron. The thiazide-sensitive Na/Cl cotransporter (TSC) is present in the apical membrane of distal tubule cells. This Cl-dependent transporter belongs to the electroneutral cation-chloride-coupled cotransporter gene family (SLC12) which also includes the Na/K/2Cl and K-Cl cotransporters.[36] While TSC is essential for transepithelial NaCl absorption in the distal convoluted tubule, very little is known about its regulation or whether its activity may be affected by NO.

The K-Cl cotransporters are also present in various nephron segments such as the proximal tubule, thick ascending limb and distal convoluted tubule where they play an important role in NaCl absorption. Despite their importance, it is not known whether NO regulates K-Cl cotransport in the kidney. However data from other cell types[37, 38] suggest that NO itself or other NO metabolites may be important regulators of K-Cl cotransport.

5. REGULATION OF Na/H EXCHANGER BY NO

5.1. Proximal Tubule

The proximal tubule reabsorbs 50-60% of the total filtered load of inorganic solutes and water, while organic solutes such as sugars, amino acids and other metabolites are essentially completely reabsorbed by this segment. Solutes are transported into the cell via apical Na-coupled cotransporters including Na/glucose, Na/PO_4 and Na/amino acid cotransporters or exchangers like the Na/H exchanger.[39] Similar to the thick ascending limb, the energy required for Na-coupled transport is provided by the electrochemical gradient generated by basolateral Na/K ATPase.

The Na/H exchanger NHE3 is present in the apical membrane of the proximal tubule and is one of the primary transporters that mediates Na and bicarbonate absorption in this nephron segment. Roczniak and Burns[40] studied the effect of NO on Na/H exchanger activity in primary cultures of proximal tubule cells. They found that the NO donors nitroprusside (1 mM) and S-nitroso-N-acetylpenicillamine (1 mM) decreased amiloride-sensitive, ouabain-insensitive Na uptake, indicative of decreased Na/H exchanger activity. These NO donors also stimulated cGMP production in these cells and the cGMP analogue 8-Br-cGMP likewise inhibited Na/H exchange activity. Moreover, these investigators found that the inhibitory effect of NO on the Na/H exchanger were partially prevented by pre-treatment with a guanylate cyclase inhibitor, suggesting that cGMP mediates the effects of NO. However, the mechanism by which NO inhibits Na/H exchange in the proximal tubule beyond cGMP is still not clear.

5.2. Thick Ascending Limb

The thick ascending limb is an important site for reabsorption of bicarbonate that escapes absorption by the proximal tubule. Bicarbonate absorption in this nephron segment is mediated primarily by Na/H exchanger (NHE) proteins.[41] At least two NHE isoforms are expressed in the thick ascending limb, including NHE3 in the apical membrane and NHE1 in the basolateral membrane. Because NO inhibited apical Na/H exchange activity in the proximal tubule, we studied its effect on the Na/H exchanger in the thick ascending

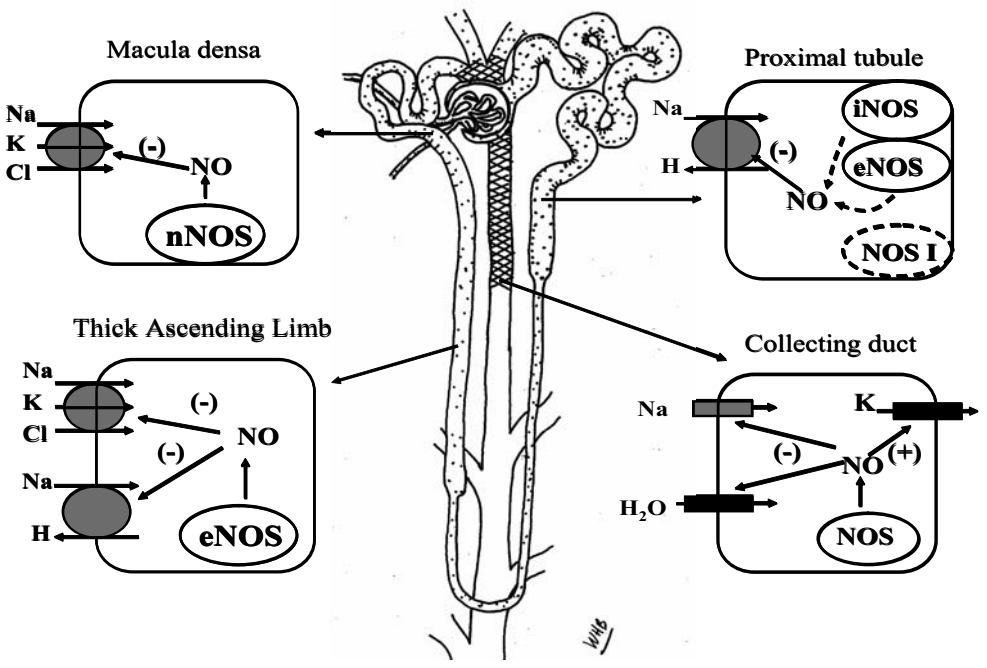

Figure 2. Effect of NO on Cl-dependent and Cl-independent transporters along the nephron.

limb. By measuring the initial rate of intracellular pH recovery (pH_i) after base loading, it was observed that pH_i recovery was slower after thick ascending limbs were treated with the NO donor spermine NONOate or nitroglycerin, suggesting that NO decreased total NHE activity.[42] When dimethyl amiloride (DMA), an NHE inhibitor, was added to the solution bathing the basolateral membrane, NO still inhibited pH_i recovery. Similarly, when DMA was present at the apical side, NO also inhibited pH_i recovery. Together, these data indicate that NO inhibits both apical and basolateral NHE activity, although the inhibitory effect was greater on apical NHE.

Because apical NHE mediates bicarbonate absorption in the thick ascending limb, we tested whether NO could also inhibit bicarbonate absorption. It was observed that endogenous NO, produced from L-arginine, reversibly decreased net bicarbonate absorption by 35%, consistent with inhibition of apical NHE.[43] We next studied whether the cascade mediating the effect of NO on NHE was similar to the mechanism by which NO inhibits Na/K/2Cl cotransport in the thick ascending limb. Pre-treatment of thick ascending limbs with a sGC inhibitor completely blocked the effect of NO on bicarbonate transport, whereas the cGMP analogues 8-Br-cGMP and dibutyryl-cGMP decreased bicarbonate absorption. In the presence of cGMP analogues, inducing NO synthesis did not further inhibit bicarbonate absorption. Together, these data indicated that NO inhibits NHE and bicarbonate absorption by stimulating sGC and inducing cGMP production. Finally, we studied whether blockade of PKG could prevent the effect of NO and found that the PKG inhibitor KT-5823 completely abolished the inhibitory effect of NO on bicarbonate absorption.[43] In agreement with the role of cGMP and PKG in the inhibition of NHE3, it

has recently been reported that this signaling cascade also mediates the inhibitory effect of NO on NHE3 activity in cultured intestinal epithelial cells.[44]

Overall, our data suggest that the effect of endogenous NO on NHE and Na/K/2Cl cotransport activity in the thick ascending limb is mediated by cGMP but the final mechanism by which cGMP inhibits these transporters is different, involving PKG in the case of the NHE and PDE II in the case of the Na/K/2Cl cotransporter.

6. CONCLUSIONS

During the past years, NO has been shown to be an important regulator of ion transport in most epithelial cells. While it is evident that NO regulates Cl-dependent Na transporters such as the Na/K/2Cl cotransporter in the kidney, its role in the regulation of other Cl-dependent transporters such as Na/Cl and K/Cl cotransport has not yet been studied. In this review, we have focused on the regulation of a Cl-independent Na transporter by NO, the Na/H exchanger, because of its importance in NaCl, water, and bicarbonate reabsorption along the nephron. Again, not only in kidney epithelial cells but also in other tissues, NO has been shown to be an important regulator of this transporter. However, the precise mechanism by which NO modulates these transport systems is not fully understood and further work is needed in this area.

In addition to its role in modulating Na/K/2Cl cotransport and Na/H exchanger, NO has also been shown to modulate the activity of K channels in the thick ascending limb as well as Na and K channels in the collecting duct.[1] A regulatory role for NO in Na/K ATPase has been reported in the proximal tubule, and regulation of paracellular permeability of this nephron segment by NO has also been suggested by other investigators.[45] Due to space constraints, we have been unable to focus on the effects of NO in modulating these transporters and channels along the nephron which have been discussed in other reviews.

Overall, the inhibitory effect of NO on the activity of individual transporters along the nephron is in agreement with its natriuretic and diuretic effect in the whole animal, emphasizing the importance of NO in the regulation of sodium and water balance.

7. REFERENCES

1. P.A. Ortiz and J.L. Garvin, Role of nitric oxide in the regulation of nephron transport, *Am J Physiol (Renal Physiol)* **282**, F777-F784 (2002).
2. S.M. Gibbs, Regulation of neuronal proliferation and differentiation by nitric oxide, *Mol Neurobiol*, **27**, 107-120 (2003).
3. J.M. Hare and W.S. Colucci, Role of nitric oxide in the regulation of myocardial function, *Prog Cardiovasc Dis*, **38**, 155-166 (1995).
4. G.P. Ahern, V.A. Klyachko and M.B. Jackson, cGMP and S-nitrosylation: two routes for modulation of neuronal excitability by NO, *Trends Neurosci*, **25**, 510-517 (2002).
5. O.W. Griffith and D.J. Stuehr, Nitric oxide synthases: properties and catalytic mechanism, *Ann Rev Physiol*, **57**, 707-736 (1995).
6. A. Roczniak, J. Zimpelmann, K.D. Burns, Effect of dietary salt on neuronal nitric oxide synthase in the inner medullary collecting duct, *Am J Physiol*, **275**:F46-F54 (1998).
7. A. Tojo, S.S. Gross, L. Zhang, C.C. Tisher, H.H. Schmidt, C.S. Wilcox,and K.M. Madsen, Immunocytochemical localization of distinct isoforms of nitric oxide synthase in the juxtaglomerular apparatus of normal rat kidney, *J Am Soc Nephrol*, **4**,1438-1447 (1994).

8. K.Y. Ahn, M.G. Mohaupt, K.M. Madsen and B.C. Kone BC, In situ hybridization localization of mRNA encoding inducible nitric oxide synthase in rat kidney, *Am J Physio,* **267**, F748-F757 (1994).
9. B.C. Kone and C. Baylis, Biosynthesis and homeostatic roles of nitric oxide in the normal kidney, *Am J Physiol*, **272**, F561-F578 (1997).
10. N.J. Guzman, M.Z. Fang, S.S. Tang, J.R. Ingelfinger and L.C. Garg, Autocrine inhibition of Na+/K(+)-ATPase by nitric oxide in mouse proximal tubule epithelial cells, *J Clin Invest*, **95**, 2083-2088 (1995).
11. P.A. Ortiz and J.L. Garvin, Trafficking and activation of eNOS in epithelial cells, *Acta Physiol Scand,* **179**, 107-114 (2003).
12. P.A. Ortiz, N.J. Hong, D. Wang and J.L. Garvin, Gene transfer of eNOS to the thick ascending limb of eNOS-KO mice restores the effects of L-arginine on NaCl absorption, *Hypertension,* **42**, 674-679 (2003).
13. D.A. Molony, W.B. Reeves, T.E. Andreoli, Na+:K+:2Cl- cotransport and the thick ascending limb, [Review] *Kidney Int*, **36**, 418-426 (1989).
14. G. Gamba, A. Miyanoshita, M. Lombardi, J. Lytton, W.S. Lee, M.A. Hediger, and S.C. Hebert, Molecular cloning, primary structure, and characterization of two members of the mammalian electroneutral sodium-(potassium)-chloride cotransporter family expressed in kidney, *J Biol Chem,* **269**, 17713-17722 (1994).
15. P. Igarashi, G.B. Vanden Heuvel, J.A. Payne and B. Forbush III, Cloning, embryonic expression, and alternative splicing of a murine kidney-specific Na-K-Cl cotransporter, *Am J Physiol (Renal Fluid Electrol Physiol*) **269,** F405-F418 (1995).
16. M.R. Kaplan, M.D. Plotkin, W.S. Lee, Z.C. Xu, J. Lytton and S.C. Hebert, Apical localization of the Na-K-Cl cotransporter, rBSC1, on rat thick ascending limbs, *Kidney Int*, **49**:40-47 (1996).
17. D.B. Mount, A. Baekgaard, A.E. Hall, C. Plata, J. Xu, D.R. Beier, G. Gamba and S.C. Hebert, Isoforms of the Na-K-2Cl cotransporter in murine TAL I. Molecular characterization and intrarenal localization, *Am J Physiol,* **276**, F347-F358 (1999).
18. N. Obermuller, S. Kunchaparty, D.H. Ellison and S. Bachmann, Expression of the Na-K-2Cl cotransporter by macula densa and thick ascending limb cells of rat and rabbit nephron, *J Clin Invest,* **98**, 635-640 (1996).
19. S. Nielsen, A.B. Maunsbach, C.A. Ecelbarger and M.A. Knepper, Ultrastructural localization of Na-K-2Cl cotransporter in thick ascending limb and macula densa of rat kidney, *Am J Physiol*, **275**, F885-F893 (1998).
20. S.C. Hebert and T.E. Andreoli, Control of NaCl transport in the thick ascending limb, *Am J Physiol*, **246**, F745-F756 (1984).
21. W.H. Wang, Two types of K+ channel in thick ascending limb of rat kidney, *Am J Physiol*, **267**, F599-F605 (1994).
22. R. Greger, Ion transport mechanisms in thick ascending limb of Henle's loop of mammalian nephron, *Physiol Rev,* **65**, 760-797 (1985).
23. C.F. Plato, B.A. Stoos, D. Wang and J.L. Garvin, Endogenous nitric oxide inhibits chloride transport in the thick ascending limb, *Am J Physiol,* **276**, F159-F163 (1999).
24. C.F. Plato, B.A Stoos, D. Wang and J.L. Garvin, Endogenous nitric oxide inhibits chloride transport in the thick ascending limb, *Am J Physiol,* **276**, F159-F163 (1999).
25. P.A. Ortiz, N.J. Hong and J.L. Garvin, NO decreases thick ascending limb chloride absorption by reducing Na(+)-K(+)-2Cl(-) cotransporter activity, *Am J Physiol (Renal Physiol)* **281**, F819-F825 (2001).
26. M. Lu, X. Wang and W. Wang, Nitric oxide increases the activity of the apical 70-pS K+ channel in TAL of rat kidney, *Am J Physiol,* **274**, F946-F950 (1998).
27. F. Akar, E. Skinner, J.D. Klein, M. Jena, R.J. Paul, W.C. O'Neill, Vasoconstrictors and nitrovasodilators reciprocally regulate the Na+-K+-2Cl- cotransporter in rat aorta, *Am J Physiol*, **276**, C1383-C1390 (1999).
28. H. He, T. Podymow, J. Zimpelmann and K. D. Burns, NO inhibits Na+-K+-2Cl- cotransport via a cytochrome P-450-dependent pathway in renal epithelial cells (MMDD1), *Am J Physiol (Renal Physiol*) **284**, F1235-F1244 (2003).
29. P.A. Ortiz and J.L. Garvin, NO inhibits NaCl absorption by rat thick ascending limb through activation of cGMP-stimulated phosphodiesterase, *Hypertension,* **37**, 467-471 (2001).
30. P.A. Ortiz, VAMP-2/3 mediates cAMP-induced translocation of NKCC2 to the apical membrane of the thick ascending limb, *J Am Soc Nephrol*, **14**, 9A. (2003).
31. C.F. Plato, E.G. Shesely and J.L. Garvin, eNOS mediates L-arginine-induced inhibition of thick ascending limb chloride flux, *Hypertension,* **35**, 319-323 (2000).
32. J. Schnermann and D.Z. Levine, Paracrine Factors in Tubuloglomerular Feedback: Adenosine, ATP, and Nitric Oxide, *Ann Rev Physiol,* **65**, 501-29 (2003).
33. C.S. Wilcox and W.J. Welch, Macula densa nitric oxide synthase: expression, regulation, and function, *Kidney International – Supplement,* **67**, S53-S57 (1998).
34. Y.L. Ren, J.L. Garvin, S. Ito and O.A. Carretero, Role of neuronal nitric oxide synthase in the macula densa, *Kidney Int,* **60**, 1676-1683 (2001).

35. G. Kovacs, P. Komlosi, A. Fuson, J. Peti-Peterdi, L. Rosivall and P.D. Bell, Neuronal nitric oxide synthase: its role and regulation in macula densa cells, *J Am Soc Nephrol,* **14**, 2475-2483 (2003).
36. S.C. Hebert, D.B. Mount and G. Gamba, Molecular physiology of cation-coupled Cl(-) cotransport: the SLC12 family, *Pflugers Arch,* Feb **447**(5), 580-93 (2004).
37. P.K. Lauf and N.C. Adragna, K-Cl cotransport: properties and molecular mechanism, *Cell Physiol Biochem*, **10**, 341-354 (2000).
38. N.C. Adragna and P.K. Lauf, Role of nitrite, a nitric oxide derivative, in K-Cl cotransport activation of low-potassium sheep red blood cells, *J Membr Biol,* **166**, 157-167 (1998).
39. C.A. Berry and F.C. Rector, Jr, Electroneutral NaCl absorption in the proximal tubule: mechanisms of apical Na-coupled transport, *Kidney Int,* **36**, 403-411 (1989).
40. A. Roczniak and K.D. Burns, Nitric oxide stimulates guanylate cyclase and regulates sodium transport in rabbit proximal tubule, *Am J Physiol*, **270,** F106-F115 (1996).
41. D.W. Good, The thick ascending limb as a site of renal bicarbonate reabsorption, *Semin Nephrol*, **13**, 225-235 (1993).
42. F. Tajima, S. Sagawa, J. Iwamoto, K. Miki, J.R. Claybaugh and K. Shiraki, Renal and endocrine responses in the elderly during head-out water immersion, *Am J Physiol,* **254**, R977-R983 (1988).
43. P.A. Ortiz and J.L. Garvin, Autocrine effects of nitric oxide on HCO(3)(-) transport by rat thick ascending limb, *Kidney Int,* **58,** 2069-2074 (2000).
44. R.K. Gill, S. Saksena, I.A. Syed, S. Tyagi, W.A. Alrefai, J. Malakooti, K. Ramaswamy, and P.K. Dudeja, Regulation of NHE3 by nitric oxide in Caco-2 cells, *Am J Physiol (Gastrointest Liver Physiol*), **283**, G747-G756 (2002).
45. M. Liang and F.G. Knox, Production and functional roles of nitric oxide in the proximal tubule, *Am J Physiol (Regul Integr Comp Physiol),* **278**, R1117-R1124 (2000).

15

VOLUME ACTIVATED ANION CHANNEL AND ASTROCYTIC CELLULAR EDEMA IN TRAUMATIC BRAIN INJURY AND STROKE

Harold K. Kimelberg*

1. INTRODUCTION

A number of pathological states are associated with inappropriate channel activities, e.g., dysfunction of chloride channels in kidney diseases, cystic fibrosis and myotonias,[1] and the Gardos potassium channel in sickle cell anemia.[2] Also a number of other CNS diseases such as epilepsy and cerebral ischemia are thought to be associated with ion channel dysfunction.[3] However, there has been no evidence as yet for the dysfunction of the volume regulated anion (VRAC) channel, also known as volume sensitive organic osmolyte anion channels (VSOAC) and, when monitored electrophysiologically, as $I_{Cl,swell}$. Other acronyms are VSOR (volume sensing outwardly rectifying Cl^- channel) and VRClC (volume regulated chloride channel).[4] These channels are currently known only by their electrophysiological and transport activities, and in spite of several claims, their molecular basis or bases are not known with any certainty. However, their physiology is definitive and there have been no pathological states clearly associated with that.[5, 6] Their molecular identification would, of course, make association of VRACs with pathologies easier, as it would allow manipulation of its expression and the identification of more specific inhibitors than are available to date.

The main functions of VRACs are thought to be volume regulation, ion secretion and cell proliferation. In volume regulation, they are activated when cells are swollen rapidly, as when experimentally exposed to a rapid decrease in medium osmolarity.[5, 7] They are also activated when the media osmolarity is gradually reduced as measured by release of taurine and D-aspartate but with no detectable change in relative cell volume, a process termed isovolumetric regulation.[8] Presumably, this results in activation of VRACs with a time course coincident with the rate of the osmolarity change, and the sensitivity to the volume increase is such that the amount of swelling minimally required to activate is

* Harold K. Kimelberg, Neural and Vascular Biology Theme, Ordway Research Institute, 150 New Scotland Avenue., Albany, NY 12208,USA.

below detection by the methods employed. The original physiological role of volume regulation was presumably for adaptation of unicellular or simple organisms to varying salinity in estuarine areas.[9] Later, they became adapted for the progressive changes in osmolarity seen in the cortical to medullary regions of the kidney and solute uptake and secretion required for water homeostasis in more complex animals. All these processes have the characteristic of relatively slow adaptation. The roles of VRACs in proliferation have been shown in many cell types, and several other functions have been proposed.[4-6]

In this chapter, I will review older experiments in experimental traumatic brain injury (TBI) and newer studies performed in my laboratory in experimental stroke where astrocytic swelling is an early event known to occur within an hour or less after initiation of the insult. The data shows that anion transport blockers prevent astrocytic swelling in TBI or inhibition of release of excitatory amino acids in rat ischemia models, resulting in marked neuroprotection in all cases.

2. RESULTS AND DISCUSSION

Some time ago, we developed a cat closed TBI model[10] that reproduced some characteristics of human head injury such as delayed mortality and early astrocytic swelling.[11, 12] It involved an imposed hypoxia which more recently, together with secondary ischemia, has been considered a clinically relevant sequelae of TBI.[13] The 60 minute hypoxia was imposed forty minutes after cessation of the 67 second acceleration-deceleration injury and was required to achieve significant delayed mortality. When drugs were given, they were administered i.v. twenty minutes after the acceleration-deceleration injury (see Figure1).

Based on studies on high K^+-induced bicarbonate-dependent swelling of brain slices, we developed very effective non-diuretic inhibitors of this swelling.[14-17] One of the most effective of these, L644,711 or (R(+) [5,6-Dichloro9a-propyl-2,3,9,9a-tetrahydro 3-oxo-1H fluoren -7-yl)oxy]acetic acid) was tested in the cat TBI model.

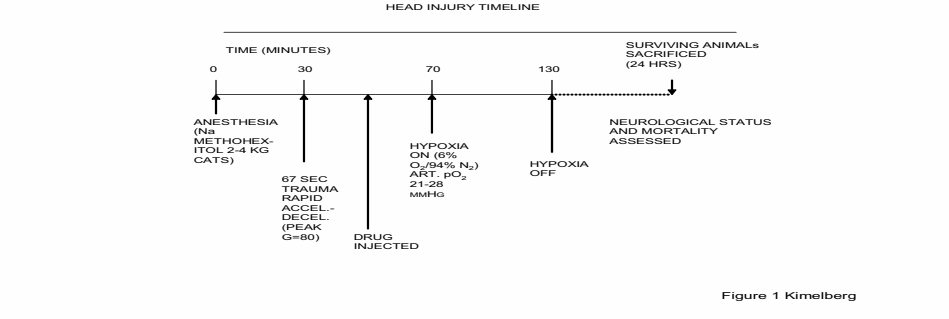

Figure 1. Time line of closed head rapid acceleration-deceleration in the cat.[17, 18]

Quantitative electron microscopy showed that L644,711 completely inhibited astrocytic swelling that normally peaked in the model at forty minutes after cessation of the

injury (Figure 2 and Ref.[12]). This was also associated with a remarkable decrease in mortality (Figure 3) and was found at a dose of 5-10 mg/kg when given i.v. However, because the compound is negatively charged at physiological pH, it does not readily enter the brain[14]. Therefore, we also undertook a series of experiments in which the compound was given by intra-cerebroventricular injection. Here, protection equally effective to the i.v dose of 5 mg/kg was found at a dose one hundredfold less (Figure 3 and Ref.[18]).

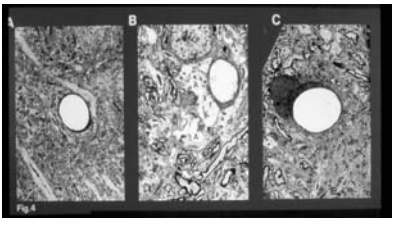

CONDITIONS	ASTROCYTIC AREA AS % AREA OF NEUROPIL AROUND A CAPILLARY
CONTROL	10.70(±1.50) 12.01(±0.24)
CONTROL HEAD INJURY + 40 MIN (i.e. NO HYPOXIA)	25.40(±2.80) 29.10(±3.47) 20.04(±1.34) 13.60(±0.76)
AS ABOVE + TREATMENT WITH L644,711 (10MG/KG)	10.31(±0.76) 11.10(±0.53) 11.31(±0.77) 10.99(±0.47)

EACH VALUE REPRESENTS THE MEAN±S.E. M OF 25 OBSERVATIONS OF DIFFERENT FIELDS FROM A SINGLE ANIMAL.

Figure 2. Inhibition of perivascular astrocytic swelling in cat TBI. Electron micrographs (EM) illustrate inhibition of such swelling when animals were treated with L641,711 twenty minutes after TBI. **A.** Sham animal. **B.** 40 min after TBI. Areas of astrocytic swelling are denoted as A. **C.** as in B except animals were treated i.v with 10 mg/kg L644,711. Table summarizes all the EM data from the number of animals shown. Total area refers to area outside basement membrane circumscribed by a circle of radius twice that of capillaries measured from the center of the capillary to the basement membrane.[12]

In both TBI and ischemia, marked perivascular astrocytic swelling is seen within 1 hour after initiation of ischemia or TBI in cat models.[12, 19] Indeed, if the decreased apparent diffusion coefficient (ADC) of water after ischemia, as measured by MRI, is primarily due to water movements from a less hindered extracellular to a more hindered intracellular environment, then cellular swelling occurs within minutes and persists for several hours after the onset of ischemia.[20] However, this interpretation of the ADC changes has been questioned and others have found that the ADC values of the intra- and extracellular spaces are essentially the same, with the intracellular signal representing about 80% of the total signal.[21] Based on the similar ADCs for extracellular markers and comparable intracellular compounds, it was suggested that the decrease in ADC seen

after ischemia is due to an increased viscosity of the intracellular space due to ischemia-induced changes such as proteolysis.[22] It remains to be resolved if such viscosity changes are consistent with the rapid onset of decreased ADC in ischemia. Such an effect is consistent with movement of more water from the extra- to intracellular spaces, as shown by EM studies,[12, 19] but does not necessarily indicate it. We have not yet measured effects on astrocytic swelling by anion transport inhibitors by morphometry in ischemia models, nor do we currently have access to small animal MRI facilities. However, we have shown that several of these inhibitors reduce the increase in extracellular EAAs and taurine, as measured by microdialysis, in the striatum after global ischemia, as will now be described.

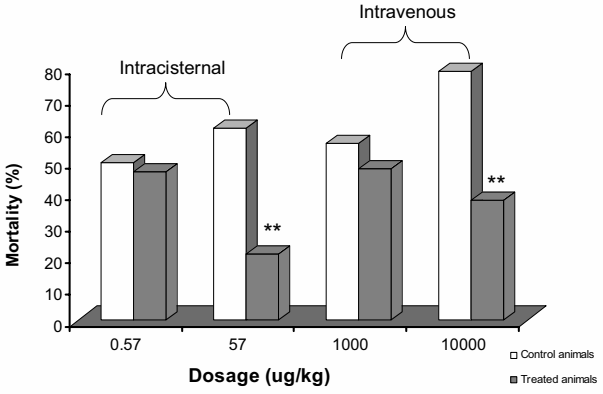

Figure 3 Kimelberg

Figure 3. Effect of L-644,711 on the mortality of cats subjected to an acceleration–deceleration plus hypoxia head injury. Bar graph of decreased mortality seen after intravenous or intracisternal injection of the drug 20 min after TBI in cat model. Treated vs. control level of significance, ** $p<0.025$.[18]

As shown in Figure 4A, approximately 40% of the glutamate increase is inhibited when the VRAC inhibitor DNDS[23] is perfused through the microdialysis probe or, as shown in Figure 4B, when the lipid soluble VRAC inhibitor tamoxifen.[4, 5] known to accumulate in the CNS.[24] when given i.v., is given systemically. The remaining approximately 60% of total release is reduced to around 20% when the astrocyte-specific EAA transport blocker dihydrokainate (DHK) is administered through the probe.[25] This implicates reversal of the astrocyte-specific GLT-1 transporter as a source of nearly half of the EAAs released during ischemia.[26] In more recent studies, we have shown that in a penumbral cortical region, DHK actually increases EAA levels while tamoxifen has a more complete and extended inhibitory effect.[27]

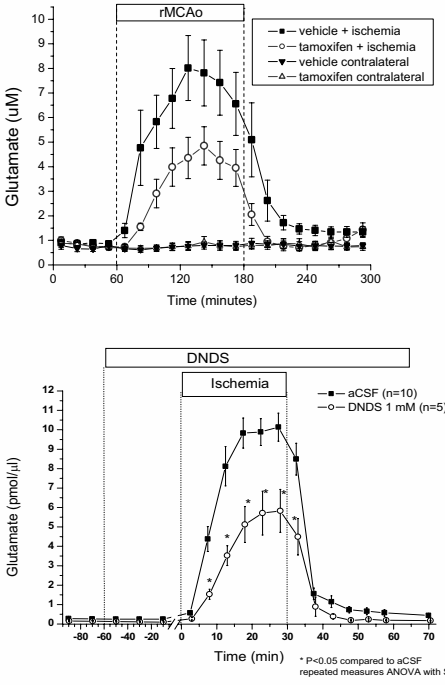

Figure 4 Kimelberg

Figure 4. Decrease in glutamate levels measured by microdialysis in the striatum with tamoxifen given i.v 25 min prior to the initiation of rMCAo at a dose of 5 mg/kg min. (upper figure), and 10 µM DNDS perfused through the probe for the period shown (lower figure).

The action of L644,711 can be interpreted on the basis that its ability to reduce astrocytic swelling will thereby inhibit VRAC activation and release of EAAs via this route.This may be because L644,711 inhibits other chloride channels needed for Donnan-induced uptake of K^+ and Cl^-, considered a major reason for the early astrocytic edema seen after TBI and ischemia where it is known that extracellular [K^+] can reach levels as high as 80 mM.[26] Although we have not determined whether tamoxifen inhibits astrocytic swelling in an ischemia model, we have done so in primary astrocytic monolayer cultures. We found that, unlike L644,711, tamoxifen did not inhibit high K^+-induced cell swelling in primary astrocyte cultures as measured by extracellular impedance increases (Figure 5A). However, it did inhibit high K^+-induced and hypotonic-induced EAA release.[28] The most parsimonious explanation for these data is shown in Figure 5B.

To show if the inhibition of EAA release correlates with neuroprotection, we asked the question whether treatment with tamoxifen conferred protection against ischemic cerebral damage. To do this, we used focal ischemia where protection can be readily measured as a decrease in the infarct volume as measured by staining with triphenyltetrazolium chloride (TTC). Tamoxifen was given systemically at a dose of 5 mg/kg which, from the data shown in Figure 3, we know decreases EAA levels. However, the decrease is only ~50%, and we need to know if there is a threshold effect. However, in more

recent studies, we have shown that the decrease in EAA levels caused by tamoxifen is around 80% in the penumbra.[27]

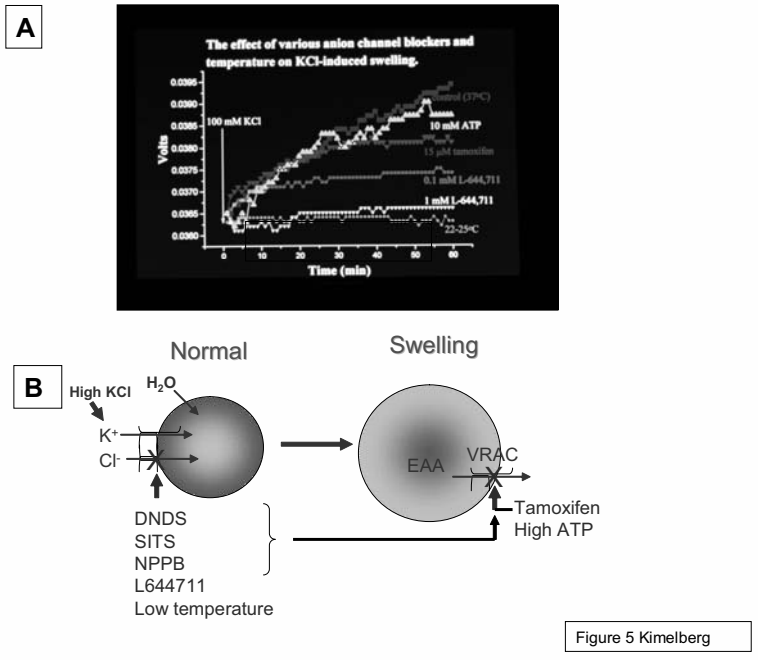

Figure 5A. L677,411 inhibits high K^+-induced swelling in primary astrocyte cultures as measured by changes in extracellular impedance, whereas tamoxifen and extracellularly-added ATP (an inhibitor of VRACs at high extracellular concentrations) do not. Also shown is the marked inhibition of the impedance increase by reduction of temperature to room temperature.[28] **B**. Proposed sites of interaction of L644,711 and tamoxifen to explain the data shown in **A** and the ability of both to inhibit high K^+ -induced release of EAAs from astrocytes. DNDS (4,4'-dinitrostilbene-2,2'-disulphonic acid), SITS (4,4'diisothiocyano-2,2'-disulfonic acid), NPPB (5-nitro-2-(3-phenylpropylamine)benzoic acid) and L644,711 are proposed to inhibit a Cl^- channel required for Cl^- entry with K^+ to produce Donnan swelling and inhibit VRACs. Tamoxifen and high $[ATP]_o$ are proposed to block only VRAC type anion channels.

In 2 hour reversible focal ischemia, (MCAo) treatment i.v. with tamoxifen up to 3 hours after initiation (1 hour post reperfusion) caused a uniform ~80 % reduction in infarct size.[29] There was an abrupt loss of protection when tamoxifen was given 4 hours after initiation of ischemia (Figure 6). Similarly, an 80% reduction in infarct size was seen up to 3 hours after initiation of permanent MCAo with tamoxifen given at a dose of 20 mg/kg plus sustaining doses every 12 hours.[30] Varying the dose showed the same effect at 5 mg/kg. Protection was also seen at 1 mg/kg but was statistically insignificant.

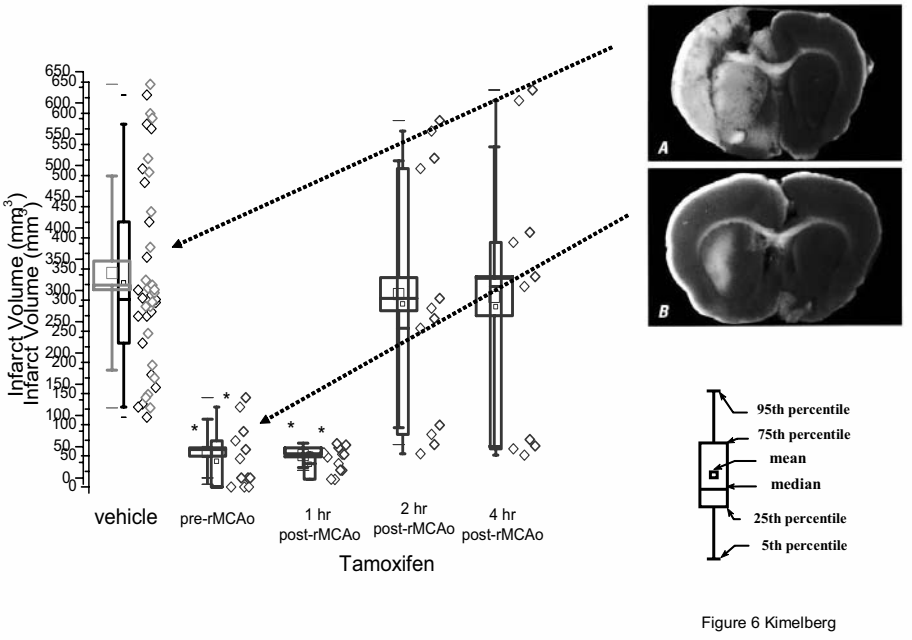

Figure 6 Kimelberg

Figure 6. Neuroprotection conferred by tamoxifen given at 5 mg/kg prior to and at varying times after initiation of two hours reversible MCAo induced by the thread model. Data redrawn from.[29] Insert shows typical reduced infarct in coronal sections of the brain with tamoxifen as measured with TTC.

Our data implicate VRACs in the release of EAA in cerebral ischemia and suggest that the marked neuroprotection noted with tamoxifen could be ascribed to this effect. The involvement of increased EAAs as a very early initiating event of the damaging ischemic cascade has been codified into the excitotoxicity hypothesis.[31] Perhaps the strongest evidence for this has been that protection with specific inhibitors of EAA receptors administered within a few hours after initiation of ischemia has always been shown to be neuroprotective with experimental ischemia[32-34] rather than the observation that a large increase in released EAAs, measured using microdialysis, is always seen in ischemia, as this could be an epiphenomenon. One of the characteristics of the release that has not been satisfactorily explained as a cause of ischemia-induced damage is that the EAA increase is transient and subsides following reperfusion while clear damage is seen only 12-24 hours later.[34] The rationalization for this is that the activation of EAA receptors does not lead immediately to damage but initiates a time-delayed cascade of events. However, without specifying and thus being able to precisely test this concept, one is simply redescribing the phenomena in seemingly more mechanistic terms. The existence of secondary and delayed release of EAAs, exacerbated by processes such as spreading depression, spreading out from the core to convert penumbra to core has been one such process.[35]

In the clinic, the EAA receptor blockers so successful in ischemia models have completely failed.[36, 37] There are numerous possible reasons: not measuring protection in

animal studies for extended periods up to months post ischemia; not checking effects on behavior; and not using older animals as most strokes occur in the elderly.[36] Also, it is important to adhere to the therapeutic windows indicated by the animal work. Experimentally, neuroprotective drugs are usually effective at one-three hours after initiation of the ischemia.[34] Clinically, such a narrow therapeutic window is not easily achieved and often, delays of 6-10 hours after apparent initiation of stroke symptoms were allowed.[37]

3. CONCLUSIONS, VRACS AND NEUROPROTECTION

The interpretation that part of the EAA efflux in experimental ischemia is via VRACs depends on tamoxifen's specificity as a VRAC inhibitor. With perhaps the exception of a compound DCPIB (4-(2-Butyl-6,7-dichlor-2-cyclopental-indan-1-obn-5yl) oxybutyric acid, there are still no truly specific inhibitors of VRACS.[38] The specificity of this compound was tested for its effect on $I_{Cl,Swell}$ in dissociated guinea pig myocytes, cultured calf pulmonary artery endothelial cells and several heteroexpression systems. It inhibited only $I_{Cl,Swell}$ and did not inhibit a variety of other channel currents. DCPIB is actually one of a group of indane (aryloxy) alkanoic acids derivatives synthesized by E.J. Cragoe, based on ethacrynic acid, and related to [(1H-fluoren-7-yl)oxy] alkanoic acids typified by L644,711.[14-16] These proprietary drugs were and are currently unavailable and their efficacy in inhibiting high K^+-induced, HCO_3^- dependent swelling of cat brain slices was tested by our group to find non-diuretic drugs for preventing brain cellular edema in a former Merck-sponsored project. The most effective were also tested in our animal TBI model[14-18, 39] and against astrocytic swelling in cat cortex superfused with adenosine.[40] Thus, the effectiveness of L644,711 in inhibiting astrocytic swelling and leading to increased protection adds extra data to support the protectiveness of inhibition of release from swollen astrocytes of EAAs via VRACs. However, the question arises why both L644,711 and DCPIB similarly inhibited high K^+-induced, HCO_3^- dependent swelling of cat brain slices if their only action is to inhibit VRACs. Decher, et al., obviously could not test all Cl^- channels,[38] and it might well be that these compounds also inhibit a depolarization activated Cl^- channel responsible for Cl^- uptake with K^+ to effect swelling (Figure 5). Further, it is not known how long the VRACs remain open and sufficient EAAs remain inside astrocytes so they can efflux. Things are clearly more complex with both known and unknown Cl^- channels that may be involved.

Tamoxifen is more widely non-specific. It is known as a specific estrogen modulator or SERM[41] which means it not only acts as an antagonist at the estrogen receptor (ER) but also can act as an agonist,[42] depending on the tissue. Because estrogens are known to be neuroprotective, this would appear to add to the mechanisms whereby tamoxifen can be neuroprotective. However, it seems unlikely that tamoxifen mimics the effects of estrogens on estrogen receptors (ER), as the protection is usually only seen with several days pre-treatment in ovarectomized females and is likely mediated by estrogen activating synthesis of endogenous neuroprotective protein compounds via its action on transcription factors.[43] Estrogens are added at low doses consistent with their action via ERs.[44] The concentrations at which we find tamoxifen neuroprotective[29, 30] is higher than the concentrations needed for its action at ERs, either as an antagonist or agonist.[42] To further complicate matters, tamoxifen is known to scavenge free radicals and also inhibits nNOS and peroxynitrite formation in the brain.[45,46] Finally, not as a complication but to

increase the likelihood that tamoxifen acts directly on brain processes, tamoxifen readily crosses the BBB and accumulates in the CNS.[24]

Thus, the hypothesis that release of damaging EAAs via VRACs contributes to the excitotoxic damage in the CNS awaits more conclusive tests. Like further knowledge of the physiology of what are operationally referred to as VRACs, VSOACs, etc., real knowledge of their pathological roles will require molecular identification. Then, the molecular engineering techniques such as complete or conditional knockouts or different transgenic animals as well as the development of specific inhibitors will allow more definitive studies. If the interpretation of the experiments described in this article are correct, the administration of a specific inhibitor or knockout of VRACs should decrease the damage caused by ischemia. At present, we have only suggestive evidence that this occurs from the L644,711 and tamoxifen data, but pursuit of this hypothesis uncovered a possibly clinically useful neuroprotective compound in tamoxifen, in the serendipitous, empirical, scientific tradition.

4. ACKNOWLEDGMENTS

The financial support of NIH through grants NS 23750 and 35205 for the studies from my laboratory quoted is gratefully acknowledged. I thank my colleagues Drs. Paul Feustel and Alexander Mongin for reading the manuscript and their helpful suggestions.

5. REFERENCES

1. O. Devuyst and W.B. Guggino, Chloride channels in the kidney: lessons learned from knockout animals, *Am. J. Physiol Renal Physiol.* **283**, F1176-F1191 (2002).
2. A.D. Maher and P.W. Kuchel, The Gardos channel: a review of the Ca $^{2+}$-activated K^+ channel in human erythrocytes, *Int. J. Biochem. Cell Biol.* **35**, 1182-1197 (2003
3. P. Calabresi, L.M. Cupini, D. Centonze, F. Pisani and G. Bernardi, Antiepileptic drugs as a possible neuroprotective strategy in brain ischemia, *Ann. Neurol.* **53**, 693-702 (2003).
4. B. Nilius and G. Droogmans, Amazing chloride channels: an overview, *Acta Physiol Scand.* **177**, 119-147 (2003).
5. B. Nilius, J. Eggermont, T. Voets, G. Buyse, V. Manolopoulos and G. Droogmans, Properties of volume-regulated anion channels in mammalian cells, *Prog. Biophys. Mol. Biol.* **68**, 69-119 (1997).
6. T. J. Jentsch, V. Stein, F. Weinreich and A.A. Zdebik, Molecular structure and physiological function of chloride channels, *Physiol Rev.* **82**, 503-568 (2002).
7. K. Strange, F. Emma and P.S. Jackson, Cellular and molecular physiology of volume-sensitive anion channels, *Am. J. Physiol. Cell Physiol.* **270**, C711-C730 (1996).
8. K. Tuz, B. Ordaz, L. Vaca, O. Quesada and H. Pasantes-Morales, Isovolumetric regulation mechanisms in cultured cerebellar granule neurons, *J. Neurochem.* **79**, 143-151 (2001).
9. M.E. Chamberlin and K. Strange, Anisosmotic cell volume regulation: a comparative view, *Am. J. Physiol.* **257**, C159-C173 (1989).
10. L.R. Nelson, R.S. Bourke, A.J. Popp, J. Cragoe, A. Signorelli, V.V. Foster and W. Creel, Evaluation of treatment modalities in severe head injuries using an animal model, *in* "Neural Trauma" (A.J. Popp, R.S. Bourke, L.R. Nelson and H.K. Kimelberg, Eds.), Raven Press, New York (1979).
11. R. Bullock, W.L. Maxwell, D.I. Graham, G.M. Teasdale and J.H. Adams, Glial swelling following cerebral contusion: an ultrastructural study, *J. Neurology, Neurosurgery and Psychiatry* **54**, 427-434 (1991).
12. K.D. Barron, M.P. Dentinger, H.K. Kimelberg, L.R. Nelson, R.S. Bourke, S. Keegan, R. Mankes and E.J. Cragoe, J., Ultrastructural features of a brain injury model in cat. I. Vascular and neuroglial changes and the prevention of astroglial swelling by a fluorenyl (aryloxy) alkanoic acid derivative (L-644, 711), *Acta Neuropathol. (Berl.)* **75**, 295-307 (1988).

13. Y. Matsushita, K. Shima, H. Nawashiro and K. Wada, Real-time monitoring of glutamate following fluid percussion brain injury with hypoxia in the rat, *J. Neurotrauma* **17**, 143-153 (2000).
14. E.J. Cragoe, Jr, Drugs for the treatment of traumatic brain injury, *Med. Res. Rev.* **7**, 271-305 (1987).
15. E.J. Cragoe, Jr, N.P. Gould, O.W. Woltersdorf, Jr, C. Ziegler, R.S. Bourke, L.R. Nelson, H.K. Kimelberg, J.B. Waldman, A.J. Popp and N. Sedransk, Agents for the treatment of brain injury. 1. (Aryloxy)alkanoic acids, *J. Med. Chem.* **25**, 567-579 (1982).
16. E.J. Cragoe, Jr, O.W. Woltersdorf, Jr, N.P. Gould, A.M. Pietruszkiewicz, C. Ziegler, Y. Sakurai, G.E. Stokker, P.S. Anderson, R.S. Bourke, H.K. Kimelberg, L.R. Nelson, K.D. Barron, J.E. Rose, D. Szarowski, A.J. Popp and J.B. Waldman, Agents for the treatment of brain edema. 2. [2,3,9,9a-Tetrahydro-3-oxy-substituted-1 H-fluoren-7-yl) oxyalkanoic acids and some of their analogues, *J. Med. Chem.* **29**, 825-841 (1986).
17. H.K. Kimelberg, J.W. Rose, K.D. Barron, R.A. Waniewski and E.J. Cragoe, Jr, Astrocytic swelling in head injury: beneficial effects of an inhibitor of anion exchange transport and glutamate uptake in glial cells, *Molec. Chem. Neuropathol.* **11**, 1-31 (1989).
18. H.K. Kimelberg, E.J. Cragoe, Jr, L.R. Nelson, A.J. Popp, D. Szarowski, J.W. Rose, O.W. Woltersdorf, Jr and A.M. Pietruszkiewicz, Improved recovery from a traumatic-hypoxic brain injury in cats by intracisternal injection of an anion transport inhibitor, *Cent. Nerv. Syst. Trauma.* **4**, 3-14 (1987).
19. J.H. Garcia, H. Kalimo, Y. Kamijyo and B.F. Trump, Cellular events during partial cerebral ischemia. I. Electron microscopy of feline cerebral cortex after middle-cerebral-artery occlusion, *Virchow's Arch. B Cell Path.* **25**, 191-206 (1977).
20. K.F. Liu, F.H. Li, T. Tatlisumak, J.H. Garcia, C.H. Sotak, M. Fisher and J.D. Fenstermacher, Regional variations in the apparent diffusion coefficient and the intracellular distribution of water in rat brain during acute focal ischemia, *Stroke* **32**, 1897-1905 (2001).
21. M.D. Silva, T. Omae, K.G. Helmer, F. Li, M. Fisher and C.H. Sotak, Separating changes in the intra- and extracellular water apparent diffusion coefficient following focal cerebral ischemia in the rat brain, *Magn Reson. Med.* **48**, 826-837 (2002).
22. T.Q. Duong, J.V. Sehy, D.A. Yablonskiy, B.J. Snider, J.J. Ackerman and J.J. Neil, Extracellular apparent diffusion in rat brain, *Magn Reson. Med.* **45**, 801-810 (2001).
23. T. Pearson and B.G. Frenguelli, Volume-regulated anion channels do not contribute extracellular adenosine during the hypoxic depression of excitatory synaptic transmission in area CA1 of rat hippocampus, *Eur. J. Neurosci.* **12**, 3064-3066 (2000).
24. A. Biegon, M. Brewster, H. Degani, E. Pop, D. Somjen and A.M. Kaye, A permanently charged tamoxifen derivative idsplays anticancer activity and improved tissue selectivity in rodents., *Cancer Res.* **56**, 4328-4331 (1996).
25. Y. Seki, P.J. Feustel, R.W. Keller, Jr, B.I. Tranmer and H.K. Kimelberg, Inhibition of ischemia-induced glutamate release in rat striatum by dihydrokainate and an anion channel blocker, *Stroke* **30**, 433-440 (1999).
26. H.K. Kimelberg, Cell volume in the CNS: Regulation and implications for nervous system function and pathology, *The Neuroscientist* **6**, 13-24 (2000).
27. P.J. Feustel, Y. Jin, and H.K. Kimelberg, Volume regulated anion channels are the predominant contributors to release of excitatory amino acids in the ischemic cortical penumbra. *Stroke*, in press (2004).
28. E. -M. Rutledge, M. Aschner and H. -K. Kimelberg, Pharmacological characterization of swelling-induced D- [^{3}H]aspartate release from primary astrocyte cultures, *Am. J. Physiol.:Cell Physiol.* **274**, C1511-C1520 (1998).
29. H.K. Kimelberg, P.J. Feustel, Y. Jin, J. Paquette, A. Boulos, R.W. Keller and B.I. Tranmer, Acute treatment with tamoxifen reduces ischemic damage following middle cerebral artery occlusion, *Neuro Report* **11**, 2675-2679 (2000).
30. H.K. Kimelberg, Y. Jin and P.J. Feustel, Neuroprotective activity of tamoxifen in permanent focal ischemia, *J. Neurosurgery* **99**, 138-142 (2003).
31. D.W. Choi, Excitotoxic cell death, *J.Neurobiol.* **23**, 1261-1276 (1992).
32. M.D. Ginsberg, Neuroprotection in brain ischemia: an update I. *The Neuroscientist* **1**, 95-103 (1995).
33. M.D. Ginsberg, Neuroprotection in brain ischemia: an update II. *The Neuroscientist* **1**, 164-175 (1995).
34. M.D. Ginsberg, Adventures in the pathophysiology of brain ischemia: penumbra, gene expression, neuroprotection. Tthe 2002 Thomas Willis lecture, *Stroke* **34**, 214-223 (2003).
35. J.A. Hartings, M.L. Rolli, X.C. Lu and F.C. Tortella, Delayed secondary phase of peri-infarct depolarizations after focal cerebral ischemia: relation to infarct growth and neuroprotection, *J.Neurosci.* **23**, 11602-11610 (2003).
36. S.B. DeBow, D.L. Clark, C.L. MacLellan and F. Colbourne, Incomplete assessment of experimental cytoprotectants in rodent ischemia studies, *Can. J. Neurol. Sci.* **30**, 368-374 (2003).

37. D.J. Gladstone, S.E. Black and A.M. Hakim, Toward wisdom from failure: lessons from neuroprotective stroke trials and new therapeutic directions, *Stroke* **33**, 2123-2136 (2002).
38. N. Decher, H.J. Lang, B. Nilius, A. Bruggemann, A.E. Busch and K. Steinmeyer, DCPIB is a novel selective blocker of I(Cl,swell) and prevents swelling-induced shortening of guinea-pig atrial action potential duration, *Br. J. Pharmacol* **134**, 1467-1479 (2001).
39. L.R. Nelson, E.L. Auen, R.S. Bourke, K.D. Barron, A.B. Malik, J. Cragoe, A.J. Popp, J.B. Waldman, H.K. Kimelberg, V.V. Foster, W. Creel and L. Schuster, Comparison of animal head injury models developed for treatment modality evaluation, *in* "Head Injury: Basic and Clinical Aspects" (R.G. Grossman and P.L. Gildenberg, Eds.), Raven Press, New York (1982).
40. R.S. Bourke, J.B. Waldman, H.K. Kimelberg, K.D. Barron, B.D. San Filippo, A. J. Popp and L.R. Nelson, Adenosine-stimulated astroglial swelling in cat cerebral cortex in vivo with total inhibition by a non-diuretic acylaryloxyacid derivative, *J. Neurosurgery* **55**, 364-370 (1981).
41. S.H. Mehta, K.M. Dhandapani, L.M. De Sevilla, R.C. Webb, V.B. Mahesh and D. W. Brann, Tamoxifen, a selective estrogen receptor modulator, reduces ischemic damage caused by middle cerebral artery occlusion in the ovariectomized female rat, *Neuroendocrinol.* **77**, 44-50 (2003).
42. J.I. MacGregor and V.C. Jordan, Basic Guide to the Mechanisms of Antiestrogen Action, *Pharmacological Reviews* **50**, 151-196 (1998).
43. N.J. Alkayed, S. Goto, N. Sugo, H.D. Joh, J. Klaus, B.J. Crain, O. Bernard, R.J. Traystman and P.D. Hurn, Estrogen and Bcl-2: gene induction and effect of transgene in experimental stroke, *J. Neurosci.* **21**, 7543-7550 (2001).
44. P.D. Hurn and L.M. Brass, Estrogen and stroke: a balanced analysis, *Stroke* **34**, 338-341 (2003).
45. H. Wiseman, Tamoxifen: new membrane-mediated mechanisms of action and therapeutic advances, *Trends Pharmacol Sci* **15**, 83-89 (1994).
46. K. Osuka, P.J. Feustel, A.A. Mongin, B I. Tranmer and H.K. Kimelberg, Tamoxifen inhibits nitrotyrosine formation after reversible middle cerebral artery occlusion in the rat, *J. Neurochem.* **76**, 1842-1850 (2001).

16

EFFECTORS AND SIGNALING EVENTS ACTIVATED BY CELL SHRINKAGE IN EHRLICH ASCITES TUMOR CELLS

Implications for cell proliferation and programmed cell death

Else K. Hoffmann and Stine Falsig Pedersen*

1. INTRODUCTION: CELL VOLUME CHANGES AS SIGNALING EVENTS

Ample evidence testifies to the pivotal importance of cell volume regulation for cell function.[1, 2] In addition to the maintenance of a stable steady-state volume, this includes the ability to recover cell volume after perturbations resulting either from variations in the tonicity of the environment or from cellular events such as secretion, uptake, or metabolic processes.[1, 2] Moreover, it is now well recognized that cell volume control is closely connected to the control of, on one hand, cell growth and proliferation, and on the other, cell death by either programmed cell death (PCD) or necrosis.[2, 3] Cell proliferation is augmented by cell swelling and inhibited by cell shrinkage.[4, 5] Consistent with this notion, increased activity of the shrinkage-activated membrane transport protein NHE1[6, 7] and NKCC1[8] is associated with cancer cell phenotypes and increased proliferation. Conversely, cell shrinkage is an integral part of the events leading to PCD,[3, 9, 10] and osmotic shrinkage *per se* can also elicit PCD.[5, 11-13] In the mammary cancer cell line Ehrlich ascites tumor cells (EATC) and the adherent Ehrlich Lettré tumor cells, the volume-activated signaling events and effector proteins have been studied in detail. Thus, this cell line makes an attractive model system for furthering the understanding of the pathophysiological implications of cell shrinkage. In the present review, we summarize the current knowledge regarding the signaling events and membrane transport proteins activated by cell shrinkage in EATC.

* Else K. Hoffmann and Stine Falsig Pedersen, Dept. of Biochemistry, August Krogh Institute, 13, Universitetsparken, DK-2100 Copenhagen Ø, Denmark.

2. EFFECTORS IN REGULATORY VOLUME INCREASE IN EHRLICH CELLS

Three shrinkage-activated membrane transport proteins contribute to Regulatory Volume Increase (RVI) in EATC: a Na^+-K^+-$2Cl^-$ cotransporter (NKCC1), a Na^+/H^+ exchanger (NHE1) and a non-selective cation channel. As discussed by Cala and Maldonado,[14] the contribution of a Na^+/H^+ exchanger to RVI is positively correlated with the magnitude of the cellular H^+ buffering capacity (β_i) and the activity of the Cl^-/HCO_3^- exchanger. Under nominally HCO_3^-free conditions, RVI in EATC is mediated by NKCC1,[15] while in the presence of HCO_3^-, NHE1 operating in parallel with the Cl^-/HCO_3^- exchanger contributes significantly (about 35%) to RVI.[16] The quantitative contribution of the non-selective cation channel to RVI has not been established in EATC, but a significant contribution has been demonstrated in other cell types.[17]

2.1 Na^+-K^+-$2Cl^-$ Cotransport

In the late 70's, it was demonstrated in EATC that Cl^- transport was completely dominated by exchange diffusion processes[18] rather than simple diffusion as previously thought. The rate constant for Cl^- flux was shown to be increased both after cell swelling and cell shrinkage, the former reflecting increased Cl^- conductance and the latter electroneutral anion-cation cotransport.[19, 20] It was subsequently demonstrated that upon osmotic shrinkage using the "RVI after RVD" protocol, bumetanide-sensitive Cl^- and K^+ influx, which is essentially zero in isotonically incubated cells, increased substantially; however, a distinction between Na^+-K^+-$2Cl^-$ cotransport with a recycling of K^+ or Na^+ Cl^- cotransport could not be made at the time.[21] If the cells were shrunken by adding sucrose to increase extracellular osmolarity, RVI was not observed. It was suggested that this difference reflected that the lower $[Cl^-]_i$ in the "RVI after RVD" situation was re-quired for cotransporter activation.[21, 22] The relationship between shrinkage and $[Cl^-]_i$ has been discussed in numerous publications and is still incompletely understood.[23] In 1993, a non-steady-state flux ratio analysis of the bumetanide-sensitive Cl^- and K^+ fluxes in the presence of Ba^{2+} to block K^+ recycling and ouabain to block the Na^+/K^+ ATPase demonstrated unequivocally that the fluxes reflected Na^+,K^+,$2Cl^-$ cotransport.[15] The Na^+-K^+-$2Cl^-$ cotransport in EATC was later shown to be at least 90% homologous with the NKCC1 isoform cloned from mouse kidney[24] (B.S. Jensen, unpublished). In addition to being activated by osmotic cell shrinkage, NKCC1 in EATC has been shown to be activated by bradykinin,[15] thrombin, histamine,[25] and by the Ser/Thr protein phosphatase inhibitor, Calyculin A.[26] Inhibition of cell shrinkage prevented activation of NKCC1 as measured 1-2 min after stimulation by bradykinin, indicating that activation was secondary to Ca^{2+}-induced cell shrinkage.[27] Similar results were obtained with thrombin.[28] The "first on-first off" model for Na^+-K^+-$2Cl^-$ cotransport,[29] was confirmed in EATC, in which K^+ occlusion during the transport cycle was furthermore demonstrated using $^{86}Rb^+$ as a tracer.[73] Using [^{3}H] bumetanide, the density of NKCC1 molecules in the EATC plasma membrane was estimated at 1,446 bumetanide sites per μm,[30] under isotonic as well as hypertonic conditions.[31] Long-term hypertonic exposure elicits a marked upregulation of NKCC1 expression.[32]

2.2 Na^+/H^+ Exchange

The presence of a Na^+/H^+ exchange system in EATC was established in the mid-80's.[33] The expression of three NHE isoforms: NHE1, NHE2, and NHE3, has been found in EATC.[34] Osmotic cell shrinkage elicits robust Na^+/H^+ exchange activity in EATC,[16, 35] and pharmacological evidence indicates that NHE1 is the primary isoform activated by osmotic cell shrinkage.[34] In addition to its activation by osmotic cell shrinkage, Na^+/H^+ exchange in EATC is also activated by intracellular acidification[36] and by stimulation with Ca^{2+}-mobilizing agents such as ATP,[33, 37] LPA,[38] thrombin, and bradykinin.[39] At least in EATC, activation of Na^+/H^+ exchange by Ca^{2+}-mobilizing agents is secondary to cell shrinkage resulting from Ca^{2+}-induced activation of Cl^- and K^+ channels.[33, 37-39] Similar to findings in other cell types, shrinkage-induced Na^+/H^+ exchange in EATC is ATP-dependent, but the mechanism(s) underlying the requirement for ATP remains elusive.[40]

2.3 Non-Selective Cation Channels

A shrinkage-activated Na^+ conductance was demonstrated in EATC in 1978.[19] The presence of a 14 pS non-selective cation channel was subsequently demonstrated.[41] This channel has a selectivity ratio $P_{Na}:P_{Li}:P_K;P_{Choline}:P_{NMDG}$ of 1.00:0.97:0.88:0.03:0.01 and is inhibited by gadolinium, benzamil, amiloride, and EIPA and is possibly related to the epithelial Na^+ channels (ENaCs).[41]

3. SIGNALING EVENTS ACTIVATED BY CELL SHRINKAGE IN EHRLICH CELLS

A wide range of signaling events are activated by osmotic cell shrinkage in EATC. In the following, we summarize current knowledge of these events. Effects of various signaling events on shrinkage-induced NHE1 and NKCC1 activity are seen in Table 1.

3.1 Ca^{2+} and Calmodulin

Osmotic cell shrinkage does not elicit a detectable increase in $[Ca^{2+}]_i$ in EATC.[39] Shrinkage-induced NKCC1 activation is dependent on a basal level of $[Ca^{2+}]_i$[26] and is inhibited by the calmodulin antagonist pimozide[15] suggesting the involvement of Ca^{2+}-calmodulin, in agreement with findings by others.[42]

Shrinkage-induced NHE1 activation is unaffected by depletion of intracellular Ca^{2+} or removal of Ca^{2+} from the incubation medium[16] but is partially inhibited by pimozide.[16] This lack of requirement for Ca^{2+}, but dependence on calmodulin, is similar to what has been shown in other cell types[43, 44] and is likely to reflect the direct binding of calmodulin to NHE1.[43]

3.2 Protein Kinases and Phosphatases

In EATC, osmotic cell shrinkage has been directly shown to elicit rapid activation of protein kinase C (PKC)[45] and a biphasic activation of p38 kinase with a rapid minor

activation phase, followed by a second robust activation between 10 and 30 min after hypertonic exposure[34] (Figures 1A and 1C).

Table 1. Signaling events involved in control of NKCC1 and NHE1 in EATC by osmotic cell shrinkage. The studies reported are based on the effect of inhibitors, and thus should be interpreted with caution.

	NKCC1	NHE1
Signaling Event		
Protein kinases		
PKC	(Yes) [a45]	Yes[16, 34]
MLCK	Yes[26]	No[34]
P38	ND	Yes[34]
ERK1/2	ND	No[34]
CaMKII	No[26]	ND
PKA	(Yes)[b26]	(No)[c72]
ROK	ND	No[55]
Tyrosin kinases	ND	(No)[d49]
Protein phosphatases		
PP1/PP2A	Yes[26]	Yes[16]
PP2B	No[26]	ND
$[Ca^{2+}]_i$	Basal level required[26]	No[16]
Calmodulin	Yes[15]	Yes[16]
F-actin	Yes[59, 62, 64]	ND

Abbreviations: PKC: Protein kinase C; MLCK: myosin light chain kinase; p38: p38 mitogen activated protein kinase; ERK1/2: extracellular signal regulated kinase 1/2; CaMKII: Calmodulin-dependent protein kinase II; PKA: protein kinase A; ROK: Rho kinase; PP: protein phosphatase; ND: not determined

[a] The PKC inhibitor chelerythrine inhibited shrinkage-induced NKCC activity by only 20%.[45]

[b] PKA appears to be required for NKCC1 activity, but not for the shrinkage-induced activition *per* se.[26]

[c] A slight inhibitory effect of 8-Br-cAMP was noted.[72]

[d] No effect of the tyrosine kinase inhibitor Lavendustin A.[49]

The shrinkage-induced activation of NKCC1 is potently inhibited by the myosin light chain kinase (MLCK) inhibitor ML-7 (IC_{50} = 0.4 μM).[26] The ML-7 sensitive fraction of NKCC1 activity was increased two-fold during RVI,[26] suggesting that MLCK is also shrinkage-activated in EATC, in agreement with findings in other cell types.[46-48] The protein kinase A (PKA) inhibitor H89 partially inhibited shrinkage-induced NKCC1 activation, but the PKA-sensitive fraction of NKCC1 activity was not increased upon cell shrinkage.[26] Arguing against a major role for PKC in shrinkage-activation of NKCC1, the PKC inhibitor chelerythrine inhibited shrinkage-induced NKCC activity by only 20%.[45] Finally, the Ca^{2+}-calmodulin-dependent kinase II (CaMKII) inhibitor KN-62 had no effect on shrinkage-induced NKCC1 activity.[26]

Shrinkage-induced NHE1 activation is inhibited by several inhibitors of PKC (chelerythrine, Gö6976, and Gö6850)[26] and by the p38 kinase inhibitor SB20358063 but not by ML-7 or PD98059 (PD98059 inhibits MEKK1 and consequently, the MEKK1 effectors,

ERK1/2[34]). NHE1 is also not inhibited by the Rho kinase (ROK) inhibitor Y-2763255 or the tyrosine kinase inhibitor lavendustin A.[49]

Ser/Thr protein phosphatases play a major role in the control of both NKCC1 and NHE1 in EATC,[26, 34] similar to findings in other cell types.[50-53] Calyculin A, an inhibitor of Ser/Thr protein phosphatases PP1 and PP2A potently activates NKCC1 and NHE1 in EATC under isotonic conditions and potentiates and prolongs their activation by osmotic shrinkage.[26, 34] Calyculin A-induced NKCC1 activation is highly transient, possibly reflecting that the substantial $[Cl^-]_i$ and water uptake mediated by NKCC1 inhibits the activity of the cotransporter.[26]

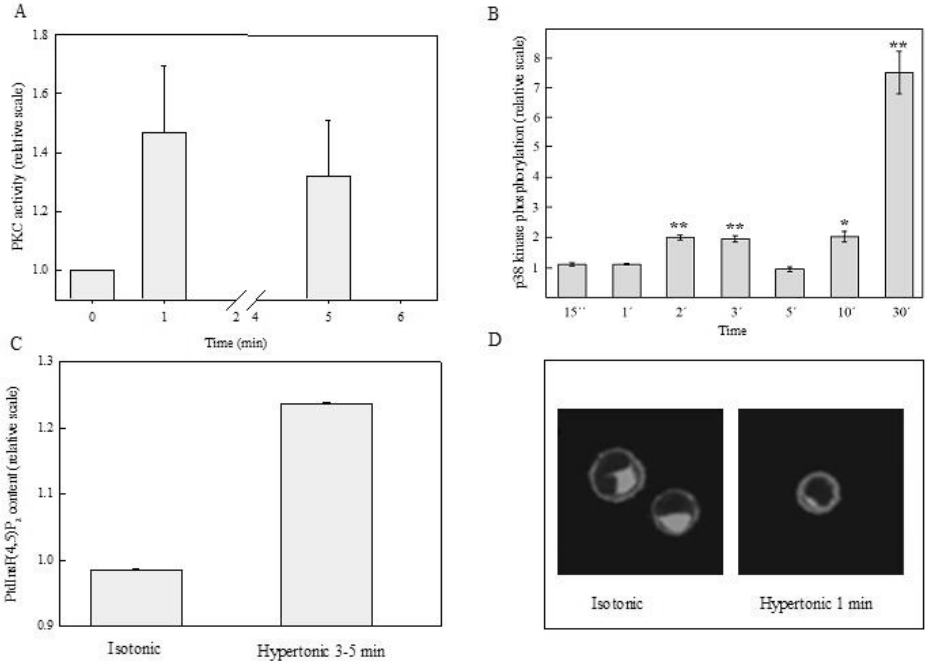

Figure 1. Signaling events activated by osmotic cell shrinkage in Ehrlich Ascites Tumor cells. A. Protein kinase C activity as a function of time after transfer to hypertonic medium (600 mOsm). Data from[45]. B. Level of p38 kinase phosphorylation as a function of time after transfer to hypertonic medium. Data from[34]. C. PtdIns (4,5)P_2 content in isotonic medium and mean value 3-5 min after transfer to hypertonic (450 mOsm) medium. Data from L.O. Simonsen, personal communication, and [54]. D. F-actin (red) and non-muscle myosin II (green) in isotonic medium and 1 min after transfer to hypertonic (600 mOsm) medium. Data from [55].

3.3 Lipid Mediators

Osmotic shrinkage of EATC increases the cellular concentration of phosphatidyl-inositol(4,5) bisphosphate (PtdIns[4,5]P_2) (Fig. 1B;[54] L.O. Simonsen, personal communication). The mechanism(s) underlying this effect is unknown. Based on findings from other cell types, one possibility could be that shrinkage-induced activation of Rho[56] could

elicit activation of phosphatidylinositol 4-phosphate 5 kinase.[57] In agreement with this, the cellular PtdIns(4) P level is conversely decreased by cell shrinkage (L.O. Simonsen, personal comment). The possible role of PtdIns(4,5)P_2 in shrinkage-induced transporter activation is not known; however, it is intriguing to note that acidification-induced NHE1 activity was shown to be dependent on PtdIns(4,5)P_2.[30]

3.4 Cytoskeleton

Using confocal laser scanning microscopy in combination with a quantitative F-actin assay, we demonstrated that osmotic shrinkage of EATC elicits a rapid (within 1 min) increase in cortical F-actin and a net cellular F-actin polymerization.[58] Moreover, myosin II was translocated from the cytosol to the cortical region[55] (Figure 1D). The shrinkage-induced myosin II reorganization appeared to be dependent on p38 kinase and Rho-dependent kinase, while the shrinkage-induced increase in F-actin was independent of p38 kinase, Rho kinase, MLCK, and PKC.[55] In contrast, recovery of F-actin appeared to be dependent on MLCK and PKC, consistent with their role in activation of NKCC1 and NHE1, respectively.[55] The mechanism of shrinkage-induced F-actin polymerization in EATC is thus currently unknown but a likely candidate is the increase in PtdIns(4,5)P_2 (See 3.3), an event well known to elicit F-actin polymerization.[58]

In EATC as well as in other cell types, the possible role of the cytoskeleton in RVI is not fully understood, at least in part due to methodological problems with the use of cytochalasins (for discussion, see Reference [59]). The RVI process in EATC is inhibited by the F-actin-disrupting fungal metabolite cytochalasin B but not by cytochalasin D which is more specific for F-actin.[74]

The role of F-actin in regulation of NKCC1 has been studied in a number of cell types including EATC.[59, 60] Based on a series of studies in EATC, a three-state model for NKCC1 was proposed:[59, 61] (I) silent state - NKCC1 inactive; (II) contact with the cytoskeleton disrupted - NKCC1 partially active; and (III) activated state, initiated by cell shrinkage in an F-actin dependent manner – NKCC1 fully active. This model was based on the following observations: cytochalasin B increases NKCC1 activity under isotonic conditions[62] in isolated plasma membrane vesicles shown to be devoid of F-actin and myosin II;[63] NKCC1 is constitutively in a partially active state;[64] in these vesicles, NKCC1 cannot be further activated by cell shrinkage and is ML-7-insensitive.[59]

4. PERSPECTIVES: PHYSIOLOGY AND PATHOPHYSIOLOGY OF SHRINKAGE-ACTIVATED TRANSPORTERS

Altered function of shrinkage-activated membrane transport proteins is associated with several important pathophysiological states. In recent years, evidence has accumulated that inhibition of shrinkage-activated transport proteins contributes to cell shrinkage associated with programmed cell death (PCD), and conversely, that proliferation is augmented by increased activity of these transporters. Thus, cell shrinkage is an early event in PCD,[3, 9, 10] and osmotic shrinkage *per se* can also elicit PCD.[5, 11-13] The signaling events leading from cell shrinkage to PCD are still incompletely understood, although some players have been described in recent years.[5, 12] PCD is facilitated in cells incapable

of RVI,[11] and consistent with this, inhibition of NHE1 has been found to augment or elicit PCD in several cell types.[65, 66]

Cell proliferation is dependent on cell volume, being augmented by cell swelling and inhibited by cell shrinkage.[4, 5] Inhibition of the shrinkage-activated transporters, NHE1 and NKCC1, inhibits proliferation in many cell types.[67, 68] Moreover, many cancer cells exhibit increased NHE1 activity and/or expression, and NHE1 has been shown to play an important role in cancer cell proliferation, migration and invasion.[6, 7, 69] Similarly, overexpression of NKCC1 has been shown to elicit cell proliferation and transformation.[8]

On the other hand, the picture is more complex than simply that inhibition and activation of the shrinkage-activated transport proteins is always associated with PCD and proliferation, respectively. For instance, the NKCC1 inhibitor bumetanide inhibited amphotericin B-induced apoptosis in human mesothelioma cells[70] and activation of NKCC1 was found to induce apoptosis in human hepatoblastoma cells, possibly via reverse-mode stimulation of the Na^+/Ca^{2+} exchanger, leading to increased $[Ca^{2+}]_I$.[71] Moreover, increases in both cell volume and pH_i could contribute to the effects of increased NHE1 activity in proliferation. Finally, the roles of changes in ion content versus changes in cell volume in the effect of transporter activation require further clarification.

Together with many other examples of pathological conditions associated with altered function of NHE1 and NKCC1,[2, 64] the above examples underscore the importance of obtaining a detailed understanding of the cellular events activated by cell shrinkage and changes in ion content, and of the similarities and differences between these events and those involved in PCD and proliferation.

5. ACKNOWLEDGMENTS

The work was supported by the Carlsberg foundation (EKH, grant 0894/10 and SFP, grant 0544/20) and the Danish Natural Science Research Council (EKH grant 21-01-0579 and SFP, grant 22-01-0055).

6. REFERENCES

1. E.K. Hoffmann and P.B. Dunham, Membrane mechanisms and intracellular signaling in cell volume regulation, *Int Rev Cytol* **161**, 173-262 (1995).
2. F. Lang, G.L. Busch, M. Ritter, H. Volkl, S. Waldegger, E. Gulbins and D. Haussinger, Functional significance of cell volume regulatory mechanisms, *Physiol Rev* **78**, 247-306 (1998).
3. Y. Okada, E. Maeno, T. Shimizu, K. Dezaki, J. Wang and S. Morishima, Receptor-mediated control of regulatory volume decrease (RVD) and apoptotic volume decrease (AVD), *J Physiol* **532**, 3-16 (2001).
4. K. Anbari and R.M. Schultz, Effect of sodium and betaine in culture media on development and relative rates of protein synthesis in preimplantation mouse embryos *in vitro*, *Mol Reprod Dev* **35**, 24-28 (1993).
5. M.B. Burg, Response of renal inner medullary epithelial cells to osmotic stress, *Comp Biochem Physiol A Mol Integr Physiol* **133**, 661-666 (2002).
6. L.A. McLean, J. Roscoe, N.K. Jorgensen, F.A. Gorin and P.M. Cala, Malignant gliomas display altered pH regulation by NHE1 compared with nontransformed astrocytes, *Am J Physiol Cell Physiol* **278**, C676-C688 (2000).
7. S.J. Reshkin, A. Bellizzi, S. Caldeira, V. Albarani, I. Malanchi, M. Poignee, M. Alunni-Fabbroni, V. Casavola and M. Tommasino, Na^+/H^+ exchanger-dependent intracellular alkalinization is an early event in

malignant transformation and plays an essential role in the development of subsequent transformation-associated phenotypes, *FASEB J* **14**, 2185-2197 (2000).
8. R. Panet, M. Marcus and H. Atlan, Overexpression of the Na(+)/K(+)/Cl(-) cotransporter gene induces cell proliferation and phenotypic transformation in mouse fibroblasts, *J Cell Physiol* **182**, 109-118 (2000).
9. C.D. Bortner and J.A. Cidlowski, A necessary role for cell shrinkage in apoptosis, *Biochem Pharmacol* **56**, 1549-1559 (1998).
10. A.H. Wyllie, J.F. Kerr and A.R. Currie, Cell death: the significance of apoptosis, *Int Rev Cytol* **68**, 251-306 (1980).
11. C.D. Bortner and J.A. Cidlowski, Absence of volume regulatory mechanisms contributes to the rapid activation of apoptosis in thymocytes, *Am J Physiol* **271**, C950-C961 (1996).
12. K.S. Lang, S. Fillon, D. Schneider, H.G. Rammensee and F. Lang, Stimulation of TNF alpha expression by hyperosmotic stress, *Pflugers Arch* **443**, 798-803 (2002).
13. Y. Terada, S. Inoshita, S. Hanada, H. Shimamura, M. Kuwahara, W. Ogawa, M. Kasuga, S. Sasaki and F. Marumo, Hyperosmolality activates Akt and regulates apoptosis in renal tubular cells, *Kidney Int* **60**, 553-567 (2001).
14. P.M. Cala and H.M. Maldonado, pH regulatory Na/H exchange by Amphiuma red blood cells, *J Gen Physiol* **103**, 1035-1053 (1994).
15. B.S. Jensen, F. Jessen and E.K. Hoffmann, Na^+, K^+, Cl^- cotransport and its regulation in Ehrlich ascites tumor cells. Ca2+/calmodulin and protein kinase C dependent pathways, *J Membr Biol* **131**, 161-178 (1993).
16. S.F. Pedersen, B. Kramhoft, N.K. Jorgensen and E.K Hoffmann, Shrinkage-induced activation of the Na^+/H^+ exchanger in Ehrlich ascites tumor cells: mechanisms involved in the activation and a role for the exchanger in cell volume regulation, *J Membr Biol* **149**, 141-159 (1996).
17. F. Wehner, T. Shimizu, R. Sabirov and Y. Okada, Hypertonic activation of a non-selective cation conductance in HeLa cells and its contribution to cell volume regulation, *FEBS Lett* **551**, 20-24, 2003.
18. E.K. Hoffmann, L.O. Simonsen and C. Sjoholm, Membrane potential, chloride exchange, and chloride conductance in Ehrlich mouse ascites tumour cells, *J Physiol* **296**, 61-84 (1979).
19. E.K. Hoffmann, Regulation of cell volume by selective changes in the leak permeabilities of Ehrlich ascites tumor cells, *Alfred Benzon Symposium* **XI**, 397-417 (1978).
20. E.K. Hoffmann, Anion exchange and anion-cation co-transport systems in mammalian cells, *Philos Trans R Soc Lond B Biol Sci* **299**, 519-535 (1982).
21. E.K Hoffmann, C. Sjoholm and L.O. SimonseN, Na^+,Cl^- cotransport in Ehrlich ascites tumor cells activated during volume regulation (regulatory volume increase), *J Membr Biol* **76**, 269-280 (1983).
22. E.K. Hoffmann and H.H. Ussing, Membrane mechanisms in volume regulation in vertebrate cells and epithelia, *In: Membrane Transport in Biology (GH Giebisch, J Schaefer, HH Ussing, and P Kristensen, Eds)* **5**, 317-399 (2004).
23. C. Lytle and T. McManus, Coordinate modulation of Na-K-2Cl cotransport and K-Cl cotransport by cell volume and chloride, *Am J Physiol Cell Physiol* **283**, C1422-C1431 (2002).
24. E. Delpire, M.I. Rauchman, D.R. Beier, S.C. Hebert and S.R. Gullans, Molecular cloning and chromosome localization of a putative basolateral Na^+-K^+-2Cl^- cotransporter from mouse inner medullary collecting duct (mIMCD-3) cells, *J Biol Chem* **269**, 25677-25683 (1994).
ascites cells measured with [3H]bumetanide, *Am J Physiol* **250**, C688-C693 (1986).
25. E.K. Hoffmann, L.O. Simonsen and I.H. Lambert, Cell volume regulation: intracellular transmission, *Adv Comp Env Physiol* **14**, 187-248 (1993).
26. T. Krarup, L.D. Jakobsen, B.S. Jensen and E.K. Hoffmann, Na^+-K^+-2Cl^- cotransport in Ehrlich cells: regulation by protein phosphatases and kinases, *Am J Physiol* **275**, C239-C250 (1998).
27. E.K. Hoffmann, Control of volume regulatory ion transport processes in a mammalian cell: signaling by secondary messengers, *Alfred Benzon Symposium* **34**, 273-294 (1993).
28. H. Harbak and L.O. Simonsen, Cell shrinkage couples agonist-induced receptor stimulation to activation of the Na,K,2Cl cotransport system in Ehrlich mouse ascites tumor cells, *J Physiol* **467**, 334p (1993).
29. C. Lytle, T.J. McManus and M.A. Haas, A model of Na-K-2Cl cotransport based on ordered ion binding and glide symmetry, *Am J Physiol* **274**, C299-C309 (1998).
30. O. Aharonovitz, H.C. Zaun, T. Balla, J.D. York, J. Orlowski and S. Grinstein, Intracellular pH regulation by Na^+/H^+ exchange requires phosphatidylinositol 4,5-bisphosphate, *J Cell Biol* **150**, 213-224 (2000).
31. E.K. Hoffmann, M. Schiodt and P.B. Dunham, The number of chloride-cation cotransport sites on Ehrlich
32. B.S. Jensen and E.K. Hoffmann, Hypertonicity enhances expression of functional $Na^+/K^+/2Cl^-$ cotransporters in Ehrlich ascites tumour cells, *Biochim Biophys Acta* **1329**, 1-6 (1997).
33. E. Wiener, G. Dubyak and A. Scarpa, Na^+/H^+ exchange in Ehrlich ascites tumor cells. Regulation by extracellular ATP and 12-O-tetradecanoylphorbol 13-acetate, *J Biol Chem* **261**, 4529-4534 (1986).

34. S.F. Pederson, C. Varming, S.T. Christensen and E.K. Hoffmann, Mechanisms of activation of NHE by cell shrinkage and by calyculin A in Ehrlich ascites tumor cells, *J Membr Biol* **189**, 67-81 (2002).
35. C. Levinson, Inability of Ehrlich ascites tumor cells to volume regulate following a hyperosmotic challenge, *J Membr Biol* **121**, 279-288 (1991).
36. B. Kramhoft, I.H. Lambert and E.K. Hoffmann, Na^+/H^+exchange in Ehrlich ascites tumor cells: activation by cytoplasmic acidification and by treatment with cupric sulphate, *J Membr Biol* **102**, 35-48 (1988).
37. S.F. Pedersen, S. Pedersen, I.H. Lambert and E.K. Hoffmann, P2 receptor-mediated signal transduction in Ehrlich ascites tumor cells, *Biochim Biophys Acta* **1374**, 94-106 (1998).
38. S. Pedersen, E.K. Hoffmann, C. Hougaard and I.H. Lambert, Cell shrinkage is essential in lysophosphatidic acid signaling in Ehrlich ascites tumor cells, *J Membr Biol* **173**, 19-29 (2000).
39. S.F. Pedersen, N.K. Jorgensen and E.K. Hoffmann, Dynamics of Ca2+i and pHi in Ehrlich ascites tumor cells after Ca2+-mobilizing agonists or exposure to hypertonic solution, *Pflugers Arch* **436**, 199-210 (1998).
40. O. Aharonovitz, N. Demaurex, M Woodside and S. Grinstein, ATP dependence is not an intrinsic property of Na^+/H^+ exchanger NHE1: requirement for an ancillary factor, *Am J Physiol* **276**, C1303-C1311 (1999).
41. P. Lawonn, E.K. Hoffmann, C. Hougaard and F. Wehner, A cell shrinkage-induced non-selective cation conductance with a novel pharmacology in Ehrlich-Lettre-ascites tumour cells, *FEBS Lett* **539**, 115-119 (2003).
42. M.E. O'Donnell, Endothelial cell sodium-potassium-chloride cotransport. Evidence of regulation by Ca2+ and protein kinase C, *J Biol Chem* **266**, 11559-11566 (1991).
43. B. Bertrand, S. Wakabayashi, T. Ikeda, J. Pouyssegur and M. Shigekawa, The Na^+/H^+ exchanger isoform 1 (NHE1) is a novel member of the calmodulin-binding proteins. Identification and characterization of calmodulin-binding sites, *J Biol Chem* **269**, 13703-13709 (1994).
44. A. Dascalu, Z. Nevo and R. Korenstein, Hyperosmotic activation of the Na^+/H^+ exchanger in a rat bone cell line: temperature dependence and activation pathways, *J Physiol* **456**, 503-518 (1992).
45. A.K Larsen, B.S. Jensen and E.K. Hoffmann, Activation of protein kinase C during cell volume regulation in Ehrlich mouse ascites tumor cells, *Biochim Biophys Acta* **1222**, 477-482 (1994).
46. J.D. Klein and W.C. O'Neill, Volume-sensitive myosin phosphorylation in vascular endothelial cells: correlation with Na-K-2Cl cotransport, *Am J Physiol* **269**, C1524-C1531 (1995).
47. L.D. Shrode, J.D. Klein, W.C. O'Neill and R.W. Putnam, Shrinkage-induced activation of Na^+/H^+ exchange in primary rat astrocytes: role of myosin light-chain kinase, *Am J Physiol* **269**, C257-C266 (1995).
48. M. Takeda, T. Homma, M.D. Breyer, N. Horiba, R.L. Hoover, S. Kawamoto, I. Ichikawa and V. Kon, Volume and agonist-induced regulation of myosin light-chain phosphorylation in glomerular mesangial cells, *Am J Physiol* **264**, F421-F426 (1993).
49. C. Varming, S.F. Pedersen and E.K. Hoffmann, Protein kinases, phosphatases, and the regulation of the Na^+ /H^+ exchanger in Ehrlich ascites tumor cells, *Acta Physiol Scand* **163**, a24 (1998).
50. l. Bianchini, M. Woodside, C. Sardet, J. Pouyssegur, A. Takai and S. Grinstein, Okadaic acid, a phosphatase inhibitor, induces activation and phosphorylation of the Na^+/H^+ antiport, *J Biol Chem* **266**, 15406-15413 (1991).
51. S. Leung, M.E. O'Donnell, A. Martinez and H.C. Palfrey, Regulation by nerve growth factor and protein phosphorylation of Na/K/2Cl cotransport and cell volume in PC12 cells, *J Biol Chem* **269**, 10581-10589 (1994).
52. H.C. Palfrey and E.B. Pewitt, The ATP and Mg2+ dependence of Na(+)-K(+)-2Cl- cotransport reflects a requirement for protein phosphorylation: studies using calyculin A, *Pflugers Arch* **425**, 321-328 (1993).
53. S.F. Pedersen, S.A. King, R.R. Rigor, Z. Zhuang, J.M. Warren and P.M. Cala, Molecular cloning of NHE1 from winter flounder RBCs: activation by osmotic shrinkage, cAMP, and calyculin A, *Am J Physiol Cell Physiol* **284**, C1561-C1576 (2003).
54. H. Harbak, D.K. Nielsen, S. Christensen and L.O. Simonsen, Cell volume-induced changes in phosphatidylinositol (4,5) bisphosphate in Ehrlich mouse ascites tumor cells, *J Physiol* **489**, 114P (1995).
55. S.F. Pedersen and E.K. Hoffmann, Possible interrelationship between changes in F-actin and myosin II, protein phosphorylation, and cell volume regulation in Ehrlich ascites tumor cells, *Exp Cell Res* **277**, 57-73 (2002).
56. C. Ciano-Oliveira, G. Sirokmany, K. Szaszi, W.T. Arthur, A. Masszi, M. Peterson, O.D. Rotstein and A. Kapus, Hyperosmotic stress activates Rho: differential involvement in Rho kinase-dependent MLC phosphorylation and NKCC activation, *Am J Physiol Cell Physiol* **285**, C555-C566 (2003).
57. K. Burridge and M. Chrzanowska-Wodnicka, Focal adhesions, contractility, and signaling *Annu Rev Cell Dev Biol* **12**, 463-518 (1996).
58. S.F. Pedersen, J.W. Mills and E.K. Hoffmann, Role of the F-actin cytoskeleton in the RVD and RVI processes in Ehrlich ascites tumor cells, *Exp Cell Res* **252**, 63-74 (1999).

59. S.F. Pedersen, E.K. Hoffmann and J.W. Mills, The cytoskeleton and cell volume regulation, *Comp Biochem Physiol A Mol Integr Physiol* **130**, 385-399 (2001).
60. P.W. Flatman, Regulation of Na-K-2Cl cotransport by phosphorylation and protein-protein interactions, *Biochim Biophys Acta* **1566**, 140-151 (2002).
61. E.K. Hoffmann and J.W. Mills, Membrane events involved in volume regulation, *Current Topics in Membranes* **48**, 123-196 (1999).
62. F. Jessen and E.K. Hoffmann, Activation of the $Na^+/K^+/Cl^-$ cotransport system by reorganization of the actin filaments in Ehrlich ascites tumor cells, *Biochim Biophys Acta* **1110**, 199-201 (1992).
63. J.W. Mills, P.S. Falsig, P.S. Walmod and E.K. Hoffmann, Effect of cytochalasins on F-actin and morphology of Ehrlich ascites tumor cells, *Exp Cell Res* **261**, 209-219 (2000).
64. E.K. Hoffmann, F. Jessen and P.B. Dunham, The Na-K-2Cl cotransporter is in a permanently activated state in cytoplasts from Ehrlich ascites tumor cells, *J Membr Biol* **138**, 229-239 (1994).
65. I.N. Rich, D. Worthington-White, O.A. Garden and P. Musk, Apoptosis of leukemic cells accompanies reduction in intracellular pH after targeted inhibition of the Na^+/H^+exchanger, *Blood* **95**, 1427-1434 (2000).
66. M. Thangaraju, K. Sharma, D. Liu, S.H. Shen and C.B. Srikant, Interdependent regulation of intracellular acidification and SHP-1 in apoptosis, *Cancer Res* **59**, 1649-165 (1999).
67. R. Panet, I. Amir, D. Snyder, L. Zonenshein, H. Atlan, R. Laskov and A. Panet, Effect of Na + flux inhibitors on induction of c-fos, c-myc, and ODC genes during cell cycle, *J Cell Physiol* **140**, 161-168 (1989).
68. R. Panet, M. Markus and H. Atlan, Bumetanide and furosemide inhibited vascular endothelial cell proliferation, *J Cell Physiol* **158**, 121-127 (1994).
69. A. Lagana, J. Vadnais, P.U. Le, T.N. Nguyen, R. Laprade, I.R. Nabi and J. Noel, Regulation of the formation of tumor cell pseudopodia by the Na(+)/H(+) exchanger NHE1, *J Cell Sci* **113** (Pt 20), 3649-3662 (2000).
70. L. Marklund, R. Henriksson and K. Grankvist, Amphotericin B-induced apoptosis and cytotoxicity is prevented by the Na^+, K^+, $2Cl^-$ cotransport blocker bumetanide, *Life Sci* **66**, L319-L324 (2000).
71. J.A. Kim, Y.Y. Kang and Y.S. Lee, Activation of Na(+), K(+), Cl(-)-cotransport mediates intracellular Ca(2+) increase and apoptosis induced by Pinacidil in HepG2 human hepatoblastoma cells, *Biochem Biophys Res Commun* **281**, 511-519 (2001).
72. S.F. Pedersen, B. Kramhoft, N.K. Jorgensen and E.K. Hoffmann, The Na^+/H^+ exchange system in Ehrlich ascites tumor cells. Effects of cell volume, phosphorylation, and calcium, *Acta Physiol Scand* **151**, 26a (1994).
73. T. Krarup, B.S. Jensen and E.K. Hoffmann, Occlusion of K+ in the $Na^+/K^+/2Cl^-$ cotransporter of Ehrlich ascites tumor cells, *Biochim Biophys Acta* **1284**, 97-108 (1996).
74. T.P. Stossel, From signal to pseudopod. How cells control cytoplasmic actin assembly, *J Biol Chem* **264**, 18261-18264 (1989).

17

WATER MOVEMENT DURING APOPTOSIS

A role for aquaporins in the apoptotic volume decrease (AVD)

Elizabeth Jablonski, Ashley Webb and Francis M. Hughes, Jr.*

1. INTRODUCTION

Recently, the field of volume regulation has turned its attention in a new direction to the study of volume changes during cell death. It is well known that cells can die by one of two mechanisms: necrosis or apoptosis. These processes can be differentiated by many characteristics including a change in cell volume. During necrosis, the plasma membrane is compromised, water enters and the cells experience an increase in volume termed the Necrotic Volume Increase (NVI). In contrast, one of the first morphological changes seen during apoptosis is the Apoptotic Volume Decrease (AVD) (for review of AVD/NVI, see [1].). This morphological change is highly conserved across almost all models of cell death. Recent studies concerning AVD have focused on the movement of ions during this process (for reviews, see[2-5]). Early in apoptosis, K^+ is extruded from the cell, creating an osmotic gradient that is favorable for water efflux. The subsequent loss of water is responsible for the decrease in cell size. K^+ efflux and apoptosis were originally linked in studies which showed that a K^+ ionophore could induce DNA fragmentation and apoptosis.[6, 7] Other studies confirmed these findings and showed that blockage of K^+ channels inhibited the AVD in eosinophils[8] and HL-60 cells.[9] Subsequent research has shown that inhibiting K^+ loss using a high K^+ medium could block downstream biochemical events including caspase and nuclease activation, ultimately leading to inhibition of cell death.[10-13] Many labs have focused on the role of K^+ channels in the AVD, most likely because this is the major ion inside the cell. However, recent studies have also begun to examine the roles of Cl^- channels[14, 15] and Na^+ channels in this process.[16-18] Clearly, there are numerous studies which focus on the ionic changes during the AVD; however, little attention has been given to the role of water movement during this process.

* E.M. Jablonski, A.N. Webb and F.M. Hughes, Jr., University of North Carolina at Charlotte, Charlotte, NC 28223.

The primary barrier to water movement is the plasma membrane, and water can cross this barrier in two ways. The first is by simple diffusion through the predominantly hydrophobic interior of the bilayer, a process generally regarded as slow and unable to be regulated. In contrast, water can also move through channels termed aquaporins (AQPs). Water movement through these proteins is comparatively fast and has been shown to be regulated in many cell types including the kidney and lung.[19, 20] Currently, there are 11 known AQP family members denoted AQPs 0-10. Structurally, all members of the AQP family contain six transmembrane segments and two "hemi-channels" that fold together into an hourglass conformation to mediate water movement (For review of AQP structure, see[21]). While each AQP monomer appears to be fully capable of functioning as an individual unit to transport water, these proteins typically are found as a homotetrameric complex in the plasma membrane. With the exception of AQPs 3 and 7, most AQPs possess a cysteine residue on the extracellular side of the membrane between the fifth transmembrane segment and the second hemi-channel. This cysteine residue binds $HgCl_2$ which sterically blocks the flow of water through the channel. Thus, $HgCl_2$ acts as an effective and general inhibitor of most AQPs.[22-24]

Since the discovery of AQPs in 1988 and the characterization of AQP-1 in 1992,[25] these water channels have been found to be regulated in a plethora of tissues by a multitude of mechanisms ranging from simple transcriptional regulation to post-translational modification (For review, see[19]). For example, extensive research has investigated the expression of AQPs in the kidney and the regulation of AQP-2 by vasopressin in this tissue. In this model, vasopressin activates PKA which phosphorylates AQP-2 found in vesicles underneath the apical membrane of renal collecting duct cells. In response to this phosphorylation, AQP-2 is inserted into the apical plasma membrane via membrane fusion (For review of AQP-2 in the kidney, see[20]).

Intuitively during apoptosis, one would predict that as K^+ leaves the cell the water would continue to follow in balance with the amount of extruded K^+. This balanced efflux would consequently retain an intracellular K^+ concentration ($[K^+]_i$) of ~ 140 mM in the cell. However, studies have shown that in the shrunken apoptotic cell, the $[K^+]_i$ can be as low as 35 mM[10, 26] which is significantly decreased from that of the non-apoptotic cell. It has also been shown that this reduction in the $[K^+]_i$ is required for the activation of various downstream apoptotic enzymes such as effector caspases and endonucleases.[10-13]

Previous data from our lab have explored the importance of the water movement during the AVD to apoptosis and suggested that the water loss occurs through AQPs.[27] In support of this, we have shown that AQP inhibition suppresses the appearance of apoptotic characteristics while overexpression of AQPs enhances the rate of cell death. Together, these data suggest a novel role for AQPs in mediating water movement during the AVD and provide evidence that the plasma membrane water permeability, dictated by the expression level of AQPs, may be a rate-limiting step in this process. In the present study, we investigate the activity of these water channels following the AVD. As stated above and illustrated in Figure 1, one might predict that K^+ loss was equally balanced by water loss resulting in no net change in the $[K^+]_i$. However, there is a dramatic and well characterized decrease in intracellular K^+ levels in the shrunken cells. Thus, we hypothesize that following the AVD, AQPs are inactivated. This inactivation, coupled with the continued efflux of ions, would then reduce the ionic strength of the cytoplasm

to levels conducive to the activation of apoptotic enzymes. Accordingly, we have examined the water permeability characteristics of apoptotic cells to determine if these water channels are inhibited following the AVD.

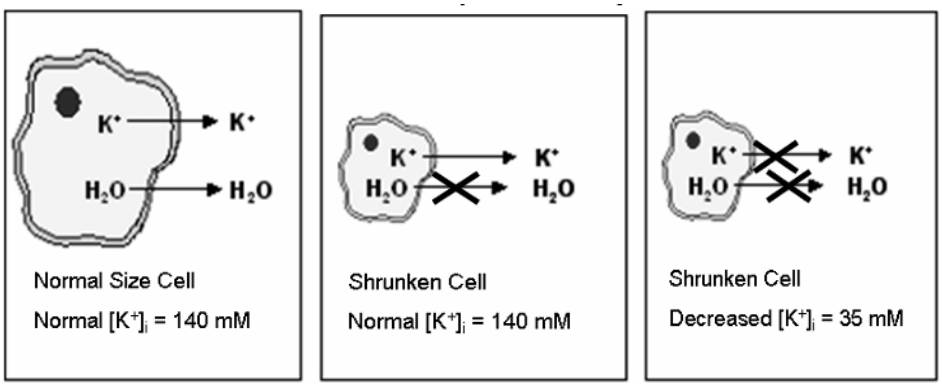

Figure 1. Schematic representation of the hypothesis that AQPs are inactivated following the AVD. At the induction of apoptosis, intracellular K^+ is extruded from the cell with the concomitant exit of water through AQPs. Following the AVD, water loss is inhibited while K^+ efflux continues, bringing about the decrease in $[K^+]_i$ needed to facilitate activation of apoptotic enzymes.

2. EXPERIMENTAL METHODS

2.1 Animals

All experimental protocols were approved by the Institutional Animal Care and Use Committee at the University of North Carolina at Charlotte and were performed in accordance with the guidelines set forth in the "NIH Guide for the Care and Use of Laboratory Animals" published by the Public Health Service. Immature 21-day old Sprague-Dawley female rats were utilized for all experiments. The animals were raised in-house and allowed food and water *ad libitum*. The rats were sacrificed by CO_2 asphyxiation, and the thymus was removed and cleaned. Thymocytes were isolated from the thymus with a pestle and screen, centrifuged at 750 x g for 5 min. Viable cells were counted by trypan blue exclusion and cells were resuspended at 10^7 cells/ml of serum-free McCoy's 5a media (Fischer Scientific, Pittsburg, PA).

2.2. Cell Culture and Treatment

Thymocytes were harvested as stated above. For freshly isolated cells, samples were pre-incubated in the presence or absence of 50 μM $HgCl_2$, 50 mM β- mercaptoethanol (Sigma Chemical Co., St. Louis, MO) or both, at room temperature while rocking for 20 minutes. Cells were washed twice and then resuspended at 10^6 cells/ml of an isotonic

buffer, Isoflow (Becman Coulter, Miami, FL). For induction of apoptosis, cells were resuspended at 10^7 cells/ml in serum-free McCoys 5a medium and cultured in 500 µl in 5 ml polystyrene round bottom tubes. Two tubes were prepared for each time point (0 h, 2 h, 4 h, 8 h, and 24 h) using either 2 µM thapsigargin (Sigma Chemical Company, St. Louis, MO) or 20 ng/ml fas ligand (fasL; Alexis Biochemicals, San Diego, Ca). The cells were then incubated in 95% air, 5% CO_2 at 37° C for the indicated time. For the experiments with latex beads, Coulter CC Size Standard L10: nominal 10 μm^3 latex beads (Beckman Coulter, Miami, Fl) were brought to room temperature and then vortexed vigorously. 0.5 ml (10^6 beads) of the size standard solution was pre-incubated ± 50 µM $HgCl_2$ for 20 min at room temperature. The beads were washed twice and then resuspended in 14.5 ml of Isoflow.

2.3 Cell Swelling Assay

To explore the plasma membrane permeabilities of both normal and apoptotic cells, 100 µl (10^6 cells) from each time point was added to a 30 ml cuvette containing 14.9 ml Isoflow. An initial measurement of cell volume was taken by the Z2 coulter counter (Beckman Coulter, Miami, Fl). 1.5 ml of deionized water was added to the cuvette and the cells were gently rocked by hand for 30 s. A final measurement of cell volume was taken by the coulter counter, and the mean cell volume for the thymocyte population at 0 and 30 s was determined through Accucomp software provided by the manufacturer. The change in mean cell volume was then used to calculate Pf by the following equation:

$$Pf = [V_0 d(V/V_0) / dt] / A_0 V_w (osm_{out} - osm_{in}) \quad (1)$$

V_0 is the initial volume of the cell, V is the final volume of the cell, A_0 is the initial area of the cell (calculated from the initial volume), V_w is the partial molar volume of water (18 cm^3/ mol), and (osm_{out} – osm_{in}) represents the osmotic gradient (with osm_{in} = 280 mOsM).[28].

2.4 Propidium Iodide (PI) analysis

In order to analyze DNA content, 100 µl (10^6 cells) were removed from each culture and placed in a separate 5 ml polystyrene round bottom tube. The cells were fixed by dripping ice-cold 70% ethanol while vortexing the cells vigorously. All fixed cells were stored at 4° C up to 24 h so that all time points could be analyzed simultaneously. The cells were washed twice in ice cold PBS and then resuspended in PBS containing 20 µg/ml propidium iodide (Sigma Chemical Co., St. Louis, MO) and 1 mg/ml DNAse-free, RNAse-A (Sigma Chemical Co., St. Louis, MO). Cell cycle analysis was performed by flow cytometry on a Becton Dickenson FACSCalibur Flow Cytometer (San Jose, CA).

2.5 Statistical Analysis

Statistics for all experiments in this manuscript were performed using Sigma Stat software. For the Pf of thymocytes stimulated by thapsigargin or FasL, a two-way

ANOVA was performed. For the increases in percent of apoptosis over 24 hours with both apoptotic inducers, a one-way ANOVA was used. Statistical significance is indicated by $P < 0.05$.

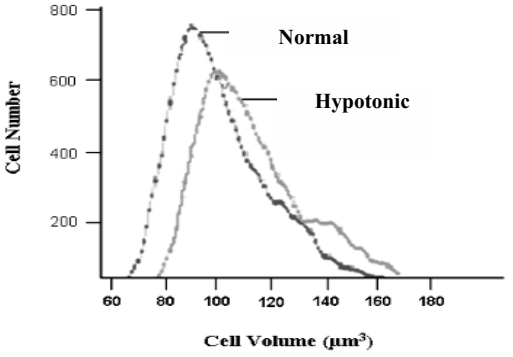

Figure 2. Primary data obtained from the Z2 coulter counter during the cell swelling assay. Curves are the cell size distribution of a freshly isolated population of thymocytes before (normal) and 30 seconds after (hypotonic) hypotonic media is added.

3. RESULTS AND DISCUSSION

3.1 Characterization of the Coulter Counter Assay for Thymocytes

We have focused our attention on the rat thymocyte as our model system for a variety of reasons. First, these cells are immature immune cells, of which 98% undergo the process of apoptosis in the thymus. Thus, these cells are primed to die. Furthermore, it is relatively easy to obtain large numbers of a pure population of thymocytes very quickly. Finally, this cell type has been regarded as the gold standard of apoptotic research because they possess most of the intrinsic and extrinsic apoptotic pathways studied in different models. In order to evaluate the role of AQPs and the plasma membrane water permeability of thymocytes during the apoptotic process, it was necessary to begin by evaluating the water permeability characteristics of normal thymocytes and the contribution of AQPs to this parameter. The mean size of the cells before and after exposure to a hypotonic medium was measured using the Z2 Coulter Counter Assay. Primary data obtained directly from the Coulter Counter can be seen in Figure 2. Freshly isolated thymocytes clearly swell 30 seconds after exposure to a hypotonic medium. From this data, a mean cell volume is obtained and these results were used to calculate the permeability coefficient (Pf) as described above. As seen in Figure 3, the mean Pf of this population was 37.26±2.58 μm/sec. We optimized this cell swelling assay and found that the largest change in cell volume occurred between 0 and 30 seconds of exposure. Furthermore, cells have a similar Pf, regardless of the osmotic strength used in the assay (data not shown). This further validates our assay because the Pf calculation is designed to be independent of osmotic stress. In all subsequent experiments, a time point of 30

seconds and a hypotonic environment of 250 mOsM were used. In order to assess the contribution of AQPs to the permeability of the cells, cells were pre-treated with $HgCl_2$, a general inhibitor of AQPs. $HgCl_2$ treatment significantly reduced the Pf value to 5.85±1.45 μm/sec. Hg^{2+} binds to a free sulfhydral group; therefore, the effects should be freely reversible with reducing agents such as β-mercaptoethanol (β-ME). Indeed, cells treated with both $HgCl_2$ and β-ME displayed a Pf value not significantly different from freshly isolated cells. Likewise, treatment with β-ME alone did not affect the Pf value, suggesting that the presence of β-ME did not have any non-specific effects on the water permeability other than to break the mercury-cysteine sulfide bond.

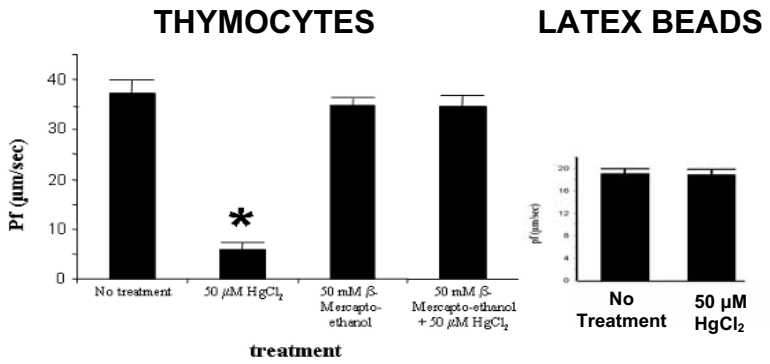

Figure 3. Evaluation of the Pf of freshly isolated thymocytes. Thymocytes were evaluated in the absence or presence of a pre-incubation with 50 μM $HgCl_2$, 50 mM β- mercaptoethanol, or both. In the right graph, the swelling characteristics and effect of $HgCl_2$ was evaluated for 10 um^3 latex beads.

The Z2 coulter counter analyzes electrical impulses created by the displacement of a conducting fluid and relates change in voltage to cell volume. Since $HgCl_2$ is a charged molecule, it is possible that it could interfere with data collected by the equipment by altering the electrical pulse measured. To show there was no effect of $HgCl_2$ on the electronics involved, the Pf values of 10 μm^3 nominal latex beads (coulter counter size L10) were examined in the presence or absence of $HgCl_2$. The water permeability of these beads and their swelling capacity was confirmed by this assay and the beads displayed a Pf of 18.97 ± 0.92 μm/sec which is significantly higher than thymocytes treated with $HgCl_2$. Importantly, pre-treatment with $HgCl_2$ did not significantly affect the swelling of these beads, suggesting that the effects of $HgCl_2$ in these experiments were limited to inhibition of AQP function only and not to changes in the electronics of the system.

3.2 Mean Pf of Normal and Apoptotic Thymocytes

As described above, the first morphological change of a dying cell is a marked decrease in cell size known as the AVD. We have shown that AQPs are a major contributor to water transport across the thymocyte cell membrane. Moreover, we have hypothesized that their inactivation following the AVD leads to a decrease in water permeability of the

apoptotic cell. Coupled with a continued loss of K^+, AQP inactivation would result in a decrease in the $[K^+]_i$ to levels conducive to activation of key downstream apoptotic enzymes. Thus, one could predict that a population of dying cells would have a significant decrease in the mean Pf value compared to a freshly isolated population.

To explore water permeability of thymocytes after the induction of apoptosis, cells were treated with either thapsigargin or FasL. Thapsigarin induces the intrinsic apoptotic pathway by causing a sustained increase in intracellular Ca^{2+} levels in the cytoplasm, while FasL activates the extrinsic death receptor mediated by Fas. We used two inducers of the apoptotic pathway, both intrinsic and extrinsic, to determine if results from our cell swelling assay were a general characteristic or were specific to a given pathway.

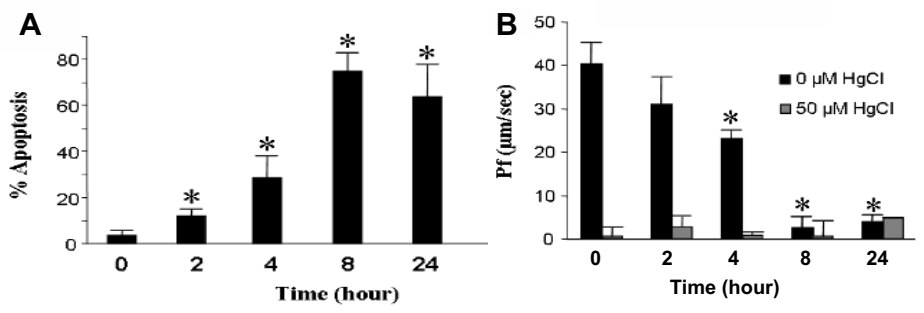

Figure 4. The mean Pf of thymocytes decreases as apoptosis increases. Cells were induced to undergo apoptosis by treatment with 2 µM thapsigargin for 0, 2, 4, 8 or 24 hours and Pf values were then measured using the coulter counter assay. As apoptosis increases in the population, mean water permeability decreases and the permeability above simple diffusion can be inhibited by $HgCl_2$.

For all time points, thapsigargin-induced apoptosis within the cell population was measured using flow cytometry and propidium iodide staining to detect cells with hypodiploid amounts of DNA, a characteristic of cells undergoing apoptosis. As seen in Figure 4A, there was a significant time-dependent increase in apoptosis beginning at 2 hours after induction of apoptosis by thapsigargin compared to the untreated population of cells. No significant difference was seen between 8 and 24 hours of treatment, indicating the induction of cell death was maximal after 8 hours.

The plasma membrane water permeability over a 24 hour period following the induction of apoptosis by thapsigargin was analyzed and the contribution of AQPs to this permeability was assessed by pre-incubation with 50 µM $HgCl_2$. During incubation with thapsigarin, water permeability of the thymocytes gradually decreases over 24 hours. As seen in Figure 4B, freshly isolated cells (T = 0) retained a Pf of 40.39 ± 4.79 µm/sec. Two hours after apoptosis was induced, the mean Pf of the population decreased, although, it did not prove to be significantly different from the Pf of T = 0 cells. However, from 4 to 24 hours after apoptosis, there was a significant time-dependent decrease in the water permeability of the population.

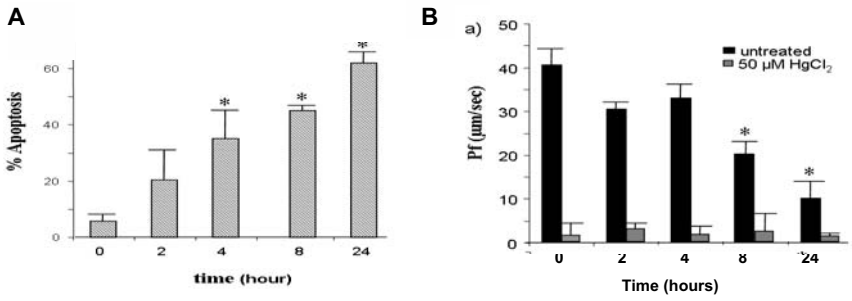

Figure 5. The mean Pf of thymocytes decreases as apoptosis increases. Cells were induced to undergo apoptosis by treatment with 20 ng/ml FasL for 0, 2, 4, 8 or 24 hours and Pf values were then measured using the coulter counter assay. As apoptosis increases in the population, mean water permeability decreases and the permeability above simple diffusion can be inhibited by $HgCl_2$.

In order to assess the contribution of AQPs to this permeability, cells were pre-treated with 50 μM of $HgCl_2$. $HgCl_2$ suppressed the Pf at each time point to essentially equivalent levels, i.e., levels equal to simple diffusion across the lipid bilayer. However, at higher time points of 8 and 24 hours where apoptosis was maximum, Pf values were so suppressed $HgCl_2$ no longer had an effect. Thus, water movement across the thymocyte membrane after 8 hours of thapsigargin treatment is strictly through simple diffusion.

These results were repeated in cells stimulated to undergo apoptosis by FasL which acts through the extrinsic, i.e., receptor-mediated pathway. As seen in Figure 5, apoptosis in the population is increased in a time-dependent manner from 2 to 24 hours. As seen with thapsigargin-treated cells, the mean water permeability (Pf) of the cell population is inversely correlated with the appearance of apoptosis. This water permeability is decreased to equivalent levels at all time points with the AQP inhibitor $HgCl_2$. This data confirms our previous data with thapsigargin (Figure 4) and suggests the decrease in water permeability in apoptotic cells following the AVD is not a signal-specific phenomenon but occurs in both intrinsically and extrinsically-stimulated pathways.

The time-dependent decrease in mean Pf of the population seen in Figures 4 and 5 can be interpreted in two ways. One possibility is this decrease represents an equivalent decrease of water permeability in all cells. For example, a 50% decrease in permeability could indicate that all cells have lost 50% of their permeability, i.e., 50% of their AQP function. However, previous studies have shown that as a population undergoes apoptosis, only normal and shrunken cells are detected with few cells in between.[10, 11] Moreover, apoptotic enzyme activity is restricted to the shrunken cells.[10, 11] Thus, increases in apoptotic parameters appear to represent increases in the percentage of cells that have died and undergone AVD, while the remaining cells are still alive. Therefore, a more likely explanation of the suppression of mean water permeability is its all or none phenomenon. Specifically, a 50% reduction in mean Pf actually represents 50% of the thymocyte population with water permeability equal to that of simple diffusion, while 50% retain normal Pf. This should be detectable in the primary data from the Coulter Counter Assay as a subpopulation of cells, i.e., shrunken cells resistant to hypotonic swelling. As

seen in Figure 6, after induction of apoptosis by thapsigargin for 4 hours, two peaks of cell size are apparent. The larger peak, which is equivalent to the cell size seen in a freshly isolated population, shows a shift in mean cell size after exposure to a hypotonic insult. In contrast, the smaller peak, representing the shrunken population of cells, showed essentially no change in size compared to the initial size measurement. This indicates that the shrunken cells possess a significantly suppressed water permeability. We have, therefore, concluded that the decrease in mean Pf of the population following induction of apoptosis is due to the decreased water permeability of the shrunken population.

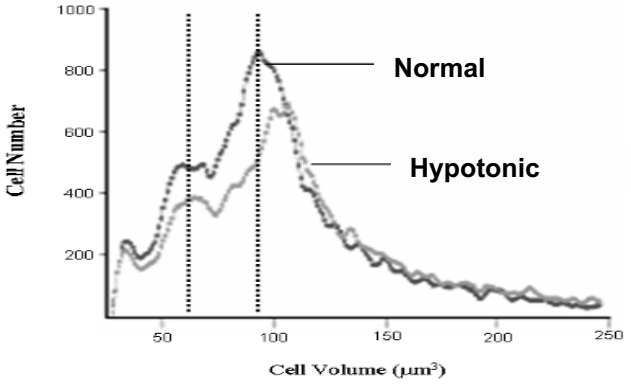

Figure 6. Cell size distribution, before (normal) and after (hypotonic) exposure to a hypotonic buffer, of a population of thymocytes induced to undergo apoptosis by treatment with 2 μM thapsigargin for 4 hr. Normal-sized cells exhibit swelling 30 sec after a hypotonic insult while shrunken cells retain the same size.

4. CONCLUSIONS

Ongoing experiments in our lab are exploring the importance and regulation of AQPs during the apoptotic process, specifically the role of these water channels prior to and after the AVD. Previous studies in our lab have shown that AQPs are the primary route of water movement across a cell's membrane as the cell undergoes the AVD and that the plasma membrane water permeability of a cell can control the rate of induced apoptosis.[27] Furthermore, in the present study, we have shown that these water channels are inhibited following the AVD, which we propose is necessary for the decrease in the intracellular K^+ concentration to levels conducive for the activation of apoptotic enzymes.

5. REFERENCES

1. Y. Okada, E. Maeno, T. Shimizu, K. Dezaki, J. Wang, and S. Morishima, Receptor-mediated control of regulatory volume decrease (RVD) and apoptotic volume decrease (AVD), *J Physiol* **532**(Pt 1), 3-16 (2001).
2. F.M. Hughes, Jr., C.D. Bortner, G.D. Purdy, and J.A. Cidlowski, Intracellular K+ suppresses the activation of apoptosis in lymphocytes, *J Biol Chem* **272**(48), 30567-76 (1997).

3. S.P. Yu, L.M. Canzoniero, and D.W. Choi, Ion homeostasis and apoptosis, *Curr Opin Cell Biol*, **13**, 405-411 (2001).
4. S.P. Yu, and D.W. Choi, Ions, cell volume, and apoptosis, *Proc Natl Acad Sci U S A* **97**(17), 9360-2 (2000).
5. M. Gomez-Angelats, C.D. Bortner, and J.A. Cidlowski, Cell volume regulation in immune cell apoptosis, *Cell Tissue Res* **301**(1), 33-42 (2000).
6. C.D. Bortner, and J.A. Cidlowski, Apoptotic Volume Decrease and the Incredible Shrinking Cell, *Cell Death Differ* **9**, 1307-1310 (2002).
7. N. Allbritton, C. Verret, R. Wolley, and H. Eisen, Calcium ion concentrations and DNA fragamentation in target cell destruction by murine cloned cytotoxic T lymphocytes, *J Exp Med* **167**(2), 514-27 (1988).
8. D. Ojcius, A. Zychlinski, L. Zheng, and J. Young, Ionophore-induced apoptosis: role of DNA fragmentation and calcium fluxes, *Exp Cell Res* **197**(1), 43-9 (1991).
9. F. Beauvais, L. Michel, and L. Dubertret, Human eosinophils in culture undergo a striking and rapid shrinkage during apoptosis. Role of K+ channels, *J Leukoc. Biol* **57**(6), 851-855 (1995).
10. J. McCarthy, and T. Cotter, Cell shrinkage and apoptosis: a role for potassium and sodium ion efflux, *Cell Death Differ* **4**, 756-770 (1997).
11. C.D. Bortner, F.M. Hughes, Jr., and J.A. Cidlowski, A primary role for K+ and Na+ efflux in the activation of apoptosis, *J Biol Chem* **272**, 32436-32442 (1997).
12. F.M. Hughes, Jr., and J.A. Cidlowski, Potassium is a critical regulator of apoptotic enzymes in vitro and in vivo, *Adv Enzyme Regul* **39**, 157-71 (1999).
13. G.I. Perez, D.V. Maravei, A.M. Trbovich, J.A. Cidlowski, J.L. Tilly, and F.M. Hughes, Jr., Identification of potassium-dependent and -independent components of the apoptotic machinery in ovarian germ cells and granulosa cells, *Biol Reprod* **63**, 1358-1369 (2000).
14. H.H. Nietsch, M.W. Roe, J.F. Fiekers, A.L. Moore, and S.D. Lidofsky, Activation of potassium and chloride channels by tumor necrosis factor alpha. Role in liver cell death, *J Biol Chem* **275**(27), 20556-20561 (2000).
15. I. Szabo, A. Lepple-Wienhues, K.N. Kaba, M. Zoratti, E. Gulbins, and F. Lang, Tyrosine kinase-dependent activation of a chloride channel in CD95-induced apoptosis in T lymphocytes, *Proc Natl Acad Sci U S A* **95**(11), 6169-6174 (1998).
16. C.D. Bortner, M. Gomez-Angelats, and J.A. Cidlowski, Plasma membrane depolarization without repolarization is an early molecular event in anti-Fas-induced apoptosis, *J Biol Chem* **276**(6), 4304-14 (2001).
17. C.D. Bortner, and J.A. Cidlowski, Uncoupled cell shrinkage from Apoptosis Reveals Na+ Influx required for Volume Loss during Programmed Cell Death, *J Biol Chem* **278**(40), 39176-84 (2003).
18. A. Rasola, D. Farahi Far, P. Hofman, and B. Rossi, Lack of internucleosomal DNA fragmentation is related to Cl(-) efflux impairment in hematopoietic cell apoptosis, *FASEB J* **13**(13), 1711-23 (1999).
19. A.S. Verkman, and A.K. Mitra, Structure and function of aquaporin water channels, *Am J Physiol Renal Physiol* **278**(1), F13-28 (2000).
20. S. Nielsen, J. Frokiaer, D. Marples, T.H. Kwon, P. Agre, and M.A. Knepper, Aquaporins in the kidney: from molecules to medicine, *Physiol Rev* **82**(1), 205-44 (2002).
21. D. Kozono, M. Yasui, L. King, and P. Agre, Aquaporin water channels: atomic structure molecular dynamics meet clinical medicine., *J Clin Invest* **109**(11), 1395-9 (2002).
22. P. Agre, M. Bonhivers, and M.J. Borgnia, The aquaporins, blueprints for cellular plumbing systems*, J Biol Chem* **273**(24), 14659-62 (1998).
23. G.M. Preston, J.S. Jung, W.B. Guggino, and P. Agre, The mercury-sensitive residue at cysteine 189 in the CHIP28 water channel, *J Biol Chem* **268**(1), 17-20 (1993).
24. E. Beitz, and J.E. Schultz, The mammalian aquaporin water channel family: A promising new drug target, *Curr Med Chem* **6**(6), 457-67 (1999).
25. G.M. Preston, T.P. Carroll, W.B. Guggino, and P. Agre, Appearance of water channels in Xenopus Oocytes Expressing Red Blood Cell CHIP28 Protein, *Science* **256**, 385 (1992).
26. G. Barbiero, F. Duranti, G. Bonelli, J. Amenta, and F. Baccino, Intracellular ionic variations in the apoptotic death of L cells by inhibitors of cell cycle progression, *Exp Cell Res* **217**(2), 410-8 (1995).
27. E. Jablonski, A. Webb, N.A. McConnell, M. Riley, and F.M. Hughes, Jr., Plasma Membrane Aquaporin Activity Can Affect the Rate of Apoptosis but is Inhibited Following the Apoptotic Volume Decrease, Am *J Physiol Cell Physiol* In press (2003).
28. R.B. Zhang, K. A. Logee, and A.S. Verkman, Expression of mRNA coding for kidney and red cell water channels in Xenopus oocytes, *J Biol Chem* **265**(26), 15375-8 (1990).

18

APOPTOSIS AND CELL VOLUME REGULATION

The importance of ions and ion channels

Gerd Heimlich, Carl D. Bortner and John A. Cidlowski*

1. INTRODUCTION

The shrinkage of cells is one of the earliest recognized morphological characteristics of apoptosis or programmed cell death. Even though the mechanisms underlying volume regulation of cells as a response to anisotonic conditions have been intensively studied for decades, the mechanisms, ion channels and transporters involved in cell shrinkage during apoptosis are far less understood. However, it is clear that the movement of ions and the resulting change in the ionic intracellular environment are important components of programmed cell death. They are ultimately involved in both the activation of the biochemical signaling cascades and the volume changes that occur during apoptosis. In this article, we review the general mechanisms of volume regulation and the distinct differences to the cell volume decrease associated with apoptosis. We also address the role of certain ions and how they are involved in the regulation of the signaling cascades.

2. APOPTOSIS – PROGRAMMED CELL DEATH

2.1 Types of Cell Death

The number of cells in multicellular organisms often remains constant throughout life and is dictated by a tightly regulated balance between cellular differentiation, cell proliferation and also cell death. The ability to remove unwanted cells from tissue and organs is crucial for the normal homeostatic function of an organism. Based on their different morphological and biochemical characteristics**,** two types of cell death can be readily distinguished.

Necrosis is considered to be a pathological or accidental form of cell death. It is characterized by massive cell swelling, destruction of intracellular organelles and finally

* G. Heimlich, C. B. Bortner, J. A. Cidlowski, National Institute of Environmental Health Sciences, National Institutes of Health, Research Triangle Park, North Carolina 27709

a rupture of the plasma membrane.[1] Subsequently, the cellular content is liberated into the surrounding tissue resulting in an inflammatory response from adjacent cells. The observed increase in cell volume occurs in both the cytoplasm and cellular organelles, while the volume of the nucleus is largely unchanged. Cellular DNA, RNA and proteins are randomly degraded and DNA appears as a smear when examined by agarose gel electrophoresis. Necrosis is usually caused by severe forms of damage or by the loss of a positive energy balance of a cell.[2] Under this condition, impaired ATP dependent ion pumps are unable to preserve the intracellular ion balance, resulting in an influx of water into the cell causing massive cellular swelling and finally rupture of the cell membrane.

In contrast, apoptosis is characterized by cell shrinkage, selective degradation of proteins, condensation of the nuclear chromatin and a characteristic fragmentation of the DNA.[1] Cellular shrinkage can be observed in both the cytoplasm and the nucleus of apoptotic cells and is a universal characteristic of the programmed cell death process. During apoptosis, the DNA is specifically cleaved at the linker region between adjacent nucleosomes by endogenous endonucleases. The resulting 180-200 bp DNA fragments appear as a characteristic ladder-like pattern when visualized by agarose gel electrophoresis. Often, plasma membrane surrounded particles, so-called apoptotic bodies, appear which are engulfed by neighboring cells or macrophages.[3] The morphological changes characteristic of apoptosis are based on a highly regulated, conserved endogenous cell death program that effectively removes unwanted cells from the organism in a non-inflammatory manner.[4] Apoptosis is a metabolically active energy-demanding process which maintains plasma membrane integrity and cellular energy levels until late in the cell death process.

Functionally, apoptosis plays a significant role during the embryonic development of an organism. Furthermore, auto-responsive immune cells or infected cells are removed by programmed cell death. Considering the growing number of diseases that are linked to abnormal rates of apoptosis, the importance in understanding the biochemical processes defining programmed cell death becomes obvious. “Excessive” apoptosis can lead to neurodegenerative diseases,[5] rheumatoid arthritis,[6] and AIDS,[7] whereas “insufficient” programmed cell death can lead to inflammation,[8] autoimmunity,[9] tumorigenic growth and cancer.[10]

2.2 The Apoptotic Signaling Cascades

In contrast to the blunt trauma resulting in necrosis, the selective removal of cells by apoptosis is induced by either specific extracellular (extrinsic) or intracellular (intrinsic) stimuli. These stimuli trigger endogenous signaling cascades that activate apoptosis resulting in specific morphological and biochemical cellular changes (Figure 1).

Extrinsically, apoptosis is induced by activating receptors of the tumor necrosis factor family (TNFR-family) by binding of a specific ligand (e.g., FasL) to its corresponding receptor (e.g., FasR) on the extracellular surface of a cell. The resulting aggregation of the receptor leads to the formation of an intracellular complex called death-inducing-signaling-complex (DISC).[11] This complex recruits various adaptor molecules and a zymogene of a special class of proteases known as caspases. Caspases are a family of cysteine-proteases that stand in the center of the apoptotic signaling cascade. Their activation by either dimerization (initiator caspases) or cleavage of the inactive pro-enzyme (effector caspases) is of considerable importance for the apoptotic progression. For example, after the initiator caspase-8 has been activated in the DISC, it further

activates downstream effector caspases like caspase-3, -6 and -7. These effector caspases are responsible for the cleavage of various cellular substrates. Death substrates include endonucleases which once proteolytically activated are responsible for the specific degradation of the DNA as well as kinases, cytoskeletal structures, ion pumps, and regulatory proteins, all of which coordinate the morphological and biochemical changes observed during programmed cell death.

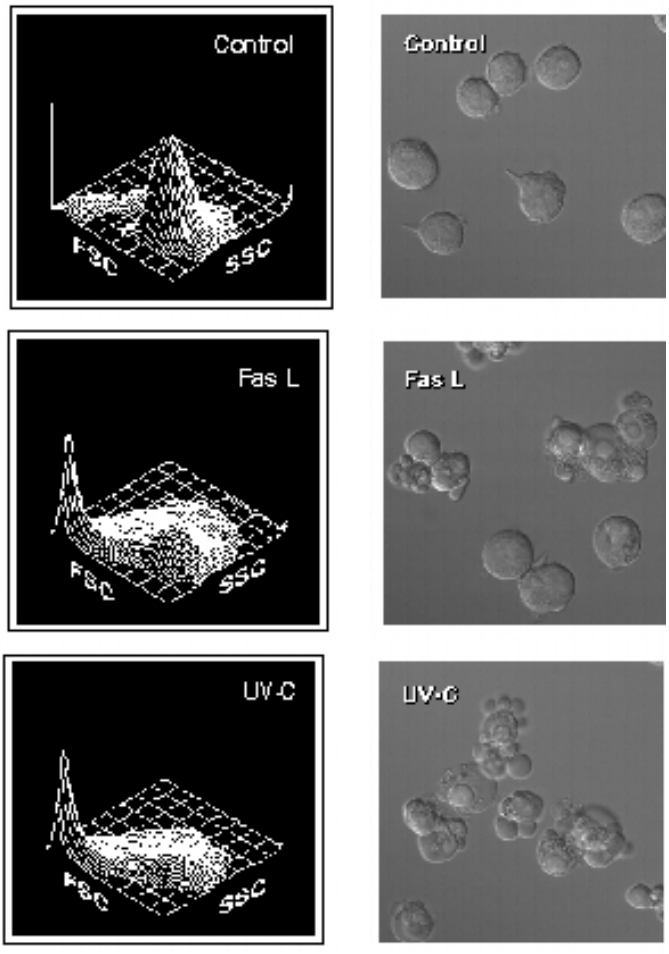

Figure 1. Cell shrinkage and apoptotic body formation occurs during Fas ligand- and UV-induced apoptosis in Jurkat T-cells. Jurkat cells treated in the presence and absence of 50 ng/ml Fas Ligand or 60 mJ/cm^2 UV-C for 4 hours were initially examined for changes in cell size by flow cytometry. Cells were analyzed on a forward-scatter (FSC; cell size) versus side-scatter (SSC; cell granularity) 3D plot. A decrease in FSC indicates a loss in cell size. Morphological examination of Jurkat cells treated with either Fas ligand or UV-C using Differential Interference Contrast (DIC) microscopy showed the classical apoptotic morphology for the Fas ligand and UV-C treated cells.

Apoptosis can also be induced intrinsically by a variety of stimuli including UV-irradiation, various pharmacological stimuli like staurosporine or actinomycin D, removal of growth factors and survival signals as well as intracellular generation of reactive oxygen species (ROS). The hallmarks of the intrinsic, apoptotic, signaling pathway are centered on alterations in the mitochondria. These include changes in the mitochondrial morphology, the mitochondrial membrane potential and other bioenergetic changes depending on the respiratory chain. The mitochondria sequester in the intermembrane space a variety of apoptogenic factors like cytochrome c, apoptosis inducing factor (AIF) and Smac/DIABLO that are released into the cytosol during programmed cell death. However, release of these proteins is often, but not exclusively, regulated by a protein family called the Bcl-2 family. Once the apoptogenic factors are released into the cytosol, they participate in the progression of the apoptotic-signaling cascade. Best characterized is the formation of a high molecular weight complex called the apoptosome consisting of the apoptosis-protease-activating-factor-1 (APAF-1), cytochrome c, ATP and pro-caspase-9. In the apoptosome, the initiator caspase-9 becomes activated which in turn activates effector caspases by proteolytic cleavage, resulting in further degradation/activation of the death substrates.

It should be noted that many of the morphological changes involving proteins and other characteristics of programmed cell death often depend on the apoptotic stimulus and the cell type undergoing cell death. Furthermore, during programmed cell death, not all the characteristics of apoptosis are necessarily observed in every situation. Variation of the actual outcome of certain apoptotic hallmarks can be observed in different cell lines or after triggering programmed cell death with different stimuli suggesting that not all the features of apoptosis are necessary for cell death.

3. VOLUME REGULATION AND APOPTOSIS

In general, mammalian cells maintain a constant shape and cellular volume in the environment of a tissue. However, during cell division, differentiation, migration, and apoptosis, tremendous volume changes can occur in cells as the result of ion movement. The plasma membrane of all cells contains various ion channels and transporters that allow the cell to maintain a homeostatic plasma membrane potential and counteract osmotic imbalances. Additionally, during their life span, cells get exposed to anisotonic conditions in accordance to their tissue location. Therefore, the ability to regulate their cellular volume is crucial for their survival and function.

3.1 Regulatory Volume Increase (RVI)

The plasma membrane of cells is highly permeable to water due to the presence of water permeable channels called aquaporins. By exposing cells to a hyperosmotic condition, an immediate and rapid cell shrinkage occurs.[12] This shrinkage is the result of an efflux of intracellular water brought about by the higher extracellular osmolarity. This "stress-induced shrinkage" activates a cellular response known as regulatory volume increase (RVI). By activating an influx of Na^+ and Cl^-, cells recover their original volume. The net uptake of NaCl takes place through a coupled activation of the Na^+/H^+ antiporter, the $Na^+/K^+/2Cl^-$ cotransporter, and the $Cl^-/HCO3^-$ exchanger. Their activation is probably achieved by reversible changes in phosphorylation.[13] The uptake of organic

osmolytes like amino acids and sugars also contributes to the increase of the intracellular osmolarity during RVI.[14] The co-uptake of these non-perturbing or inert small organic solutes protects the cell from the harmful effects of an elevated electrolyte concentration which may provoke irreversible changes in cellular physiology.[15, 16] The Na^+/K^+-ATPase exchanges this excess of intracellular Na^+ for K^+ and restores normal, homeostatic ionic balance in an energy-dependent manner.

3.2 Regulatory Volume Decrease (RVD)

On the other hand, placing cells into a hypotonic environment results in rapid cell swelling due to an influx of water that triggers a regulatory volume decrease (RVD). The loss of intracellular water is mainly achieved by a massive extrusion of intracellular K^+, Cl^- and to a lesser extent Na^+ ions.[17] K^+ channels, K^+/Cl^- cotransporters, K^+/H^+ and Cl^-/HCO_3^- exchangers and some amino acid transporters participate in this ion efflux. A high external K^+ concentration abolishes the RVD response, providing evidence for the importance of the K^+ loss. The Cl^- conductance activated by cell swelling appears to occur to a lesser degree as a result of the loss of K^+ and contributes to depolarization of the plasma membrane. Both RVI and RVD clearly involve short-term and long-term changes of ion fluxes, osmolyte transport, and changes in gene expression.

Mechanical changes in the plasma membrane, the integrin network, and macromolecular crowding have been postulated to represent potential cellular osmosensors responsible for triggering the volume regulatory mechanisms.[18] Osmosensing and the resulting changes in the cellular volume induce a profound reorganization of the cytoskeleton which in turn might immediately affect the transduction of extracellular signals.[19] In general, cell swelling and cell shrinkage affect the cytoskeletal architecture. Swollen cells are known to contain depolymerized actin filaments, possibly due to Ca^{2+} binding to gelsolin.[20] However, an intact actin filament network is required for Na^+ channel activity, insertion of volume regulatory channels into membranes, regulation of channels by kinases and phospholipids, activation of mechanosensitive anion channels by membrane stretch, and activation of the Na^+/H^+ exchanger as well as the $Na^+/K^+/2Cl^-$ cotransporter.[20]

3.3. Apoptotic Volume Decrease (AVD)

The loss of cell volume or cell shrinkage, termed apoptotic volume decrease (AVD) is a general morphological event associated with apoptosis that clearly differentiates programmed cell death from necrosis. The reason for the loss of cellular volume is still unknown; although, one could hypothesize that engulfment of a dying cell is favored by a decreased cell volume. However, as described in detail below, the changes in ions involved in AVD also play a key role in the actual activation of the programmed cell death signaling cascade. The time frame in which apoptotic cell shrinkage can be detected appears to be cell type-, apoptotic stimulus-dependent and is often stochastic in cultured cells. The loss of cell volume is the result of the combined action of ion channel fluxes, plasma membrane transporter activity, and cytoskeletal reorganization, all leading to a massive extrusion of intracellular water. It is noteworthy that cellular shrinkage during AVD is not counteracted by a regulatory volume increase response (RVI). In fact, cells undergoing AVD after induction of apoptosis appear to react with a facilitated RVD response to application of hypotonic stress.[21] This has lead to the assumption that the

volume-regulatory K^+ and Cl^- channels that participate in AVD are most likely, in part, the same channels activated during RVD response. Furthermore, it is now well-established that the loss of intracellular ions, specifically potassium and sodium are important for AVD.[22] To maintain electroneutrality, the loss of anions like chloride should accompany the loss of sodium and potassium. Additionally, as previously described, a potential involvement of cytoskeleton should not be ruled out as important for sensing and mediating volume changes. It has been shown that the cytoskeleton-associated protein fodrin was cleaved by a caspase-dependent mechanism during apoptosis.[23] Fodrin is also important in anchoring a variety of proteins to the plasma membrane, including ion channels and transporters.[24] This suggests a potential role for fodrin in a late (post-caspase) stage of apoptotic cell shrinkage.

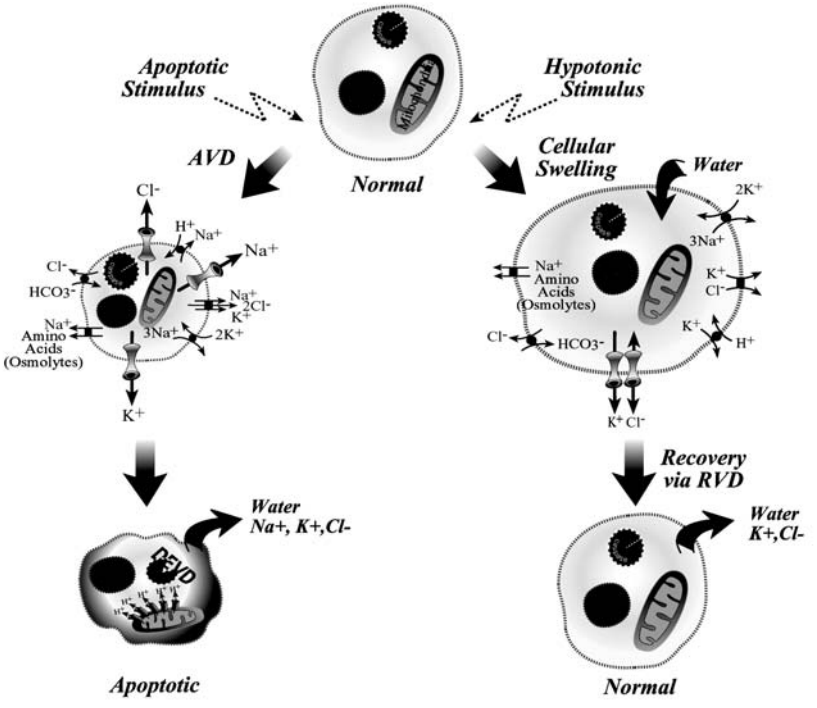

Figure 2. A loss of cell volume occurs during both AVD and RVD; however, AVD occurs in an isotonic environment while RVD occurs as a response to a decrease in extracellular osmolality. Both responses may utilize similar channels and ionic transporters to achieve the overall goal of a reduction in cell size.

It is noteworthy that while sharing similar characteristics, the apoptotic volume decrease (AVD) response is different from a regulatory volume decrease (RVD) response (Figure 2). In both cases, the loss of intracellular water by extrusion of ions and organic osmolytes might involve the same ion channels, exchangers and transporters. However, differences in the activation and signaling processes must exist because RVD appears to

occur exclusively as a response to hypotonic stress, whereas AVD is triggered by multiple and unique stimuli and occurs in an isotonic environment. Additionally, differences in the movement of water may also exist between RVD and AVD. In a study examining water movement during apoptosis, inhibition of aquaporin activity or overexpression of aquaporins was shown to prevent or enhance AVD, respectively.[25] Interestingly, swelling assays showed that the shrunken, apoptotic population of cells had a very low permeability to water compared with the normal non-apoptotic cells, suggesting that aquaporins become inactive after the AVD process. Thus, aquaporin inhibition after AVD may facilitate the occurrence of a low intracellular ionic environment shown to be essential for optimal activation of apoptotic enzymes (see below). It will be a challenging future task to characterize the osmosensors involved in RVD and the key regulators activated during programmed cell death that make use of the same mechanisms to reach the ultimate goal of cellular volume decrease.

4. THE ROLE OF IONS FOR THE ACTIVATION OF APOPTOSIS

The loss of ions and other organic osmolytes appears to be a driving force for the AVD response during the progression of apoptosis. The resulting decrease in ionic strength is not only necessary for the AVD response, but it also plays a pivotal role in the activation of the apoptotic-signaling cascade. In many cases, caspase and nuclease activity could not be detected prior to apoptotic cell shrinkage, suggesting that these classes of enzymes are in some way regulated by changes in cell volume and ionic fluxes.

Using FACS analysis to physically sort cells, it was shown that in Jurkat cells after induction of apoptosis with an anti-Fas antibody only the shrunken cell population contained significantly reduced levels of intracellular K^+ and Na^+.[22] Furthermore, active caspase-3, one of the most important executioner caspases, as well as significant DNA degradation were restricted to the cell population with decreased cellular volume. Culturing Jurkat cells in medium composed of high K^+, thus preventing the loss of K^+, resulted in inhibition of the apoptotic signaling cascade and cell shrinkage.[22] It was also shown that apoptosis was enhanced after decreasing the intracellular K^+ concentration by application of a prior RVD response. Jurkat cells cultured under hypotonic conditions showed an 85% faster apoptotic progression after stimulation with anti-Fas antibody. Interestingly, the decreased K^+ concentration only potentiated the cell death process, because hypotonic conditions alone did not induce programmed cell death. Altogether, this provided the first evidence for a direct link between the apoptotic machinery and changes in the intracellular ionic composition and suggested that the loss of intracellular K^+ is required for the activation of the programmed cell death-signaling cascade.

In vitro studies have also shown that the dATP/cytochrome c-dependent activation of caspase-3 is highly dependent on the K^+ concentration. A physiological K^+ concentration actually inhibited caspase-3 activation, whereas a decrease of the K^+ concentration resulted in dose dependent caspase-3 activation.[26] Furthermore, formation of the apoptosome, a high molecular weight protein complex in which caspase-9 is processed to its active form, is inhibited *in vitro* by increasing K^+ concentrations.[27] Similarly, the activation of interleukin-1ß-converting enzyme (ICE, a synomym for caspase-1) is also directly influenced by K^+ flux and local K^+ concentration.[28] Together, these data suggest that the efficient activation of caspases depends on changes in the intracellular K^+ concentration.

In vitro studies have also shown that nucleases are inhibited by physiological K^+ concentrations.[26] Additionally, substituting the K^+ ions in the buffer for other monovalent ions like Na^+, Cs^+ or Li^+ led to a similar dose-dependent repression of the nuclease activity. This data suggested that the ionic strength and not necessarily K^+ itself is responsible for impairment of nuclease activity. Using isolated nuclei from HeLa cells exposed to buffers with increasing K^+ concentrations, it was directly shown that increasing concentrations of K^+ prevented internucleosomal DNA cleavage, characteristic for apoptosis, in a dose-dependent manner.[29] Furthermore, DNA fragmentation was blocked by physiological K^+ concentrations, indicating that the ionic strength and/or the ionic composition might act as a safeguard against accidental DNA degradation. In the case of caspase activated DNase (CAD), an important nuclease in the execution of apoptosis, the dependence on ionic strength was directly shown with naked DNA *in vitro*.[30]

Together these data on the activation of caspases and the activity of nucleases, both of which share a central role in the progression and execution of apoptosis, provide evidence for the critical prerequisite of a decrease in intracellular ionic strength. Since K^+ is the most prominent intracellular ion, a decrease in the K^+ concentration is pivotal and may act as a regulator of apoptosis triggered by various stimuli. Furthermore, it is also possible homeostatic levels of potassium act as a safeguard against the accidental activation of the enzymes usually engaged to execute the cell death program.

5. THE ROLE OF ION CHANNELS DURING APOPTOSIS

As indicated above, the loss of K^+ appears to be an important ion-related regulator for the activation of at least two different classes of enzymes required for apoptosis as well as the apoptotic volume decrease. However, the involved ion channels, exchangers or transporters as well as the exact communication between the apoptotic trigger and ion channel activation are not well characterized. Because of the obvious analogy between K^+ extrusion during a RVD response and an AVD response, the importance of K^+ channels during apoptosis has been extensively studied. Using K^+ channel blockers like 4-aminopyridine (4-AP), sparteine or quinine, the shrinkage of human eosinophils was abrogated after induction of apoptosis by cytokine withdrawal.[31] Furthermore, 4-aminopyridine prevented UV-C evoked K^+ current as measured by patch-clamp techniques and prevented the loss of viability after UV-C treatment of myeloblastic leukemia cells (ML-1). The UV-C stimulated K^+ channel activity appears upstream of the JNK signaling pathway, and Ca^{2+} influx does not play a significant role in the JNK signaling of UV-C induced apoptosis. Interestingly, 4-AP did not prevent cell death induced by etoposide in the same cell line.[32] Additionally, in a rat liver cell line (HTC), activation of an outwardly rectifying K^+ channel after apoptotic stimulation with TNF-α was shown to be sensitive to Ba^{2+} and quinine (a K^+ channel blocker). In this study, the channel opening was Ca^{2+}, ATP and PKC, but not calmodulin kinase II, dependent.[33] However, in other cell types such as astrocytes, TNF-α has been shown to be a potent inhibitor of inwardly rectifying K^+ currents.[34] In monocytic cells (U937), cell shrinkage was prevented by Ba^{2+} and quinine and various Cl^- channel blockers (NPPB, DIDS and SITS).[21] Altogether, these examples demonstrate the variation in the activation pathway

of apoptosis depending on the stimulus and cell type, thus distinguishing the characteristic ion fluxes of AVD from RVD.

The n-type K^+ channels are an important target for tyrosine phosphorylation. Stimulation of apoptosis in Jurkat T-cells with anti-Fas antibody resulted in a fast inhibition of the voltage-dependent n-type K^+ channel ($K_V1.3$). The current inhibition correlated with tyrosine phosphorylation of the channel protein, indicating a link between induction of apoptosis, tyrosine kinases and n-type K^+ channels.[35] Interestingly, in a second study, acute treatment of human Jurkat T-lymphocytes (E6.1) with anti-Fas antibody resulted in activation of a K^+ current within 30 minutes. This current was blocked by nanomolar concentrations of margatoxin or ShK-Dap selective blockers of $K_V1.3$ channels.[36] The activation of $K_V1.3$ channel mediated K^+ current was caspase-8 dependent and independent of *de novo* protein synthesis. This current appeared before detectable cellular shrinkage, suggesting an early role in the apoptotic signaling cascade upstream of caspase-3. Furthermore, activation of PKC activity known to decrease Fas-induced apoptosis also decreased $K_V1.3$ channel mediated K^+ currents. However, it is noteworthy that blocking the $K_V1.3$ channel mediated K^+ currents with ShK-Dap still resulted in cellular shrinkage after triggering apoptosis by Fas ligation.[36] This implicates other ion channels in the loss of K^+ during apoptosis and highlights the complex nature of ion movement during the cell death process.

Subsequently, it was shown that CTLL-2 T-lymphocytes deficient in $K_V1.3$ are resistant to apoptosis induction by actinomycin D. Transfecting the $K_V1.3$ channel back into these cells restored sensitivity to this apoptotic stimulus.[37] Actinomycin D triggers the release of ROS and induces intracellular acidification. Furthermore, actinomycin D might sensitize cells to Fas ligation by downregulation of FLIP, an inhibitor of caspase-8. Cells deficient in $K_V1.3$ showed no release of cytochrome c from the mitochondria, no loss of the mitochondrial membrane potential, and no DNA fragmentation, indicating an early requirement of this ion channel in the activation phase of apoptosis. However, the activation of $K_V1.3$ mediated K^+ currents appeared late after application of actinomycin D, suggesting a secondary role of $K_V1.3$, independent of its ion channel function.[37] In this scenario, $K_V1.3$ might function as a platform required for assembling of pro-apoptotic proteins.

Interestingly, in thymocytes from $K_V1.3$-deficient mice, no voltage-dependent K^+ current was detected; however, transcripts for other voltage-dependent K^+ channel proteins such as $K_V1.4$ were upregulated. To compensate for this loss of $K_V1.3$, a 50-fold increased Cl^- current was observed in the $K_V1.3^{-/-}$ thymocytes compared to the wild-type cells which could be blocked by NPPB.[38] This data indicates that impaired ion flux through a specific ion channel influences the protein expression and activity of similar or compensatory ion channels. The appearance of a compensatory anion current, in this case of Cl^-, provides an interconnection and importance of ion movement and suggests the movement of more than one ion during programmed cell death. A compensatory ion movement also indicates that once initiated, programmed cell death seals the fate of a cell and dooms it to death. This is important for immune cells which are critical for the overall well-being of a multicellular organism.

It appears that the K^+ channels involved and the signaling pathways that lead to their activation depend on the apoptotic stimulus and the cell type. Furthermore, these studies prove the importance of ion channel inhibitors as modulators for the progression of apoptosis. However, simply inhibiting ion flux *in vivo* is of lesser value in the prevention

of apoptotic cell death due to the diversity of cell types and the multiple stimuli that can induce cell death through numerous pathways in any given organism.

Knowing the importance of K^+ and Cl^- efflux during a RVD response, the possible involvement of Cl^- channels has also been evaluated during apoptosis. It was shown that induction of apoptosis by Fas ligation triggers the activation of an outwardly rectifying chloride channel (ORCC) in Jurkat T-lymphocytes. The activation is mediated by Src-like tyrosine kinase dependent phosphorylation.[39] Furthermore, inhibition of ORCC with glibenclamide or indoleacetic acid (IAA) resulted in decreased intracellular acidification and also decreased apoptotic cell death, indicating that Cl^- efflux is required for apoptotic progression. The occurrence of a separate Cl^- efflux through ORCC during the AVD response suggests that the efflux of K^+ and Cl^- may occur in parallel, similar to a RVD response, through two separate efflux pathways. However their activation must somehow be coordinated during the progression of programmed cell death.

Apoptotic cell death in HeLa, U937, NG108-15 and PC12 cells induced by either staurosporine or TNF/CHX was significantly reduced by a variety of volume-regulatory chloride channel inhibitors including NPPB, SITS, DIDS, niflumic acid, glibenclamide and phloretin.[21] Interestingly, in all cases, application of the volume-regulatory chloride channel inhibitors prevented cell shrinkage, release of cytochrome c from mitochondria, effector caspase activation and DNA laddering. In contrast, blockers of cAMP-activated (CFTR) Cl^- channels and epithelial Ca^{2+}-activated Cl^- channels were found to be ineffective in preventing apoptosis.[21] These results clearly underline the importance of Cl^- extrusion most likely through a volume-regulated chloride channel during the early phase of apoptosis upstream of the mitochondria.

In hematopoietic cells after induction of apoptosis by hyperosmotic shock, staurosporine or Fas ligation, oligonucleosomal (DNA laddering) but not high molecular weight (50-150 kbp) DNA degradation was abolished by preventing Cl^- efflux.[40] The efflux was prevented by a raise in extracellular Cl^- or by application of Cl^- channel blockers (NPPB, ddFSK). However, other apoptotic parameters such as PARP cleavage, chromatin condensation and nuclear envelope disruption were still observed. These data suggest that a reduction of intracellular Cl^- through ORCC is required for caspase-activated DNAse (CAD) activation but not for execution of programmed cell death. Additionally, in a rat liver cell line (HTC), apoptosis triggered with TNF-α elicited a 5-fold increase in Cl^- current that was sensitive to NPPB and DPC (Cl^- channel blockers). Furthermore, substitution of Cl^- in the medium also abolished the TNF-α induced Cl^- current. Interestingly, a TNF-induced K^+ current was also inhibited by Cl^- removal but not by Cl^- channel blockers, suggesting that the K^+ channel opening does not depend on Cl^- movement. However, Cl^- binding might affect K^+ channel kinetics. The channel opening was also Ca^{2+}, ATP and PKC, but not calmodulin kinase II, dependent.[33]

In conclusion, these data in concert indicate that a loss of intracellular chloride is important for the apoptotic signaling cascade either directly by enabling activation of caspases and nucleases or indirectly by affecting plasma membrane potential and/or intracellular pH. The efflux of Cl^- possibly occurs through a volume-regulated chloride channel in the early phase of apoptosis upstream of mitochondria.

6. SODIUM MOVEMENT DURING THE APOPTOTIC RESPONSE

As described above, potassium and chloride have been the primary focus in most studies examining the role and movement of intracellular ions during apoptosis. The significance of these ions during apoptosis is due mainly to the high concentration of intracellular potassium that occurs in most mammalian cells and chloride's ability to act as a counter ion during the cell death process. In contrast, the normally low concentration of intracellular sodium has not afforded this ion the same attention as those for potassium in relation to cell shrinkage or AVD. Thus, studies examining a role for sodium during apoptosis have lagged behind. Recently, however, a defining role for changes in intracellular sodium during apoptosis has been reported specifically in regard to cell shrinkage and the AVD process.

Early studies on ions and apoptosis have suggested a change in intracellular sodium as part of the programmed cell death process. Treatment of peripheral-blood human T-lymphocytes with nanomolar concentrations of *Staphylococcus aureus* alpha-toxin gave rise to small membrane pores that permitted movement of monovalent, but not divalent, ions.[41] This permeabilization and subsequent ion movement resulted in characteristics of apoptosis including internucleosomal DNA degradation. Interestingly, treatment of human T-lymphocytes with low concentrations of alpha-toxin in the absence of extracellular sodium did not permit the occurrence of internucleosomal DNA cleavage, suggesting a role for Na^+ ions in precipitating the programmed cell death process. Additionally, in a study of dopamine-induced apoptosis in mouse thymocytes, an increase in intracellular sodium using X-ray microanalysis of cellular elements was observed.[42] Furthermore, in studies involving oxidized low-density lipoprotein (LDL) treatment of human monocytes and UV-irradiated human monoblastoid cells (U937), X-ray microanalysis of total element content suggested a higher sodium content in cells undergoing apoptosis which occurred prior to the loss of membrane integrity.[43, 44] Thus, these early studies on ion movement during apoptosis have implied a critical role for sodium flux during the programmed cell death process.

Our work has shown that multiple apoptotic stimuli induce an increase in intracellular sodium that occurs prior to the loss of membrane integrity.[45] In this study, Jurkat T-cells treated with an anti-Fas antibody, the calcium ionophore A23187, or thapsigargin showed a time-dependent increase in intracellular sodium that occurred not only prior to the loss of membrane integrity but also preceded the loss of cell volume. Additionally, this sodium influx was reflected in depolarization of the plasma membrane that again occurred prior to cell shrinkage. Using flow cytometry to examine cells that had not shrunk at the single-cell level, a direct correlation between cells with increased intracellular sodium and a depolarized plasma membrane was observed.[45] In primary rat thymocytes, dexamethasone was shown to induce plasma membrane depolarization both *in vivo* and *in vitro*, in a time- and dose-dependent manner.[46] The cellular depolarization of thymocytes was shown to be a direct effect of glucocorticoid-induced apoptosis since HeLa cells, which contain a functional glucocorticoid receptor but do not die in response to hormone, did not alter their plasma membrane potential in response to steroid treatment.

Once the apoptotic stimulated cells depolarize, this change in plasma membrane potential was sustained throughout the cell death process, suggesting an inability of dying cells to repolarize to a normal membrane potential. Further study into anti-Fas treated Jurkat cells showed that the ability of these cells to maintain cellular depolarization was

due in part to an early inhibition/degradation of the Na^+/K^+-ATPase.[45, 47] Inhibition of the Na^+/K^+-ATPase would not only facilitate an increase in intracellular sodium and membrane depolarization, but also promote a loss of intracellular potassium through loss of the cells primary K^+ uptake mechanism. Furthermore, the addition of the cardiac glycoside ouabain that inhibits the Na^+/K^+-ATPase was shown to enhance anti-Fas induced apoptosis in Jurkat cells.[45, 48] Treatment of cultured cortical neurons or human prostatic smooth muscle cells with ouabain alone results in both necrotic and apoptotic components depending not only on the cell type, but also on the concentration of ouabain employed.[49, 50] Additionally, cardiac glycosides, including ouabain, were shown to induce apoptosis in androgen-independent human prostate cancer cell lines.[51]

A critical role for the Na^+/K^+-ATPase in its efforts to maintain ionic homeostasis during apoptosis has also been described in several other studies [reviewed by Yu[52]]. In early studies, the onset of apoptosis in freshly isolated proximal tubule cells was accompanied by a decline in Na^+/K^+-ATPase activity.[53] Treatment of mouse cortical neurons with low concentrations of ouabain resulted in a slight loss of Na^+/K^+-ATPase activity but did not affect potassium homeostasis or cell viability.[54] However, in combination with non-lethal doses of various apoptotic stimuli such as C_2-ceramide or -amyloid, low concentrations of ouabain induced apoptosis, suggesting that slight impairment of the Na^+/K^+-ATPase and disruption of potassium homeostasis can lead to the apoptotic cascade. In a different study involving cultured cortical neurons, Na^+/K^+-ATPase activity was directly suppressed by apoptotic insults including serum deprivation, staurosporine, and C_2-ceramide.[55] Additionally, these authors suggested preserving pump activity might provide a neuroprotective effect in certain pathological conditions. In contrast, studies in porcine renal proximal tubular cells, cultured rat cerebellar granule cells, and vascular smooth muscle cells suggest that inhibition of the Na^+/K^+-ATPase protects cells from apoptosis,[56-58] implying the role of the Na^+/K^+-ATPase during programmed cell death may be cell-type specific.

We have recently defined an important role for sodium flux in controlling AVD during apoptosis.[59] Treatment of Jurkat cells with anti-Fas in the presence of sodium-substituted media abolished the increase in intracellular sodium and resulted in cellular swelling which is characteristic of necrosis. However, further characterization of these swollen, anti-Fas treated cells revealed numerous traits associated with apoptosis including chromatin condensation, externalization of the phosphatidylserine, caspase activation and activity, along with internucleosomal DNA degradation. Interestingly, a loss of intracellular potassium was observed in the swollen cells that accompanied the apoptotic events. The addition of sodium back into the extracellular environment led to the loss of cell volume and the typical apoptotic morphology associated with apoptosis. Therefore, apoptotic cell shrinkage can be uncoupled from other programmed cell death characteristics, thus defining specific roles for both sodium and potassium; sodium controlling cell size while potassium controls the apoptotic machinery.

7. CONCLUSION AND PERSPECTIVES

The understanding of programmed cell death or apoptosis has become one of the most studied and fastest growing fields in the life science area. The implication of volume regulatory mechanisms, ion channels as well as ion movements, are recognized

as playing an important role during the activation of programmed cell death and for the regulation of the cell shrinkage characteristic of apoptosis. The knowledge gained through decades of studying cellular volume regulation and the mechanisms counterbalancing osmo-changes provide a great resource in the current application to identify and characterize apoptosis related ion fluxes and regulated ion channels. Although many similarities between RVD and AVD are known**,** obvious differences exist between these two responses. Understanding the mechanisms regulating apoptosis related volume changes and the ion movements resulting in the activation of the cell death program may lead to the development of drugs that target ion channels or transporters and tip the balance between cell life and death.

8. REFERENCES

1. J. F. Kerr, A. H. Wyllie, and A. R. Currie, Apoptosis: a basic biological phenomenon with wide-ranging implications in tissue kinetics, *Br J Cancer*, **26** (4), 239-57 (1972).
2. L. F. Barros, T. Hermosilla, and J. Castro, Necrotic volume increase and the early physiology of necrosis, *Comp Biochem Physiol A Mol Integr Physiol*, **130** (3),401-9 (2001).
3. J. Savill and V. Fadok, Corpse clearance defines the meaning of cell death, *Nature*, **407** (6805), 784-8 (2000).
4. A. H. Wyllie, J. F. Kerr, and A. R. Currie, Cell death: the significance of apoptosis, *Int Rev Cytol*, **68**, 251-306 (1980).
5. J. Yuan and B. A. Yankner, Apoptosis in the nervous system, *Nature*, **407** (6805), 802-9 (2000).
6. G. S. Firestein, M. Yeo, and N. J. Zvaifler, Apoptosis in rheumatoid arthritis synovium, *J Clin Invest*, **96** (3), 1631-8 (1995).
7. M. W. Cloyd, J. J. Chen, and I. Wang, How does HIV cause AIDS? The homing theory, *Mol Med Today*, **6** (3), 108-11 (2000).
8. V. Baud and M. Karin, Signal transduction by tumor necrosis factor and its relatives, *Trends Cell Biol*, **11** (9), 372-7 (2001).
9. E. Baixeras, L. Bosca, C. Stauber, A. Gonzalez, A. C. Carrera, J. A. Gonzalo, and C. Martinez, From apoptosis to autoimmunity: insights from the signaling pathways leading to proliferation or to programmed cell death, *Immunol Rev*, **142**, 53-91 (1994).
10. J. C. Reed, Dysregulation of apoptosis in cancer, *Cancer J Sci Am*, **4 Suppl 1**, S8-14 (1998).
11. F. C. Kischkel, S. Hellbardt, I. Behrmann, M. Germer, M. Pawlita, P. H. Krammer, and M. E. Peter, Cytotoxicity-dependent APO-1 (Fas/CD95)-associated proteins form a death-inducing signaling complex (DISC) with the receptor, *Embo J*, **14** (22), 5579-88 (1995).
12. S. Waldegger, J. Matskevitch, G. L. Busch, and F. Lang, Introduction to cell volume regulatory mechanisms, *Contrib Nephrol*, **123**, 1-7 (1998).
13. W. C. O'Neill, Physiological significance of volume-regulatory transporters, *Am J Physiol*, **276** (5 Pt 1), C995-C1011 (1999).
14. D. F. Perlman and L. Goldstein, Organic osmolyte channels in cell volume regulation in vertebrates, *J Exp Zool*, **283** (7), 725-33 (1999).
15. M. B. Burg, Molecular basis of osmotic regulation, *Am J Physiol*, **268** (6 Pt 2), F983-96 (1995).
16. J. D. McGivan and M. Pastor-Anglada, Regulatory and molecular aspects of mammalian amino acid transport, *Biochem J*, **299 (Pt 2)**, 321-34 (1994).
17. J. L. Eveloff and D. G. Warnock, Activation of ion transport systems during cell volume regulation, *Am J Physiol*, **252** (1 Pt 2), F1-10 (1987).
18. M. B. Burg, Macromolecular crowding as a cell volume sensor, *Cell Physiol Biochem*, **10** (5-6), 251-6 (2000).
19. A. Moustakas, P. A. Theodoropoulos, A. Gravanis, D. Haussinger, and C. Stournaras, The cytoskeleton in cell volume regulation, *Contrib Nephrol*, **123**, 121-34 (1998).
20. F. Lang, G. L. Busch, M. Ritter, H. Volkl, S. Waldegger, E. Gulbins, and D. Haussinger, Functional significance of cell volume regulatory mechanisms, *Physiol Rev*, **78** (1), 247-306 (1998).
21. E. Maeno, Y. Ishizaki, T. Kanaseki, A. Hazama, and Y. Okada, Normotonic cell shrinkage because of disordered volume regulation is an early prerequisite to apoptosis, *Proc Natl Acad Sci U S A*, **97** (17), 9487-92 (2000).

22. C. D. Bortner, F. M. Hughes, Jr., and J. A. Cidlowski, A primary role for K+ and Na+ efflux in the activation of apoptosis, *J Biol Chem*, **272** (51), 32436-42 (1997).
23. S. J. Martin, G. A. O'Brien, W. K. Nishioka, A. J. McGahon, A. Mahboubi, T. C. Saido, and D. R. Green, Proteolysis of fodrin (non-erythroid spectrin) during apoptosis, *J Biol Chem*, **270** (12), 6425-8 (1995).
24. W. J. Nelson and R. W. Hammerton, A membrane-cytoskeletal complex containing Na+,K+-ATPase, ankyrin, and fodrin in Madin-Darby canine kidney (MDCK) cells: implications for the biogenesis of epithelial cell polarity, *J Cell Biol*, **108** (3), 893-902 (1989).
25. E. M. Jablonski, A. N. Webb, N. A. McConnell, M. C. Riley, and F. M. Hughes, Jr., Plasma membrane aquaporin activity can affect the rate of apoptosis but is inhibited after apoptotic volume decrease, *Am J Physiol Cell Physiol*, **286** (4), C975-85 (2004).
26. F. M. Hughes, Jr., C. D. Bortner, G. D. Purdy, and J. A. Cidlowski, Intracellular K+ suppresses the activation of apoptosis in lymphocytes, *J Biol Chem*, **272** (48), 30567-76 (1997).
27. G. J. Thompson, C. Langlais, K. Cain, E. C. Conley, and G. M. Cohen, Elevated extracellular [K+] inhibits death-receptor- and chemical-mediated apoptosis prior to caspase activation and cytochrome c release, *Biochem J*, **357** (Pt 1), 137-45 (2001).
28. I. Walev, K. Reske, M. Palmer, A. Valeva, and S. Bhakdi, Potassium-inhibited processing of IL-1 beta in human monocytes, *Embo J*, **14** (8), 1607-14 (1995).
29. F. M. Hughes, Jr. and J. A. Cidlowski, Potassium is a critical regulator of apoptotic enzymes in vitro and in vivo, *Adv Enzyme Regul*, **39**, 157-71 (1999).
30. P. Widlak and W. T. Garrard, Ionic and cofactor requirements for the activity of the apoptotic endonuclease DFF40/CAD, *Mol Cell Biochem*, **218** (1-2), 125-30 (2001).
31. F. Beauvais, L. Michel, and L. Dubertret, Human eosinophils in culture undergo a striking and rapid shrinkage during apoptosis. Role of K+ channels, *J Leukoc Biol*, **57** (6), 851-5 (1995).
32. L. Wang, D. Xu, W. Dai, and L. Lu, An ultraviolet-activated K+ channel mediates apoptosis of myeloblastic leukemia cells, *J Biol Chem*, **274** (6), 3678-85 (1999).
33. H. H. Nietsch, M. W. Roe, J. F. Fiekers, A. L. Moore, and S. D. Lidofsky, Activation of potassium and chloride channels by tumor necrosis factor alpha. Role in liver cell death, *J Biol Chem*, **275** (27), 20556-61 (2000).
34. H. Koller, N. Allert, D. Oel, G. Stoll, and M. Siebler, TNF alpha induces a protein kinase C-dependent reduction in astroglial K+ conductance, *Neuroreport*, **9** (7), 1375-8 (1998).
35. I. Szabo, E. Gulbins, H. Apfel, X. Zhang, P. Barth, A. E. Busch, K. Schlottmann, O. Pongs, and F. Lang, Tyrosine phosphorylation-dependent suppression of a voltage-gated K+ channel in T lymphocytes upon Fas stimulation, *J Biol Chem*, **271** (34), 20465-9 (1996).
36. N. M. Storey, M. Gomez-Angelats, C. D. Bortner, D. L. Armstrong, and J. A. Cidlowski, Stimulation of Kv1.3 potassium channels by death receptors during apoptosis in Jurkat T lymphocytes, *J Biol Chem*, **278** (35), 33319-26 (2003).
37. J. Bock, I. Szabo, A. Jekle, and E. Gulbins, Actinomycin D-induced apoptosis involves the potassium channel Kv1.3, *Biochem Biophys Res Commun*, **295** (2), 526-31 (2002).
38. P. A. Koni, R. Khanna, M. C. Chang, M. D. Tang, L. K. Kaczmarek, L. C. Schlichter, and R. A. Flavella, Compensatory anion currents in Kv1.3 channel-deficient thymocytes, *J Biol Chem*, **278** (41), 39443-51 (2003).
39. I. Szabo, A. Lepple-Wienhues, K. N. Kaba, M. Zoratti, E. Gulbins, and F. Lang, Tyrosine kinase-dependent activation of a chloride channel in CD95-induced apoptosis in T lymphocytes, *Proc Natl Acad Sci U S A*, **95** (11), 6169-74 (1998).
40. A. Rasola, D. Farahi Far, P. Hofman, and B. Rossi, Lack of internucleosomal DNA fragmentation is related to Cl(-) efflux impairment in hematopoietic cell apoptosis, *Faseb J*, **13** (13), 1711-23 (1999).
41. D. Jonas, I. Walev, T. Berger, M. Liebetrau, M. Palmer, and S. Bhakdi, Novel path to apoptosis: small transmembrane pores created by staphylococcal alpha-toxin in T lymphocytes evoke internucleosomal DNA degradation, *Infect Immun*, **62** (4), 1304-12 (1994).
42. D. Offen, I. Ziv, S. Gorodin, A. Barzilai, Z. Malik, and E. Melamed, Dopamine-induced programmed cell death in mouse thymocytes, *Biochim Biophys Acta*, **1268** (2), 171-7 (1995).
43. J. N. Skepper, I. Karydis, M. R. Garnett, L. Hegyi, S. J. Hardwick, A. Warley, M. J. Mitchinson, and N. R. Cary, Changes in elemental concentrations are associated with early stages of apoptosis in human monocyte-macrophages exposed to oxidized low-density lipoprotein: an X-ray microanalytical study, *J Pathol*, **188** (1), 100-6 (1999).
44. E. Fernandez-Segura, F. J. Canizares, M. A. Cubero, A. Warley, and A. Campos, Changes in elemental content during apoptotic cell death studied by electron probe X-ray microanalysis, *Exp Cell Res*, **253** (2), 454-62 (1999).

45. C. D. Bortner, M. Gomez-Angelats, and J. A. Cidlowski, Plasma membrane depolarization without repolarization is an early molecular event in anti-Fas-induced apoptosis, *J Biol Chem*, **276** (6), 4304-14 (2001).
46. C. L. Mann and J. A. Cidlowski, Glucocorticoids regulate plasma membrane potential during rat thymocyte apoptosis in vivo and in vitro, *Endocrinology*, **142** (1), 421-9 (2001).
47. C. L. Mann, C. D. Bortner, C. M. Jewell, and J. A. Cidlowski, Glucocorticoid-induced plasma membrane depolarization during thymocyte apoptosis: association with cell shrinkage and degradation of the Na(+)/K(+)-adenosine triphosphatase, *Endocrinology*, **142** (12), 5059-68 (2001).
48. C. S. Nobel, J. K. Aronson, D. J. van den Dobbelsteen, and A. F. Slater, Inhibition of Na+/K(+)-ATPase may be one mechanism contributing to potassium efflux and cell shrinkage in CD95-induced apoptosis, *Apoptosis*, **5** (2), 153-63 (2000).
49. A. Y. Xiao, L. Wei, S. Xia, S. Rothman, and S. P. Yu, Ionic mechanism of ouabain-induced concurrent apoptosis and necrosis in individual cultured cortical neurons, *J Neurosci*, **22** (4), 1350-62 (2002).
50. S. C. Chueh, J. H. Guh, J. Chen, M. K. Lai, and C. M. Teng, Dual effects of ouabain on the regulation of proliferation and apoptosis in human prostatic smooth muscle cells, *J Urol*, **166** (1), 347-53 (2001).
51. D. J. McConkey, Y. Lin, L. K. Nutt, H. Z. Ozel, and R. A. Newman, Cardiac glycosides stimulate Ca2+ increases and apoptosis in androgen-independent, metastatic human prostate adenocarcinoma cells, *Cancer Res*, **60** (14), 3807-12 (2000).
52. S. P. Yu, Na(+), K(+)-ATPase: the new face of an old player in pathogenesis and apoptotic/hybrid cell death, *Biochem Pharmacol*, **66** (8), 1601-9 (2003).
53. M. J. Tang, Y. R. Cheng, and H. H. Lin, Role of apoptosis in growth and differentiation of proximal tubule cells in primary cultures, *Biochem Biophys Res Commun*, **218** (3), 658-64 (1996).
54. A. Y. Xiao, X. Q. Wang, A. Yang, and S. P. Yu, Slight impairment of Na+,K+-ATPase synergistically aggravates ceramide- and beta-amyloid-induced apoptosis in cortical neurons, *Brain Res*, **955** (1-2), 253-9 (2002).
55. X. Q. Wang, A. Y. Xiao, C. Sheline, K. Hyrc, A. Yang, M. P. Goldberg, D. W. Choi, and S. P. Yu, Apoptotic insults impair Na+, K+-ATPase activity as a mechanism of neuronal death mediated by concurrent ATP deficiency and oxidant stress, *J Cell Sci*, **116** (Pt 10), 2099-110 (2003).
56. X. Zhou, G. Jiang, A. Zhao, T. Bondeva, P. Hirszel, and T. Balla, Inhibition of Na,K-ATPase activates PI3 kinase and inhibits apoptosis in LLC-PK1 cells, *Biochem Biophys Res Commun*, **285** (1), 46-51 (2001).
57. N. K. Isaev, E. V. Stelmashook, A. Halle, C. Harms, M. Lautenschlager, M. Weih, U. Dirnagl, I. V. Victorov, and D. B. Zorov, Inhibition of Na(+),K(+)-ATPase activity in cultured rat cerebellar granule cells prevents the onset of apoptosis induced by low potassium, *Neurosci Lett*, **283** (1), 41-4 (2000).
58. S. N. Orlov, N. Thorin-Trescases, S. V. Kotelevtsev, J. Tremblay, and P. Hamet, Inversion of the intracellular Na+/K+ ratio blocks apoptosis in vascular smooth muscle at a site upstream of caspase-3, *J Biol Chem*, **274** (23), 16545-52 (1999).
59. C. D. Bortner and J. A. Cidlowski, Uncoupling cell shrinkage from apoptosis reveals that Na+ influx is required for volume loss during programmed cell death, *J Biol Chem*, **278** (40), 39176-84 (2003).

19

ANION CHANNEL INVOLVED IN INDUCTION OF APOPTOSIS AND NECROSIS

Yasunobu Okada, Emi Maeno, and Shin-ichiro Mori*

1. INTRODUCTION

Even under anisotonic conditions, most animal cells can show volume regulation by responding to osmotic swelling and shrinkage with the regulatory volume decrease (RVD) and the regulatory volume increase (RVI), respectively.[1, 2] However, it appears that volume-regulatory mechanisms are impaired during cell death processes, since persistent cell shrinkage and swelling are major hallmarks of the early phases of apoptosis and necrosis, respectively.[3-5]

Apoptotic cell shrinkage is divided into two phases: the early-phase whole-cell shrinkage, termed the apoptotic volume decrease (AVD),[6] and the late-phase cell fragmentation into apoptotic bodies that are to be rapidly cleaned up by phagocytes (Figure 1).

Necrotic cells exhibit persistent swelling, termed the necrotic volume increase (NVI),[7] until cell membrane rupture which gives rise to cytolytic release of harmful substances, especially proteins associated with nuclear materials,[8] resulting in tissue injury and inflammation (Figure 1).

* Yasunobu Okada, Emi Maeno, and Shin-ichiro Mori, Department of Cell Physiology, National Institute for Physiological Sciences, Okazaki 444-8585, Japan

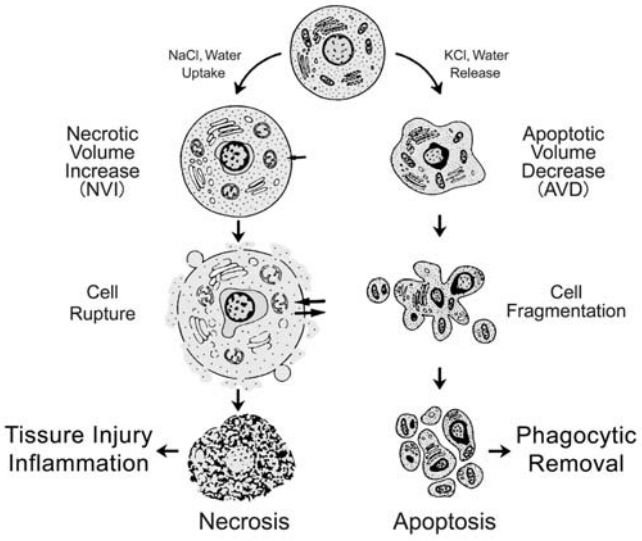

Figure 1. Cell volume changes in association with cell death processes.

2. ANION CHANNEL ACTIVATION INVOLVED IN AVD

Prior to apoptotic body formation which starts 2-3 h after stimulation, epithelial HeLa, lymphoid U937 and neuronal PC12 and NG108-15 cells rapidly (within 1-2 h) respond with AVD to stimulation of the intrinsic apoptotic pathway by a mitochondrion-mediated apoptosis inducer, staurosporine (STS) as well as of the extrinsic apoptotic pathway by a death receptor-mediated apoptosis inducer, TNFα[6] or Fas ligand.[7] The AVD induction was found to be coupled to facilitation of the RVD observed after osmotic swelling in response to a hypotonic challenge.[6, 7] Since the RVD is attained by water outflow driven by KCl efflux due to activation of volume-regulatory K^+ and Cl^- channels in most cell types,[2, 9] it is suggested that the AVD induction also results from activation of these K^+ and Cl^- channels. In fact, the AVD induction was abolished by broad-spectrum blockers of K^+ channels (quinine and Ba^{2+}) and of Cl^- channels (NPPB, DIDS and SITS) as well as by phloretin which is a blocker relatively selective to volume-sensitive outwardly rectifying (VSOR) Cl^- channels[10] in all four cell types.[6] Furthermore, STS, a Fas ligand, and TNFα have recently been found to rapidly (within 10 min) activate outwardly rectifying Cl^- currents in HeLa cells.[11]

During apoptosis, activated caspases are known to induce cleavage of a number of proteins including cytoskeletons.[12, 13] The activity of the VSOR Cl^- channel has been shown to be dependent on cytoskeletal components.[9, 14] Thus, it is natural to assume that anion channels involved in the AVD are activated by proteolytic cleavage of the cytoskeletal proteins or of channel protein *per se*. However, the onset of the AVD was found to precede caspase-3 activation in HeLa, U937, PC12 and NG108-15 cells stimulated with STS or TNFα.[6] In addition, we found that pancaspase blockers (zVAD-

fmk and zD-dcb) failed to abolish the AVD induction in U937 cells stimulated with STS, although, these broad-spectrum caspase blockers abolished caspase-3 activation.[6] Also, it was found that the AVD onset preceded release of cytochrome *c* from mitochondria in HeLa, U937 and PC12 cells stimulated with STS.[6] Thus, it is concluded that activation of AVD-inducing channel is an early event upstream of caspase activation and cytochrome *c* release (Figure 2).

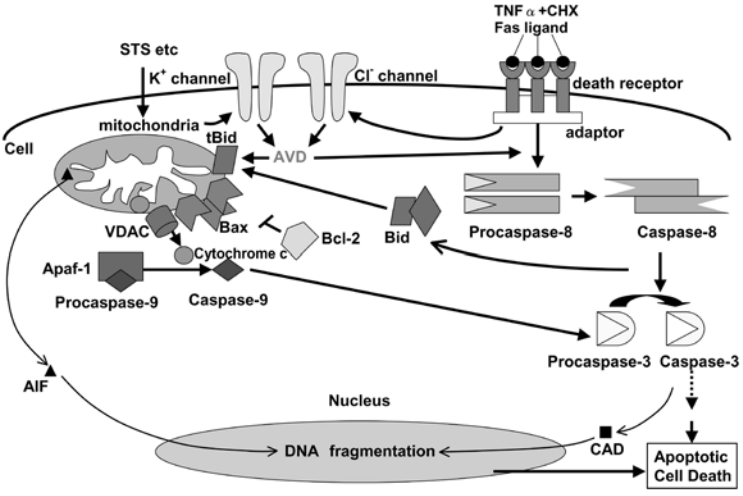

Figure 2. Activation of AVD-inducing channels upstream to caspase activation and mitochondrial cytochrome *c* release in both mitochondrion-mediated intrinsic and death receptor-mediated extrinsic pathways leading to apoptotic cell death.

3. ANION CHANNEL INHIBITION INVOLVED IN NVI

Prior to cell rupture, necrotic cells exhibit persistent cell swelling, NVI, due to uptake of osmolytes, especially NaCl. Accidental cell damage or injury should result in Na^+ inflow via membrane leakage and eventually in ATP depletion due to constrained overwork of the Na^+ pump and to ATP leak-out. ATP depletion should also be brought about by ischemic and hypoxic insults. Under ATP-deficient conditions, cell swelling would be induced by an impairment of Na^+ pump-mediated steady-state cell volume regulation working against oncotic osmotic pressure due to intracellular localization of macromolecular polyvalent anion.[15, 16] Furthermore, such cell swelling must persist, because activity of VSOR anion channels which are involved in the RVD process is inhibited not only by subsequent reduction of cellular ATP but also by elevation of cytosolic free Mg^{2+}.[9, 17] Such persistent cell swelling may eventually result in cell membrane rupture, thus the NVI.[7]

Cell acidosis may induce NVI due to NaCl accumulation within cells, because acidosis-mediated production of H_2CO_3 results in NaCl uptake by stimulation of Na^+-H^+ antiporter (NHE) and Cl^--HCO_3^- antiporter (AE) (Figure 3). Acidosis with lactate

accumulation due to augmented glycolysis-fermentation reactions is frequently associated with cerebral ischemia or trauma and results in necrosis of glial and neuronal cells. Under such conditions called lactacidosis, cell swelling must further be strengthened by entry of lactate and proton via monocarboxylate transporters (MCT)[18] (Figure 3). Our recent *in vitro* studies using cultured neuronal and glial cells showed persistent swelling was in fact induced by lactacidosis but neither by acidosis in the absence of lactate nor by application of lactate at normal pH.[19, 20] Furthermore, the succeeding RVD was impaired under lactacidosis conditions due to inhibition of VSOR Cl^- channels by protons over-accumulated within the cells (Figure 3). When lactacidosis-resistant anion channels were exogenously introduced by applying an anion channel-forming toxin protein purified from *Helicobacter pylori*, VacA, glial cells restored the RVD ability after demonstrating transient swelling under lactacidosis conditions[20] (Figure 3). Thus, we conclude that inhibition of volume-regulatory VSOR Cl^- channels is involved in the NVI in glial cells.

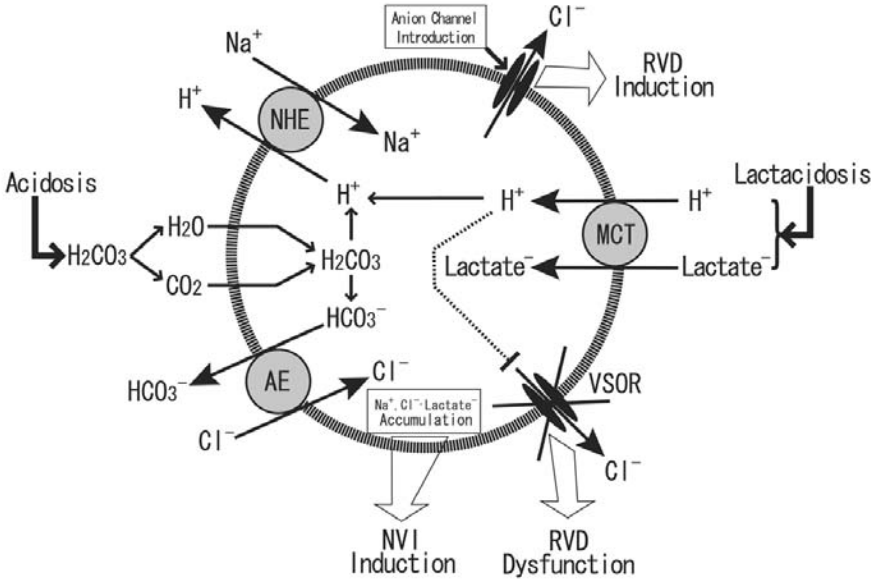

Figure 3. Induction of NVI under lactacidosis conditions and recovery therefrom by introduction of exogenous anion channels.

4. REFERENCES

1. E.K. Hoffmann and L.O. Simonsen, Membrane mechanisms in volume and pH regulation in vertebrate cells, *Physiol Rev.* **69**, 315-382 (1989).
2. Y. Okada and A Hazama, Volume-regulatory ion channels in epithelial cells, *News Physiol. Sci.* **4,** 238-242 (1989).
3. A.H. Wyllie, J.F.R. Kerr and A.R. Currie, Cell death: the significance of apoptosis, *Int. Rev. Cytol.* **68**, 251-306 (1980).

4. E. Duvall and A.H. Wyllie, Death and the cell, *Immun. Today* 7, 115-119(1986).
5. G. Kroemer, B. Dallaporta, and M. Resche-Rigon, The mitochondrial death/life regulator in apoptosis and necrosis, *Annu. Rev. Physiol.* **60**, 619-642 (1998).
6. E. Maeno, Y. Ishizaki, T. Kanaseki, A. Hazama, and Y. Okada, Normotonic cell shrinkage because of disordered volume regulation is an early prerequisite to apoptosis, *Proc. Natl. Acad. Sci. USA* **97**, 9487-9492 (2000).
7. Y. Okada, E. Maeno, T. Shimizu, K. Dezaki, J. Wang, and S. Morishima, Receptor-mediated control of regulatory volume decrease (RVD) and apoptotic volume decrease (AVD), *J. Physiol.* **532**, 3-16 (2000).
8. P. Scaffidi, T. Misteli, and M.E. Bianchi, Release of chromatin protein HMGB1 by necrotic cells triggers inflammation, *Nature* **418**, 191-195 (2000).
9. Y. Okada, Volume expansion-sensing outward-rectifier Cl^- channel: fresh start to the molecular identity and volume sensor, *Am. J. Physiol.* **273**, C755-C789 (1997).
10. H.-T. Fan, S. Morishima, H. Kida, and Y. Okada, Phloretin differentially inhibits volume-sensitive and cyclic AMP-activated, but not Ca-activated, Cl^- channels, *Br. J. Pharmacol.* **133**, 1096-1106 (2001).
11. T. Shimizu, and Y. Okada, Electrophysiological characteristics of Cl^- channel currents activated by apoptosis inducers,) *Jpn. J. Physiol.* **53** (in press) (2003).
12. D.W. Nicholson, and N.A. Thornberry, Caspases: killer proteases, *Trends Biochem. Sci.* **22**, 299-306 (1997).
13. X. Tan, and J.Y. Wang, The caspase-RB connection in cell death, *Trends Cell Biol.* **8**, 116-120 (1998).
14. S. Morishima, T. Shimizu, H. Kida, and Y. Okada, Volume expansion sensitivity of swelling-activated Cl^- channel in human epithelial cells, *Jpn. J. Physiol.* **50**, 277-280 (2000).
15. A. Leaf, On the mechanism of fluid exchange of tissues in vitro, *Biochem. J.* **62**, 241-248 (1956).
16. D.C. Tosteson and J.F. Hoffman, Regulation of cell volume by active cation transport in high and low potassium sheep red cells, *J. Gen. Physiol.* **44**, 169-194 (1960).
17. S. Oiki, M. Kubo, and Y. Okada, Mg^{2+} and ATP-dependence of volume-sensitive Cl^- channels in human epithelial cells, *Jpn. J. Physiol.* **44**, S77-S79 (1994).
18. R. Lomneth, S. Medrano, and E.I. Gruenstein, The role of transmembrane pH gradients in the lactic acid induced swelling of astrocytes, *Brain Res.* **523**, 69-77 (1990).
19. S. Mori, S. Morishima, M. Takasaki, and Y. Okada, Impaired activity of volume-sensitive anion channel during lactacidosis-induced swelling in neuronally differentiated NG108-15 cells, *Brain Res.* **957**, 1-11 (2002).
20. T. Nabekura, S. Morishima, T.L. Cover, S. Mori, H. Kannan, S. Komune, and Y. Okada, Recovery from lactacidosis-induced glial cell swelling with the aid of exogenous anion channels, *Glia* **41**, 247-259 (2003).

20

ERYTHROCYTE ION CHANNELS IN REGULATION OF APOPTOSIS

Florian Lang, Christina Birka, Svetlana Myssina, Karl S. Lang, Philipp A. Lang, Valerie Tanneur, Christophe Duranton, Thomas Wieder, Stephan M. Huber*

ABSTRACT

Erythrocytes lack mitochondria and nuclei, key organelles in the regulation of apoptosis. Until recently, erythrocytes were thus not considered subject to this type of cell death. However, exposure of erythrocytes to the Ca^{2+} ionophore ionomycin was shown to induce cell shrinkage, cell membrane blebbing and breakdown of phosphatidylserine asymmetry with subsequent phosphatidylserine exposure at the cell surface, all typical features of apoptosis. Further studies revealed the participation of ion channels in the regulation of erythrocyte "apoptosis." Osmotic shock, oxidative stress and energy depletion all activate a Ca^{2+}-permeable non-selective cation channel in the erythrocyte cell membrane. The subsequent increase of Ca^{2+} concentration stimulates a scramblase leading to breakdown of cell membrane phosphatidylserine asymmetry and activates Ca^{2+} sensitive K^+ (Gardos) channels leading to KCl loss and (further) cell shrinkage. Phosphatidylserine exposure and cell shrinkage are blunted in the nominal absence of extracellular Ca^{2+}, in the presence of the cation channel inhibitors amiloride or ethylisopropylamiloride, at increased extracellular K^+ or in the presence of the Gardos channel inhibitors clotrimazole or charybdotoxin. Thus, increase of cytosolic Ca^{2+} and cellular loss of K^+ participate in the triggering of erythrocyte scramblase. Nevertheless, phosphatidylserine exposure is not completely abrogated in the nominal absence of Ca^{2+}, pointing to additional Ca^{2+}-independent pathways. One of those is activation of sphingomyelinase with subsequent formation of ceramide which in turn leads to stimulation of erythrocyte scramblase. The exposure of phosphatidylserine at the extracellular face of the cell membrane stimulates phagocytes to engulf the apoptotic erythrocytes. Thus, sustained activation of the cation channels eventually leads to clearance of affected erythrocytes from peripheral blood. Erythropoietin inhibits the non-selective cation channel and thus interferes with erythrocyte "apoptosis." Susceptibility to scramblase activation is

* Florian Lang, Christina Birka, Svetlana Myssina, Karl S. Lang, Philipp A. Lang, Valerie Tanneur, Christophe Duranton, Thomas Wieder, Stephan M. Huber, Department of Physiology,Eberhard-Karls-University of Tuebingen, Gmelinstrasse 5, D-72076 Tuebingen, Germany

enhanced in thalassemia, sickle cell disease and glucose-6-phosphate dehydrogenase deficiency. Infection with *Plasmodium falciparum* leads to activation of the cation channel eventually triggering erythrocyte "apoptosis."

1. INTRODUCTION

Apoptosis, a physiological mechanism eliminating abundant and potentially harmful cells, is characterised by nuclear condensation, DNA fragmentation, mitochondrial depolarization, cell shrinkage and breakdown of phosphatidylserine asymmetry of the plasma membrane.[1, 2] The exposure of phosphatidylserine at the cell surface triggers and the decrease of cell volume facilitates the engulfment of the dying cells by phagocytes.[3, 4] Thus, apoptosis allows the elimination of the cells without release of intracellular proteins which would otherwise cause inflammation.[2]

Erythrocytes lack mitochondria and nuclei, intracellular organelles involved in the apoptosis of nucleated cells. However, erythrocytes exposed to the Ca^{2+} ionophore ionomycin undergo shrinkage, membrane blebbing and breakdown of cell membrane phosphatidylserine asymmetry, all typical features of apoptosis in nucleated cells.[5-7] In the following, the role of ion channels in the regulation of erythrocyte apoptosis will be discussed.

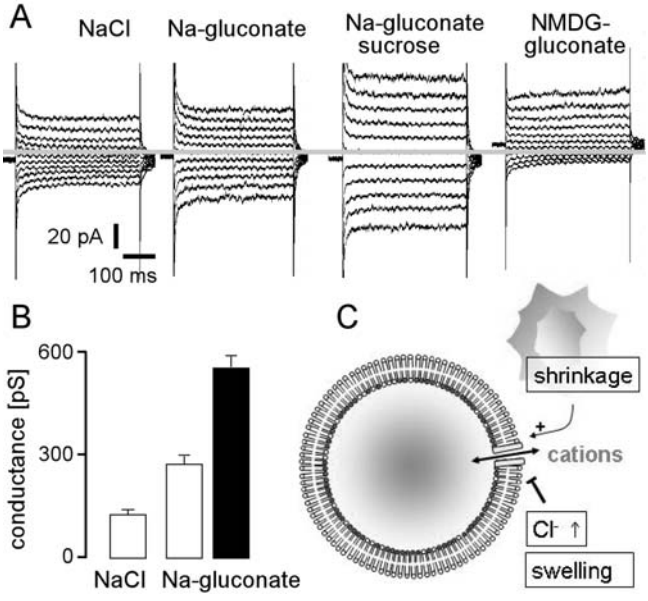

Figure 1. Activation of non-selective cation channels by osmotic shock in the absence of Cl^-. **A.** Original whole-cell current tracings recorded in a human erythrocyte with isotonic NaCl (outer left) and Na-gluconate bath solution (inner left) and upon increasing the osmolarity of the Na-gluconate bath solution by adding 250 mM sucrose (inner right; Na-gluconate pipette solution). The cell shrinkage-induced conductance was further recorded upon replacement of Na^+ in the bath solution by the impermeant cation N-methyl-D-glucamine$^+$ (NMDG-gluconate; outer right). **B.** Mean whole cell conductance (± SE) recorded as in (A) with isotonic NaCl and Na-gluconate bath solution (open bars) or upon cell shrinkage in Na-gluconate bath solution (closed bar). **C.** Scheme summarizing the regulation of the human erythrocyte cation channels by cell volume and Cl^- ions.

2. ACTIVATION OF NON-SELECTIVE CATION CHANNELS

Osmotic shock[8] and oxidative stress[9] open non-selective cation channels in the erythrocyte cell membrane. The same channels can be activated by removal of intracellular and extracellular Cl^-[8, 9] (Fig. 1). This property is reminiscent of the Na^+ and K^+ permeability activated by incubating human erythrocytes in low ionic strength (LIS) medium.[10-12] Similar to what has been shown for the LIS permeability,[11, 13] activation of the volume and oxidant sensitive cation channel by removal of extracellular Cl^- is inhibited by the anion channel/transport inhibitor 4,4'-diisothiocyanostilbene-2,2'-disulfonic acid (DIDS).[9] Moreover, the cation channels are inhibited by amiloride and ethylisopropylamiloride (EIPA).[14] Cation channels are permeable to calcium ions.[9, 15, 16] Accordingly, exposure to osmotic shock or oxidative stress triggers erythrocyte Ca^{2+} uptake.[16]

3. ROLE OF NON-SELECTIVE CATION CHANNELS IN ERYTHROCYTE APOPTOSIS

Compelling evidence points to a role of the volume sensitive cation channels in the induction of erythrocyte apoptosis. An increase of cytosolic Ca^{2+} concentration stimulates a scramblase thus leading to the breakdown of phosphatidylserine asymmetry.[5-7, 16] Exposure of phosphatidylserine is detected by determination of annexin binding, together with cell shrinkage, a typical feature of apoptosis in nucleated cells.[2] The erythrocyte annexin binding is triggered by osmotic shock and oxidative stress,[16] both maneuvers activating the cation channel.[8, 9] Furthermore, energy depletion leads to enhanced annexin binding.[16] Presumably, energy depletion impairs the replenishment of GSH and thus weakens the antioxidative defence of the erythrocytes.[17, 18] The annexin binding following osmotic shock and oxidative stress is blunted following chelation of extracellular calcium ions.[16] Moreover, the annexin binding is blunted by amiloride[16] and ethylisopropylamiloride (EIPA),[19] both putative inhibitors of the cation channel.[14, 16, 19]

4. ROLE OF THE CA^{2+} SENSITIVE GARDOS K^+ CHANNEL

The entry of Ca^{2+} further activates Ca^{2+} sensitive K^+ (Gardos) channels[20-24] (Fig. 2) leading to KCl loss and (further) cell shrinkage.[25] Phosphatidylserine exposure and cell shrinkage are blunted at increased extracellular K^+ or in the presence of the Gardos channel inhibitors clotrimazole or charybdotoxin.[26-32] Thus, cellular loss of K^+ participates in the triggering of erythrocyte scramblase. Cellular loss of K^+ has been shown to be critical for apoptosis of nucleated cells.[26-32]

5. PHYSIOLOGICAL AND PATHOPHYSIOLOGICAL IMPLICATIONS

The non-selective cation channel and thus erythrocyte apoptosis is inhibited by erythropoietin.[33] The hormone is known to increase the number of circulating erythrocytes by inhibition of apoptosis of erythroid precursor cells.[34] The influence of erythropoietin on the cation channel suggests that the hormone is, in addition, effective

by preventing apoptosis of mature erythrocytes. Erythropoietin has indeed been shown to prolong the life span of circulating erythrocytes.[35]

As phosphatidylserine exposure at the cell surface triggers the phagocytosis of affected erythrocytes,[3, 4] erythrocyte apoptosis may well participate in the clearance of aged, defective, energy depleted, leaky or infected erythrocytes from the blood stream. Aged erythrocytes expose more phosphatidylserine which contributes to the elimination of the senescent cells[3]. The capacity for oxidative defence decreases with erythrocyte age,[36, 37] a phenomenon paralleled by increase of passive cation permeability[38] and cytosolic free Ca^{2+} concentration.[39-44] Therefore, it is tempting to propose that the cation channels sense cell age.

Energy depletion and oxidative stress activate the cation channels, presumably increasing cytosolic Ca^{2+} and triggering erythrocyte apoptosis. Energy depletion impairs the function of the Na^+/K^+ATPase, thus jeopardizing maintenance of ionic gradients across the cell membrane which are required for cell volume regulation (For review, see Reference [45]). Thus, energy depletion would eventually lead to cell swelling and hemolysis. The triggering of apoptosis leads to elimination of the cells prior to hemolysis. The parallel activation of the Ca^{2+} sensitive K^+ channels delays cell swelling and provides extra time for the clearance of the defective erythrocytes.

Infection with *Plasmodium falciparum* similarly imposes oxidative stress on the host cell.[8, 9] The oxidation of the host cell membrane opens the so-called "new permeability pathway"[46] which is essential for nutrient uptake and waste disposal. On the other hand, the activation of the cation channel triggers erythrocyte apoptosis and limits the intraerythrocyte lifetime of the pathogen.

Erythrocytes from patients with thalassemia, sickle cell anemia and glucose-6-phosphate dehydrogenase deficiency are more sensitive to apoptotic stimuli.[47] Similarly, increased scramblase activity and phosphatidylserine exposure have been demonstrated for erythrocytes in sickle cell and thalassemia mouse models.[48] At least in desoxygenized sickle cells, deranged regulation of the Ca^{2+} sensitive K^+ channels[20-24] could contribute to the enhanced sensitivity to osmotic shock and oxidative stress. It is tempting to speculate that enhanced susceptibility to apoptosis provides some protection against severe malaria following infection with *Plasmodium falciparum*.

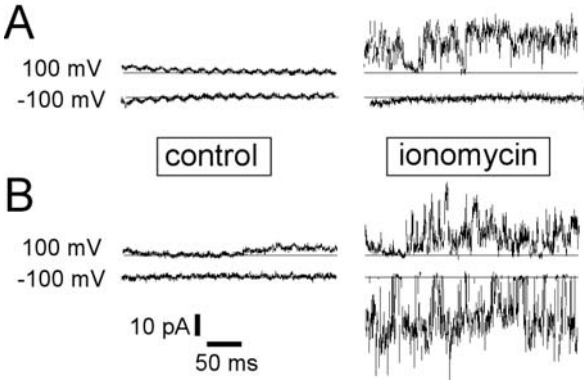

Figure 2. Activation of Gardos K^+ channels in human erythrocytes by increase of the cytosolic Ca^{2+} activity. Original current tracings recorded in cell-attached mode with Na-gluconate (**A**) and K-gluconate (**B**) pipette- and NaCl Ringer bath solution before (control) and after bath application of the Ca^{2+} ionophore ionomycin (1 μM). Records were obtained at 100 mV and -100 mV voltage, as indicated.

6. ADDITIONAL MECHANISMS

Erythrocyte apoptosis does not result only from channel activation with subsequent increase of cytosolic Ca^{2+} and decrease of cytosolic K^+ but involves further mechanisms. One of those mechanisms is activation of erythrocyte sphingomyelinase with subsequent release of ceramide[49] which triggers phosphatidylserine exposure without increasing cytosolic Ca^{2+}.[49] Ceramide added to extracellular fluid similarly stimulates phosphatidylserine exposure and enhances the sensitivity of the erythrocytes to increases of cytosolic Ca^{2+}. Moreover, a decrease of cytosolic ATP concentration may foster erythrocyte apoptosis not only by impairment of oxidant defence and break down of cation gradients. Thus, additional studies are required to fully understand the complex machinery leading to erythrocyte apoptosis.

7. ACKNOWLEDGMENTS

The authors acknowledge the technical assistance of E. Faber and the meticulous preparation of the manuscript by Lejla Subasic. Research of the authors was supported by the Deutsche Forschungsgemeinschaft, Nr. La 315/4-3, La 315/6-1, DFG Schwerpunkt Intrazelluläre Lebensformen La 315/11-1, and the Bundesministerium für Bildung, Wissenschaft, Forschung und Technologie (Center for Interdisciplinary Clinical Research) 01 KS 9602.

The authors congratulate Peter Lauf for his 70th birthday and more importantly, for his outstanding achievements in erythrocyte physiology over the past few decades. Similar to countless scientists dedicated to erythrocyte physiology, cell volume and/or membrane transport, we have been inspired and guided by his brilliant ideas and seminal observations.

8. REFERENCES

1. D. R. Green and J. C. Reed, Mitochondria and apoptosis, *Science*. **281,** 1309-1312 (1998).
2. E. Gulbins, A. Jekle, K. Ferlinz, H. Grassme, and F. Lang, Physiology of apoptosis, *Am. J. Physiol Renal Physiol*. **279,** F605-F615 (2000).
3. F. E. Boas, L. Forman, and E. Beutler, Phosphatidylserine exposure and red cell viability in red cell aging and in hemolytic anemia, *Proc. Natl. Acad. Sci. U. S. A*. **95,** 3077-3081 (1998).
4. S. Eda and I. W. Sherman, Cytoadherence of malaria-infected red blood cells involves exposure of phosphatidylserine, *Cell. Physiol. Biochem.* **12,** 373-384 (2002).
5. C. P. Berg, I. H. Engels, A. Rothbart, K. Lauber, A. Renz, S. F. Schlosser, K. Schulze-Osthoff, and S. Wesselborg, Human mature red blood cells express caspase-3 and caspase-8, but are devoid of mitochondrial regulators of apoptosis, *Cell Death. Differ.* **8,** 1197-1206 (2001).
6. D. Bratosin, J. Estaquier, F. Petit, D. Arnoult, B. Quatannens, J. P. Tissier, C. Slomianny, C. Sartiaux, C. Alonso, J. J. Huart, J. Montreuil, and J. C. Ameisen, Programmed cell death in mature erythrocytes: a model for investigating death effector pathways operating in the absence of mitochondria, *Cell Death. Differ.* **8,** 1143-1156 (2001).
7. E. Daugas, C. Cande, and G. Kroemer, Erythrocytes: death of a mummy, *Cell Death. Differ.* **8,** 1131-1133 (2001).
8. S. M. Huber, N. Gamper, and F. Lang, Chloride conductance and volume-regulatory nonselective cation conductance in human red blood cell ghosts, *Pflugers Arch.* **441,** 551-558 (2001).
9. C. Duranton, S. M. Huber, and F. Lang, Oxidation induces a Cl(-)-dependent cation conductance in human red blood cells, *J. Physiol.* **539,** 847-855 (2002).
10. I. Bernhardt, A. C. Hall, and J. C. Ellory, Effects of low ionic strength media on passive human red cell monovalent cation transport, *J. Physiol.* **434,** 489-506 (1991).

11. G. S. Jones and P. A. Knauf, Mechanism of the increase in cation permeability of human erythrocytes in low-chloride media. Involvement of the anion transport protein capnophorin, *J. Gen. Physiol.* **86,** 721-38 (1985).
12. P. L. LaCelle and A. Rothstein, The passive permeability of the red blood cell to cations, *J. Gen. Physiol.* **50,** 171-88 (1966).
13. S. J. Culliford, I. Bernhardt, and J. C. Ellory, Activation of a novel organic solute transporter in mammalian red blood cells, *J Physiol*. **489 (Pt 3),** 755-65 (1995).
14. K. S. Lang, S. Myssina, V. Tanneur, T. Wieder, S. M. Huber, F. Lang, and C. Duranton, Inhibition of erythrocyte cation channels and apoptosis by ethylisopropylamiloride, *Naunyn Schmiedebergs Arch. Pharmacol.* **367,** 391-396 (2003).
15. L. Kaestner, P. Christophersen, I. Bernhardt, and P. Bennekou, The non-selective voltage-activated cation channel in the human red blood cell membrane: reconciliation between two conflicting reports and further characterisation, *Bioelectrochemistry*. **52,** 117-25 (2000).
16. K. S. Lang, C. Duranton, H. Poehlmann, S. Myssina, C. Bauer, F. Lang, T. Wieder, and S. M. Huber, Cation channels trigger apoptotic death of erythrocytes, *Cell Death and Differentiation*. **10(2),** 249-256 (2003).
17. S. Bilmen, T. A. Aksu, S. Gumuslu, D. K. Korgun, and D. Canatan, Antioxidant capacity of G-6-PD-deficient erythrocytes, *Clin Chim Acta*. **303,** 83-6 (2001).
18. I. Mavelli, M. R. Ciriolo, L. Rossi, T. Meloni, G. Forteleoni, A. De Flora, U. Benatti, A. Morelli, and G. Rotilio, Favism: a hemolytic disease associated with increased superoxide dismutase and decreased glutathione peroxidase activities in red blood cells, *Eur J Biochem*. **139,** 13-8 (1984).
19. K. S. Lang, C. Weigert, S. Braedel, S. Fillon, M. Palmada, E. Schleicher, H. G. Rammensee, and F. Lang, Inhibition of interferon-gamma expression by osmotic shrinkage of peripheral blood lymphocytes, *Am. J. Physiol Cell Physiol*. **284,** C200-C208 (2003).
20. R. M. Bookchin, O. E. Ortiz, and V. L. Lew, Activation of calcium-dependent potassium channels in deoxygenated sickled red cells, *Prog Clin Biol Res*. **240,** 193-200 (1987).
21. C. Brugnara, L. de Franceschi, and S. L. Alper, Inhibition of Ca(2+)-dependent K+ transport and cell dehydration in sickle erythrocytes by clotrimazole and other imidazole derivatives, *J. Clin. Invest.* **92,** 520-6 (1993).
22. R. S. Franco, M. Palascak, H. Thompson, D. L. Rucknagel, and C. H. Joiner, Dehydration of transferrin receptor-positive sickle reticulocytes during continuous or cyclic deoxygenation: role of KCl cotransport and extracellular calcium, *Blood*. **88,** 4359-65 (1996).
23. C. H. Joiner, Cation transport and volume regulation in sickle red blood cells, *Am J Physiol*. **264,** C251-C270 (1993).
24. V. L. Lew and R. M. Bookchin, Osmotic effects of protein polymerization: analysis of volume changes in sickle cell anemia red cells following deoxy-hemoglobin S polymerization, *J Membr. Biol.* **122,** 55-67 (1991).
25. P. A. Lang, S. Kaiser, S. Myssina, T. Wieder, F. Lang, and S. M. Huber, Role of Ca2+ activated K+ channels in human erythrocyte apoptosis, *Am J Physiol - Cell Physiol*. **285,** C1553-C1560 (2003).
26. C. D. Bortner, F. M. Hughes, Jr., and J. A. Cidlowski, A primary role for K+ and Na+ efflux in the activation of apoptosis, *J Biol. Chem.* **272,** 32436-32442 (1997).
27. C. D. Bortner and J. A. Cidlowski, Caspase independent/dependent regulation of K(+), cell shrinkage, and mitochondrial membrane potential during lymphocyte apoptosis, *J Biol Chem*. **274,** 21953-62 (1999).
28. M. Gomez-Angelats, C. D. Bortner, and J. A. Cidlowski, Protein kinase C (PKC) inhibits fas receptor-induced apoptosis through modulation of the loss of K+ and cell shrinkage. A role for PKC upstream of caspases, *J Biol. Chem.* **275,** 19609-19619 (2000).
29. F. M. Hughes, Jr., C. D. Bortner, G. D. Purdy, and J. A. Cidlowski, Intracellular K+ suppresses the activation of apoptosis in lymphocytes, *J Biol. Chem.* **272,** 30567-30576 (1997).
30. F. M. Hughes, Jr. and J. A. Cidlowski, Potassium is a critical regulator of apoptotic enzymes in vitro and *in vivo*, *Adv. Enzyme Regul.* **39,** 157-171 (1999).
31. J. W. Montague, C. D. Bortner, F. M. Hughes, Jr., and J. A. Cidlowski, A necessary role for reduced intracellular potassium during the DNA degradation phase of apoptosis, *Steroids*. **64,** 563-569 (1999).
32. G. I. Perez, D. V. Maravei, A. M. Trbovich, J. A. Cidlowski, J. L. Tilly, and F. M. Hughes, Jr., Identification of potassium-dependent and -independent components of the apoptotic machinery in mouse ovarian germ cells and granulosa cells, *Biol. Reprod.* **63,** 1358-1369 (2000).
33. S. Myssina, S. M. Huber, C. Birka, P. A. Lang, K. S. Lang, T. Wieder, and F. Lang, Inhibition of erythrocyte cation channels by erythropoietin, *J Am Soc Nephrol*. **14,** 2750-2757 (2003).
34. W. Jelkmann, Erythropoietin: structure, control of production, and function, *Physiol Rev.* **72,** 449-489 (1992).

35. M. Polenakovic and A. Sikole, Is erythropoietin a survival factor for red blood cells?, *J Am Soc Nephrol*. **7,** 1178-1182 (1996).
36. H. Imanishi, T. Nakai, T. Abe, and T. Takino, Glutathione metabolism in red cell aging, *Mech Ageing Dev*. **32,** 57-62 (1985).
37. G. Piccinini, G. Minetti, C. Balduini, and A. Brovelli, Oxidation state of glutathione and membrane proteins in human red cells of different age, *Mech Ageing Dev*. **78,** 15-26 (1995).
38. C. H. Joiner and P. K. Lauf, Ouabain binding and potassium transport in young and old populations of human red cells, *Membr Biochem*. **1,** 187-202 (1978).
39. N. R. Aiken, J. D. Satterlee, and W. R. Galey, Measurement of intracellular Ca2+ in young and old human erythrocytes using 19F-NMR spectroscopy, *Biochim. Biophys. Acta.* **1136,** 155-60 (1992).
40. D. Allan and P. J. Raval, The role of Ca2+-dependent biochemical changes in the ageing process in normal red cells and in the development of irreversibly sickled cells, *Folia Haematol Int Mag Klin Morphol Blutforsch*. **114,** 499-503 (1987).
41. I. L. Cameron, W. E. Hardman, N. K. Smith, G. D. Fullerton, and A. Miseta, Changes in the concentration of ions during senescence of the human erythrocyte, *Cell Biol Int*. **17,** 93-8 (1993).
42. J. J. Kramer and N. I. Swislocki, The effects of pentoxifylline on rat erythrocytes of different age, *Mech Ageing Dev*. **32,** 283-98 (1985).
43. P. J. Romero, E. A. Romero, and M. D. Winkler, Ionic calcium content of light dense human red cells separated by Percoll density gradients, *Biochim Biophys Acta*. **1323,** 23-8 (1997).
44. N. W. Seidler and N. I. Swislocki, Ca2+ transport activities of inside-out vesicles prepared from density-separated erythrocytes from rat and human, *Mol Cell Biochem*. **105,** 159-69 (1991).
45. F. Lang, G. L. Busch, M. Ritter, H. Völkl, S. Waldegger, E. Gulbins, and D. Häussinger, Functional significance of cell volume regulatory mechanisms, *Physiol Rev.* **78,** 247-306 (1998).
46. K. Kirk, Membrane transport in the malaria-infected erythrocyte, *Physiol Rev.* **81,** 495-537 (2001).
47. K. S. Lang, B. Roll, S. Myssina, M. Schittenhelm, H. G. Scheel-Walter, L. Kanz, J. Fritz, F. Lang, S. M. Huber, and T. Wieder, Enhanced erythrocyte apoptosis in sickle cell anemia, thalassemia and glucose-6-phosphate dehydrogenase deficiency, *Cell Physiol Biochem*. **12,** 365-72 (2002).
48. L. S. Kean, L. E. Brown, J. W. Nichols, N. Mohandas, D. R. Archer, and L. L. Hsu, Comparison of mechanisms of anemia in mice with sickle cell disease and beta-thalassemia: peripheral destruction, ineffective erythropoiesis, and phospholipid scramblase-mediated phosphatidylserine exposure, *Exp Hematol*. **30,** 394-402 (2002).
49. K. S. Lang, S. Myssina, V. Brand, C. Sandu, P. A. Lang, S. M. Huber, F. Lang, and T. Wieder, Involvement of ceramide in hyperosmotic shock-induced death of erythrocytes, *Cell Death. Differ.* **11**, 231-243 (2004).

21

APOPTOSIS *VS.* ONCOSIS: ROLE OF CELL VOLUME AND INTRACELLULAR MONOVALENT CATIONS

Sergei N. Orlov and Pavel Hamet*

SUMMARY

Several research teams have proposed that shrinkage and swelling in cells undergoing apoptosis and oncosis are not only the earliest morphological markers of the two modes of cell death but are also obligatory steps in the development of the death machinery. We examined this hypothesis as well as the role of monovalent cations as major intracellular osmolytes using vascular smooth muscle cells (VSMC) from the rat aorta and C7-MDCK cells derived from the Madin-Darby canine kidney. 48-hr inhibition of the Na^+-K^+ pump with ouabain did not affect VSMC survival and delayed serum deprivation-induced apoptosis at a step upstream of caspase-3 via elevation of the $[Na^+]_i/[K^+]_i$ ratio and the expression of Na^+_i-sensitive antiapoptotic genes including mortalin. Transient and modest (15-20%) shrinkage observed in serum-deprived VSMC did not contribute to triggering of the apoptotic machinery. In contrast to VSMC, ouabain led to oncosis of C7-MDCK cells, indicated by swelling and resistance to the pan-caspase inhibitor z-VAD.fmk. In these cells, the death signal was mediated by interaction of ouabain with the Na^+-K^+-ATPase α-subunit but was independent of the inhibition of Na^+-K^+ pump-mediated ion fluxes and elevation of the $[Na^+]_i/[K^+]_i$ ratio.

1. INTRODUCTION

The maintenance of protein concentration in the range of ~300 mg per ml of intracellular water is a ubiquitous feature of all cell types studied thus far. In nucleated cells with $P_K > P_{Cl} >> P_{Na}$, such extensive macromolecular crowding is under control of the Na^+-K^+ pump as well as membrane transporters whose activities are sensitive to cell volume modulation such as inwardly-directed Na^+/H^+ exchange, Na^+-K^+-Cl^- cotransport

* Sergei N. Orlov and Pavel Hamet, Centre de recherche du Centre hospitalier de l'Université de Montréal (CHUM)-Hôtel-Dieu, 3850, rue Saint-Urbain, Montreal, Québec H2W 1T7, Canada

and Na^+-coupled symport of organic osmolytes providing regulatory volume increase (RVI), and outwardly-directed K^+,Cl^- cotransport, K^+ and anion channels providing regulatory volume decrease (RVD).[1-3]

The first description of the death of clustering neighboring cells in injured tissues, indicated by their swelling and known as necrosis, came from Virchow's classic pathomorphological studies. More recently, the death of single cells without formation of an injury area and characterized by initial shrinkage was observed during embryogenesis, metamorphosis, aging, endocrine- and neuronal-dependent tissue atrophy and was called apoptosis.[4-8] The different pattern of cell volume modulation in these two modes of cell death is so impressive that the term "shrinkage-mediated necrosis" was adopted for the initial description of apoptosis in immune system cells.[9] To underline the striking difference of cell volume behaviour, a revised terminology has been proposed claiming that necrosis was originally offered as a concept to characterize any postmortem changes in cell morphology. In accordance with this nomenclature, the label oncosis, derived from the Greek word for swelling, describes cell death that is distinct from apoptotic shrinkage.[10]

Several researchers including our team have suggested that the distinct patterns of volume modulation in cells undergoing apoptosis and oncosis are not solely the earliest morphological markers of the two modes of cell death but are also obligatory steps in development of the death machinery.[11-15] We examined this attractive hypothesis in vascular smooth muscle cells (VSMC) from rat aorta and Madin-Darby canine kidney C7 cells (C7-MDCK) resembling principal cells from collecting ducts. The data obtained in these studies are reviewed below.

2. INVERSION OF THE $[Na^+]_i/[K^+]_i$ RATIO INHIBITS APOPTOSIS IN VSMC AT A STEP UPSTREAM OF CASPASE 3

Similar to fibroblasts,[16] transfection of VSMC with the functional analogue of c-Myc E1A adenoviral protein sharply accelerates apoptosis triggered by serum deprivation. Video tape recording indicated exposure of phosphatidyl serine on the outer surface of plasma membranes, caspase-3 activation, accumulation of intracellular chromatin fragments, internucleosomal DNA degradation, and suppression by the pan-caspase inhibitor z-VAD.fmk.[17-21] Similar to other cells undergoing apoptosis, the death of serum-deprived VSMC-E1A is respectively suppressed and potentiated by transfection with bcl-2 and p53.[17, 18, 22] With this well-established cell culture model of apoptosis, we noted that pretreatment with ouabain, a highly selective Na^+-K^+ pump inhibitor, delayed VSMC death triggered by distinct apoptotic stimuli such as serum deprivation, inhibition of serine-threonine phosphatases, cytochrome c release, and DNA damage triggered by extensive labeling with [^{3}H]-thymidine at a step upstream of caspase-3.[21, 23] Later, protection against apoptosis by Na^+-K^+ pump inhibitors was documented in neuronal cells,[24] and renal epithelial cells.[25]

The antiapoptotic action of ouabain might be caused by rapid membrane depolarization due to electrogenicity of the Na^+-K^+ pump, elevation of $[Na^+]_i$ or loss of intracellular K^+. In addition, the interaction of ouabain with targets distinct from the Na^+-K^+ pump cannot be excluded. To further examine this issue, we compared the effect of ouabain on the intracellular content of monovalent ions and apoptosis in K^+-free and high-K^+/low-Na^+ media. These experiments allowed us to conclude that protection

against apoptosis in VSMC-E1A is caused by elevation of the $[Na^+]_i/[K^+]_i$ ratio[21] However, this approach was unable to dissect the relative role of $[Na^+]_i$ vs. $[K^+]_i$.

3. ANTIAPOPTOTIC ACTION OF THE INVERTED $[Na^+]_i/[K^+]_i$ RATIO IS MEDIATED BY GENE EXPRESSION

This statement is supported by three initial observations. *First*, inhibitors of macromolecular synthesis, such as actinomycin D and cycloheximide,[26] abolished the antiapoptotic action of ouabain in VSMC-E1A. *Second*, 6-hr exposure of VSMC to ouabain led to ~6-fold elevation of RNA synthesis.[27] *Third*, analysis of ^{35}S-labeled proteins by 2D electrophoresis revealed more than 50 new protein spots after 3-hr preincubation with ouabain (Fig. 1A).

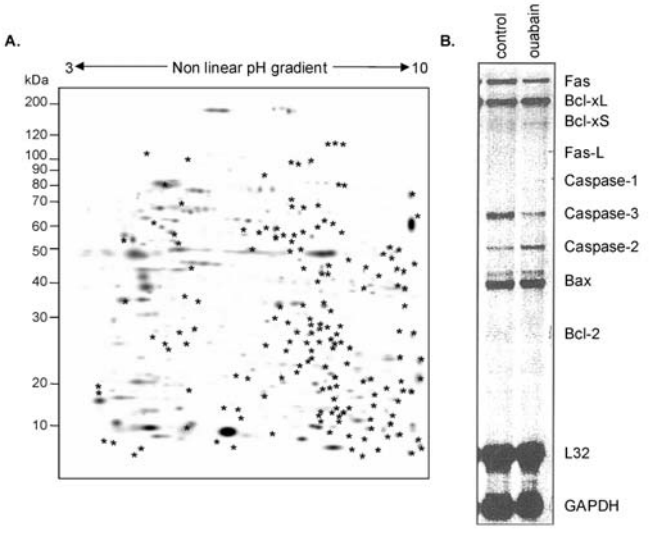

Figure 1. Effect of ouabain on gene expression in VSMC. **A.** 2D electrophoresis of VSMC proteins. Serum-deprived cells were treated for 3 hr with Trans ^{35}S cocktail in the absence or presence of 1 mM ouabain. Map shows data obtained in 3 independent experiments. Asterisks flag proteins whose expression was triggered by ouabain. **B.** Autoradiogram utilizing the Multi-Probe template set (rAPO-1 #45601P, PharMingen) with mRNA obtained after 24-hr incubation of serum-deprived cells in the absence or presence of 1 mM ouabain.

Deploying the rAPO-1 Multi-probe template set, we failed to detect, in ouabain-treated VSMC, sustained elevation of expression of the major pro- and antiapoptotic genes Bcl-2, Bcl-xL, Bcl-xS, Bax, and caspase 1-3 (Fig. 1B). Keeping in mind these negative data, we took a proteomics approach to identify genes whose expression is triggered by ouabain.[28] To increase the resolution of this approach, we separated soluble, membrane-bound and cytoskeleton proteins. Twelve soluble proteins whose expression is triggered by ouabain have been identified by mass spectrometry including mortalin. Previous studies have demonstrated the pancytosolic and mitochondrial/juxtanuclear localization of mortalin in mortal and immortal cells, respectively.[7, 29-31] Northern and

Western blotting confirmed the induction of mortalin expression in ouabain-treated VSMC and documented its mitochondrial localization. We also established that, similar to ouabain, transfection with mortalin delayed the development of apoptosis in serum-deprived VSMC-E1A, probably via its interaction with p53.[28]

4. EVIDENCE FOR Na^+_i-MEDIATED Ca^{2+}_i-INDEPENDENT EXCITATION-TRANSCRIPTION COUPLING

In the last decade, it was found that Na^+-K^+ pump inhibition in cardiomyocytes, hepatocytes and renal epithelial cells triggers the expression of the α1- and 1-subunits of the Na^+-K^+ pump, myosin light chain, skeletal muscle actin, atrial natriuretic factor and tumour growth factor (for recent review, see[32, 33]). These data as well as the induced expression of numerous genes detected in ouabain-treated VSMC (Fig. 1A) suggest that this effect is at least partially mediated by expression of early response genes (ERG) such as c-Fos, c-Jun, and c-Myc. Indeed, Na^+-K^+ pump inhibition led to activation of c-Fos mRNA expression in leukemia and melanoma cells,[34-36] renal epithelial cells,[37] fibroblasts, HeLa cells,[35] and cardiomyocytes.[38, 39] We observed that accumulation of c-Fos mRNA in ouabain-treated cells was correlated with elevation of $[Na^+]_i$ and preceded the loss of intracellular K^+.[40] c-Fos expression, seen under elevated $[Na^+]_i$, can be mediated by activation of the Na^+/Ca^{2+} exchanger. The latter hypothesis is consistent with the presence of (Ca^{2+}+cAMP) response element (CRE) within the c-Fos promoter (Fig. 2). Indeed, we have demonstrated that K^+_o-induced depolarization leads to c-Fos

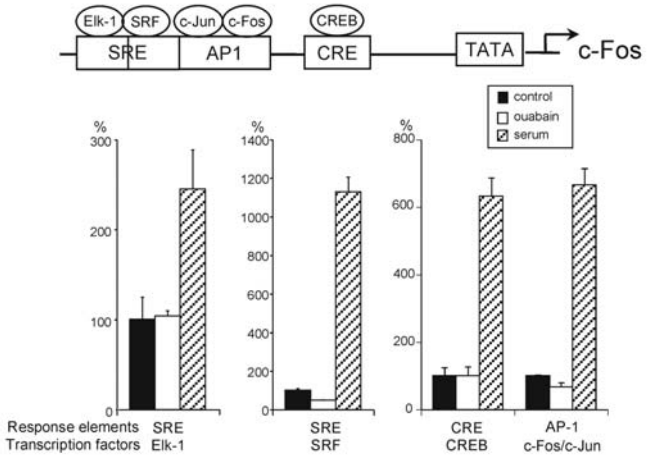

Figure 2. Structure of the c-Fos promoter and effect of 10% serum and 1 mM ouabain on the activity of c-Fos transcriptional elements, measured as luciferase luminescence in *trans*- and *cis*-reporter systems. The activity of transcriptional factors in the absence of serum and ouabain was taken as 100%. For more details, see[40].

expression that is completely abolished by the selective L-type Ca^{2+} channel blocker nicardipine.[40] However, the data listed below strongly indicate that c-Fos expression in ouabain-treated VSMC is not mediated by $[Ca^{2+}]_i$ elevation. *First*, c-Fos expression in

ouabain-treated cells is not sensitive to nicardipine. *Second*, neither $[Ca^{2+}]_i$ nor total exchangeable Ca content in VSMC is affected by ouabain. *Third*, neither omission of Ca^{2+}_o nor addition of extracellular (EGTA) and intracellular (BAPTA-AM) Ca^{2+} chelators abolishes ouabain-induced c-Fos expression.[40] *Fourth*, in contrast to serum, ouabain does not affect expression of the three major elements detected in the c-Fos promoter, including CRE (Fig. 2). Viewed collectively, these data allow us to hypothesize that inhibition of apoptosis in ouabain-treated VSMC is mediated by a novel Na^+_i-dependent, Ca^{2+}_i-insensitive mechanism of excitation-transcription coupling.

5. ONCOSIS IN OUABAIN-TREATED C7-MDCK CELLS: EVIDENCE FOR A NOVEL Na^+-K^+ PUMP FUNCTION

In contrast to VSMC,[27] ouabain leads to massive oncosis in C7-MDCK cells indicated by 1.5-fold elevation of cell volume after 6 hr incubation[41] and followed by the appearance of swollen, floating cells (Fig. 3). We have also revealed that unlike the apoptosis of serum-deprived VSMC-E1A, the death of ouabain-treated C7-MDCK cells is resistant to the pan-caspase inhibitor z-VAD.fmk and inhibitors of macromolecular synthesis.[41]

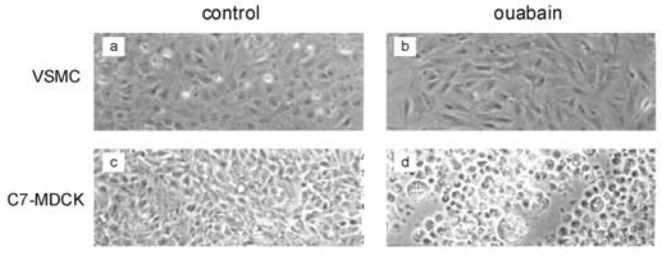

Figure 3. Phase-contrast microscopy of control (**a,c**) and ouabain-treated (**b,d**) VSMC (**a,b**) and C7-MDCK cells (**c,d**). The cells were treated with 1 mM (VSMC) or 10 μM (C7-MDCK cells) ouabain for 24 hr.

In accordance with the hypothesis postulated more than two decades ago, cell swelling caused by dissipation of the Gibbs-Donnan equilibrium under inhibition of the Na^+-K^+ pump is *per se* sufficient to disrupt plasma membrane integrity.[42] Indeed, we failed to detect any significant modulation of cell volume in ouabain-treated VSMC.[19] To further examine the chemiosmotic mechanism of oncosis, we subjected C7-MDCK cells to incubation in media with different contents of monovalent cations. Surprisingly, we observed that more than 500-fold inhibition of the Na^+-K^+ pump in K^+-free medium does not affect the survival of these cells.[41] As predicted, 6-hr incubation of C7-MDCK cells in K^+-free medium led to a sharp $[Na^+]_i$ elevation and addition of ouabain only slightly altered this parameter, whereas incubation in high-K^+/low-Na^+ medium did not impact the baseline values of $[Na^+]_i$ and $[K^+]_i$ but completely abolished K^+_i loss triggered by ouabain. However, similar to control medium, ouabain killed cells to the same extent in K^+-free and high-K^+/low-Na^+ media.[41]

Two alternative hypotheses could be generated by analysis of these intriguing results. *First*, ouabain leads to oncosis of C7-MDCK cells via its interaction with targets distinct from the Na^+-K^+-ATPase α-subunit. *Second*, ouabain-triggered oncosis is caused by its interaction with Na^+-K^+-ATPase independently of the inhibition of ion fluxes and inversion of the $[Na^+]_i/[K^+]_i$ ratio controlled by this enzyme. The first hypothesis should probably be ruled out. Indeed, keeping in mind well-documented data on the modulation of Na^+/K^+ pump affinity for ouabain by extracellular K^+,[43-45] we compared the effect of ouabain on the rate of ^{86}Rb influx and cell survival in control and K^+-free medium. Table 1 shows that preincubation in K^+-free medium increases the sensitivity of ^{86}Rb influx to ouabain by one order of magnitude. The same leftward shift of dose-dependencies is observed by analysis of the ouabain effect on cell survival.

Table 1. Effect of ouabain on the Na^+K^+ pump activity and survival of C7-MDCK cells in control and K-free medium

K^+ and Na^+ concentration in the incubation medium, mM	Cell survival under baseline conditions, %	Cell survival in the presence of 3 μM ouabain, %	Concentration of ouabain causing half-maximal inhibition of ^{86}Rb uptake, nM	Concentration of ouabain causing half-maximal attenuation of cell survival, nM
K^+ 5; Na^+ - 140	100±6	25±3	800±72	265±45
K^+ 0; Na^+ - 145	102±7	24±4	50±8	23±6

The survival of C7-MDCK cells after 6-hr incubation in K^+-containing medium in the absence of ouabain was taken as 100%. Means + S.E. obtained in experiments performed in quadruplicate are shown. For methodological details, see[41].

It should be underlined that these data do not obligatorily mean the lack of involvement of cell swelling in the triggering of oncosis in ouabain-treated epithelial cells. Indeed, similar to cell survival, incubation in K^+-free medium did not significantly affect the volume of C7-MDCK cells, whereas ouabain led to about the same cell swelling in this as well as in high-K^+/low-Na^+ medium (unpublished data). The mechanism of $[Na^+]_i/[K^+]_i$-independent volume increase should be examined further.

6. APOPTOSIS IN HYPEROSMOTICALLY-SHRUNKEN CELLS

Initially, the hypothesis of the involvement of cell shrinkage in triggering apoptosis was based on data showing that hyperosmotic shrinkage with 250 mM mannitol evokes apoptosis of cultured lymphocytes.[12] Apoptosis activation was also detected in hyperosmotically-shrunken Jurkat cells,[21] vascular endothelial cells,[46] the mIMCD3 renal epithelial cell line,[47] and HeLa cells.[48] Unlike the above-listed cell types, the addition of 300 mM mannitol slightly affected apoptosis in SH-SY5Y neuroblastoma cells[49] and had no effect in VSMC, MDCK,[15] Cos-7, GH_3 and HeLa cells.[12]

Recently, we observed that in contrast to immune system cells undergoing massive apoptosis in the presence of 200 mM mannitol, 400 and 500 mM of mannitol should be

added to induce apoptosis in C7-MDCK and VSMC (Fig. 4). Similar to serum-deprived medium, VSMC apoptosis triggered by hyperosmotic medium was sharply potentiated by transfection with E1A-adenoviral protein (Fig. 5B). Importantly, the volume of mannitol-treated VSMC and VSMC-E1A was about the same (Fig. 5A), suggesting that distinct sensitivity to hyperosmotic medium rather than a cell type-specific pattern of cell volume modulation determines the distinct susceptibility of cells to apoptosis.

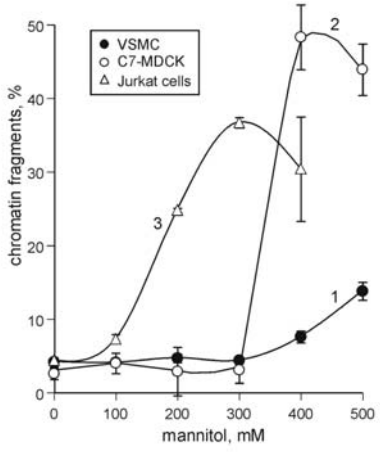

Figure 4. Dose-dependency of the effect of mannitol on chromatin cleavage in VSMC (**1**), C7-MDCK (**2**) and Jurkat cells **(3)**. The cells were incubated for 24 hr in DMEM containing 5% (Jurkat cells) or 10% serum (VSMC and C7-MDCK) and mannitol at concentrations indicated in the X axis. Means ± S.E. obtained from experiments performed in quadruplicate are given. For more details, see[19].

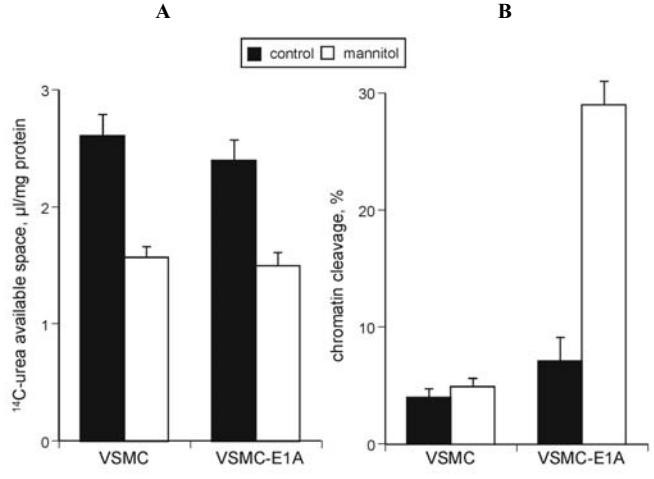

Figure 5. Effect of mannitol on cell volume (**A**) and chromatin cleavage (**B**) in VSMC and VSMC-E1A. Mannitol was added at a concentration of 375 mM in DMEM containing 10% serum for 2 (A) or 24 (B) hr. Means ± S.E. obtained from experiments performed in quadruplicate are given. For more details, see[19].

In contrast to rapid shrinkage of VSMC-E1A in hyperosmotic medium, we failed to detect any accumulation of intracellular chromatin fragments with 3 hr of mannitol addition. Moreover, in contrast to "classic" apoptotic stimuli, apoptosis in hyperosmotically-shrunken VSMC-E1A was potentiated rather than inhibited by ouabain.[19] These data allowed us to speculate that the mechanisms of apoptosis triggered by hyperosmotic shrinkage and physiological stimuli might be different. To further examine this issue, we compared cell volume modulation in hyperosmotically-shrunken and serum-deprived VSMC-E1A.

Electronic sizing, cell density measurement by isopyknic centrifugation and flow cytometry have been employed to quantify apoptotic volume decrease (AVD) in the range from 20 to 50% of the initial size (for review, see[13]). In human T cells treated with ionomycin and phytohemaglutinin[50] as well as in HeLa, U973 and NG108-15 cells,[51] shrinkage preceded the appearance of apoptotic nuclei and membrane blebbing. In contrast, in X-irradiated rat thymocytes[52] and Fas-L-treated Jurkat cells,[12, 53, 54] the kinetics of cell volume modulation and accumulation of dead cells were identical, suggesting that cell shrinkage is at least partially a consequence of apoptosis rather than its primary event. The secondary mechanism of AVD is also supported by observations on the inhibition of cell volume decrease under suppression of apoptosis with the pan-caspase inhibitor z-VAD.fmk.[55]

To escape the impact of the degradation phase of apoptosis on cell volume estimation, we measured [^{14}C]-urea available space, a common marker of intracellular water volume.[56] This approach allowed us to avoid volume measurement in the portion of floating apoptotic cells. We observed that 1-hr incubation of VSMC-E1A in serum-deprived medium resulted in attenuation of [^{14}C]-urea available space by 10-15%.[19] These results are consistent with modest (from 10 to 25%) volume reduction in non-transfected VSMC, HeLa, U973, NG108-15, lymphoblastoid cells and cultured cortical neurons measured before the appearance of apoptotic markers.[15, 51, 57, 58] They also show that AVD in serum-deprived VSMC is less than threshold for the induction of apoptosis in hyperosmotic medium.

7. THE SEARCH FOR TRANSPORTERS INVOLVED IN AVD

Isosmotic AVD can be triggered by efflux of major intracellular osmolytes via activated K^+ channels, electroneutral K^+-Cl^- cotransport or anion channels permeable to organic osmolytes. In thymocytes undergoing apoptosis, intracellular K^+ content measured by inductively-coupled plasma/mass spectrometry or as ^{86}Rb content was decreased by two to threefold.[59, 60] It should be noted, however, that the kinetics of K^+_i decline and DNA fragmentation in dexamethasone-treated thymocytes are similar,[60] indicating a secondary rather than a primary mechanism of K^+ loss. Indeed, a negligible decrease in total K^+_i content was observed in dexamethasone-treated CEM-C7A before the development of morphologically-defined apoptosis, whereas the sharp increment in the apoptotic cell number was accompanied by the loss of ~40% of intracellular K^+.[57] About the same reduction of K^+ was noted in mouse L cells with complete apoptosis in the presence of inhibitors of cell cycle progression.[61] Because attenuation of K^+_i content in immune system cells undergoing apoptosis was accompanied by two to threefold elevation of Na^+_i content,[61] a secondary rather than a primary mechanism of perturbation of intracellular ion homeostasis is suspected. Indeed, in dexamethasone-treated

thymocytes and Fas-L-treated Jurkat cells, fluorescence of the K^+ chelator PBFI was attenuated by more than 10-fold compared to control cells,[54, 60] whereas in cell-free system, the decrease of KCl from 135 to 5 mM reduced PBFI fluorescence by twofold only.[61, 62] These data strongly suggest that the sharp decrease of PBFI fluorescence in dexamethasone-treated thymocytes was mainly caused by loss of PBFI rather than K^+. This conclusion is consistent with a 15-fold decreased fluorescence of the Na^+ chelator SBFI observed in shrunken Fas-L-treated Jurkat cells.[54]

Several laboratories have reported that the development of apoptosis is accompanied by activation of voltage- (K_V) and Ca^{2+}-gated (K_{Ca}) K^+ channels.[63-67] In contrast, in rat cortical neurons, long-term treatment with TNF triggered K_V expression involved in cell survival rather than death.[68] Lang with co-workers documented decreased activity of N-type voltage-gated K^+ channels ($K_V1.3$) in Jurkat cells undergoing apoptosis in the presence of Fas-L[69] or ceramides.[70] In protonophore-treated VSMC, freshly-isolated neurons and leukemia cells, inhibitors of K^+ channels partially suppressed the development of apoptosis.[51, 66, 71, 72] In contrast, Nobel et al.[55] did not observe any protection against apoptosis in Fas-L-treated Jurkat cells in the presence of K_{Ca} and K_V blockers, such as charibdotoxin, dendrotoxin, apamin, TEA, glibenclamide and quinidine. We failed to find any protection by the above-listed compounds against apoptosis in serum-deprived VSMC-E1A.[19] These negative results are consistent with the thermodynamic model of cell volume regulation. Indeed, activation of K^+ channels leads to extensive shrinkage in a limited number of cells, such as mammalian erythrocytes, where E_m is much lower than E_K and is close to E_{Cl} values of ~-10 mV. In these cells, a sharp elevation of P_K caused by activation of charibdotoxin-sensitive K_{Ca} elicits shrinkage and full-scale apoptosis indicated by the loss of lipid asymmetry and membrane blebbing.[73] In contrast, in the majority of nucleated cells, E_K and E_{Cl} are close to E_m, and activation of K^+ or Cl^- channels exerts an opposite effect on Cl^- and K^+ fluxes, minimizing their impact on cell volume.

Less is known about the role of anion channels in AVD. Maeno with co-workers[51] reported that in HeLa, U937, PC12 and NG108-15 cells, inhibitors of anion channels such as NPBB and DIDS, completely blocked AVD triggered by two distinct inducers of apoptosis and restored cell survival, whereas other inhibitors of anion channels (anthracene-9-carboxylate) and Na^+-K^+-Cl^- and K^+,Cl^- cotransporters (furosemide) were ineffective. Activation of NPPB-sensitive Cl- channels was observed in rat hepatoma cells undergoing apoptosis in the presence of TNFα.[65] In contrast, Gottlieb and Dosanjh[71] reported that transfection with mutationally-inactivated cystic fibrosis transmembrane regulator anion channels suppresses apoptosis in epithelial cells. Taurine is known to be a major organic osmolyte in the overwhelming number of cell types studied so far.[74] Massive [^{3}H]-taurine release occurs from Jurkat cells after 1 hr of their stimulation with Fas-ligand.[75] Taurine release has also been observed in apoptotic cerebellar granule neurons.[76] The relative contribution of organic osmolyte efflux in AVD remains unknown.

8. CELL SHRINKAGE DOES NOT CONTRIBUTE TO APOPTOSIS IN SERUM-DEPRIVED VSMC

Keeping in mind that apoptosis in VSMC treated with 375 mM mannitol was accompanied by ~40% cell volume decrease (Fig. 5), we undertook additional experiments to characterize the role of modest shrinkage seen in serum-deprived VSMC-E1A before

their detachment. We observed that similar to other cell types studied so far,[2] VSMC-E1A transferred from hyposmotic to isosmotic medium undergo transient shrinkage with maximal amplitude ~2-fold higher than in serum-deprived cells. However, this isosmotic shrinkage does not affect baseline apoptosis and apoptosis triggered by serum deprivation.[19]

Isosmotic shrinkage is caused by loss of intracellular osmolytes and should be abolished under dissipation of their transmembrane gradient. It has been shown that extracellular taurine prevents high glucose-induced apoptosis in endothelial cells.[77] In HeLa,[48] Jurkat[54] and neuronal cells,[63] apoptosis is partially suppressed under dissipation of the K^+ transmembrane gradient. Modest inhibition of caspase-3 activity by high-K^+ medium is also observed in dexamethasone-, thapsigargin- and staurosporine-treated thymocytes[60] as well as in VSMC treated with protonophore.[64] In HeLa cells, addition of 200 mM KCl completely blocks apoptosis triggered by 400 mM sorbitol.[78] However, the same protecttion is observed under equimolar substitution of KCl with NaCl. These results strongly suggest that the antiapoptotic effect of high-salt medium is not related to K^+_o-dependent cell volume modulation and is caused by elevation of ionic strength of the medium.

Table 2. Effect of high-K^+ and organic osmolytes on apoptosis in serum-deprived VSMC-E1A

Medium	Chromatin Fragments %	
	10% serum	*Serum-free*
Low-K^+ medium (control)	7.0±1.2	40.4±3.0
High-K^+ medium$^-$	6.3±1.0	34.3±3.8
DMEM (control)	5.3±1.6	33.4±4.1
DMEM + betaine, myo-inositol, alanine, taurine	5.6±0.9	28.3±2.4
DMEM + mannitol, 100 mM	5.4±0.6	27.7±3.0

Cells were incubated for 6 hr in low- or high-K^+ media or in DMEM in the presence or absence of serum and with organic osmolytes at concentrations of 25 mM each. To control the effect of medium osmolality, mannitol was added at a concentration of 100 mM. Low-K^+ medium contained 121 mM NaCl, 5 mM KCl, 1.8 mM $CaCl_2$, 0.8 mM $MgSO_4$, 5 mM glucose, 12 mM $NaHCO_3$, 4.2 mM HEPES (pH 7.3) and amino acids at concentrations indicated for DMEM. In high-K^+ medium, NaCl was equimolarly substituted by KCl. Means ± S.E. from experiments performed in quadruplicate are given.

Neither extracellular K^+ nor organic osmolytes protect serum-deprived VSMC-E1A from apoptosis (Table 2). These data strongly suggest that the modest cell shrinkage seen in serum-deprived VSMC is a parallel phenomenon rather than an obligatory intermediate of the apoptotic machinery. The role of shrinkage in the apoptosis of immune system and hematopoietic cells possessing higher sensitivity to hyperosmotic medium,[12, 13] the massive loss of intracellular K^+[53, 60] and protection from apoptosis by K^+ channel blockers[66, 72, 79, 80] should be examined further.

9. UNRESOLVED ISSUES AND FUTURE DIRECTIONS

Data obtained in our recent studies and summarized in Figure 6 raise several questions. Which protein(s) interact(s) with the Na^+-K^+-ATPase α-subunit in the presence

of ouabain to transform the death signal triggering oncosis in epithelial cells? Which intermediate(s) of this signaling cascade is missing/suppressed in VSMC and other cells resistant to ouabain? What is the origin of the intracellular Na^+ sensor triggering antiapoptotic signals? Does enhanced production of endogenous ouabain-like factors documented in hypertension[81] and several other chronic diseases[82] contribute to renal damage and vascular remodeling? We will address these questions in forthcoming studies.

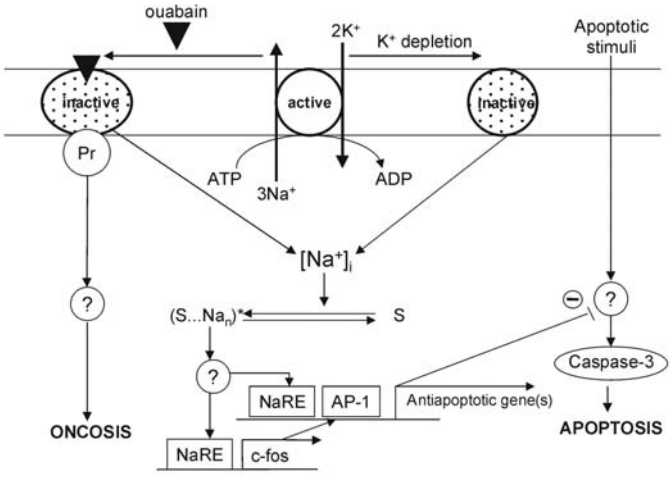

Figure 6. Mechanisms underlying the dual role of Na^+/K^+-ATPase in apoptosis and oncosis. Ouabain and K^+ depletion lead to inactivation of Na^+/K^+-ATPase, fixing its α-subunit in two distinct conformations. In the presence of ouabain, Na^+/K^+-ATPase interacts with an unknown protein (**Pr**) that triggers signal evoking oncosis. In contrast, elevation of $[Na^+]_i$ activates an unidentified intracellular Na^+ sensor (**S**) and expression of ERG and late response antiapoptotic genes including mortalin. **NaRE** – sodium response element within the promoter; **?** – unknown intermediates of intracellular signaling. For more details, see text.

10. ACKNOWLEDGMENTS

This work was supported by grants from the Canadian Institutes of Health Research. The technical assistance of Monique Poirier and the editorial help of Ovid Da Silva are appreciated.

11. REFERENCES

1. E. K. Hoffmann and L. O. Simonsen, Membrane mechanisms in volume and pH regulation in vertebrate cells, *Physiol Rev* **69**, 315-382 (1989).
2. F. Lang, G. L. Busch, M. Ritter, H. Volkl, S. Waldegger, E. Gulbins, and D. Haussinger, Functional significance of cell volume regulatory mechanisms, *Physiol Rev* **78**(1), 247-306 (1998).
3. A. A. Mongin, S. N. Orlov, Mechanisms of cell volume regulation and possible nature of the cell volume sensor, *Pathophysiology* **8**(2), 77-88 (2001).

4. T. G. Cotter, S. V. Lennon, J. G. Glynn, and S. J. Martin, Cell death via apoptosis and its relation to growth, development and differentiation of both tumor and normal cells., *Anticancer Res* **10**(5A), 1153-1160 (1990).
5. E. Duvall, A. H. Wyllie, Death and the cell, *Immunol Today* **7**, 115-119 (1986).
6. D. L. Vaux, A. Strasser, The molecular biology of apoptosis, *Proc Natl Acad Sci USA* **93**, 2239-2244 (1996).
7. R. Wadhwa, O. M. Pereira-Smith, R. R. Reddel, Y. Sugimoto, Y. Mitsui, and S. C. Kaul, Correlation between complementation group for immortality and the cellular distribution of mortalin, *Exp Cell Res* **216**(1), 101-106 (1995).
8. A. H. Wyllie, The 1992 Frank Rose memorial lecture, *Br J Cancer* **67**, 205-208 (1993).
9. J. F. R. Kerr, A. H. Wyllie, and A. R. Currie, Apoptosis: a basic biological phenomenon with wide-ranging implications in tissue kinetics., *Br J Cancer* **26**, 239-257 (1972).
10. L. B. Jordan, D. J. Harrison, Apoptosis: a distinctive form of cell death, in: *Apoptosis in Cardiac Biology*, edited by H. Schunkert, G. A. J. Riegger (Kluwer Academic Publishers, Boston-Dordrecht-London, 1999), pp. 124-135.
11. L. F. Barros, T. Hermosilla, and J. Castro, Necrotic volume increase and the early physiology of necrosis, *Comp Biochem Physiol A Mol Integr Physiol* **130**(3), 401-409 (2001).
12. C. D. Bortner, J. A. Cidlowski, Absence of volume regulatory mechanisms contributes to the rapid activation of apoptosis in thymocytes, *Am J Physiol* **271**, C950-C961 (1996).
13. C. D. Bortner, J. A. Cidlowski, A necessary role for cell shrinkage in apoptosis, *Biochem Pharmacol* **56**, 1549-1559 (1998).
14. Y. Okada, E. Maeno, T. Shimizu, K. Dezaki, J. Wang, and S. Morishima, Receptor-mediated control of regulatory volume decrease (RVD) and apoptotic volume decrease (AVD), *J Physiol* **532**(Pt 1), 3-16 (2001).
15. S. N. Orlov, T. V. Dam, J. Tremblay, and P. Hamet, Apoptosis in vascular smooth muscle cells: role of cell shrinkage, *Biochem Biophys Res Commun* **221**(3), 708-715 (1996).
16. G. I. Evan, A. H. Wyllie, C. S. Gilbert, T. D. Littlewood, H. Land, M. Brooks, C. M. Waters, L. Z. Penn, and D. C. Hancock, Induction of apoptosis in fibroblasts by c-myc protein, *Cell* **69**(1), 119-128 (1992).
17. M. R. Bennett, G. I. Evan, and A. C. Newby, Deregulated expression of the *c-myc* oncogene abolishes inhibition of proliferation of rat vascular smooth muscle cells by serum reduction, interferon-α, heparin, and cyclic nucleotide analogues and induces apoptosis., *Circ Res* **74**, 525-536 (1994).
18. M. R. Bennett, G. I. Evan, and S. M. Schwartz, Apoptosis of rat vascular smooth muscle cells is regulated by p53 dependent and independent pathways., *Circ Res* **77**, 266-273 (1995).
19. S. N. Orlov, D. Pchejetski, S. Taurin, N. Thorin-Trescases, G. V. Maximov, A. V. Pshezhetsky, A. B. Rubin, and P. Hamet, Apoptosis in serum-deprived vascular smooth muscle cells: evidence for cell volume-independent mechanism, *Apoptosis* **9**, 55-56 (2004).
20. S. N. Orlov, N. Thorin-Trescases, T. V. Dam, M. A. Fortuno, N. O. Dulin, J. Tremblay, and P. Hamet, Activation of cAMP signaling transiently inhibits apoptosis in vascular smooth cells in a site upstream of caspase-3, *Cell Death Differ* **6**(7), 661-672 (1999).
21. S. N. Orlov, N. Thorin-Trescases, S. V. Kotelevtsev, J. Tremblay, and P. Hamet, Inversion of the intracellular Na+/K+ ratio blocks apoptosis in vascular smooth muscle at a site upstream of caspase-3, *J Biol Chem* **274**(23), 16545-16552 (1999).
22. M. R. Bennett, K. MacDonald, S.-W. Chan, J. P. Luzio, R. Simari, and P. Weissberg, Cell surface trafficking of Fas: a rapid mechanism of p53-mediated apoptosis, *Science* **282**, 290-293 (1998).
23. S. N. Orlov, D. Pchejetski, S. Der Sarkissian, V. A. Adarichev, S. Taurin, A. V. Pshezhetsky, J. Tremblay, G. V. Maximov, D. deBlois, M. R. Bennett, and P. Hamet, [^{3}H]Thymidine labelling of DNA triggers apoptosis potentiated by E1A-adenoviral protein, *Apoptosis* **8**, 199-208 (2003).
24. N. K. Isaev, E. V. Stelmashook, A. Halle, C. Harms, M. Lautenschlager, M. Weih, U. Dirnagl, I. V. Victorov, and D. B. Zorov, Inhibition of Na(+),K(+)-ATPase activity in cultured rat cerebellar granule cells prevents the onset of apoptosis induced by low potassium, *Neurosci Lett* **283**(1), 41-44 (2000).
25. X. Zhou, G. Jiang, A. Zhao, T. Bondeva, P. Hirszel, and T. Balla, Inhibition of Na,K-ATPase activates PI3 kinase and inhibits apoptosis in LLC-PK1 cells, *Biochem Biophys Res Commun* **285**(1), 46-51 (2001).
26. S. N. Orlov, S. Taurin, N. Thorin-Trescases, N. O. Dulin, J. Tremblay, and P. Hamet, Inversion of the intracellular Na^+/K^+ ratio blocks apoptosis in vascular smooth muscle cells by induction of RNA synthesis, *Hypertension* **35**(5), 1062-1068 (2000).
27. S. N. Orlov, S. Taurin, J. Tremblay, and P. Hamet, Inhibition of Na^+-K^+ pump affects nucleic acid synthesis and smooth muscle cell proliferation via elevation of the $[Na^+]_i/[K^+]_i$ ratio: possible implication in vascular remodelling, *J Hypertens* **19**, 1559-1565 (2001).

28. S. Taurin, V. Seyrantepe, S. N. Orlov, T. L. Tremblay, P. Thibault, M. R. Bennett, P. Hamet, and A. V. Pshezhetsky, Proteome analysis and functional expression identify mortalin as an antiapoptotic gene induced by elevation of $[Na^+]_i/[K^+]_i$ ratio in cultured vascular smooth muscle cells, *Circ Res* **91**(10), 915-922 (2002).
29. S. Takano, R. Wadhwa, Y. Yoshii, T. Nose, S. C. Kaul, and Y. Mitsui, Elevated level of mortalin expression in human brain tumors, *Exp Cell Res* **237**(1), 38-45 (1997).
30. R. Wadhwa, S. Takano, Y. Mitsui, and S. C. Kaul, NIH 3T3 cells malignantly transformed by mot-2 show inactivation and cytoplasmic sequestration of the p53 protein, *Cell Res* **9**(4), 261-269 (1999).
31. R. Wadhwa, S. Takano, M. Robert, A. Yoshida, H. Nomura, R. R. Reddel, Y. Mitsui, and S. C. Kaul, Inactivation of tumor suppressor p53 by mot-2, a hsp70 family member, *J Biol Chem* **273**(45), 29586-29591 (1998).
32. S. Taurin, P. Hamet, and S. N. Orlov, Na/K pump and intracellular monovalent cations: novel mechanism of excitation-transcription coupling involved in inhibition of apoptosis, *Mol Biol* **37**(3), 371-381 (2003).
33. Z. Xie, A. Askari, Na^+/K^+-ATPase as a signal transducer, *Eur J Biochem* **269**, 2434-2439 (2003).
34. Y. Nakagawa, E. F. Petricoin, H. Akai, P. M. Grimley, B. Rupp, and A. C. Larner, Interferon-alpha-induced gene expression: evidence for a selective effect on activation of the ISGF3 transcription complex, *Virology* **190**, 210-220 (1992).
35. Y. Nakagawa, V. Rivera, and A. C. Larner, A role for the Na/K-ATPase in the control of human c-fos and c-jun transcription, *J Biol Chem* **267**(13), 8785-8788 (1992).
36. S. Numazawa, N. Inoue, H. Nakura, T. Sugiyama, E. Fujino, M. Shinoki, T. Yoshida, and Y. Kuroiwa, A cardiotonic steroid bufalin-induced differentiation of THP-1 cells. Involvement of Na^+ ,K(+)-ATPase inhibition in the early changes in proto-oncogene expression, *Biochem Pharmacol* **52**(2), 321-329 (1996).
37. M. Joannidis, L. G. Cantley, K. Spokes, A. K. Stuart-Tilley, S. L. Alper, and F. H. Epstein, Modulation of c-fos and egr-1 expression in the isolated perfused kidney by agents that alter tubular work, *Kidney Int* **52**(1), 130-139 (1997).
38. M. Peng, L. Huang, Z. Xie, W. H. Huang, and A. Askari, Partial inhibition of Na+/K+-ATPase by ouabain induces the Ca2+- dependent expressions of early-response genes in cardiac myocytes, *J Biol Chem* **271**(17), 10372-10378 (1996).
39. Z. Xie, P. Kometiani, J. Liu, J. I. Shapiro, and A. Askari, Intracellular reactive oxygen species mediate the linkage of Na^+/K^+-ATPase to hypertrophy and its marker genes in cardiac myocytes, *J Biol Chem* **274**, 19323-19328 (1999).
40. S. Taurin, N. O. Dulin, D. Pchejetski, R. Grygorczyk, J. Tremblay, P. Hamet, and S. N. Orlov, c-Fos expression in ouabain-treated vascular smooth muscle cells from rat aorta: evidence for an intracellular-sodium-mediated, calcium-independent mechanism, *J Physiol* **543**(Pt 3), 835-847 (2002).
41. D. Pchejetski, S. Taurin, S. Der Sarkissian, O. D. Lopina, A. V. Pshezhetsky, J. Tremblay, D. deBlois, P. Hamet, and S. N. Orlov, Inhibition of Na^+-K^+-ATPase by ouabain triggers epithelial cell death independently of inversion of the $[Na^+]_i/[K^+]_i$ ratio, *Biochem Biophys Res Commun* **301**, 735-744 (2003).
42. A. D. C. Macknight, A. Leaf, Regulation of cell volume, *Physiol Rev* **57**, 510-573 (1977).
43. T. Akera, Y.-C. Ng, I. S. Shien, E. Bero, T. M. Brody, and W. E. Braselton, Effects of K^+ on the interaction between cardiac glycosides and Na,K-ATPase, *Eur J Pharmacol* **111**, 147-157 (1985).
44. J. B. Lingrel, M. L. Croyle, and J. M. Argüello, Ligand binding sites of Na,K-ATPase, *Acta Physiol Scand* **163**(Suppl. 643), 69-77 (1998).
45. E. T. Wallick, A. Schwartz, Interaction of cardiac glycosides with Na^+-K^+-ATPase, *Methods in Enzymology* **156**, 201-213 (1988).
46. A. M. Malek, G. G. Goss, L. Jiang, S. Izumo, and S. L. Alper, Mannitol at clinical concentrations activates multiple signaling pathways and induces apoptosis in endothelial cells, *Stroke* **29**(12), 2631-2640 (1998).
47. L. Michea, D. R. Ferguson, E. M. Peters, P. M. Andrews, M. R. Kirby, and M. B. Burg, Cell cycle delay and apoptosis are induced by high salt and urea in renal medullary cells, *Am J Physiol Renal Physiol* **278**(2), F209-F218 (2000).
48. A. J. Bilney, A. W. Murray, Pro- and anti-apoptotic effects of K^+ in HeLa cells, *FEBS Lett* **424**(3), 221-224 (1998).
49. C. C. Matthew, E. L. Feldman, Insulin-like growth factor I rescues SH-SY5Y human neuroblastoma cell from hyperosmotic induced programmed cell death, *J Cell Physiol* **166**, 323-331 (1996).
50. S. Wesselborg, D. Kaberlitz, Activation-driven death of human T cell clones: time course kinetics of the induction of cell shrinkage, DNA fragmentation, and cell death, *Cell Immunol* **148**(1), 234-241 (1993).
51. E. Maeno, Y. Ishizaki, T. Kanaseki, A. Hazama, and Y. Okada, Normotonic cell shrinkage because of disordered volume regulation is an early prerequisite to apoptosis, *Proc Natl Acad Sci USA* **97**, 9487-9492 (2000).
52. H. Ohyama, T. Yamada, and I. Watanabe, Cell volume reduction associated with interphase death in rat thymocytes, *Radiat Res* **85**, 333-339 (1981).

53. C. D. Bortner, J. A. Cidlowski, Caspase independent/dependent regulation of K+, cell shrinkage and mitochondrial membrane potential during lymphocyte apoptosis, *J Biol Chem* **274**, 21953-21962 (1999).
54. C. D. Bortner, F. M. Hughes, and J. A. Cidlowski, A primary role for K^+ and Na^+ efflux in activation of apoptosis, *J Biol Chem* **272**, 32436-32442 (1997).
55. C. S. I. Nobel, J. K. Aronson, D. J. van den Dobbelsteen, and A. F. G. Slater, Inhibition of Na^+/K^+-ATPase may be one mechanism contributing to potassium efflux and cell shrinkage in CD995-induced apoptosis, *Apoptosis* **5**(2), 153-163 (2000).
56. S. N. Orlov, J. Tremblay, and P. Hamet, Cell volume in vascular smooth muscle cells is regulated by bumetanide-sensitive ion transport., *Am J Physiol* **270**, C1388-C1397 (1996).
57. R. S. Benson, S. Heer, C. Dive, and A. J. Watson, Characterization of cell volume loss in CEM-C7A cells during dexamethasone-induced apoptosis, *Am J Physiol* **270**, C1190-C1203 (1996).
58. A. Y. Xiao, L. Wei, S. Xia, S. Rothman, and S. P. Yu, Ionic mechanism of ouabain-induced concurrent apoptosis and necrosis in individual cultured cortical neurones, *J Neurosci* **22**, 1350-1362 (2002).
59. M. Gomez-Angelats, C. D. Bortner, and J. A. Cidlowski, Protein kinase C (PKC) inhibits Fas receptor-induced apoptosis through modulation of the loss of K^+ and cell shrinkage, *J Biol Chem* **275**, 19609-19619 (2000).
60. F. M. Hughes, C. D. Bortner, G. D. Purdy, and J. A. Cidlowski, Intracellular K^+ suppresses the activation of apoptosis in lymphocytes, *J Biol Chem* **272**, 30567-30576 (1997).
61. G. Barbiero, F. Duranti, G. Bonelli, J. S. Amenta, and F. M. Baccino, Intracellular ionic variations in the apoptotic death of cells by inhibitors of cell cycle progression, *Exp Cell Res* **217**, 410-418 (1995).
62. A. Minta, R. Y. Tsien, Fluorescent indicators for cytosolic sodium, *J Biol Chem* **264**, 19449-19457 (1989).
63. L. V. Colom, M. E. Diaz, D. R. Beers, A. Neely, W. J. Xie, and S. H. Appel, Role of potassium in amyloid-induced cell death, *J Neurochem* **70**, 1925-1934 (1998).
64. S. Krick, O. Platoshyn, M. Sweeney, H. Kim, and J. X. J. Yuan, Activation of K^+ channels induces apoptosis in vascular smooth muscle cells, *Am J Physiol* **280**, C970-C979 (2001).
65. H. H. Nietsch, M. W. Roe, J. F. Fiekers, A. L. Moore, and S. D. Lidofsky, Activation of potassium and chloride channels by tumor necrosis factor α, *J Biol Chem* **275**, 20556-20561 (2000).
66. L. Wang, D. Xu, W. Dai, and L. Lu, An ultraviolet-activated K+ channel mediates apoptosis of myeloblastic leukemia cells, *J Biol Chem* **274**, 3678-3685 (1999).
67. S. P. Yu, C. H. Yeh, S. L. Sensi, B. J. Gwag, L. M. Canzoniero, Z. S. Farhangrazi, H. S. Ying, M. Tian, L. L. Dugan, and D. W. Choi, Mediation of neuronal apoptosis by enhancement of outward potassium current, *Science* **278**(5335), 114-117 (1997).
68. M. J. Mann, V. J. Dzau, Therapeutic applications of transcription factor decoy oligonucleotides, *J Clin Invest* **106**, 1071-1075 (2000).
69. I. Szabo, E. Gulbins, H. Apfel, X. Zhang, P. Barth, A. E. Busch, K. Schlottmann, O. Pongs, and F. Lang, Tyrosine phosphorylation-dependent suppression of a voltage-gated K+ channel in T lymphocytes upon Fas stimulation, *J Biol Chem* **271**, 20465-20469 (1996).
70. E. Gulbins, I. Szabo, K. Baltzer, and F. Lang, Ceramide-induced inhibition of T-lymphocyte voltage gated potassium channel is mediated by tyrosine kinases, *Proc Natl Acad Sci USA* **94**, 7661-7666 (1997).
71. R. A. Gottlieb, A. Dosanjih, Mutant cystic fibrosis transmembrane conductance regulator inhibits acidification and apoptosis in C127 cells: possible relevance to cystic fibrosis, *Proc Natl Acad Sci USA* **93**, 3587-3591 (2001).
72. I. Szabo, A. Lepple-Wienhues, K. N. Kaba, M. Zoratti, E. Gulbins, and F. Lang, Tyrosine kinase-dependent activation of a chloride channel in CD95-induced apoptosis in T-lymphocytes, *Proc Natl Acad Sci USA* **95**, 6169-6174 (1998).
73. K. S. Lang, C. Duranton, H. Poehlmann, S. Myssina, C. Bauer, F. Lang, T. Wieder, and S. M. Huber, Cation channels trigger apoptotic death of erythrocytes, *Cell Death Differ* **10**(2), 249-256 (2003).
74. H. Pasantes-Morales, R. M. del Rio, Taurine and mechanisms of cell volume regulation, in: *Taurine: Functional Neurochemistry, Physiology and Cardiology*, edited by R. Cohen (Wiley-Liss Inc., New York, 1990), pp. 317-328.
75. F. Lang, J. Madlung, A. C. Uhlemann, T. Risler, and E. Gulbins, Cellular taurine release triggered by stimulation of the FAS (CD95) receptor in Jurkat lymphocytes, *Pflugers Arch* **436**(3), 377-383 (1998).
76. J. Moran, X. Hernandez-Pech, H. Merchant-Larios, and H. Pasantes-Morales, Release of taurine in apoptotic cerebellar granule neurones in culture, *Pflugers Arch* **439**(3), 271-277 (2000).
77. Q. D. Wu, J. H. Wang, F. Fennesy, H. P. Redmond, and D. Bouchier-Hayes, Taurine prevents high-glucose-induced human vascular endothelial cell apoptosis, *Am J Physiol* **277**, C1229-C1238 (1999).
78. J. B. Smith, M. B. Wade, N. S. Fineberg, and M. H. Weinberger, Influence of race, sex, and blood pressure on erythrocyte sodium transport in humans, *Hypertension* **12** (3), 251-258 (1988).

79. F. Beauvais, L. Michel, and L. Dubertret, Human eosinophils in culture undergo a striking and rapid shrinkage during apoptosis, *J Leukoc Biol* **57**, 851-855 (1995).
80. B. Dallaporta, P. Marchetti, M. A. de Pablo, C. Maisse, H. T. Duc, D. Métivier, N. Zamzani, M. Geuskens, and G. Kroemer, Plasma membrane potential in thymocyte apoptosis, *J Immunol* **162**, 6534-6542 (1999).
81. P. A. Doris, Abnormalities of sodium pump function in hypertension and the role of endogenous cardiotonic steroids, *Cell Mol Biol* **47**(2), 391-401 (2001).
82. E. Berendes, P. Cullen, H. van Aken, W. Zidek, M. Erren, M. Hubschen, T. Weber, S. Wirtz, M. Tepel, and M. Walter, Endogenous glycosides in critically ill patients, *Crit Care Med* **31**, 1331-1337 (2003).

22

POLYCYSTIN-2 AS A SIGNAL TRANSDUCER

H. F. Cantiello, N. Montalbetti, G. A. Timpanaro,
and S. González-Perrett*

1. INTRODUCTION

The human syncytiotrophoblast (hST) is a differentiated syncytial epithelium that covers the villous tree of the maternal-facing surface of the human placenta.[1-3] The hST is covered by apical microvilli which are bathed by the maternal blood. This brush border epithelial membrane displays a number of transport properties including the ability to selectively transfer ions.[4] Ion channels in hST allow the permeation of cations such as K^{+}[5-7] and Ca^{2+},[6] and anions such as Cl^{-}.[8, 9] We recently identified the Ca^{2+}-permeable, non-selective cation channel of hST as being a functional polycystin-2, the gene product of one of the ADPKD-causing genes, *PKD2*.[6] Little is known, however, about the mechanisms that control and regulate ion channel activity, in particular polycystin-2, in this syncytial epithelium. The chorionic villous tree presents an intricate structure which is continuously growing by branching during gestation.[3] This process requires a dynamic cytoskeleton. The hST apical membrane is supported by an intricate network of cytoskeletal structures. The apical cytoskeleton in hST encompasses a supramolecular structure known as the "syncytioskeletal layer" of a potentially supporting nature.[10] Major cytoskeletal components[11] including microtubules,[12, 13] intermediate filaments,[14-16] and actin-based networks[17, 18] have been identified which may have distinct and interactive roles in the developing placenta. Apical hST microvilli have highly organized actin filaments,[10] and apical hST membrane vesicles retain prominent microfilamental structures associated with the presence of structured actin.[12] Thus, the microvillous actin cytoskele-

* H.F. Cantiello, Laboratorio de Canales Iónicos, Departamento de Fisicoquímica y Química Analítica, Facultad de Farmacia y Bioquímica, Buenos Aires, Argentina, 1113 and Renal Unit, Department of Medicine, Massachusetts General Hospital and Harvard Medical School, Charlestown, MA 02129. N. Montalbetti and G.A. Timpanaro, Laboratorio de Canales Iónicos, Departamento de Fisicoquímica y Química Analítica, Facultad de Farmacia y Bioquímica, Buenos Aires, Argentina, 1113. S. González-Perrett, Laboratorio de Canales Iónicos, Departamento de Fisicoquímica y Química Analítica, Facultad de Farmacia y Bioquímica, Buenos Aires, Argentina, 1113 and Departamento de Fisiología, Facultad de Medicina, Buenos Aires, Argentina, 1121.

ton may play important, yet unknown, regulatory functions in the hST. The apical hST, for example, contains the actin-bundling protein α-actinin[19] which is excluded from the basal membrane cytoskeleton.[20] The actin cytoskeleton anchoring protein EBP50 co-localizes with ezrin and actin only in the apical microvilli of epithelial ST[21, 22] and the cytoskeletally-related annexins are developmentally expressed in the placenta.[23] Both α-actinin[24] and EBP50-related proteins[25] regulate ion channels. Thus, distinct organizational aspects of actin networks may be functional effectors of ion channel regulation in the apical aspect of hST. This is supported by the fact that actin filamental dynamics is an important regulator of ion channel function in a variety of tissues and cell types.[26, 27] A number of epithelial channels are controlled by the actin cytoskeleton including Na^+-[28, 29] K^+-[30] and Cl^--[31, 32] permeable channels. Thus, the possibility exists for cytoskeletal structures to also enable channel regulation in the human placenta.

Here, we report new findings and discuss the implications of cytoskeletal and osmotic/hydrostatic regulation of the Ca^{2+}-permeable, non-selective cation channels in the hST. This channel activity represents the functional expression of polycystin-2 (PC2), the gene product of *PKD2* in hST.[6] Addition of actin filament disrupting agents such as cytochalasin D activates channel function which, interestingly, was mimicked by addition of the actin bundling protein α-actinin and physical changes mediated by hydrostatic gradients. These data suggest that channel regulation in hST is effected by a functional interface linking changes in actin filamental dynamics and changes in membrane structure. This functional interface may regulate the hydroelectrolytic homeostasis in term human placenta.

2. EXPERIMENTAL

Human placenta syncytiotrophoblast apical membrane vesicles were reconstituted in a lipid bilayer system as recently reported.[6] Briefly, term human placenta were obtained within 20 min of normal vaginal delivery and immediately processed. Villous tissue was fragmented, washed with unbuffered NaCl saline (150 mM), and minced into small pieces. The fragmented tissue was stirred in a solution containing 10 mM HEPES, pH 7.4, and 0.1 mM EGTA. The solution also contained 0.2 mM PMSF, 1 μg pepstatin A, 1 μg/ml aprotinin, 1-5 μg/ml leupeptin, 1-5 μg p-aminobenzamidine, and 250 mM sucrose. The tissue preparation was filtered and centrifuged for 10 min at 3,100 rpm. The supernatant was again centrifuged for 10 min at 11,000 rpm and for 90 min at 14,000 rpm, in an ultracentrifuge. The final pellet was resuspended in a buffer solution containing HEPES-KOH, 10 mM, pH 7.4, sucrose, 250 mM, and KCl, 20 mM. The membrane suspension was aliquoted and stored at -20°C until the time of the experiment. The apical membrane enrichment (~26:1 initial homogenate) and total protein were determined as recently described.[6]

Lipid bilayers were formed with a mixture of synthetic phospholipids (Avanti Polar Lipids, Birmingham, AL) in n-decane as reported.[6] The lipid mixture was made of 1-palmitoyl-2-oleoyl phosphatydil-choline and phosphatydil-ethanolamine in a 7:3 ratio. The lipid solution (~20-25 mg/ml) was used to form lipid membranes in a polystyrene cuvette (CP13-150) of a bilayer chamber (model BCH-13, Warner Instruments Corp.). Both sides of the lipid bilayer were bathed with a solution containing MOPS-KOH, 10 mM, and MES-KOH, 10 mM, pH 7.40, and 10-15 μM Ca^{2+}. The final K^+ concentration in

the trans solution was approximately 15 mM and 150 mM the cis compartment. Electrical signals were obtained with a PC501A patch-clamp amplifier (Warner Instruments, Hamden, CT) with a 10 Gohm feedback resistor. Signals were low-pass filtered at 700 Hz (-3 dB) with an eight pole, Bessel type filter (Frequency Devices, Haverhill, MA). Signals were displayed on an oscilloscope and processed with pCLAMP Version 5.5.1 (Axon Instruments, Foster City, CA). Sigmaplot Version 2.0 (Jandel Scientific, Corte Madera, CA) was used for statistical analysis and graphic design.

2.1 Cytoskeleton-Related Compounds

Cytochalasin D (CD, Sigma) was dissolved in DMSO and used at concentrations ranging from 1 to 50 μM. Actin was obtained from original vendors (Sigma-Aldrich, Milwaukee WI). G-actin (monomeric, 5-10 mg/ml) and stored at -80°C in a depolymerizing buffer containing, in mM: Tris-HCl, 2.0; ATP, 0.5; $CaCl_2$, 0.2; and -mercaptoethanol, 0.5; pH 8.0. The actin bundling protein α-actinin[33, 34] was obtained from Sigma (2.5 mg/ml) and used at a final concentration of 25 μg/ml.

3. RESULTS AND DISCUSSION

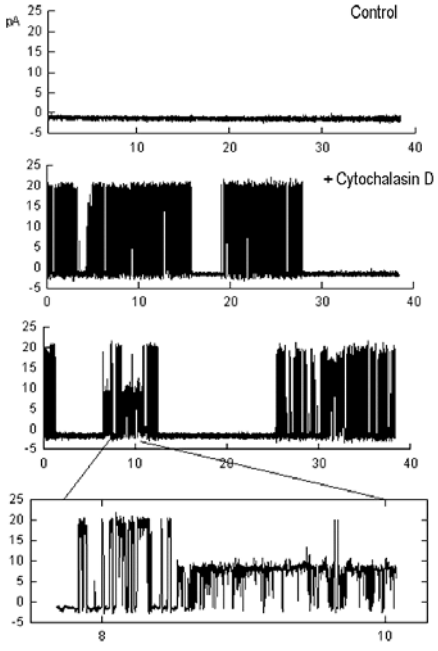

Figure 1. Effect of cytochalasin D on hST cation channels. Addition of cytochalasin D (5 μg/ml) to the *cis* (cytoplasmic) side of the reconstituted hST apical vesicles induced a transient channel activation. Membranes were reconstituted in the presence of a KCl chemical gradient. Holding potential was 60 mV. Time is indicated in seconds. Data are representative of 17 experiments.

3.1 Effect of Cytochalasin D on Channel Activity in hST

To assess a regulatory role of the actin cytoskeleton in channel function in hST, apical membranes were reconstituted in a lipid bilayer system. Experiments were conducted in the presence of a K^+ chemical gradient, with 150 mM in the *cis* chamber and 15 mM KCl in the *trans* chamber, respectively. Experiments where no or little spontaneous activity was originally observed at the beginning of the experiment were chosen. Addition of cytochalasin D (CD, 5 μg/ml) to the *cis* side of the reconstitution chamber induced a transient activation of K^+-permeable ion currents (Figure 1) which peaked at approximately seven min after addition of the drug.

The CD-activated channels (Figure 1) were highly cation-selective, had a mean single channel conductance of 135 pS, presented substates, and were further characterized as those previously observed as mediated by polycystin-2.[6] The pharmacological profile, including inhibition by La^{3+} and 50 μM amiloride was also similar to that of the spontaneously active channels (data not shown). To further test the role of endogenous actin networks on cation channel activity, hST plasma membranes were also incubated for 1-3 days at 4 ^oC in the presence of cytochalasin D (5 μg/ml), to completely collapse the actin networks. Under these conditions channel activity was spontaneously absent but was re-activated by addition of actin to the *cis* chamber (1 mg/ml, data not shown).

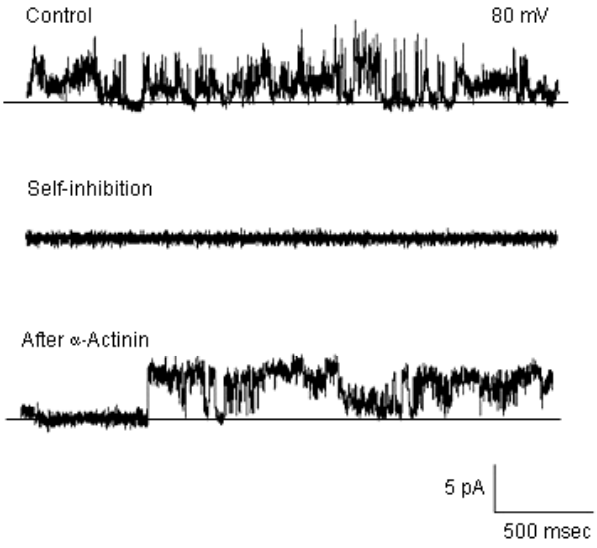

Figure 2. Effect of α-actinin on hST cation channel activity. Representative single-channel tracings of hST apical membranes in asymmetrical KCl. Addition of the F-actin bundling protein α-actinin to the *cis* chamber induced cation channel activity. Data suggest that cytoskeletal dynamics plays a regulatory role in channel function in human placenta. Data are representative of 7 experiments.

3.2 Effect of α-actinin on Cation Channels in hST

To assess whether the stimulatory effect of CD on K^+ channel activity in hST was affected by changes in cortical actin network organization in the proximity of the channels, the effect of the actin-bundling protein α-actinin was also tested. This actin-binding protein arranges tightly packed actin filaments.[35]

Alpha-actinin also shares functionally similar domains with a number of other actin binding proteins including the actin-severing protein gelsolin[36] and the actin-anchoring protein dystrophin,[37] entailing a high plasticity in cytoskeletal re-modeling. Interestingly, α-actinin is preferentially localized to the apical domain of the hST.[20] Addition of α-actinin (25 μg/ml) to the *cis* chamber induced and/or increased hST cation channel activety previously inactivated by voltage (Figure 2), suggesting cytoskeletal configurations do control basal channel activity in hST. Interestingly, the actin-binding domains of α-actinin also share homology with the actin-crosslinking proteins filamins[35] which are known to regulate epithelial channel function.[38] Thus, the encompassed evidence suggests that changes in gel configuration of the actin networks may be an important contributor to channel regulation in hST.

The above data forward a regulatory role of endogenous actin networks and likely actin associated proteins in the control of K^+ channel activity in hST. However, the spontaneous and cytoskeletally-induced channel activity observed herein occurs in the presence of an osmotic gradient (ΔΠ) constantly imposed by the KCl chemical gradient to the plasma membrane.[6, 39] This indicates that changes in the properties of the membrane, including its capacitance,[40, 41] tonically control channel activity in the hST.

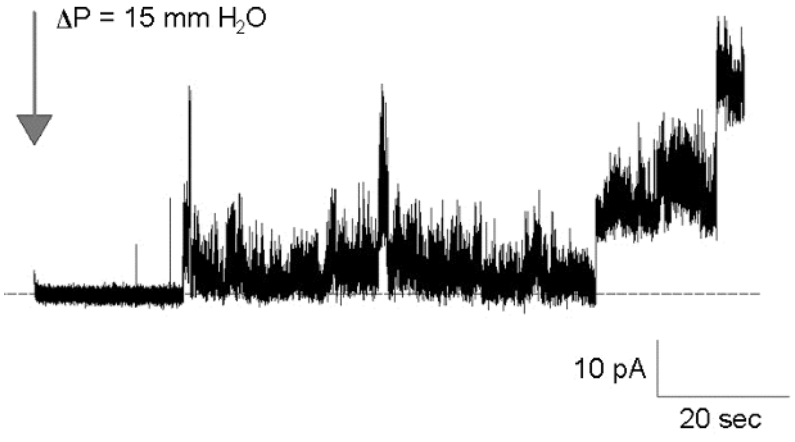

Figure 3. Effect of hydrostatic pressure on hST cation channel activity. Cation channel activity was first observed and allowed to spontaneously inactivate (data not shown). Hydrostatic pressure was imposed by reducing volume in *cis* and addition of isosmotic saline in the *trans* chambers, respectively. Data are representative of 3 experiments.

3.3 Effect of Hydrostatic Pressure on hST Channel Regulation

To assess a regulatory role of the physical membrane parameters on the cation channel function of hST, osmotically challenged ($\Delta\Pi$) membranes were subjected to a compensatory hydrostatic gradient (ΔP) which normally counters osmotic interactions.[40] A decrease in *cis* volume and increase in volume to the *trans* chamber (total ΔP = 15 mm water, Figure 3) was sufficient to elicit a stimulatory response on cation channel function in the hST reconstituted membrane. Thus, physical challenge indeed exerts a functional control on hST channel activity. Whether this phenomenon is directly linked to elastic changes in the reconstituted membrane, as opposed to cytoskeletal reorganization observed above, is currently under investigation. Recent studies from our laboratory determined that the K^+ channel activity is largely mediated by the gene product of the ADPKD causing gene *PKD2*, the Trp-type channel polycystin-2.[6] Little evidence is yet available for cytoskeletal interactions with PC2. However, recent studies suggest that various cytoskeletal proteins including Hax-1, a cytoskeletal protein that interacts with the F-actin-binding protein cortactin,[42] troponin-I[43] and tropomyosin-1[44] all bind to PC2. Interestingly, PC2 has been co-localized with tubulin, in cilia of renal epithelial cells.[45] This location in a sensory organelle suggests an important role by transducing environmental signals such as volume flow to the stimulation of Ca^{2+} signals.[46] Thus, PC2 channels may be part of a novel mechano-transduction signaling mechanism regulated or at least interacting with cytoskeletal structures. Conversely, physical forces imposed onto the membrane may also affect the osmotic behavior of lipid bilayers and cell membranes.[47] The elastic pressure from bilayer osmotic deformation should be compensated by both inter-bilayer pressure and the difference in hydrostatic pressure across the membrane. In turn, hydrostatic pressure differences which counteract the osmotic stress produce a mechanical imbalance on the membrane which is compensated by changes in the surface pressure of the membrane. This surface pressure modifies the membrane surface area,[48, 49] a phenomenon manifested by changes in membrane capacitance.[41] Thus, our data support two not mutually exclusive and likely cooperative, regulatory mechanisms in hST channel regulation. Namely, elastic compliance of the membrane and cytoskeletal reorganization may act in concert to gate channel function.

The human syncytiotrophoblast is a highly dynamic structure whose function depends on the growth and branching of the invading trophoblast into the uterine mucosa.[10, 50] The membrane-cytoskeleton interface may play a critical role in cation-dependent signaling pathway(s) associated with placental function (Figure 4), in particular the control of osmo-electrolytic homeostasis in placental metabolism. Changes in hydrostatic pressure may be important contributors to water and solute transport in the placental environment.[51, 52] Further, regulatory mechanisms linking the cytoskeleton to cation transport may also be essential for fetal development, as water and solute transfer across the human placenta are directly and positively correlated to fetal growth.[4] The actin bundling protein α-actinin, for example, is released from the actin cytoskeleton in hST in a Ca^{2+}-dependent fashion.[20] This is particularly interesting in the context of the present study as α-actinin plays a role in the regulation of epithelial cation channels[24] and Ca^{2+} is transported by the channel complexes described in this study.[6]

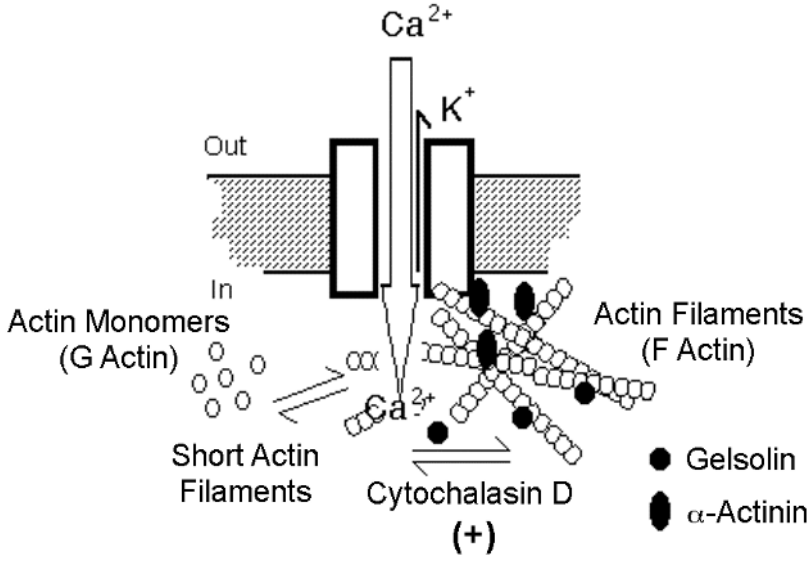

Figure 4. Schematics of actin cytoskeleton-pressure regulation of cation channels in hST. In term human placenta, the hST apical membrane contains an organized actin cytoskeleton comprised of actin and actin-binding proteins. Actin de-polymerization by toxins such as cytochalasin D, or changes in cytoskeletal dynamics elicited by either addition of actin bundling proteins such as α-actinin, or changes in physical parameters as changes in hydrostatic pressure activate channel function.

4. CONCLUSION

In summary, the present study demonstrates that dynamic changes in the endogenous actin cytoskeleton regulate K^+-permeable cation channels in term hST. This effect was mimicked by either early cytoskeletal disruption with such drugs as CD or addition of the actin-bundling protein α-actinin. The encompassed data suggest a regulatory role of actin filaments on channel function by either direct interaction with actin and/or the control of tightly associated proteins such that changes in the actin conformations may modify channel function. Our data also provide the first demonstration for environmental signals such as changes in hydrostatic pressure playing an important role in cation transport in hST. Our studies suggest that hST channel regulation may be controlled by cortical actin cytoskeletal structures and physical changes in membrane properties. At present, little is known about the potential regulatory role of cytoskeletal structures in PC2 function. Nevertheless, actin-associated proteins including tropomyosin-1[44] and troponin-I[43] have recently been reported to bind to polycystin-2 and thus, may have a regulatory role in channel function which remains to be determined. Interestingly, recent evidence also indicates that the PC2-related PCL channel which shares a number of functional properties with PC2 is controlled by troponin-I.[53] Further studies will be required to determine whether osmo-electrolytic changes themselves may convey changes in membrane properties expected to play a role in placental metabolism. Both direct actin interactions and cytoskeletal coupling through scaffolding proteins may control channel activity in hST. Conversely, other channel functions may also be targeted by the actin cytoskeleton.

Cl^- channels, for example, are regulated by cytoskeletal structures.[32, 54] Thus, it is possible and rather likely that the actin cytoskeleton may help concert various channel functions in this syncytial epithelium.

5. REFERENCES

1. A.C. Enders, Formation of syncitium from cytotrophoblast in the human placenta, *Obstet Gynecol.* **25**, 378-386 (1965).
2. P. Truman, J.S. Wakefield, J.S. & H.C. Ford, Microvilli of the human term placenta, Isolation and subfractionation by centrifugation in sucrose density gradients. *Biochem. J.* **196**, 121-132 (1981).
3. R. Demir, G. Kosanke, G. Kohnen, S. Kertschanska, P. Kaufmann, Classification of human placental stem villi: review of structural and functional aspects, *Microsc. Res. Tech.* **38**, 29-41 (1997).
4. J. Stulc, Placental transfer of inorganic ions and water, *Physiol. Rev.* **77**, 805-836 (1997).
5. C. Grosman, I.L. Reisin, Single-channel characterization of a nonselective cation channel from human placental microvillus membranes. Large conductance, multiplicity of conductance states, and inhibition by lanthanides, *J. Membr. Biol.* **174**, 59-70 (2000).
6. S. González-Perrett, K. Kim, C. Ibarra, A.E. Damiano, E. Zotta, M. Batelli, P.C. Harris, I.L. Reisin, M.A. Arnaout & H.F. Cantiello, Polycystin-2, the protein mutated in autosomal dominant polycystic kidney disease (ADPKD), is a Ca^{2+}-permeable nonselective cation channel, *Proc. Natl. Acad. Sci. USA* **98**, 1182-1187 (2001).
7. P. Llanos, M. Henriquez, & G. Riquelme, A low conductance, non-selective cation channel from human placenta, *Placenta* **23**, 184-191 (2002).
8. M. Berryman, & A. Bretscher, Identification of a novel member of the chloride intracellular channel gene family (CLIC5) that associates with the actin cytoskeleton of placental microvilli, *Mol. Biol. Cell.* **11**, 1509-1521 (2000).
9. L. Bernucci, F. Umana, P. Llanos, & G. Riquelme, Large chloride channel from pre-eclamptic human placenta, *Placenta* **24**, 895-903. (2003).
10. C.D. Ockleford, J. Wakely, & R.A. Badley, Morphogenesis of human placental chorionic villi: cytoskeletal, syncytioskeletal and extracellular matrix proteins, *Proc. R. Soc. Lond. B Biol. Sci.* **212**, 305-316 (1981).
11. P. Truman, & H.C. Ford, Proteins of human placental microvilli: I. Cytoskeletal proteins, *Placenta* **7**, 95-110 (1986).
12. C.H. Smith, D.M. Nelson, B.F. King, T.M. Donohue, S. Ruzycki, & L.K. Kelley, Characterization of a microvillous membrane preparation from human placental syncytiotrophoblast: a morphologic, biochemical, and physiologic study, *Am. J. Obstet. Gynecol.* **128**, 190-196 (1977).
13. G.C. Douglas, & B.F. King, Colchicine inhibits human trophoblast differentiation *in vitro, Placenta* **14**, 187-201 (1993).
14. R.K. Clark, & I. Damjanov, Intermediate filaments of human trophoblast and choriocarcinoma cell lines, *Virchows Arch. A. Pathol. Anat. Histopathol.* **407**, 203-208 (1985).
15. M. Hesse, T. Franz, Y. Tamai, M.M. Taketo, & T.M. Magin, Targeted deletion of keratins 18 and 19 leads to trophoblast fragility and early embryonic lethality, *EMBO J.* **19**, 5060-5070 (2000).
16. P.C. de Souza, & S.G. Katz, Coexpression of cytokeratin and vimentin in mice trophoblastic giant cells, *Tissue Cell* **33**, 40-45 (2001).
17. A. Beham, H. Denk, H. & G. Desoye, The distribution of intermediate filament proteins, actin and desmoplakins in human placental tissue as revealed by polyclonal and monoclonal antibodies, *Placenta* **9**, 479-492 (1988).
18. M.M. Parast, & C.A. Otey, Characterization of palladin, a novel protein localized to stress fibers and cell adhesions, *J. Cell Biol.* **150**, 643-656 (2000).
19. A.G. Booth, & O.A. Vanderpuye, Structure of human placental microvilli, *Ciba Found. Symp.* **95**, 180-194 (1983).
20. O.A. Vanderpuye, H.C. Edwards, & A.G. Booth, Proteins of the human placental microvillar cytoskeleton, alpha-Actinin. *Biochem J.* **233**, 351-356 (1986).
21. M. Berryman, R. Gary, & A. Bretscher, Ezrin oligomers are major cytoskeletal components of placental microvilli: a proposal for their involvement in cortical morphogenesis, *J. Cell Biol.* **131**, 1231-1242 (1995).
22. D. Reczek, M. Berryman, & A. Bretscher, Identification of EBP50: A PDZ-containing phosphoprotein that associates with members of the ezrin-radixin-moesin family, *J. Cell Biol.* **139**, 169-179 (1997).

23. D. Kaczan-Bourgois, J.P. Salles, F. Hullin, J. Fauvel, A. Moisand, I. Duga-Neulat, A. Berrebi, G. Campistron, & H. Chap, Increased content of annexin II (p36) and p11 in human placenta brush-border membrane vesicles during syncytiotrophoblast maturation and differentiation, *Placenta* **17**, 669-676 (1996).
24. H.F. Cantiello, Role of the actin cytoskeleton on epithelial Na^+ channel regulation, *Kidney Int.* **48**, 970-984 (1995).
25. T. Ogura, T. Furukawa, T. Toyozaki, K. Yamada, Y.J. Zheng, Y. Katayama, H. Nakaya, N. Inagaki, ClC-3B, a novel ClC-3 splicing variant that interacts with EBP50 and facilitates expression of CFTR-regulated ORCC, *FASEB J.* **16**, 863-865 (2002).
26. H.F. Cantiello, & A.G. Prat, Role of actin filament organization in ion channel activity and cell volume regulation, in *Membrane Protein-Cytoskeleton Interactions*, Vol. 43 (ed. Nelson, W.J.) 373-396 (Acad. Press, San Diego, 1996).
27. P. Janmey, The cytoskeleton and cell signaling: component localization and mechanical coupling, *Physiol. Rev.* **78**, 763-781 (1998).
28. H.F. Cantiello, J. Stow, A.G. Prat, & D.A. Ausiello, Actin filaments control epithelial Na^+ channel activity, *Am. J. Physiol.* **261**, C882-C888 (1991).
29. B. Berdiev, A.G. Prat, H.F. Cantiello, D.A. Ausiello, C.M. Fuller, B. Jovov, D.J. Benos, & I.I. Ismailov, Regulation of epithelial sodium channels by short actin filaments, *J. Biol. Chem.* **271**, 17704-17710 (1996).
30. W.-H. Wang, A. Cassola, & G. Giebisch, Involvement of actin cytoskeleton in modulation of apical K^+ channel activity in rat collecting duct, *Am. J. Physiol.* **267**, F592-F598 (1994).
31. H.F. Cantiello, Role of the actin cytoskeleton in the regulation of the cystic fibrosis transmembrane conductance regulator, *Exp. Physiol.* **83**, 505-514 (1996).
32. E.M. Schwiebert, J.W. Mills, & B.A. Stanton, Actin-based cytoskeleton regulates a chloride channel and cell volume in a renal cortical collecting duct cell line, *J. Biol. Chem.* **269**, 7081-7089 (1994).
33. A. Blanchard, V. Ohanian, & D. Critchley, The structure and function of α-actinin, *J. Muscle Res. Cell. Motil.* **10**, 280-289 (1989).
34. D.H. Wachsstock, W.H. Schwarz, & T.D. Pollard, Affinity of α-actinin for actin determines the structure and mechanical properties of actin filament gels, *Biophys. J.* **66**, 205-214 (1993).
35. P. Matsudaira, Modular organization of actin crosslinking proteins, *Trends Biol. Sci.* **16**, 87-92 (1991).
36. M. Way, B. Pope, & A.G. Weeds, Evidence for functional homology in the F-actin binding domains of gelsolin and α-actinin: Implications for the requirements of severing and capping, *J. Cell Biol.* **119**, 835-842 (1992).
37. L. Hemmings, P.A. Kuhlman, & D.R. Critchley, Analysis of the actin-binding domain of α-actinin by mutagenesis and demonstration that dystrophin contains a functionally homologous domain, *J. Cell Biol.* **116**, 1369-1380 (1992).
38. H.F. Cantiello, A.G. Prat, J.V. Bonventre, C.C. Cunningham, J. Hartwig, & D.A. Ausiello, Actin-binding protein contributes to cell volume regulatory ion channel activation in melanoma cells, *J. Biol. Chem.* **268**, 4596-4599 (1993).
39. S. González-Perrett, M. Batelli, K. Kim, M. Essafi, G. Timpanaro, N. Montalbetti, I.L. Reisin, I.L. M.A. Arnaout, & H.F. Cantiello, Voltage dependence and pH regulation of human polycystin-2 mediated cation channel activity, *J. Biol. Chem.* **277**, 24959-24966 (2002).
40. I.I. Ismailov, V.G. Shlyonsky, & D.J. Benos, Streaming potential measurements in α γ-rat epithelial Na^+ channel in planar lipid bilayers, *Proc. Natl. Acad. Sci. USA* **94**, 7651-7654 (1997).
41. B. Schuster, & U.B. Sleytr, The effect of hydrostatic pressure on S-layer-supported lipid membranes, *Biochim. Biophys. Acta* **1563**, 29-34 (2002).
42. A.R. Gallagher, A. Cedzich, N. Gretz, S. Somlo, & R. Witzgall, The polycystic kidney disease protein PKD2 interacts with Hax-1, a protein associated with the actin cytoskeleton, *Proc. Natl. Acad. Sci. USA* **97**, 4017-4022 (2000).
43. Q. Li, P.Y. Shen, G. Wu, & X.Z. Chen, Polycystin-2 interacts with troponin I, an angiogenesis inhibitor, *Biochemistry* **42**, 450-457 (2003).
44. Q. Li, Y. Dai, L. Guo, Y. Liu, C. Hao, G. Wu, N. Basora, M. Michalak, & X.Z. Chen, Polycystin-2 associates with tropomyosin-1, an actin microfilament component, *J. Mol. Biol.* **325**, 949-962 (2003).
45. B.K. Yoder, X. Hou, & L.M. Guay-Woodford, The polycystic kidney disease proteins, polycystin-1, polycystin-2, polaris, and cystin, are co-localized in renal cilia, *J. Am. Soc. Nephrol.* **13**, 2508-2516 (2002).
46. S.M. Nauli, F.J. Alenghat, Y. Luo, E. Williams, P. Vassilev, X. Li, A.E..H. Elia, W. Lu, E.M. Bown, S.J. Quinn, D.E. Ingber, & J. Zhou, Polycystins 1 and 2 mediate mechanosensation in the primary cilium of kidney cells, *Nature Genet* . **33**, 129-137 (2003).

47. T. Ito, Y. Masahito, & S.-I. Ohnishi, Osmoelastic coupling in biological structures: A comprehensive thermodynamic analysis of the osmotic response of phospholipid vesicles and a reevaluation of the "dehydration force" theory, *Biochemistry* **28**, 5626-5630 (1989).
48. D.M. LeNeveu, & R.P. Rand, Measurement and modification of forces between lecithin bilayers, *Biophys. J* . **18**, 209-230 (1977).
49. V.A. Parsegian, N. Fuller, & R.P. Rand, Measured work of deformation and repulsion of lecithin bilayers, *Proc. Natl. Acad. Sci. USA* **76**, 2750-2754 (1979).
50. J. Kingdom, B. Huppertz, G. Seaward, & P. Kaufmann, Development of the placental villous tree and its consequences for fetal growth, *Eur. J. Obstet. Gynecol. Reprod. Biol.* **92**, 35-43 (2000).
51. A. Umur, M.J. Van Gemert, & M.G. Ross, Amniotic fluid and hemodynamic model in monochorionic twin pregnancies and twin-twin transfusion syndrome, *Am. J. Physiol.* **280**, R1499-R1509 (2001).
52. S.J. Ladella, M.Y.C Desai, & M.G. Ross, Maternal plasma hypertonicity is accentuated in the postterm rat, *Am. J. Obstet. Gynecol.* **189**, 1439-1444 (2003).
53. Q. Li, Y. Liu, P.Y. Shen, X.Q. Dai, S. Wang, L.B. Smillie, R. Sandford, & X.Z. Chen, Troponin I binds polycystin-L and inhibits its calcium-induced channel activation, *Biochem.* **42**, 7618-7625 (2003).
54. A.G. Prat, Y.-F. Xiao, D.A. Ausiello, & H.F. Cantiello, cAMP-independent regulation of CFTR by the actin cytoskeleton,. *Am. J. Physiol.* **268**, C1552-C1561 (1995).

23

FURTHER CHARACTERIZATION OF THE NEMATODE IClnN2 PROTEIN RECONSTITUTED IN LIPID BILAYERS

M. Ritter, C. Bertocchi, M. Jakab, J. Fürst, M. Paulmichl*

1. INTRODUCTION

ICln is a highly conserved and ubiquitously expressed, multifunctional protein which is indispensable for cell viability and essential for cell volume regulation. In addition to its role in the RNA splicing process,[1-4] ICln is involved in the generation of the anion currents activated during regulatory volume decrease after cell swelling (RVDC). In *Xenopus laevis* oocytes overexpression of ICln results in the occurence of ion currents with properties closely resembling RVDC.[5] ICln knock down with specific antibodies[6] or antisense oligodeoxynucleotides reduces, and overexpression of ICln increases RVDC in native cells.[7-9]

ICln can primarily be found in the cytosol as a water-soluble protein but some fraction can also be detected within or in close association with the cell membrane. Recently we have shown that cell swelling leads to a cellular redistribution of ICln and that the portion of membrane associated ICln increases during RVD.[10]

If reconstituted in artificial bilayers, ICln can form ion channels with biophysical properties related to RVDC.[11-13] The proposed ion channel model of ICln is described in the contribution of Jakab *et al.* in this issue.[14]

In the nematode *Caenorhabditis elegans* we recently identified two splice variants of the ICln protein termed IClnN1 and IClnN2. While IClnN1 is highly homologous to all ICln proteins identified so far, IClnN2 is characterized by an additional string of 20 amino acids, which carries clusters of positively and negatively charged amino acids and which is encoded by the exon 2a.[5] Figure 1A schematically shows the alternative splicing of the polycistronic ICln mRNA and Figure 1B displays the sequence alignment of human ICln, canine ICln and the two nematode ICln splice variants. According to the proposed ion channel model of ICln, these 20 amino acids are located on the cytosolic

* M. Ritter, Institute of Physiology, University of Innsbruck, Fritz-Pregl Straße 3, A-6020 Innsbruck, Austria

side immediately after the predicted second transmembrane β-sheet, i.e., adjacent to the inner mouth of the putative channel pore (figure 1C).

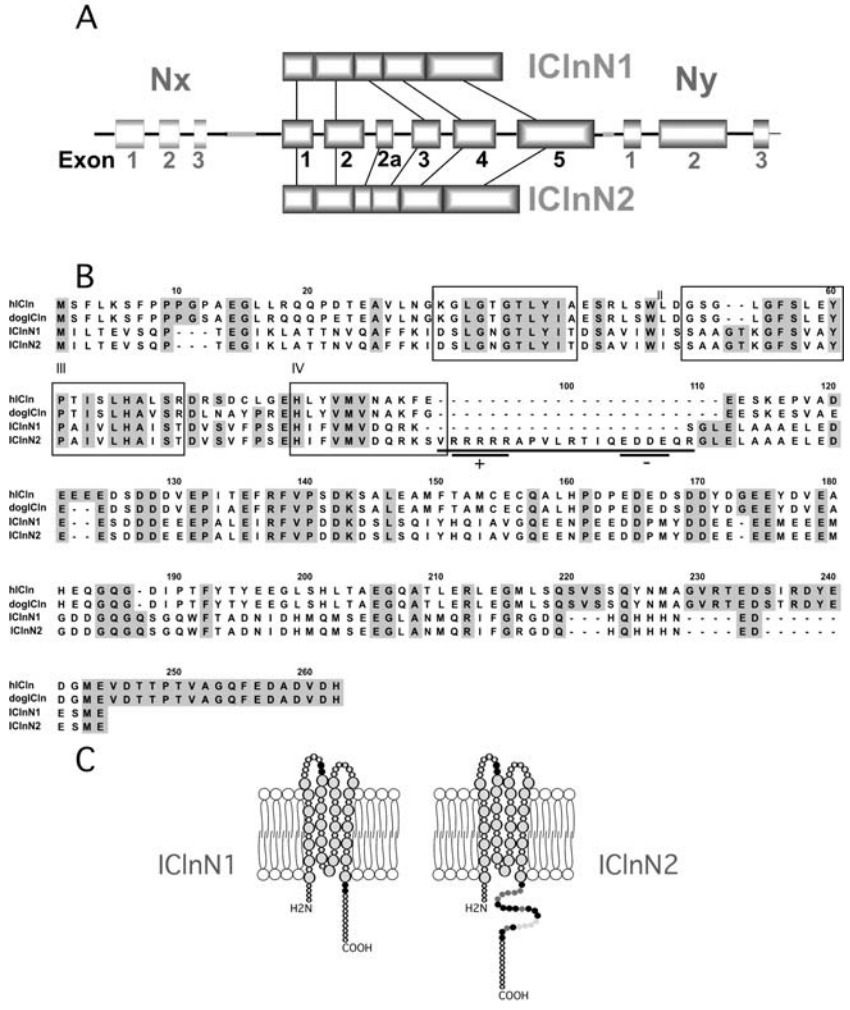

Figure 1. A: Operon organization of ICln, Nx and Ny in *Caenorhabditis elegans*. Alternative splicing of the polycistronic mRNA leads to the expression of IClnN1 and IClnN2. IClnN1 is lacking the amino acids encoded by exon 2a. The operon is housing two additional proteins termed Nx and Ny. **B:** Sequence alignment of ICln from *Homo sapiens* (hICln), *Canis familiaris* (dogICln) and *Caenorhabditis elegans* (IClnN1 and IClnN2). Identical and similar amino acids are indicated by dark and light gray shading, respectively. The string of 20 amino acids encoded by exon 2a of the IClnN2 splice variant is underlined and charged amino acids within this sequence are indicated. The putative transmembrane domains formed by β-sheets are indicated by the boxes marked I-IV. **C:** Putative transmembrane organisation of IClnN1 and IClnN2. The model suggests a transmembrane domain that is composed of a four-stranded β-sheet. To form a functional channel the formation of an ICln dimer is required. The string of amino acids encoded by exon 2a is supposed to be located in close vicinity to the inner mouth of the channel pore. Figures are modified from Fürst et al.[15]

In a previous study we demonstrated that both nematode ICln variants exhibit identical single channel conductances of ≈3 pS if reconstituted in planar lipid bilayers. The open probabilities (P_o) of both variants are identical at negative (pipette vs. bath) holding potentials (0.3-0.4). However, at positive potentials the P_o of IClnN2 rapidly drops to a value close to zero, whereas the P_o of IClnN1 remains unaffected, indicating voltage-dependent inactivation of IClnN2. By reconstitution of IClnN1, the splice variant lacking the exon 2a derived amino acid sequence, in the presence of synthetic peptides comprising the entire sequence from exon 2a or fragments thereof, we could show that inactivation can be conferred to this channel. From these experiments it was concluded that the voltage-dependent inactivation of IClnN2 is mainly due to a cluster of positively charged amino acids, i.e, five consecutive arginines.[15]

In addition to the presence of the unique splice variant, the ICln gene in *Caenorhabditis elegans* is organized in an operon and ICln is transcribed along with two other proteins which have been termed Nx and Ny (figure 1A). Coreconstitution of IClnN2 and protein Nx revealed, that this protein is able to suppress the voltage-dependent inactivation of IClnN2. This indicates a functional interaction between IClnN2 and Nx.[15]

The present study was performed to further investigate the inactivation behavior of reconstituted IClnN2 by use of antibodies directed against the amino acid sequence comprised by exon 2a.

2. EXPERIMENTAL

Salts, chemicals, drugs: All salts, chemicals and drugs were of *pro analysis* grade and purchased from Sigma, Germany, unless otherwise stated.

Nematodes: The nematode strain (N2) used was provided by the Caenorhabditis Genetics Center funded by the NIH National Center for Research Resources (NCRR).

Purification of the ICln proteins: The open reading frame (ORF) of IClnN1 and IClnN2 were cloned in frame into the pET3-His vector, which adds a histidine tag (H-tag) to the N-terminus of the protein. The H-tag allows for purification of the protein on a Ni-NTA agarose column (Qiagen, Germany). As shown earlier, overexpression of the ICln proteins in *Escherichia coli* (strain BL21 (DE3)) and the subsequent purification leads to single protein bands of the expected sizes.[11] The purified proteins were stored at –74°C in elution buffer (50 mM K_2HPO_4 and 200 mM imidazole, pH 7.40–8.00) at a concentration of ≈0.4 µg/µl.

Antibodies: Polyclonal rabbit antibodies were raised against a synthetic peptide with the sequence SVRRRRRAPVLRTIQEDDEQ, which comprises the amino acid sequence encoded by exon 2a, employing standard methods (Davids Biotechnologie, Germany). For experiments, the immunoserum (IS) was used at a dilution of 1:1000. Control experiments were performed using the corresponding preimmunoserum (PIS) at the same dilution. The specificity of the affinity purified antibody was verified by Western blot analysis of preparations from whole worms as well as from purified IClnN1 and IClnN2 proteins.

SDS-PAGE and Western blotting: Purified proteins and homogenized worms were heated to 100 °C for 5 min, separated on a 12% SDS-PAGE and electroblotted onto a

nitrocellulose membrane (Amersham).[16, 17] Membranes were blocked in TBST containing 0.5% blocking substrate (Roche) for 1 h at room temperature, incubated with affinity purified polyclonal antibody (1:3000) for 1 h, washed and incubated with secondary antibody (1:7000) in TBST. Antibody-detection was performed by enhanced chemiluminescence (Roche) (Figure 2).

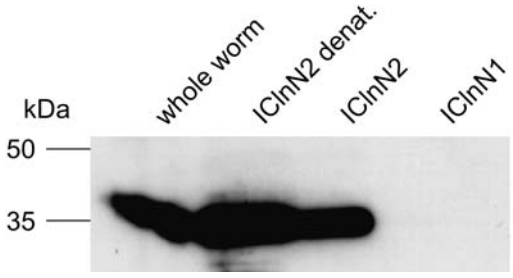

Figure 2. Western blot of lysates of whole *Caenorhabditis elegans* worms (lane 1) and purified IClnN2 (lanes 2 and 3) and IClnN1 (lane 4) proteins using an antibody raised against the amino acid sequence encoded by exon 2a (SVRRRRRAPVLRTIQEDDEQ). The antibody specifically recognizes purified IClnN2 protein, whereas no signal can be detected with IClnN1 protein.

Single-channel current recordings: Single-channel currents of reconstituted IClnN2 proteins were measured using the "tip-dip" method as described previously.[15] The planar lipid bilayer was established on patch pipettes using 1% (w/v) of 1,2-diphytanoyl-sn-glycero-3-phosphocholine (Diph-PC; Avanti Polar Lipids, USA). Diph-PC was dissolved in n-decane for membrane formation. All measurements were made in symmetrical KCl solutions (pipette and bath: 300 mM KCl, 10 mM HEPES, pH 7.40) using an EPC-8 patch-clamp amplifier (HEKA, Germany) and the data were stored on a hard disk. Membranes were voltage-clamped at a holding potential of -120 mV (pipette *versus* bath). The protein was added to the bath solution at a final concentration of ≈1 µg/ml, which was usually followed by the appearance of single channel currents. Where indicated, PIS or IS was added to the bath solution (1:1000). Voltage steps were performed from -120 mV to +120 mV at intervals of five seconds and the single channel open propability (P_o) was determined at the two potentials at intervals of 2.5 seconds before and immediately after the voltage step using the TAC/TACfit (Bruxton) and MS-Excel software. For the analysis, the data were filtered at 0.2 kHz. All experiments were conducted at room temperature.

Statistical analysis: All values are given as mean±SEM. Data were tested for differences in the means by Student's t-test. A statistically significant difference was assumed at $p<0.05$.

3. RESULTS AND DISCUSSION

Reconstitution of IClnN2 in planar Diph-PC bilayers led to the appearance of single channel currents like those shown in Figure 3A. Under these control conditions, the open

probability (P_o) was 0.45±0.06 (n=14). In agreement with our previous study,[15] the P_o of the observed currents rapidly dropped to a value of 0.20±0.06 (n=14) upon a step increase of the holding potential to +120 mV, indicating voltage-dependent inactivation of IClnN2.

Subsequently, 5µl of either preimmunoserum (PIS) or immunoserum (IS) were added to the bath solution (Figure 3A and B). The single channel conductance in the presence of PIS was 2.1±02 pS at -120 mV (n=29) and 2.3±0.3 pS (n=28) at +120 mV, respectively. Addition of IS did not significantly alter these values (2.2±0.3 pS, n=28 and 2.0±0.3 pS, n=28 at -120 mV and +120 mV, respectively). Addition of PIS did not alter the inactivation behavior of reconstituted IClnN2. The P_o at -120 mV was 0.38±0.05 (n=10) and dropped significantly to 0.19±0.03 (n=10) at +120 mV. In the presence of IS, however, the inactivation of IClnN2 was annihilated. The P_o was 0.31±0.07 (n=10) at -120 mV and 0.35±0.05 (n=10) at +120 mV. Thus, in contrast to control conditions or to the presence of PIS, no significant change in the P_o could be observed in the presence of IS.

These results clearly indicate that antibodies specifically recognizing the amino acid sequence encoded by exon 2a do not interfere with the ion conducting part of the molecule, but that they are able to disturb the intramolecular entity responsible for the voltage-dependent inactivation of IClnN2. This entity is most likely comprised by the additional string of 20 amino acids, which are located in close vicinity to the inner mouth of the putative ion-conducting pore of the channel. These amino acids are thought to act as an inactivating particle, closing the channel pore in a voltage-dependent manner as described for other ion channels.[18] It is feasible to assume that the antibodies immobilize the inactivation particle, thus preventing it from binding to a putative intramolecular acceptor site.

Analysis of the amino acid composition of the exon 2a-encoded sequence revealed the presence of two charged clusters, one bearing a net positive charge at the N-terminal part and one bearing a net negative charge at the C-terminal part of the sequence. Reconstitution of IClnN1, the splice variant which is lacking the string of additional amino acids and which does not exhibit inactivation, *per se*, with synthetic peptides composed of these amino acids of exon 2a, or fragments thereof, showed that inactivation can be conferred to IClnN1 by those peptides that contain the positively charged amino acids.[15]

It has to be stated, however, that IClnN2 is so far the only known isoform of ICln that exhibits the exon 2a encoded sequence. In *Caenorhabditis elegans* both IClnN1 and IClnN2 are expressed. In embryonic cells of this organism, RVDC diplays inward rectification. This is in contrast to RVDC found in virtually all other cells investigated so far, in which hypotonicity elicits outwardly rectifying currents.[19] The unique biophysical behavior of IClnN2 may contribute to the regulation of RVDC in this organism. Moreover reconstitution of IClnN2 and protein Nx revealed that the latter is able to counteract the inactivation of IClnN2, thus disclosing a functional interaction of these proteins.[15] Recently we were able to demonstrate that the highly conserved human orthologue of Nx, a protein termed HSPC038, is also able to interact with human ICln if overexpressed in NIH 3T3 fibroblasts.[20] Although the physiological significance of this interaction has to be determined, this study demonstrates that the analysis of the nematode operon organization is a powerful tool to identify functionally interacting partner-proteins.[20]

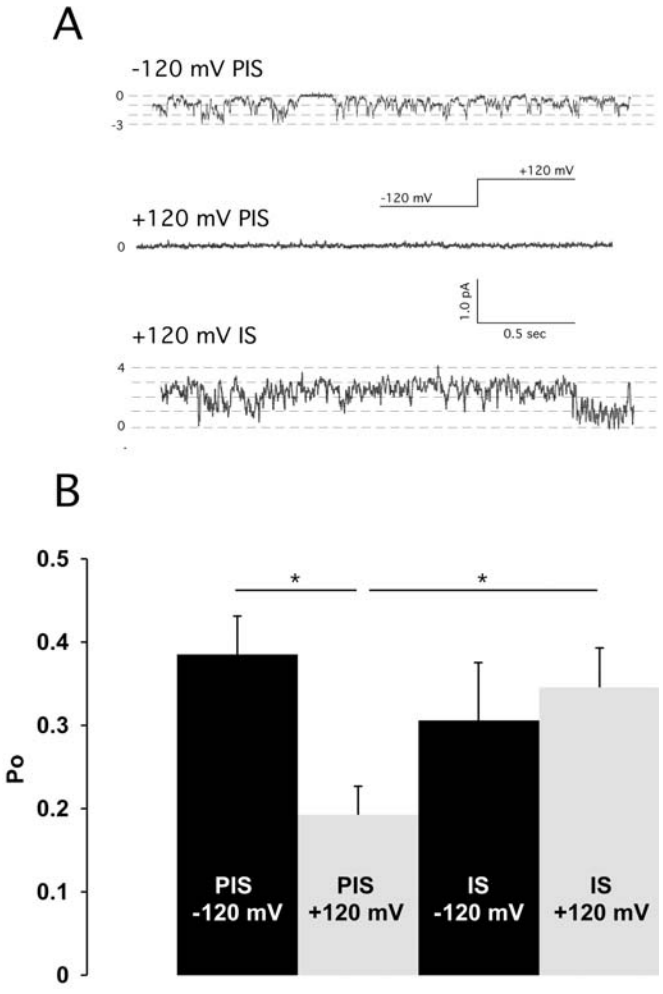

Figure 3. Functional interaction of IClnN2 with antibodies raised against the amino acid sequence encoded by exon 2a. The reconstitution of IClnN2 led to a single channel currents that inactivated at positive potentials (i.e. a voltage step from -120 mV to +120 mV) due to a drop in the open probability (P_o) of the channels. This 'inactivation was unaffected in the presence of preimmunoserum (PIS, left bars) but was completely annhilated in the presence of immunoserum containing the specific antibodies (IS, right bars). **A :** Original tracings from a single channel recording. **B :** Means±SEM of 10 individual experiments.

4. CONCLUSIONS

The results presented in this study confirm previous findings demonstrating voltage-dependent inactivation of the nematode ICln splice variant IClnN2. Furthermore they demonstrate that antibodies directed against the additional 20 amino acids encoded by exon 2a are able to suppress the inactivation of IClnN2, thus mimicking the action of the ICln operon partner protein Nx on reconstituted IClnN2. The results further substantiate

the assumption that the amino acids encoded by exon 2a are responsible for the voltage-dependent inactivation of IClnN2.

5. ACKNOWLEDGMENTS

We thank E. Wöll, G. Meyer and G. Botta for helpful discussion and A. Baumgartner for the technical assistance. This work was supported by grants from the Austrian Science Foundation (FWF; P14102-Med) and the Austrian National Bank (8444) to MR.

6. REFERENCES

1. W.T. Pu, G.B. Krapivinsky, L. Krapivinsky, and D.E. Clapham, pICln inhibits snRNP biogenesis by binding core spliceosomal proteins, *Molecular and Cellular Biology* **19**, 4113-20 (1999).
2. W.J. Friesen, The methylosome, a 20S complex containing JBP1 and pICln, produces dimethylarginine-modified Sm proteins, *Mol Cell Biol* **21**, 8289-300. (2001).
3. W. Friesen, A novel WD repeat protein component of the methylosome binds Sm proteins, *J Biol Chem* **277**, 8243-7. (2002).
4. G. Meister, Methylation of Sm proteins by a complex containing PRMT5 and the putative U snRNP assembly factor pICln, *Curr Biol* **11**, 1990-4. (2001).
5. M. Paulmichl, New mammalian chloride channel identified by expression cloning, *Nature* **356**, 238-41 (1992).
6. G.B. Krapivinsky, M.J. Ackerman, E.A. Gordon, L.D. Krapivinsky,and D.E. Clapham, Molecular characterization of a swelling-induced chloride conductance regulatory protein, pICln, *Cell* **76**, 439-448 (1994).
7. L. Chen, L. Wang, and T.J. Jacob, Association of intrinsic pICln with volume-activated Cl- current and volume regulation in a native epithelial cell, *American Journal of Physiology* **276**, C182-92 (1999).
8. M. Gschwentner, Antisense oligonucleotides suppress cell-volume-induced activation of chloride channels, *Pflügers Archiv. European Journal of Physiology* **430**, 464-70 (1995).
9. M.D. Hubert, Modulation of volume regulated anion current by I(Cln), *Biochimica Et Biophysica Acta* **1466**, 105-14 (2000).
10. M. Ritter, Cell swelling stimulates cytosol to membrane transposition of ICln, J Biol Chem (2003).
11. J. Fürst, Functional reconstitution of ICln in lipid bilayers, *Pflügers Arch* **440**, 100-15. (2000).
12. J. Fürst, Molecular and functional aspects of anionic channels activated during regulatory volume decrease in mammalian cells, *Pflügers Arch* **444**, 1-25. (2002).
13. M. Jakab, Mechanisms sensing and modulating signals arising from cell swelling, *Cell Physiol Biochem* **12**, 235-58 (2002).
14. M. Jakab, C. Bertocchi, M. Jakab, J. Fürst, and M. Paulmichl. Probing of the ICln channel pore by cysteine mutagenesis and cadmium-block, Presentation: *2003 International Symposium, Dayton, OH*, Sep 20-25, 2003.
15. J. Fürst, ICln ion channel splice variants in Caenorhabditis elegans: voltage dependence and interaction with an operon partner protein, *J Biol Chem* **277**, 4435-45 (2002).
16. U. K. Laemmli, Cleavage of structural proteins during the assembly of the head of bacteriophage T4, *Nature* **227**, 680-685 (1970).
17. J. Sambrook, E.F. Fritsch, and T. Maniatis, Molecular Cloning, *Laboratory Manual, Cold Spring Harbour, New York* (1989)
18. B. Hille, Ionic channels of excitable membranes, *Sinauer Associates, Inc*., Sunderland, Mass. (1992).
19. K. Strange, From genes to integrative physiology: ion channel and transporter biology in Caenorhabditis elegans, *Physiol Rev* **83**, 377-415 (2003).
20. S. Eichmüller, A new gene-finding tool: Using the caenorhabditis elegans operons for identifying functional partner-proteins in human cells, *J Biol Chem* (2003).

24

HYPERTONICITY-INDUCED CATION CHANNELS IN RAT HEPATOCYTES AND THEIR INTRACELLULAR REGULATION

Frank Wehner and Heidrun Olsen*

1. INTRODUCTION

For an efficient regulatory volume increase (RVI) to occur, the osmolyte content of a shrunken cell has to be augmented rapidly. To this end, transport systems for inorganic osmolytes are activated as the first cellular response. In most instances, an uptake of Na^+ is employed which is due to the favorable driving forces for this cation across the plasma membrane. As the second step, Na^+ is then exchanged for K^+ by the activation of Na^+/K^+-ATPase and thus the Na^+ gradient is restored. On balance, a net uptake of K^+ (plus Cl^-) and osmotically obliged water is achieved and the original cell volume is regained.

The rates of ion transport through channels are approximately 4 to 5 orders of magnitude higher than those found for carriers. Modulations of ion channel activity in response to changes in cell volume may therefore serve as fast and efficient mechanisms of regulatory osmolyte transport. Conductive Na^+ entry under hypertonic conditions was already proposed by Hoffmann[1] for Ehrlich ascites tumor cells and by Okada and Hazama[2] for intestine 407 cells. In 1995, our lab proved the significance of this mechanism in rat hepatocytes and defined the activation of Na^+ channels as a novel mechanism of RVI.[3]

Here, we will first review the physiological significance of Na^+ channels for the RVI of rat hepatocytes and address the possible molecular entity of these channels. We will then focus on the intracellular mechanisms by which the hypertonic activation of Na^+ channels in rat hepatocytes is controlled. A brief overview on hypertonicity-induced cation channels in other systems is also presented.

* F. Wehner and H. Olsen, Max-Planck-Institut für molekulare Physiologie, Abteilung Epithelphysiologie, Otto-Hahn-Strasse 11, 44227 Dortmund, Germany

2. THE CONTRIBUTION OF Na^+ CHANNELS TO RVI

It was generally assumed that the RVI of rat hepatocytes is mediated by Na^+/H^+ antiport and Na^+/K^+-ATPase operating in concert: Activation of Na^+/H^+ antiport leads to an increase of cell Na^+ which is then exchanged for K^+ via activation of the Na^+ pump[4,5] (Figure 1). In addition, evidence for a role of Na^+-K^+-$2Cl^-$ symport in hormone- (insulin)-induced increase of rat hepatocyte cell volume was reported which suggested this transporter's role in the RVI process as well.[6]

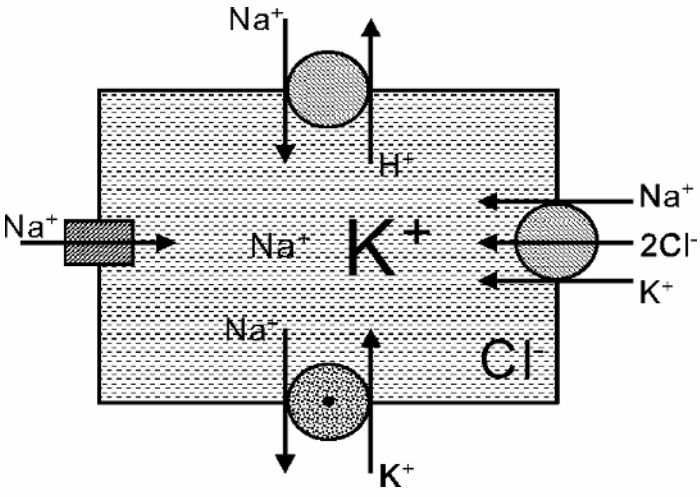

Figure 1. The initial event in the RVI of rat hepatocytes is an import of Na^+ that is channel mediated (left), driven by Na^+/H^+ antiport (top) as well as Na^+-K^+-$2Cl^-$ symport (right). Na^+ is then exchanged for K^+ via activetion of Na^+/K^+-ATPase (bottom). Together, these processes lead to a pronounced increase of cell K^+ (plus a small amount of Na^+). Uptake of Cl^- as well as HCO_3^- will parallel this cation import by (electro-) chemical processes not under consideration here.

Our laboratory was the first to demonstrate a significant contribution of amiloride-sensitive Na^+ channels to the RVI of rat hepatocytes[3] (Figure 1). In a quantitative study, it was then shown that the relative contribution of Na^+ channels, Na^+/H^+ antiport and Na^+-K^+-$2Cl^-$ symport to the hypertonicity-induced Na^+ uptake equals 4:1:1 (upon change from 300 to 400 mosmol/l). Moreover, the amount of Na^+ imported by these transporters was in excellent balance with the actual increase of cell Na^+ plus the amount of Na^+ extrusion via Na^+/K^+-ATPase. In other words, a complete osmolyte and Na^+ transport balance was obtained.[7] When testing for the osmotic sensitivity of the Na^+ transporters employed in RVI, it was found that in the range of 20% to 50% hypertonicity, the activation of Na^+ channels was clearly the dominant mechanism of cell volume regulation in rat hepatocytes[8] (Figure 2).

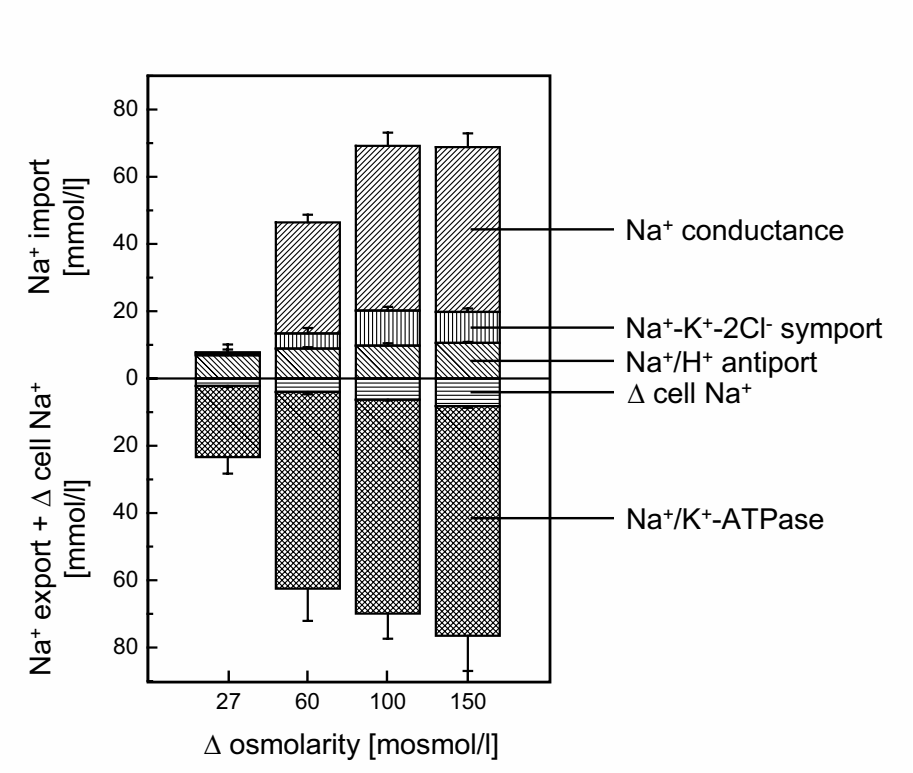

Figure 2. Na^+ transport balance during rat hepatocyte RVI. Four degrees of hypertonicity were tested (changes from 300 to 327, 360, 400 and 450 mosmol/l, respectively). For each series, the Na^+ import occurring via Na^+ conductance, Na^+-K^+-$2Cl^-$ symport and Na^+/H^+ antiport during a 10-min exposure to hypertonic stress is compared with the amount of Na^+ export via Na^+/K^+-ATPase plus the actual increase of cell Na^+ [8] (with kind permission).

3. THE MOLECULAR CORRELATE OF Na^+ CHANNELS

The hypertonicity-induced Na^+ channel of rat hepatocytes was inhibited by amiloride with an apparent K_i of some 5 μmol/l and its overall sensitivity was ethyl-isopropyl-amiloride (EIPA) > amiloride > benzamil.[9, 10] Hence, at first sight, the channel may reflect a low (amiloride) affinity type rather than an epithelial Na^+ channel (ENaC). The latter typically exhibits K_i values in the upper nanomolar range and an inverse pharmacological profile.[11, 12] Nevertheless, all three subunits of rENaC could be detected in Western blots on rat hepatocytes (Figure 3) and fragments of 400 - 500 bp and with 100 % identity to α-, -, γ-rENaC could be amplified by RT-PCR techniques.[10]

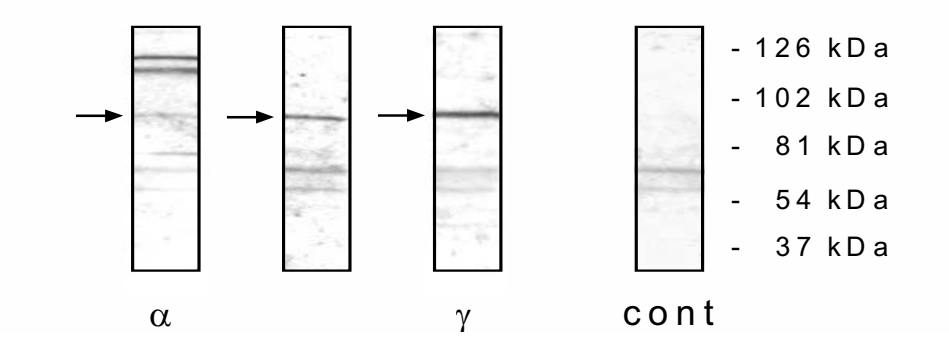

Figure 3. Immunoblot detection of α-, -, and γ-rENaC in rat hepatocytes[10] (with kind permission).

Interestingly, when specific antisense oligo-nucleotides directed against α-rENaC were injected into rat hepatocytes hypertonicity-induced currents were reduced to 30% of control values (Figure 4).[13] This was the first direct evidence for a role of the ENaC in cell volume regulation in a native system. Of note, however, a permeability ratio P_{Na}/P_K = 1.4 could be derived from these measurements which is very low when compared to data obtained for a "typical" ENaC with all three subunits. The actual contribution of -, γ-rENaC to the hypertonicity-induced Na^+ channel of rat hepatocytes is currently under investigation.

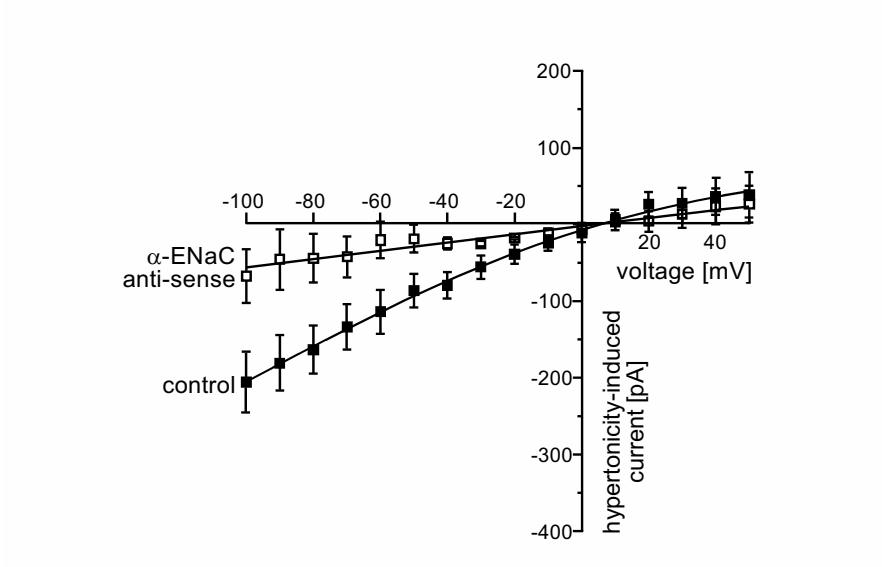

Figure 4. Current-voltage relations of hypertonicity-induced membrane currents in rat hepatocytes. The differences between currents obtained at 400 and 300 mosmol/l were computed for cells injected with a control oligo-DNA [filled squares] or anti-α-rENaC oligo-DNA[13] [open squares] (with kind permission).

4. MECHANISMS OF Na^+ CHANNEL ACTIVATION

As was determined by means of cable-analysis (Figure 5) as well as in ion-substitution experiments with low Na^+ pulses (not shown), PKC is one of the key players in intracellular activation of Na^+ channels. Whereas under control conditions hypertonic stress decreased the specific membrane resistance of rat hepatocytes by 20% (reflecting Na^+ channel activation), this response was completely inhibited in the presence of 400 nmol/l bis-indolyl-maleimide I which (at this concentration) is a highly selective blocker of PKC.[14] It is likely that PKC is functioning quite proximal to Na^+ channel activation. The actual PKC isoform involved in these processes is currently under investigation.

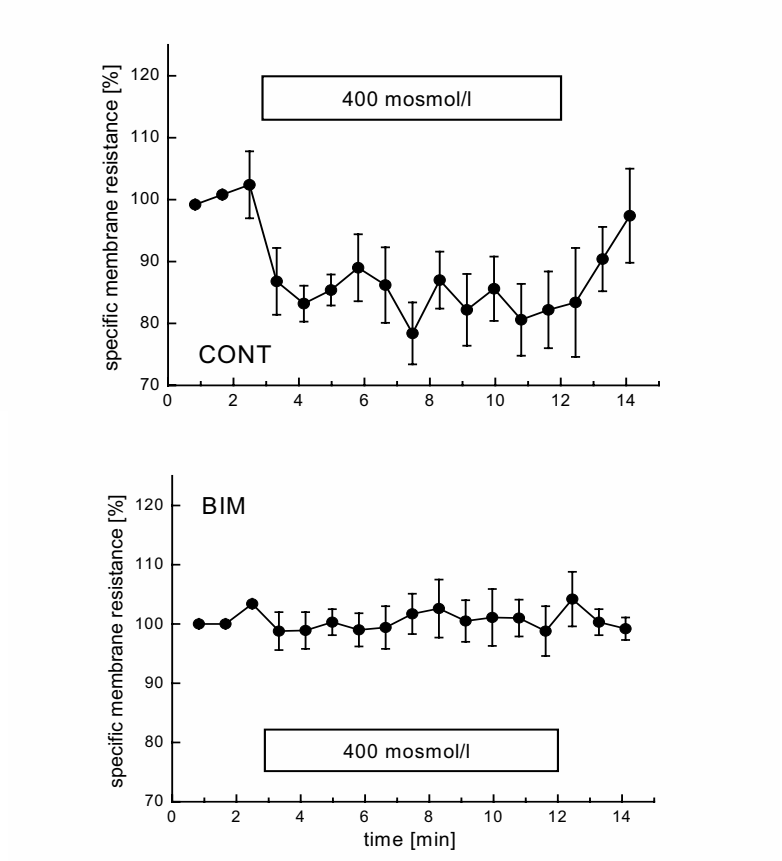

Figure 5. Cable analysis of the hypertonic activation of rat hepatocyte Na^+ conductance. The effects of hypertonic stress (change from 300 to 400 mosmol/l) on specific membrane resistance were determined under control conditions (CONT) and in the presence of 400 nmol/l bis-indolyl-maleimide I (BIM), a selective blocker of PKC[14] (with kind permission).

In addition to the activation of Na^+ channels, PKC stimulated Na^+-K^+-$2Cl^-$ symport[14] which also explains the very similar osmotic sensitivity of both transporters (Figure 2). Of note, stimulation of Na^+/H^+ antiport did not depend on PKC.[14] Likewise, this transporter exhibited a significantly lower osmotic threshold with 65% of its maximal activation already at 9% hypertonicity (327 mosmol/l; Figure 2). Therefore, we hypothesized that cell alkalinization via stimulation of Na^+/H^+ antiport may be part of the signaling machinery employed in Na^+ channel activation. It was found, however, that experimental cell alkalinization (under isotonic conditions) did not significantly alter the activity of rat hepatocyte Na^+ channels[15]).

The signaling events further upstream to PKC are under extensive investigation. A contribution of G-proteins, tyrosine kinases, phospholipase C, and PI3-kinase is very likely and the interplay between these actors is currently characterized in our laboratory.

In addition, as in many other systems, changes in cell volume were found to significantly modify the cytoskeleton of rat hepatocytes. Within a few minutes, the cell actin is rearranged and stress fibres are formed (Figure 6). Interestingly, this effect appeared to occur in concert with changes in the activity of RhoA (not shown).

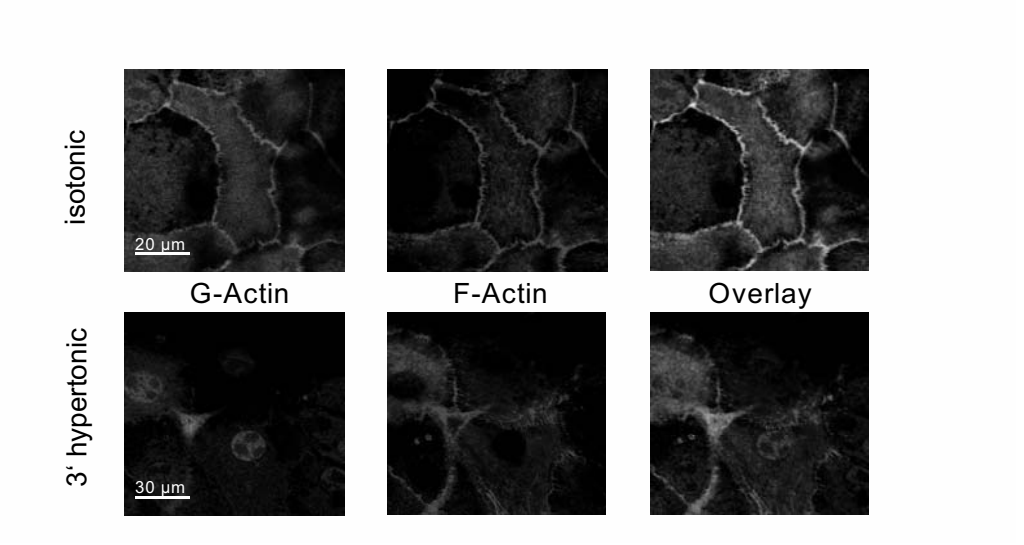

Figure 6. Confocal analysis of hypertonicity-induced stress fibres in rat hepatocyte monolayers. G-actin and F-actin were stained with DNAse I – Alexa 488 and phalloidin – TRITC, respectively, under isotonic conditions and at 3 min after change to 400 mosmol/l.

Our aim is to characterize and further understand the signaling network that finally leads to the hypertonic activation of rat hepatocyte Na^+ channels. Our final goal will be to define the sensors by which cells actually perceive changes in their volume and, at present, integrins and cadherins are some of the most likely candidates. The understanding of these signaling events will be of considerable (patho-) physiological relevance for all of the very many processes that are interrelated to changes in cell volume. The interplay between proliferation (tumor genesis) and apoptosis is only one of them.

5. COMPARISON WITH OTHER SYSTEMS

In addition to rat hepatocytes, hypertonicity-induced and amiloride-*sensitive* cation channels have been reported from the human hepatoma cell line HepG2,[16] Ehrlich Lettre-ascites tumour cells,[17] and human ciliary epithelium[18] (Table 1). In some instances, these channels are even more sensitive to benzamil, supporting the notion of a possible molecular correlation to the ENaC.[19]

Table 1. Pharmacology, ion-selectivity, and molecular correlate of hypertonicity-induced cation channels

	Gd^{3+}	Fluf	EIPA	Amil	Benz	P_{Na}/P_K	Mol[a]
Rat Liver	-	-	++	+	+/-	1.4	α-ENaC
HepG2	+	+	-	+	-	?	?
Ehrlich Lettre	++	?	+/-	+	++	1.14	?
Ciliary Epithelium	?	?	?	+	++	?	?
NSCs[b]	++	++	?	-	?	1.2	TRP[c]?

[a] Molecular correlate
[b] "classical" amiloride-insensitive channels
[c] transient receptor-potential channels

In contrast, "classical" non-selective cation channels (NSCs) are typically *insensitive* to amiloride in concentrations up to 10^{-4} mol/l. In every instance however, these channels are blocked by the anti-inflammatory drug flufenamate (10^{-4} mol/l) as well as Gd^{3+} (from 10^{-5} to 10^{-3} mol/l). NSCs are expressed in human nasal epithelial cells[20] in the human colon cell lines CaCo-2 and HT_{29},[21, 22] in the mouse cortical collecting duct cell line M1,[23] as well as in BSC-1 renal epithelium cells (derived from the African green monkey), A10 vascular smooth muscle cells (established from rat embryonic aorta), Neuro-2a cells (derived from mouse neuroblastoma),[22] and the human cervix carcinoma cell line HeLa.[24]

Little is known about the molecular entities of amiloride-sensitive or insensitive channels. The only exceptions are rat hepatocytes where α-ENaC is one component of the channel and possibly HeLa cells from which a correlation to transient receptor potential (TRP) channels was reported[24] (See[19] for review). Concerning future studies in the field, Ehrlich Lettre cells may be the preparation of choice because they combine a pronounced sensitivity to both benzamil and Gd^{3+}, the typical blockers of amiloride-sensitive and insensitive channels (Table 1). In this respect, also note that wherever tested, the P_{Na}/P_K ratio is in the very narrow range of 1.1 to 1.4, which may be interpreted in terms of a possibly closer relation between both types of channels than was originally proposed.

6. CONCLUSIONS

Our recent work on the RVI of rat hepatocytes has led to a complete understanding of the osmolyte and Na^+ transport balance in this system, and the osmotic sensitivity of the transporters employed were defined. Clearly, the activation of an amiloride-sensitive

Na^+ channel is the main mechanism mediating RVI which is a novel mechanism of cell volume regulation. On the molecular level, at least α-rENaC is a functional component of this channel. With respect to regulation, PKC is one of the triggering mechanisms rather close to channel activation. The intracellular network that is in charge further upstream to PKC, including possible sensors of cell volume changes, is currently under investigation.

7. ACKNOWLEDGMENTS

We wish to thank Dr. R.K.H. Kinne for his continuous support of the project and for many stimulating discussions. The invaluable secretarial help of Daniela Mägdefessel is also gratefully acknowledged.

8. REFERENCES

1. E.K. Hoffmann, Regulation of cell volume by selective changes in the leak permeabilities of Ehrlich ascites tumor cells, In: *Osmotic and Volume Regulation. Alfred Benzon Symposium XI*, C. B. Jørgensen and E. Skadhauge, ed., Munksgard, Copenhagen, 397-417 (1978).
2. Y. Okada and A. Hazama, Volume-regulated ion channels in epithelial cells, *News Physiol. Sci.* **4**, 238-242 (1989).
3. F. Wehner, H. Sauer, and R.K.H. Kinne, Hypertonic stress increases the Na^+ conductance of rat hepatocytes in primary culture, *J. Gen. Physiol.* **105**, 507-535 (1995).
4. P. Haddad and J. Graf, Volume-regulatory K^+ fluxes in the isolated perfused rat liver: characterization by ion transport inhibitors, *Am. J. Physiol.* **257**, G357-G363 (1989).
5. F. Lang, M. Ritter, H. Völkl and D. Häussinger, Cell volume regulatory mechanisms - an overview, *Adv. Comp. Environ. Physiol.* **14**, 1-31 (1993).
6. C. Hallbrucker, S. vom Dahl, F. Lang, W. Gerok, and D. Häussinger, Modification of liver cell volume by insulin and glucagon, *Pflugers Arch.* **418**, 519-521 (1991).
7. F. Wehner and H. Tinel, Role of Na^+ conductance, Na^+-H^+ exchange, and Na^+-K^+-$2Cl^-$ symport in the regulatory volume increase of rat hepatocytes, *J. Physiol.* **506**, 127-142 (1998).
8. F. Wehner and H. Tinel, Osmolyte and Na^+ transport balances of rat hepatocytes as a function of hypertonic stress, *Pflugers Arch*. **441**, 12-24 (2000).
9. F. Wehner, H. Tinel and R.K.H. Kinne, Pharmacology of volume activated Na^+ conductance in rat hepatocytes, *Physiologist* **40**, A-4 (1997).
10. C. Böhmer, C.A. Wagner, S. Beck, I. Moschen, J. Melzig, A. Werner, J.-T. Lin, F. Lang, and F. Wehner, The shrinkage-activated Na^+ conductance of rat hepatocytes and its possible correlation to rENaC, *Cell. Physiol. Biochem.* **10**,187-194 (2000).
11. H. Garty and L.G. Palmer, Epithelial sodium channels: Function, structure, and regulation, *Physiol. Rev.* **77**, 359-396 (1997).
12. G.K. Fyfe, A. Quinn and C.M. Canessa, Structure and function of the Mec-ENaC family of ion channels, *Semin. Nephrol.* **18**,138-151 (1998).
13. C. Böhmer and F. Wehner, The epithelial Na^+ channel (ENaC) is related to the hypertonicity-induced Na^+ conductance in rat hepatocytes, *FEBS Lett.* **494**,125-128 (2001).
14. H. Heinzinger, F. van den Boom, H. Tinel and F. Wehner, In rat hepatocytes, the hypertonic activation of Na^+ conductance and Na^+-K^+-$2Cl^-$ symport – but not Na^+-H^+ antiport – is mediated by protein kinase C, *J. Physiol.* **536**, 703-715 (2001).
15. F. Wehner, R.K.H. Kinne, H. Tinel, Hypertonicity-induced alkalinization of rat hepatocytes is not involved in activation of Na^+ conductance or Na^+, K^+-ATPase, *Biochim. Biophys. Acta* **1328**,166-176 (1997).
16. F. Wehner, P. Lawonn and H. Tinel, Ionic mechanisms of regulatory volume increase (RVI) in the human hepatoma cell line HepG2, *Pflugers Arch.* **443**, 779-790 (2002).

17. P. Lawonn, E.K. Hoffmann, C. Hougaard, and F. Wehner, A cell shrinkage-induced non-selective cation conductance with a novel pharmacology in Ehrlich-Lettre-ascites tumour cells, *FEBS Lett.* **539**, 115-119 (2003).
18. M.M. Civan, K. Peterson-Yantorno, J. Sánchez-Torres and M. Coca-Prados, Potential contribution of epithelial Na^+ channel to net secretion of aqueous humor*, J. Exp. Zool.* 279, 498-503 (1997).
19. F. Wehner, H. Olsen, H. Tinel, E. Kinne-Safran and R.H.K. Kinne, Cell volume regulation: osmolytes, osmolyte transport, and signal transduction, *Rev. Physiol. Biochem. Pharmacol.* **148**, 1-80 (2003).
20. H.C. Chan and D.J. Nelson, Chloride-dependent cation conductance activated during cellular shrinkage, *Science* **257**, 669-671 (1992).
21. D.J. Nelson, X.Y. Tien, W.W. Xie, T.A. Brasitus, M.A. Kaetzel, and J.R. Dedman, Shrinkage activates a nonselective conductance: Involvement of a Walker-motif protein and PKC, *Am. J. Physiol.* **270**, C179-C191 (1996).
22. J.P. Koch and C. Korbmacher, Osmotic shrinkage activates nonselective cation (NSC) channels in various cell types, *J. Membr. Biol.* **168**, 131-139 (1999).
23. T. Volk, E. Frömter and C. Korbmacher, Hypertonicity activates nonselective cation channels in mouse cortical collecting duct cells, *Proc. Natl. Acad. Sci. USA* **92**, 8478-8482 (1995).
24. F. Wehner, T. Shimizu, R. Sabirov and Y. Okada, Hypertonic activation of a non-selective cation conductance in HeLa cells and its contribution to cell volume regulation, *FEBS Lett.* **551**, 20-24 (2003).

25

CELL VOLUME SENSING AND REGULATION IN SKELETAL MUSCLE CELLS

Lessons from an Invertebrate

Hector Rasgado-Flores, Jillian Theobald, Jesus Ruiz, John B. Bitner, Susan Markowitz, Darryl Zlatnick, Pei-Ang Yee, Pei-Ping Yee, Lauren Trais, Kathy Gohar, David Hergan, Robert Buechler, Robert Lajvardi and Cecilia Pena-Rasgado*

1. INTRODUCTION

Human skeletal muscle cells, in addition to their contractile role, serve as reservoirs for 45% of the total body water and ~35% and ~73% of body Mg^{2+} and K^{+}, respectively. Furthermore, these cells contain relatively large concentrations of intracellular free amino acids (FAA) or related compounds, e.g., ~16 mM taurine and 6 mM glycine,[1] known to act as osmolytes in numerous cells. Thus, net membrane fluxes of water, K^{+} and FAA in skeletal muscle have the potential of affecting not only the volume of the contracting muscle cell but also that of neighboring muscle cells and perhaps the body's electrolyte balance as well.[2] Under isosmotic conditions, skeletal muscle contraction is accompanied by increases in intracellular osmolality (due to accumulation of lactate, creatine and inorganic phosphate) and thus cell volume. While subsequent efflux of osmolytes from the contracting cell restores its volume, it may affect the plasma osmolality thereby compromising the volume of non-contracting neighboring muscle cells. Furthermore, cell volume changes affect the muscle's contractile capability.[3] This complex array of cause-effect relationships has interested physiologists and biophysicists for more than 100 years,[4-6] but the underlying details are just beginning to be unveiled as understanding of volume regulatory mechanisms increases. The muscle cell from the barnacle, *Balanus nubilus*, is an ideal model to study these interactions. The cell's large size (2 cm length x 2 mm

* Dept. Physiology and Biophysics Rosalind Franklin University of Medicine and Science/The Chicago Medical School 3333 Green Bay Road North Chicago, IL 60064

diameter) permits measurement and/or control of all known relevant parameters involved in contraction and cell volume regulation, e.g., membrane potential, intracellular pressure, cell shape and volume, force generation, lattice spacing, and sarcomere length. Further-more, these cells undergo large volume and shape changes during isometric contraction.[7] To understand the interactions between cell volume and muscle contraction, it is essential to know how volume changes are sensed by muscle cells as well as the mechanisms re-sponsible for effecting volume recovery. We will review how barnacle muscle cells sense hypotonicity-induced swelling and the mechanisms responsible for volume recovery.

2. MATERIALS AND METHODS

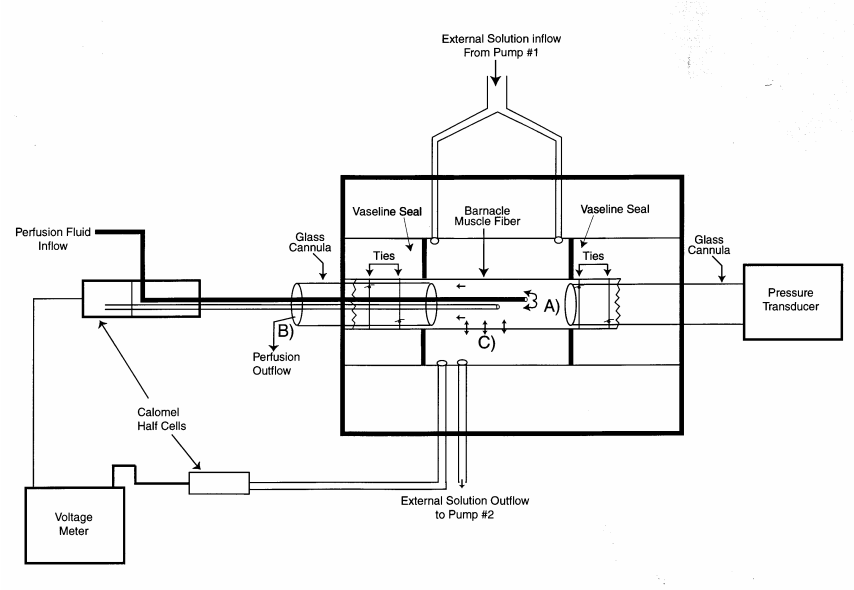

Figure 1. Diagram representing the experimental set-up used for barnacle muscle perfusion and simultaneous measurement of intracellular pressure and osmolality. The perfusion solution is dispensed into the cell via a perfusion pump #1 at the end of the perfusion capillary tube at a rate of 0.83 µl/min [see Eq. 4]. Subsequently, the perfusate flows back to the left cannula where it is collected every 30 min for measurement of its osmolality. The rate of perfusate efflux at the opening of the left cannula (B) can be identical or different than the rate I depending on whether there is any net gain or loss of water across the sarcolemma (Q_V) [see Eq. 3]. Net transport of water across the sarcolemma will affect the osmolality of the perfusate collected at the left cannula. See text for details. (Reproduced from Bitner et al.,[17] with permission).

Four different types of barnacle muscle cell preparations were used depending on the experimental needs. The **first** consists of bundles (30-40 cells) of intact cells detached from each other but attached to the carapace at their basal end. This arrangement is used to maintain integrity of the cells as much as possible. Examples of the use of this preparation include measurement of the intracellular content of osmolyte and cyclic nucleotides under various experimental manipulations.[8-10] The **second** preparation consists of cells cut from the carapace at their basal end, cannulated at this region and mounted in an experimental cham-

ber. The cannula is used to impale the otherwise intact cell with an intracellular electrode and a current-passing wire; there is no intracellular perfusion. This arrangement permits con-tinuous superfusion of a single cell, monitoring of its volume, and measurement and control of its membrane potential (V_M). For example, this setup is used to determine the effects of isosmotic removal of extracellular Ca^{2+} (Ca_o) or Na^+ (Na_o) on cell volume and V_M.[11-13] The **third** setup consists of internally perfused cells, accomplished by impaling the cannulated basal end of the cell with an additional capillary tube connected to a perfusion syringe.[14] This setup permits simultaneous control of intra- and extracellular environments and V_M. It is used for numerous purposes including: i) determination of the effect on cell volume of changes in intracellular ionic strength or macromolecular crowding while maintaining the membrane stretch and intracellular tonicity constant; ii) assessment of the effect of increas-ing, under isosmotic conditions, the intracellular concentrations of Ca^{2+} or cyclic nucleotides (e.g., cAMP, cGMP) on cell volume and the efflux of radiolabeled osmolytes added to the perfusates (e.g., K^+, Cl^-, and FAA); or iii) determination of the effect of exposure to hypoto-nicity on cell volume and the efflux of radiolabeled osmolytes.[15, 16] The **fourth** preparation is similar to the third except both the tendon and basal ends of the cell are cannulated (Figure 1). The basal end is used to impale the cell with the perfusion and V_M electrodes while the tendon end is connected to a pressure transducer via a sealed liquid bridge. This set-up allows direct measurement of the apparent sarcolemmal water permeability, intracellular osmolality, and hydrostatic pressure under isosmotic and anisosmotic conditions.[17]

Techniques to isolate the cells, measure their apparent sarcolemmal water permeability,[17] cell volume,[11] extracellular space,[11] intracellular content of ions and FAA,[10] ionic fluxes[14] and for internally perfusing,[18] voltage-clamping, and modifying the intracellular macro-molecular crowding have been published.[19] Additional, recently developed, unpublished procedures follow:

2.1. Determination of Intracellular cAMP and cGMP Levels

Bundles of 30-40 intact barnacle muscle cells, attached to the carapace but separated from each other, are incubated in the absence or presence of extracellular Ca^{2+} (Ca_0) under isosmotic (1hr) and hyposmotic (additional 3 hrs) conditions. Every 10 min, cells are cut from the bundle, rapidly frozen in liquid nitrogen, freeze-dried and weighed. Subsequently, they are homogenized in trichloroacetic acid and their cAMP and cGMP levels are determined by radioimmunoassay (Dupont, Boston, MA). The units are in nmoles (for cAMP) or pmoles (for cGMP) x g dry wt^{-1}.

2.2. Modification of Intracellular Ionic Strength

The experimental strategy consists of assessing the effect on cell volume of perfused cells resulting from modifying the intracellular ionic strength while maintaining isosmotic and constant the intra- and extracellular osmolalities (1000 mOsm x Kg^{-1}, the intracellular macromolecular crowding and the sarcolemmal stretching. The value of the ionic strength of the internal perfusion solutions is calculated using:

$$\text{Ionic strength} = \tfrac{1}{2} \Sigma_i \, c_i \, z^2_i \qquad (1)$$

where the suffix i represents a given ion present in the solution, c is the concentration of each

ion, and z is the valence of such ion. The values of the ionic strength of control and experimental solutions are 279 and 63 mM, respectively.

2.3. Determination of Membrane Tension

In experiments in which it was necessary to maintain the membrane tension constant, care was taken to ensure all the cells possessed similar membrane compliance and developed comparable membrane tension before changes in either ionic strength or the concentration of intracellular macromolecules were made. Similar compliance was assured by discarding cells (5% of the cases) that swelled too quickly or too slowly (as compared to the majority of the cells) in response to intracellular perfusion. Membrane tension was calculated by solving the Laplace equation, i.e., tension = radius x intracellular pressure. Knowing the radii attained after the initial 90 min of the experiment were 0.01 to 0.014 cm, the intracellular pressure was ~5 cm H_2O when steady volume was reached, and the measured density of the perfusion fluid was 1 g/cm^3, the value of membrane tension was 33-51 dynes/cm.

2.4 Basic Extracellular and Intracellular Solutions

Two methods for preparing isosmotic (1000 mOsm x Kg^{-1}) and anisosmotic external sodium seawater solutions were used: i) All the solutions contained the same ionic composi-tion, and the osmolality was adjusted with various concentrations of sucrose. The composi-tion of this solution was as follows (in mM): NaCl, 230; KCl, 10; $CaCl_2$, 11; $MgCl_2$, 25; along with a mixture of Trizma base and Tris-HCl to adjust the pH to 7.8; ii) The hyposmotic solutions were prepared by diluting a standard isosmotic seawater (NaSW)with the following composition (in mM): NaCl, 456; KCl, 10; $CaCl_2$, 11; $MgCl_2$, 25; and a mixture of Trizma base and Tris-HCl (pH =7.8). Concentrations of Ca^{2+} were varied by replacing Ca^{2+} mole for mole with Mg^{2+}.

Several internal solutions were used depending on the experimental needs. The basic composition of these solutions was (in mM): 6 Na-Hepes, 172 K-Aspartate, 38 KCl, 4 Mg-ATP, 7 $MgCl_2$, 1.5 phosphoenolpyruvate, 3.5 caffeine, 0.025 FCCP, 0.56 $CaCl_2$, 8 EGTA, 60 HEPES and 0.08 mg/ml of pyruvate kinase. The measured free Ca^{2+} was 10 nM. All internal solutions were isosmotic (1000 mOsm x Kg^{-1}) with a pH of 7.3. All experiments were carried out at room temperature.

3. RESULTS

3.1. Osmotic Properties of Barnacle Muscle Cells: Effect of Ca_o

There is an intimate relationship between Ca^{2+} concentration and hypotonicity-induced cell volume regulation in barnacle muscle cells (see below). To understand the role of this divalent cation on volume regulation, it is necessary first to know what effect, if any, this ion might have on the basic osmotic properties of these muscle cells. The pertinent osmotic properties which could affect the volume regulatory responses are: i) the rate and magnitude of the cell volume changes induced by exposure to anisosmotic conditions; ii) the apparent sarcolemmal hydraulic water permeability (L'_p); and iii) the value of the extracellular space.

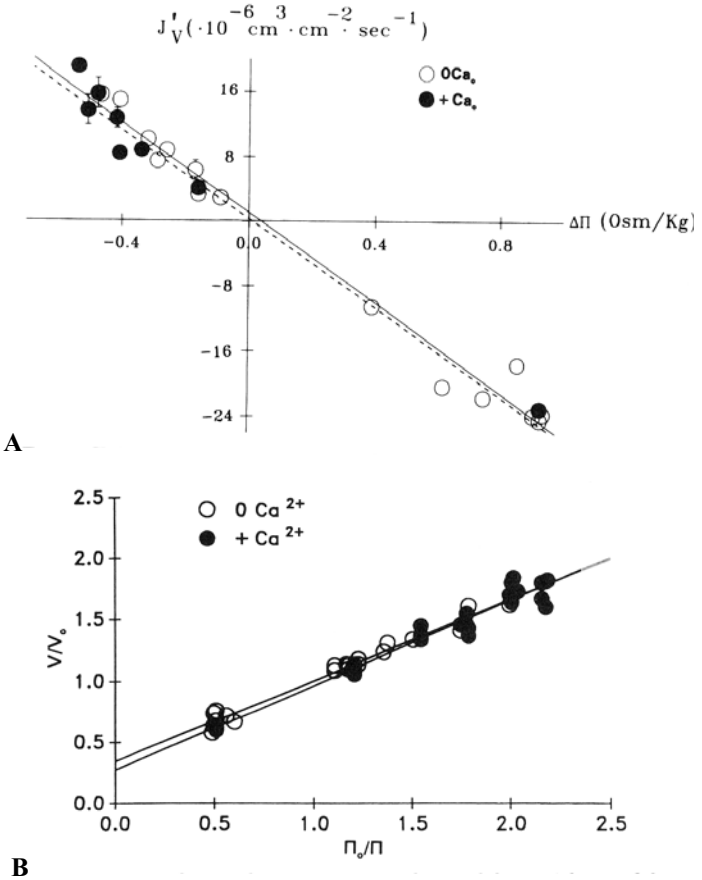

Figure 2. A. Effect of various external osmolalities (Δ) on apparent cell water fluxes (J'_v) in single isolated barna-cle muscle cells mounted in the experimental chamber. Δ is the difference between experimental osmolality and isosmotic osmolality. J'_v values were obtained from initial rates of cell volume changes (during the first 5 min of hypotonic challenge) in response to anisotonic conditions from 21 cells superfused with Ca^{2+}-free media (O) and from 37 cells superfused with the media containing normal Ca^{2+} (11 mM, ●). Continuous (0 Ca^{2+}) and discon-tinuous (11 mM Ca^{2+}) lines are the best fit (slope) for results and represent values of apparent hydraulic water per-meability (L'_p) Negative Δ and positive J'_v values represent hyposmotic challenges and cell swelling, respectively; positive Δ and negative J'_v values indicate hyperosmotic challenges and cell shrinking, respectively. Extracellular Ca^{2+} (Ca_o) had no effect on J'_v. Data points represent values from either single experiments or average 3-7 experiments performed at the same Δ . Error bars represent SE where their values extend beyond the symbols. **B.** Effects of Ca_o and various extracellular osmolalities on peak cell volume changes in single isolated barnacle muscle cells. Intact cells mounted in the experimental chamber were continuously exposed to either Ca^{2+}-free (O) or Ca^{2+}-containing (11 mM ●) solutions. Abscissa, relative media osmolality challenges ($_o$/ , where $_o$, and are the tonicity of the isotonic and anisotonic solutions, respectively). Ordinate, relative peak cell volume changes (V/V_o, where V_o = volume under isosmotic conditions just prior to changing the external solution and V = peak volume reached following exposure to the anisosmotic conditions. Slope of regression line and extrapolated intercept (dead volume) obtained in the absence of Ca^{2+} were 0.65 ± 0.02 and 0.35 ± 0.03 (n= 21), respectively. Corresponding slope and intercept values obtained in the presence of Ca^{2+} were 0.69 ± 0.02 and 0.27± 0.04 (n=37) (reproduced from Berman et al.,[11] with permission).

The volume of intact (not perfused) barnacle muscle cells varies with the size of the

animal, but the volume of cells commonly used experimentally is ~80 µl for intact, dissected cells left attached to the carapace[12] and 20 - 40 µl for cut cells mounted in the experimental chamber.[11, 12, 17] Because of the very large surface/volume ratio, the volume changes induced by exposure to anisosmotic external conditions are very slow ($t_{1/2}$ = 20-30 min) and can be readily calculated by directly measuring the cell's dimensions using a calibrated microscope eye piece and/or from pictures of the cells taken at pertinent incubation times.[11, 18, 19] The initial rates of volume changes are measured during the first 5 min of anisotonic challenge; the maximal (peak) volume changes are measured 45-60 min after the anisotonic challenge.

Figure 2 A[58] displays the effect of Ca_o and of various externally applied osmolalities on apparent cell water fluxes (J'_v) in single isolated barnacle muscle cells mounted in the exper-imental chamber. The graph depicts the initial rates of volume changes induced by exposure to anisotonic solutions. The figure shows that both in the absence and presence of Ca_o, J'_v was linearly related to the nominal differences in extracellular osmolality (Δ) and Ca_o did not significantly ($p<0.05$) affect the initial rates of volume changes at all the osmolalities tested. Figure 2B[58] shows the relationship between the relative peak cell volume changes and the relative media osmolality challenges in the absence and presence of Ca_o, i.e., 11 mM, closed symbols. The figure shows a linear relationship between V/V_o and $_o/$ and no significant difference ($p<0.2$) between the slope and extrapolated intercepts of the regression lines in the absence or presence of Ca_o. Thus, barnacle muscle cells behave like osmometers, obeying the Boyle-van't Hoff relationship, and Ca^{2+} has no effect on this parameter.

3.2. Sarcolemmal Hydraulic Water Permeability in Barnacle Muscle Cells: Effect of Ca_o

Two methods were used to determine L'_p. The first one consisted of measuring the rates of cell volume changes in response to exposure to anisosmotic external solutions in intact isolated cells mounted in the experimental chamber.[11] L'_p was calculated from:

$$L'_p = \frac{J'_v}{\sigma \times \Delta} \qquad (2)$$

where J'_v is the apparent water flow (in mL/cm^2), σ is the reflection coefficient of sucrose and Δ is the difference between the tonicity of the isosmotic and anisosmotic solutions; J'_v was calculated from measurements of the initial rates of cell volume changes in response to exposure to the anisosmotic conditions. Presence or absence of Ca_o had no effect on the value of L'_p which was ~2.7 x 10^{-5} cm x sec^{-1} x Osm^{-1} x kg H_2O^{-1}.[11]

The second method to determine L'_p consisted of measuring the effect of a positive intracellular hydrostatic pressure (ΔP) on inducing a positive (outflow) plasmalemmal water flow (Q_v) under isosmotic conditions. Thus, the actual measurement of Q_v consisted of a sar-colemmal water filtration in the absence of an osmotic gradient, i.e., Δ = 0.[17] To accom-plish this goal, cells were cut and cannulated at their basal and tendon ends (Figure 1). The right cannula served to measure the intracellular pressure. This was accomplished by estab-lishing direct contact of the myoplasm with a pressure transducer *via* a liquid sealed bridge. The left cannula was not sealed but was left open to the air and was used for three purposes: i) monitoring of V_M; ii) internal perfusion; and iii) collection of the perfusion fluid once it had perfused the cell.

L'_p was calculated from Equation 3:

$$Q_v = A\, L'_p\, (\Delta P - \sigma\, \Delta\pi) \quad (3)$$

where A is the sarcolemmal surface area and the other coefficients have their usual meaning (see above). Q_v could be calculated from the difference between the rate at which the cell is being perfused (pump #1) [see Figure 1] and the rate at which the perfusates emerge from the left cannula (B) according to the following equation:

$$Q_v = \text{Inflow} - \text{Outflow} \quad (4)$$

However, accurate measurements of O are difficult to obtain; therefore, Q_v was calculated by measuring the difference in osmolality between the perfusion fluid before perfusing the cell (Osm_I; in mOsm x kg x H_2O^{-1}) and the osmolality of the perfusates exiting the left cannula after having perfused the cell (Osm_O). Equation 5 shows how the terms are related:[17]

$$L'_p = I\,[1 - (Osm_I \times Osm_O^{-1})]\;\; [A\,(\Delta P - \sigma\,\Delta\pi)]^{-1} \quad (5)$$

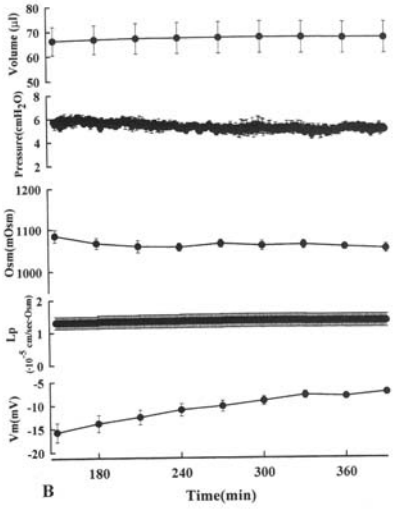

Figure 3. Time-course of changes in cell volume (67.2 ± 6 µl, top panel), intracellular pressure (5.6 ± 0.4 cm H_2O, second panel from top), osmolality of perfusion fluid collected after having perfused the cell (1052 ± 10 mOsm/kg H_2O, middle panel), calculated value of L'_p (1.35 x 10^{-5} cm x sec^{-1} x Osm^{-1} x kg H_2O^{-1}, second panel from bottom), and membrane potential (V_M, 16 ± 2.5 mV, bottom panel) in 5 perfused barnacle muscle cells. The graph displays the values of these parameters after 150 m of perfusion when steady values have been reached. Prior to this time, intracellular perfusion increased cell volume (from original average value of 45.1 ± 6.9 µl) and intracellular pressure. Cell swelling results from the interaction between intracellular hydrostatic pressure generated by the perfusion and membrane compliance (reproduced from Bitner et al.,[17] with permission).

Figure 3 shows the values of cell volume, intracellular pressure, osmolality of the collected, L'_p and V_M, after the cell has been per-fused for 2 hours. The results show that except for V_M which follows a trend of continuous slow depolarization (resulting from the

intracellular perfusion) all other parameters reached steady values. The value of L'_p was 1.35 x 10^{-5} cm x sec^{-1} x Osm^{-1} x kg H_2O^{-1}.

The values of L'_p obtained using the two very different methodologies described above are in very close agreement. This is remarkable because these values are one to two orders of magnitude smaller than those reported for other cells.[20] Underestimation of L'_p could result from the fact that this value was estimated using osmotic volume measurements (as opposed to radiotracer flux measurements). Osmotic measurements are subject to water flow retardation, not only by the plasmalemma but also by the cytoplasm which behaves as an internal unstirred layer.[21] The similarity of the L'_p values obtained suggests either that unstirred layers affected intracellular water movements in both studies in a similar fashion or that these studies would require measurement of L'_p under conditions in which the unstirred layers play no role in the calculations, i.e., by using tracer H_2O.

3.3. Time-Course of the Hypotonicity-Induced Swelling: Effect of Ca_o and Verapamil

Animal cells swell when placed in hyposmotic solutions. However, despite continuous exposure to hypotonicity, most cells shrink back to almost their original volume. This process is termed regulatory volume decrease (RVD) and is due to a net loss of intracellular osmolytes followed by osmotically-obliged water. There is controversy regarding the role of intracellular Ca^{2+} in signaling the loss of osmolytes in animal cells. Many groups report Ca^{2+} dependence for RVD in a variety of animal cell types, while others claim Ca^{2+} independent RVD in others.[22, 23]

To assess whether Ca^{2+} is involved in promoting RVD in barnacle muscle cells, the effect of Ca_o was studied on the time-course of hypotonicity-induced cell volume changes in three types of muscle cell preparations: i) intact, dissected cells attached to the carapace;[10] ii) unperfused cells cut and mounted in the experimental chamber;[11] and iii) internally perfused cells.[18] Interestingly, in all cases, even in perfused cells where the myoplasm has been replaced by the perfusion fluid, the muscle cells displayed Ca_o-dependent RVD.

Figure 4 A[10] depicts the time-course of the average relative volume (V/Vo) of intact muscle cells attached to the carapace exposed to isosmotic and hyposmotic external solutions in the absence or presence of Ca^{2+}. The figure shows that, under isosmotic conditions, replacement of Ca_o for Mg^{2+} for 1 h induced a significant and surprising volume reduction of 6%. Since the relative volume just prior to exposure to the hyposmotic solution has a fixed value of 1, the relative volume in the absence of Ca_o at time 0 in the graph appears as significantly larger than the one measured in the presence of Ca_o. Exposure to analogous hyposmotic solutions produced a similar muscle swelling regardless of the presence of Ca_o. In the absence of Ca_o, the cells remained swollen during the hypotonic challenge. However, if Ca_o was present, the cells underwent RVD, manifested by a significant drop of the swollen volume, reaching a reduction of ~ 49% after 3 h of exposure to hypotonicity.

The fact that replacement of Ca_o for Mg^{2+} under isosmotic conditions produced a small but significant volume reduction was surprising and was studied in detail using isolated, unperfused but voltage-clamped cells mounted in the experimental chamber.[12] Results showed Ca_o removal induced a verapamil-sensitive, extracellular Na^+-dependent membrane depolarization which induced in turn a volume reduction in cells in which the sarcoplasmic reticulum (SR) was loaded with Ca^{2+}. This was interpreted as suggesting Ca_o removal releases an inhibition on Na^+ permeation through verapamil-sensitive Ca^{2+} channels. The subsequent influx of Na^+ following its electrochemical gradient produces a membrane

depolarization which in turn induces SR Ca^{2+} release in cells in which this organelle is loaded with Ca^{2+}. The subsequent increase in $[Ca^{2+}]_i$ under isosmotic conditions induces the loss of osmolytes followed by water, leading to the cell volume reduction. As will be shown, the osmolytes responsible for this process have been identified.[10]

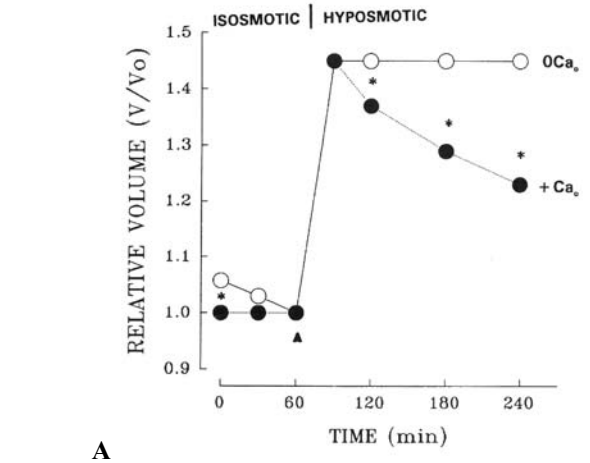

A

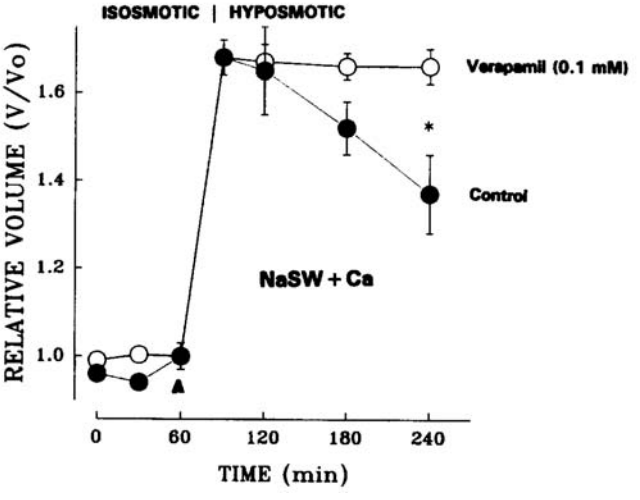

B

Figure 4. A. Time-course of the effect of extracellular Ca^{2+} (Ca_o) and exposure to hypotonicity on the relative cell volume of intact barnacle muscle cells attached to the carapace. Ordinate, ratio of cell volume measured at time indicated (V) to volume measured before exposing (V_o, arrowhead at 60 min of incubation) cells to either Ca^{2+}-free (O) or Ca^{2+}-containing (11 mM, ●) hyposmotic (575 mOsm/kg H_2O) solutions. Data points represent the average ± SE of 60 (●) or 40 cells (O). In this and all figures, the asterisk indicates significant ($p<0.05$) difference between control and experimental cells. Ca^{2+}-free solutions contained 2 mM of the Ca^{2+}-chelator, EGTA. (Reproduced from Pena-Rasgado et al.,[10] with permission.) **B.** Comparison of the effect of hypotonicity (496 mosm/kg H_2O; arrowhead, at 60 min of incubation) on cell volume of cells attached to carapace exposed to 11 mM Ca_o (NaSW+Ca) and to either the absence (●, n=24) or presence of 0.1mM externally applied verapamil (O, n=28) (reproduced from Pena-Rasgado et al.,[12] with permission).

Once it was shown that barnacle muscle cells undergo RVD and that this process has an absolute requirement for Ca_o, the next step in understanding the underlying mechanisms in volume recovery was to test the hypothesis that this Ca_o-dependence resulted from a swelling-induced activation of sarcolemmal Ca^{2+} channels.

Since it has been reported that verapamil is the most effective and most available blocker of barnacle muscle Ca^{2+} channels at a 0.1 mM concentration,[24] the effect of this con-centration of the blocker was assessed on the Ca_o-dependent RVD in cells attached to the carapace[18] and in isolated cells mounted in the experimental chamber.[25] In either case, verapamil completely blocked the Ca_o-dependent RVD. Figure 4B[18] displays the time-course of the average relative volume (V/V_o) of intact cells attached to the carapace exposed to isosmotic and hyposmotic solutions containing Ca^{2+} and of cells exposed to the same conditions but in the presence of 0.1 mM verapamil. The figure shows that either in the absence or presence of the blocker, the cells swelled similarly in response to an identical hyposmotic challenge, indicating that this blocker did not affect the osmotic properties. However, as expected, the control cells, in the presence of Ca_o, gradually recovered a portion (~56 %) of their original isosmotic volume, i.e., RVD, while they were exposed to the hyposmotic conditions. On the other hand, in the presence of the blocker, the RVD process was significantly ($p<0.05$) inhibited. The fact that the presence of Ca_o is necessary for RVD and that verapamil blocks this process in the presence of Ca_o strongly suggests that swelling activates a verapamil-sensitive Ca^{2+} influx pathway, inducing an increase in $[Ca^{2+}]_i$ which in turn activates volume reduction. This is further supported by the observation that activation of the verapamil-sensitive Ca^{2+} influx pathway under isosmotic conditions via reduction of macromolecular crowding (see below),[19] induces a measurable influx of Ca^{2+} as demonstrated by using radiolabeled Ca^{2+}. These results, however, do not rule out the possibility that verapamil, at the concentration tested, could act like the phenylalkylamine Ca^{2+} channel blocker D-600, which inhibits skeletal muscle contraction by entering the cell and preventing SR Ca^{2+} release.[26] If this is the case, then the chain of events leading to RVD could be swelling activates Ca^{2+} influx via verapamil-sensitive, sarcolemmal Ca^{2+} channels. The subsequent increase in $[Ca^{2+}]_i$ would promote Ca^{2+} release from the SR, which in turn would stimulate loss of osmolytes leading to volume reduction. Support for this hypothesis is provided by the fact that under isosmotic conditions, membrane depolarization induces volume reduction in cells exposed to isosmotic Ca_o-free conditions provided the SR is first loaded with Ca^{2+}.[12, 13] Definitive proof of this hypothesis would be provided by showing that in Ca_o-free conditions, addition of Ca_o at the peak of hyposmotic swelling would induce RVD only in cells in which the SR is loaded with Ca^{2+} but not in SR Ca^{2+}-depleted cells.

In summary, an increase in $[Ca^{2+}]_i$ is necessary for inducing volume reduction under isosmotic and hyposmotic conditions. Ca^{2+} influx via a verapamil-sensitive pathway is necessary for RVD; Ca^{2+} release from the SR via membrane depolarization can induce volume reduction under isosmotic conditions. The possibility that RVD is exclusively induced by Ca^{2+} release from the SR cannot be ruled out at present.

3.4. Extracellular Space: Effect of Hypotonicity and Ca_o

The next step in studying the underlying mechanisms responsible for RVD in barnacle muscle cells consisted of determining the osmolytes responsible for the Ca_o-dependent RVD. Knowledge of an accurate value of extracellular space is an essential prerequisite for measuring the content of intracellular ionic concentrations during isosmotic and anisosmotic

conditions. This is particularly true for cells exposed to the large extracellular ionic concentrations present in seawater. To determine the extracellular space, the experimental protocol consisted of measuring the time-course equilibration of a membrane impermeant, radiolabeled extracellular marker. The molecule chosen was ^{14}C-polyethyleneglycol (4,000 Da), and its distribution at the cell surface was studied from 30 to 330 min in intact cells attached to the carapace exposed to the absence or presence of Ca_o under isosmotic and hyposmotic (500 mOsm Kg^{-1}) conditions. Figure 5 shows the time-course of equilibration of the extracellular marker in Ca_o-free (panel A) and Ca^{2+}-containing (panel B) isotonic and hypotonic solutions. The graph demonstrates the following: i) under all conditions there were two components of polyethylene glycol equilibration: a fast component that reached saturation in less than 30 min of incubation and a slow component that required three hours of incubation to equilibrate; ii) hypotonicity (550 mOsm/kg H_2O) reduced the fast component by ~40% but did not affect the slow component; and iii) presence of normal Ca_o (11 mM) reduced the fast component by ~47 % without affecting the slow component. To facilitate interpretation of these results, a three-dimensional reconstruction of autoradiographs of sectioned cells incubated in the presence of ^{14}C-polyethylene-glycol under isosmotic and hyposmotic conditions in the absence and presence of Ca_o were made. Analysis of the stereograms indicated that under isosmotic conditions the cells retained large quantities of radioactivity at the outer layer, probably from entrapment of the marker at the

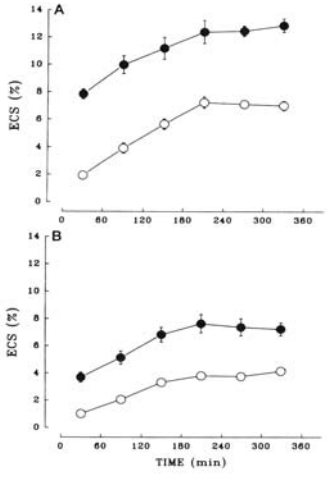

Figure 5. [^{14}C] polyethylene glycol (4,000 Da) equilibration in bundles of intact dissected barnacle muscle cells attached to the carapace. Cells were incubated either under isosmotic (●) or hyposmotic (550 mosmol/kg H_2O, O) conditions in the absence (panel A) or presence (panel B) of Ca_o. **A.** Results in Ca^{2+}-free seawater solutions. Each symbol represents mean ± SE (where errors extend beyond symbols) of 3-17 cells obtained from 6 different bundles of muscle cells. After 210-230 min of incubation the marker reached equilibration. The value of extracellular space (ECS) reached was 12.56± 0.38% and 7.11 ± 0.33% under isosmotic (●) and hyposmotic (O) conditions, respec-tively. **B.** Results obtained from cells incubated in the presence of normal Ca_o. Symbols represent means ± SEM (where errors extend beyond symbols) of 17-20 cells from 6 different bundles of muscle cells. ECS values measured when marker had equilibrated were 7.42 ± 0.34 and 3.89 ± 0.11% for cells exposed to isosmotic and hyposmotic conditions, respectively. Hyposmotic solutions were obtained by diluting the isosmotic solutions (reproduced from Berman et al.,[11] with permission).

external (wider) portions of the sarcolemmal invaginations. Exposure to hyposmotic conditions significantly reduced the amount of radioactivity entrapped at the cell surface. This may result from a decrease in the diameter of the invaginations as cells swell. Cells incubated in the presence of Ca_o showed reduction of radioactivity at the surface which may result from extrusion of water from the invaginations as the cells contract when cut in the presence of Ca_o. The values of extracellular space obtained from these studies are consistent with values obtained from other laboratories using different techniques and extracellular markers.[11] These values have been used to determine the loss of intracellular osmolytes in response to increases in $[Ca^{2+}]_i$ under isosmotic and hyposmotic conditions.[10]

3.5. Osmolytes Responsible for Volume Reduction under Isotonic and Hypotonic Conditions

In barnacle muscle cells, volume reduction occurs in response to increases in $[Ca^{2+}]_i$ under both isosmotic and hyposmotic conditions (see Figure 4A). Since water is in thermodynamic equilibrium between the intra- and extracellular environments, cell volume is largely determined by the intracellular osmolyte concentration. Therefore the volume reductions observed in Figure 4A under isosmotic and hyposmotic conditions must result from a net loss of intracellular osmolytes followed by osmotically-obliged water. The next step in elucidating the chain of events linking cell swelling to RVD consisted of identifying the osmolytes responsible for volume reduction under isosmotic and hyposmotic conditions. The experimental protocol consisted of exposing bundles of 30-40 muscle cells, separated from each other but left attached to the carapace, to the absence and presence (11 mM) of Ca_o under isotonic and hypotonic (535-575 mOsm/Kg H_2O) conditions. At the end of each experimental period (60 or 120 min), three to five cells were cut from the bundle for intracellular osmolyte analysis. The intracellular content of Na^+ and K^+ was measured using flame photometry, the content of Cl^- was determined with chloridometry and the content of FAA was assessed using HPLC.[10] To permit comparison of osmolyte content independently of the cell volume, the values were expressed as μmol/g dry wt.

Table 1[10] shows the effect of isosmotic removal of Ca_o on the intracellular osmolyte content. The experimental manipulation produced a significant ($p<0.05$) loss of K^+, Cl^-, glycine and taurine. The loss of K^+ and Cl^- had a ratio of $1K^+$:$1Cl^-$.

Table 1. Effect of isosmotic removal of extracellular Ca^{2+} on the intracellular osmolyte content in intact barnacle muscle cells.

Condition	NaSW+Ca	NaSW0Ca	Δ	n	p
IONS					
Na	60.1 ± 1.4	60.8 ± 7.4	- 0.7 ± 7.5	90	-
K	371.8 ± 2.9	353.1 ± 3.6	18.7 ± 4.6	90	*
Cl	163.0 ± 1.3	144.4 ± 10.2	18.6 ± 10.2	90	*
Total Ions	594.9 ± 3.4	558.3 ± 13.1	36.6 ± 13.5		*
FAA					
Gly	406.0 ± 12	376.3 ± 9.1	29.7 ± 15	25	*
Tau	170.3 ± 3	157.2 ± 2.5	13.1 ± 3.9	25	*
Arg	140.6 ± 2.8	139.2 ± 1.4	1.4 ± 3.2	25	-
Asp	20.0 ± 2	21.6 ± 0.8	- 1.6 ± 2.1	25	-

Table 1. (continued)

Leu	9.5 ± 0.7	10.4 ± 0.7	- 0.9 ± 0.9	25	-
Val	13.1 ± 0.8	12.0 ± 0.5	1.1 ± 0.9	25	-
Sar	10.4 ± 0.5	10.1 ± 0.9	0.3 ± 1.0	25	-
Thr	19.3 ± 5.4	12.0 ± 0.4	7.2 ± 5.4	25	-
Ser	5.8 ± 2.2	4.4 ± 0.3	1.4 ± 2.3	25	-
Glu	15.4 ± 1.9	15.3 ± 0.5	0.1 ± 1.9	25	-
Ala	34.5 ± 2.5	29.7 ± 1.2	4.8 ± 2.7	25	-
Tyr	6.8 ± 0.5	5.4 ± 0.3	1.4 ± 1.0	25	-
Glut	10.5 ± 2	9.6 ± 0.3	0.9 ± 2.2	25	-
Total FAA	862.2 ± 14.6	803.2 ± 9.8	59.3 ±17.6		*
TOTAL	1457.1 ± 15	1361.5 ± 16.4	95.9 ± 22.2		*

The second and third columns are the osmolyte content (expressed as μmol/g dry weight) of cells exposed to either isosmotic seawater containing 11 mM Ca^{2+} (NaSW + Ca) or ○ Ca^{2+} (NaSW ○ Ca), respectively. The fourth column (Δ) is the difference between the second and third columns. (n) number of individual cells measured from various barnacles C5-10 cells/barnacle). (p) defines if the value of Δ is statistically significant. * indicates $p<0.05$.

Table 2. Effect of exposure to hyposmotic conditions (575 mosm) on intracellular osmolyte content expressed in intact barnacle muscle cells exposed to seawater with 11 mM Ca^{2+} or 5.5 mM Ca^{2+} for the isosmotic or hyposmotic solutions, respectively.

Condition	Isosmotic	Hyposmotic	Δ	n	p
IONS					
Na	60.1 ± 1.4	63.7 ± 1.3	- 3.6 ± 2	130	-
K	371.8 ± 2.9	349.0 ± 1.7	22.8 ± 3.3	130	*
Cl	163.0 ± 1.3	152.2 ± 0.9	10.8 ± 2.5	130	*
Total Ions	594.9 ± 3.4	564.9 ± 2.3	30.0 ± 4.5		*
FAA					
Gly	406.0 ± 12	304.2 ± 16	101.8 ± 20	45	*
Tau	170.3 ± 3	152.2 ± 8.3	18.1 ± 8.8	45	*
Arg	140.6 ± 2.8	139.2 ± 8.0	1.4 ± 8.4	45	-
Asp	20.0 ± 2	20.0 ± 3.5	0.0 ± 4	45	-
Leu	9.5 ± 0.7	9.0 ± 0.3	0.5 ± 0.7	45	-
Val	13.1 ± 0.8	11.8 ± 0.8	1.3 ± 1.1	45	-
Sar	10.4 ± 0.5	9.7 ± 1.0	0.7 ± 1.1	45	-
Thr	19.3 ± 5.4	11.5 ± 1.1	7.8 ± 5.5	45	-
Ser	5.8 ± 2.2	3.8 ± 0.1	2.0 ± 2.2	45	-
Glu	15.4 ± 1.9	12.8 ± 2.1	2.6 ± 1.9	45	-
Ala	34.5 ± 2.5	31.5 ± 1.5	3.0 ± 2.9	45	-
Tyr	6.8 ± 0.5	4.8 ± 0.3	2.0 ± 0.5	45	-
Glut	10.5 ± 2	8.1 ± 1.0	2.4 ± 2.2	45	-
Total FAA	862.2 ± 14.6	718.7 ± 20.3	143.5 ± 23.4		*
TOTAL	1457.1 ± 15.0	1283.6 ± 20.4	173.5 ± 23.8		*

Second and third columns are the intracellular osmolyte content (expressed as μmol/g dry weight) of cells exposed to isosmotic (second column) or hyposmotic (third column) solutions containing Ca^{2+}. The meaning of n, p and * are as indicated in Table 1.

Table 2 shows a comparison between the effect of exposure to hypotonicity on the intracellular osmolyte content in the absence/presence of Ca_o. As expected, exposure to hypotonicity in the absence of Ca_o produced neither volume changes nor alteration in the intracellular osmolyte content.[10] In contrast, exposure to hypotonicity in the presence of Ca_o produced a significant net loss of KCl, gly and tau. In this instance, the ratio of K^+ to Cl^- loss was of $2K^+$:$1Cl^-$. Interestingly, the relative contribution of inorganic ions (46%) and FAA (48%) to the total osmolyte content under hyposmotic conditions was similar to that found under isosmotic conditions (42% and 52%, respectively).

The Ca_o-dependent loss of FAA observed during RVD could result from actual trans-port of these osmolytes from the intra- to the extracellular environment[27] or from their metabolism or incorporation into proteins.[28] To differentiate between these possibilities, the appearance of these molecules in the extracellular media was measured in response to expo-sure to the hyposmotic solution in either the absence or presence of Ca_o. Since the intracellu-lar FAA loss and the appearance of these osmolytes in the extracellular environment were expressed in the same units (μmol/g dry wt), the values were directly comparable. The comparison indicated that ~92% of the FAA loss during RVD appeared in the extracellular environment.[10] It was concluded that under either isosmotic (in response to Ca_o removal) or hyposmotic conditions (in the presence of Ca_o), volume reduction was due to an increase in $[Ca^{2+}]_i$ which in turn induced the loss of osmolytes followed by osmotically obliged water.

3.6. Changes in Extracellular pH during RVD

Comparison of Tables 1 and 2 shows a change in the ratio of K:Cl loss from 1:1 under isosmotic conditions to $2K^+$:$1Cl^-$ under hyposmotic conditions. To explain this result, a hypothesis was formulated which proposed that loss of $2K^+$:$1Cl^-$ during RVD was due to K^+ efflux not only as the ion pair KCl but also as being exchanged with H^+ via a putative K^+/H^+ exchanger or being cotransported with OH^-. A similar K^+/H^+ exchanger activated by osmotic swelling has been identified in Amphiuma erythrocytes[29] and an osmotic swelling-activated K^+-OH^- cotransporter has been reported in trout erythrocytes.[30] To test the aforementioned hypothesis, changes in extracellular pH were measured in cells exposed to hyposmotic solu-tions either in the absence or presence of Ca_o. The experimental protocol consisted of plac-ing the 1 mm tip of a pH microelectrode in the core of a bundle of 25-35 cells separated from each other but left attached to the carapace. The concentration of the extracellular buf-fer solution (10 mM Hepes) was a compromise between being low enough to permit the measurement of changes in extracellular pH yet high enough to prevent a large acidification resulting from cellular metabolism.

Figure 6[10] depicts the time-course of the change in extracellular pH induced by intact barnacle muscle cells incubated in either Ca^{2+}-free or Ca^{2+}-containing hyposmotic solutions. The cells were exposed to Ca^{2+}-containing or to Ca^{2+}-free isosmotic solutions for 75 min prior to the hyposmotic challenge. Subsequently, the cells were challenged with the homologous hyposmotic solutions. To normalize the data from seven different barnacles, the pH values were expressed as the difference from the pH measured under isosmotic conditions just prior to the hyposmotic exposure. Consequently, the first data point in the graph has a value of zero, and a positive and negative deviation from this value represents alkalinization and acidification, respectively. The graph shows that in the absence of Ca_o, hypotonicity is accompanied by a continuous trend toward extracellular acidification probably resulting from cell metabolism. However, in the presence of Ca_o, during RVD, the

cells produced a significant ($p<0.05$) alkalinization of ~0.5 pH units that reached a steady-state value after 90 min of exposure to the hypotonic challenge.

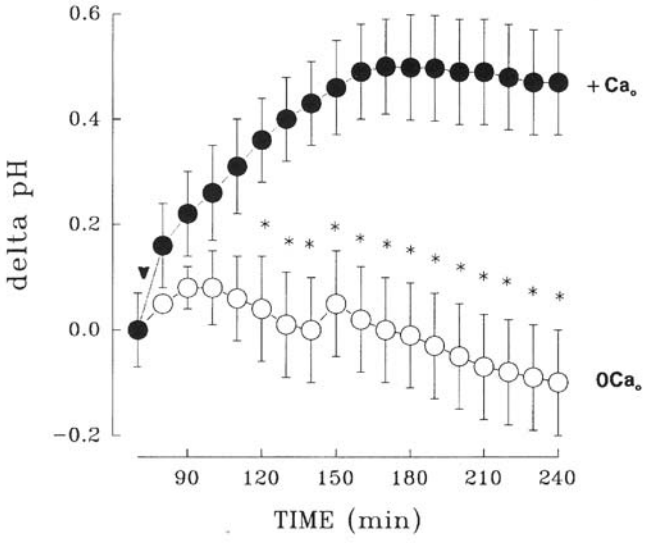

Figure 6. Time-course of changes in extracellular pH in response to exposure of bundles (25-35 cells) of barnacle muscle cells attached to the carapace to hyposmotic media containing 11mM Ca^{2+} (●) or 0 Ca^{2+} and 2 mM EGTA (O). To normalize data from different barnacles, pH values are expressed in relation to the pH measured under isos-motic conditions (7.6-7.8) just prior to exposure to the hyposmotic condition at 75 min incubation. Ordinate, delta pH is the difference between pH measured under hyposmotic conditions minus pH measured under isosmotic con-ditions. Consequently, the first data point has a value of zero, and a positive and negative deviation from this value represents alkalinization and acidification, respectively. At the arrow, the isosmotic solution was replaced by the hyposmotic one. Data points represent average ± SEM of pH values obtained from 7 independent experiments (Reproduced from Pena-Rasgado et al.,[10] with permission).

Interestingly, removal of Ca_o under isosmotic conditions induced a cell volume reduction without affecting the extracellular pH. This observation, together with the fact that RVD was accompanied by external alkalinization, raised the possibility that neither an increase in $[Ca^{2+}]_i$ nor swelling *per se* induced activation of the putative K^+/H^+ exchanger. However, the simultaneous increase in $[Ca^{2+}]_i$ and cell swelling or the alteration of an intracellular factor accompanying swelling (e.g., reduction in intracellular osmotic strength or in protein con-centration, see below) may be responsible for activating the K^+-OH^- cotransport (or K^+/H^+ exchange). Assessment of these possibilities requires a detailed future analysis.

3.7. Role of Cyclic Nucleotides on Cell Volume in Barnacle Muscle Cells

The next step in understanding the underlying mechanisms linking cell swelling to RVD consisted of assessing a possible role of cyclic nucleotides in the Ca^{2+}-dependent cell volume reduction It has been shown that in some cells either mechanical deformation[31] or hypotonic swelling[32, 33] is accompanied by increases in cAMP levels. Similarly, the presence of hor-

mones or other agents that produce cell shrinkage[34] or swelling[35] induce increases in cAMP. On the other hand, in a variety of cells, cAMP and cGMP interact in mediating second mes-senger signals.[36-39] This includes barnacle muscle cells where, for example, insulin-promoted glucose uptake is accompanied by a reduction in cAMP and an increase in cGMP.[40] Likewise, in these cells, Ca^{2+} influx produces a simultaneous increase in cAMP and cGMP levels.[41] Since it has been reported that changes in cGMP may accompany the changes in cAMP levels in response to cell volume alterations,[42, 43] the effect of both cyclic nucleotides on cell volume regulation was explored. To accomplish this goal, the effect of intracellularly perfusing cAMP and/or cGMP on isosmotic cell volume was studied.

To eliminate the possibility that these nucleotides could affect cell volume via modifying the $[Ca^{2+}]_i$, cells were perfused with either control or cyclic nucleotide-containing solutions in which the $[Ca^{2+}]_i$ was strongly buffered at 10nM with 8 mM EGTA. Figure 7A[18] shows a comparison of the time-course of the effect of internally perfusing barnacle muscle cells with either a control isosmotic solution or isosmotic perfusion solutions containing (1 mM) cAMP, cGMP or cAMP plus cGMP. The graph shows that internal perfusion (at 0.5 μl/min) of control cells induced a swelling which reached a steady value of 10-15 % at about 90 min. Addition of cAMP (at arrow) induced a significant ($p<0.05$) cell volume reduction of ~12 % which reached a stable value after 150 min. This effect was abolished if cGMP was also present in the perfusate. On the other hand, addition of cGMP alone induced a slight additional swelling of ~6% which became significant ($p<0.05$) with respect to control cells after 180 min. Thus, these results indicate that these cyclic nucleotides play opposite roles in mediating volume reduction in barnacle muscle cells: cAMP promotes this process while cGMP has the reverse effect.[18] The results also suggest the volume reduction induced by an increase in $[Ca^{2+}]_i$ may in fact be mediated by an increase in cAMP.

Once it was demonstrated that increases in both $[Ca^{2+}]_i$ and cAMP induce volume reduction, an attempt was made to elucidate their physiological role and possible linkage during volume regulation. Figure 7A demonstrated increases in cAMP induce volume reduction in cells in which $[Ca^{2+}]_i$ is heavily buffered with EGTA. This is evidence that cAMP nucleotide effects volume reduction independently of $[Ca^{2+}]_i$. However, it was unknown whether increases in $[Ca^{2+}]_i$ could lead to volume reduction independently of changes in cAMP levels. To answer this question, an experimental protocol was designed consisting of assessing the effect of various levels of $[Ca^{2+}]_i$ buffering and of the presence of a specific cAMP antagonist (cAMP monophosphorothioate Rp-isomer, Rp-cAMPS) on hypotonicity-induced RVD. Figure 7B[18] shows a comparison of volume changes in response to an identical hyposmotic challenge in cells internally perfused with solutions containing a low $[Ca^{2+}]_i$ of 10^{-8} M. However, these solutions contained either a weak or strong Ca^{2+} buffering capacity consisting of the presence of 2 mM or 8 mM EGTA, respectively. The graph also depicts the effect of the same hyposmotic challenge on the time-course of volume changes of cells perfused with 2 mM EGTA plus 1mM Rp-cAMPS. The figure shows that exposure to an identical hyposmotic challenge produced similar swellings in all cells regardless of the composition of the perfusate solution. However, the cells perfused with 2 mM EGTA underwent a significant RVD which reached 61% of the swollen volume after 150 min of the hyposmotic challenge. In contrast, the cells perfused with 8 mM EGTA remained swollen during the entire time of exposure to the hyposmotic challenge. Furthermore, presence of Rp-cAMPS completely prevented the RVD otherwise observed in cells perfused with 2 mM EGTA. These results demonstrated that hyposmotic swelling only promotes RVD in weakly $Ca^{2+}{}_i$ –buffered cells and that inhibition of protein kinase A (due to the presence of Rp-

cAMPS) activity precludes RVD in these weakly Ca_i-buffered cells. Thus, these results led to the formulation of the hypothesis that the sequence of events linking Ca^{2+} and volume reduction under isosmotic and hyposmotic conditions is an increase in $[Ca^{2+}]_i$ leading to the synthesis of cAMP which induces in turn the loss of osmolytes accompanied by water.

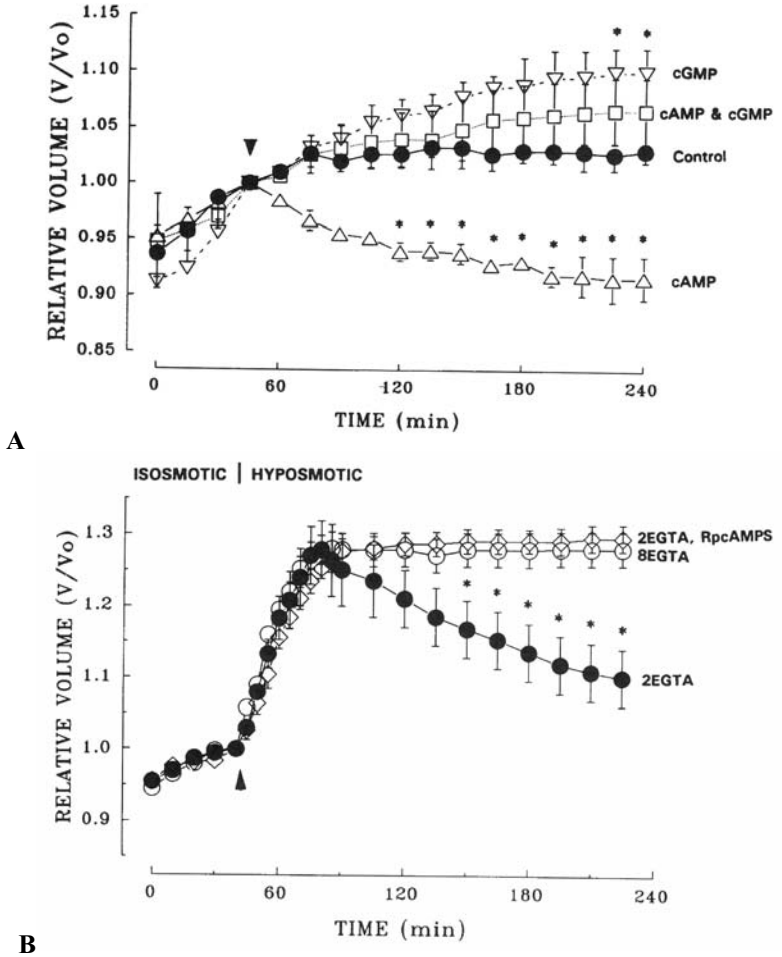

Figure 7. A. Time-course of the effect of intracellular perfusion with control perfusate or media containing various cyclic nucleotides on cell volume in barnacle muscle cells exposed to the absence of Ca_o. At arrowhead, internal perfusion was switched to fresh perfusates. These solutions consisted of same control perfusate (●, n = 3) or control perfusate containing 1mM cAMP (Δ, n = 4), 1mM cAMP plus 1mM cGMP (□, n = 5), or 1mM cGMP (▽, n = 5). Data from control perfusate (absence of cyclic nucleotides) and from media containing either cAMP or cGMP are significantly different. (*, $P < 0.05$). **B.** Time-course of effect of $[Ca^{2+}]_i$-buffering and 1mM [*R*]-*p*-adenosine 3', 5'-cyclic monophospho-thioate (*R*p-cAMP[S]) on cell volume response to a hyposmotic challenge (550 mosmol/kgH_2O) in internally per-fused barnacle muscle cells. Data points represent average ± SE of relative volume of 5 control cells perfused with a solution containing 8mM EGTA (O), 4 cells perfused with 2mM EGTA (●) and 5 cells perfused with 2 mM EGTA plus 1 mM *R*p-cAMP[S] (◊). At arrowhead, isosmotic solution was replaced with hyposmotic one. Cells perfused with 2mM EGTA underwent a significant (*) volume reduction (RVD) in response to hyposmotic challenge with respect to cells perfused with 8 mM EGTA or with 2 mM EGTA and 1 mM *R*p-cAMP[S], $P < 0.05$. External solution contained normal 11 mM Ca^{2+} (reproduced from Pena-Rasgado et al.,[18] with permission).

An important corollary of the aforementioned hypothesis linking $[Ca^{2+}]_i$, cAMP and cell volume is that under both isosmotic and hyposmotic conditions, the increase in $[Ca^{2+}]_i$ should promote synthesis of cAMP. In addition, if cGMP is also physiologically involved in volume regulation (Figure 7A), the intracellular levels of this cyclic nucleotide should also increase during volume regulation, perhaps later than those of cAMP. To test this hypothe-sis, the intracellular levels of cAMP and cGMP were measured under well-established con-ditions known to produce volume reduction under isosmotic and hyposmotic environments. The experimental protocol consisted of measuring the intracellular nucleotide levels (using radioimmunoassays) in cells separated from each other but left attached to the carapace. Cells were initially exposed for 1 h to isosmotic conditions either in the absence or presence of Ca_o and were subsequently challenged hyposmotically for 3 additional hrs. Every 20 min, cells were cut from the bundle and analyzed for their cAMP or cGMP levels.

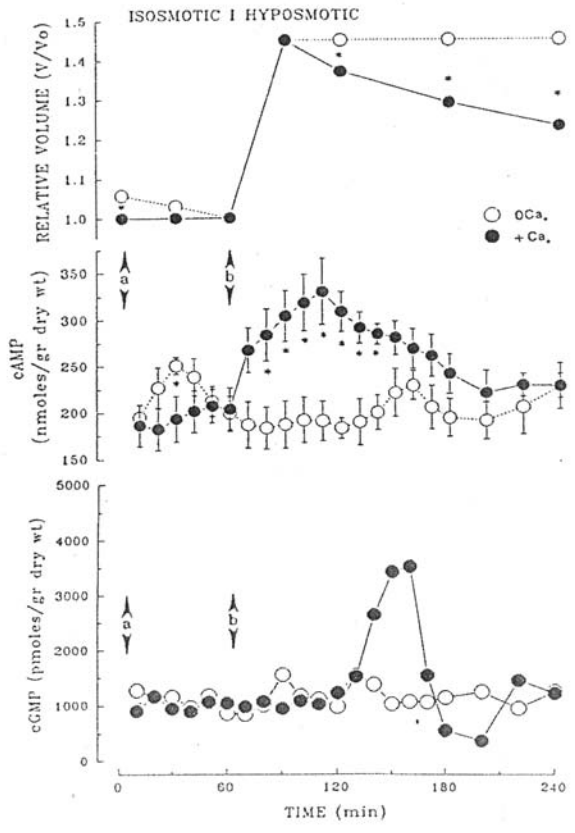

Figure 8. Time-course of the effect of the presence or absence of Ca_o under isosmotic or hyposmotic conditions on the intracellular levels of cAMP and cGMP of intact barnacle muscle cells attached to the carapace. All cells were initially exposed to the standard isosmotic seawater solution containing 11 mM Ca^{2+}. At time zero in the graph (a), groups of cells were exposed to Ca_o-free conditions ( ) while other groups were left in Ca_o-containing solutions (●). Top panel, relative volume changes of 90 control (O) and 120 experimental (●) cells. Middle panel, average cAMP levels (nmoles/mg dry wt) of six cells. Bottom panel, cGMP levels (in pmoles/mg dry wt) of six cells. At 60 min of incubation, the cells were exposed to the hyposmotic solution (500 mosm/kg; at b).

Figure 8 shows simultaneous measurements of the intracellular levels of cAMP, cGMP and cell volume in response to exposure to isosmotic and hyposmotic conditions in the absence and presence of Ca_o. All cells were initially exposed to the standard isosmotic seawater solution containing Ca^{2+}. At time zero, groups of cells were exposed to Ca_o-free conditions while other groups were left in Ca_o-containing solutions. The middle panel shows the average cAMP levels of six cells; the bottom panel shows the cGMP levels (in pmoles/mg dry wt) of six cells; the top panel shows the relative volume changes of 90 control and 120 experimental cells. At 60 min of incubation, the cells were exposed to the hyposmotic solution. The figure shows that removal of Ca_o at time zero produced a small but significant ($p<0.05$) transient increase in cAMP accompanied by a significant cell volume reduction. Further, cell swelling in response to exposure to hyposmotic conditions in the presence of Ca_o, but not in its absence, induced a larger and transient increase in cAMP. This increase was followed by a significant reduction in cell volume (RVD). Finally, it should be noted that the basal levels of cGMP are about two orders of magnitude smaller than those of cAMP. The levels of cGMP did not appear to increase in response to isosmotic replacement of Ca_o. However, cGMP levels increased in response to cell swelling providing Ca_o was present, i.e., presence of RVD. Interestingly, the increase in cGMP occurred later in time than the increase in cAMP, a result consistent with the hypothesis that cGMP may serve the purpose of turning off RVD.

In sum, these results demonstrated that under both isosmotic (in response to Ca_o removal) and hyposmotic conditions (in the presence of Ca_o), volume reduction is accompanied by an increase in the intracellular levels of cAMP. The results also showed that levels of cGMP increase during RVD, but this increase occurs after the increase in cAMP.

3.8. Nature of the Sensor that Detects Cell Volume Increases

RVD occurs because of the existence of a feedback loop containing at least two functional elements: a sensor that detects the volume increase and a sensor-activated effector responsible for restoring the original volume. Although effector mechanisms for volume regu-lation have been extensively studied, little is known about how changes in volume are de-tected by cells. There are two major hypotheses. One proposes that the volume signal arises from mechanical events such as bending or stretching of the membrane or rearrangement of structures within the cell.[44-47] Another postulates that volume changes are sensed by changes in concentration of some cell component such as water, salt, or cytoplasmic protein pool.[48, 49]

Barnacle muscle cells offer the remarkable possibility of dissecting the role of each of the postulated volume sensors independently of the others. Using internally perfused cells, it is feasible to modify membrane stretch, intracellular ionic strength or intracellular macromolecular crowding while maintaining the other two parameters as well as V_m constant.

3.8.1. Mechanical Membrane Deformation

Support for the hypothesis of mechanical deformation as volume sensor is provided by the widespread presence of mechano-sensitive membrane channels in prokaryotes and eukaryotes.[45, 50, 51] These channels respond to negative or positive pressure as well as cell swelling by altering their conductance to cations or anions.[51-53] Recently, these channels have been cloned,[54] reconstituted, and their molecular mechanisms of activation are beginning to be

uncovered.[55, 56] However, in spite of the aforementioned arguments, some critical observations argue against the role of mechanical deformation as a volume sensor in numerous cells. Among these is the fact that membrane deformations induced by amphiphilic reagents in rabbit erythrocyte membranes have no effect on K^+-Cl^- cotransport.[57] Similarly, in human erythrocytes, swelling-induced transport pathways are activated at much lower degrees of cell swelling (1.05-1.1 times normal volume) than those necessary to make the cells spherical and therefore produce membrane stretch (1.6 times normal volume).[58] Further-more, when the tonicity of the medium which bathes rabbit proximal tubules is gradually reduced, there is no detectable volume change but the cells adapt to the hypotonicity by ex-truding solute. Thus, cells can activate transport pathways despite the absence of swelling.[59]

A preliminary report using internally perfused barnacle muscle cells[60] indicates that under conditions of constant osmolality (1000 mOsm/kg), ionic strength, and intracellular macromolecular concentration, an increase in cell volume of 50% resulting from increasing the intracellular hydrostatic pressure to 18 mm of H_2O did not induce volume reduction. This suggests that membrane stretch *per se* does not act as a volume sensor in these cells. However, this result does not rule out the possibility that membrane stretch, acting synergistically with other changes in the cellular properties accompanying cell swelling, e.g., a reduction in macromolecular crowding, could behave as a volume sensor.

3.8.2. Intracellular Ionic Strength

Support for the ionic strength hypothesis as a volume sensor is provided by observations in several cell types including trout red cells.[48] In these cells, swelling can be produced by exposing the cells to hypotonicity or to an isotonic medium containing catecholamines, NH_4Cl, or urea. Interestingly, swelling induced in response to either condition activates transport mechanisms leading to cell shrinking, but the nature of these mechanisms depends on the intracellular ionic strength changes that result from the swelling rather than on the increase in cell volume *per se*. For example, swelling may be caused by an increase in intracellular ionic strength. This occurs when trout erythrocytes are exposed to catecholamines because this manipulation leads to an increase in the intracellular Na^+ concentration via activation of the Na/H exchanger. Similarly, when these cells are exposed to NH_4Cl, there is a subsequent increase in intracellular NH_4Cl. In both cases, the activated RVD pathway consists of an intracellular Cl^- (Cl_i)-dependent K^+ efflux which is not accompanied by the efflux of the osmolyte taurine. Conversely, when swelling induces a reduction in ionic strength, as when the erythrocytes are exposed to isotonic urea (due to urea and water influx) or when they are exposed to hypotonicity, the transport pathway activated consists of a Cl_i-dependent, K^+ efflux accompanied by taurine. Thus, ionic strength appears to be the swelling sensor that determines which volume re-establishing transport pathway is activated. However, this does not appear to be true for dog erythrocytes, because the transport pathway which is activated is the same whether their volume is altered by changing the ionic strength of the external medium or by keeping external ionic strength constant and varying internal solute content.[61]

To test whether ionic strength plays a volume sensing role in barnacle muscle, the effect of reduction in the ionic strength (from a normal value of 278.6 mM to 62.6 mM) was tested in cells internally perfused under conditions of constant membrane stretch (see 2. Methods), intra- and extracellular osmolality and the concentration of intracellular macromolecules.

The reduction in ionic strength was attained by isosmotically replacing the salts of Na^+ and K^+ in the perfusate with sucrose.

Figure 9 shows the time-course of the effect on cell volume and V_M of isosmotically reducing the intracellular ionic strength in internally perfused cells. The figure shows that after 90 minutes of pre-incubation with the perfusate containing the high ionic strength, the cell volume and V_M had reached steady values. At this point in the experiment, cells were separated into a control and an experimental group. The control cells were continuously perfused with the high ionic strength solution. The average cell volume and V_M of these control cells are depicted in the graph as a discontinuous line. The experimental cells were subjected to a reduction of the intracellular ionic strength which produced a significant ($p<0.05$) volume reduction and membrane depolarization which, respectively, reached values of 15% and 15 mV, after 240 min of incubation. This result clearly shows that reduction in ionic strength, under conditions in which the other postulated volume sensors are maintained constant, produces a volume reduction. However, this effect could be due either to the reduction in the ionic strength *per se*, the membrane depolarization accompanying the reduction in ionic strength, or a combination of both factors.

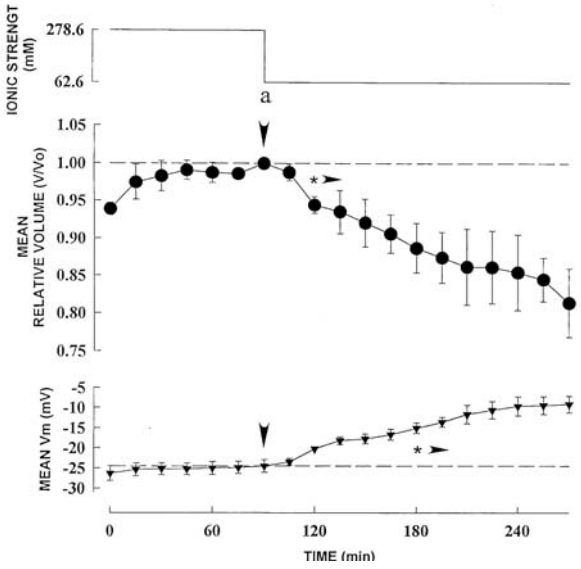

Figure 9. Time-course of the effect of isotonically reducing the intracellular ionic strength from 278.6 to 62.6 mM (top panel) on cell volume (middle panel) and membrane potential (bottom panel, V_M) in internally perfused barnacle muscle cells (n=3). V/V_o, ratio of cell volume (± SEM) measured at time indicated (arrowhead) to volume obtained before intracellular IS was reduced (V_0, at 90 min of incubation indicated by "a"). Dashed lines, average relative volume (*top, SE,* ± 0.01) and V_M (*bottom*, SE, ± 1 mV) of control cells (n=6) that were continuously perfused with the standard perfusate (IS=278.6 mM). Time that relative volume and/or V_M became significantly different from controls is indicated by asterisk and rightward arrowhead.

To dissect the relative roles of V_M and of the reduction in ionic strength on effecting cell volume reduction, experiments were performed in which V_M was controlled. Figure 10 A

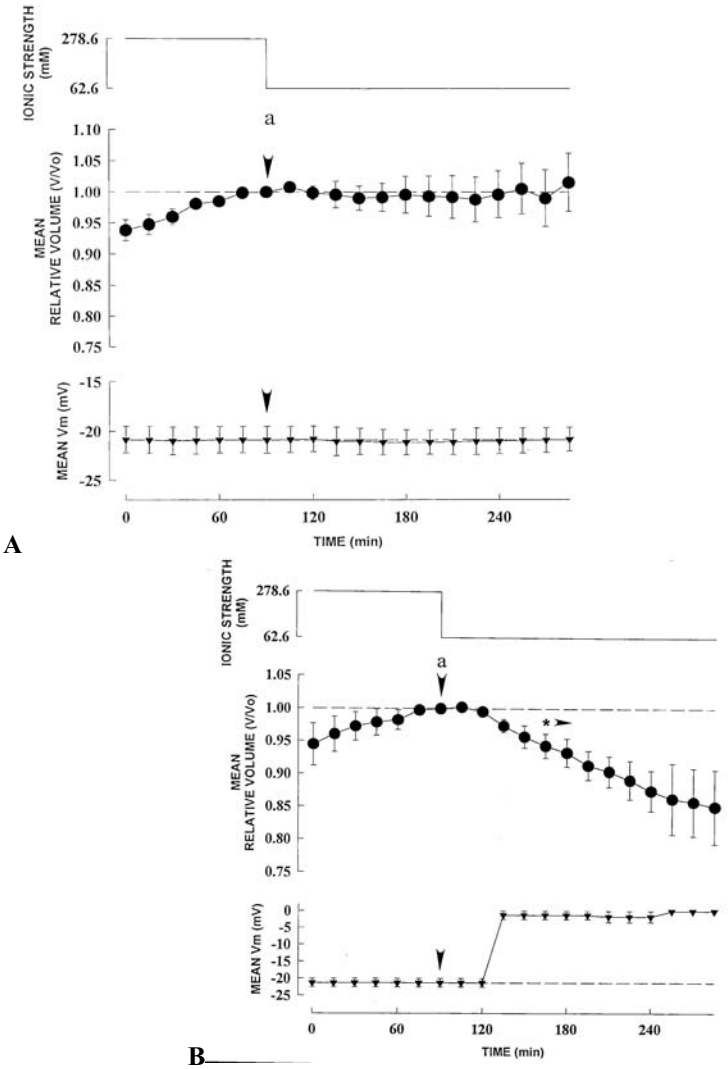

Figure 10. A. Time-course of the effect of isotonically reducing the intracellular ionic strength (IS, top) and of membrane potential (V_M, bottom) on mean relative cell volume (middle) of internally perfused, voltage-clamped barnacle muscle cells. At 90 min of incubation, the IS was reduced from 278.6 to 62.6 mM (at **a)** while V_M was maintained constant at -22 ± 1.0 mV. This manipulation did not induce a significant change in the mean relative volume (V/V_o) of the cells. The symbols (●,▼) represent the means ± SE of 6 independent experiments. Dashed lines, average volume (middle panel; SE, ± 0.01) and V_M (bottom panel; SE, ± 0.5 mV) of control cells (n=6) continuously perfused with the standard solution containing 278.6 mM IS. **B.** Time-course of effect of isotonically reducing intracellular ionic strength from 278.6 to 62.6 mM at 90 min incubation and of depolarizing V_M (bottom,▼) on cell volume (middle,●). All cells originally voltage-clamped at -22 mV. At 120 min incubation, V_M of mean relative experimental cells (n=4) was depolar-ized to 0 mV. Dashed lines, average volume (middle; SE, ± 0.01) and V_M of control cells (n=6) whose V_M was maintained at -22 ± 1 mV and continuously perfused with the standard solution containing 278.6 mM IS. Time-relative volume became significantly different from controls is indicated by * and rightward arrowhead.

depicts an experiment in which the experimental cells were subjected to the identical reduce-tion in ionic strength as described in Figure 9, but the membrane depolarization was prevented via voltage-clamping. The graph demonstrates that blockage of the membrane depolarization completely inhibited the otherwise observed volume reduction upon reduction of the ionic strength. Further evidence for the role of membrane depolarization as the actual factor inducing the volume reduction is provided in Figure 10B. The exper-imental protocol was identical to that used for Figure 10A except that after 30 minutes of the reduction in the ionic strength the experimental cells were depolarized from -20 to 0 mV. As expected, the graph illustrates that reduction of the ionic strength did not affect the volume under voltage clamp conditions, but depolarization was immediately followed by a significant volume reduction which reached a value of 15 % at 240 min of incubation.

Interpretation of the above results led to formulation of the following hypothesis: reduction in ionic strength produces a membrane depolarization due to diminution in the concentration of intracellular K^+.[25] This membrane depolarization activates a verapamil-sensitive Ca^{2+} influx pathway which in turn induces loss of intracellular osmolytes, water, and cell volume. A critical test of this hypothesis consisted of assessing whether inhibition of the Ca^{2+} influx pathway could inhibit the depolarization-induced volume reduction.

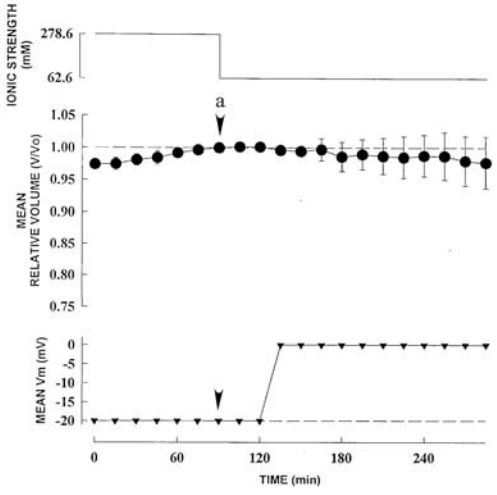

Figure 11. Time-course of effect of V_M, verapamil (0.1 mM) and of isotonically reducing the intracellular ionic strength (top) from 278.6 to 62.6 mM (at 90 min incubation, at **a**) on the average relative cell volume (V/V_o, middle) in internally perfused, voltage-clamped barnacle muscle cells. Symbols (●,) represent the means ± SE of 3 independent experiments. Dashed lines, average volume (SE, ± 0.01) and V_M (SE, ± 0.5 mV) of control cells (n=6) continuously perfused with standard solution containing 278.6 mM IS. All cells were originally voltage-clamped at -20 mV. Control and experimental cells were exposed to 0.1 mM verapamil 30 min prior to time 0 in the graph. At 120 min incubation, V_M of experimental cells was depolarized to 0 mV.

Figure 11 shows the time-course of the effect of a reduction in ionic strength and membrane depolarization on the volume of cells continuously exposed to 0.1 mM of the Ca^{2+} channel blocker verapamil. The graph shows that, similar to Figure 10B, reduction in

ionic strength did not affect cell volume under voltage-clamp conditions, but in the presence of verapamil, membrane depolarization was not followed by the previously observed volume reduction.

In sum, the experimental results demonstrate that, at least in barnacle muscle cells, a reduction in ionic strength does not play a major volume sensor role. Care must be taken in interpreting the volume-sensing role of ionic strength in other cells. The possible role of changes in V_M accompanying the reduction in ionic strength should be prudently considered.

3.8.3 Intracellular Macromolecular Crowding

An alternative hypothesis for the putative volume sensor is the changes in intracellular macromolecular crowding.[62-64] It postulates that small, localized changes in cell volume can greatly modify the concentration of ambient, inert macromolecules. This effect can signify-cantly alter the thermodynamic activity of enzymes, therefore affecting their kinetics and equilibria. If these enzymes regulate plasmalemmal osmolyte transporters, channels and/or pumps, cell volume changes lead to modification in the net transport of osmolytes that pro-duce cell volume modification or recovery. A quantitative model has been developed which predicts how small dilutions of total cytosolic protein resulting from swelling can exert nonspecific effects of the required magnitude to affect osmolyte transport rates.[63] This model also predicts that the effectiveness of a macromolecule to produce crowding is related to its molecular weight. At similar concentrations, macromolecules with larger molecular weights are more efficient in producing crowding as compared to molecules of smaller molecular weight. Likewise, the model successfully postulates how changes in reaction rates are explained by changes in intracellular protein concentration.

To test whether macromolecular crowding plays a volume-sensing role in barnacle mus-cle cells, an experimental strategy was developed consisting of testing the effect of modify-ing the concentration of intracellular inert macromolecules (polymers) on the volume of internally perfused cells in which the intracellular and extracellular osmolalities, membrane stretch, ionic strength and V_M were maintained constant.[19] The following five major predictions of the macromolecular crowding theory were tested: 1) Intracellular isotonic replacement of large and inert macromolecules (polymers and albumin) by sucrose should produce volume reduction; 2) there should be a minimal effective size of the macromole-cules to produce the expected crowding effect; 3) there should also be a minimal concen-tration for large enough macromolecules to produce the crowding effect; 4) even very large concentrations of small macromolecules should not produce the crowding effect; and 5) reductions in the concentration of large enough macromolecules should produce proportional reductions in volume. The experimental results demonstrated that all the predictions were met.[19]

Figure 12A[19] shows the time-course of the effect on cell volume of isotonically replacing various intracellular concentrations of the polymer polyvinyl pyrrolidone (40 KDa, PVP-40K) by sucrose. Cells were originally perfused for 90 minutes (before time 0 in the graph) with either 36, 31, 27, 18, or 10 mg/ml of PVP-40K. For the duration of the experiment, control cells were perfused with 36 mg/ml PVP-40K, and their average volume is depicted in the graph as a discontinuous line. With the exception of the cells originally perfused with 10 mg/ml PVP-40K, the graph illustrates that the volume of all the other cell groups diminished with time in response to replacing PVP-40K with sucrose. This volume

reduction reached steady values after 165 min of the replacement of the perfusate, and these values were proportional to the original concentration of the polymer present prior to its removal. With the exception of the comparison between the volume of the control and the 10 mg/ml group, statistical analysis revealed all the other groups were significantly ($p<0.05$) different than the control cells. This result strongly supports the role of macromolecular crowding as a volume sensor in barnacle muscle cells.

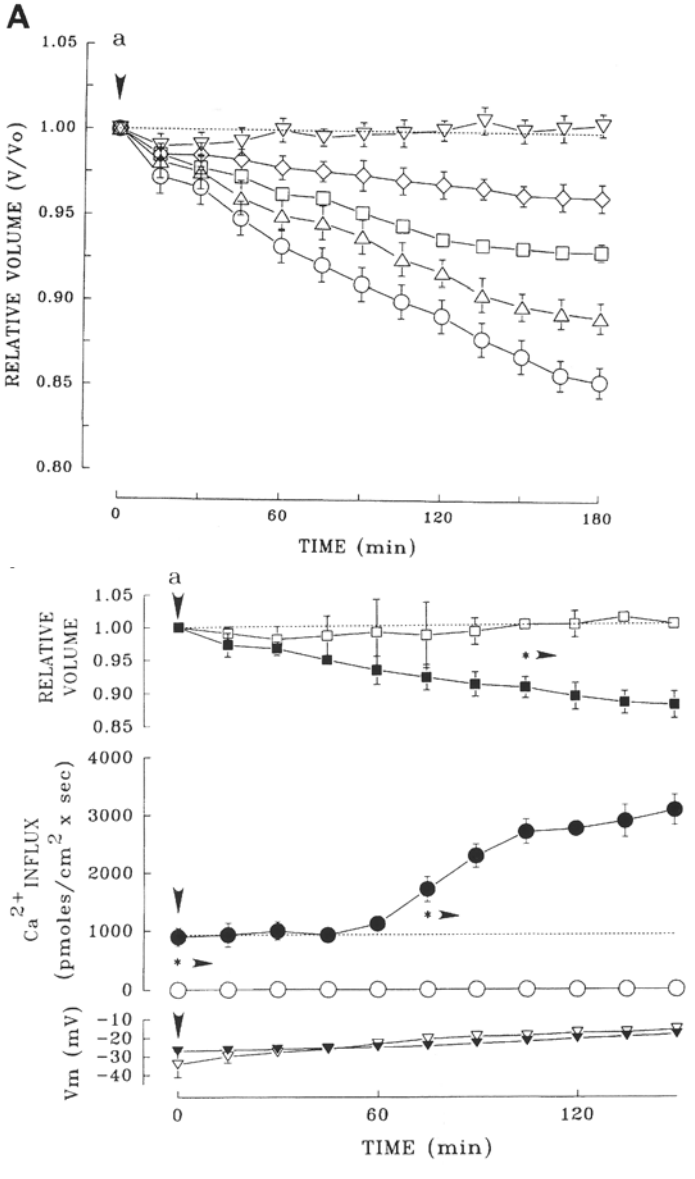

Figure 12 A. Time-course of effect of isotonically replacing (at time 0, AT"a" and down arrow) vari-ous intracellular concentrations of polymers by sucrose on cell volume in internally perfused barnacle muscle cells. At "a", either 36 (n = 6; ○), 31 (n = 5; △), 27 (n = 5; ف), 18 (n = 4; ◇) or 10 (n = 10; ▽) mg/ml poly-vinyl

pyrrolidone-40K (PVP-40K) were isotonically replaced by sucrose. Dashed line, average relative volume (SE, ±0.01) of control cells (n = 6) continuously exposed to 0.036 g/ml PVP-40K. (Reproduced from Summers et al.,[19] with permission.) **12B.** Time-course of effect of isotonically replacing 0.036 g/ml PVP-40K by sucrose (at time 0, at "a") on relative cell volume (V/V_o, top (□;■)), Ca^{2+} uptake (in pmoles x cm^{-2} x sec, middle(○;●)) and V_M (bottom(▽;▼)) in cells exposed to presence of extracellular Ca^{2+} (Ca_o^{2+}), Na^+ seawater in presence of 0.01 mM Ca_o^{2+} (n = 3; open symbols) or 11 mM Ca_o^{2+} (n = 5; closed symbols). Cells exposed to 0.01 mM Ca_o^{2+} were pre-equilibrated for 30 min under this condition before intracellular perfusion began (120 min before time 0). Dashed lines, average relative volume (top; SE, ±0.01) and Ca^{2+} influx (middle; SE, ±150 $pmol \cdot cm^{-2} \cdot s^{-1}$) of control cells (*n* = 6) continuously exposed to 0.036 mg/ml PVP-40K in presence of 11 mM Ca_o^{2+}. Times at which relative volume and Ca^{2+} influx became significantly different from controls are indicated by * and right arrowheads (reproduced from Summers et al.,[19] with permission).

A critical additional prediction of macromolecular crowding as a volume sensor in barnacle muscle cells is that an isotonic reduction of a large enough macromolecule at a large enough concentration should produce activation of a verapamil-sensitive Ca^{2+} influx pathway leading to cell volume reduction. To test this hypothesis, cells were internally perfused and exposed to the presence of normal (11 mM) or very low (0.01 mM) extracellular Ca^{2+}. To measure Ca^{2+} uptake, ^{45}Ca was added to the superfusion solution. The appearance of ^{45}Ca in the intracellular fluid was determined by collecting aliquots of the perfusion fluid every 15 min as it emerged from the cannula at the basal end of the cell.

Figure 12 B[19] shows the time-course of the effect on cell volume, Ca^{2+} uptake and V_M of isotonically replacing PVP-40K by sucrose. Control cells were continuously perfused with PVP-40K in the presence of 11 mM Ca_o. Following 90 min of pre-incubation, at time 0 in the graph, PVP-40K was replaced by sucrose. In the presence of low Ca_o, this manipulation affected neither the influx of Ca^{2+} nor the relative cell volume. In contrast, in the presence of 11 mM Ca_o, replacement of PVP-40K by sucrose induced a significant increase in Ca^{2+} influx and a cell volume reduction with respect to control cells. In additional experiments[19] presence of 0.1 mM verapamil completely blocked the volume reduction otherwise observed upon isosmotic replacement of PVP-40K by sucrose. These results demonstrate that reduction in macromolecular crowding activates a Ca^{2+} influx pathway which leads to cell volume reduction. In addition, presence of 0.1mM verapamil completely abolishes the cell volume reduction otherwise observed upon isotonically replacing PVP-40K by sucrose. [19] These results support the role of macromolecular crowding as sensor of volume changes in barnacle muscle cells.

4. SUMMARY AND FUTURE WORK

Figure 13 depicts a diagram summarizing the working hypothesis herein reviewed. It postulates how osmotic swelling is sensed by barnacle muscle cells as well as how RVD is effected. Exposure to hypotonicity (a) induces a net influx of water into the cell driven by its chemical gradient (b). The entrance of water produces two main effects: 1) dilution of intracellular macromolecules (c) leading to activation of a Ca^{2+} influx pathway (d) which can be inhibited by verapamil (e); and 2) dilution of intracellular $[K^+]$ which in turn produces membrane depolarization (f) leading to activation of Ca^{2+} release from the sarcoplasmic reticulum (SR; h). A possible direct role of cytosolic Ca^{2+} in inducing SR Ca^{2+} release cannot be discarded at present. The increase in $[Ca^{2+}]_i$, resulting from either the influx of Ca^{2+} and/or

SR Ca^{2+} release (g), induce the synthesis of cAMP (i). This nucleotide activates a pathway through which the osmolytes K^+, Na^+ and glycine exit the cell (j) following their electrochemical gradients. The combination of cell swelling and the increase in $[Ca^{2+}]_i$ (or the synthesis of cAMP) simultaneously activates a K^+/OH or OH^-/Cl^- exchanger (k). The osmotically obligated efflux of water following the net loss of intracellular osmolytes produces volume recovery.

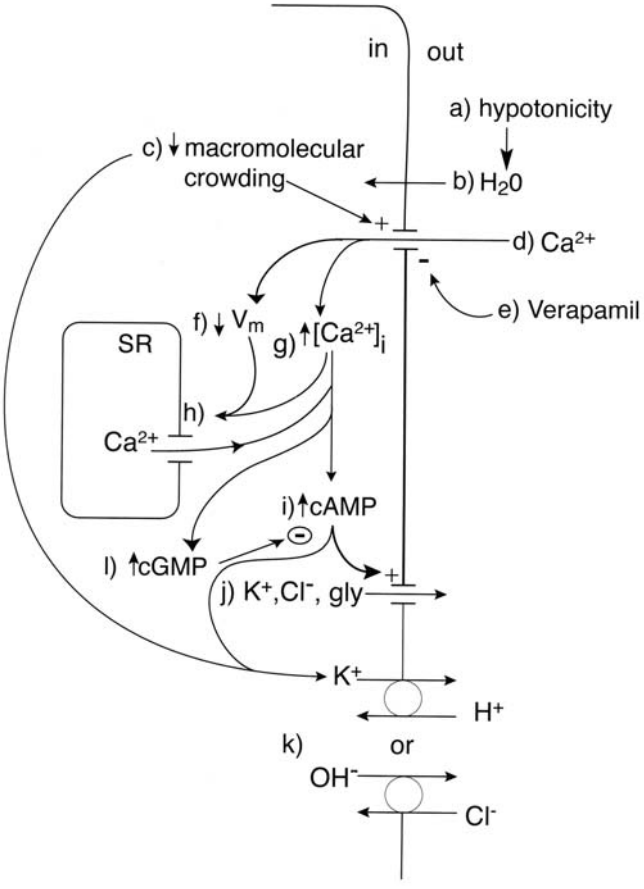

Figure 13. Diagram illustrating summary of experimental results and proposed mechanisms presented and discussed in this review. "+" and "-" indicate activation and inhibition, respectively. The sequence of events is indicated by the lower case letters followed by the right-facing parenthesis. SR is sarcoplasmic reticulum; see text for details.

The aforementioned hypothesis raises numerous questions that must be addressed: 1) What are the mechanisms by which a reduction in macromolecular crowding activates the Ca^{2+} influx pathway? 2) To what extent does SR Ca^{2+} release and Ca^{2+} influx contribute to synthesis of cAMP? 3) How is it that increase in $[Ca^{2+}]_i$ activates synthesis of cAMP? 4)

Which mechanism is responsible for activating the synthesis of cGMP later than cAMP; is it the increase in $[Ca^{2+}]_i$ or cAMP? 4) How does cAMP activate the efflux pathway for K^+, Cl^- and glycine? 5) By which mechanism does cGMP inhibit the action of cAMP in promoting the loss of osmolytes? and 6) How is the K^+/OH or OH^-/Cl^- exchanger activated and what physiological role does it play? Current work is aimed at answering these questions. Further-more, perhaps the most physiologically relevant work is yet to be undertaken. Barnacle muscle cells undergo cell volume and shape changes during isometric contraction, and these changes significantly affect their contractile ability.[7] The physiological relevance of these studies may include the key to deciphering the as yet poorly understood phenomena of mus-cle fatigue. Study of the underlying mechanisms linking muscle contraction and cell volume changes is just beginning. The authors suggest that the use of barnacle muscle cells will prove very helpful in elucidating these very relevant physiological questions.

5. ACKNOWLEDGMENTS

The authors are indebted to Dr. Seymour Ehrenpreis for critical reading of the manuscript. This work was supported by an American Heart Association (Midwest Consortium) Grant-in-Aid (to H.R-F).

6. REFERENCES

1. M. Ando and W.L. Nyhan, *Heritable Disorders of Aminoacid Metabolism*, New York: Wiley (1974).
2. A.R. Gosmanov, M.I. Lindinger and D.B. Thomason, Riding the Tides:K^+ concentration and volume regulation by muscle Na^+-K^+-$2Cl^-$ cotransport activity, *NIPS* **18**, 196-200 (2003).
3. A.R. Gosmanov, E.G. Schneider and D.B. Thomason, NKCC activity restores muscle water during hyperosmotic challenge independent of insulin, ERK, and p38 MAPK, *Am J Physiol Regul Integr Comp Physiol* **284**, R655-R665 (2003).
4. B.C. Abbott and R.J. Baskin, Volume changes in frog muscle during contraction, *J Physiol* (Lond) **161**, 379-391 (1962).
5. R.J. Baskin and P.J. Paolini, Muscle volume changes, *J Gen Physiol,* **49**, 387-404 (1966).
6. R.S. Taylor, I.R. Neering, L.A. Quesenberry and V.A. Morris, Volume changes during contraction of isolated frog muscle fibers, In: Excitation-Contraction Coupling in *Skeletal, Cardiac and Smooth Muscle*, edited by G.B. Frank, New York: Plenum Press, 91-101 (1992).
7. J. Theobald, S.R. Taylor, J.P.R. Orgel, T.C. Irving, H. Gonzalez-Serratos, C. Pena-Rasgado, M. Gamboa, and H. Rasgado-Flores, Preferential regional contraction in barnacle muscle cells may be due to local structural variations, *FASEB J.* **18,** A749 (2004).
8. W. Lu, C. Pena-Rasgado, S. Markowitz and H. Rasgado-Flores, Inhibition of regulatory volume decrease by lithium in barnacle muscle cells, *FASEB J* **10**, A388 (1996).
9. S. Markowitz, C. Peña-Rasgado, J.C. Summers, D. Zlatnik and H. Rasgado-Flores, Relationship between cAMP levels and volume reduction in barnacle muscle cells, *Biophys J* **70**, A348 (1996).
10. C. Peña-Rasgado, S.K. Pierce and H. Rasgado-Flores, Osmolytes responsible for volume reduction under isosmotic or hyposmotic conditions in barnacle muscle cells, *Cell Mol Biology* **47**, 841-853 (2001).
11. D.M. Berman, C. Peña-Rasgado, M. Holmgren, P. Hawkins and H. Rasgado-Flores, External Ca effect on water permeability, regulatory volume decrease and extracellular space in barnacle muscle cells, *Am J Physiol* **265**(Cell Physiol.34) C1128-C1137 (1993).
12. C. Peña-Rasgado, K.D. McGruder, J.C. Summers and H. Rasgado-Flores, Effect of isosmotic removal of extracellular Ca and of membrane potential on cell volume in muscle cells, *Am J Physiol* **267** (Cell Physiol 36) C768-C775 (1994).
13. C. Peña-Rasgado, J.C. Summers, K.D. McGruder, J. deSantiago and H. Rasgado-Flores, Effect of isosmotic

removal of extracellular Na on cell volume and membrane potential in muscle cells, *Am J Physiol* **267** (Cell Physiol 36) C759-C767 (1994).
14. H. Rasgado-Flores, E.M. Santiago and M.P. Blaustein, Kinetics and stoichiometry of coupled Na efflux and Ca influx (Na/Ca exchange) in barnacle muscle cells, *J Gen Physiol* **93**, 1219-1241 (1989).
15. D.C. Ferguson, K.D. McGruder, C. Peña-Rasgado and H. Rasgado-Flores, Isosmotic intracellular Ca-dependent volume loss and KCl efflux in internally perfused barnacle muscle cells, *Biophys J,* **68,** A43 (1995).
16. K.D. McGruder, C. Peña-Rasgado and H. Rasgado-Flores H, Characterization of glycine efflux and volume reduction in barnacle muscle cells, *FASEB J **10,*** A388 (1996).
17. J.B. Bitner, C. Peña-Rasgado, J. Ruiz, J. Cardona and H. Rasgado-Flores, Osmotic properties of internally perfused barnacle muscle cells, I. Isosmotic Conditions, *Cell Mol Biology* **47**, 855-864 (2001).
18. C. Peña-Rasgado, V.A. Kimler, K.D. McGruder, J. Tie and H. Rasgado-Flores, Opposite roles of cAMP and cGMP on volume decrease in muscle cells, *Am J Physiol* **267** (Cell Physiol 36) C-1319-C-1328 (1994).
19. J.C. Summers, L. Trais, R. Lajvardi, D. Hergan, R. Buechler, H. Chang, C.Peña-Rasgado and H. Rasgado-Flores, Role of concentration and size of intracellular macromolecules in cell volume regulation, *Am J Physiol* (Cell Physiol) **42**, C360-C370 (1999).
20. D.A.T. Dick, Structure and properties of water in the cell, In: *Mechanisms of Osmoregulation in Animals,* edited by R. Gilles, New York: John Wiley & Sons, 3-45 (1979).
21. D.A.T. Dick, The permeability coefficient of water in the cell membrane and the diffusion coefficient in the cell interior, *J Theor Biol* **7**, 504-531(1964).
22. N.K. Jorgensen, S. Christensen, H. Harbak, A.M. Brown, I.H. Lambert, E.K. Hoffman and L.O. Simonsen, On the role of calcium in the regulatory volume decrease (RVD) response in Ehrlich mouse ascites tumor cells, *J Membr Biol* **157**(3), 281-299 (1997).
23. M. Weskamp, W. Seidl and S. Grissmer, Characterization of the increase in $[Ca^{2+}]_i$ during hypotonic shock and the involvement of Ca^{2+}-activated K^+ channels in the regulatory volume decrease in human osteoblast-like cells, *J Membr Biol* **178**, 11-20 (2000).
24. H. Xie and E.E. Bittar, Nicardipine as a Ca channel blocker in single barnacle muscle fibers, *Biochim Biophys Acta* **1014**, 207-209 (1989).
25. D.M. Berman, C. Peña-Rasgado and H. Rasgado-Flores, Changes in membrane potential associated with cell swelling and regulatory volume decrease in barnacle muscle cells, *J Exp Zool* **268**, 97-103 (1994).
26. H. Gonzalez-Serratos, G. Inesi and A. Ortega, Effects of D-600 on isolated fibres and isolated sarcoplasmic reticulum of frog skeletal muscle, *J Physiol* (Lond) **418**,119P, (1989).
27. L.M. Amende and S.K. Pierce, Free amino acid mediated volume regulation of isolated Noetia ponderosa red blood cells: control by Ca^{2+} and ATP, *J Comp Physiol* **138**, 291-298 (1980).
28. M.E. Clark, The osmotic role of amino acids: discovery and function, In: *Transport Processes, Iono- and Osmoregulation*, edited by R. Gilles and M. Gilles-Baillien, Berlin:Springer-Verlag, 412-423 (1985).
29. P.M. Cala, Volume regulation by amphiuma red blood cells: The membrane potential and its implications regarding the nature of the ion-flux pathways, *J Gen Physiol* **76**, 683-708 (1980).
30. H. Guizouarn, B.J. Harvey, F. Borgese, N. Gabillat, F. Garcia-Romeu and R. Motais, Volume-activated Cl-independent and Cl-dependent K pathways in trout red blood cells, *J Physiol* (Lond) **462**, 609-626 (1993).
31. P.A. Watson, Function follows form: generation of intracellular signals by cell deformation, *FASEB J* **5**, 2013-2019 (1991).
32. H.E. Morgan, X.P. Xenophontos, T. Haneda, S. McGlaughlin and P.A. Watson, Stretch-anabolism transduction, *J Appl Cardiol* **4**, 415-422 (1989).
33. P.A. Watson, Direct stimulation of adenylate cyclase by mechanical forces in S49 mouse lympoma cells during hyposmotic swelling, *J Biol Chem* **265**, 6569-6575 (1990).
34. S. vom Dahl, C. Hallbrucker, F. Lang and D. Häussinger, Regulation of cell volume in the perfused rat liver by hormones, *Biochem J* **280**, 105-109 (1991).
35. A. Salama and M. Nikinmaa, Effect of oxygen tension on catecholamine-induced formation of cAMP and on swelling of carp red blood cells, *Am J Physiol Cell Physiol* **259**, C723-C726 (1990).
36. S.R. Bolsover, SH Gilbert and I. Spector, Intracellular cyclic AMP produces effects opposite to those of cyclic GMP and calcium on shape and motility of neuroblastoma cells, *Cell Motil Cytoskeleton* **22**, 99-116 (1992).
37. N.D. Goldberg, M.K. Haddox, S.E. Nicol, D.B. Glass, C.H. Sanford, F.A. Kuehl, Jr. and R. Estensen, Biological regulation through opposing influences of cGMP and cAMP: The Yin-Yang hypothesis, *Advan Cyclic Nucleotide Res* **5**, 307-330 (1975).
38. R.P. Mecham, B.D. Levy, S.L. Morris, J.G. Madaras and D.S. Wrenn, Increased cyclic GMP levels lead to a

stimulation of elastin production in ligament fibroblasts that is reversed by cyclic AMP, *J Biol Chem* **260**, 3255-3258 (1985).
39. L.L. Rubin, D.E. Hall, S. Porter, K. Barbu, C. Cannon, H.C. Horner, M. Janatpour, C.W. Liaw, K. Manning, J. Morales, L.I. Tanner, K.J. Tomaselli and F. Bard, A cell culture method of the brain-blood barrier, *J Cell Biol* **115**, 1725-1735 (1991).
40. P.F. Baker and A. Carruthers, Insulin regulation of sugar transport in giant muscle fibres of the barnacle, *J Physiol* (Lond) **336**, 397-431 (1983).
41. K.G. Beam, E.J. Nestler and P. Greengard, Increased cyclic GMP levels associated with contraction in muscle fibres of the giant barnacle, *Nature* **267**, 534-536 (1977).
42. D.A. Carter and D. Murphy, Cyclic nucleotide dynamics in the rat hypothalamus during osmotic stimulation: *In vivo* and *in vitro* studies, *Brain Res* **487**, 350-356 (1989).
43. D. Häussinger and F. Lang, Cell volume and hormone action, *TIPS* **13**, 371-373 (1992).
44. O. Christensen, Mediation of cell volume regulation by Ca influx through stretch-activated channels, *Nature* **330**, 66-68 (1987).
45. F. Sachs, Mechanical transduction by membrane ion channels: A mini review, *Mol Cell Biochem* **104**, 57-60 (1991).
46. H. Sackin, A stretch-activated K^+ channel sensitive to cell volume, *Proc Natl Acad Sci USA* **86**, 1731-1735 (1989).
47. S.I. Sukharev, B. Martinac, V.Y. Arshavky and C. Kung, Two types of mechanosensitive channels in the E. coli cell envelop: Solubilization and functional reconstitution, *Biophys J* **65**, 177-183 (1993).
48. R. Motais, H. Guizouarn and F. Garcia-Romeu, Red cell volume regulation: The pivotal role of ionic strength in controlling swelling-dependent transport systems, *Biochim Biophys Acta Gen Subj* **1075**, 169-180, 1991.
49. B. Sarkadi and J.C. Parker, Activation of ion transport pathways by changes in cell volume, *Biochim Biophys Acta Rev Biomembr* **1071**, 407-427 (1991).
50. B. Martinac, Mechanosesnsitive Ion Channels: Biophysics and Physiology, In: *Thermodynamics of membrane receptors and channels,* edited by MB. Jackson, Boca Raton: CRC Press (1993).
51. H. Sackin, Stretch-activated ion channels, edited by Strange K. CRC Press (1994).
52. D. Kim, Novel cation-selective mechanosensitive ion channel in the atrial cell membrane, *Circ Res* **72**, 225-231 (1993).
53. S. Sorota, Swelling-induced chloride-sensitive current in canine arterial cells revealed by whole-cell patch-clamp method, *Circ Res* **70**, 679-687 (1992).
54. O.P. Hamill and D.W. McBride, Jr., The cloning of a mechano-gated membrane ion channel, *Trends Neurosci* **17**, 439-443 (1994).
55. F. Maingret, E. Honore, M. Lazdunski and A.J. Patel, Molecular basis of the voltage-dependent gating of TREK-1, a mechano-sensitive K channel, *Biochem Biophys Res Commun* **292**, 339-346 (2002).
56. E, Perozo, D.M. Cortes, P. Sompornpisut, A. Kloda and B. Martinac, Open channel structure of MscL and the gating mechanism of mechanosensitive channels, *Nature* **418**, 942-948 (2002).
57. M.L. Jennings and R.K. Schulz, Swelling-activated KCl cotransport in rabbit red cells: Flux is determined mainly by cell volume rather than shape, *Am J Physiol Cell Physiol* **259**, C960-C967 (1990).
58. J.F. Hoffman, M. Eden, J.S. Barr and H.S. Bedell, The hemolytic volume of human erythrocytes, *J Cell Comp Physiol* **51**, 405-414 (1958).
59. J.W. Lohr and J.J. Grantham, Isovolumetric regulation of isolated S2 proximal tubes in anisotonic media, *J Clin Invest* **78**, 1165-1172 (1986).
60. L. Trais, J.C. Summers, R. Lajvardi, K. Goharderakhshan, D. Hergan, R. Buechler H. Chang, C. Pena-Rasgado and H. Rasgado-Flores, Identification of the volume sensor in barnacle muscle cells, *Biophysical Journa*l **72**, A410 (1997).
61. J.C. Parker, Volume-responsive sodium movements in dog red blood cells, *Am J Physiol* **244**, C324-C330 (1983).
62. A.P. Minton, The effect of volume occupancy upon the thermodynamic activity of proteins: Some biochemical consequences, *Mol Cell Biochem* **55**, 119-140 (1983).
63. A.P. Minton, C.C. Colclasure and J.C. Parker, Model for the role of macromolecular crowding in regulation of cellular volume, *Proc Natl Acad Sci USA* **89**, 10504-10506 (1992).
64. J.C. Parker, In defense of cell volume? *Am J Physiol* **34**, C1191-C1200 (1993).

26

Q-VD-OPh, NEXT GENERATION CASPASE INHIBITOR

Thomas L. Brown*

1. INTRODUCTION

Apoptotic cell death is an active process characterized by the lack of an inflammatory response, crosslinking of the plasma membrane, caspase activation, DNA laddering, and the formation of apoptotic bodies.[1] Apoptosis is mediated by specific initiator and effector cysteine proteases (caspases) that are unique in cleaving substrates specifically following aspartate residues.[2-5] The activation of specific caspases has defined three major pathways that can carry out the apoptotic process. Caspase 9 can be activated by the release of cytochrome c from the mitochondria into the cytosol and triggered by addition of actinomycin D or etoposide or indirectly by anti-fas antibody.[6-9] The caspase 8/10 pathway is activated via ligand binding to death receptor systems of the Fas/CD95 and tumor necrosis factor alpha families.[7] Caspase 12 is activated in response to thapsigargin and other endoplasmic reticulum stressors in rodent cells; however, a recent report suggests that caspase 12 is not functional in human cells.[10-12]

Recent advances have led to commercially available inhibitors that prevent caspase activation. Specific as well as broad-spectrum caspase inhibitors consist of methylated monopeptides to tetrapeptides conjugated to carboxyterminal groups such as chloromethyl ketone (cmk), fluoromethyl ketone (fmk), or aldehyde (cho) that enable them to act as competitive inhibitors. These cell-permeable inhibitors alkylate the active site cysteine of caspases and irreversibly block apoptosis by preventing caspase activation, substrate cleavage, and DNA ladder formation.

The broad-spectrum inhibitor, ZVAD-fmk, can prevent apoptosis of the major pathways at high concentrations and has a preference for the caspase 3 pathway at somewhat lower doses. Boc-D-fmk (B-D-fmk) consists of a single aspartate residue and is capable of preventing apoptosis mediated by any of the three pathways at about one half the effective concentration of ZVAD-fmk. Although these broad-spectrum inhibitors have been effective in identifying caspase-mediated events, the relatively high doses

* Thomas L. Brown, Department of Anatomy and Physiology, Wright State University, 3640 Colonel Glenn Highway, 042 Biological Sciences, Dayton, Ohio 45435, USA. Ph 937-775-3809, Fax 937-775-3391, Thomas.l.brown@wright.edu

required can limit their usefulness in some systems and may have nonspecific or cytotoxic effects.[13-16] Recently, a new generation of broad-spectrum caspase inhibitor, Q-VD-OPh, was developed to circumvent *in vivo* toxicity of existing caspase inhibitors as well as to try to reduce the effective concentration to increase specificity.[15]

2. EXPERIMENTAL

WEHI 231 mouse immature B cells were cultured in RPMI 1640 containing 10% FBS and 29 μM 2-mercaptoethanol. Jurkat human T lymphoma cells were cultured in RPMI 1640 containing 10% FBS. The rat trophoblast cell line, HRP-1, was cultured in 2.5% fetal bovine serum in DMEM. All cells were cultured at 37°C and 95% O_2/5% CO_2. Apoptosis was determined by oligonucleosomal DNA laddering and quantitated by flow cytometry after TUNEL assay.[5, 16-20] Caspase inhibitors were added at the indicated concentrations 1 h prior to treatment. Cell number and viability were determined by trypan blue exclusion. Protein concentrations and Western blotting were performed as described previously.[5, 16-20]

3. RESULTS AND DISCUSSION

Caspase activation is an essential and irreversible enzymatic event during apoptosis. Caspase inhibitors have been routinely used to identify specific caspases and analyze particular mechanisms involved in the cell death process. Two of the most widely used caspase inhibitors are the broad-spectrum fluoromethyl ketone caspase inhibitors, B-D-fmk and Z-VAD-fmk. The amino terminal Boc and Z groups serve to block the amino acids D (aspartate) or VAD (Val-Ala-Asp) while the carboxy terminal fluoromethyl ketone facilitates cell permeability. We determined the effectiveness of known broad-spectrum caspase inhibitors to prevent apoptosis in comparison to the next generation caspase inhibitor, Q-VD-OPh.[15, 16]

Actinomycin D has previously been shown to induce caspase activation in WEHI 231 immature B cells.[18, 19] To analyze the effects of broad-spectrum caspase inhibitors on actinomycin D-induced apoptosis in WEHI 231 cells, DNA fragmentation was analyzed. Incubation with decreasing concentrations of ZVAD-fmk, B-D-fmk, or Q-VD-OPh in the presence of 1 μg/ml actinomycin D demonstrated that each inhibitor prevented apoptosis in a dose dependent manner (Figure 1).

ZVAD-fmk was only partially effective at inhibiting DNA laddering at 50 μM, consistent with observations in other systems (Figure 1A). This result was also confirmed by TUNEL assay and flow cytometry (data not shown). The broad-spectrum caspase inhibitor B-D-fmk completely prevented apoptosis in WEHI 231 cells at 50 μM but was ineffective at lower doses (Figure 1B). In striking contrast to ZVAD-fmk and B-D-fmk, the caspase inhibitor Q-VD-O-phenoxy (Q-VD-OPh) exhibited the ability to prevent DNA fragmentation at concentrations as low as 5 μM (Figure 1C). Q-VD-OPh uses an amino-terminal quinoline group conjugated to the amino acids valine and aspartate and a carboxyl ester attached to a phenoxy ring. Q-VD-OPh used in these studies contained an O-methyl group; however, a modified Q-VD-OPh (No Methyl) was even more effective with an apoptotic inhibitory concentration of 2.5 μM (TLB, unpublished data).

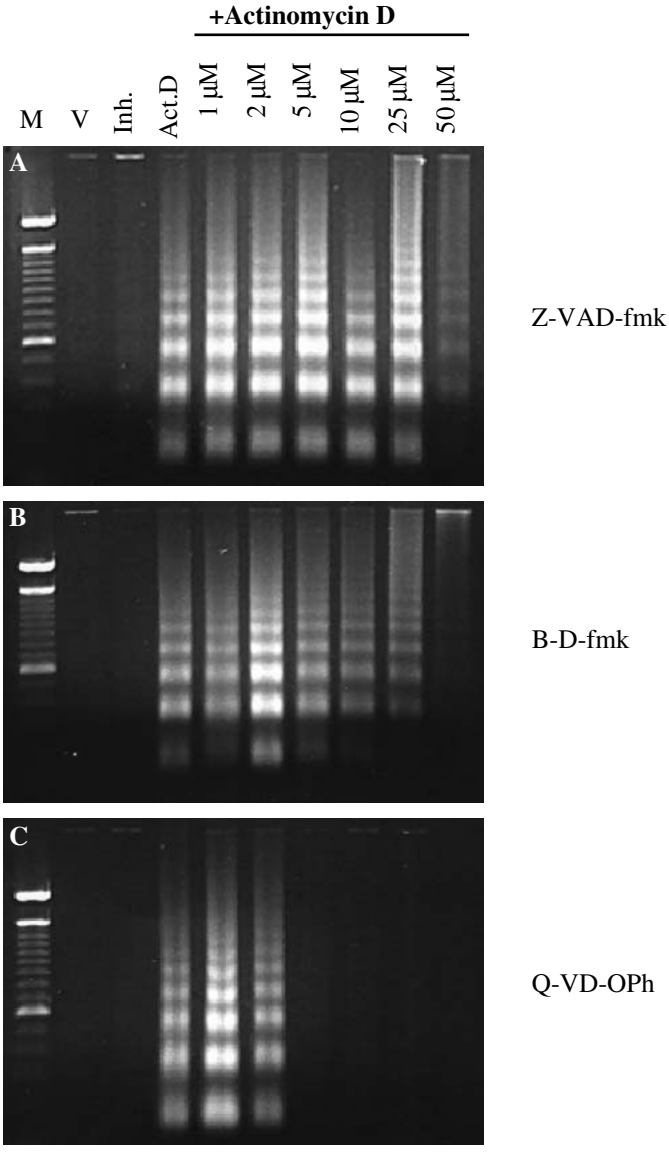

Figure 1. Caspase inhibitors dose-dependently inhibit Actinomycin D induced DNA laddering. Panel A=Z-VAD-fmk. Panel B=Boc-D-fmk. Panel C=Q-VD-OPh. WEHI-231 cells ($1x10^5$ cells/ml) were treated for 4 hrs with (V) vehicle, (Inh) 50 μM caspase inhibitor alone, (Act.D) 1 μg/ml actinomycin D, or caspase inhibitor (at either 1 μM, 2 μM, 5 μM, 10 μM, 25 μM, or 50 μM as indicated) preincubated 1 hr prior to addition of actinomycin D. DNA was isolated, separated on a 1.2% agarose gel and stained with ethidium bromide to determine the effective dose of each inhibitor. (M) denotes the 100bp DNA molecular weight marker.

Effects of Q-VD-OPh on cellular toxicity were also examined in WEHI 231 cells. Concentrations of dimethylsulfoxide greater than 0.33% can induce apoptosis in WEHI 231 cells. The presence of 500 μM Q-VD-OPh, which results in a DMSO vehicle

concentration of 5%, resulted in 4% apoptosis, whereas 1 mM Q-VD-OPh (10% DMSO concentration) resulted in 21% apoptosis.[16] Chemical breakdown is often a limiting factor in the efficacy of small peptide inhibitors for use in long-term studies and B-D-fmk has been shown to be stable for 48 h in cultured cells treated continuously with actinomycin D.[13] Analysis of 5 μM Q-VD-OPh in the presence of actinomycin D for at least 48 h resulted in no change in cell number and complete cellular viability (author's unpublished data).

In addition to the WEHI 231 mouse B cell line, the human Jurkat T cell line was also analyzed to determine if the effective inhibitory concentration of Q-VD-OPh would be similar. Jurkat cells, incubated for 4 h with actinomycin D, displayed a significant amount of apoptosis as indicated by DNA laddering. Similar to WEHI 231 cells, the presence of 5 μM Q-VD-OPh completely prevented apoptosis in Jurkat T cells (data not shown).[16] WEHI 231 or Jurkat cells in the presence of Q-VD-OPh and actinomycin D were completely viable, as determined by trypan blue exclusion, but were strongly growth-inhibited (data not shown). Q-VD-OPh alone did not interfere with cell growth or viability. To determine if receptor-mediated apoptosis would also be inhibited by Q-VD-OPh, the multifunctional cytokine TGF beta was used to induce apoptosis in rat trophoblast HRP-1 cells. TGF beta induced apoptosis in HRP-1 cells within 24 h, as determined by DNA laddering, and was completely inhibited by 5 μM Q-VD-OPh (data not shown).

Actinomycin D treatment also resulted in activation of caspase 3 which was prevented by Q-VD-OPh. In addition to the caspase 3 pathway, we also determined whether Q-VD-OPh was capable of inhibiting the other known major pathways of apoptosis at this low concentration (Figure 2). DNA laddering representative of apoptosis occurred in WEHI 231 cells by the caspase 9/3 pathway activated by actinomycin D and the caspase 12 pathway after treatment with thapsigargin as well as the caspase 8 pathway which was induced in Jurkat T cells after stimulation with anti-Fas. Western blotting was performed to demonstrate substrate cleavage (data not shown) as well as actual caspase cleavage and the ability of Q-VD-OPh to prevent the enzymatic activation (Figure 3). All three apoptotic pathways were completely inhibited in the presence of 5 μM Q-VD-OPh.

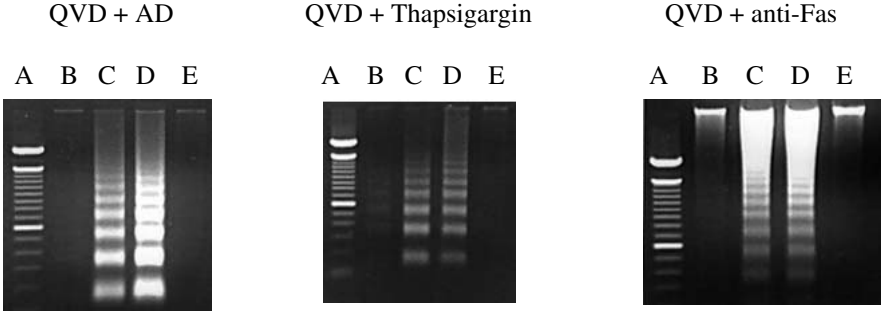

Figure 2. Q-VD-OPh inhibits all major apoptotic pathways. Panel 1: WEHI-231 cells treated for 4 h with (**B**) vehicle, (**C**) 1 μg/ml actinomycin D, (**D**) DMSO + 1 μg/ml actinomycin D or (**E**) 5 μM Q-VD-OPh pre-incubated 1 hr prior to actinomycin D addition. (**A**) indicates a 100 bp DNA molecular wt marker. Panel 2: WEHI-231 cells treated for 4 h with (**B**) vehicle, (**C**) 1 μM thapsigargin, (**D**) DMSO + 1 μM thapsigargin or (**E**) 5 μM Q-VD-OPh pre-incubated 1 h prior to thapsigargin addition. Panel 3: Jurkat cells treated with (**B**) vehicle, (**C**) 100 ng/ml anti Fas (Clone CH-11), (**D**) DMSO + 100 ng/ml anti Fas or (**E**) 5 μM Q-VD-OPh pre-incubated 1 h prior to anti-Fas addition. DNA was isolated from treated cells and DNA laddering determined.

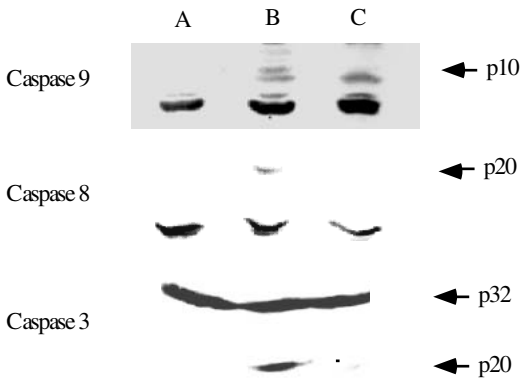

Figure 3. Q-VD-OPh prevents activation of initiator and effector caspases. Jurkat T cells were treated with **A**) 100 ng/ml anti-Fas clone CH-11 for 4 h or (**B, C**) 25 μM etoposide for 6 h in the absence or presence of Q-VD-OPh. Whole cell lysates were separated by SDS-PAGE and Western blotting was performed using caspase 3 proform and p20, caspase 8 p10 or caspase 9 p10 polyclonal or monoclonal antibodies.

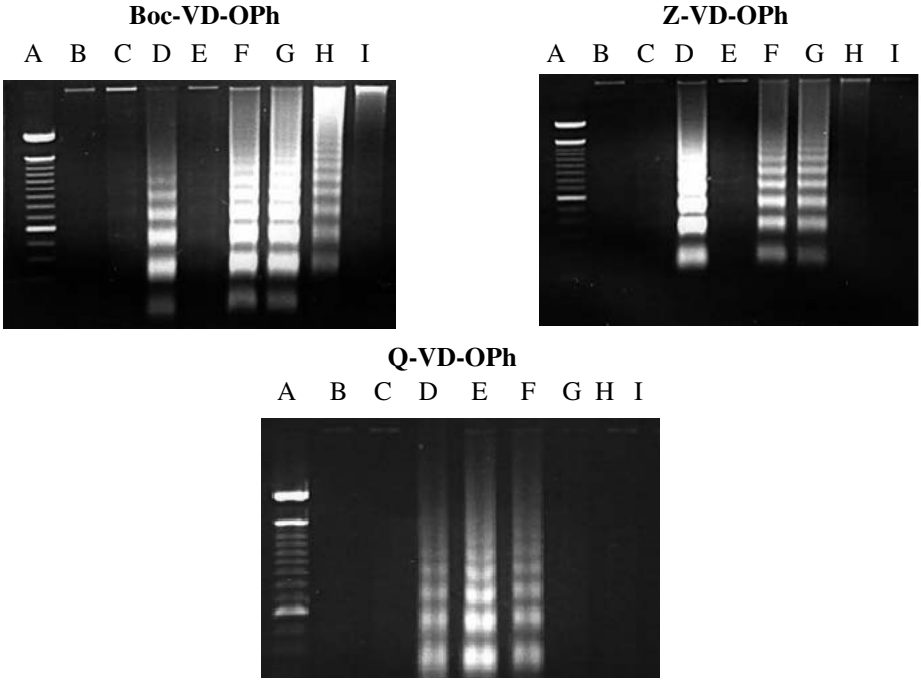

Figure 4. The carboxyterminal O-phenoxy group is responsible for increased apoptotic inhibition. WEHI-231 cells treated with (**B**) 10 μM inhibitor alone, (**C**) vehicle (**D**) 1 μg/ml actinomysin D, (**E**) 0.1% DMSO. Samples (**F-I**) pretreated with either 1 μM, 2 μM, 5 μM, 10 μM inhibitor (Boc-VD-OPh or Z-VD-OPh) one h prior to 1 μg/ml actinomysin D treatment for 4 h. DNA isolated, separated on a 1.2% agarose gel and stained with ethidium bromide to determine effective dose of each inhibitor. (**A**) indicates the 100 bp DNA molecular wt marker. Lower Panel: no DMSO control shown and lines **E-H** represent 1,2,5 and 10 μM Q-VD, respectively.

The development of Q-VD-OPh relies on carboxy and amino-terminal modifications to increase cell permeability, stability and efficacy. To determine if the carboxyterminal blocking group contributes to the high level of effectiveness of Q-VD-OPh, WEHI 231 cells were treated with actinomycin D for 4 h in the presence or absence of decreasing concentrations of Boc-VD-OPh, Z-VD-OPh, or Q-VD-OPh and analyzed by DNA laddering. As shown in Figure 4, the increased ability to protect against apoptosis induced by actinomycin D is directly related to the carboxyterminal modification contributed by the -OPh group. Substitution of the -OPh group for the -fmk group decreased the effective concentration of Boc-VD-OPh to 10 μM (compared to 50 μM Boc-D-fmk) and Z-VD-OPh to 5 μM. Suprisingly, the substitution of an amino terminal "Mu" blocking group conjugated to VD-OPh in an attempt to make a water soluble inhibitor was completely ineffective at preventing actinomycin D-induced apoptosis in WEHI 231 cells at concentrations as high as 10 μM (data not shown).

4. DISCUSSION

Next generation, broad-spectrum caspase inhibitors can have dramatic differences in effectiveness depending upon specific amino and carboxy-terminal modifications. Q-VD-OPh was effective at inhibiting the three major cell death pathways, caspase 8/10, caspase 9, and caspase 12. Q-VD-OPh inhibited apoptosis in human, mouse and rat cell lines, and prevented terminal caspase activation, substrate cleavage, and DNA ladder formation. Q-VD-OPh was found to be maximal at one tenth the concentration of the most currently effective caspase inhibitors, suggesting the addition of a quinolyl and phenoxy moieties may greatly enhance cellular permeability and/or substrate access.

The specificity of this caspase inhibitor was demonstrated in that Q-VD-OPh did not affect the growth arrest function of the RNA synthesis inhibitor, actinomycin D but did prevent caspase 3 specific cleavage of a target substrate, poly ADP-ribose polymerase (PARP). Addition of the carboxy terminal O-phenoxy (-OPh) group was primarily responsible for the increased effectiveness as an apoptotic inhibitor as indicated by similar results obtained using the amino terminal Z or Boc groups conjugated to -VD-OPh. Aminoterminal modifications, however, can also alter the effectiveness of the inhibitor as indicated by the slightly less effective Boc blocking group when compared to Z- or Q- blocking groups conjugated to -VD-Oph and the loss of effectiveness by Mu-VD-OPh.

Commercial caspase inhibitors are hydrophobic and as such require suspension in DMSO to solubilize them. This can present particular problems in DMSO sensitive cells such as lymphocytes since inhibitors such as Z-VAD-fmk require a dose of greater than 50 μM to be effective. High concentrations of caspase inhibitors may also lead to some nonspecificity and binding to other cellular proteins not involved in the apoptotic pathway further compounding analysis.[13, 14, 17] The ability to use a caspase inhibitor at such a low effective dose eliminates the problems associated with vehicle concentrations or nonspecificity associated with the widely used fluoromethyl ketone caspase inhibitors, not to mention the increased cost effectiveness.

The effective concentration of Q-VD-OPh may provide a unique reagent when trying to revive hard to propagate cell lines from liquid nitrogen. The addition of this inhibitor to thawed cells would give the cells adequate time to recover from the stress of thawing,

even in the presence of standard DMSO concentrations, and begin to proliferate in the absence of toxicity. Q-VD-OPh is stable in solution for several months and is effective in culture for at least 2.5 days. This would provide an ideal timeframe for cell recovery whereas, the subsequent decrease in effectiveness over time would be fortuitous in that the cells would return to standard culture conditions with minimal manipulation. It is likely that the decreased inhibitory effect on apoptosis in cell culture over time is due to uptake and cellular depletion of the inhibitor.

In this study, we determined the effectiveness of several broad spectrum caspase inhibitors to prevent DNA laddering and caspase activation during apoptosis induced via several stimuli. Actinomycin D rapidly induces substantial apoptosis and can be dramatically inhibited by the caspase inhibitor, Q-VD-OPh (quinolyl-valyl-O-methylaspartyl-[-2,6-difluorophenoxy]-methyl ketone). Q-VD-OPh was significantly more effective in preventing apoptosis than the widely used inhibitors, ZVAD-fmk and B-D-fmk. Q-VD-OPh was also equally effective in preventing apoptosis mediated by the three major apoptotic pathways, caspase 9/3, caspase 8/10, and caspase 12. In addition to the increased effectiveness, Q-VD-OPh was minimally toxic to cells, even at very high concentrations. Our data indicate that the specificity, effectiveness, and reduced toxicity of caspase inhibitors will be significantly enhanced using aminoterminal quinolyl and carboxyterminal o-phenoxy groups.

5. CONCLUSION

The broad spectrum caspase inhibitor, Q-VD-OPh, provides not only a cost effective, non-toxic, and highly specific means of apoptotic inhibition but also new insight into next generation caspase inhibitors. Our data indicate that the specificity and effectiveness of next generation caspase inhibitors will be significantly enhanced by incorporating conjugated aminoterminal quinolyl and carboxyterminal O-phenoxy groups. A major disadvantage of fluoromethyl ketone and other carboxyterminal-conjugated caspase inhibitors has been the resultant toxicity *in vivo* which has hampered their use. Future studies examining other amino terminal modifications to 0-phenoxy conjugates to decrease hydrophobicity as well as nonpeptide, selective caspase inhibitors should provide even greater effectiveness. Studies assessing *in vivo* specificity, clearance, and toxicity of Q-VD-OPh will determine the potential use of this new generation of O-phenoxy caspase inhibitor conjugates as promising new therapeutics.

6. ACKNOWLEDGMENTS

I would like to thank Dr. Tomaselli, Idun Pharmaceuticals, for providing the caspase 3 antibody; Dr. Vincenz, University of Michigan, for antibodies to caspase 8 and 9; and Dr. Lessard, Cincinnati Childrens Hospital Medical Center, for providing the beta actin antibody. We also thank Dr. Hughes, University of North Carolina-Charlotte, and Dr. Larner, Cleveland Clinic Foundation, for providing Jurkat cells and Dr. Soares, University of Kansas City Medical Center, for kindly providing the rat HRP-1 trophoblast cells. We would also like to acknowledge Steve Ledbetter, Genzyme, Inc., for generously providing TGF beta and Enzyme Systems Products, Inc., for caspase

inhibitors. Figures 1-4 were used with permission of Kluwer Academic/Plenum Publishers (Apoptosis. 2003, **8**:345-352).

7. REFERENCES

1. D.R. Plas and CB Thompson, Cell metabolism in the regulation of programmed cell death, *Trends Endocrinol Metab.* **13**, 75-8 (2002).
2. W.C. Earnshaw, L.M. Martins, S.H. Kaufmann, Mammalian caspases: structure, activation, substrates, and functions during apoptosis, *Ann Rev Biochem*. **68**, 383-424 (1999).
3. G.S. Salvesen and V.M. Dixit, Caspases: intracellular signaling by proteolysis, *Cell* **91**, 443–446 (1997).
4. G.M. Cohen, Caspases: the executioners of apoptosis, *Biochem. J.* **326**, 1–16 (1997).
5. T.L. Brown**,** S. Patil and P.H. Howe, Analysis of TGFβeta-Inducible Apoptosis, In *Methods in Molecular Biology –"Transforming growth factor-beta protocols,"* P. Howe, ed., (Totowa, NJ: Humana Press) **142**, 149-67 (2000).
6. J.C. Goldstein, N.J. Waterhouse, P. Juin, G.I. Evan, and D.R. Green, The coordinate release of cytochrome c during apoptosis is rapid, complete and kinetically invariant, *Nat Cell Biol*. **2**, 156-62 (2000).
7. X.M. Yin, Signal transduction mediated by Bid, a pro-death Bcl-2 family proteins, connects the death receptor and mitochondria apoptosis pathways, *Cell Res.* **10**, 161-7 (2000).
8. M. Fujino, X.K. Li, Y. Kitazawa, L. Guo, M. Kawasaki, N. Funeshima, T. Amano, and S. Suzuki, Distinct pathways of apoptosis triggered by FTY720, etoposide, and anti-Fas antibody in human T-lymphoma cell line (Jurkat cells), *J Pharmacol Exp Ther*. **300**, 939-45 (2002).
9. J.D. Robertson, M. Enoksson, M. Suomela, B. Zhivotovsky, S. Orrenius, Caspase-2 acts upstream of mitochondria to promote cytochrome c release during etoposide-induced apoptosis, *J Biol Chem* **277**, 9803-9 (2002).
10. T. Nakagawa, H. Zhu, N. Morishima, E. Li, J. Xu, B.A. Yankner, and J. Yuan, Caspase-12 mediates endoplasmic-reticulum-specific apoptosis and cytotoxicity by amyloid-beta, *Nature*. **403**, 98-103 (2000).
11. R.V. Rao, E. Hermel, S. Castro-Obregon, G. del Rio, L.M. Ellerby, H.M. Ellerby, and D.E. Bredesen, Coupling endoplasmic reticulum stress to the cell death program: Mechanism of caspase activation, *J Biol Chem*. **276**, 33869-74 (2001).
12. H. Fischer, U. Koenig, L. Eckhart, E.Tschachler, Human caspase 12 has acquired deleterious mutation. *Biochem Biophys Res Commun*. May 3;**293**(2), 722-6 (2002).
13. P. Schotte, W. Declercq, S.Van Huffel, P. Vandenabeele, and R. Beyaert, Non-specific effects of methyl ketone peptide inhibitors of caspases, *FEBS Lett*. **442**, 117-21 (1999).
14. C.J. Van Noorden, The history of Z-VAD-FMK, a tool for understanding the significance of caspase inhibition, *Acta Histochem*. **103**, 241-51 (2001).
15. R. Mischak, ICN/ESP Caspase inhibitors: Applications *in vivo* and *in vitro*. *ICN Bioconcepts* **8**, 1-5 (2002).
16. T.M. Caserta, A.N. Smith, A.D. Gultice, M.A. Reedy, and TL. Brown, Q-VD-OPh, a broad spectrum caspase inhibitor with potent antiapoptotic properties, *Apoptosis* **8**, 345-352 (2003).
17. T.L. Brown, S. Patil, R.K. Basnett, and P.H. Howe, Caspase inhibitor BD–fmk distinguishes transforming growth factor beta–induced apoptosis from growth inhibition, *Cell Growth Diff*. **9**, 869–875 (1998).
18. T.L. Brown, S. Patil, C.D. Cianci, J.S. Morrow, and P.H. Howe, TGF beta induces caspase 3 independent cleavage of alpha II spectrin (alpha–fodrin) coincident with apoptosis, *J. Biol. Chem*. **274**, 23256-23262 (1999).
19. S.T. Williams, A.N. Smith, C.D. Cianci, J.S. Morrow, and T.L. Brown, Identification of the primary caspase 3 cleavage site in alpha II spectrin during apoptosis, *Apoptosis* **8**, 353-361 (2003).
20. S. Patil, G.M. Wildey, T.L. Brown, L. Choy, R. Derynck, and P.H. Howe, Smad7 is induced by CD40 and protects WEHI 231 B-lymphocytes from transforming growth factor-beta-induced growth inhibition and apoptosis, *J Biol Chem*. **275**, 38363-70 (2000).

27

ARE MEMBRANE TYROSINE KINASE RECEPTORS INVOLVED IN OSMOTRANSDUCTION?

H. Pasantes-Morales, R. Lezama and R. Franco*

1. INTRODUCTION

The adaptive cell response to swelling after a reduction in external osmolarity, known as regulatory volume decrease (RVD), involves a complex series of reactions that in most cells ultimately leads to the extrusion of osmotically active solutes directed to re-establish the osmotic equilibrium with the new extracellular condition. The overall response involves three main steps: 1) the volume-sensing mechanisms detecting the change in cell volume set by the lineage of each cell type. The volume sensor machinery acts also as a memory of the original cell size, necessary for arresting the adaptative response once this size has been attained; 2) a volume transducing cascade connecting the sensor signal to the osmolyte extrusion mechanisms, and 3) the setting in motion of the osmolyte efflux pathways, resulting in a decrease in intracellular osmolarity to equilibrate with the external medium. Early studies in the field were directed toward characterizing the mechanisms of release of the main osmolytes involved in RVD. The efflux pathways for Cl and K were identified as separate channels in most cases,[1-3] and those for organic osmolytes were recognized as leak pathways.[4, 5] Thereafter, interest was extended to aspects of volume sensing and osmotransduction. It was soon evident that volume sensors and signaling cascades involve the convergence of multiple elements and complex mechanisms with an active interplay.[6, 7] With our current state of knowledge, we are still unable to define whether the mechanisms of volume sensing involve interactions between the molecules in the membrane and extracellular entities or instead, are responses to variations in some intracellular condition or signal. At the membrane side, proposed elements for volume sensing include adhesion molecules (integrins in particular), mechanical changes leading to membrane stretch and unfolding or molecules acting as osmolarity receptors. At the intracellular side, changes in the cytoskeleton, a reduction in the macromolecular crowding, or a decrease in ionic strength have been

* H. Pasantes-Morales, R. Lezama and R. Franco, Departamento de Biofísica, Instituto de Fisiología Celular, Universidad Nacional Autónoma de México, UNAM, Ciudad Universitaria, 04510, Mexico City, Mexico.

proposed as volume or osmolarity detectors. In the present work, we discuss our recent findings on the potential participation of the membrane tyrosine kinase receptors as elements of the sensor and/or osmotransduction signaling cascades. TKR are well suited to sense changes in the cell environment and to transmit that message to the intracellular compartment.

2. TYROSINE KINASE RECEPTORS (TKR) ARE INVOLVED IN THE SENSING/TRANSDUCTION CASCADE IN RVD

2.1 Protein Tyrosine Kinases Are Involved in the Operation of Cl^- and Amino Acid Efflux Pathways

One of the antecedents to consider as a role for TKR in the signaling mechanisms connecting the change in cell volume to the osmolyte efflux pathways was the importance of protein tyrosine kinases in the mechanisms operating the hyposmotic efflux of Cl^- and taurine.[7-9] A feature characteristic of TKR is the presence at the intracellular domain of an intrinsic protein tyrosine kinase activity which is the initial step for setting in motion a complex network of many other reactions.[10-13] The question is then raised whether some of the tyrosine kinases required for the operation of Cl^- and taurine hyposmotic fluxes may be those present in TKR. This possibility is suggested by a comparison between the effect of different tyrosine kinase blockers on the osmolyte fluxes. Tyrphostins are often considered rather specific blockers of the tyrosine kinase activity in TKR, while other blockers such as herbimycin and lavendustin affect the intracellular tyrosine kinases more. What has been seen in a number of cell types is that volume-activated taurine and Cl^- pathways are clearly more sensitive to tyrphostins than to other tyrosine kinase blockers.[7-9]

3. CHANGES IN EXTERNAL OSMOLARITY ACTIVATE TYROSINE KINASE RECEPTORS

By their nature as transmembrane molecules, TKR are well positioned to be a link between the external environment, including changes in the cell surrounding fluids or in the extracellular matrix proteins, and the intracellular compartment. In fact, TKR are now identified as crucial elements in the operation and interplay of a variety of intracellular downstream signaling pathways, ultimately regulating the expression and activity of numerous cell functions.[10-12] TKR activate by dimerization and the subsequent activation of the intrinsic tyrosine kinase activity. Tyrosine phosphorylation of TKR can be elicited either by specific ligands, or in the absence of the physiological ligands, by a number of other stimuli. Ligand-independent activation of TKR is known to occur through radiation, oxidative stress, heavy metal ions and alkylating agents.[13] TKR may also be activated by membrane stretch.[14] Changes in external osmolarity could be also sensed by TKR as suggested by the activation of EGFR by hyperosmolarity.[15] Considering these antecedents, we are interested in investigating whether an increase in cell volume and/or a reduction in osmolarity are able to activate TKR, thus including these molecules as early membrane signals or elements in osmotransduction. We selected EGFR in the Swiss3T3

fibroblasts as the experimental model for this study. EGFR is one the best characterized members of the superfamily of TKR and is expressed in most cell types. In addition, pharmacological tools are available to manipulate its activity.

Results from this study[16] showed a marked activation of EGFR in fibroblasts when cells were exposed for 3 min to a 35% hyposmotic medium. It is noteworthy that phosphorylation of EGFR by hyposmolarity is higher than that evoked by a saturating concentration of the ligand EGF.

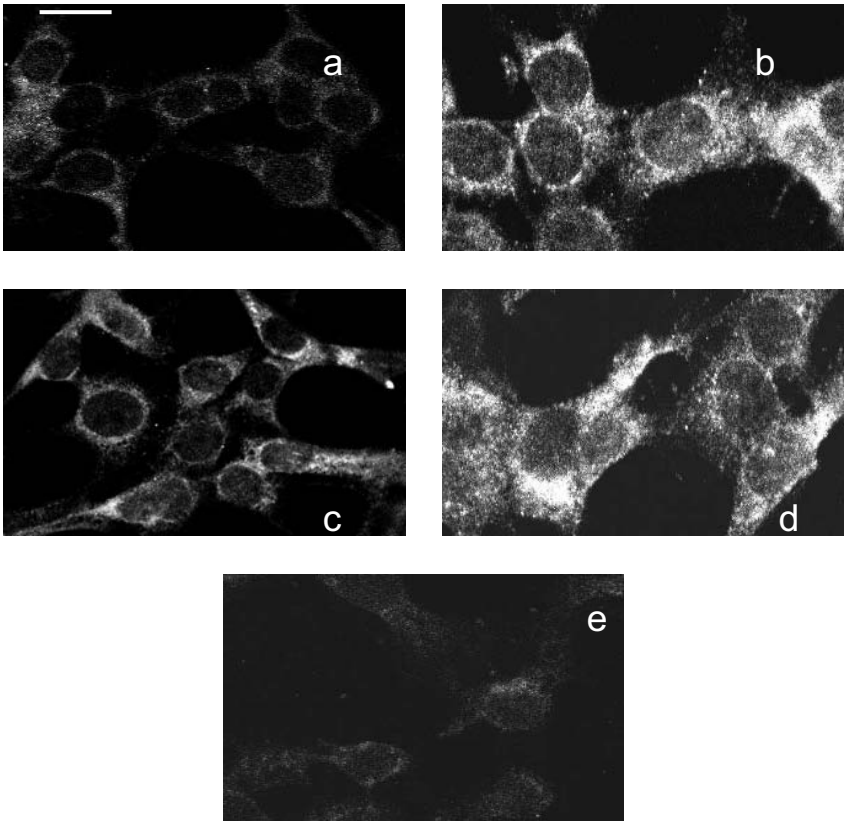

Figure 1. Hyposmolarity-induced EGFR phosphorylation in Swiss 3T3 fibroblast cell line cultures. Serum-starved cells (24 h) were treated for 3 min in the indicated conditions and then fixed and incubated overnight with phospho-EGFR (Tyr 845) antibody. Cells were then incubated with a secondary fluorescent antibody and visualized by confocal microscopy in sections collected at 0.5 μM intervals. Images shown are from the fifth section in the series. Isosmotic medium (a); 35% hyposmotic medium (b); isosmotic medium plus EGF (200ng/ml) (c); 35% hyposmotic medium plus EGF added at the same time as the hyposmotic medium (d) and 35% hyposmotic medium plus 50 μM AG213 (e). Bar = 10 μ. Quantitative expression of fluorescence intensity was carried out by analysis of five fields, containing 10-15 cells each from at least three independent experiments. This analysis showed a 3.4-fold fluorescence increase by hyposmolarity, 2.9-fold by EGF and 5.2-fold for hyposmolarity plus EGF. In the presence of the EGF blocker AG213, the hyposmolarity effect is abolished (Data from [16]).

Quantitation of the fluorescence intensitiy showed an increase over fluorescence in isosmotic conditions of 3.4-fold after the hyposmotic stimulus, while the increase in the EGF/isosmotic condition was 2.9-fold. The effect of hyposmolarity is increased by saturating concentrations of EGF, although the effect of the two stimuli is not additive (Figure 1). EGFR activation was markedly reduced by the tyrphostin AG213, a fairly specific blocker of EGFR phosphorylation (Figure 1). The mechanism of EGFR activation by hyposmolarity is still unknown. Several conditions or reactions modified by hyposmolarity and/or by subsequent cell swelling may be implicated. An interaction with integrins is one of these possibilities, as integrins are known to cooperate with an extensive repertoire of TKR including EGFR.[17, 18] On the other hand, integrins also activate in response to events of cell adhesion and mechanical stimuli associated with changes in cell volume.[19] Other adhesion molecules like p125FAK may also be participating. p125FAK is closely linked to EGFR phosphorylation and is activated by osmolarity reduction.[20]

Additionally or alternatively, hyposmolarity-induced EGFR activation may result from the convergence of stress phenomena which concur with the change in external osmolarity and the swelling of cells. Stress-activated MAP kinase p38 is activated by hyposmotic swelling,[21, 22] and its blockade results in a decrease in the EGFR activation by hyperosmolarity.[23] Generation of reactive oxygen species, known to occur in hyposmotic conditions,[24] is another possible cause of TKR activation in hyposmolarity. The receptor activation by reactive oxygen species may result from an increase in the phosphorylation state of the protein after inhibition of the phosphotyrosine phosphatase reactions by the oxidative stimulus. Finally, EGFR activation may be elicited by swelling-induced mechanical stress, by overexposure of the kinase domain of the receptor or by inducing subcellular redistribution and clustering of the receptor, all ultimately leading to EGFR activation.[14, 25] Elucidation of the predominance and relative contribution of all these factors and the details of the mechanism responsible in each case remains. However, the coincidence of situations leading to EGFR activation and the swelling and volume regulation processes, as well as the concurrence of signaling networks for the two phenomena, is suggestive of a link between these two responses and makes EGFR a likely participant in the osmotransduction signaling cascade. It is still unknown whether other TKR besides EGFR respond in the same way to the change in external osmolarity. This is one of the most relevant questions raised by current findings.

4. EGFR ACTIVATION INFLUENCES THE EFFLUX PATHWAYS OF THE MAIN OSMOLYTES INVOLVED IN CELL VOLUME REGULATION AFTER SWELLING

The first suggestion about a link between TKR and the adaptive fluxes of osmolytes after swelling came from a report by Tilly et al. in Intestin 407 cells[8] showing potentiation by EGF of the hyposmotic efflux of Cl^- (traced as ^{125}I). Evidence of an influence of EGFR in the volume-sensitive Cl^- current also came from a study in C127 cells in which overexpression of the receptor results in modulation of the channel.[26] We found in Swiss3T3 fibroblasts that EGFR is connected with the osmosensitive taurine efflux by the following evidence. Figure 2A shows the time course of ^3H-taurine release from fibroblasts exposed to a medium of reduced osmolarity (35%). In isosmotic

conditions, taurine is released at a rate of about 0.3% per min. Upon reduction in osmolarity, the efflux increases rapidly with a maximal peak of 4.6% reached after 3 min. Thereafter, the release progressively decreases, approaching basal levels despite the persistence of the hyposmotic condition. This is the typical response of taurine to hyposmolarity observed in a large variety of cell types. Addition of EGF (200 ng/ml) to the hyposmotic medium results in a more rapid activation of taurine release as well as a marked potentiation of the efflux, particularly at the initial fractions. In the presence of EGF, the maximal taurine efflux, reached at min 1 after stimulus, is 7.8 %, i.e., an increase of more than 67% over the maximal release in the absence of the factor. Consistent with the stimulatory effect of EGF, the blocker of EGFR activation, AG213, had an inhibitory effect on taurine efflux as shown in Figure 2A. These results are suggestive of EGFR involvement in the mechanism of taurine release in hyposmotic conditions. When EGF was tested on taurine efflux at various osmolarities, an effect was observed on the set point activation, indicative of an increase in sensitivity to hyposmolarity (Figure 2B). In isosmotic conditions, EGF elicits only a marginal increase in taurine efflux suggesting that elements other than the sole activation of the EGFR are necessary to fully operate the osmolyte efflux pathway.

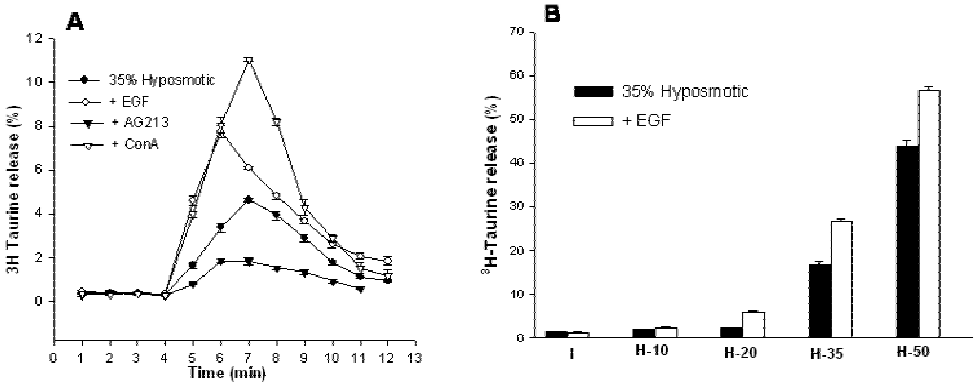

Figure 2. Taurine efflux increased by hyposmolarity and the effect of activation or inhibition of the EGFR. Cells preloaded with ^{3}H-taurine (0.5 μCi/ml during 1 h) were washed and superfused with isosmotic medium for 4 min and then for 8 min with 35% hyposmotic medium (●) or with hyposmotic medium containing EGF (200ng/ml) (○) or Con A (500 ng/ml) ( ). In (▼), cells were preincubated with 50μM AG213 for 30 min and the drug was present in all solutions throughout the experiment. **B**. Stimulatory effect of EGF on ^{3}H-taurine efflux at hyposmolarity reductions of -10% to -50%. Data represent taurine released in fractions 2-5th after the hyposmotic stimulus, with or without the addition of 200ng/ml EGF. (Data obtained from[15]).

In addition to EGF, another mechanism which activates EGFR is treatment with lectins. Some of these compounds are known to activate EGFR and trigger the characteristic signal transduction pathways associated with the activation of the intrinsic tyrosine kinase reactions.[27] Two lectins, concanavalin A (Con A) and wheat germ agglutinin (WGA), in particular, induce receptor dimerization and the subsequent tyrosine kinase phosphorylation. The effect of these lectins on EGFR phosphorylation was examined in the Swiss3T3 fibroblasts, and results are shown in Figure 3. The two lectins elicited a marked phosphorylation of EGFR, even more potent than that evoked by

hyposmolarity or by the ligand EGF itself. In accordance with the effect of EGFR activation on the hyposmotic taurine release, Con A and WGA highly potentiated this efflux. The maximal peak release increased up to 10.9% in the presence of both agents, approximately 140% higher than in the absence of the lectins. This potentiation was prevented by AG213, the EGFR phosphorylation blocker, indicating that the increase in taurine efflux by the lectins is indeed mediated by an effect on the EGFR phosphorylation.

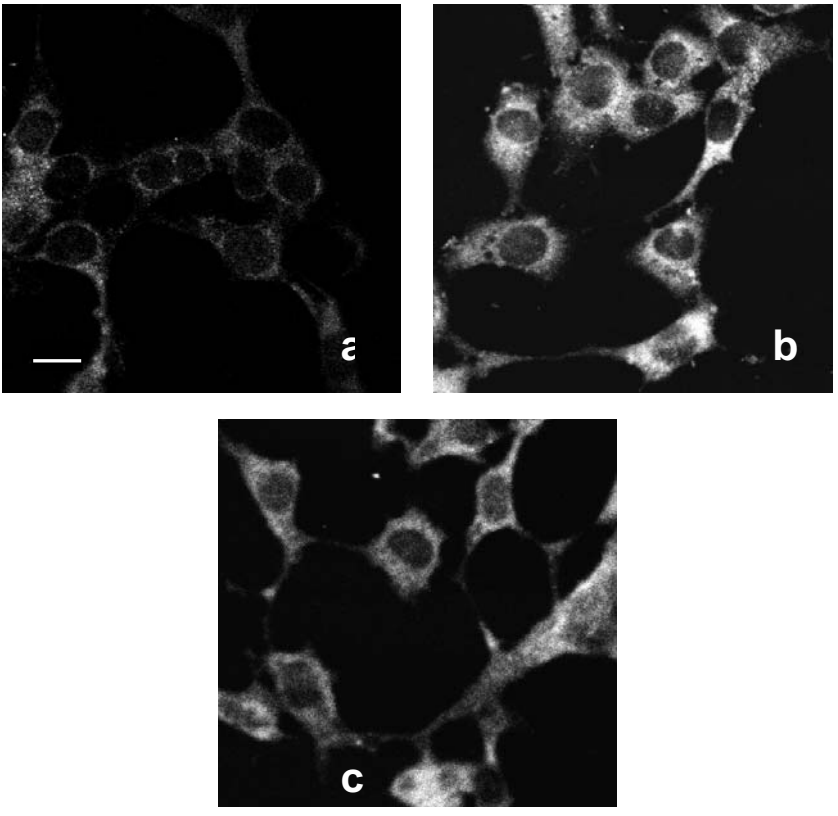

Figure 3. EGFR phosphorylation by Con A and WGA. Cells were incubated for 10 min in isosmotic medium (a) or in medium containing 500ng/ml of Con A (b) or wheat germ agglutinin (WGA) (c). Preparation of samples for visualization and quantification by immunofluorescence was the same as in Figure 1. The quantitative expression of results, calculated as described in Figure 1, showed an increase in fluorescence of 5-fold and 3.5-fold for Con A and WGA, respectively.

Compared to EGF, the more potent effect of the lectins in potentiating taurine efflux may be due to the higher EFGR phosphorylation observed in our study or to a possible effect of the lectins activating other TKR, which may converge at the same signalling pathways, increasing the factors responsible for the potentiated taurine efflux.

These results, together with those previously discussed about volume-sensitive Cl^- fluxes, point to an influence of EGFR on the efflux pathway of two of the main osmolytes involved in the volume regulatory response, i.e., the volume-activated Cl^- channel and the osmosensitive taurine efflux pathway (often considered as representative of the pathway release for other organic osmolytes). There has been a controversy whether the hyposmotic taurine efflux, as well as that of other organic osmolytes, occurs through the volume-sensitive Cl^- channel. The idea of this common pathway resulted from the consistently observed inhibitory effect of Cl^- channel blockers on the hyposmotic efflux of organic osmolytes including taurine and other amino acids, as well as on the efflux of other organic osmolytes.[4] Although this point is still debated,[28] the common pharmacological profile indicates a close interconnection of the two pathways which is further supported by the similar effect of EGF on taurine and Cl^-.

The effect of EGF on the hyposmotic K^+ fluxes (followed as ^{86}Rb) was also examined in our study.[16] EGF seems to potentiate the hyposmotic K^+ efflux, but in contrast to that observed for Cl^- and taurine, EGF and Con A markedly increased K^+ release in isosmotic conditions. This result raises the question of whether the potentiation observed in hyposmotic conditions is not an effect of the factor on the K^+ hyposmotic release but rather the isosmotic efflux overlapping the hyposmotic release. This seems to be the case, since the sum of these two fluxes fully accounts for the potentiation by EGF in hyposmotic conditions. In addition, EGFR blockade did not affect the hyposmotic K^+ efflux, suggesting the above discussed overlap as the most likely explanation for the observed increase elicited by EGF. The conclusion of these results is that EGF activates a K^+ pathway different from the hyposmotic pathway, as it is known that a number of K^+ channels respond to EGF.[29] In any event, and whatever the mechanism involved might be, the conclusion is that EGFR activation increases the efflux of the three types of major osmolytes responsible for the cell volume recovery after hyposmotic swelling and may strongly modulate RVD.

5. MECHANISMS CONNECTING EGFR ACTIVATION AND TAURINE OSMOSENSITIVE FLUXES

TKR including EGFR are very well positioned to act as transducers of the change in external osmolarity or changes in cell volume, as they are crosspoint of numerous upstream and downstream chains of reactions. Tyrosine phosphorylation of specific residues of EGFR and other members of this family of TKR provides specific docking sites for intracellular signal transducers and adaptors and/or to the assembly of numerous signaling complexes. Some of these chains of reactions are known to activate during cell exposure to hyposmolarity.

5.1 Protein Kinases, Protein Tyrosine Kinases and Small GTPases

Hyposmolarity leads to activation of a variety of kinases and tyrosine kinases including FAK, Src, PI3-kinase and the MAP kinases ERK, JNK and p38.[7, 9, 30] Members of the Ras family of small GTPases are also activated during hyposmolarity. Most of these enzymes are related to EGFR activation. Not all of them, however, appear to be coupled to the efflux pathways of Cl^- or taurine. This is not unexpected, since cell

swelling and the subsequent volume regulatory mechanisms are complex phenomena involving cell reactions to stress, cell adhesion or retraction and cytoskeleton reorganization, among others. All these processes activate their own signals which may or may not be implicated in the activation of corrective osmolyte fluxes. For instance, the Ras/MAPK pathway is consistently activated in response to hyposmolarity in a large variety of cells,[7] but its blockade has no effect on the volume sensitive efflux of Cl^- or taurine in most cell types;[8, 22] an exception is the volume-sensitive Cl^- channel in astrocytes.[31] The same lack of correlation is found in most but not all cells for the stress-activated protein kinases p38 and JNK.[21, 22, 32, 33] An EGFR-connected element more directly linked to the osmosensitive taurine efflux is PI3K. TKR can activate PI3K through at least two distinct pathways, a Ras-dependent pathway or via the adaptor proteins Shc, Grb-2 and Gab-1 which provide the docking site to bind the p85 subunit of PI3K. Activation of PI3K by EGFR may also be mediated by Src phosphorylation. We could establish a link between EGFR activation by hyposmolarity and PI3K in Swiss3T3 fibroblasts, since activation of PI3K in the hyposmotic condition is prevented by blockade of EGFR (Figure 4). This pathway appears linked to the osmolyte fluxes involved in cell volume regulation as shown by the effect of PI3K inhibition by wortmannin, LY294002 or treatment with antibodies to the 110-catalytic subunit, impairing cell volume recovery, as well as the volume-sensitive Cl^- channel and the osmosensitive ^{125}I and taurine fluxes[21, 22, 34] (Figure 4).

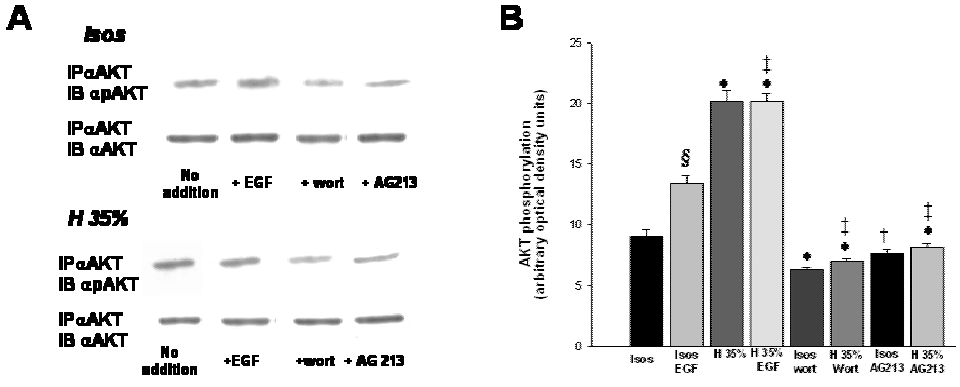

Figure 4. PI3K activation by hyposmolarity and the effect of EGFR blockade. **A**. Activation of PI3K by EGF in isosmotic medium and the effect wortmannin and AG213. *Upper panel*: Cell lysates prepared after treatment in the indicated conditions were immunoprecipitated overnight with anti-AKT antibody (IP) and analyzed by Western blotting with anti-pAKT (IB). Blots reprobed with AKT antibody after stripping, to detect protein levels. *Lower pannel:* PI3K activity in hyposmotic (H35) conditions and effects of EGF, wortmannin and AG213. **B.** Quantitative expression of results in A with bars representing the percentage increase of AKT phosphorylation by hyposmotic medium over that in isosmotic medium under the indicated conditions. Results are means ± SE of 4-6 experiments. Significantly different from isosmotic condition *P<0.001; §P< 0.005. Significantly different from 35% hyposmotic *P< 0.001. (Data from[16]).

A downstream PI3K signaling pathway relates this kinase with the small G proteins of the Cdc-42/Rac/Rho family. These are proteins regulating a wide range of phenomena such as the structure of the actin cytoskeleton, cell/cell contacts and adhesion, and

reactive oxygen species generation, most of which are related to swelling and regulatory volume decrease. A connection between p21Rho and the volume-sensitive Cl^- channel has already been established.[20, 35] Such a link has also recently been found for taurine fluxes.[36]

5.2 Phosholipases, Ca^{2+} and Ca^{2+}-calmodulin

Implication of phospholipases (PLAs) in osmolyte fluxes came from the early work in Ehrlich ascites cells[37] showing an effect of leukotrienes accelerating RVD and enhancing taurine efflux under isotonic conditions. Also in the neuroblastoma CP100 cells, swelling increases arachidonic acid release which, if prevented by blockade of the PLA2, inhibits taurine and Cl^- fluxes.[38]

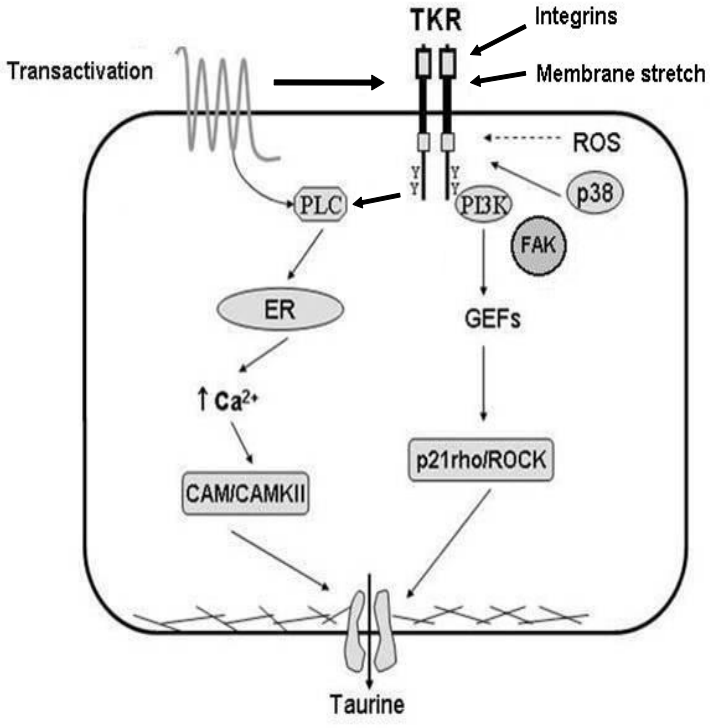

Figure 5. Proposed signaling cascades involved in the activation of EGFR by hyposmolarity and the transduction resulting in the osmosensitive taurine efflux. Activation of the receptor may occur by membrane stretch, interaction with adhesion molecules, transactivation by metabotropic receptors, activation of stress protein and generation of reactive oxygen species. The downstream cascade to trigger or modulate the taurine efflux involves the PLCγ-induced Ca^{2+} release from the endoplasmic reticulum, and CAM/CAMKII signaling as well as PI3K-p21rho-ROCK signaling. CAM: calmodulin; CAMKII: calmodulin dependent kinase II; ER: endoplasmic reticulum; FAK: p125 focal adhesion kinase; PLCγ: phospholipase Cγ; PI3K, phosphatidyl inositide-3 kinase; ROCK: p21rho-kinase; ROS: reactive oxygen species.

An alternate route connecting EGFR activation and taurine osmosensitive fluxes is that mediated by the stimulation on PLCγ or PLD which may both be activated directly by EGFR, while PLA2 is indirectly regulated by other EGF-mediated reactions. Once activated, PLCγ, via generation of diacylglycerol and IP3, leads to Ca^{2+} release from intracellular stores, thereby affecting Ca^{2+}-dependent pathways. The hyposmotic taurine efflux may be Ca^{2+}-dependent or independent according to the cell type, but regardless of the condition, an increase in cytosolic Ca^{2+} markedly potentiates this efflux. Ca^{2+}-calmodulin and Ca^{2+}-calmodulin kinase II appear to be part of the Ca^{2+} effects associated with the swelling-activated taurine efflux.[39]

6. CONCLUSIONS AND PERSPECTIVES

The activation of EGFR and possibly of other TKR by hyposmolarity suggests a role for these receptors in the mechanisms of cell volume sensing or as early signals in osmotransduction. The plethora of interplaying connections with both external and internal messengers, molecules and signaling cascades, a characteristic feature of these receptors, make them exceptionally well-positioned as transducers of the changes in cell volume and the adaptive mechanisms to re-establish normal volume. Moreover, TKR receptors may also offer an interesting link to be considered in cell functions in which both changes in cell volume and TKR activation concur such as proliferation, adhesion and survival.

5. ACKNOWLEDGMENTS

We wish to thank the excellent technical assistance of Claudia Peña-Segura and Alicia Sampieri. This study was supported in part by grants No. IN206403-3 from DGAPA, UNAM and 3586-N from CONACyT.

6. REFERENCES

1. A. Sardini, J.S. Amey, K.H. Weylandt, M. Nobles, M.A. Valverde and C.F. Higgins, Cell volume regulation and swelling-activated chloride channels, *Biochim. Biophys. Acta* **1618**, 153 (2003).
2. H. Pasantes-Morales and M. Morales-Mulia, Influence of calcium on regulatory volume decrease role of potassium channels, *Nephron,* **86**, 414 (2000).
3. J. Furst, M. Gschwentner, M. Ritter, G. Botta, M. Jakab, M. Mayer, C. Bazzini, G. Meyer, S. Eichmuller, E. Woll and M. Paulmilch, Mechanisms sensing and modulating signals arising from cell swelling, *Eur. J. Physiol.* **441**, 1(2002).
4. K. Kirk and K. Strange, Functional properties and physiological roles of organic solute channels, *Ann. Rev. Physiol.* **60**, 719 (1998).
5. H. Pasantes-Morales, R. Franco, M. E. Torres-Márquez and A. Ortega, Amino acid osmolytes in regulatory volume decrease and isovolumetric regulation in brain cells: contribution and mechanisms, *Cell Physiol. Biochem.* **10**, 361 (2000).
6. H.K. Hoffmann. Intracellular signalling involved in volume regulatory decrease, *Cell Physiol. Biochem.* **10**, 273 (2000).
7. T. Van der Wijk, S. Tomassen, H. De Jonge and B.C. Tilly, Signalling mechanisms involved in volume regulation of intestinal epithelial cells, *Cell Physiol. Biochem.* **10**, 289 (2000).

8. B.C. Tilly, N. Van den Berghe, L.G. Tertoolen, M.J. Edixhoven and H.R. de Jonge, Protein tyrosine phosphorylation is involved in osmoregulation of ionic conductances *J. Biol. Chem.* **268**, 19919 (1993).
9. H. Pasantes-Morales, V. Cardin and K. Tuz, Signalling events during swelling and regulatory volume decrease, *Neurochem. Res.* **25,** 1301 (2000).
10. P.O. Hackel, E. Zwick, N. Prenzel and A. Ullrich, Epidermal growth factor receptors: critical mediators of multiple receptor pathways, *Curr. Opinion Cell Biol.* **11,** 184 (1999).
11. R.N. Jorissen, F. Walker, N. Pouliot, T.P.J.Garret, C.W. Ward and A.W. Burgess, Epidermal growth factor receptor: mechanism of activation and signalling, *Exp. Cell Res.* **284,** 31, (2003).
12. N. Prenzel, E. Zwick, M. Leserer and A. Ullrich, Tyrosine kinase signalling in breast cancer epidermal growth factor receptor: convergence point for signal integration and diversification, *Breast Cancer Res.* **2,** 184 (2000).
13. P. Dent, A. Yacoub, J. Contessa, R. Caron, G. Amorino, K. Valerie, M.P. Hagan, S. Grant and R. Schmidt-Ullrich, Stress and radiation-induced activation of multiple intracellular signalling pathways, *Radiation Res.* **159,** 283 (2003).
14. C. Li and Q. Xu, Mechanical stress-initiated signal transductions in vascular smoth muscle cells, *Cellular Signalling,* **12,** 435 (2000).
15. C. Rosete and M. Karin, Ultraviolet light and osmotic stress: activation of JNK cascades through multiple growth factor and cytokine receptors, *Science,* **274,** 1194, (1996).
16. R. Franco, R. Lezama, B. Ordaz B and H. Pasantes-Morales, Epidermal growth factor receptor is activated by hyposmolarity and is an early signal modulating osmolyte efflux pathway in Swiss3T3 fibroblasts, *Eur. J. Physiol.* **447,** 830 (2004).
17. N.J. Boudreau and P.L. Jones, Extracellular matrix and integrin signaling: the shape of things to come, *Biochem. J.* **339,** 481 (1999).
18. L. Moro, M. Venturino, C. Bozzo, L. Silengo, F. Altruda, L. Beguinot, G. Tarone and P. Defilippi, Integrins induce activation of EGF receptor: role in MAP kinase induction and adhesion dependent cell survival *EMBO J.* **17,** 6622 (1998).
19. S. vom Dahl, S. Schliess, R. Reissmann, B. Gorg, O. Weiergraber, M. Kocalkova, F. Dombrowsky and D. Haussinger, Involvement of integrins in osmosensing and signaling toward autophagic proteolysis in rat liver, *J. Biol. Chem.* **278,** 27088 (2003).
20. B.C. Tilly, M.J. Edixhoven, L.G. Tertoolen, N. Morii, Y. Saitoh, S. Narumiya and H.R. de Jonge, Activation of the osmosensitive chloride conductance involves p21Rho and is accompanied by a transient reorganization of the F-actin cytoskeleton, *Mol. Biol. Cell,* **7,** 1419 (1996).
21. B.C. Tilly, M. Gaestel, K. Engel, M.J. Edixhoven and H.R. de Jonge, Hypo-osmotic cell swelling activates the p38 MAPK signaling cascade, *FEBS Lett.* **395,** 133 (1996).
22. S. Morales-Mulia, V. Cardin, M.E. Torres-Márquez, A, Crevenna and H. Pasantes-Morales, Influence of protein kinases on the osmosensitive release of taurine from cerebellar granule neurons *Neurochem. Int.* **38,** 153 (2001).
23. H. Cheng, J. Kartenbeck, K. Kabsch, X. Mao, M. Marques and A. Alonso, Stress kinase p38 mediates EGFR transactivation by hyperosmolar concentrations of sorbitol, *J. Cell Physiol.* **192,** 234 (2002).
24. H.I. Lambert, Reactive oxygen species regulates swelling-induced taurine efflux in NIH3T3 mouse fibroblasts, *J. Membrane Biol.* **192,** 19 (2003).
25. M.S. Crouch, D.A. Davy, F.S. Willard and L.A. Berven, Activation of endogenous thrombin receptors causes clustering and sensitization of epidermal growth factor receptors of Swis3T3 cells without transactivation, *J. Cell. Biol.* **152,** 263 (2001).
26. I:F.Abdullaev, R.Z. Sabirov and Y. Okada, Upregulation of swelling-activated Cl-channel sensitivity to cell volume by activation of EGF receptors in murine mammary cells, *J Physiol* **549,** 749 (2003).
27. F.Y. Zeng, A. Benguria, S. Kafert, S. Andre, H.J. Gabius and A. Villalobo, Differential response of epidermal growth factor receptor tyrosine kinase activity to several plants and mammalian lectins, *Mol. Cell. Biochem.* **142,** 117 (1995).
28. A. Stutzin, R. Torres, M. Oporto, P. Pacheco, A.L. Eguiguren, L.P. Cid and F.V. Sepúlveda, Separate taurine and chloride efflux pathways activated during regulatory volume decrease, *Am.J. Physiol.* **277,** C392 (1999).
29. S.G. Rane, Ion channels as physiological effectors for growth factor receptors and ras/erk signaling pathway, *Adv. Sec. Mess. Phosph. Res.* **33,** 107 (1999).
30. M. Jakab, J. Furst, G. Botta, M.L. Garavaglia, C. Bazzini, S. Rodighiero, G. Meyer, E. Woll, S. Chwatal, M. Ritter and M. Paulmichl, Mechanisms sensing and modulating signals arising from cell swelling, *Cell Physiol. Biochem.* **12,** 235 (2002).
31. V. Crepel, W. Panenka, M.E. Kelly and B.A. MacVicar, Mitogen-activated protein and tyrosine kinases in the activation of astrocyte volume-activated chloride current, *J. Neurosci.* **18,** 1196 (1998).

32. N. Niisato, M. Post, W.Van Driessche and Y. Marunaka, Cell swelling activates stress-activated protein kinases, p38 MAP kinase and JNK, in renal epithelial A6 cells, *Biochem. Biophys. Res Commun.* **266,** 547 (1999).
33. D. Haussinger, F. Schliess, F. Dombrowski and S.vom Dahl, Involment of p38 MAPK in the regulation of proteolysis by liver cell hydration, *Gastroenterology.* **116,** 921 (1999).
34. A.P. Feranchak, R.M. Roman, E.M. Schweibert and J.G. Fitz, Phosphatidylinositol 3-kinase contributes to cell volume regulation through effects on ATP release, *J. Biol. Chem.* **273,** 14906 (1998).
35. B. Nilius, T. Voets, J. Prenen, H. Barth, K. Aktories, K. Kaibuchi, G. Droogmans and J. Eggermont, Role of Rho and Rho kinase in the activation of volume-regulated anion channels in bovine endothelial cells *J. Physiol.* **516,** 67 (1999).
36. R. Franco, R. Martínez and H. Pasantes-Morales, Mechanisms of the ATP potentiation of hyposmotic taurine release in Swiss3T3 fibroblasts (submitted).
37. I. H. Lambert, Regulation of taurine content in Ehrlich ascites tumour cells, *Adv. Exp. Med. Biol.* **442,** 269 (1998).
38. S. Bassavappa, S.F. Pedersen, N.K. Jorgensen, J.C. Ellory and E.K. Hoffmann, Swelling-induced arachidonic acid release via the 85-kDa cPLA2 in human neuroblastoma cells, *J. Neurophysiol.* **79,** 1441 (1998).
39. V. Cardin, R. Lezama, M.E. Torres-Márquez and H. Pasantes-Morales, Potentiation of the osmosensitive taurine release and cell volume regulation by cytosolic Ca^{2+} rise in cultured cerebellar astrocytes, *GLIA* **44,** 119 (2003).

28

GLIAL-NEURONAL SIGNALING AND ASTROGLIAL SWELLING IN PHYSIOLOGY AND PATHOLOGY

Elisabeth Hansson and Lars Rönnbäck*

1. INTRODUCTION

The central nervous system (CNS) consists of 10^{11} neurons and three to five times as many glial cells. These glial cells make up four major groups: 1) astrocytes; 2) oligodendrocytes; 3) microglia; and 4) ependymal cells, of which the astrocytes or astroglial cells are the most frequent in terms of number and occupy a prominent volume in the CNS. The long processes of the astrocytes encapsulate synapses, neuronal cell bodies, and blood vessels and form the blood-brain barrier (BBB) together with the endothelial cells of the blood vessel walls. Of particular importance is the strategic position of the astrocytes between the vasculature and the synapses. Synaptic activity regulates the support of metabolic substrates provided to the neurons from the astrocytic networks.[1,2] There is extensive Ca^{2+} signaling within the astrocytic gap junction-coupled networks.[3] With the aid of adenosine triphosphate (ATP) as mediating factor, such signaling has been demonstrated to also involve astroglial networks which are not gap junction-coupled,[4,5] and there seems to be a tight regulation of gap junction- and ATP-mediated signaling pathways in a coordinated manner.[6,7]

Astrocytes also express a set of functional and neurochemical properties previously considered specific to neurons. For instance, the cells are supplied with membrane receptors for most known neurotransmitters and neuromodulators.[8] Receptors found on astrocytes can be divided into three categories: 1) those coupled to heterotrimeric G proteins or ion channels such as glutamate and gamma-aminobutyric acid (GABA) receptors and receptors for monoamines such as noradrenaline, dopamine, serotonin, and histamine; 2) other membrane receptors coupled to intracellular protein kinases; and 3) nuclear receptors associated with either mitochondria or cell nuclei.

*Elisabeth Hansson and Lars Rönnbäck, Institute of Clinical Neurosciene, Goteborg University, P.O. Box 420, Medicinaregatan 5, SE 405 30 Goteborg, Sweden, Tel.: +46-31-773-3363, Fax: +46-31-773-3330, elisabeth.hannson@anatcell.gu.se

Furthermore, the astrocytes have a capacity to monitor extracellular glutamate and maintain it at low levels with the aid of the glutamate aspartate transporter (GLAST) and the glutamate transporter 1 (GLT-1).[9,10] Astrocytes utilize glucose taken up from the blood and supply substrates of energy metabolism and amino acids to neurons, mainly lactate, α-ketoglutarate, and alanine.[11] The interactions between astrocytes and neurons are crucial not only for the energy metabolism in the brain, but also, for *de novo* synthesis of the amino acid transmitters glutamate and GABA[12,13] (for aspects on astroglial properties and characteristics, see Figure 1).

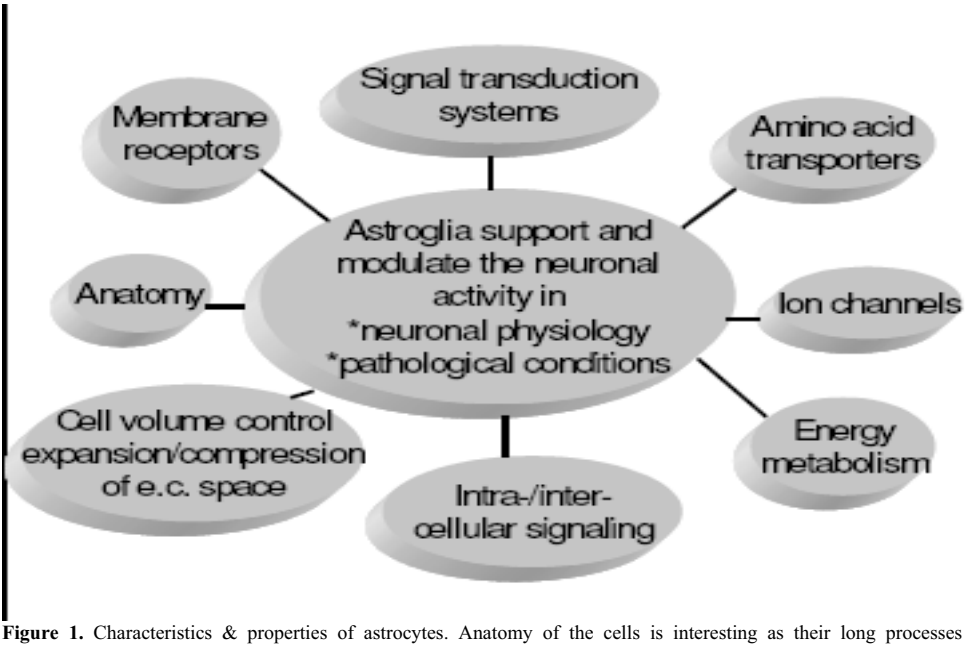

Figure 1. Characteristics & properties of astrocytes. Anatomy of the cells is interesting as their long processes encapsulate synapses and blood vessels and reach neuronal cell bodies. In addition, astrocytic processes establish contacts with each other, forming a network in which signals pass and low molecular weight substances are transported. Astroglia express membrane receptors for most neurotransmitters and neuromodulators, amino acid transporters, and ion channels. The cells have a multitude of signal transduction systems for intra- and intercellular signaling, serving energy substrates to neurons and have well-developed systems for volume regulation. Changes in astroglial intracellular volume affect the volume and shape of the extracellular space, thus the concentration of neuroactive substances within this space. The astroglial networks have a strategic position vis-à-vis the neuronal networks, and data indicate that neuronal excitability level can be influenced, at least in part, by the activity and physiological status of the astroglial networks.

Taken together, this provides a prominent cellular and molecular basis for two-way signaling and interactions between astrocytic and neuronal networks.[14] Furthermore, a large amount of data has accumulated on the importance of signaling events in the neuron-glial unit for the establishment of higher brain functions including learning and memory (for further reading, see reference 15,16). In this context, it should be remembered that most studies on glial properties, reactions, and signaling have been

performed in primary cultures or brain slice preparations because the tightly interwoven cellular networks and large array of substances active in cell signaling have made it easier to evaluate the role of individual substances at the single cell level. Therefore, most knowledge on glial biology should be verified in *in vivo* systems.

2. NEURON-GLIAL SIGNALING IN THE GLUTAMATERGIC SYNAPTIC REGION

When the action potential of the axon reaches the presynaptic region, the neuronal depolarization induces a release of K^+ into the extracellular space. Glutamate is released from the presynaptic terminal and when it interacts with the postsynaptic membrane receptors, there is neuronal depolarization, resulting in an increased level of $[K^+]_e$ around the postsynaptic area. The increased $[K^+]_e$ is recognized by the astrocytic membranes and K^+ is taken up by these cells. The astrocytes function as a sink for K^+ which can be transported within the astroglial gap junction-coupled network to places of lower neuronal activity.[17,18] Activation of astroglial metabotropic glutamate receptors (mGluRs) induces the formation of inositol-1,4,5-trisphosphate (IP_3) which leads to mobilization of intracellular Ca^{2+} ($[Ca^{2+}]_i$) and formation of Ca^{2+} oscillations and/or Ca^{2+} waves that travel within the cell and further, to other cells in the astrocytic network.[3] On the basis of appropriate signals passing from one cell type to the other, a coordination of glial activity can be formed. In mGluRs bearing astrocytes, the synaptic release of glutamate has been shown to evoke periodic increases in $[Ca^{2+}]_i$ which are tunable in frequency, according to the level of neuronal activity.[19] Glutamate-mediated neuronal-astrocyte signaling may therefore represent a refined communication system which allows neurons to transfer information to astrocytes at the level of their activity.[20] These observations have changed the common concept that information intake and processing in the form of learning and establishment of memory are exclusive activities of neuronal cells. It has been shown that mGluRs control the release of glutamate and prostaglandins from astrocytes which can be pulsatile and synchronous with mGluR-mediated oscillations in $[Ca^{2+}]_I$.[21-23]

Furthermore, astrocytes release ATP[24] after triggering $[Ca^{2+}]_i$. Adenosine triphosphate is a key extracellular messenger that mediates propagation of Ca^{2+} waves in the astrocytic networks which may play a critical role in astrocyte proliferation and differentiation and in modulating neuronal activity. Adenosine triphosphate in the extracellular space stimulates the P_{2x} purinoceptors on astrocytes[25] and the P_{2X} purinoceptors[26] on microglia. The astrocytes seem to play an important regulatory role in the process of microglial differentiation and deactivation.[14] Astrocytic Ca^{2+} waves and concomitant ATP release could communicate injury to uninjured areas by activation of the microglial cells which can release cytokines such as tumor necrosis factor α (TNF-α) and interleukin 1 (IL-1).[27] These released factors could then influence the Ca^{2+} wave which could lead to state-dependent changes in morphology and consequently, the relationship and functional interactions in the synaptic region. Subsequent synaptic remodeling can result in altered numbers of GABA-ergic (inhibitory), glutamatergic (excitatory), or noradrenergic (excitatory) synapses. The neuronal-glial and synaptic changes occur rapidly, possibly within hours.[28]

3. ASTROGLIAL CELL VOLUME REGULATION AND VOLUME TRANSMISSION

The volume of the extracellular space composes up to 20% of the total brain volume.[29] It constitutes the microenvironment for neurons and glia and is a site for communication between the different cell types. The neurons communicate by synaptic transmission and diffusion of ions and neurotransmitters through the extracellular space, while the preferential communication between neurons and glia or between different glial cell types is based on extrasynaptic signaling. Neuroactive substances, released non-synaptically, diffuse via the extracellular space to their targets which can be located near or far from the release sites. This type of extracellular signaling is called "volume transmission" as the neuroactive substances move through the volume of extracellular space.[30, 31] Extrasynaptic transmission is dependent on the structure and physiochemical properties of this microenvironment.[29]

As astrocytes are the glial cells occupying comparatively most of the brain tissue volume, alterations in astroglial intracellular volume have a great impact upon the shape and volume of the local extracellular space, thereby altering concentrations of extracellular neuroactive substances, with a subsequent influence on the glial-neuronal signaling. The astrocytes have a well-developed capacity for cell volume regulation.[32, 33] One main function of cell volume changes is to keep the osmolarity at a constant level, both outside and inside the cell. Cell swelling is rapidly seen after a brain injury but may also occur under normal conditions when there is intense neuronal activity with changes in the composition of neuroactive substances in the extracellular milieu as a result.[34] Astrocytic swelling can be attributable to an uptake of osmoles such as Na^+, Cl^-, K^+, or glutamate from the extracellular to the intracellular space. The active exchange transporters, the Na^+-K^+-$2Cl^-$ transporter, and the Na^+-K^+-adenosine triphosphatase (ATPase) are involved as are volume-sensitive Cl^- channels. Another important mechanism for volume changes may be transmitter-stimulated carbonic anhydrase activities such as H^+ and HCO_3^- created by the hydration of CO_2 and transported out of the cell via the Na^+/H^+ and Cl^-/HCO_3^- carriers. This would lead to an accumulation of NaCl and therefore to a net increase in osmolarity, driving water into the cell.[35] There seems to be an intimate relationship between cell volume control, ion fluxes, and intracellular pH. Some free amino acids such as taurine may participate in cell volume regulation as osmoregulatory molecules.[36] Even the excitotoxic amino acid aspartate has been demonstrated to be released by swollen astroglial cells in primary culture.[37] Due to the tentative importance of the extracellular space for the active transport of neuroactive substances, it may be that in addition to its osmoregulatory function, astroglial volume control is a much more active process than previously thought.[38]

4. ALTERED GLIAL-NEURONAL SIGNALING DUE TO IMPAIRMENT OF ASTROGLIAL GLUTAMATE UPTAKE MAY INDUCE MENTAL FATIGUE

Glutamate, the most extensively studied excitatory neurotransmitter in the brain, is indispensable to information intake, processing, and memory formation.[16,39,40] After glutamate has exerted its effects on the postsynaptic and adjacent glial membrane receptors, the astroglial glutamate uptake carriers GLT-1 and GLAST remove excess

glutamate from the extracellular space. Inhibition of the astroglial glutamate transporters GLAST or GLT-1 by knock-out techniques has been demonstrated to produce elevated extracellular glutamate levels, while inhibition of the neuronal glutamate transporter EAAC1 does not elevate the extracellular glutamate level.[41] The extracellular concentration of glutamate should be below 3 μM in order for the glutamatergic neurotransmission to be effective.[42] In nervous tissue pathology, i.e., stroke, trauma, degeneration, infection, inflammation, and metabolic or toxic disturbances, the production of substances has been demonstrated to impair astroglial glutamate uptake, as have altered conditions. An increased extracellular glutamate level has also been demonstrated in most of these states.[43] Taken together, it is highly probable that astroglia are responsible for keeping the extracellular glutamate at low levels by clearing glutamate from this space. Examples of the above-mentioned substances which decrease astroglial glutamate uptake are: free oxygen radicals, arachidonic acid, lactic acid, endothelins, cytokines and leukotriens (such as TNF-α, interferon-γ (INF-γ), IL1- , and leukotriene B4), amyloid peptides, nitric oxide (NO), peroxynitrite, hemosiderin (in cases of little bleeding), and glucocorticoids.[44-51] The altered conditions mentioned above include disturbed energy metabolism or acidosis.[52] The production of such substances or altered conditions may precede CNS pathology such as inflammation or degeneration and may also continue in the CNS for variable time periods after damage, infection or inflammation. Activated microglial cells can produce many of these substances in response to all forms of pathology, both within the CNS and in the periphery.[53]

4.1. What Could the Consequences Be, for Cognitive Functions, of a Slightly Impaired Astroglial Glutamate Uptake?

In conditions of impaired astroglial uptake of extracellular glutamate, extracellular glutamate levels increase and long-term stimulation of the N-Methyl-D-Aspartate (NMDA) receptors leads to a Ca^{2+} influx into NMDA-receptor-bearing neurons. A subsequent neuronal cell death by excitotoxicity may follow. We will not go into the problems of excitotoxicity in this chapter. Instead, we present a hypothesis focusing on possible consequences of slightly impaired astroglial uptake for higher cortical functions, resulting in decreased endurance over time of information processing. With this hypothesis, we try to give one explanation, at the cellular level, to the mental fatigue symptom with the feeling of being exhausted, tense and irritable which occurs in connection with almost every mild to moderate dysfunction of the brain regardless of the location of the lesion (see also under "mild cognitive disorder" DSM-IV,[54] the classification system by Lindqvist and Malmgren[55] and Figure 2).

In conditions of slightly impaired astroglial glutamate uptake, mental activity will lead to slightly increased glutamate levels around the neurons and synaptic regions over time (Figure 2, bottom). Increases in extracellular glutamate concentration slightly over 3-5μM could reduce the efficiency of the glutamate signaling and decrease the signal-to-noise ratio in the glutamate transmission. As a consequence, less precise or less distinct signals will be processed within the brain.[56] We propose that under these conditions, incoming stimuli will be recognized by the brain as being less distinct. Due to difficulties in selecting "old" from "new," information recognized as "new" due to its indistinct character will travel up to the cortex to be processed there. This was an adequate reaction of the brain in old days when people were living as farmers. Then, even in situations of

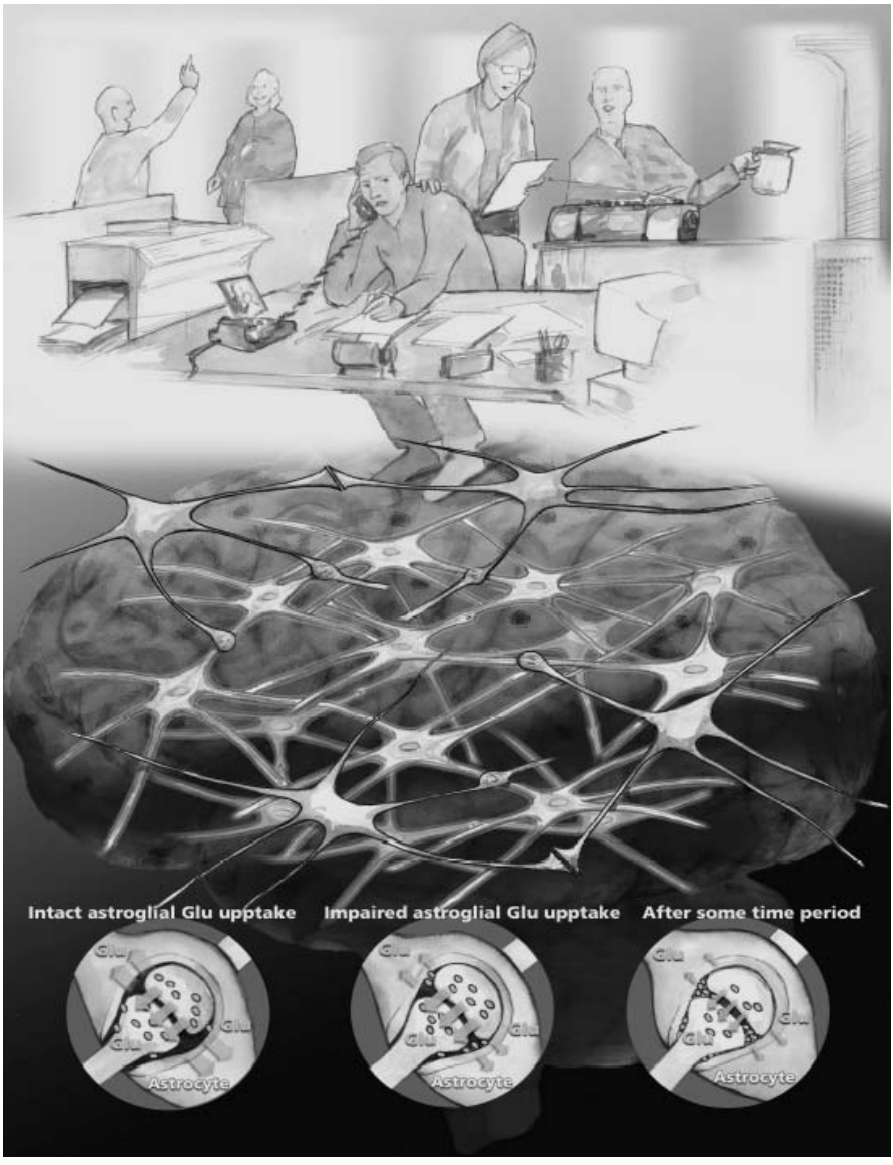

Figure 2. In connection with almost every organic or psychologically-induced mild to moderate dysfunction of the brain, e.g., during rehabilitation after a brain injury, inflammation or long-term stress reaction, the person suffers from mental fatigue, noise and light sensitivity, irritability, affect lability, and stress intolerance. Symptoms probably reflect a decreased capacity of the brain to handle and process information due to brain dysfunction. According to our hypothesis herein, one cellular mechanism underlying the symptoms is an impaired astroglial glutamate uptake capacity, resulting in slightly increased extracellular glutamate levels and decreased signal-to-noise ratio in the glutamate transmission over time. When the brain is exposed to a multitude of sensory stimulation (upper part of the Figure), the cerebral cortex will be overstimulated, and in the situation of decreased astroglial glutamate extracellular clearance, the end point will be cellular exhaustion expressed as mental fatigue.

mild brain dysfunction, it was important to be able to recognize threatening danger such as the roaring of wild animals. At that time, sensory stimulation was limited. Today, it is quite different; there is a massive sensory influx to the brain. At a modern place of work, there is prominent sound, noise and light stimulation (Figure 2, top). When exposed to such a stimuli enriched milieu, many neuronal circuits will be activated at the same time.

If there is an impaired astroglial glutamate clearance of the extracellular space, the information reaching the cerebral cortex will be handled with more noise and less precision. In addition, activation of astroglial networks, with induction of Ca^{2+} oscillations both within and between the gap junction-coupled astroglial networks and with a subsequent astroglial release of glutamate, can increase the excitability level in neighboring neuronal circuits. The overall result may be that more and larger neuronal circuits will be activated over time.

Furthermore, in states of decreased astroglial glutamate uptake capacity, even astroglial glucose uptake, thereby the supply of metabolic substrates for the neurons will decrease,[57] and there may be relative energy insufficiency at the cellular level in neuronal circuits. Experimental investigations in the rat and monkey have demonstrated a feedback loop from the left basal frontal cortex, with an inhibitory influence on the locus coeruleus in the brain stem.[58] If this loop also exists in humans, a slight increase in the neuronal firing, due to slightly elevated glutamate levels during prolonged time in the basal frontal cortex, could lead to a decrease in noradrenaline and 5-HT release in the cerebral cortex which would also decrease glucogenolysis,[59, 60] and furthermore impair metabolic substrates for cortical neurons. A disturbed noradrenaline-/5-HT turnover could further explain the disturbed attention and "filter" function of sensory information typical of such human patients.[61, 62]

Taken together, since many neuronal circuits are activated in parallel with a decreased capacity for supply and utilization of cellular metabolic substrates, there will be an increasing energy deficiency at the cellular level over time. In addition, glutamate release from the presynaptic terminals could decrease due to factors such as a decreased glutamine supply of the neurons. The result will be metabolic exhaustion, experienced as increased mental fatigue, with secondary learning and memory impairment.

When the composition of the extracellular milieu is disturbed, microglial cells are activated and could produce cytokines, among which for instance TNF-*a*, if released, could induce a vicious cycle by further decreasing the astroglial glutamate uptake capacity. Furthermore, glucocorticoids produced due to anxiety or stress experienced by the affected person may have similar effects, at least on the astroglial glutamate transport.[45] Our hypothesis could serve as a biological basis for understanding and recognizing the symptoms which are regarded as unspecific by many clinicians and are therefore underestimated. The hypothesis could then lead to formulation and further investigation of strategies for treatment.[40]

4.2. Testing the Hypothesis

The hypothesis should be tested in humans suffering from mental fatigue due to an organic brain process or a long period of psychological suffering. Brain imaging techniques with the ability to identify, determine and follow over time, during heavy mental activity, the extracellular concentrations of glutamate and/or K^+, or cellular energy consumption would be suitable. At present, however, this is not possible for technical reasons. Specific parts of the hypothesis can, however, be tested. Neuroactive substances

produced or altered conditions related to brain pathology can be evaluated with regard to their effects on astroglial glutamate transport capacity, especially following the production of such substances over time. The role of the intact astroglial network in higher brain functions can be studied in animal models. Effects of astroglial dysfunction with regard to glutamate transport capacity would be of special interest. Even clinical studies with different treatment strategies may be important in casting some light on the accuracy of the hypothesis.

4.3. Strategies for Treatment

When considering treatment, it is important to recognize the mental fatigue symptoms as they constitute a concealed disability and can cause additional anxiety and stress for the patient. Providing information about the prognosis, which mostly is a positive process, is important for breaking the vicious cycle which brings with it the risk for secondary anxiety and depression. Furthermore, it is of utmost importance to avoid too much sensory stimulation. If our hypothesis is correct, at least theoretically, it would be possible to provide additional improvement to the symptoms by suppressing the production of proinflammatory cytokines, reactive oxygen species, and NO, and thus, increase the glial glutamate uptake. In this context, xanthine derivatives may be of some interest.[63] However, due to the cellular signaling discussed above, it would be probable that there would be a rebuilding of neuronal circuits. It would therefore be important to identify the symptoms and treat them as early as possible to avoid formation of new and functionally disturbing neuronal circuits due to overstimulation of neuronal-glial units.

5. CONCLUSIONS AND PERSPECTIVES

Recent knowledge of neuronal-glial signaling has increased our understanding of dynamic and plastic changes in the nervous system including formation of new synapses. Signaling has been demonstrated to occur both within and between gap junction-coupled astroglial networks. Therefore, at least tentatively, flexible astroglial cell networks could be formed with the possibility to act as functional units. Within these networks, low molecular weight substances are transported through the gap junction channels. The astroglial networks nourish, protect, and interact with the surrounding neuronal networks. Two-way signaling is made possible as the cells are supplied with a multitude of membrane ionic channels, transporters and receptors, making them able to receive, integrate, and transmit signals. The pH_i is important since the Na^+-HCO_3^- transporter, which is electrogenic, is sensitive to any changes in the membrane potential. Recent results also demonstrate that astroglial cells signal back to neurons through the excitatory amino acid glutamate. Thus, the neuronal excitability level could be influenced by the functional status of the astroglial networks. The highly regulated astroglial cell volume has an influence upon the volume and shape of the extracellular space in which a prominent amount of neuroactive substances is transported, another dimension of brain cell signaling. Due to this intricate cell signaling, it has been postulated that higher cortical functions such as learning, memory and language take place not only due to neuronal interactions and to the glia acting as mere passive supportive cells. There also seems to be close interaction and signaling between glia and neurons underlying plasticity. In this context, the microglial cells are of utmost significance. At rest, these

cells produce neurotrophic substances of importance for neuronal survival and function. Microglia also sense even extremely small alterations in the composition of substances in the extracellular space. In pathology, microglia produce and release cytokines and other substances which, through astroglial and neuronal mechanisms, can influence neuronal excitability. Knowledge of such signaling could help us understand symptoms such as the mental fatigue experienced during rehabilitation after stroke, brain injury or states of extreme and long-term stress reactions. With this knowledge, it is also easy to imagine that, with the formation of new synapses due to neuronal-glial signaling, the plasticity can go wrong and result in the formation of non-functional neuronal circuits. Resulting symptoms could be chronic even if the pathological agents have been removed (cf., e.g., the situation at chronic pain[64]).

6. ACKNOWLEDGMENTS

The work performed in the authors´ laboratories was supported by grants from the Swedish Research Council (projects no. 33X-06812 and 21X-13015), Edith Jacobson´s Foundation, and the Swedish Council for Working Life and Social Research. The technical assistance of the authors´ research by Ulrika Björklund, Barbro Eriksson and Mona Brantefjord is greatly appreciated. Figure 2 was drawn by Eva Kraft, Göteborg, Sweden.

7. REFERENCES

1. D.O. Keyser, and T.C. Pellmar, Synaptic transmission in the hippocampus: critical role for glial cells, *GLIA*, **10**, 237-243 (1994).
2. A. Araque, V. Parpura, R.P. Sanzgiri, and P.G. Haydon, Tripartite synapses: glia, the acknowledged partner, *Trends Neurosci*. **22**, 208-215 (1999).
3. F. Blomstrand, S. Khatibi, H. Muyderman, E. Hansson, T. Olsson, and L. Rönnbäck, 5-Hydroxytryptamine and glutamate modulate velocity and extent of intercellular calcium signalling in hippocampal astroglial cells in primary culture, *Neuroscience*, **88**, 1241-1253 (1999).
4. M.L. Cotrina, J.H. Lin, A. Alves-Rodrigues, S. Liu, J. Li, H. Azmi-Ghadimi, J. Kang, C.C. Naus, and M. Nedergaard, Connexins regulate calcium signalling by controlling ATP release, *Proc. Natl. Acad. Sci. USA* **95**, 15735-15740 (1998).
5. P.B. Guthrie, J. Knappenberger, M. Segal, M.V.L. Bennett, A.C. Charles, and S.B. Kater, ATP released from astrocytes mediates glial calcium waves, *J. Neurosci*. **19**, 520-528 (1999).
6. G.R. John, E. Scemes, S.O. Suadicani, J.S.H. Liu, P.C. Charles, S.C. Lee, D.C. Spray, and C.F.Brosnan, IL-1β differentially regulates calcium wave propagation between primary human fetal astrocytes via pathways involving P2 receptors and gap junction channels, *Proc. Natl. Acad. Sci. USA*. **96**, 11613-11618 (1999).
7. N. Rouach, J. Glowinski, and C. Giaume, Activity-dependent neuronal control of gap-junctional communication in astrocytes, *J. Cell Biol*. **149**, 1513-1526 (2000).
8. E. Hansson, and L. Rönnbäck, Astrocytic receptors and second messenger systems, *Advances in Molecular and Cell Biology* (Elsevier Science B.V. **31**, pp. 475-502 (2003).
9. G. Gegelashvili, Y. Dehnes, N.C. Danbolt, and A. Shousboe, The high-affinity glutamate transporters GLT, GLAST, and EAAT4 are regulated via different signalling mechanisms, Neurochem. Int. 37, 163-170 (2000).
10. N.C. Danbolt, Glutamate uptake, *Progr. Neurobiol*. **65**, 1-105 (2001).
11. M Tsacopoulus, Metabolic signaling between neurons and glial cells: a short review, *J. Physiol., Paris*, **96**, 283-288 (2002).
12. L. Hertz, R. Dringen, A. Schousboe, and S.R. Robinson, Astrocytes: Glutamate producers for neurons, *J. Neurosci. Res*. **57**, 417-428 (1999).

13. L. Hertz, A.C.H. Yu, G. Kala, and A. Schousboe, Neuronal-astrocytic and cytosolic mitochondrial metabolite trafficking during brain activation, hyperammonemia and energy deprivation, *Neurochem. Int.* **37**, 83-102 (2000).
14. E. Hansson, and L. Rönnbäck, Glial neuronal signaling in the central nervous system, *FASEB J,* **17**, 341-348 (2003).
15. J.M. Robertson, The astrocentric hypothesis: proposed role of astrocytes in consciousness and memory function, *J. Physiol. Paris* **96**, 251-255 (2002).
16. L. Hertz, E. Hansson, and L. Rönnbäck, Signaling and gene expression in the neuron-glia unit during brain function and dysfunction: Holger Hydén in memorian, *Neurochem. Int*. **39**, 227-252 (2001).
17. R.K. Orkand, J.G. Nicholls, and S.W. Kuffler, Effect of nerve impulses on the membrane potential of glial cells in the nervous system in amphibian, *J Neuropysiol.* **29**, 788-806 (1966).
18. R.K. Orkand, Glial-interstitial fluid exchange, *Ann NY Acad Sci*. **481**, 269-272 (1986).
19. L. Pasti, A. Volterra, T. Pozzan, and G. Carmignoto, Intracellular calcium oscillations in astrocytes : a highly plastic, bidirectional form of communication between neurons and astrocytes in situ, *J. Neurosci*. **17**, 7817-7830 (1997).
20. G. Carmignoto, Reciprocal communication systems between astrocytes and neurones, *Progr. Neurobiol*. **62**, 561-581 (2000).
21. H. Muyderman, M. Ängehagen, M. Sandberg, U. Björklund, T. Olsson, E. Hansson, and M. Nilsson, α_1-Adrenergic modulation of metabotropic glutamate receptor-induced calcium oscillations and glutamate release in astrocytes, *J. Biol. Chem*. **276**, 46504-46514 (2001).
22. M. Zonta, and G. Carmignoto, Calcium oscillations encoding neuron-to-astrocyte communication, *J. Physiol. Paris* **96**, 193-198 (2002).
23. M. Zonta, A. Sebelin, S. Gobbo, T. Fellin, T. Pozzan, and G. Carmignoto, Glutamate-mediated cytosolic calcium oscillations regulate a pulsatile prostaglandin release from cultured rat astrocytes, *Physiology* **17**, 1-16 (2003).
24. P.B. Guthrie, J. Knappenberger, M. Segal, M.V.L. Bennett, A.C. Charles, and S.B. Kater, ATP released from astrocytes mediates glial calcium waves, *J. Neurosci*. **19**, 520-528 (1999).
25. S.R. Fam, C.J. Gallagher, L.V. Kalia, and M.W. Salter, Differential frequency dependence of $P2Y_1$- and $P2Y_2$- mediated Ca^{2+} signalling in astrocytes, *J. Neurosci*. **23**, 4437-4444 (2003).
26. C. Verderio, and M. Matteoli, ATP mediates calcium signalling between astrocytes and microglial cells: modulation by IFN-γ, *J. Immunol*. **166**, 6383-6391 (2001).
27. C.G. Schipke, C, Boucsein, C, Ohlemeyer, F. Kirchhoff, and H. Kettenmann, Astrocyte Ca^{2+} waves trigger responses in microglial cells in brain slices, *FASEB J*. **16**, 255-257 (2002).
28. S.L. Langle, D.A. Poulain, and D.T. Theodosis, Neuronal-glial remodelling: a structural basis for neuronal-glial interactions in the adult hypothalamus, *J. Physiol. Paris* **96**, 169-175 (2002).
29. E. Syková, Glial diffusion barriers during aging and pathological states, *Progr. Brain Res*. **132**, 339-363 (2001).
30. K. Fuxe, and L.F. Agnati, *Volume transmission in the brain: novel mechanisms for neural transmission,* Raven Press, New York, (1991).
31. C. Nicholson, and E. Syková, Extracellular space structure revealed by diffusion analysis, *Trends Neurosci.* **21**, 207-215 (1998).
32. H.K. Kimelberg, S.K. Goderie, S. Higman, S. Pang, and R.A. Waniewski, Swelling-induced release of glutamate, aspartate, and taurine from astrocyte cultures, *J. Neurosci.* **10**, 1583-1591 (1990).
33. E. Hansson, Metabotropic glutamate receptor activation induces astroglial swelling, *J. Biol. Chem.* **269**, 21955-21961 (1994).
34. B.R. Ransom, C.L Yamate, and B.W. Connors, Activity-dependent shrinkage of extracellular space in rat optic nerve: a developmental study, *J. Neurosci.* **5**, 532-535 (1985).
35. O. Kempski, F. Staub, M. Jansen, and A. Baethmann, Molecular mechanisms of glial swelling in acidosis, *Adv. Neurol*. **52**, 39-45 (1990).
36. A.A. Mongin, Z. Cai, and K.H. Kimelberg, Volume-dependent taurine release from cultured astrocytes requires permissive $[Ca^{2+}]_i$ and calmodulin, *Am. J. Physiol*. **277**, C823-C832 (1999).
37. E.M. Rutledge, M. Aschner, and H.K. Kimelberg, Pharmacological characterization of swelling-induced D-[^{3}H]aspartate release from primary astrocyte cultures, *Am. J. Physiol.* **274**, C1511-C1520 (1998).
38. E. Hansson, and L. Rönnbäck, Astrocytes in glutamate neurotransmission, *FASEB J*. **9**, 343-350 (1994).
39. G. Riedel, Function of metabotropic glutamate receptors in learning and memory, *Trends Neurosci*, **19**, 219-224 (1996).
40. E. Hansson, T. Olsson, and L. Rönnbäck, eds. *On astrocytes and glutamate neurotransmission* (Landes Bioscience Company, Springer, Austin, TX, 1997).

41. J.D. Rothstein, M. Dykes-Hoberg, C.A. Pardo, L.A. Bristol, L. Jin, R. Kuncl,Y.Kanai, M.A. Hediger, Y. Wang, J.P Schielke, and D.F. Welty, Knockout of glutamate transporters reveals a major role of astroglial transport in excitotoxicity and clearance of glutamate, *Neuron*,**16**, 675-686 (1996).
42. M. Yudkoff, I. Nissim, Y. Daikhin, Z-P. Lin, D. Nelson, D. Pleasure, and M. Erecinska, Brain glutamate metabolism: neuronal-astroglial relationships, *Dev. Neurosci.* **15**,343-350 (1993).
43. D. Scheller, S. Szathmary, J. Kolb, and F. Tegtmeier, Observations on the relationship between the extracellular changes of taurine and glutamate during cortical spreading depression, during ischemia, and within the area surrounding a thrombotic infarct, *Amino Acids* **19**, 571-583 (2000).
44. B. Barbour, M. Szatkowski, N. Ingledew, and D. Attwell, Arachidonic acid induces a prolonged inhibition of glutamate uptake into glial cells, *Nature* **342**, 918-919 (1989).
45. C.E. Virgin Jr, T.P. Ha, D.R. Packan, G.C. Tombaugh, S.H. Yang, H.C. Horner, and R.M. Sapolsky, Glucocorticoids inhibit glucose transport and glutamate uptake in hippocampal astrocytes: implications for glucocorticoid neurotoxicity, *J. Neurochem.* **57**,1422-1428 (1991).
46. H. Köller, M. Siebler, M. Pekel, and H.W. Muller, Depolarization of cultured astrocytes by leukotriene B4. Evidence for the induction of a K^+ conductance inhibitor, *Brain Res.* **612**, 28-34 (1993).
47. J.P. Bolanos, and J.M. Medina, Induction of nitric oxide synthase inhibits gap junction permeability in cultured rat astrocytes, J. Neurochem. 66, 2091-2099 (1996).
48. S.M. Fine, R.A. Angel, S.W. Perry, L.G. Epstein, J.D. Rothstein, S. Dewhurst, and H.A. Gelbard, Tumor necrosis factor alpha inhibits glutamate uptake by primary human astrocytes. Implications for pathogenesis of HIV-1 dementia, *J. Biol. Chem.* **271**, 15303-15306 (1996).
49. O. Sorg, T.F. Horn, N. Yu, D.L. Gruol, and F.E. Bloom, Inhibition of astrocyte glutamate uptake by reactive oxygen species: role of antioxidant enzymes, *Mol. Med.* **3**, 431-440 (1996).
50. F. Blomstrand, C. Giaume, E. Hansson, and L. Rönnbäck, Distinct pharmacological properties of ET-1 and ET-3 on astroglial gap junctions and Ca^{2+} signaling, *Am. J. Physiol. Cell. Physiol.* **277**, C616-C627 (1999).
51. J. Leonova, T. Thorlin, N.D. Åberg, P.S. Eriksson, L. Rönnbäck, and E. Hansson, Endothelin-1 decreases glutamate uptake in primary cultured rat astrocytes, *Am. J. Physiol. Cell. Physiol.* **281**,C1495-C1503 (2001).
52. R.A. Swanson, K. Farrell , R.P. Simon, Acidosis causes failure of astrocyte glutamate uptake during hypoxia, *J. Cereb. Blood Flow Metab.* **15**,417-424 (1995).
53. G.W. Kreutzberg, Microglia: a sensor for pathological events in the CNS, *Trends Neurosci.* **19**, 312-318 (1996).
54. American Psychiatric Association, *Diagnostic and statistical manual of mental disorders*, 4th ed. Washington DC: American Psychiatric Association (1994).
55. G. Lindqvist, and H. Malmgren, Organic mental disorders as hypothetical pathogenetic processes, *Acta Psychiatr. Scand.* **88**, Suppl 373:5-17 (1993).
56. F.W Pfrieger, and B.A. Barres, Synaptic efficacy enhanced by glial cells in vitro, *Science* **277**, 1684-1687 (1997).
57. P. Magistretti, and L. Pellerin, Regulation by neurotransmitters of glial energy metabolism, *Adv. Exp. Med. Biol.* **429**, 137-143 (1997).
58. S.J. Sara, and A. Hervé-Minvielle, Inhibitory influence of frontal cortex on locus coeruleus neurons, *Proc. Natl. Acad. Sci. USA* **92**,6032-6036 (1995).
59. K.V. Subbaru, and L. Hertz, Effect of adrenergic agonists on glycogenolysis in primary cultures of astrocytes, *Brain Res.* **536**, 220-226 (1009).
60. C.C. Hsu, and C.S. Hsu, Effect of isoproterenol on the uptake of ^{14}C-glucose into glial cells, *Neurosci. Res.* **9**, 54-58 (1990).
61. N.I. Bohnen, J. Jolles, A. Twijnstra, R. Mellink, and G. Winjen, Late neurobehavioural symptoms after mild head injury, *Brain Injury* 9, 27-33 (1995).
62. S.J. Granr, G. Aston-Jones, and E. Redmond, Jr, Responses of primate locus coeruleus neurons to simple and complex sensory stimuli, *Brain Res. Bull.* **21**, 401-410 (1988).
63. S.M. Sweitzer, P. Schubert, and J.A. DeLeo, Propentofylline, a glial modulating agent exhibits anti-allodynic properties in a rat model of neuropathic pain, *J. Pharmacol. Exp. Ther.* **297**, 1210-1217 (2001).
64. E. Hansson, and L. Rönnbäck, Altered neuronal-glial signaling in glutamatergic transmission as a unifying mechanism in chronic pain and mental fatigue, *Neurochem. Res.* **29**, 987-994 (2004).

29

CELL SWELLING-INDUCED PEPTIDE HORMONE SECRETION

Vladimir Strbák, Julius Benicky, Susan E. Greer, Zuzana Bacova, Miroslava Najvirtova, and Monte A. Greer*

ABSTRACT

Cell volume changes induced in various ways (anisosmotic environment, hormones, oxidative stress, substrate uptake) are an integral part of a signal transduction network regulating cell function.[1, 2, 3] Cell swelling has received increasing attention as a stimulus for a variety of intracellular phenomena.[4] One of the most remarkable effects of cell swelling is its powerful effect in inducing exocytosis of material in intracellular secretory vesicles. Secretion of essentially all so-packaged hormones[5-24] including those from hypothalamus (thyrotropin-releasing hormone, TRH; gonadotropin-releasing hormone, GnRH), pituitary (LH, FSH, ACTH, MSH, TSH, prolactin, beta endorphin), pancreas (insulin, somatostatin, glucagon), heart (atrial natriuretic hormone) and kidney (renin) are stimulated in a concentration-related manner by medium hyposmolarity or isosmolar medium containing permeant molecules such as ethanol or urea (reviewed in Ref. 21). Cell swelling-induced exocytosis is not restricted to endocrine cells and hormones; medium hyposmolarity also induces secretion of exocrine pancreatic enzymes[5] and myeloperoxidase from human polymorphonuclear leukocytes.[25]

Vladimir Strbák, Julius Benicky, Zuzana Bacova, and Miroslava Najvirtova, Institute of Experimental Endocrinology, Slovak Academy of Sciences, Bratislava 83306, Slovakia. Susan E. Greer and Monte A. Greer, Oregon Health Sciences University, Portland, OR, USA

1. EXPERIMENTAL

Dynamics of secretion induced by cell swelling closely resembles that induced by specific secretagogues.[9, 10, 26] Perifusion of pituitary cells with 10 nM TRH (prolactin natural secretagogue) as well as cell swelling induced by hypotonic solution (medium dilution with 30% H_2O) or depolarizing 30 mM KCl stimulates an immediate dose-related high-amplitude prolactin secretory burst, reaching a peak at 1-2 minutes followed by a decline to a low plateau within 5-10 minutes during continuous exposure to the same stimulus (Figure 1A). Repeated stimuli with 30 sec. interstimulus interval produce the same secretory response as continuous stimulation (Figure 1B). For all three types of stimuli, the secretory response to continuous exposure and refractory periods to repeated stimulation (less than 1 minute) were essentially identical (1A, 1B and 1C). An identical high-amplitude secretory burst was induced by exposure to TRH for times varying from 6 to 600 sec. In contrast, for 30% H_2O and high KCl, the secretory amplitude was proportional to the exposure time between 6 and 60 sec (Figure 1D). While the TRH response was triggered by rapid specific receptor binding, a very short pulse would not have time to produce sufficient transmembrane osmotic gradient or K^+ difference. It is concluded that hyposmotic medium does not trigger peptide release by the specific receptor-ligand binding.[26]

The most striking and unusual feature of cell swelling-induced secretion is that it stimulates regulated secretion independent of intracellular Ca^{2+} concentration,[5, 7, 8, 12, 13, 17-24] in contrast to most types of regulated secretion. When Ca^{2+} influx is prevented by removing extracellular Ca^{2+} or by adding Ca^{2+} channel blockers, cell swelling does not induce a rise in intracellular Ca^{2+}, but hormone release is present and even enhanced. These peculiar features indicate a specific signal transduction pathway for cell swelling-induced peptide secretion. However, in clonal tumor-derived rat pituitary cells (GH_4C_1 and MMQ), the situation was different. In contrast to normal freshly isolated pituitary cells, Sato et al.[13] found that hyposmolarity induced hormone secretion in clonal cells only in the presence of extracellular Ca^{2+}. It was suggested that this is a possible important hallmark for tumor cells.[13] It is of interest that Straub et al. found two distinct mechanisms in the presence and absence of extracellular Ca^{2+} in clonal cells secreting insulin (βHC9).[27] While we did not see this dichotomy in isolated rat pancreatic islets,[28] we believe that at least some tumor cells have special requirements for extracellular Ca^{2+} in cell swelling-induced hormone release.

Inhibition of stretch-activated channels by 10 μM $GdCl_3$ did not affect cell swelling-induced TRH secretion from the posterior pituitary, hypothalamic paraventricular nucleus (Figure 2) or isolated pancreatic islets.[29] It is of interest, however, that this stimulus did not induce release of oxytocin from the same tissue explants (Figure 2).[29] It was therefore concluded that cell swelling-induced exocytosis possesses limited selectivity; cells specifically involved in water and salt metabolism retain their specific response to osmotic stimuli.[29] However, our recent unpublished results suggest that inhibition of a specific response also unmasks general exocytotic response in these cells.

Swelling-induced secretion can be triggered in different parts of neurons – similar TRH release was evoked from the hypothalamic paraventricular nucleus (mostly perikarya) and the median eminence and posterior pituitary (exclusively axon terminals).[17, 19, 24, 29]

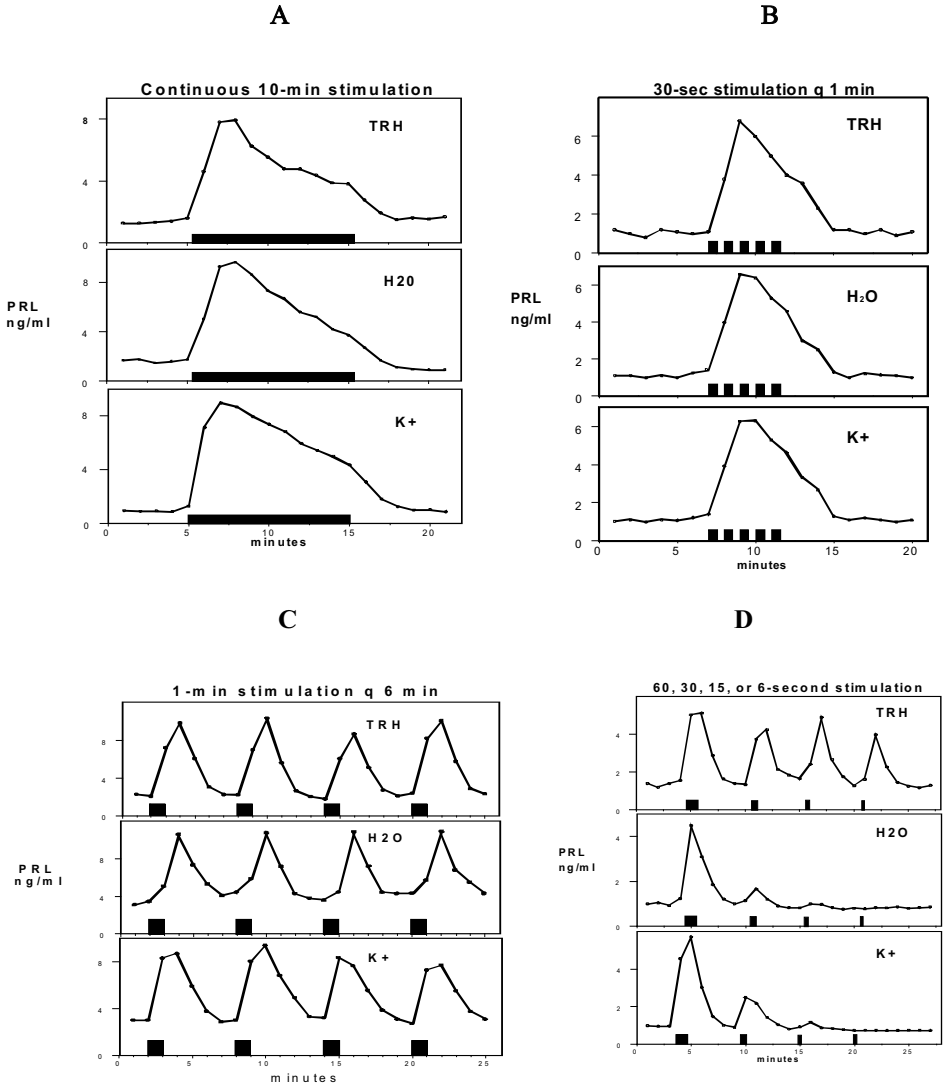

Figure 1. Dynamics of prolactin secretory response of perifused pituitary cells to 10 mM thyrotropin releasing hormone (TRH, prolactin natural secretagogue), hypotonic solution (H_2O, medium diluted with 30% water) or 30 mM KCl (K^+, membrane depolarizing solution – non-specific stimulus). Continuous stimulation (A) or repeated stimuli lasting 30 sec within 1 min (or with 30 sec interstimulus interval) (B), 1 min stimulation with 6 min interstimulus interval (C) or stimuli lasting 6-60 sec with 6 min interval (D) were compared. Differences were found only if stimulus lasted less than 1 min.

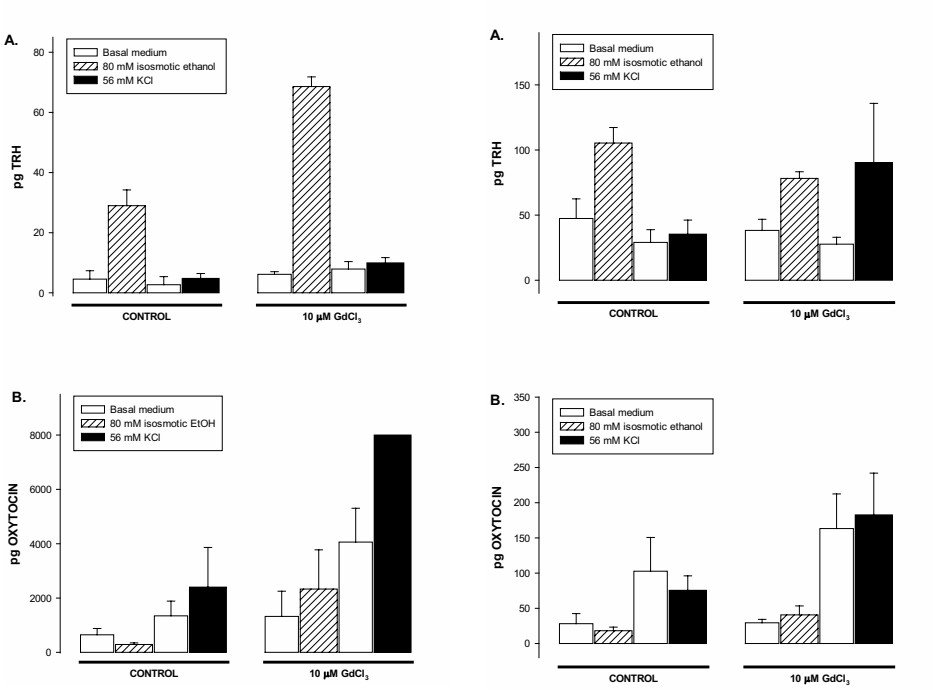

Figure 2. Cell swelling-induced TRH (A) and oxytocin (B) secretion from posterior pituitary (left) and hypothalamic paraventricular nucleus (right). 80 mM ethanol in isosmotic medium was used as cell swelling stimulus. TRH but not oxytocin release was induced by cell swelling. $GdCl_3$ in 10 μM concentration did not affect the release. From Najvirtova et al.[29]

The signal transduction pathway for cell swelling-induced exocytosis remains obscure. Using various tissues (pituitary, pancreatic islets, brain structures), hormones (prolactin, insulin, thyrotropin releasing hormone - TRH, oxytocin) and inhibitors, we found that hormone secretion induced by cell swelling is not depressed by inhibition of stretch activated channels ($GdCl_3$), mercury-sensitive aquaporins,[29] protein kinase C (bisindolylmaleimide VIII), microtubules and microfilaments (colchicine, cytochalasin)[12] and does not involve the arachidonic acid metabolites prostaglandins and leukotriens (indomethacin, NDGA).[29] Blocking Na^+-K^+-dependent ATPase, Na^+ channels or K^+ channels[12] or VSOR had no inhibiting effect on hyposmolarity-induced hormone secretion in pituitary cells. Cell swelling-induced exocytosis overrides physiological inhibition: glucose stimulated but not hypotonicity evoked insulin secretion from the isolated pancreatic islets was inhibited by norepinephrine.[28]

2. CONCLUSION

Previous studies suggest that signaling of cell swelling-induced exocytosis bypasses conventional transduction pathways and might be effective at the distal end of the

cascade. There are data suggesting that secretory vesicle swelling is critical for exocytosis.[30-32] Stretching of vesicular and plasma membranes in the region of contact results in exposing areas of hydrophobic acyl chains leading to subsequent merging and fusion. Fusion rates are orders of magnitude higher if an osmotic gradient is applied.[30] The externalization of hormones or transmitters upon exocytosis of vesicles is augmented by secretion of water from the vesicle membrane through the widened fusion pore.[32] Considering these data, we hypothesize that cell swelling triggered exocytosis involves a biophysical effect of the osmotic gradient on secretory vesicles.

3. ACKNOWLEDGMENTS

The work was supported by projects #2/7178/20 and 23191/23 of the Grant Agency of the Ministry of Education and Slovak Academy of Sciences (VEGA), by the project supported by European Commission ICA 1-CT-2000-70008, by project #017/2001 of the US-Slovak Science and Technology Program and APVT-51-016002 (Agency for Support of Sciences and Technology) and SP 51/0280800/02808. We thank Professor Ian Robinson (MRC, National Institute for Medical Research, London) for rabbit antiserum against oxytocin and the National Hormone and Pituitary Program NIDDK, NIH, USA for the reagents for prolactin radioimmunoassay.

4. REFERENCES

1. F. Wehner, H. Olsen, H. Tinel, E. Kinne-Saffran and R.K.H Kinne, Cell volume regulation: osmolytes, osmolyte transport, and signal transduction, *Rev. Physiol. Biochem. Pharmacol.* **148**,1-80 (2003).
2. F. Lang, G.L. Busch, M. Ritter, H. Volkl, S. Waldegger, E. Gulbins and D. Haussinger, Functional significance of cell volume regulatory mechanisms, *Physiol. Rev.* **78**, 247-306 (1998).
3. F. Lang, M. Ritter, N. Gamper, S. Huber, S. Fillon, V. Tanneur, A. Lepple-Wienhues, I. Szabo and E. Gulbins, Cell volume in the regulation of cell proliferation and apoptotic cell death, *Cell. Physiol. Biochem*. **10**, 417-428. (2000).
4. M. Jakab, J. Fürst, M. Gschwentner, G. Bottà, M.-.L Garavaglia, C. Bazzini, S. Rodighiero, G. Meyer, S. Eichmüller, E. Wöll, S. Chwatal, M. Ritter and M. Paulmichl, Mechanisms sensing and modulating signals arising from cell swelling, *Cell. Physiol. Biochem*. **12**, 235-258 (2002).
5. W.G. Blackard, M. Kikuchi, A. Rabinovitch and AE. Renold, An effect of hyposmolarity on insulin release in vitro, *Am J. Physiol*. **228**, 706-713 (1975).
6. M.A. Greer, S.E. Greer, Z. Opsahl, L. McCafferty and S. Maruta, Hyposmolar stimulation of in vitro pituitary secretion of luteinizing hormone: a potential clue to the secretory process, *Endocrinology*, **113**, 1531-1533 (1983).
7. M.A. Greer, S.E. Greer, Z. Opsah and S. Maruta, Comparison of hyposmolar and hyperosmolar effects on in vitro luteinizing hormone secretion by anterior pituitary cells, *Proc. Soc. Exp. Biol. Med*. **178**, 24-28 (1985).
8. O. Skott, Calcium and osmotic stimulation in renin release from isolated rat glomeruli, *Pflugers Arch*. **406**, 485-491 (1986).
9. L. D. Keith, B. Tam, H. Ikeda, Z. Opsahl and M.A. Greer, Dynamics of thyrotropin-releasing hormone-induced thyrotropin and prolactin secretion by acutely dispersed rat adenohypophysial cells, Evidence for "all-or-none" secretion by heterogenous secretory units, each with a specific response threshold, *Neuroendocrinology* **43**, 445-452 (1986).
10. X. Wang, N. Sato, M.A. Greer, S.E. Greer and S. McAdams, Cell swelling induced by the permeant molecules urea or glycerol induces immediate high amplitude thyrotropin and prolactin secretion by perifused adenohypophyseal cells, *Biochem. Biophys. Res. Commun*.**163**, 471-475 (1989).

11. J.E. Greenwald, M. Apkon, K.A. Hruska and P. Needleman, Stretch-induced atriopeptin secretion in the isolated rat myocyte and its negative modulation by calcium, *J. Clin. Invest*. **83**, 1061-1065 (1989).
12. M.A. Greer, S.E. Greer and S. Maruta, Hyposmolar stimulation of secretion of thyrotropin, prolactin, and luteinizing hormone does not require extracellular calcium and is not inhibited by colchicine, cytochalasin B, ouabain, or tetrodotoxin, *Proc. Soc. Exp. Biol. Med*. **193**, 203-209 (1990).
13. N. Sato, M. Murakami, X. Wang and M.A. Greer, The contrasting role of calcium influx in secretion induced by cell swelling can differentiate normal and tumor-derived rat pituitary cells, *Endocrinology* **129**, 2541-2546 (1991).
14. N. Sato, X. Wang and M.A. Greer, Hormone secretion stimulated by ethanol-induced cell swelling in normal rat adenohypophyseal cells, *Am. J. Physiol*. **260**, E946-E950 (1991).
15. T. Inukai, X. Wang, S.E. Greer and M.A. Greer, Cell swelling induced by medium hyposmolarity or isosmolar urea stimulates gonadotropin-releasing hormone secretion from perifused rat median eminence, *Brain Res*. **599**, 161-164. (1992).
16. T. Inukai, X. Wang, M.A. Greer and S.E. Greer, Isotonic but not hypertonic ethanol stimulates LHRH secretion from perifused rat median eminence, *Neuroendocrinology* **58**, 258-262 (1993).
17. M. Nikodemova, V. Strbak, S.E. Greer and MA. Greer, Isosmolar ethanol or urea stimulate hypophysiotropic TRH secretion from both the hypothalamic paraventricular nuclei and median eminence, *Thyroid* **5** S161 (1995).
18. J. Benicky, M.A. Greer and V. Strbak, Hyposmolar medium and ethanol in isosmotic solution induce release of thyrotropin-releasing hormone (TRH) by isolated rat pancreatic islets, *Life Sci*. **60**, 865-872 (1997).
19. M. Nikodemova, M.A. Greer and V. Strbak, Hyposmolarity stimulates and high sodium concentration inhibits thyrotropin releasing hormone secretion from rat hypothalamus, *Neuroscience* **88**, 1299-1306, (1999).
20. J. Benicky, M.A. Greer and V. Strbak, Hyposmolar medium and ethanol in isosmotic solution induce release of thyrotropin-releasing hormone (TRH) by isolated rat pancreatic islets, *Life Sci*. **60**. 865-872 (1997).
21. V. Strbak and M.A. Greer, Regulation of hormone secretion by acute cell volume changes: Ca^{2+}-independent hormone secretion, *Cell. Physiol. Biochem*. **10,** 393-402 (2000).
22. N. Back, S. Soinila and K. Tornquist, Monensin and hypo-osmolar medium cause calcium independent beta-endorphin secretion from melanotropes, *Neuroendocrinology* **71**, 99-106 (2000).
23. J. Kucerova, and V. Strbak, The osmotic component of ethanol and urea action is critical for their immediate stimulation of thyrotropin-releasing hormone (TRH) release from rat brain septum, *Physiol. Res*. **50**, 309-314 (2001).
24. M. Najvirtova, L. Baqi, J. Kucerová and V. Strbák, Cell swelling induced secretion of TRH by posterior pituitary, hypothalamic paraventricular nucleus and pancreatic islets: effect of L-canavanine, *Cell. Mol. Neurobiol*. **22**, 35-46 (2002).
25. N. Sato, X. Wang and M.A. Greer, Hyposmolarity stimulates exocytosis from human polymorphonuclear leukocytes, *Am. J. Med. Sci*. **289**, 309-312 (1990).
26. MA Greer, and SE Greer, Evidence that desensitization is not receptor-modulated. Comparison of PRL secretory dynamics induced by three diverse stimuli (TRH, depolarizing K^+, cell swelling), Abstracts *81st Ann. Mtg. Endocrine Soc*., San Diego, p. 383 (1999).
27. S Straub, S Daniel, and GWG Sharp, Hyposmotic shock stimulates insulin secretion by two distinct mechanism, Studies with HC9 cell, *Am. J. Physiol*. *Endocrinol. Metab*. **282**: E1070-E1076 (2002).
28. J. Benicky, Z. Bacova, M. Najvirtova and V. Strbak, Cell volume and physiological regulation of insulin secretion, Presentation: International Symposium Cell Volume and Signal Transduction, Dayton, OH, Sep 20-25, 2003.
29. M. Najvirtova, S. E. Greer, M.A. Greer, L. Baqi, J. Benicky and V. Strbak, Cell volume induced hormone secretion: Studies on signal transduction and specificity, *Cell. Physiol. Biochem*. **13,** 113-122 (2003).
30. A. Finkelstein, J. Zimmerberg and F. S. Cohen, Osmotic swelling of vesicles: Its role in the fusion of vesicles with planar phospholipid bilayer membranes and its possible role in exocytosis, *Ann. Rev. Physiol*. **48**, 163-174 (1986).
31. G. Alvarez de Toledo, R. Fernandez-Chacon and J.M. Fernandez, Release of secretory products during transient vesicle fusion, *Nature* **363**, 554-558 (1993).
32. T. Tsuboi, T. Kikuta, T. Sakurai, and S. Terakawa, Water secretion associated with exocytosis in endocrine cells revealed by micro forcemetry and evanescent wave microscopy, *Biophys. J*. **83**, 173-182 (2002).

30

VOLUME REGULATION OF THE HIPPOCAMPUS

James E. Olson and Norman R. Kreisman*

1. INTRODUCTION

Numerous studies have examined mechanisms of cellular volume regulation using cultured neurons or glial cells.[1-8] While cell cultures provide a relatively pure cell population that can be easily manipulated, the environment is vastly different from that which the cells experience *in situ*. In particular, the size of the extracellular space is greatly enlarged while interactions between cells are minimized. Other studies have used *in vivo* models to measure volume regulation and mobilization of osmolytes in intact brain.[9-13] Such whole animal studies inherently model the physiological cellular environment very well; however, manipulation and measurement of parameters relevant for mechanisms of cellular volume regulation are difficult to perform. Brain slices are an appropriate compromise of these model systems since cellular interactions between cell types are maintained while control and measurement of the extracellular environment is readily accomplished.[14-16] In this study, we examine volume regulation of brain tissue using slices from adult rat hippocampus.

In previous studies we found control hippocampal slices prepared without the addition of taurine to incubation solutions demonstrated no cellular volume regulation over 60 min following swelling in hyposmotic (200 mOsm) saline solution.[16] In contrast, slices incubated with 1 mM taurine showed the same degree of swelling as control slices yet had a significant volume regulatory response. These slices also lost taurine during the period of hyposmotic exposure. Control slices had taurine contents that were approximately 25% of that found in the intact hippocampus *in vivo* while slices incubated in taurine had normal taurine contents. Contents of potassium and free amino acids other than taurine were similar in control and taurine-treated slices and were not affected by hyposmotic exposure. Additionally, hyposmotic volume regulation and taurine loss from taurine-treated slices was sensitive to the anion channel blocker NPPB. These results suggested that taurine is an important osmolyte used for osmotic volume regulation of the

* James E. Olson, Department of Emergency Medicine and Department of Anatomy and Physiology, Wright State University, Dayton, Ohio 45435. Norman R. Kreisman, Department of Physiology, Tulane University School of Medicine, New Orleans, Louisiana, 70112

hippocampus. To extend these results we examined the importance of taurine for volume regulation during oxidative stress, a treatment known to lead to swelling of the hippocampus.[17] A preliminary report of this investigation has appeared elsewhere.[18]

2. EXPERIMENTAL

The Laboratory Animal Care and Use Committees of Wright State University and Tulane University School of Medicine approved all procedures involving animals. Adult Sprague-Dawley rats of either sex were anaesthetised to apnea using halothane and then perfused via the left cardiac ventricle with ice-cold artificial cerebrospinal fluid (aCSF) consisting of 124 mM NaCl, 3.5 mM KCl, 2.0 mM $CaCl_2$, 1.0 mM $MgSO_4$, 1 mM Na_2HPO_4, 10 mM glucose and 26 mM Na_2HCO_3. Animals were then decapitated and the brain quickly removed and placed in a slurry of frozen aCSF. After five minutes, hippocampi were dissected from each hemisphere. Tissue slices (400 μm) were prepared from the middle third of each hippocampus by cutting in an orientation that maintains the integrity of the Schaffer Collateral connection from pyramidal cells in CA3 to those in CA1. Slices were then incubated at room temperature for at least 120 min in aCSF bubbled with 95% O_2 plus 5% CO_2 before being placed on a recording stage and perfused for 60 min at 35°C with the same O_2 plus CO_2-equilibrated aCSF. For taurine-treated slices, the aCSF used during room temperature incubation and the first 30 min of perfusion at 35°C contained 1 mM taurine. Control slices were not exposed to exogenous taurine during the experimental protocol. After population spikes and light transmission was recorded for 60 min, 2 mM H_2O_2 was added to the perfusion solution.

Light transmission through the slice was used as an index of cellular volume.[19] Slices were illuminated with a DC-regulated halogen light source via a fiber optic light guide. Images of the entire slice were acquired every 60 sec with a fixed-gain CCD video camera. We subsequently processed these data using NIH-image software provided by Scion Corporation (Frederick, MD). Regions of interest outlining the stratum radiatum of CA1 or the entire CA3 region (stratum radiatum, stratum pyramidale plus stratum oriens) were defined and the average intensity determined on each image. These data were then normalized to the mean intensity determined from the last five images acquired while slices were perfused in aCSF prior to changing to experimental perfusion solution.

Water content was determined in some slices by measuring the specific gravity with a hydrophobic density gradient column.[20, 21] At various times, slices were removed from the recording stage, blotted dry and placed in a drop of kerosene. Adherent portions of entorhinal cortex and fimbria were removed and the slices were placed at the top of a linear density gradient column of kerosene plus bromobenzene in a graduated cylinder. After the slice had fallen in the column for 2 min, the position of the slice was recorded and compared with positions of standard density glass beads.

We monitored the population spike from pyramidal neurons in the CA1 portion of the hippocampus following stimulation of Schaffer collaterals. A bipolar tungsten stimulating electrode was placed in stratum radiatum of CA3 using a micromanipulator. A glass pipette filled with aCSF (approximately 30 MΩ) was similarly placed in the pyramidal cell layer of CA1 and connected to a high-input impedance electrometer. Stimulating pulses (0.2-2.0 mA, 200 μsec) were delivered every 30 sec and the resulting waveform from CA1 was recorded on digital tape. In many studies, the pre-synaptic volley was measurable in the signal recorded in the pyramidal cell layer of CA1. This wave arises from synchronous action potentials in Schaffer Collateral fibers. We subsequently

determined the amplitudes of the population spike and pre-synaptic volley of each stimulus event using a digital storage oscilloscope and computer interface.

Slices fixed for immunohistochemical localization of cellular taurine were treated on the recording stage with 4% paraformaldehyde in 0.1 M Na_2HPO_4 (pH=7.4) for 5 min and were then placed in the same fixative solution at 4°C. After 24 hours, the fixative solution was replaced with 15% sucrose in the same buffer for cryoprotection. Slices were frozen at 77°K in isopentane and 20 μm sections cut with a cryostat. Sections were permeablized with 0.1% triton X-100 and non-specific staining blocked using 20% goat serum. The tissue was then probed for taurine-like immunoreactivity by overnight incubation at 4°C in a 1:200 dilution of primary rabbit anti-taurine antibody (Chemicon International Inc., Temecula, CA) followed by overnight incubation with 1:100 goat anti-rabbit antibody conjugated with Texas Red (Jackson Immunoresearch Laboratories Inc., West Grove, PA). Sections were also probed for glial fibrillary acidic protein using a 1:5000 dilution of primary mouse monoclonal antibodies provided by Sternberger Monoclonals (Lutherville, MD) followed by incubation with goat anti-mouse antibody conjugated with fluroescein (Jackson Immunoresearch Laboratories Inc., West Grove, PA). Sections were mounted on glass slides and visualized with a standard epifluorescence microscope.

3. RESULTS AND DISCUSSION

Exposure of control slices to 2 mM H_2O_2 for 30 min caused an increase in light transmission indicating an increase in cell volume (Figure 1). All regions of the hippocampus became more transparent; however, the CA3 region showed the largest percent change in transmitted light intensity. In contrast, slices incubated with 1 mM taurine during preparation showed substantially smaller changes in light transmission during and after H_2O_2 exposure. Quantitative analysis of image intensities in stratum radiatum of CA1 showed changes in transmitted light intensity of control slices that began immediately upon introduction of H_2O_2 to the aCSF perfusate (Figure 2). No recovery of transmitted light intensity occurred following removal of H_2O_2 from the aCSF. However, for taurine-treated hippocampal slices, transmitted light intensity was not altered during or after H_2O_2 exposure. Similar results were obtained for quantitative analysis of the CA3 region (data not shown).

Oxidative stress has been shown to lead to increased water content of hippocampal slices.[17] Ascorbate loading of hippocampal slices reduces this edema. Measurements of transmitted light intensity described above suggest taurine-treated slices have an increased capacity for volume regulation during oxidative stress; however, recent data have suggested factors other than volume may contribute to the light transmission signal.[22, 23] Therefore, we wished to verify these indirect results on cell volume changes with direct measurements of slice water content. We measured hippocampal slice water content at various times of H_2O_2 exposure using specific gravity determinations. Prior to H_2O_2 exposure, control and taurine-treated slices had a similar specific gravity with a combined mean±SEM of 1.03079±0.00044 (N=18). After 30 min in 2 mM H_2O_2, control slice specific gravity fell significantly to 1.02703±0.00122 (N=7) indicating an increase in water content ($p<0.05$). The specific gravity of taurine-treated slices after 30 min of H_2O_2 exposure was 1.02944±0.00038 (N=7), a value not significantly different from the initial value. For the entire hippocampal slice, these results confirm the optical measurements of transmitted light intensity made on selected regions of the hippocampus. The data provide strong evidence that hippocampal slices with diminished taurine content also

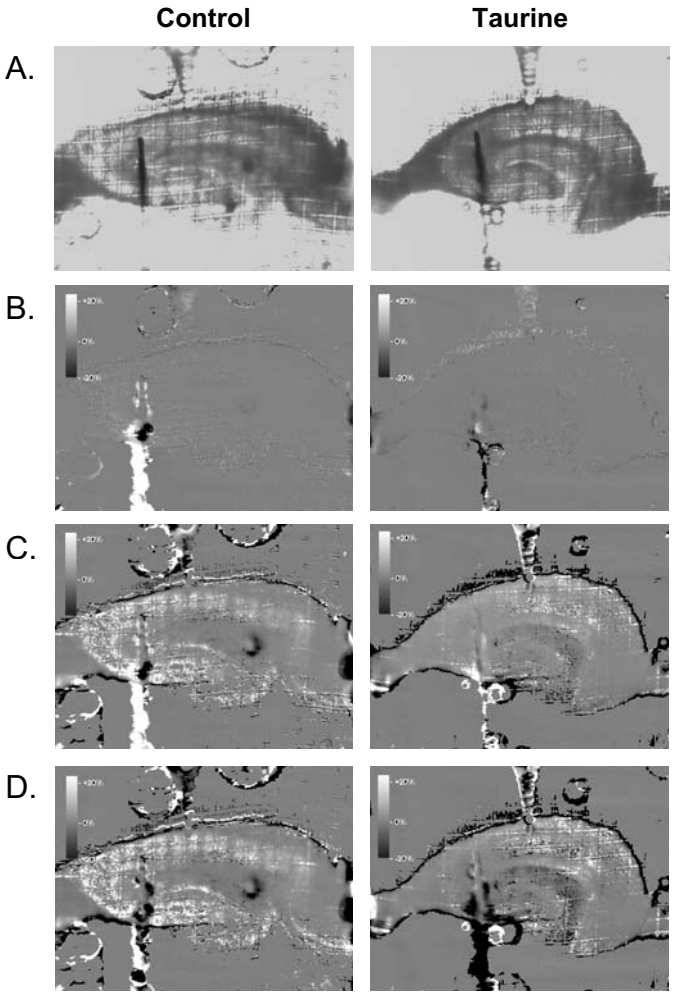

Figure 1. Images of control and taurine-treated rat hippocampal slices during exposure to aCSF containing 2 mM H_2O_2. **A.** Unprocessed video images shown for orientation. In each slice, a stimulating electrode was placed in stratum radiatum of CA3 and a glass recording electrode was placed in stratum pyramidale of CA1. **B, C, and D.** Video images normalized pixel by pixel to the average of five images acquired prior to the introduction of H_2O_2 to the perfusing aCSF. The scale indicates percent changes in transmitted light intensity. **B.** Images acquired prior to H_2O_2 exposure. **C.** Images acquired after 30 min of H_2O_2 exposure. **D.** Images acquired after 30 min of H_2O_2 exposure followed by 30 min in normal aCSF perfusate.

have a significantly reduced capacity for volume regulation during oxidative stress. A similar effect of taurine content on volume regulation during hyposmotic exposure has been reported previously.[16]

The amplitude of the population spike in CA1 is known to be sensitive to oxidative stress.[24, 25] Thus, we measured this electrophysiological response in control and taurine-treated slices during H_2O_2 exposure to determine whether accumulated taurine may act

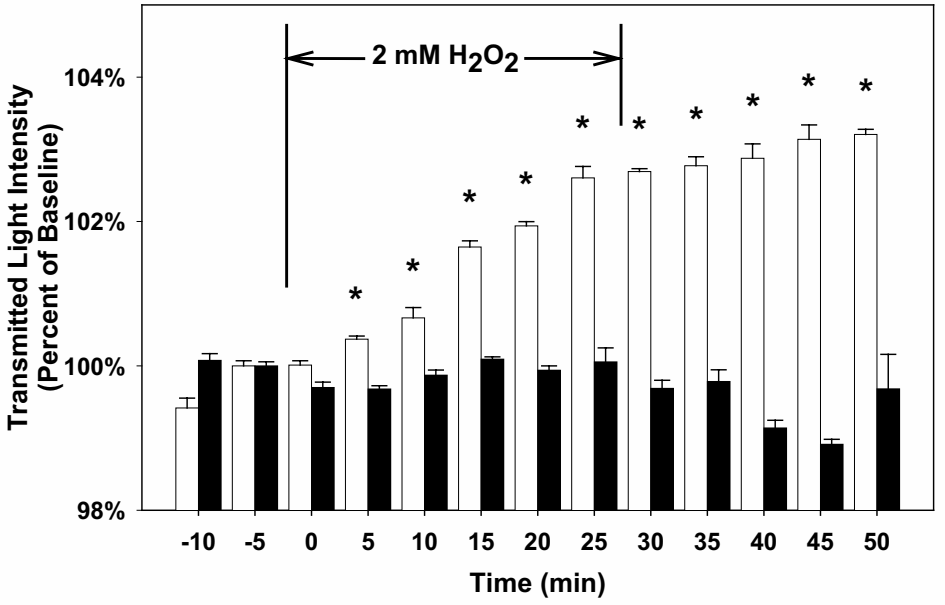

Figure 2. Percent change in transmitted light intensity for stratum radiatum of CA1. Values for each time point are the average of a defined region of interest in five sequential images and are expressed relative to the value measured just prior to the start of H_2O_2 exposure. Data shown are the mean±SEM of three independent experiments with control (open bars) and taurine-treated (solid bars) slices. * indicates mean values significantly different from the measurement obtained prior to H_2O_2 exposure ($p<0.05$).

act as an antioxidant.[26, 27] We found that the amplitude of the CA1 population spike was similarly reduced during 2 mM H_2O_2 exposure in both control and taurine-treated slices (Figure 3). After 30 min, the amplitude was significantly reduced by 40-45% for both slice treatments. Recovery of the population spike amplitude was apparent when slices were returned to normal aCSF perfusate following H_2O_2 exposure. In contrast, with either group of slices, the amplitude of the pre-synaptic volley was not altered by H_2O_2 exposure indicating the excitation of Schaffer Collateral fibers and transmission of action potentials to the CA1 region was not affected by H_2O_2 (data not shown).

In a separate series of studies, the iron chelator,1 mM deferoxamine was added to the perfusate of control slices 15 min prior to and throughout exposure to 2 mM H_2O_2. This treatment has previously been shown to block the NMDA-dependent inhibition of population spike amplitude caused by H_2O_2 treatment.[25] We observed no change in either population spike amplitude or transmitted light intensity in slices treated with deferoxamine. Thus, the responses to H_2O_2 exposure in the absence of deferoxamine appear to be mediated by oxidative stress imposed via the generation of hydroxyl radicals.

Immunohistochemical analysis of taurine-like immunoreactivity in taurine-treated hippocampal slices demonstrated significant staining in pyramidal cell bodies and dendrites of CA1 and CA3 regions (Figure 4). Staining appeared to be confined to the cytoplasm with little reactivity in nuclei. Cell bodies and processes of astroglial cells could also be identified with positive taurine-like immunoreactivity by comparison with GFAP staining in double-labeled sections. Substantially less taurine-like immunoreactivity was

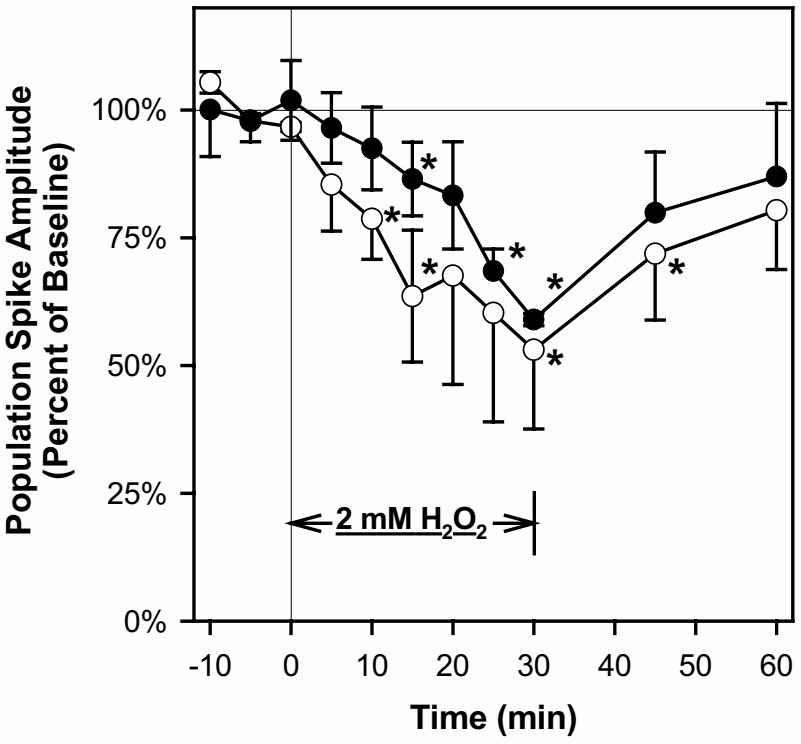

Figure 3. Population spike amplitude recorded in stratum pyramidale of CA1. Values for each time point are the average of six sequential responses to Schaffer collateral stimulation and are expressed relative to the value measured just prior to the start of H_2O_2 exposure. Data shown are the mean±SEM of three independent experiments with control (open circles) or taurine-treated (solid circles) slices. * indicates mean values that are significantly different from the measurement obtained prior to H_2O_2 exposure ($p<0.05$).

observed in control slices (data not shown). No taurine-like immuno-reactivity was observed if primary anti-taurine antibody was omitted from the staining procedure, and staining was largely reduced if the primary anti-taurine antibody was treated for 24 hours with taurine conjugated with paraformaldehyde. Treatment of the primary anti-taurine antibody with conjugates of glutamine, glutamate, or aspartate had no effect on taurine-like immunoreactivity (data not shown). We have previously described taurine loss as more sensitive to reductions in osmolality in cultured hippocampal neurons than in cultured hippocampal astrocytes.[28] A similar preferential loss of taurine from cerebellar Purkinje cells and accumulation by adjacent astroglial cells has been described during *in vivo* hyposmotic hyponatremia.[29] Future studies using laser confocal microscopy will examine whether a preferential loss of taurine from hippocampal pyramidal neurons correlates with regulation of cell volume.

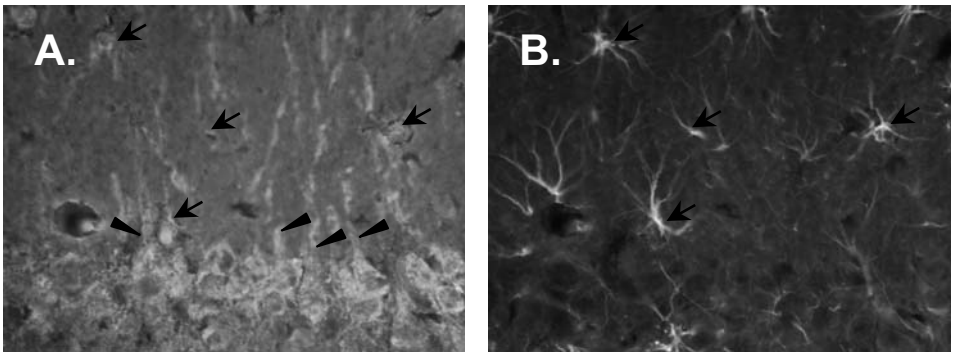

Figure 4. Localization of taurine-like (**A**) and GFAP (**B**) immunoreactivities. Images are epifluorescence micrographs of the CA1 region of a 20 μm section of rat hippocampal slice that had been incubated with 1 mM taurine and then fixed with 4% paraformaldehyde after perfusion on the recording stage for 60 min in aCSF. Panel **A** shows strong labeling of taurine-like immunoreactivity in pyramidal neurons of the CA1 layer and their broad proximal apical dendrites (arrow heads). Taurine-like immunoreactivity is also apparent in the more delicate processes and some cell bodies of glial cells which can be identified in the corresponding image in panel **B** showing GFAP immunoreactivity (arrows).

4. CONCLUSIONS

We conclude that cellular taurine is critical for volume regulation of the hippocampus during swelling caused by oxidative stress. Both pyramidal neurons and astroglial cells accumulate taurine in slices treated to restore normal taurine contents. Since H_2O_2 exposure alters synaptic function via an oxidative mechanism in slices with normal or diminished slice taurine contents, we conclude the effects of taurine are not mediated by the antioxidant properties of the taurine molecule. We suggest loss of taurine from the slice exposed to oxidative stress facilitates regulation of normal cell volume via osmotic effects.

5. ACKNOWLEDGMENTS

We acknowledge our productive collaboration with Dr. Robert Fyffe and the Brain Research Center of Wright State University on the immunohistochemical studies. We also gratefully acknowledge the technical assistance of James Leasure. Funding for this project was provided by the NIH (NS 37485).

6. REFERENCES

1. Pasantes-Morales, H., et al., *Osmosensitive release of neurotransmitter amino acids: relevance and mechanisms.* Neurochem Res, 2002. **27**(1-2): p. 59-65.
2. Sanchez-Olea, R., H. Pasantes-Morales, and A. Schousboe, *Neurons respond to hyposmotic conditions by an increase in intracellular free calcium.* Neurochem Res, 1993. **18**(2): p. 147-52.
3. Schousboe, A., et al., *Hypoosmolarity-induced taurine release in cerebellar granule cells is associated with diffusion and not with high-affinity transport.* J Neurosci Res, 1991. **30**(661-665).
4. Pasantes Morales, H. and A. Schousboe, *Volume regulation in astrocytes: a role for taurine as an osmoeffector.* J Neurosci Res, 1988. **20**(4): p. 503-9.

5. Mongin, A.A., Z. Cai, and H.K. Kimelberg, *Volume-dependent taurine release from cultured astrocytes requires permissive [Ca2+]i and calmodulin.* Am J Physiol Cell Physiol, 1999. **277**(4): p. C823-832.
6. O'Connor, E.R. and H.K. Kimelberg, *Role of calcium in astrocyte volume regulation and in the release of ions and amino acids.* J Neurosci, 1993. **13**(6): p. 2638-50.
7. Kimelberg, H.K. and M.V. Frangakis, *Furosemide- and bumetanide-sensitive ion transport and volume control in primary astrocyte cultures from rat brain.* Brain Res, 1985. **361**(1-2): p. 125-34.
8. Olson, J.E., et al., *Energy-dependent volume regulation in primary cultured cerebral astrocytes.* J Cell Physiol, 1986. **128**(2): p. 209-15.
9. Verbalis, J.G. and S.R. Gullans, *Hyponatremia causes large sustained reductions in brain content of multiple organic osmolytes in rats.* Brain Res, 1991. **567**(2): p. 274-82.
10. Solis, J.M., et al., *Does taurine act as an osmoregulatory substance in the rat brain?* Neurosci Lett, 1988. **91**: p. 53-58.
11. Melton, J.E., et al., *Volume regulatory loss of Na, Cl, and K from rat brain during acute hyponatremia.* Am J Physiol, 1987. **252**(4 Pt 2): p. F661-9.
12. Cserr, H.F., et al., *Extracellular volume decreases while cell volume is maintained by ion uptake in rat brain during acute hypernatremia.* J Physiol, 1991. **442**: p. 277-95.
13. Wade, J.V., et al., *A possible role for taurine in osmoregulation within the brain.* J Neurochem, 1988. **51**(3): p. 740-5.
14. Andrew, R.D. and B.A. MacVicar, *Imaging cell volume changes and neuronal excitation in the hippocampal slice.* Neuroscience, 1994. **62**(2): p. 371-83.
15. Ballyk, B.A., S.J. Quackenbush, and R.D. Andrew, *Osmotic effects on the CA1 neuronal population in hippocampal slices with special reference to glucose.* J Neurophysiol, 1991. **65**(5): p. 1055-66.
16. Kreisman, N.R. and J.E. Olson, *Taurine enhances volume regulation in hippocampal slices swollen osmotically.* Neuroscience, 2003. **120**(3): p. 635-42.
17. Brahma, B., et al., *Ascorbate inhibits edema in brain slices.* J Neurochem, 2000. **74**(3): p. 1263-70.
18. Olson, J.E. and J.E. Leasure, *Intracellular taurine protects the hippocampus from swelling during H_2O_2 exposure.* 2002 Abstract Viewer and Itinerary Planner. Washington, DC: Society for Neuroscience, 2002: p. Program No. 389.13.
19. Andrew, R.D., C.R. Jarvis, and A.S. Obeidat, *Potential sources of intrinsic optical signals imaged in live brain slices.* Methods, 1999. **18**(2): p. 185-96, 179.
20. Nelson, S.R., M.L. Mantz, and J.A. Maxwell, *Use of specific gravity in the measurement of cerebral edema.* J Appl Physiol, 1971. **30**: p. 268-271.
21. Olson, J.E., L. Mishler, and R.V. Dimlich, *Brain water content, brain blood volume, blood chemistry, and pathology in a model of cerebral edema.* Ann Emerg Med, 1990. **19**(10): p. 1113-21.
22. Fayuk, D., et al., *Two different mechanisms underlie reversible, intrinsic optical signals in rat hippocampal slices.* J Neurophysiol, 2002. **87**(4): p. 1924-37.
23. Sykova, E., et al., *The relationship between changes in intrinsic optical signals and cell swelling in rat spinal cord slices.* Neuroimage, 2003. **18**(2): p. 214-30.
24. Avshalumov, M.V. and M.E. Rice, *NMDA receptor activation mediates hydrogen peroxide-induced pathophysiology in rat hippocampal slices.* J Neurophysiol, 2002. **87**(Jun): p. 2896-903.
25. Avshalumov, M.V., B.T. Chen, and M.E. Rice, *Mechanisms underlying H(2)O(2)-mediated inhibition of synaptic transmission in rat hippocampal slices.* Brain Res, 2000. **882**(Nov 3): p. 86-94.
26. Lauschke, H., et al., *Use of taurine as antioxidant in resuscitating livers from non-heart-beating donors by gaseous oxygen persufflation.* J Invest Surg, 2003. **16**(1): p. 7-11.
27. Aruoma, O.I., et al., *The antioxidant action of taurine, hypotaurine and their metabolic precursors.* Biochem J, 1988. **256**(1): p. 251-5.
28. Olson, J.E. and G.Z. Li, *Osmotic sensitivity of taurine release from hippocampal neuronal and glial cells.* Adv Exp Med Biol, 2000. **483**: p. 213-8.
29. Nagelhus, E.A., A. Lehmann, and O.P. Ottersen, *Neuronal-glial exchange of taurine during hypo-osmotic stress: a combined immunocytochemical and biochemical analysis in rat cerebellar cortex.* Neuroscience, 1993. **54**(3): p. 615-31.

31

CELL VOLUME REGULATION IN INTESTINAL EPITHELIAL CELLS

Sebastian F.B.Tomassen, Hugo R. de Jonge and Ben C. Tilly*

1. INTRODUCTION

Most cells have to perform their physiological functions under a variable osmotic stress caused by the uptake or release of osmotically active substances (amino acids, sugars etc.), the formation or degradation of macromolecules (proteins, glycogen) or changes in the osmolarity of the surrounding fluid. As a consequence of the high permeability of the plasma membrane for water, an osmotic imbalance will immediately lead to a redistribution of intracellular water and, subsequently, to a rapid change in cell volume. Because alterations in cell size are potentially deleterious and may result in a loss of function, almost all cell types have developed compensatory mechanisms. In general, compensation is achieved by the activation of transport pathways in the plasma membrane, leading to a net accumulation (Regulatory Volume Increase or RVI) or loss (Regulatory Volume Decrease or RVD) of osmotically active intracellular substances. Whereas the RVI involves the uptake of NaCl through stimulation of the Na^+/H^+- and Cl^-/HCO_3^--exchangers or by activation of Na^+-K^+-$2Cl^-$- and Na^+-Cl^--symporters, the RVD largely depends on the release of KCl, either through specific K^+ and Cl^- selective ion channels or by the activation of K^+-Cl^--symporters (For reviews, see 1-3). In addition, osmotic cell swelling is often accompanied by an efflux of small organic osmolytes such as taurine and betaine through a release pathway whose molecular identity has not yet been elucidated (For reviews, see [4, 5]).

Because the osmolarity of the interstitial fluid in mammals is carefully regulated, osmotic stress almost always originates from (hormone-induced) alterations in cell metabolism.[6] Notable exceptions are the intestinal and renal epithelia that experience

* Sebastian F.B.Tomassen, Hugo R. de Jonge and Ben C. Tilly, Department of Biochemistry, Erasmus University Medical Center, 3000DR Rotterdam, the Netherlands. Email: b.tilly@ErasmusMC.nl.

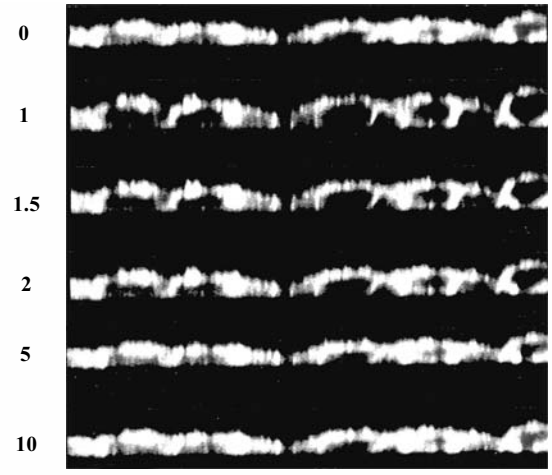

Figure 1. Hypotonicity-induced increase in cell volume. Cells were loaded with DII-C14 and changes in height were quantitated by constructing optical sections perpendicular to the substratum at the indicated times after changing to a hyposmotic medium.

alterations in the osmolarity of the luminal fluid and cells in the circulation which periodically traverse the osmotic gradients present in the kidneys. To study the RVD in intestinal epithelia, we used monolayers of cultured Intestine 407 cells, an epithelial cell line with stem cell-like properties derived from human foetal jejunum,[7] as a model. This cell line is particularly suitable for studying cell swelling-regulated Cl^- channels because no other anion channels, i.e., Ca^{2+}-, voltage-activated or cAMP/protein kinase A-activated CFTR Cl^- channels, are expressed.[8] In this review, we will discuss the cellular responses triggered by osmotic cell swelling of Intestine 407 cells which include the activation of compensatory osmolyte fluxes and the release of ATP by exocytosis as well as the signaling pathways involved.

2. REGULATORY VOLUME DECREASE IN INTESTINE 407 CELLS

Upon hyposmotic stimulation, Intestine 407 cells immediately respond with an increase in cell height, indicative of an increase in volume (Fig.1). Rapidly, compensatory mechanisms are activated and within 1 – 2 min the RVD is completed, resulting in an almost full recovery of the original cell volume. Underlying the RVD response is the activation of specific Cl^-- and K^+-selective ion channels. Whereas the K^+ conductance involvement has been identified by the Okada group[9] as a Ca^{2+}-dependent intermediate K^+ channel (I_K) in these cells, the molecular identity of the anion channel has not yet been elucidated. Several potential candidates have been proposed, including MDR-1/P-glycoprotein, ClC-2 and 3 and ICln. None of them, however, have *all* the electrical and

pharmacological properties of the Volume Regulated Anion Channel or VRAC (for Reviews, see 10, 11).

3. PROPERTIES OF VOLUME REGULATED ANION CONDUCTANCE

Although the molecular identity of VRAC remains to be established, the volume-sensitive anion conductance has been studied in numerous different cell types. The electrical characteristics of the conductance are very similar in all models studied and include: 1) a strong outward rectification; 2) a marked inactivation at depolarising potentials; and 3) a permeability sequence that corresponds to the Eisenman's sequence I ($SCN^- > I^- > NO_3^- > Br^- > Cl^- > F^-$ > gluconate$^-$ (For reviews, see [10, 11]. Activation of VRAC can de inhibited by common Cl^--channel blockers like 4-acetamido-4'-isothiocyanostilbene (SITS), 4,4'-Diisothiocyanatostilbene-2,2'-disulfonic acid (DIDS), 5-nitro-2-(3-phenyl-propylamino)-benzoate (NPPB) and diphenylamine-2-carboxylate (DPC). In addition, extracellularly-applied nucleotides, e.g., ATP and UTP in millimolar concentrations as well as the purinoceptor antagonists suramin and Reactive Blue, inhibit the cell swelling-induced anion conductance.[12] This inhibition is most prominent at depolarising membrane potentials and apparently does not involve purinoceptor activation.

Previously, we demonstrated that protein tyrosine phosphorylation is required for the activation of the cell swelling-induced anion conductance.[8] Treatment of the cells with tyrosine kinase inhibitors like herbimycin A or genistein largely reduced the cell swelling-induced anion efflux and vice versa, promoting tyrosine phosphorylation by (per)vanadate-mediated inhibition of phosphotyrosine phosphatases potentiated the anion efflux triggered by non-saturating hyposmotic stimulation.[8] Involvement of protein tyrosine phosphorylation in the regulation of VRAC has now been established in several other but not all cell types. To date, the identity of the kinase(s) and phosphatase(s) leading to channel regulation has not yet been established in most models studied. For Jurkat T lymphocytes however, strong evidence exists that the Src-like $p56^{lck}$ tyrosine kinase is both essential and adequate for the activation of volume-sensitive anion channels.[13] This notion is supported by our observations that in Intestine 407 cells, the hypotonicity-provoked anion efflux is largely reduced after treating the cells with damnacanthal, an inhibitor of $p56^{lck}$ (B.C. Tilly, unpublished results).

Intracellular administration of GTPγS, and thereby activation of G proteins, was found to activate anion-selective conductance in several cell types including human HT29cl19A colonocytes,[14] and this activation could be inhibited by GDP S.[15, 16] Using *Clostridium botulinum* exoenzyme C3 as a tool to ADP-ribosylate and inactivate p21Rho, we have demonstrated that this G-protein, but not the related p21Ras or p21Rac, is involved in the activation of the osmo-sensitive anion efflux in Intestine 407 cells.[17] Although a functional Rho pathway is required for the opening of osmo-sensitive anion channels, recent studies in bovine endothelial cells, however, have shown that Rho activation alone is not adequate.[18] Most plausibly, Rho exerts its function through the induction of cytoskeletal remodelling. Indeed, immediately after hyposmotic stimulation, a rapid and transient remodeling of the actin cytoskeleton has been observed in Intestine 407 cells as well as in other cell types.[17, 19, 20] Therefore, it seems likely that a reorganization of the actin cytoskeleton is necessary but not sufficient to activate VRAC. This notion is supported by the observation that hormones and growth factors capable of activating Rho and inducing cytoskeletal rearrangements are able to potentiate but not to

activate the anion conductance.[21] Linking these signaling pathways to an independent, yet unidentified 'volume sensor' has two important physiological consequences. First, activation of VRAC occurs only during cell swelling, thereby preserving the specificity of the response. Second, by coupling the volume response to pathways activated upon hormonal stimulation, small changes in cell volume which may occasionally take place during hormone-induced changes in cellular metabolism[6] are more adequately corrected.

4. RELEASE OF ORGANIC OSMOLYTES

In a number of tissues, the release of small organic osmolytes contribute significantly to the RVD response. In several cell types, these molecules were even found to be the major determinants of the volume correction mechanism involved.[22, 23] In Intestine 407 cells, osmotic cell swelling also leads to a stimulation of an organic anion release pathway readily permeable to taurine and phosphocholine.[24] Unlike activation of the cell swelling-induced anion conductance, activation of the organic anion release pathway occurred only after a distinct lag time of approximately 30-60 s. The hypotonicity-induced release of organic osmolytes was not sensitive to tyrosine kinase or phosphatase inhibition and did not require p21Rho or PtdIns-3-kinase activity,[24] indicating the efflux is regulated independently of VRAC. As compared to the Cl^- efflux, the threshold for activation of taurine release was reached only at a relatively strong hypotonic stimulation[24] suggesting the release of organic osmolytes acts a second line of defence or may facilitate the re-uptake of ions and restoration of the membrane potential in Intestine 407 cells.

5. ACTIVATION OF VESICLE CYCLING AND THE RELEASE OF ATP

In addition to activation of osmolyte release pathways and like many other forms of mechanical stress, osmotic cell swelling promotes the release of ATP, an auto- or paracrinic factor acting through plasma membrane purinoceptors.[12, 25-27] Extracellular ATP has been shown to regulate the RVD in a number of different cell types,[25, 26, 28, 29] by either stimulating Ca^{2+} -dependent K^+ efflux[28] or activating VRAC.[25, 29] In Intestine 407 cells, extracellular ATP was not able to directly activate volume-sensitive Cl^- channels nor did addition of purinoceptor antagonists or the ATP hydrolase apyrase prevent the development of the conductance.[12] However, (sub)micromolar concentrations of ATP were able to potentiate the hypotonicity-provoked Cl^- efflux in a Ca^{2+}-dependent manner.[12]

Osmotically-induced ATP release was found to be critically involved in the activation of extracellular signal-regulated protein kinase-1/2 (ERK-1/2) in Intestine 407 cells.[12] Although activation of ERK-1/2 as well as other members of the MAP kinase family (p38 and JNK) has been observed in most cell models studied, their function during the RVD response has not yet been fully understood.

Several mechanisms have been proposed to underlie the release of ATP including (1) leakage due to (local) membrane damage, (2) activation of specific channel(s) or transporter(s), and (3) exocytotic events. Unlike activation of VRAC, ATP release from Intestine 407 cells was abolished after treatment of the cells with 1,2-bis-(2-aminophenoxy)-ethane-*N*,*N*,*N′*,*N′*-tetra-acetic acid acetoxymethyl ester (BAPTA-AM) acting as a buffer

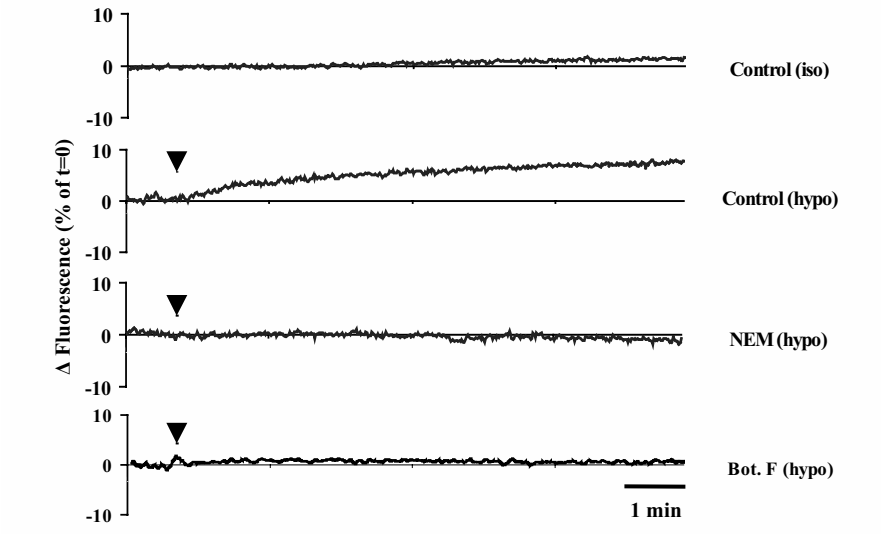

Figure 2. Hypotonicity-provoked change in FM 1 – 43 fluorescence. Cells grown on coverslips were treated with N-ethylmaleimide (NEM, 1 mM) or Chariot™-conjugated *C. botulinum* toxin F for respectively 15 min or 2 h. Thereafter, the coverslips were placed in a cuvette with isotonic medium containing 1 μM FM 1-43. Arrow indicates a shift to a hypotonic medium (for experimental details see [30]).

of intracellular free Ca^{2+} levels or with cytochalasin B.[12] It was concluded that ATP does not permeate through volume-sensitive anion channels. This notion was supported by our observations that the cell-swelling-induced ATP release developed rather slowly and continued for at least 15 min.[12] Notably, the RVD response under these conditions is completed within approx. 2~3 min.[8]

Osmotic swelling of Intestine 407 cells leads to an immediate increase in cell surface membrane area as determined using the fluorescent membrane dye FM 1-43 (Figure 2). Like the release of ATP, the increase in FM 1-43 fluorescence was abolished after loading the cells with BAPTA-AM or after cytochalasin B treatment, indicating that the increase in surface labelling is dependent on intracellular Ca^{2+} and on an intact actin cytoskeleton.[30] To investigate whether exocytosis is involved in the increase in fluorescence, cells were treated with N-ethylmaleimide (NEM) to inactivate SNAP-25, one of the SNARE (soluble-NEM-sensitive factor–attachment protein receptor) proteins involved in vesicle docking and fusion. Alternatively, *Clostridium botulinum* toxin F was introduced into the cells using the Chariot™ protein delivery kit to inactivate the vesicle-associated SNARE protein VAMP2 by proteolytic cleavage.[30] As shown in Figure 2, both NEM treatment and intracellular delivery of *C. botulinum* toxin F almost completely abolished the cell swelling-induced increase in fluorescence, suggesting that exocytosis occurs rapidly upon osmotic cell swelling.

Because exocytosis is often accompanied by subsequent internalisation of membrane fragments, we studied endocytosis in Intestine 407 cells by quantitating intracellular accumulation of TRITC-dextran. After a distinct lag time of 2-3 minutes, a robust (> 100 fold) increase in rate of endocytosis was observed in hyposmolarity-stimulated cells that lasted for approx. 10-15 minutes.[30] The delayed onset of endocytosis may suggest it is

Table 1. Effects of Cl^- and K^+ channel inhibition on the hypotonicity-induced TRITC-dextran uptake (% of hypotonic control).

		Isotonic	Hypotonic
Control		9 ± 9	100 ± 39
Cl^- channel	SITS	8 ± 7	11 ± 45
	Suramin	5 ± 5	7 ± 5
	ATP (5 mM)	1 ± 1	22 ± 10
K^+ channel	Quinidine	26 ± 22	545 ± 159
	Gd^{3+}	2726 ± 914	5443 ± 1685
	High $[K^+]_{out}$ (50 mM)	7 ± 4	229 ± 107

triggered by the prior increase in exocytosis. In Intestine 407 cells, however, we found that exo- and endocytosis are regulated independently because cytochalasin B treatment and BAPTA-AM loading, both strong inhibitors of exocytosis, did not affect the cell swelling-induced endocytosis. In contrast, our observation that the hypotonicity-provoked endocytosis is inhibited by inactivation of VRAC and promoted by K^+ channel blockers and high extracellular $[K^+]$ (Table 1) suggests that membrane depolarisation, a known consequence of VRAC activation,[31] may promote or trigger endocytosis.

Using *C. botulinum* toxin F treated cultures, a putative role for exocytosis in the release of ATP was investigated. To summarise the results, both basal and hypotonicity-induced ATP release was strongly reduced in toxin-treated cultures, supporting the notion that the efflux of ATP is mediated by exocytosis. Furthermore, we found that inhibition of ERK-1/2 activation or apyrase-catalysed removal of extracellular ATP strongly reduced the exocytosis rate, suggesting that purinergic activation of ERK-1/2 plays a role in a positive feedback loop that may contribute to the release of ATP from hyposmotically-stimulated cells.[30]

6. REGULATION OF VRAC BY LIPID RAFTS

Recently, a putative role for lipid rafts, cholesterol-rich domains of the plasma membrane, in the regulation of cell-swelling activated Cl^- channels has been indicated.[32-34] Trouet et al.[32] demonstrated that the volume-sensitive anion conductance was limited in caveolin-1 deficient cell types but could be enhanced robustly by overexpression of this protein. In addition, they found that transfection of calf pulmonary artery endothelial (CPAE) cells with mutant caveolin-1, thereby disturbing the formation of caveolea, markedly reduced the hypotonicity-induced anion current,[34] suggesting that intact caveolea play an important role in VRAC regulation. However, disruption of caveolea in Intestine 407 cells, brought about by extracting plasma membrane cholesterol using 2-hydroxypropyl-β-cyclodextrin in the presence of acceptor lipid vesicles, did not reduce the volume-sensitive anion

conductance but was found instead to potentiate the response. This potentiation was also observed in caveolin-1 deficient CaCo-2 colonocytes as well as in sphingomyelinase-treated cells, indicating that these cholesterol-rich micro domains do not play a crucial role in VRAC activation in this cell type.

Alternative targets for the action of cyclodextrin/lipid vesicles are the rapidly recycling endosomes or retrosomes involved in cholesterol transport between intracellular compartments and the plasma membrane.[35] Treatment of the cells with cyclodextrin may accelerate endosome cycling in an attempt to replenish plasma membrane cholesterol. Vesicle cycling during the RVD response is not unprecedented because, as described above, osmotic swelling of Intestine 407 cells is accompanied by exo- and endocytosis. Treatment of the cells with *Clostridium botulinum* toxin F to abolish exocytosis (c.f. see Section 5) partly inhibited the volume sensitive anion efflux, indicating insertion of additional channels by vesicle fusion with the plasma membrane. Together, these results support a model in which the recruitment of volume-sensitive anion channels to the plasma membrane acts as an important step in the mechanism of VRAC activation and suggest a role for rapidly recycling endosomes in the response to osmotic cell swelling.

7. CONCLUSIONS

A plethora of signaling cascades is activated upon hyposmotic stimulation of mammalian cells. In Intestine 407 cells, p21Rho as well as tyrosine kinase(s) and PtdIns-3-kinase were found to be a prerequisite for VRAC activation, whereas protein kinase C is likely to be involved in the regulation of a distinct organic osmolyte release pathway. In addition, a number of cellular responses are able to modulate the volume-sensitive anion conductance including Ca^{2+} mobilization, cytoskeletal re-arrangements and vesicle cycling. The molecular mechanism(s) by which these signaling molecules affect ion channel opening is still fragmentary and detailed investigations into the mode of activation including reconstitution studies are hampered by the current lack of information about the molecular identity of the channel(s) involved. Our observation that at least part of the anion channel activation occurs through their recruitment from intracellular compartments to the plasma membrane now adds intracellular Cl^- channels to the list of potential VRAC candidates.

Other signaling pathways, like the stress kinases p38 and Jnk as well as the ATP-provoked activation of Erk-1/2, are apparently not involved in channel regulation. Although their physiological role in the RVD response remains to be elucidated, it is tempting to speculate that they may have a function in restoring cellular homeostasis and in maintaining cell viability.

8. REFERENCES

1. W.C.O'Neill, Physiological significance of volume-regulatory transporters, *Am.J.Physiol*. **276**, C995-C1011 (1999).
2. A.A.Mongin and S.N.Orlov, Mechanisms of cell volume regulation and possible nature of the cell volume sensor, *Pathophysiology* **8**, 77-88 (2001).

3. F.Wehner, H.Olsen, H.Tinel, E.Kinne-Saffran and R.K.Kinne, Cell volume regulation: osmolytes, osmolyte transport and signal transduction, *Rev. Physiol. Biochem. Pharmacol.* **148**, 80 (2003).
4. P.R.Junankar and K.Kirk, Organic osmolyte channels: a comparative view, *Cell Physiol. Biochem.* **10**, 355-360 (2000).
5. H.Pasantes-Morales, R.Franco, L. Ochoa and B.Ordaz, Osmosensitive release of neurotransmitter amino acids: relevance and mechanisms, *Neurochem. Res.* **27**,59-65 (2002).
6. D.Häussinger, The role of cellular hydration in the regulation of cell function, *Biochem. J*., **313**, 697-710 (1996).
7. G.Henle and F.J.Deinhardt, The establishment of strains of human cells in tissue culture, *J. Immunol.* **79**, 54-59 (1957).
8. B.C.Tilly, N.van den Berghe, L.G.J.Tertoolen, M.J.Edixhoven and H.R. de Jonge, Protein tyrosine phosphorylation is involved in osmoregulation of ionic Conductances, *J. Biol. Chem.* **268**, 19919-19922 (1993).
9. J.Wang, S.Morishima and Y.Okada, IK channels are involved in the regulatory volume decrease in human epithelial cells, *Am. J.Physiol.* **284**, C77-C84 (2003).
10. T.J.Jentsch, V.Stein, F.Weinreich and A.A.Zdebik, Molecular structure and physiological function of chloride channels, *Physiol. Rev.* **82**, 503-568 (2002).
11. B.Nilius and G.Droogmans, Amazing chloride channels: an overview, *Acta Physiol. Scand* **177**, 119-147 (2003).
12. T.van der Wijk T, H.R.de Jonge and B.C.Tilly, Osmotic cell swelling-induced ATP release mediates the activation of extracellular signal-regulated protein kinase (Erk)-1/2 but not the activation of osmo-sensitive anion channels, *Biochem. J.* **343**, 579-586 (1999).
13. A.Lepple-Wienhues, I.Szabo, T.Laun, N.K.Kaba, E.Gulbins and F.Lang, The tyrosine kinase p56lck mediates activation of swelling-induced chloride channels in lymphocytes, *J. Cell Biol.* **141**, 281-286 (1998).
14. B.C.Tilly, G.M.Mancini, J.Bijman, P.G.van Gageldonk, C.E.Beerens, R.J.Bridges, H.R.de Jonge and F.W.Verheijen, Nucleotide-activated chloride channels in lysosomal membranes, *Biochem. Biophys. Res. Commun.* **187**, 254-260(1992).
15. P.Doroshenko, P.Penner and E.Neher, Novel chloride conductance in the membrane of bovine chromaffin cells activated by intracellular GTPγS, *J. Physiol*. **436**, 711-24 (1991).
16. T.Voets, V.Manolopoulos, J.Eggermont, C.Ellory, G.Droogmans, B.Nilius, Regulation of a swelling-activated chloride current in bovine endothelium by protein tyrosine phosphorylation and G proteins, *J. Physiol.* **506**, 341-345 (1998).
17. B.C.Tilly, M.J.Edixhoven, L.G.J.Tertoolen, N.Morii, Y.Saitoh, S.Narumiya and H.R. de Jonge, Activation of the osmo-sensitive chloride conductance involves P21rho and is accompanied by a transient reorganization of the F-actin cytoskeleton, *Mol. Biol. Cell* **7**, 1419-1427 (1996).
18. I.Carton, D.Trouet, D.Hermans, H.Barth, K.Aktories, G.Droogmans, N.K.Jorgensen, E.K.Hoffmann, B.Nilius and J.Eggermont, RhoA exerts a permissive effect on volume-regulated anion channels in vascular endothelial cells, *Am. J. Physiol.* **283**, C115-C125 (2002).
19. S.F.Pedersen, J.W.Mills and E.K.Hoffmann, Role of the F-actin cytoskeleton in the RVD and RVI processes in Ehrlich ascites tumor cells, *Exp. Cell Res.* **252**, 63-74 (1999).
20. I.Carton, D.Hermans and J.Eggermont, Hypotonicity induces membrane protrusions and actin remodeling via activation of small GTPases Rac and Cdc42 in Rat-1 fibroblasts, *Am. J. Physiol.* **285**, C935-C944 (2003).
21. B.C.Tilly, M.J.Edixhoven, N.van den Berghe, A.G. M.Bot and H.R.de Jonge, Ca^{2+}-mobilizing hormones potentiate hypotonicity-induced activation of ionic conductances in Intestine 407 cells, *Am. J. Physiol.* **267**, C1271-C1278 (1994).
22. T.Nakanishi, O.Uyama and M.Sugita, Osmotically regulated taurine content in rat renal inner medulla, *Am. J. Physiol.* **261**, F957-F962 (1991).
23. H.Pasantes-Morales, R.Franco, M.E.Torres-Marquez, K.Hernandez-Fonseca and A.Ortega, Amino acid osmolytes in regulatory volume decrease and isovolumetric regulation in brain cells: contribution and mechanisms, *Cell. Physiol. Biochem.* **10**,361-370 (2000).
24. S.F.B.Tomassen, D.Fekkes, H.R.de Jonge and B. C.Tilly, Osmotic swelling provoked release of organic osmolytes in human intestinal epithelial cells, *Am. J. Physiol.*, in press.
25. Y.Wang, R.Roman, S.D.Lidofsky and J.G.Fitz, Autocrine signaling through ATP release represents a novel mechanism for cell volume regulation, *Proc. Natl. Acad.* USA **93**, 12020-12025 (1996).
26. A.L.Taylor, B.A.Kudlow, K.L.Marrs, D.C.Gruenert, W.B.Guggino and E.M.Schwiebert, Bioluminescence detection of ATP release mechanisms in epithelia, *Am. J. Physiol.* **275**, C1391-C1406 (1998).
27. A.Hazama, T.Shimizu, Y.Ando-Akatsuka, S.Hayashi, S.Tanaka, E.Maeno and Y.Okada, Swelling-induced, CFTR-independent ATP release from a human epithelial cell line: lack of correlation with volume-sensitive Cl^- channels Y. *J. Gen. Physiol.* **114**, 525-533 (1999).

28. D.B.Light, T.L.Capes, R.T.Gronau and M.R.Adler, M.R., Extracellular ATP stimulates volume decrease in Necturus red blood cells, *Am. J. Physiol.* **277**, C480-C491 (1999).
29. R.M.Roman, A.P.Feranchak, K.D.Salter, Y.Wang and J.G.Fitz, Endogenous ATP release regulates Cl^- secretion in cultured human and rat biliary epithelial cells, *Am. J. Physiol.* **276**, G1391-G1400 (1999).
30. T.van der Wijk, S.F.B.Tomassen, A.B.Houtsmuller, H.R.de Jonge and B.C.Tilly, Increased vesicle recycling in response to osmotic cell swelling. Cause and consequence of hypotonicity-provoked ATP release, *J. Biol.Chem.* **278**, 40020-40025 (2003).
31. A.Hazama and Y.Okada, Biphasic rises in cytosolic free Ca^{2+} in association with activation of K^+ and Cl^- conductance during the regulatory volume decrease in cultured human epithelial cells, *Pflügers Arch.***416**, 710-714 (1990).
32. D.Trouet, B.Nilius, A.Jacobs, C.Remacle, G.Droogmans and J.Eggermont, Caveolin-1 modulates the activity of the volume-regulated chloride channel, *J. Physiol.* **520,** 113-119 (1999).
33. I.Levitan, A.E.Christian, T.N.Tulenko and G.H.Rothblat, Membrane cholesterol content modulates activation of volume-regulated anion current in bovine endothelial cells, *J. Gen. Physiol*. **115**, 405-416 (2000).
34. D.Trouet, D.Hermans, G.Droogmans, B.Nilius and J.Eggermont, Inhibition of volume-regulated anion channels by dominant-negative caveolin-1, *Biochem. Biophys. Res. Commun*. **284**, 461-465 (2001).
35. J.P.Incardona and S.Eaton, Cholesterol in signal transduction, *Curr. Opin. Cell Biol.* **12**, 193-203 (2000).

32

REGULATION OF EPITHELIAL ELECTROLYTE TRANSPORTERS THROUGH PROTEIN-PROTEIN INTERACTIONS

Carole M. Liedtke*

1. INTRODUCTION

Two Cl transport proteins, a basolateral Na-K-2Cl (NKCC1) cotransporter and an apical Cl channel designated cystic fibrosis transmembrane regulator (CFTR), act in a highly coordinated manner to mediate salt and water secretion in epithelial cells lining the airways, sweat glands, and salivary glands. In airway epithelial cells, fluid movement into the conducting airways humidifies inspired air, maintains a periciliary fluid layer, hydrates mucus and maintains optimal electrolyte and water homeostasis necessary for optimal mucociliary clearance. Control of electrolyte and fluid secretion is directed at the activity of CFTR and NKCC1 through intracellular signaling mechanisms coupling hormonal and environmental stimuli to the Cl transporter. Our studies demonstrate that NKCC1 expressed in human tracheal epithelial cells and in a Calu-3 airway epithelial cell line is quiescent until activated by α_1-adrenergic stimulation through the effector enzyme protein kinase C (PKC). More recent studies using an antisense approach identified PKC-δ as the PKC isotype required for NKCC1 activation.[1, 2] Secretagogues that elevate cAMP levels rapidly activate CFTR. Although CFTR is regulated primarily by protein kinase A (PKA), PKC stimulates it to a modest extent. We and others have now shown regulation of cAMP-dependent CFTR function by PKC,[3-5] specifically a PKC-ε isoform.[6]

The highly specific signaling of PKC regulation of epithelial Cl transporters at the isotype level points to a fidelity to appropriate extracellular and intracellular signaling pathways associated with protein-protein interactions. In other cells, a molecular network of adapter, anchoring and scaffold proteins maintain kinases and phosphatases in defined subcellular compartments.[7] Indeed, active and inactive PKC isotypes have been localized near their target substrates by binding to anchoring or scaffold proteins.[8-10] In these studies, we examined protein-protein interactions necessary for activation of NKCC1 by PKC-δ and of CFTR by PKC-ε.

* Carole. M. Liedtke, Case Western Reserve University, Cleveland, OH 44106.

2. METHODS

2.1. Cell Culture

Calu-3 cells were grown in cell culture on tissue culture plastic or on 0.4 μm pore size Transwell-Clear polyester filter inserts (Corning Costar, Cambridge, MA) for transport experiments and for immunofluorescence. Cell monolayers were assessed for confluence by microscopic examination and by measurement of electrical resistance across the cell monolayers grown on filter inserts. Electrical resistance was quantitated using chopstick electrodes and EVOM (Epithelial Voltohmmeter, World Precision Instruments, New Haven, CT). Values were corrected for background resistance of filter alone bathed in HEPES-buffered Hank's balanced salt solution (HPSS).

2.2. Measurement of Transport Function

NKCC1 transporter activity was measured by radioisotopic uptake of ^{86}Rb, a congener of K^2 in serum-deprived cells. Cells were pre-incubated for 30 min at 32°C following addition of vehicle or 10 μM bumetanide. In some experiments, recombinant peptides were delivered into cells using a BioPORTER™ protein delivery system. Radiotracer uptake was initiated by transferring filter inserts to a six well tissue culture dish, each well containing HPSS, 1 μCi ^{86}Rb and drugs to be tested. Influx was measured for a 4 min time interval and then terminated by rapidly immersing filters four times in an ice-cold isotonic buffer of 100 mM $MgSO_4$ and 137 mM sucrose. Intracellular radioactivity was extracted by incubating cell monolayers in 0.1 N NaOH. Aliquots of extract were assayed for radioactive counts by liquid scintillation counting and for protein with a Pierce protein assay kit using bovine serum albumin as the standard. Intracellular radioisotopic content was calculated as nmol K/mg protein.

2.3. Immunoprecipitation, Pulldown Analysis and Immunoblot Analysis

Protein analyses were performed as previously described.[1, 2, 5, 9, 10] Cells were grown to confluence, serum deprived overnight and lysed in ice-cold lysis buffers supplemented with 1% NP-40 and 0.25% sodium deoxycholate. Lysates were clarified by pretreatment with agarose beads then incubated with an antibody directed against the protein of interest. NKCC1 was immunoprecipitated from lysates in a buffer supplemented with 0.3% Triton X-100 and 1 mM benzamide. A 0.5 ml aliquot of lysate was incubated with 1.1% sodium dodecyl sulfate (SDS) for 1 hr at room temp. The SDS-solubilized lysate was combined with 1.4 ml of 3.0% Triton X-100 in lysis buffer and incubated for 1 hr on ice, then overnight with T4 monoclonal antibody to immunoprecipitate NKCC1. For CFTR, the lysis buffer contained 1% Triton X-100, 1% Na deoxycholate, and 0.1% SDS. Non-muscle actin was pulled down using anti-actin antibody conjugated to agarose beads. Immune complexes were recovered using Protein A agarose (CFTR, NHERF1), Protein G-agarose (NKCC1, PKC-δ, PKC-ε) or Protein L agarose (RACK1) beads. Samples were solubilized in Laemmli buffer then subjected to SDS-PAGE and immunoblot analysis. Pulldown analysis was performed using tagged recombinant proteins and antibodies to tags.

2.4. Expression of Recombinant Proteins

Recombinant δC2 domain and GST-NHERF1 fusion proteins were expressed in DH5α cells.[11, 12] A pET14b-δC2 expression vector which placed a polyhistidine tag at the N terminus of the construct was kindly provided by Dr. Lodewijk V. Dekker (Univ. Coll. London). Fusion proteins were expressed and purified using B-PER extraction. The fusion proteins were evaluated by immunoblot analysis using a polyclonal antibody to the HIS_6 tag or India HisProbe (δC2 domain) or polyclonal antibody to a GST tag. Viral stocks, kindly provided by Dr. Susan Brady-Kilnay (Case Western Reserve University), were used to infect Sf9 insect cells and to express recombinant human His6 and HA-tagged RACK1.

2.5. Actin Solutions

Monomeric actin (G-actin) was stored in G-actin buffer consisting of 2 mM Tris-HCl, pH 8.0, 0.5 mM ATP, 0.5 mM $CaCl_2$, 0.5 mM β-mercaptoethanol at a final concentration of 100 μg/ml. Filamentous actin (F-actin) was polymerized from G-actin by the addition of 2 mM $MgCl_2$ and 50 mM KCl actin in G-actin buffer. The mixture was incubated for 1 hr at room temperature.

2.6. Binding and Overlay Assays

In vitro binding of proteins was measured using solid phase binding in a slot blot apparatus or solution binding.[11, 12] To pre-activate enzymes, 200 ng recombinant human PKC-δ or PKC-ε were incubated with 30 μg/ml phosphatidylserine (PtdSer) and 2 μg/ml diacylglycerol (DAG) for 15 min at 30°C. For overlay assays, Calu-3 cell proteins were separated on SDS-PAGE, transferred to PVDF membrane paper and incubated with blocking buffer (50 mM Tris-HCl, pH 7.5, 200mM NaCl, 12 mM β-mercaptoethanol and 0.4% bovine serum albumin.[11] Membrane strips were next incubated for 1 hr. with or without preactivated PKC isotype. Unbound material was removed by washing and bound PKC isotype detected by immunoblot analysis and enhanced chemiluminescence.

3. RESULTS

3.1 PKC Isotype Binding to Cl Transporter

One model of a protein-protein interaction leading to PKC-dependent regulation of epithelial Cl transporters depicts direct interaction between PKC isotype and transporter. This model was tested by co-immunoprecipitation and overlay assay of Calu-3 cell proteins. PKC-δ was detected in total cell lysates as a 75 kDa protein band and also in immunoprecipitates of NKCC1.[10] NKCC1 was detected in immunoprecipitates of PKC-δ, indicating an association that is likely physiologically relevant. However, when tested in overlay assays, PKC-δ did not bind to immunoprecipitated NKCC1. PKC-ε was detected as a 75 kDa protein band in total cell lysates and also found in immunoprecipitates of CFTR and vice versa.[11]

To determine whether PKC isotypes directly bind to their corresponding Cl transporter, overlay assay using pre-activated, recombinant human PKC-δ or PKC-ε was performed on Calu-3 cell proteins separated on SDS gels and transferred electrophoretically to PVDF membrane paper. Overlay assay using pre-activated recombinant PKC-ε revealed binding to at least 6 protein bands; one predominant band was a 37 kDa protein corresponding in molecular mass to RACK1.[7, 8] Overlay assays on immunoprecipitates of CFTR and RACK1 from Calu-3 cells showed no specific binding of PKC-ε to immunoprecipitated CFTR. However, binding of pre-activated recombinant PKC-ε was detected in immunoprecipitates of RACK1; binding was prominent at 37 kDa, the molecular mass of RACK1, indicating binding of PKC-ε to endogenous RACK1. Next, we turned to a study of endogenous RACK1 and PKC-ε in Calu-3 cells, a human airway epithelial cell line, using immunoblot assay of immunoprecipitated RACK1 or PKC-ε. Robing of immunoprecipitates of RACK1 with antibody to PKC-ε revealed a protein band at 75 kDa immunoreactive to antibody to PKC-ε, but not to antibody to PKC-δ, indicating co-immunoprecipitation of PKC-ε with RACK1. This was confirmed by immunoblot analysis of immunoprecipitates of PKC-ε for RACK1. Overall, we conclude that in Calu-3 cells, PKC-δ and PKC-ε bind to proteins different from the Cl transporters regulated by the specific PKC isotypes.

3.2 F-actin as a Binding Partner for PKC-δ

Electrolyte transport proteins, including NKCC1, have been implicated in cytoskeletal anchoring. However, the molecular nature of the involvement is not clearly understood. Because the actin cytoskeleton is thought to bind PKC isotypes in other cell types, we examined the role of F-actin cytoskeleton on NKCC1 function in Calu-3 epithelial cells. In Calu-3 cells, baseline activity of NKCC1 represented 28.2% of the total ^{86}Rb uptake. Methoxamine, an α_1-adrenergic agent, increased NKCC1 activity 3.0-fold from 23.5 ± 2.7 (n=15) nmol K/mg protein to 111.9 ± 16.8 (n=8) nmol K/mg protein ($P<.005$). The α_1-adrenergic agent also elevated the bumetanide-sensitive K uptake from 28.2% to 61.1 % of total ^{86}Rb uptake, a 2.2-fold increase that together with stimulation of K uptake indicates activation of NKCC1. Latrunculin B did not significantly affect basal NKCC1 activity but did block methoxamine-stimulated flux. In contrast, jasplakinolide induced a 2-fold increase in baseline NKCC1 activity to 80.9 ± 14.4 (n=7) nmol K/mg protein ($P<.005$) and a 2.1-fold increase in percent bumetanide-sensitive flux, pointing to activation of NKCC1. To determine whether PKC-δ is necessary for jasplakinolide-stimulated NKCC1 activity, cells were pre-treated with rottlerin, an inhibitor of PKC-δ. Jasplakinolide stimulated a rottlerin-sensitive uptake of 58.6 ± 6 (n=6) nmol K/mg protein which was not significantly different than the bumetanide-sensitive K uptake or a combined rottlerin, bumetanide-sensitive uptake of 69.6 ± 11 (n=6) nmol K/mg protein. Results indicate that jasplakinolide stimulates NKCC1 activity as robustly as methoxamine and suggest further a role for F-actin in hormone-stimulated NKCC1 activity.

One possible explanation for the results is an interaction between F-actin and PKC-δ or NKCC1 or both proteins. Co-immunoprecipitation and pulldown experiments demonstrated that PKC-δ and NKCC1 co-immunoprecipitate with actin and that actin co-immunoprecipitates with NKCC1. The close association of the three proteins together with lack of PKC-δ binding to NKCC1 prompted us to ask whether PKC-δ directly binds

to actin. Binding of actin and PKC-δ was examined using recombinant proteins in a solution binding assay or in a slot blot apparatus with immobilized F- or G-nonmuscle actin. We found that PKC-δ binds to nonmuscle actin and that binding is enhanced 3-fold by pre-activation of enzyme. In addition, pre-activated PKC-δ binds to both nonmuscle F- and G-actin; however, there is a 3.9-fold greater binding to F-actin than G-actin, suggesting preferential binding to F-actin. This was confirmed using anti-actin drugs to manipulate actin polymerization. Non-muscle G-actin was incubated with jasplakinolide to promote polymerization of G-actin and non-muscle F-actin was incubated with latrunculin B which mimics the activity of monomer sequestering proteins, thus preventing polymerization of G-actin to F-actin. Jasplakinolide increased binding of PKC-δ by 84% and latrunculin B decreased PKC-δ binding by 28%. Binding of PKC-δ to F-actin is dose-dependent with an EC_{50} of 72 ng. Examination of dual-label immunofluorescence of confluent cell cultures demonstrated localization of actin at the cell periphery and of PKC-δ in the cytosol and cell periphery. Merged images revealed focal spots of yellow-orange indicating colocalization of PKC-δ and actin at discrete sites in the cell periphery but not the cytosol. Our conclusion from these experiments is that PKC-δ binds to F-actin and led us to hypothesize that this interaction is necessary for activation of NKCC1.

Instead of a Ca^{2+} binding function, the N-terminal C2 domain expressed in novel PKC isotypes is thought to have one of protein interaction.[18, 19] We expressed a recombinant His_6-tagged C2 domain of PKC-δ and tested its binding to non-muscle F-actin and the effects of this binding on NKCC1 function. The His_6-tagged C2 domain of PKC-δ bound to non-muscle F-actin, but not muscle actin, in a dose-dependent manner and blocked binding of activated PKC-δ to F-actin with an IC_{50} of 2.26 μg. When delivered into Calu-3 cells using a BioPORTER™ protein delivery system, the recombinant C2 domain dose-dependently decreased methoxamine-stimulated NKCC1 activity with an IC_{50} of 0.36 μg. The results demonstrate that binding of PKC-δ to the actin cytoskeleton is necessary for activation of NKCC1.

3.3 RACK1 as a Binding Partner for PKC-ε

Preliminary evidence pointed to airway epithelial RACK1 as a binding partner for preactivated PKC-ε. Immunoblot analysis demonstrated the presence of RACK1 protein in Calu-3 total cell lysates.[11] This was confirmed by sequence analysis of cDNA amplified from reverse transcribed total mRNA of Calu-3 cells with primers for human RACK1. Airway epithelial mRNA encoded RACK1, a member of a heterotrimeric G superfamily of proteins. Binding of RACK1 and PKC-ε was examined using recombinant proteins in a slot blot assay or solution binding assay. Dose-dependent binding of preactivated PKC-ε to recombinant RACK1 was detected using both assay methods. A binding site on each protein was next predicted from reports on heart muscle proteins.[20] An 8 amino acid sequence in the sixth WD40 repeat of RACK1 (DIINALCF, designated VI-RACK) was synthesized and used for binding studies. We found that VI-RACK binds to PKC-ε in a dose-dependent manner with peak binding at 5 nM peptide and that binding was dependent on the presence of PKC activators. A site on the N-terminus of PKC-ε, denoted as εV1-2, has been shown to selectively inhibit PKC-ε translocation function in intact myocytes[20] and prevents binding of PKC-ε to rat '-COP.[21] A peptide encoding this site (EAVSLKPT) was synthesized and used in competitive inhibition

experiments. Binding of preactivated PKC-ε to recombinant RACK1 was blocked by PKC-ε peptide with an IC_{50} of 80.3 μM.

In the absence of direct binding of PKC-ε or RACK1 to CFTR, we next explored a binding partner for RACK1 that is proximal to CFTR. Two closely related proteins which interact with CFTR are the PDZ-domain proteins NHERF1, a 50 kDa phosphoprotein with two PDZ domains, and NHERF2 or E3KARP, a 50 kDa protein that shares approximately 52% amino acid identity with NHERF1.[22, 23] In co-immunoprecipitation experiments, NHERF1 was detected in immune complexes of RACK1 as a 50 kDa protein band and RACK1 was detected in immune complexes of NHERF1 as a 37 kDa protein band, suggesting an association of the two proteins. Although readily detected in Calu-3 cell lysates, NHERF2 was not consistently detected in immunoprecipitates of RACK1. In pulldown assays using His_6-tagged RACK1, a protein immunoreactive with antibody to NHERF1 was recovered from Calu-3 cell lysates, and GST-tagged NHERF1 pulled down a protein immunoreactive with antibody to RACK1. These results suggest direct binding of the two endogenous proteins that was examined in more detail in slot blot assays. Using recombinant proteins, we found that RACK1 binds to NHERF1 in a dose-dependent manner with an EC_{50} of 3.1 μg of RACK1.

4. DISCUSSION

These studies have revealed two new and unique PKC binding interactions that have profound effects on the activity of epithelial electrolyte transporters. An examination of the binding of PKC-ε to Calu-3 cellular proteins demonstrates direct binding of PKC-ε to RACK1, a Receptor for Activated C-Kinase, and binding of RACK1 to NHERF1, a Na^+/H^+ exchange regulatory factor, a scaffold protein that binds four C-terminal amino acids (DTRL) of CFTR through either of its PDZ (PDZ1 and PDZ2) domains.[23-25] This implies a pivotal role for the scaffold protein RACK1 in epithelial Cl channel function. NHERF1 and CFTR bind with high affinity apparently to regulate other transport proteins (such as renal outer medullary K channel, and epithelial Na channels and NHE3)[26, 27] and to function as a membrane retention signal.[28] But, it is the potential dimerization of CFTR by bivalent NHERF1 that is thought to regulate full expression of CFTR channel function.[24] NHERF1 may act as a scaffold protein to facilitate an interaction between CFTR and RACK1 or PKC-ε to achieve optimal cAMP-dependent CFTR function. RACK1 has a unique rigid -propeller structure formed by WD-repeat regions which have been implicated in protein-protein interactions, the first being binding of activated PKC.[20] Calu-3 RACK1 binds activated PKC-ε at a site on the 6th WD repeat of RACK1 and a C2-like domain of PKC-ε at its N-terminus. Our results indicate that airway epithelial RACK1 binds multiple proteins, each directly implicated in the regulation of CFTR function and thus acts as a scaffold. The mode of interaction between RACK1 and NHERF1 is not known. RACK1 lacks a PDZ binding motif at its carboxyl terminus. However, we speculate that RACK1 might express an internal motif that binds to the PDZ domains of NHERF1. Alternatively, NHERF1 might interact with RACK1 through non-PDZ motifs such as in its interaction with ezrin.[29]

How interaction between PKC-ε and RACK1 and between RACK1 and NHERF1 regulates CFTR function is not known. RACK1 has been implicated in some of the effects of PKC-ε; however, the intracellular signaling mechanism still must be determined.

Nevertheless, our studies suggest a model in which NHERF1 recruits a stable regulatory complex near CFTR specifically for regulation of CFTR function. A protein complex of activated PKC-ε bound to RACK1, which binds NHERF1, would support cAMP-dependent CFTR function. One can conjecture that inactivation of PKC-ε would free the enzyme from RACK1, possibly to bind to another scaffold or anchor protein with a subsequent loss of cAMP-dependent CFTR function. RACK1 might, as a consequence, dissociate from NHERF1 or alter NHERF1-CFTR interaction. Thus, PKC-ε may shift between anchor proteins depending on its activity state. The activity of PKC-ε may be an important determinant of its binding partner and phosphorylation state of its target protein as well as the functional status of CFTR.

Regulation of NKCC1 function in airway epithelial cells is a process as complex as regulation of CFTR function, involving a signaling cascade in which PKC-δ is a major effector enzyme.[2, 10] As reported for colonic epithelial cells,[14, 15] our studies show that inhibitors of actin integrity have marked effects on NKCC1 function. In addition, these studies provide new information on an association of actin with NKCC1 and PKC-δ characterized by co-localization of PKC-δ with F-actin cytoskeleton and avid binding of PKC-δ to non-muscle F-actin. As with our studies with PKC-ε, we analyzed the N- and C-terminal domains of PKC-δ for a possible site(s) of binding to F-actin. A C2-like domain, encoding a 123 amino acid segment of the N-terminus, shares properties with a similar domain in PKC-ε. A recombinant C2-like domain of PKC-δ (δC2 domain) blocks binding of PKC-δ to non-muscle F-actin and prevents activation of NKCC1 by a α_1-adrenergic agonist methoxamine. Binding occurs in the absence of phosphatidylserine, indicating that the δC2 domain lacks a recognition site for phosphatidylserine. Inhibition of NKCC1 activation appears to occur because the δC2 domain prevents binding of PKC-δ to F-actin. The δC2 domain lacks the Ca^{2+}-coordinating sequences characteristic of C2 domains in conventional Ca^{2+}-dependent PKC isotypes; hence, cannot bind Ca^{2+}. A C2 domain in conventional PKC isotypes such as PKC-α and PKC- functions as a membrane anchor that promotes translocation to other cellular compartments through the binding of Ca^{2+} and lipids. Our results point to a novel phospholipid-independent binding site for interaction of a δC2 domain with non-muscle F-actin. A δC2 domain also interacts with GAP-43 or neuromodulin[30] in the absence of phospholipid at a V0/C2 region comprising amino acids 1-121, which is referred to as δC2 domain in our study. These results and our new finding of binding of δC2 domain to non-muscle actin indicates that the δC2 domain is not just a target region for a PKC cofactor but serves as a protein-protein interaction domain.

These new findings indicate a unique signaling mechanism for activation of airway epithelial NKCC1; however, a mechanism explaining the regulatory role of actin is poorly understood. The F-actin cytoskeleton interacts with specific PKC isotypes in other cell types.[31] PKC isotypes can co-localize with a range of cytoskeletal proteins and components of the actin filaments.[32, 33] However, our data bring out unique differences in the role of actin in colonic T84 cells and airway epithelial cells. In colonic cells, cytochalsin D, which inhibits actin polymerization by increasing short actin filaments, increased NKCC1 activity.[14, 15] However, latrunculin-A, which sequesters G-actin monomers and prevents polymerization of actin, did not activate or inhibit NKCC1 but did prevent hormonal stimulation of NKCC1 activity in Calu-3 airway epithelial cells. Promoting actin polymerization using jasplakinolide increased baseline activity of Calu-3 NKCC1 but blocked cAMP-elicited Cl secretion and inhibited NKCC1 in T84 cells.[14, 15, 34] These contrasting results suggest that, unlike T84 colonic cells, short actin fibers do not

regulate airway epithelial NKCC1. The results also indicate that the polymerization state of non-muscle actin is an important determinant of PKC-δ binding. Despite differences in response to actin inhibitors, NKCC1 in both colonic and airway epithelial cell types depends on an intact and dynamic actin cytoskeleton for proper regulation.

Table 1. Differential Regulation of Epithelial Cl Transporters

	CFTR	NKCC1
Localization	Apical	Basolateral
Receptor activation	β-Adrenergic	α-Adrenergic
G-protein dependence	Yes	Yes
Intracellular Mediator	cAMP	Diacylglycerol
Effector enzyme	PKA	PKC-δ
Non-receptor requirement	PKC-ε	PKC-δ
Non-receptor acivation	Phorbol ester	Hyperosmotic stress Phorbol ester
PKC targeting proteins	RACK1	F-actin
Site on PKC	C2-like domain	C2-like domain
Site on binding partner	VI^{th} WD repeat	----------

Our findings also indicate localization of at least part of the cellular PKC-δ to a specific site, the actin cytoskeleton. Subcellular localization of PKC isotypes offers advantages to epithelial cells. One is the placement of inactive PKC isotypes near their target substrates to ensure preferential and rapid phosphorylation on activation. The primary function of actin-PKC-δ binding in Calu-3 cells is not yet clear. Binding may bring PKC-δ near its substrate or near protein kinases and phosphatases which regulate its activity. Another possibility is that activated PKC-δ stabilizes the F-actin cytoskeleton, thus promoting activation of NKCC1. Because the overall result of activation of PKC-δ is rapid stimulation of NKCC1, the positioning of PKC-δ near its substrate would be advantageous for fidelity and specificity in the regulation of NKCC1 function.

Table 1 summarizes the results of our research on NKCC1 and CFTR and their regulation by PKC isotypes in airway epithelial cells. There are still many gaps in our understanding of the signaling mechanism. Important questions arise as to the kinases involved in the phosphorylation steps necessary to activate the PKC isotypes and whether activation leads to translocation from one scaffold protein to another or involves membrane lipids or subcellular organelles and vesicles. Clearly, there is fertile ground for future research.

5. ACKNOWLEDGMENTS

The author thanks Mr. Thomas S. Cole, Melinda Hubbard, Denise Hatalya and Xiangyun Wang for their technical expertise. The research was supported by grants from the National Institutes of Health, HL-58598, HL 67190 and DK 27651, and by a Cystic Fibrosis Foundation Research Development Program. Peptides were synthesized by the Molecular Biotechnology Core Facility of the Cleveland Clinic Institute (Cleveland, OH).

6. REFERENCES

1. C.M. Liedtke, T. Cole, and M. Ikebe, Differential activation of PKC-δ and PKC-ζ by α_1-adrenergic stimulation in human airway epithelial cells, *Am. J. Physiol. Cell Physiol*. **273**,C937-C943 (1997)**.**
2. C.M. Liedtke and T. Cole, Antisense oligodeoxynucleotide to PKCδ blocks α_1-adrenergic activation of Na-K-2Cl cotransport, *Am. J. Physiol. Cell Physiol.* **273**,C1632-C1640 (1997).
3. Y. Jia , C.J. Mathews, and J.W. Hanrahan, Phosphorylation by protein kinase C is required for acute activation of cystic fibrosis transmembrane conductance regulator by protein kinase A, *J. Biol. Chem*. **272**,4978-4984 (1997).
4. L.M. Middleton and R.D. Harvey, PKC regulation of cardiac CFTR Cl^- channel function in guinea pig ventricular myocytes, *Am. J. Physiol. Cell Physiol*. **275**,C293-C302 (1998).
5. C.M. Liedtke and T. Cole, Antisense oligodeoxynucleotide to PKC-ε alters cAMP-dependent stimulation of CFTR in Calu-3 cells, *Am. J. Physiol. Cell Physiol*. **275**:C1357-C1364 (1998).
6. R.V. Schillace and J.D. Scott, Organization of kinases, phosphatases, and receptor signaling complexes, *J. Clin. Invest*. **103**, 761-765 (1999).
7. S. Jaken and P.J. Parker, Protein kinase C binding partners, *BioEssays* **22**,245-254 (2000).
8. D. Mochly-Rosen and A.S. Gordon, Anchoring proteins for protein kinase C: a means for isozyme selectivity*, FASEB J.* **12**, 35-42 (1998).
9. C.M. Liedtke, D. Cody, and T.S. Cole, Differential regulation of Cl transport proteins by PKC in Calu-3 cells*, Am. J. Physiol. Lung Cell. Molec. Physiol*., **280**, L739-L747 (2001).
10. C.M. Liedtke, R. Papay , and T.S. Cole, Modulation of Na/K/2Cl cotransport by intracellular Cl and protein kinase C-δ in Calu-3 cells, *Am. J. Physiol Lung Cell. Mole. Physiol.* **282**,L1151-L1159 (2002).
11. C.M. Liedtke, C.H.C. Yun, N. Kyle, and D. Wang, PKC-ε dependent regulation of CFTR involves binding to RACK1, a Receptor for Activated C Kinase, and RACK1 binding to NHERF, *J. Biol. Chem*. **277**,22925-22933 (2002).
12. C.M. Liedtke, M. Hubbard, and X. Wang, Stability of actin cytoskeleton and PKC-δ binding to actin regulate NKCC1 function in airway epithelial cells, *Am. J. Physiol. Cell. Physiol*. **284**,C487-C496 (2003).
13. L.C. D'Andrea, C. Lytle, J.B. Matthews, P. Hofman, B. Forbush III, and J.L. Madara, Na/K/2Cl cotransporter protein of intestinal epithelial cells: surface distribution, immunoprecipitation as a protein complex and surface expression in response to cAMP, *J. Bio.l Chem.* **271**,28969-28976 (1996).
14. J.B. Matthews, J.A. Smith, and B.J. Hrnjez, Effects of F-actin stabilization or disassembly on epithelial Cl^- secretion and Na-K-2Cl cotransport, *Am. J. Physiol. Cell Physiol.* **272**,C254-C262 (1997).
15. J.B. Matthews, J.A. Smith, E.C. Mun, and J.K. Sicklick, Osmotic regulation of intestinal epithelial Na-K-Cl cotransport: role of Cl and F-actin, *Am. J. Physiol. Cell. Physiol*. **274**,C697-C706 (1998).
16. J.C. Song, B.J. Hrnjez, O.C. Farokhzad, and J.B. Matthews, PKC-ε regulates basolateral endocytosis in human intesinal epithelia: role of F-actin and MARCKS, Am. J. Physiol. Cell Physiol. **277,**C1239-C1249 (1999).
17. I. Spector, F. Braet, N.R. Shochet, and M.R. Bubb, New anti-actin drugs in the study of the organization and function of the actin cytoskeleton, *Microscopy Res. Technique* **47,**18-37 (1999).
18. J.A. Johnson, M.O. Gray, H.-H. Chen, and D. Mochly-Rosen. A protein kinase C translocation inhibitor as an isozyme-selective antagonist of cardiac function, *J. Biol. Chem*. **271**,24962-24966 (1996).
19. G. Lopez-Lluch, M.M. Bird, B. Canas, J. Godovac-Zimmerman, A. Ridley, A.W. Segala and L.V. Dekker, Protein kinase C-δ C2-like domain is a binding site for actin and enables actin redistribution in neutrophils, *Biochem. J.* **357**,39-57 (2001).
20. D. Ron, C.H. Chen, J. Caldwell, L. Jamieson, E. Orr, and D. Mochly-Rosen, Cloning of the intracellular receptor for protein kinase C: a homolog of the β subunits of G proteins, *Proc. Natl. Acad. Sci. USA* 91,839-843 (1994).
21. M. Csukai, C.-H. Chen, M.A. De Matteis, and D. Mochly-Rosen, The coatomer protein β'-COP, a selective binding protein (RACK) for protein kinase Cε, *J. Biol. Chem*. **272**,29200-29206 (1997).
22. D.B. Short, K.W. Trotter, D. Reczek, S.M. Kreda, A. Bretscher, R.C. Boucher, M.J. Stutts, and S.L. Milgram, An apical PDZ protein anchors the cystic fibrosis transmembrane conductance regulator to the cytoskeleton, *J. Biol. Chem*. **273**,19797-19801 (1998).
23. S.S. Wang, R.W. Raab, W.B. Guggino, and M. Li, *FEBS Lett*. Peptide binding consensus of the NHE-RF-PDZ1 domain matches the C-terminal sequence of cystic fibrosis transmembrane conductance regulator (CFTR), *FEBS Lett.* **427**, 103-108 (1998)
24. V. Raghuram, D.-O.D. Mak, and J.K. Foskett, Regulation of cystic fibrosis transmembrane conductance regulator single-channel gating by bivalent PDZ-domain-mediated interaction. *Proc. Natl. Acad. Sci. USA* **98**,1300-1305 (2001).

25. R.A. Hall, L.S. Ostedgaard, R.T. Premont, J.T. Blitzer, N. Rahman, M.J. Welsh, and R.J. Lefkowitz, A C-terminal motif found in the $_2$-adrenergic receptor, P2Y1 receptor and cystic fibrosis transmembrane conductance regulator determines binding to the Na^+/H^+ exchanger regulatory factor family of PDZ proteins, *Proc. Natl. Acad. Sci. USA* **95**,8496-8501 (1998).
26. W. Ahn, K.H. Kim, J.A. Lee, J.Y. Kim, J.Y. Choi, O.W. Moe, S.L. Milgram, S. Muallem, and M.G. Lee, Regulatory interaction between the cystic fibrosis transmembrane conductance regulator and CHO3-salvage mechanisms in model systems and the mouse pancreatic duct, *J. Biol. Chem*. **276**,17236-17243 (2001).
27. K. Kunzelmann, G.L. Kiser, R. Schreiber, and J.R. Riordan, Inhibition of epithelial Na^+ currents by intracellular domains of the cystic fibrosis transmembrane conductance regulator, *FEBS Lett*. 400,341-344 (1997).
28. B.D. Moyer, J. Denton, K.H. Karlson, G.R. Reynolds, W.B. Guggino, M. Li, and B.A. Stanton, A PDZ-interacting domain in CFTR is an apical membrane polarization signal, *J. Clin. Invest*. **104**,1353-1361 (1999).
29. D. Reczer, M. Berryman, and A. Bretscher, Identification of EBP50: a PDZ-containing phosphoprotein that associates with members of the ERM family. *J. Cell Biol*. **139**,169-179 (1997).
30. L.V. Dekker and P.J. Parker, Regulated binding of the protein kinase C substrate GAP-43 to the V0/C2 region of protein kinase C-δ, *J. Biol. Chem*. **272**,12747-12753, (1997).
31. C. Keenan and D. Kelleher, Protein kinase C and the cytoskeleton, *Cell Signal*. **10**:225-232 (1998).
32. B. Chasan, N.A. Geisse, K. Pedatella, D.G. Wooster, M. Teintze, M.D. Carattino, W.H. Goldmann, and H.F. Cantiello, Evidence for direct interaction between actin and the cystic fibrosis transmembrane conductance regulator, *Eur. Biophys. J*. **30**,617-624 (2002).
33. R. Prekeris, M.W. Mayhew, J.B. Cooper, and D.M. Terrian, Identification and localization of an actin-binding motif that is unique to the epsilon isoform of protein kinase C and participates in the regulation of synaptic function, *J. Cell Biol*. **132**,77-90 (1996).
34. J.C. Song, B.J. Hrnjez, O.C. Farokhzad, and J.B. Matthews, PKC-ε regulates basolateral endocytosis in human intestinal epithelia: Role of F-actin and MARCKS, *Am. J. Physiol. Cell Physiol*. **277**,C1239 C1249, (1999).

33

THE ROLE OF THE PHOSPHOINOSITIDE PATHWAY IN HORMONAL REGULATION OF THE EPITHELIAL SODIUM CHANNEL

Bonnie L. Blazer-Yost and Charity Nofziger*

1. INTRODUCTION

The phosphoinositide (PI) pathway, initiated by the activation of phosphatidylinositol 3-kinase (PI3-kinase), forms a complex, branching signal transduction mechanism involving multiple lipids and protein kinases. This pathway has been implicated in the regulation of a wide variety of cellular processes including inhibition of apoptosis, stimulation of protein synthesis, cellular trafficking, actin rearrangement, and multiple transport processes. The pathway can be activated either by hormone dependent or independent signals and may be present in a constitutively active, tonic level in some cell types.

Our laboratory was the first to show that the PI pathway is crucial for both aldosterone (steroid) and insulin (peptide) hormone stimulation of renal Na^+ reabsorption.[1-3] Subsequent work by us and others have solidified the importance of several of the components of the pathway in the natriferic (Na^+ retaining) actions of the hormones.

2. THE AMILORIDE-SENSITIVE Na^+ CHANNEL

Epithelial Na^+ channels (ENaCs) are intimately involved in fluid and electrolyte homeostasis. These amiloride-sensitive channels are found in the apical membrane of a variety of salt-absorbing epithelia and form the rate-limiting step for Na^+ reabsorption. The importance of this channel in regulating Na^+ homeostasis is underscored by the number of steroid and peptide hormones which directly modulate channel activity *in vivo*, including aldosterone, insulin, ADH (anti-diuretic hormone), and IGF1 (insulin-like growth factor 1).[1-8]

The primary components of the channel have been described at a molecular level.[9-11]

* Bonnie L. Blazer-Yost and Charity Nofziger, Biology Dept., Indiana University Purdue University at Indianapolis, Indianapolis, Indiana, 46202.

The basic building blocks consist of homologous subunits termed α, β, and γ. α is required and sufficient for transport albeit at a low level.[9, 11] In the oocyte expression system, neither the β nor γ subunit alone can confer Na^+ transport to the oocyte. However, co-expression of all three subunits leads to a 10-100 fold increase in transport as compared to rates of transport seen with the expression of α alone.[10]

Clinically, mutations in the C-terminal region of the β or γ subunit can cause Liddles syndrome, a severe form of hypertension resulting from constitutive activation of the renal ENaC.[12, 13] Mutations in α as well as amino acid substitutions in either the cytoplasmic N-terminal portion of β or the extracellular region of γ result in pseudohypoaldosteronism type 1, characterized by renal salt wasting and hyperkalemic metabolic acidosis due to loss of channel activity.[14-16] These clinical observations support the principle that ENaC is crucial for regulation of salt and water homeostasis and that mutations in the channel, particularly in the cytoplasmic domains, cause serious disturbances in the maintenance of this delicate balance.

One of the most common clinical entities arising from an imbalance of salt and water homeostasis is essential hypertension. Based on the findings of the most recent National Health and Nutrition Examination Survey (NHANES) collected from 1999-2000, 28.7% of the U.S. adult population had hypertension.[17] This is an alarming increase compared to the NHANES study from 1988 through 1991 which indicated 24% of adults had hypertension.[18] The development of essential hypertension is a multifactorial pathogenic process. Clearly, there are both genetic and environmental influences. However, many of the predisposing factors, e.g., aberrations in the renin-angiotensin-aldosterone axis; hyperinsulinemia, have the common result of stimulating Na^+ reabsorption in the renal distal tubule/collecting duct via a direct effect on the ENaC. Understanding the regulatory mechanisms controlling ENaC activity is, therefore, an essential prerequisite to designing therapeutic modalities aimed at controlling disturbances in fluid and electrolyte balance such as hypertension.

3. HORMONAL REGULATION OF ENaC

The three hormonal systems that regulate ENaC activity in the principal cells of the distal nephron—aldosterone, insulin, and ADH—have additive or synergistic actions, one to another, on the Na^+ reabsorptive transport process. Therefore, it follows that there are individual and distinct rate-limiting steps between receptor binding and channel activation.

Renal Na^+ retention can be attained by increasing the density of active ENaCs in the apical membrane, by increasing the open probability of individual channels, or by altering single channel current. In all studies to date, the single channel current appears to vary according to the electrochemical driving forces across the apical membrane rather than in response to direct hormonal stimulation. Interestingly, using blocker-induced noise analysis, we have found that both insulin and aldosterone cause an increase in the number of active channels in the apical membrane with no increase in the open probability of the channel.[2, 6] Previous noise analysis studies by Els and Helman have shown that the action of ADH also involves an increase in the number of active channels in the apical membrane.[19] These studies are in direct contrast to those using patch clamp techniques where investigators have found an increase in open probability in response to both

insulin and aldosterone.[20, 21] Reasons for this discrepancy are not immediately obvious, although, there may be some contribution from the invasive nature of the patch clamp technique.

In order to resolve the controversy, we stably transfected green fluorescent protein (GFP)-tagged ENaC subunits into model renal epithelial cells and demonstrated that the labeled channels were indeed functional.[8] Using the transfected lines, we were able to confirm, in the case of ADH and insulin, a movement of labeled channel from an internal pool into the apical plasma membrane, thus substantiating the noise analysis data.[2, 6, 8] The combined data provide strong support for the contention that the actions of all three hormones appear to culminate in the insertion of ENaC into the apical membrane. Therefore, the discriminating, rate-limiting steps in the various pathways are proximal to the insertion reaction.

4. PI3-KINASE

The PI3-kinases are a family of enzymes which phosphorylate the D-3 position of the *myo*-inositol ring of phosphatidylinositols (PtdIns) and according to relative specificity, form PI(3)P (phosphatidylinositol-3-phosphate), $PI(3,4)P_2$, or $PI(3,4,5)P_3$.[22-24] These kinases have been implicated as key regulatory components of a wide variety of cellular processes[25-32] including peptide stimulated ion transport events.[29-32]

With regard to transporters, PI3-kinase activity has been shown to be involved in insulin-stimulated insertion of vesicles containing glucose transporters (GLUT4) into the membranes of adipocytes[27] and skeletal muscle.[28] More recently, other peptide hormone-mediated transport events have been shown to be dependent on the production of PIP_3. These include insulin-stimulated K^+ uptake into fibroblasts via the $Na^+/K^+/2Cl^-$ cotransporter,[29] PDGF (platelet-derived growth factor) activation of the Na^+/H^+ exchanger,[30] EGF (epidermal growth factor) stimulation of intestinal Na^+ absorption,[31] and EGF-mediated inhibition of Ca^{2+}-dependent Cl^- secretion.[32]

We have previously identified PI3-kinase as a regulator of basal, aldosterone- and insulin-stimulated Na^+ flux.[1-3] Hormone induced increases in the enzyme activity have been demonstrated in model renal cell lines, and this heightened activity is directly correlated with changes in Na^+ transport. Thus, the phosphoinositide pathway appears to form a central control point in the regulation of both peptide- and steroid-mediated natriferic activity (Figure 1).

Specifically, in the A6 cell culture model of the principal cells of the distal nephron, we have shown that stimulation with either insulin or aldosterone results in an increase of PIP_3. In addition, basal, insulin-stimulated and aldosterone-stimulated Na^+ transport are all abolished by LY294002, a specific inhibitor of PI3-kinase.[1, 2] These results indicate that both hormones have an effect on the activity of the enzyme and that this stimulation of activity is necessary for insulin and aldosterone-stimulated Na^+ retention.

The insulin results were not unanticipated because this peptide hormone is known to activate PI3-kinase via the insulin receptor substrate (IRS) signaling intermediate in other tissues. However, the pathway stimulated in response to insulin binding in these polarized cells may be different than that described in non-polarized tissues. We have demonstrated that in response to insulin, ENaC moves from a diffuse cytoplasmic localization to the apical and lateral membranes. Co-localization studies have shown that ENaC and PI3-kinase are not co-localized under basal conditions. Rather, the two entities

co-localize and are mobilized along the lateral membrane within one minute of insulin stimulation.[3] These data indicate that insulin stimulates the migration of ENaC into the apical membrane and that this trafficking is dependent on PI3-kinase activity. The details of the trafficking pathway remain unresolved but will be of interest because they appear to be mediated by a heretofore undescribed trafficking route for integral membrane proteins in polarized epithelial cells.

Our results with regard to the importance of PI3-kinase in aldosterone's action were rather surprising. Steroid hormone regulation of ion transport had not been previously linked to the PI pathway. The aldosterone stimulated increase in PIP_3 indicates that there is a steroid hormone-stimulated event at or before PI3-kinase which may modify the amount and/or activity of the enzyme. The identification of this portion of the signaling pathway will be important as it is a likely site for the first rate-limiting step in aldosterone's natriferic action.

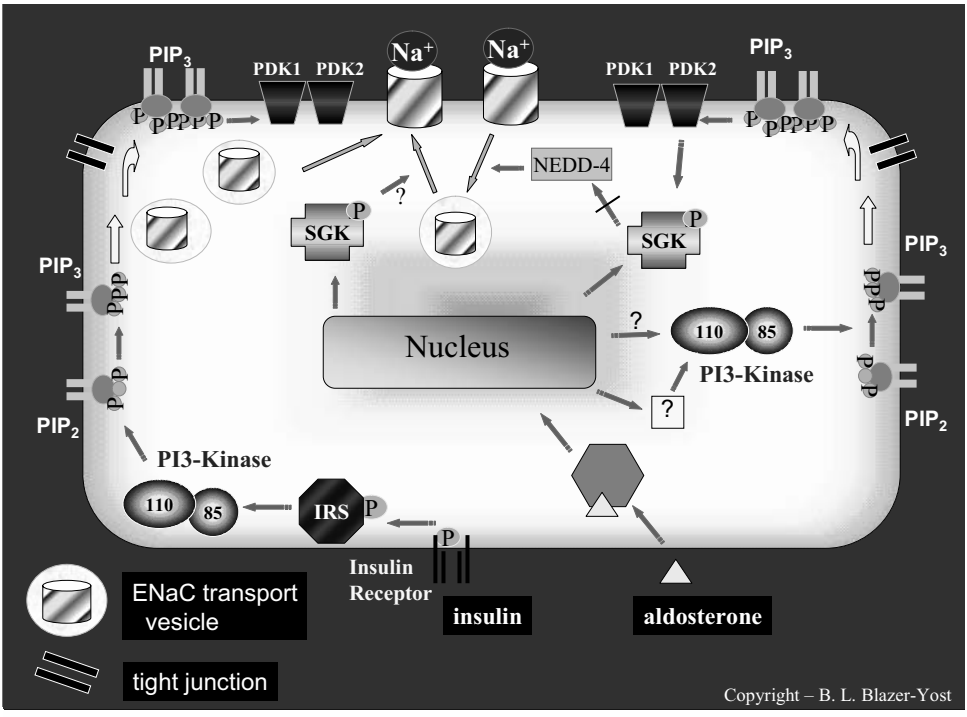

Figure 1: Working hypothesis of the signal transduction pathway followed by natriferic hormones which stimulate transcellular Na^+ transport in the principal cell of the mammalian distal nephron. This theoretical model reflects the pathways discussed in the text. ENaC = epithelial Na^+ channel; IRS = insulin receptor substrate; PIP_2 = phosphatidylinositol-4,5-bisphosphate; PIP_3 = phosphatidylinositol-3,4,5-trisphosphate; sgk = serum, glucocorticoid-induced kinase; PDK = phosphatidylinositide-dependent kinase; NEDD-4 = neuronal precursor cell developmentally downregulated gene 4.

PI3-kinase-mediated phosphorylation of the inositol headgroup of PIP_2 stimulates the activity of the serine/threonine kinases, phosphoinositide-dependent kinases (PDK) 1 and 2.[33, 34] There are a number of substrates for the PDKs which have been identified. Several have been shown to be involved in transport events, particularly Akt (related to A and C kinase) also known as PKB (protein kinase B),[33, 34] PKA (cAMP-dependent protein kinase A)[5] and sgk (serum, glucocorticoid induced kinase).[36, 37] Of these, sgk has been shown to be a crucial regulatory component in hormone-stimulated Na^+ transport.

5. SGK

Sgk, Akt and PKA all belong to the same "family" of serine/threonine kinases linked by a structural similarity in the kinase domain, particularly the activation loop. Within the activation loop, PDK1 phosphorylation of a key threonine residue is necessary for enzyme activation. The particular motif defining the single PDK1 phosphorylation site is common to these three serine/threonine kinases.[3, 35-37] Phosphorylation of these substrates by PDK2 on a serine residue outside the activation loop appears to have a permissive effect on activity.

Of the PDK substrates, sgk is potentially the most interesting because it has been shown to be an aldosterone-induced protein in A6 epithelia[38] and rat cortical collecting ducts.[39] This kinase is regulated by multiple factors including serum, steroid hormones and cell volume changes. When the mRNAs for sgk and ENaC are co-expressed in oocytes, the ENaC activity is potentiated several-fold.[38, 39]

It has been demonstrated that sgk does not phosphorylate the channel *per se.* Interestingly, however, one of the substrates for the enzyme is an ENaC regulatory protein, a ubiquitin ligase termed Nedd4-2 (neural precursor cell-expressed, developmentally downregulated gene 4, isoform 2).[40-42] Nedd4-2 has been shown to be an ENaC partner in a two hybrid system.[41] The ubiquitin ligase contains WWW domains which bind the highly conserved proline-rich PY (proline-tyrosine) motifs in the carboxyl termini of ENaC subunits. In the kidney, Nedd4-2 has been immunolocalized to the cortical collecting tubules and outer and inner medullary collecting ducts.[42] Nedd4-2 appears to be a negative regulator of ENaC which ubiquitinates the channel, thereby targeting it for endocytosis and, presumably, degradation. Sgk phosphorylation of Nedd4-2 inhibits the binding of this ubiquitin ligase to the channel, resulting in increased channel expression in the apical membrane.[40, 43-45] While expression of Nedd4-2 is not altered by elevations of serum aldosterone,[42] sgk which can negatively modulate its activity is an aldosterone-induced protein. The role of sgk in this portion of the pathway could be envisioned as an inhibitor of the "turn-off" mechanism of aldosterone's action.

It is possible that sgk may play additional roles in the natriferic action of both steroid and peptide hormones. In native, Na^+ transporting epithelial cells (A6 cell line), we have supplemented the endogenous sgk by stably transfecting with either wt or mutated enzyme and have used the resultant cell lines to show that sgk plays a role in basal as well as insulin-, ADH- and aldosterone-stimulated Na^+ transport.[46] The enzyme is required for basal and hormone-stimulated transport; a dominant negative form of the kinase abolishes all transepithelial Na^+ flux. Expression of additional wt sgk results in a potentiated response to ADH indicating that the enzyme is rate-limiting for this natriferic response. In contrast, the enzyme, while necessary, does not appear to be rate-limiting for insulin- or aldosterone-stimulated Na^+ transport.[46] These studies are in agreement with a

mouse sgk knock-out model demonstrating a milder phenotype than the corresponding ENaC or mineralocorticoid receptor knockout animals.[47]

Our results from the transfection studies have been substantiated by others who have reached the similar conclusion that sgk may also play a role in the initial steps of hormonal stimulation, possibly by mediating channel insertion into the membrane.[48] In the search for a mechanism of the action of sgk in the initial steps of Na^+ channel activation, several intriguing clues have emerged. Alvarez de la Rosa and colleagues have found that in rat kidney, sgk1, the predominant isoform of the distal tubular cells, is expressed in relatively high amounts under basal conditions with little fluctuation in response to physiological concentrations of aldosterone.[49]Sgk, a protein with no membrane spanning domains, was found associated with the microsomal fraction in tissue homogenates. Furthermore, sgk co-localized with Na^+,K^+-ATPase in immunohistochemical studies.[49] These results suggest that sgk may be part of a complex found predominately on the basolateral membrane rather than on the apical membrane where sgk would be localized to regulate the ENaC/Nedd4-2 interaction.

As noted above, we have recently found that within one minute of insulin stimulation, ENaC moves first to the vicinity of the lateral membranes where it co-localizes with PI3-kinase, an enzyme that initiates a kinase cascade which can result in the activation of sgk. Subsequently, the ENaC enters the apical membrane. If the activity of PI3-kinase is inhibited with LY294002, ENaC and PI3-kinase still undergo an insulin-mediated co-localization but are not trafficked to the lateral membrane, and ENaC does not enter the apical membrane.[3] Given the sgk localization results cited above, it could be speculated that the entire PI pathway may be assembled in a complex close to the basolaterally-located peptide hormone receptors which initiate the natriferic signal. Confirmation of this speculation awaits experimental verification.

6. INTERACTION BETWEEN THE PHOSPHOINOSITIDE AND cAMP/PKA PATHWAYS

Biochemical pathways besides the PI pathway are capable of modulating changes in Na^+ reabsorption via ENaC. For example, ADH stimulates the cAMP/PKA signaling cascade via binding to a V2 receptor on the basolateral membrane of renal epithelial cells, thereby stimulating adenylate cyclase and the production of cAMP. The increased cAMP in turn activates PKA. The end result of the hormone-receptor binding is a decrease in Na^+ excretion but the post-PKA activation steps of the pathway remain unknown.

As cited above, sgk appears to be the rate-limiting step in ADH-mediated Na^+ reabsorption.[46] Therefore, it is likely that the cAMP and PI pathways intersect. There are several plausible sites for this potential interaction. PKA and sgk are each substrates for PDK1 and 2.[50, 51] Thus, PKA could theoretically be modulated by the PI pathway in the absence of cAMP induction.

Alternatively, in the absence of PI3-kinase, the PKA pathway may activate downstream elements of the PI pathway. Sgk contains a PKA consensus sequence and Perrotti et al., have shown that 8-(4-chlorophenylthio)-cAMP caused a two-fold activation of sgk expressed in COS7 cells,[52] indicating that cAMP can regulate sgk independently of PI3-kinase. This would be consistent with our observations that stimulation of A6 cells with ADH leads to an apparent potentiated response (measured as an increase in transport) if the PI3-kinase pathway has been inhibited by LY294002.[53]

One possible explanation for this finding is that the increased PKA activity could restore the sgk activity.

PKA and sgk can also phosphorylate the same substrate. Both kinases have been shown to regulate the ROMK channel, a K^+ leak channel activated in response to aldosterone stimulation, thereby causing it to be redistributed from the endoplasmic reticulum to the plasmolemma.[54] Based on the latter findings, it would be reasonable to postulate that sgk and PKA may act on a novel, common substrate upstream of ENaC.

Clearly, the cAMP/PKA and PI pathways intersect. In model renal epithelial cells, both pathways regulate transepithelial Na^+ transport. Determining the site(s) of such complex interactions will require a melding of biochemical, electrophysiological, molecular and histological approaches.

7. SUMMARY

In summary, insulin and aldosterone stimulate phosphatidylinositol phosphorylation, thus indicating the existence of a regulated protein at or before the PI3-kinase step.[1-5] Aldosterone induces the synthesis of sgk, a downstream element of the PI pathway. Sgk is necessary, but not rate-limiting, for aldosterone- and insulin-stimulated Na^+ transport. However, the enzyme appears to be rate-limiting for the natriferic action of ADH. Insulin-stimulated Na^+ transport, an acute response, is dependent on PI3-kinase activity but the magnitude of the response is not altered by a cellular excess of sgk. ADH-stimulated transport is not dependent on PI3-kinase but is potentiated by an excess of sgk. The foregoing data indicate that the PI pathway is involved in several steps of the natriferic action of hormones and intersects with other pathways which regulate ENaC. Furthermore, the data are consistent with the hypothesis that activation of PI3-kinase may ultimately stimulate channel insertion as well as regulate channel endocytosis. Both of these phenomena can result in an increase of ENaC-mediated Na^+ transport.

8. REFERENCES

1. R.D. Record, L.L. Froelich, C.J. Vlahos and B.L. Blazer-Yost, Phosphatidylinositol 3-kinase activation is required for insulin-stimulated sodium transport in A6 cells, *Am. J. Physiol. Endocrinol. Metab*. **274**,E611-617 (1998).
2. B.L. Blazer-Yost, T.G. Paunescu, S.I. Helman, K.D. Lee and C.J. Vlahos, Phosphoinositide 3-kinase is required for aldosterone regulated sodium reabsorption, *Am. J. Physiol. Cell Physiol.* **277**, C531-536 (1999).
3. B.L. Blazer-Yost, M.A. Esterman and C.J. Vlahos, Insulin-stimulated trafficking of ENaC in renal cells requires PI 3-kinase activity, *Am. J. Physiol. Cell Physiol.* **284**, C1645-1653 (2003).
4. B.L. Blazer-Yost, M. Cox, and R. Furlanetto. Insulin and IGF1 receptor-mediated Na^+ transport in toad urinary bladders, *Am. J. Physiol. Cell Physiol.* **257**, C612-620 (1989).
5. R.D. Record, M. Johnson, S. Lee and B.L. Blazer-Yost, Aldosterone and insulin stimulate amiloride-sensitive sodium transport in A6 cells by additive mechanisms, *Am. J. Physiol Cell Physiol*. **271**, C1079-1084 (1996).
6. B.L. Blazer-Yost, X. Liu and S.I. Helman, Hormonal regulation of ENaCs: Insulin and aldosterone, *Am. J. Physiol. Cell Physiol.* **274**, C1373-C1379 (1998).
7. B.L. Blazer-Yost, Y. Fesseha and M. Cox, Aldosterone-mediated Na^+ transport in renal epithelia: Time-course of induction of a potential regulatory component of the conductive Na^+ channel, *Biochem. Intern.* **26**, 887-897 (1992).
8. B.L. Blazer-Yost, M. Butterworth, A.D. Hartman, G.E. Parker, C.J. Faletti, W.J. Els and S.J. Rhodes, Characterization and imaging of A6 epithelial cell clones expressing fluorescently labeled ENaC subunits,

Am. J. Physiol. Cell. Physiol. **281**, C624-632 (2001).
9. C.M. Canessa, J.-D. Horisberger and B.C. Rossier, Epithelial sodium channel related to proteins involved in neurodegeneration, *Nature* **36**, 467-470 (1993).
10. C.M. Canessa, L. Schild, G. Buell, B. Thorens, I. Gautschi, J.-D. Horisberger and B.C. Rossier Amiloride-sensitive epithelial Na^+ channel is made of three homologous subunits, *Nature* **367**, 463-466 (1994).
11. E.N. Lingueglia, Voilley, R. Waldmann, M. Lazdunski and P. Barbry, Expression cloning of an epithelial amiloride-sensitive Na^+ channel: A new channel type with homologies to Caenorhabditis elegans degenerins, *FEBS Lett*. **318**, 95-99 (1993).
12. J.H. Hanson, C. Nelson-Williams, H. Suzuki, L. Schild, R. Shimkets, Y. Lu, C. Canessa, T. Iwasaki, B. Rossier and R.P. Lifton, Hypertension caused by a truncated epithelial sodium channel subunit: genetic heterogeneity of Liddles syndrome, *Nature Genet*. **11**, 76-82 (1995).
13. R.A. Shimkets, D.G. Warnock, C.M. Bositis, C. Nelson-Williams, J.H. Hanson, M. Schambelan, J.R. Gill, Jr., S. Ulick, R.V. Milora, J.W. Findling, C.M. Canessa, B.C. Rossier and R.P. Lifton, Liddle's syndrome: Heritable human hypertension caused by mutations in the. subunit of the epithelial sodium channel, *Cell* **79**, 407-414 (1994).
14. S.S. Chang, S. Grunder, A. Hanukoglu, A. Rösler, P.M. Mathew, I. Hanukoglu, L. Schild, Y. Lu, R.A. Shimkets, C. Nelson-Williams, B.C. Rossier and R.P. Lifton, Mutations in subunits of the epithelial sodium channel cause salt wasting with hyperkalaemic acidosis, pseudohypoaldosteronism type 1, *Nature Genet*. **12**, 248-253 (1996).
15. S.D. Gründer, Firsov, S.S. Chang, N.F. Jaeger, I. Gautschi, L. Schild and B.C. Rossier, A mutation causing pseudohypoaldosteronism type 1 identifies a conserved glycine that is involved in the gating of the epithelial sodium channel, *EMBO J.* **16**, 899-907 (1997).
16. S. S. Strautnieks, R. J. Thompson, R. M. Gardiner and E. Chung, A novel splice-site mutation in the subunit of the epithelial sodium channel gene in three pseudohypoaldosteronism type 1 families, *Nature Genet*. **13**, 248-250 (1996).
17. I. Hajjar and T.A. Kotchen, Trends in prevalence, awarness, treatment and control of hypertension in the United States, 1988-2000, *JAMA* **290**, 199-206 (2003).
18. V.L. Burt, P. Whelton, E.J. Roccella, C. Brown, J.A. Cutler, M. Higgins, M.J. Horan and D. Labar, The prevalence of hypertension in the US adult population, *Hypertens*. **25**, 305-313 (1995).
19. W.J. Els and S.I.. Helman, Regulation of epithelial sodium channel densities by vasopressin signaling, *Cellul. Signal.* **1**, 533-539 (1989).
20. Y. Marunaka, N. Hagiwara and H. Toda, Insulin activates single amiloride-blockable Na channels in a distal nephron cell line (A6), *Am. J. Physiol. Renal Fluid Electrolyte Physiol*. **263**, F392-F400 (1992).
21. A.E. Kemendy, T.R. Kleyman and D.C. Eaton, Aldosterone alters the open probability of amiloride-blockable sodium channels in A6 epithelia, *Am J. Physiol. Cell Physiol*. **263**, C825-C837 (1992).
22. G.D. Holman and M. Kasuga, From receptor to transporter: insulin signaling to glucose transport, *Diabetol*. **40**, 991-1003 (1997).
23. P.R. Shepherd, B.T. Nave and S. O'Rahilly, The role of phosphoinositide 3-kinase in insulin signaling, *J. Mol. Endocrin.* **17**, 175-184 (1996).
24. A. Toker and L.C. Cantly, Signaling through the lipid products of phosphoinositide-3-OH kinase, *Nature* **387**, 673-676 (1997).
25. L. del Peso, M. Gonzalez-Garcia, C. Page, R. Herrera and G. Nunez, Interleukin-3-induced phosphorylation of BAD through the protein kinase Akt, *Science* **278**, 687-689 (1997).
26. B.M. Marte and J. Downward, PKB/Akt: connecting phosphoinositide 3-kinase to cell survival and beyond, *Trends in Biol. Sci.* **22**, 355-358 (1997).
27. B. Cheatham, C.J. Vlahos, L. Cheatham, L. Wang, J. Blenis and C.R. Kahn, Phosphatidylinositol 3-kinase activation is required for insulin stimulation of pp70 S6 kinase, DNA synthesis, and glucose transporter translocation, *Mol. Cell. Biol*. **14**, 4902-4911 (1994).
28. J.I. Yeh, E.A. Gulve, L. Rameh and M.J. Birnbaum, The effects of wortmannin on rat skeletal muscle, *J. Biol. Chem.* **270**, 2107-2111 (1995).
29. G. Sweeney, R. Somwar, T. Ramlal, P. Martin-Vasallo and A. Klip, Insulin stimulation of K^+ uptake into 3T3-L1 fibroblasts involves phosphatidylinositol 3-kinase and protein kinase C-zeta, *Diabetologia* **41**, 1199-1204 (1998).
30. Y.H. Ma, H.P. Reusch, E. Wilson, J.A. Escobedo, W.J. Fantl, L.T. Williams and H.E. Ives, Activation of Na^+/H^+ exchange by platelet-derived growth factor involves phosphatidylinositol 3-kinase and phosphor-lipase C gamma, *J. Biol. Chem.* **269**, 30734-30739 (1994).
31. S. Khurana, S.K. Nath, S. A. Levine, J. M. Bowser, C. Tse, M. E. Cohen and M. Donowitz, Brush border phosphatidylinositol 3-kinase mediates epidermal growth factor stimulation of intestinal NaCl absorption and $Na^{+/}H^+$ exchange, *J. Biol. Chem*. **271**, 9919-9927 (1996).
32. J.M. Uribe, S.J. Keely, A E. Traynor-Kaplan and K.E. Barrett, Phosphatidylinositol 3-kinase mediates the

inhibitory effect of epidermal growth factor on calcium-dependent chloride secretion, *J. Biol. Chem.* **271**, 26588-26595 (1996).

33. D.R. Alessi, S.R. James, C.P. Downes, A.B. Holmes, P.R., Gaffney, C.B. Reese and P. Cohen, Characterization of a 3-phosphoinositide-dependent protein kinase which phosphorylates and activates protein kinase Bα, *Curr. Biol*. **7**, 261-269 (1997).
34. D. Stokoe, L.R. Stephens, T. Copeland, P.R. Gaffney, C.B. Reese, G.F. Painter, A.B. Holmes, F. McCormick and P.T. Hawkins, Dual role of phosphatidylinositol-3,4,5,-trisphosphate in the activation of protein kinase B, *Science* **277**, 567-570 (1997).
35. X. Cheng, Y. Ma, M. Moore, B.A. Hemmings and S.S. Taylor, Phosphorylation and activation of cAMP-dependent protein kinase by phosphoinositide-dependent protein kinase*, Proc. Natl. Acad. Sci. USA.* **95**, 9849-9854 (1998).
36. T. Kobayashi and P. Cohen, Activation of serum- and glucocorticoid-regulated protein kinase by agonists that activate phosphatidylinositol 3-kinase is mediated by 3-phosphoinositide-dependent protein kinase-1 (PDK1) and PDK2, *Biochem. J*. **339**, 319-328 (1999).
37. J. Park, M.L.L. Leong, P. Buse, A.C. Maiyar, G.L. Firestone and B.A. Hemmings, Serum and glucocorticoid-inducible kinase (SGK) is a target of the PI 3-kinase-stimulated signaling pathway, *EMBO J.* **18**, 3024-3033 (1999).
38. S. Y. Chen, A. Bhargava, L. Mastroberardino, O.C. Meijer, J. Wang, P. Buse, G.L. Firestone, F. Verrey and D. Pearce, Epithelial sodium channel regulated by aldosterone-induced protein sgk, *Proc. Natl. Acad. Sci. USA* **96**, 2514-2519 (1999).
39. A. Naray-Fejes-Toth, C. Canessa, E.S. Cleaveland, G. Aldrich and G. Fejes-Toth, sgk is an aldosterone-induced kinase in the renal collecting duct, *J. Biol. Chem*. **274**, 16973-16978 (1999).
40. E. Kamynina and O. Staub, Concerted action of ENaC, Nedd4-2 and Sgk1 in transepithelial Na^+ transport. *Am. J. Physiol. Renal Physiol*, **283**, F377-F387 (2002).
41. O. Staub, S. Dho, P.C. Henry, J. Correa, T. Ishikawa, J. McGlade and D. Rotin, WWW domains of Nedd4 bind to the proline rich PY motifs in the epithelial Na^+ channel deleted in Liddle's syndrome, *EMBO J*. **15**, 2371-2380 (1996).
42. O. Staub, H. Yeger, P.J. Plant, H. Kim, S.A. Ernst and D. Rotin, Immunolocalization of the ubiquitin-protein ligase Nedd4 in tissues expressing the epithelial sodium channel (ENaC*)*, *Am. J. Physiol. Cell Physiol.* **272**, C1871-C1880 (1997).
43. C. Debonneville, S.Y. Flores, E. Kamynina, P.J. Plant, C. Tauxe, M.A. Thomas, C. Munster, A. Chraibi, J.H. Pratt, J-D. Horisberger, D. Pearce, J. Loffing and O. Staub, Phosphorylation of Nedd4-2 by Sgk1 regulates epithelial Na^+ channel cell surface expression, *The EMBO J*. **20**, 7052-7059 (2001).
44. E. Kamynina,, C. Debonneville, M. Bens, A. Vandewalle and O. Staub, A novel mouse Nedd4 protein suppresses the activity of the epithelial Na^+ channel, *FASEB J*. **15**, 204-214 (2001).
45. P.M. Synder, D.R. Olson and B.C. Thomas. Serum and glucocorticoid-regulated kinase modulates Nedd4-2-mediated inhibition of the epithelial Na^+ channel, *J. Biol. Chem*. **277**, 5-8 (2002).
46. C. J. Faletti, N. Perrotti, S.I. Taylor and B.L. Blazer-Yost, sgk: An essential convergence point for peptide and steroid hormone regulation of ENaC-mediated Na^+ transport, *Am. J. Physiol. Cell Physiol.* **282**, 494-500 (2002).
47. P. Wulff, V. Vallon, D.Y. Huang, H. Volkl, F. Yu, K. Richter, M. Jansen, M. Schlunz, K. Klingel, J. Loffing, G. Kauselmann, M.R. Bosl, F. Lang and D. Kuhl, Impaired renal Na^+ retention in the sgk1-knockout mouse, *J. Clin. Invest*. **110**, 1262-1268 (2002).
48. D. Alvarez de la Rosa and C. Canessa, Role of SGK in hormonal regulation of epithelial sodium channel in A6 cells. *Am. J. Physiol. Cell Physiol*. **284,** C404-C414, (2003)
49. D. Alvarez de la Rosa, T. Coric, N. Todorovic, D. Shao, T. Wang and C. Canessa, Distribution and regulation of expression of serum- and glucocorticoid-induced kinase-1 in the rat kidney, *J. Physiol*. **551**, 455-466 (2003).
50. X. Cheng, Y. Ma, M. Moore, B.A. Hemmings and S.S. Taylor, Phosphorylation and activation of cAMP-dependent protein kinase by phophoinositide-dependent protein kinase, *Proc. Natl. Acad. Sci. USA* **95**, 9849-9854 (1998).
51. M.J. Moore, J.R. Kanter, K.C. Jones and S.S. Taylor, Phosphorylation of the catalytic subunit of protein kinase A: autophosphorylation versus phosphorylation by phosphoinositide-dependent kinase-1, *J. Biol. Chem.* **277**, 47878-47884 (2002).
52. N. Perrotti, R.A. He, S A. Phillips, C.R. Haft and S.I. Taylor, Activation of serum- and glucocorticoid-induced protein kinase (sgk) by cyclic AMP and insulin, *J. Biol. Chem.* **276**, 9406-9412 (2001).
53. C. Nofziger and B.L. Blazer-Yost, ADH-stimulated Na^+ transport: Interaction between the cAMP/PKA and phosphoinositide signaling pathways, *2003 International Cell Symposium*, Dayton OH (Sep 20-25, 2003).

54. D. Yoo, B.Y. Kim, C. Campo, L. Nance, A. King, D. Maouyo and P.A. Welling, Cell surface expression of the ROMK (Kir 1.1) channel is regulated by the aldosterone-induced kinase, sgk-1, and protein kinase A, *J. Biol. Chem.* **278**, 23066-23075 (2003).

34

MODULATION OF VOLUME-SENSITIVE TAURINE RELEASE FROM NIH3T3 MOUSE FIBROBLASTS BY REACTIVE OXYGEN SPECIES

Ian Henry Lambert*

1. TAURINE – A COMPATIBLE OSMOLYTE

The role of organic osmolytes, i.e., methylated compounds, sugars, polyols, free amino acids, and the nitrogenous waste product urea, in the adjustment and maintenance of cellular osmotic pressure and volume has been the subject of study for several decades. It is clear that following osmotic swelling most vertebrate cells restore their cell volume by release of ions (KCl), organic osmolytes, and osmotically-obliged cell water in a process termed regulatory volume decrease (RVD). The inorganic ions at high concentrations disrupt protein function, whereas the amino acids used as osmolytes have no effect on protein function up to 1 mol/l and are consequently designated compatible osmolytes. Alanine, β-alanine, betaine, glycine, glutamate, proline and taurine are often involved in the restoration of cell volume following osmotic swelling. The essential amino acids, on the other hand, are often found in low cellular concentrations and play only a minor or no role in cell volume restoration. Taurine, amino ethane sulphonic acid, is well-suited as an organic osmolyte. By virtue of its zwitterionic nature (pK_1 = 1.5, pK_2 = 8.74) and an acidic isoelectric point (5.16), taurine is quite water soluble (837 mmol/l) and has a slight negative charge at physiological pH that decreases its lipophilicity. Furthermore, taurine is not incorporated into proteins and not oxidized in mammalian cells. The intracellular taurine concentration is a balance between (i) active taurine uptake via the Na^+, Cl^--dependent, pH-sensitive and high affinity taurine transporter TauT, (ii) synthesis from cysteine/methionine, and (iii) release via either a transport process that resembles TauT working in reverse or a volume-sensitive taurine leak pathway.[1] Taurine is abundant in the retina, heart and skeletal muscle, and the intracellular taurine concentration ranges from 10 mM in NIH3T3 cells,[2] 20–50 mM in leukocytes[3] and 40-50 mM in Ehrlich ascites tumour cells.[4, 5]

* Ian Henry Lambert, The August Krogh Institute, Biochemical Department, Universitetsparken 13, DK-2300, Copenhagen Ø, Denmark

2. ROLE OF PHOSPHOLIPASE A_2 AND 5-LIPOXYGENASE IN SWELLING-INDUCED ACTIVATION OF TAURINE RELEASE

Mammalian cells exposed to hypotonic conditions swell initially almost as perfect osmometers due to their high water permeability. This initial volume expansion inevitably results in unfolding of the plasma membrane, distortion/reorganization of the cytoskeleton, integrin clustering and/or shift in intracellular ionic strength/macromolecular crowding which elicits intracellular signaling events that lead to activation of volume-sensitive leak pathways for ions and organic osmolytes. While the initial volume-sensing mechanisms as well as the volume-sensitive taurine leak pathway still await identification, it has been found that phospholipase A_2 (PLA_2) and lipoxygenase (LO) activities are permissive elements in the swelling-induced intracellular cascades leading to taurine release in HeLa cells, fibroblasts, human platelets and Ehrlich ascites tumour cells.[1] Kinnunen and co-workers demonstrated that PLA_2 incorporated in a unilamellar lipid vesicle is activated by stretch. Consequently, they suggested a shift in the lateral packing of lipids in a plasma membrane could function as a volume-sensing mechanism.[6] In the case of Ehrlich cells, it has been determined that a cytosolic, Ca^{2+}-dependent PLA_2 ($cPLA_{2\alpha}$) actually translocates to so-called hot-spots at the nuclear envelope and arachidonic acid is released from the nucleus within the first minutes following hypotonic exposure.[7] On the other hand, NIH3T3 fibroblasts utilize a cellular, Ca^{2+}-independent PLA_2 ($iPLA_2$) as an upstream element in the swelling-induced signaling cascade.[8] The 5-LO is a nonheme iron-containing enzyme which catalyses the initial steps in the synthesis of the biologically potent leukotrienes (LTB_4, LTC_4, LTD_4, LTE_4).[9] A variety of 5-LO products[10] is produced by Ehrlich cells. Within these cells, the $cPLA_{2\alpha}$ and the 5-LO apparently translocate to the same site on the nuclear membrane following cell swelling and LTD_4 is an essential down-stream second messenger in the swelling-induced activation of the taurine efflux pathway[11] and the volume-sensitive K^+ channel.[12] On the other hand, LTD_4 is not involved in the concomitant activation of the volume-sensitive Cl^- channel in Ehrlich cells.[13] LTD_4 has also been reported to play a role in RVD response in rat colonic enterocytes[14] and rat distal colon[15] whereas, the RVD response in swollen human platelets involves the 12-LO product hepoxilin A_3.[16] It is noted that swelling-induced mobilization of arachidonic acid and oxidation via cytochrome P450 seem to be initial events in the activation of the volume-sensitive, Ca^{2+}-selective TRPV4 channel.[17] Thus, PLA_2 activation and arachidonic acid mobilization/oxidation are initial, up-stream events in activation of various types of volume-sensitive transport pathways.

3. MODULATION OF VOLUME SENSITIVE TAURINE RELEASE BY REACTIVE OXYGEN SPECIES

3.1 Reactive Oxygen Species Potentiate Swelling-Induced Taurine Release

Besides activation of PLA_2 and 5-LO activities, it is now evident that cell swelling is accompanied by modulation of protein tyrosine phosphorylation and that reactive oxygen species (ROS) play an essential role in the volume-dependent regulation of

protein tyrosine kinases and phosphatases. ROS, including the non-radical oxygen species (H_2O_2, lipid hydroperoxide) as well as the oxygen radicals (superoxides, hydroxyl

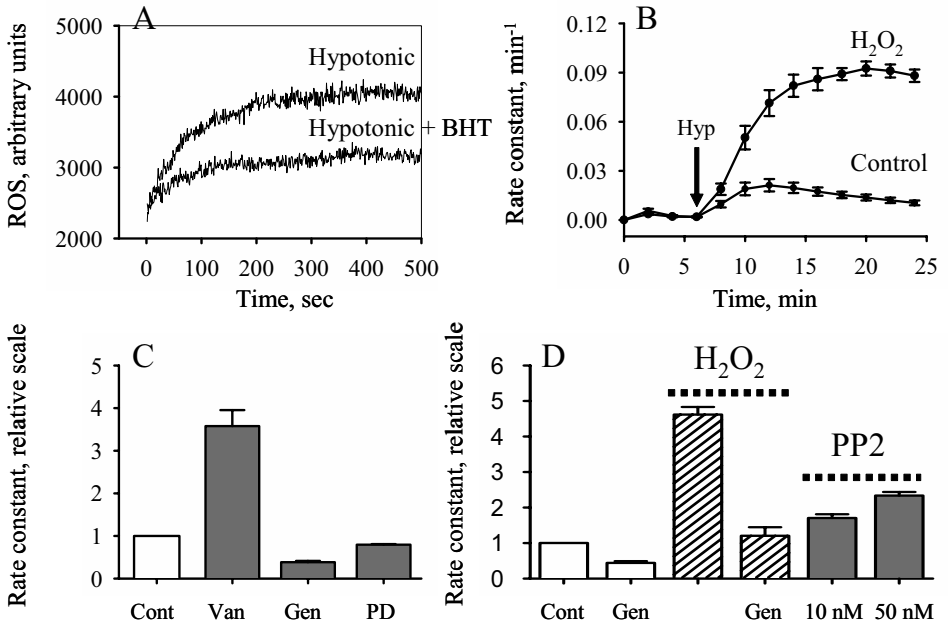

Figure 1. ROS production following hypotonic exposure and the effect of protein tyrosine kinase and phosphatase inhibitors on swelling-induced taurine release. Cells were grown at 80% confluence in Dulbecco´s Modified Eagle Medium (high glucose) containing heat-inactivated fetal bovine serum (10%) and penicillin (100 units/ml). *Panel A*: Cells grown on coverslips were loaded with the fluorescent, ROS sensitive probe carboxy-H_2DCFDA (20 μM, 2 hr) in serum-free medium. Cells were subsequently washed with isotonic NaCl medium (300 mOsm) containing in mM: 143 NaCl, 5 KCl, 1 Na_2HPO_4, 1 $CaCl_2$, 0.1 $MgSO_4$, 5 glucose, and 10 *N*-2-hydroxyethyl piperazine-*N'*-2-ethanesulfonic acid and at time zero exposed to hypotonic NaCl (200 mOsm) medium with or without 0.5 mm BHT. The ROS production was followed with time in a PTI Ratio Master fluorescence spectrometer using excitation and emission wavelengths 490 and 515 nm, respectively. Traces are representative of 3 sets of experiments. *Panel B:* Cells, grown to 80% confluence (35 mm diameter polyethylene dishes), were loaded with [^{14}C]-taurine (80 nCi/ml, 2 hr). After the final wash, 1 ml of experimental solution was added to the dish, left for 2 min, and transferred to a scintillation vial for estimation of ^{14}C activity. This procedure was repeated every 2 minutes throughout the experiment with the solution being replaced at time 6 min by hypotonic NaCl medium (indicated by an arrow). H_2O_2 (1 mM) was present throughout the efflux experiment. ^{14}C-taurine activity remaining in cells at the end of the efflux experiment was estimated by lysing the cells with 1 ml NaOH (0.5 M, 1 hr), washing the dishes twice with distilled water and estimating the ^{14}C activity in the NaOH lysate as well as in both water washouts. The natural logarithm of the fraction of ^{14}C activity remaining in the cells at the given time was plotted versus time and the rate constant for the initial taurine efflux at a given time point was estimated as the negative slope between the actual and the preceding time point. Rate constants are given as mean values ± SEM of 3 sets of paired experiments. *Panels C and D:* Experiments were performed in isotonic/hypotonic KCl medium (Na^+ being substituted by K^+, Panel C) or NaCl medium (Panel D) as outlined in Panel B. Vanadate (Van, 50 μM), Genistein (Gen, 100 μM), PD153035 (PD, 100 nM), H_2O_2 (2 mM) and PP2 were present throughout the efflux experiment. The maximal rate constant for swelling-induced taurine efflux in the presence of drugs was estimated and given relative to the control value ± SEM. Data in Panels C and D are reproduced from.[1, 8]

radicals, peroxyl radicals, alkoxyl radicals) have been demonstrated to act as intracellular signaling molecules in phagocytic as well as non-phagocytic cells.[18-20] More recently, it

has been shown that NIH3T3 cells[8] and skeletal muscle cells[21] produce ROS following hypotonic exposure. This is confirmed in Figure 1A where it is seen that ROS production in NIH3T3 cells increases dramatically within the first minute following hypotonic exposure and is impaired in the presence of the antioxidant butylated hydroxytoluene (BHT). The swelling-induced ROS production in NIH3T3 cells is also impaired following inhibition of $iPLA_2$ by bromoenol lactone (BEL), indicating that ROS production following osmotic cell swelling is down-stream to the $iPLA_2$ activation.[8] Exogenous H_2O_2 has no immediate effect on taurine release when added to NIH3T3 cells under isotonic conditions[8] but significantly potentiates the swelling-induced taurine release (Figure 1B). The effect of H_2O_2 on the volume-sensitive taurine efflux is unaffected by addition of BEL but inhibited by the 5-LO inhibitor ETH 615-139 as well as by well-known direct blockers of the volume-sensitive taurine release.[1, 8] As H_2O_2 does not affect the osmosensitivity, i.e., the degree of cell swelling required for activation of the volume-sensitive taurine efflux pathway,[8] it is assumed that ROS modulate the volume-sensitive intracellular signaling events that lead to activation of the taurine release pathway. In this context, it is noted that addition of the PLA_2 activator melittin elicits ROS production and taurine release from NIH3T3 cells under isotonic conditions by an intracellular signaling system and a taurine efflux pathway resembling pharmacologically those provoked by osmotic cell swelling.[8] Thus, activation of PLA_2 is an up-stream element in the signaling sequence which is activated by osmotic cell swelling in NIH3T3 cells and which leads to ROS production.

3.2 Reactive Oxygen Species Are Generated by the NAD(P)H Oxidase Following Hypotonic Exposure

ROS are generated in the mitochondria when electrons leak from the electron transferring systems and by xanthine and flavoprotein oxidases, cytochrome P450, the NAD(P)H oxidase and superoxide dismutase. ROS are eliminated by catalase and glutathione peroxidase. Taurine has been assigned a role as an antioxidant; it scavenges the potent oxidant hypochlorous acid generated from H_2O_2 in monocytes and neutrophiles, forming the less aggressive TauCl.[22]

The NAD(P)H oxidase in phagocytes consists of the transmembrane flavocytochrome complex ($gp91^{phox}$, $p22^{phox}$), cytosolic components ($p40^{phox}$, $p47^{phox}$, $p67^{phox}$) and a small GTP binding protein (Rac2). Oxidase activity requires assembly of the involved components at the plasma membrane.[23] The NAD(P)H oxidase in non-phagocytic cells is of a similar composition and it appears that (i) all components are constitutively associated at intracellular membranes, (ii) Rac1 is involved in NAD(P)H oxidase activity following stimulation of growth factor receptors, and (iii) ROS are released to the intracellular compartment.[24, 25] Activation of the NAD(P)H oxidase complex has also been demonstrated to involve arachidonic acid[26] and protein kinase C (PKC) activity.[27] It is thus conceivable that arachidonic acid, released by $iPLA_2$, serves as modulator of ROS generation as well as precursor for synthesis of second messengers. Expression of constitutively active forms of Rac in fibroblasts increases the ROS level[18] and improves the RVD response.[28] Exogenous addition of H_2O_2 seems to prolong the open-probability of the swelling-induced taurine efflux in NIH3T3 cells (Figure 1B);[28] whereas, addition of the NAD(P)H oxidase inhibitor diphenylene iodonium (DI) accelerates inactivation of

the volume-sensitive taurine efflux.[8] Furthermore, stimulation of PKC activity in NIH3T3 cells prior to hypotonic exposure has recently been shown to potentiate swelling-induced taurine efflux during a subsequent hypotonic exposure in a process involving NAD(P)H oxidase activity.[29] It has accordingly been suggested that ROS are produced in NIH3T3 cells following osmotic exposure at a step down-stream to the $iPLA_2$ activation by a PKC-regulated NAD(P)H oxidase.[1] It is noted that lysophospholipids are generated by PLA_2 and that lysophosphatidyl choline (LPC) is known to generate ROS and induce taurine release under isotonic conditions in porcine myotubes[21] and NIH3T3 cells.[1] Although LPC is produced following osmotic cell swelling in Ehrlich cells, for example,[48] it does not appear to contribute to swelling-induced taurine release.[1, 30]

3.3 Reactive Oxygen Species Interfere with Protein Tyrosine Phosphatases

ROS exert their effect either by alteration in the intracellular redox state or by oxidative modification of proteins (oxidation of sulphydryl group, formation of intra/intermolecular disulfide linkage, dityrosine formation). A variety of protein serine/threonine kinases (mitogen-activated protein (MAP) kinases, S6 kinase, Akt, PKC) and protein tyrosine kinases (epidermal growth factor receptor, insulin receptor, Src, Lck) are regulated by the cellular redox state.[19] Furthermore, exposure to H_2O_2 leads in general to an increased protein tyrosine phosphorylation as a consequence of oxidation of an essential cysteine residue in the catalytic centre of multiple protein tyrosine phosphatases, resulting in their inactivation.[31] Furthermore, swelling-induced taurine release from a variety of cells is inhibited/potentiated in the presence of protein tyrosine kinase and phosphatase inhibitors, respectively.[28, 30, 32-34] From Figures 1C and 1D, it is seen that genistein, which inhibits receptor-associated as well as non-receptor protein tyrosine kinase activity, reduces the volume-sensitive taurine release in NIH3T3 cells. On the other hand, vanadate (a competitive inhibitor of various protein phosphatases including the ubiquitously-expressed endoplasmatic reticulum associated protein tyrosine phosphatase PTP1B)[35] potentiates, just like H_2O_2, the swelling-induced taurine release from NIH3T3 cells (Figure 1C). The potentiating effect of H_2O_2 (Figure 1D) and vanadate[8] is severely reduced in the presence of genistein. It has been suggested that cell swelling and activation of a protein tyrosine kinase are required for ROS to potentiate the swelling-induced taurine release and that the effect of ROS most probably reflects oxidation and subsequent inhibition of protein tyrosine phosphatase (PTP1B) activity.[8]

3.4 Role of the Protein Tyrosine Kinases c-Src and pFAK^{125}

Tyrphostines, inhibitors of receptor protein tyrosine kinases, have been demonstrated to reduce the swelling-induced taurine release in primary astrocyte cultures.[36] As seen in Figure 1C, PD153035 which inhibits protein tyrosine kinase activity, coupled to the epidermal growth factor (EGF) receptor, reduces the swelling-induced taurine release from NIH3T3 cells by 20% (less than the 60% inhibition obtained by genistein). It is currently assumed that the EGF receptor plays a minor role in activation of the swelling-induced taurine release from NIH3T3 cells.[1] Non-receptor tyrosine kinases (p72Syk/p56Lyn) are considered to be involved in the phosphorylation of the Band 3 anion exchanger and to contribute to regulation of the swelling-induced taurine efflux in skate blood cells.[32] Both the non-receptor tyrosine kinase of the Src family and the focal adhesion kinase pFAK^{125}

are activated by mechanical stress, integrin clustering,[37] and ROS[38, 39] and accordingly can be activated by cell swelling.

Membrane-associated Src kinases have a catalytic domain, SH2/SH3 domains plus several tyrosine residues, and their kinase activity is modulated by phosphorylation of two tyrosine residues. Phosphorylation of Tyr^{527} by the ubiquitous protein tyrosine kinase Csk leads to an intramolecular interaction with the SH2 domain and autoinhibition, whereas phosphorylation of Tyr^{416}, presumably by an intermolecular event, correlates with enzyme activation.[40] c-Src is normally maintained in the inactive state and it is assumed that PTP1B mediates dephosphorylation of Tyr^{527} and activation of c-Src.[41] In the case of HeLa cells, it has been shown that exposure to H_2O_2 decreases c-Src kinase activity[42] and potentiates swelling-induced taurine release,[30] indicating a role of c-Src in swelling-induced taurine release. Using Western blot technique (10% SDS page, polyclonal rabbit antibodies against phosphorylated Tyr^{527} of human Src from Cell Signaling Technology, Inc.), it is estimated that phosphorylation of c-Src at Tyr^{527} in NIH3T3 cells under hypotonic conditions (66% of the isotonic value, 5 min) is increased by 23 ± 4% (n = 3) in the presence of 1 mM H_2O_2. Exposure to the antioxidant BHT (0.25 mM) reduced phosphorylation at Tyr^{527} by about 30% (single experiment). Thus, exposure to H_2O_2 shifts c-Src in NIH3T3 cells to the more phosphorylated and most probably less active state. Furthermore, the selective Src kinase inhibitor PP2 potentiates the swelling-induced taurine efflux from NIH3T3 mouse fibroblasts via the volume-sensitive taurine release pathway in a dose-dependent manner (Figure 1D).[1] Thus, it is conceivable that the volume-sensitive taurine efflux pathway in NIH3T3 cells is potentiated under conditions where Src kinase activity is reduced.

$pFAK^{125}$ is a cytoplasmic protein tyrosine kinase preferentially localized in contact with the cytoplasmatic domain of β1-integrin at the focal adhesion complex. $pFAK^{125}$ has several tyrosine residues, the focal-adhesion targeting domain, but lacks typical SH2/SH3 domains.[39] Autophosphorylation of $pFAK^{125}$ at Tyr^{397} following β1-integrin activation provides a binding site for the p85 subunit of the phosphatidyl inositol 3 kinase (PI-3K) and for c-Src.[39] The monomeric GTP-binding protein RhoA activates $pFAK^{125}$ and subsequently the PI-3K and volume sensitive Cl^- current in human intestine 407 cells.[43] PI-3K has been assigned a regulatory role in the swelling-induced taurine release from chicken retina.[33] In the case of NIH3T3 cells, it has been demonstrated that cells expressing constitutive active RhoA have an accelerated RVD following hypotonic exposure as well as a significantly increased rate constant for the swelling-induced taurine efflux when compared to wild-type cells.[28] However, neither inhibitors of the PI-3K nor of the Rho-associated kinases (ROK / ROCK) affect swelling-induced taurine efflux from NIH3T3 cells.[28] It is currently assumed that RhoA is involved in the upstream events activated by cell swelling and leading to RVD.[28]

Once associated to $pFAK^{125}$, c-Src is thought to phosphorylate $pFAK^{125}$ at Tyr^{925} in the focal adhesion targeting domain and at Tyr^{576}/Tyr^{577} in the catalytic domain.[39, 44] The Src-mediated phosphorylation of Tyr^{925} confers the binding site for the growth factor receptor binding protein (Grb) and the guanine nucleotide exchange factor Sos and consequently, initiation of a Ras-Raf-MAP kinase pathway.[39] An increased phosphorylation of $pFAK^{125}$ and the MAP kinase p38 following osmotic exposure has recently been demonstrated in chicken retina,[33] whereas the involvement of MAP kinases ERK1/2 has been demonstrated in the activation of K^+, Cl^- and taurine efflux in cervical epithelial cells.[34]

Src-mediated phosphorylation of pFAK^{125} at Tyr^{576}/Tyr^{577} affects its kinase activity. Sustained pFAK^{125} phosphorylation at Tyr^{576}/Tyr^{577} and an increased pFAK^{125} kinase activity are detected in cells over-expressing chicken pFAK^{125} following vanadate treatment.[45] Similarly, exogenous H_2O_2 induces a time-dependent phosphorylation of pFAK^{125} in bovine pulmonary artery endothelial cells which is primarily caused by an inhibition of protein tyrosine phosphatases specific to pFAK^{125}.[46] As PP2 inhibits both phosphorylation of pFAK^{125} at Tyr^{577} as well as pFAK^{125} activation in Swiss 3T3 cells,[44] it is conceivable that both c-Src and pFAK^{125} are involved in the ROS-mediated modulation of the swelling-induced taurine efflux in mouse fibroblasts. It is noted that the swelling-induced taurine efflux is potentiated in the presence of H_2O_2/vanadate and PP2 (Figure 1), whereas inactivation of the volume-sensitive taurine efflux pathway is delayed/impaired in the presence of H_2O_2 (Figure 1B) but unaffected in the presence of PP2.[1] It is currently assumed that a reduced c-Src activity leads to the potentiation of the swelling-induced taurine efflux, whereas reduced activity of yet unidentified protein tyrosine phosphatases leads to an increased open probability of the volume-sensitive taurine release pathway. At present, it is not known whether ROS also affect the activation and activity of the volume-sensitive transport systems for ions in NIH3T3 fibroblasts and thus the general RVD response.

4. MODEL FOR MODULATION OF THE CELLULAR TAURINE CONTENT FOLLOWING HYPOTONIC EXPOSURE

Taurine is accumulated by TauT and released following hypotonic exposure via the volume-sensitive taurine efflux pathway. In the case of Ehrlich ascites tumour cells, the cellular to extracellular taurine concentration gradient is dramatically diminished following hypotonic exposure and this reduction is due to both a reduced uptake via TauT and an increased release via the volume-sensitive taurine efflux pathway.[4, 28] Activation of the volume-sensitive efflux pathway in Ehrlich cells involves the sequential translocation of $cPLA_2$ to the nucleus, release of arachidonic acid from the nuclear membrane, oxidation of arachidonic acid to leukotrienes (notably LTD_4), binding of LTD_4 to a receptor (CysLT1) and subsequent activation of a DIDS-sensitive taurine release pathway.[1] The reduction of the active taurine uptake in Ehrlich cells is most probably a result of an inhibition of TauT due to the swelling-induced depolarisation of the plasma membrane.[1] Figure 2 illustrates the transport systems involved in the regulation of the taurine content in NIH3T3 fibroblasts as well as the intracellular signaling events involved in the activation and modulation of swelling-induced release of taurine. $iPLA_2$ as well as a 5-LO play a permissive role in the activation of the swelling-induced taurine efflux pathway in NIH3T3 cells. ROS are generated following hypotonic exposure at a step down-stream to $iPLA_2$ and most probably by activation of the NAD(P)H oxidase. Arachidonic acid is assumed to act as a precursor for the synthesis of essential down-stream second messengers via the 5-LO and to interact with the NAD(P)H oxidase. ROS are proposed to exert their effect via interference with the 5-LO system and via oxidation and inactivation of protein tyrosine phosphatases (PTP1B). The latter causes a shift in the general protein tyrosine phosphorylation pattern and activity of c-Src

and pFAK^{125}, consequently modulation of the open probability of the volume-sensitive taurine release pathway.[1]

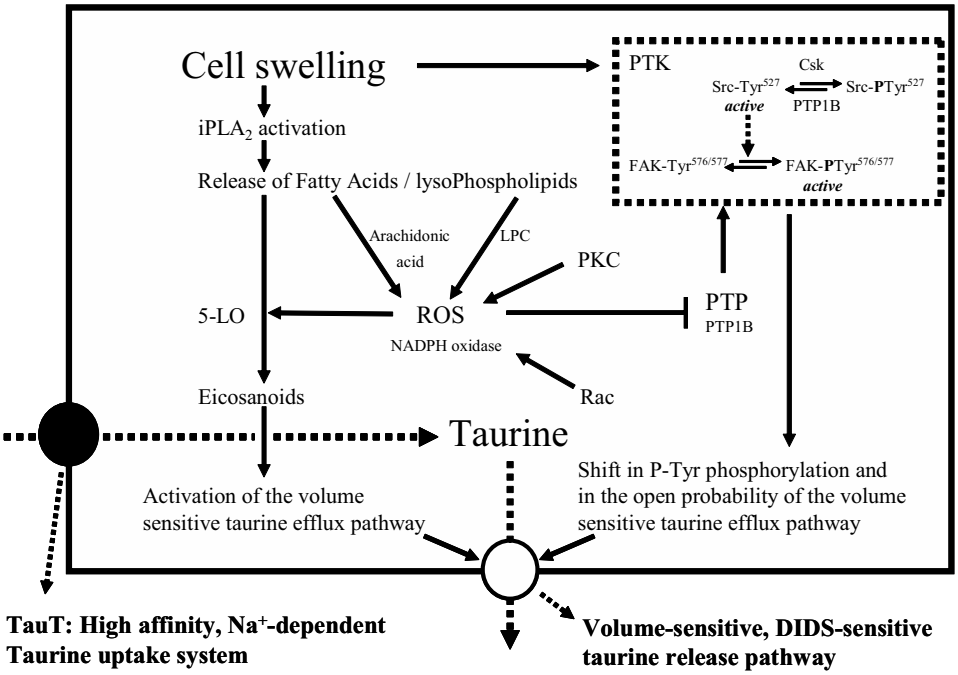

Figure 2. Regulation of the cellular taurine content in NIH3T3 fibroblasts. Taurine is taken up by TauT which in NIH3T3 cells requires 2-3 Na^+ ions to facilitate the uptake of 1 taurine.[47] Taurine is released following hypotonic exposure via an efflux system that requires $iPLA_2$ and 5-lipoxygenase (5-LO) activities for activation.[1] The swelling-induced taurine release is modulated by ROS in a process involvpng protein tyrosine kinases (c-Src, pFAK125) and tyrosine phosphatases (PTP1B).[1]

5. ACKNOWLEDGMENTS

This work was supported by the Danish Research Council and "Fonden af 1870". Dr. Stine F. Pedersen is thanked for carefully reading and commenting on the manuscript.

6. REFERENCES

1. IH Lambert, Regulation of the cellular content of the organic osmolyte taurine in mammalian cells, *Neurochem Res* **29,** 27-63 (2004).
2. J Moran, D Miranda, C Pena-Segura and H Pasantes-Morales, Volume regulation in NIH/3T3 cells not expressing P-glycoprotein. II. Chloride and amino acid fluxes, *Am J Physiol* **272**, C1804-C1809 (1997).
3. K Fukuda, Y Hirai, H Yoshida, T Hakajima and T Usii, Free amino acid content of lymphocytes and granulocytes compared, *Clin Chem* **28**, 1758-1761 (1982).

4. EK Hoffmann and IH Lambert, Amino acid transport and cell volume regulation in Ehrlich ascites tumour cells, *J Physiol* **338**, 613-625 (1983).
5. J Mollerup and IH Lambert, Calyculin A modulates the kinetic constants for the Na^+-coupled taurine transport in Ehrlich ascites tumour cells, *Biochim Biophys Acta* **1371,** 335-344 (1998).
6. PK Kinnunen, Lipid bilayers as osmotic response elements, *Cell Physiol Biochem* **10**, 243-250 (2000).
7. S Pedersen, IH Lambert, SM Thoroed and EK Hoffmann, Hypotonic cell swelling induces translocation of the alpha isoform of cytosolic phospholipase A_2 but not the gamma isoform in Ehrlich ascites tumor cells, *Eur J Biochem* **267,** 5531-5539 (2000).
8. IH Lambert, Reactive oxygen species regulate swelling-induced taurine efflux in NIH3T3 mouse fibroblasts, *J Membr Biol* **192**, 19-32 (2003).
9. S Nicosia, V Capra and GE Rovati, Leukotrienes as mediators of asthma, *Pulm Pharmacol Ther* **14**, 3-19 (2001).
10. IH Lambert, Eicosanoids and cell volume regulation, *Cellular and Molecular Physiology of Cell Volume Regulation, CRC Press, Boca Raton, FL* 279-298 (1994).
11. IH Lambert, Regulation of the taurine content in Ehrlich ascites tumour cells, *Adv Exp Med Biol* **442**, 269-276 (1998).
12. EK Hoffmann, Leukotriene D_4 (LTD_4) activates charybdotoxin-sensitive and -insensitive K^+ channels in Ehrlich ascites tumor cells, *Pflugers Arch* **438**, 263-268 (1999).
13. C Hougaard, MI Niemeyer, EK Hoffmann and FV Sepulveda, K^+ currents activated by leukotriene D_4 or osmotic swelling in Ehrlich ascites tumour cells, *Pflugers Arch* **440**, 283-294 (2000).
14. M Diener and E Scharrer, The leukotriene D_4 receptor blocker, SK&F 104353, inhibits volume regulation in isolated crypts from the rat distal colon, *Eur J Pharmacol* **238**, 217-222 (1993).
15. O Mignen, C Le Gall, BJ Harvey and S Thomas, Volume regulation following hypotonic shock in isolated crypts of mouse distal colon. *J Physiol* **515** (Pt 2), 501-510 (1999).
16. A Margalit, AA Livne, J Funder and Y Granot, Initiation of RVD response in human platelets: mechanical-biochemical transduction involves pertussis-toxin-sensitive G protein and phospholipase A_2, *J Membr Biol* **136,** 303-311 (1993).
17. H Watanabe, J Vriens, J Prenen, G Droogmans, T Voets and B Nilius, Anandamide and arachidonic acid use epoxyeicosatrienoic acids to activate TRPV4 channels, *Nature* **424**, 434-438 (2003).
18. T Finkel, Reactive oxygen species and signal transduction, *IUBMB Life* **52**, 3-6 (2001).
19. H Kamata and H Hirata, Redox regulation of cellular signaling, *Cell Signal* **11**, 1-14 (1999).
20. VJ Thannickal and BL Fanburg, Reactive oxygen species in cell signaling, *Am J Physiol (Lung Cell Mol Physiol)* **279**, L1005-L1028 (2000).
21. N Ørtenblad, JF Young, N Oksbjerg, JH Nielsen and IH Lambert, Reactive oxygen species are important mediators of taurine release from skeletal muscle cells, *Am J Physiol* **284**, C1362-C1373 (2003).
22. GB Schuller-Levis and E Park, Taurine: New implications for an old amino acid, *FEMS Microbiology Letters* **226**, 195-202 (2003).
23. LC McPhail, KA Waite, DS Regier, JB Nixon, D Qualliotine-Mann, WX Zhang, R Wallin and S Sergeant, A novel protein kinase target for the lipid second messenger phosphatidic acid, *Biochim Biophys Acta* **1439**, 277-290 (1999).
24 W Dröge, Free radicals in the physiological control of cell function, *Physiol Rev* **82**,47-95 (2003).
25. D Javesghani, SA Magder, E Barreiro, MT Quinn and SN Hussain, Molecular characterization of a superoxide-generating NAD(P)H oxidase in the ventilatory muscles, *Am J Respir Crit Care Med* **165**, 412-418 (2002).
26. X Zhao, EA Bey, FB Wientjes and MK Cathcart, Cytosolic phospholipase A_2 ($cPLA_2$) regulation of human monocyte NADPH oxidase activity. $cPLA_2$ affects translocation but not phosphorylation of p67(phox) and p47(phox), *J Biol Chem* **277**, 25385-25392 (2002).
27. A Fontayne, PM Dang, MA Gougerot-Pocidalo and J El Benna, Phosphorylation of p47phox sites by PKC alpha, beta II, delta, and zeta: effect on binding to p22phox and on NADPH oxidase activation, *Biochemistry* **41**, 7743-7750 (2002).
28. SF Pedersen, KH Beisner, C Hougaard, BM Willumsen, IH Lambert and EK Hoffmann, Rho family GTP binding proteins are involved in the regulatory volume decrease process in NIH3T3 mouse fibroblasts, *J Physiol* **541**, 779-796 (2002).
29. IH Lambert, Regulation of the volume-sensitive taurine efflux pathway in NIH3T3 mouse fibroblasts, *Taurine in the 21st century Eds JB Lombardini, SW Schaffer, J Azuma,* 115-122 (2003).

30. IH Lambert and B Falktoft, Lysophosphatidylcholine induces taurine release from HeLa cells, *J Membr Biol* **176,** 175-185 (2000).
31. TC Meng, T Fukada and NK Tonks, Reversible oxidation and inactivation of protein tyrosine phosphatases *in vivo, Mol Cell* **9**, 387-399 (2002).
32. EM Hubert, MW Musch and L Goldstein, Inhibition of volume-stimulated taurine efflux and tyrosine kinase activity in the skate red blood cell, *Pflugers Arch* **440,** 132-139 (2000).
33. LD Ochoa de la Paz, R Lezama, ME Torres-Marquez and H Pasantes-Morales, Tyrosine kinases and amino acid efflux under hyposmotic and ischaemic conditions in the chicken retina, *Pflugers Arch* **445**, 87-96 (2002).
34. MR Shen, CY Chou, JA Browning, RJ Wilkins and JC Ellory, Human cervical cancer cells use Ca^{2+} signaling, protein tyrosine phosphorylation and MAP kinase in regulatory volume decrease, *J Physiol* **537**, 347-362 (2001).
35. G Huyer, S Liu, J Kelly, J Moffat, P Payette, B Kennedy, G Tsaprailis, MJ Gresser and C Ramachandran, Mechanism of inhibition of protein-tyrosine phosphatases by vanadate and pervanadate, *J Biol Chem* **272**, 843-851 (1997).
36. AA Mongin, JM Reddi, C Charniga and HK Kimelberg, [^{3}H]taurine and D-[^{3}H]aspartate release from astrocyte cultures are differently regulated by tyrosine kinases, *Am J Physiol* **276,** C1226-C1230, 1999.
37. JT Parsons, Focal adhesion kinase: The first ten years, *J of Cell Sci* **116**, 1409-1416 (2003).
38. A Barchowsky, SR Munro, SJ Morana, MP Vincenti and M Treadwell, Oxidant-sensitive and phosphorylation-dependent activation of NF-kappa B and AP-1 in endothelial cells, *Am J Physiol* **269**, L829-L836 (1995).
39. MH Ben Mahdi, V Andrieu and C Pasquier, Focal adhesion kinase regulation by oxidative stress in different cell types, *IUBMB Life* **50**, 291-299 (2000).
40. M Minetti, C Mallozzi and AM Di Stasi, Peroxynitrite activates kinases of the Src family and upregulates tyrosine phosphorylation signaling, *Free Radic Biol Med* **33**, 744-754 (2002).
41. JD Bjorge, A Pang and DJ Fujita, Identification of Protein-tyrosine Phosphatase 1B as the major Tyrosine Phosphatase Activity Capaple of Dephosphorylating and Activating c-Src in Several Human Breast Cancer Cell Lines, *J Biol Chem* **275,** 41439-41446 (2000).
42. JM Cunnick, JF Dorsey, T Standley, J Turkson, AJ Kraker, DW Fry, R Jove and J Wu, Role of tyrosine kinase activity of epidermal growth factor receptor in the lysophosphatidic acid-stimulated mitogen-activated protein kinase pathway, *J Biol Chem* **273**, 14468-14475 (1998).
43. BC Tilly, MJ Edixhoven, LG Tertoolen, N Morii, Y Saitoh, S Narumiya and HR de Jonge, Activation of the osmo-sensitive chloride conductance involves P21rho and is accompanied by a transient reorganization of the F-actin cytoskeleton, *Mol Biol Cell* **7,** 1419-1427 (1996).
44. EP Salazar and E Rozengurt, Bombesin and platelet-derived growth factor induce association of endogenous focal adhesion kinase with Src in intact Swiss 3T3 cells, *J Biol Chem* **274**, 28371-28378 (1999).
45. MC Maa and TH Leu, Vanadate-dependent FAK activation is accomplished by the sustained FAK Tyr-576/577 phosphorylation, *Biochem Biophys Res Commun* **251**, 344-349 (1998).
46. S Vepa, WM Scribner, NL Parinandi, D English, JG Garcia and V Natarajan, Hydrogen peroxide timulates tyrosine phosphorylation of focal adhesion kinase in vascular endothelial cells, *Am J Physiol* **277**, L150-L158 (1999).
47. JM Voss, ST Christensen and IH Lambert, Characterisation and subcellular localisation of TauT in mouse fibroblasts, *Acta Physiol Scand,* **181** (1), P08-4 (2004).
48. SM Thoroed, L Lauritzen, IH Lambert, HS Hansen and EK Hoffmann, Cell swelling activates phospholipase A_2 in Ehrlich ascites tumor cells, *J Membr Biol* **160**, 47-58 (1997).

35

HYPERTENSION IN K-CL COTRANSPORTER-3 KNOCKOUT MICE

Norma C. Adragna, Yanfang Chen, Eric Delpire,
Peter K. Lauf and Mariana Morris*

1. INTRODUCTION

Hypertension is a public health problem affecting up to 25% of the population. While there is much information on the cellular mediators of vascular control, the precise etiology of hypertension remains unsolved. Nitric oxide (NO) and other reactive oxygen species have been implicated in blood pressure control.[1-11] Likewise, abnormalities in monovalent ion transport are proposed to play a role in cardiovascular disease such as hypertension.[12-17]

K-Cl cotransport (COT, KCC), the electroneutral movement of K and Cl, is critical in regulating cell volume and ionic homeostasis.[18] Four KCC genes have been characterized.[19] Several human and murine phenotypes have been associated with defects in cation-chloride cotransport.[20-22] For instance, the K-Cl cotransporter, in particular the KCC3 gene, is involved in degenerative peripheral neuropathies linked to chromosome 15q14,[23] and targeted deletion of the KCC2 gene produces a profound seizure disorder.[20-22]

In primary cultures of vascular smooth muscle cells (VSMCs), we showed that nitrovasodilators, NO donors and effective antihypertensive drugs regulate K-Cl COT activity and KCC1/KCC3 mRNA expression via the cGMP pathway.[24-29] Furthermore, KCC3 is expressed in brain, heart, skeletal muscle, kidney and blood vessels.[19] Thus, we proposed a putative role for the KCC3 gene in blood pressure regulation and consequent cardiovascular disease. These studies were conducted in a recently developed KCC3 knockout model,[23] using radiotelemetry for measurement of blood pressure and heart rate.

These results were presented in abstract form at the 2003 Experimental Biology Meeting in San Diego, CA.[23]

*N.C. Adragna, Y. Chen and M. Morris, Dept. of Pharmacology and Toxicology and Peter K. Lauf, Dept. of Pathology, Wright State University School of Medicine, 3640 Colonel Glenn Hwy, Dayton, OH, 45435. E. Delpire, Dept. of Anesthesiology, Vanderbilt University Medical Center, Nashville, TN, 37232.

2. MATERIALS AND METHODS

The mouse KCC3 gene was disrupted at exon 3 by targeted homologous recombination in embryonic stem cells as reported elsewhere.[20] Homozygous (KCC3-/-) animals are viable but exhibit a severe peripheral neuropathy.[20] Homozygous (KCC3 -/-) and controls (KCC3 +/+) were generated by mating heterozygous animals. Male mice, 5-6 months of age, were housed at 22°C under 12-h light/12-h dark cycles with access to water and standard chow. Mice were anesthetized with a ketamine:xylazine mixture (6:1 mg/kg, im) and the telemetric catheter (Data Sciences Int., St. Paul, MN) inserted into the left carotid artery. The main body of the transmitter was implanted subcutaneously on the right flank. The animals were allowed to recover from surgery for 7-10 days; sufficient recovery time is important for the measurement of basal, non-stress cardiovascular parameters. For the experiment, arterial pressure was measured continuously for 24 h (500 Hz, sampling rate) in conscious mice.[10, 21] Ten min averages were compiled to produce average mean arterial pressure (MAP) and heart rate (HR) for the light (0500 to 1700 h) and dark (1700 to 0500 h) periods. Licking activity was recorded continuously for 24 h using a drink meter system (Columbus Instruments, Columbus, OH). The system is interfaced with a computerized data acquisition system (Biopac System Inc., Santa Barbara, CA) with a sampling rate of 85 Hz.[33] The volume of water intake (ml/day) was also measured to complement the licking activity. Animals were decapitated with collection of trunk blood for measurement of hematocrit and plasma osmolality. All experi-mental protocols were approved by the Laboratory Animal Care and Use Committee of Wright State University.

3. RESULTS

Table 1. Plasma osmolality, hematocrit, drinking activity, and water consumption in KCC3-/- mice.

	Control	KCC3 -/-
Osmolality (mOsm/kg)	325.5 ± 4.3	326.3 ± 5.9
Hematocrit (%)	49.3 ± 1.7	49.3 ± 1.8
Drinking volume (ml/24hr)	4.9 ± 0 .4	6.0 ± 0.6*
Drinking activity (licks/24hr)	1,697 ± 345	2,519 ± 337*

Values are Mean ± SEM, *p<0.05, compared to controls, N=4/group

Studies were conducted using the KCC3 knockout model to evaluate the role of the ion transporter in the regulation of blood pressure, heart rate and water intake. Water intake and licking activity were significantly increased in mice lacking the KCC3 transporter (~22% for volume and 58% for licking activity/24 h, Table 1). Licking activity was concentrated during the night/active period with an increase in KCC3 -/- mice (1,463 ± 148 vs. 2,308 ± 322 licks/12 h, control +/+ vs. KCC3 -/- where $p<0.05$) with no differences seen during the day/inactive period (371 ± 200 vs. 206 ± 84 licks/12 h, control +/+ vs. KCC3 -/-). Licking activity is the more accurate measurement of water

intake, particularly in mice which consume small volumes. Hematocrit and plasma osmolality were not different between the groups, suggesting that the animals were not volume depleted (Table 1). Food intake was not measured since it is difficult to obtain accurate measurements in rodents. However, at 28 days of age, control male mice weighed 11.4 ± 2.2 g (n=10) and homozygous mice 12.6 ±1.7 g (n=10). At 16 months, control male mice weighed 32.7 ± 3.0 g (n=6) and homozygous mice 28.7 ± 2.0 g (n=6). As the data indicate, there was no significant difference in weight measurements for the two groups.

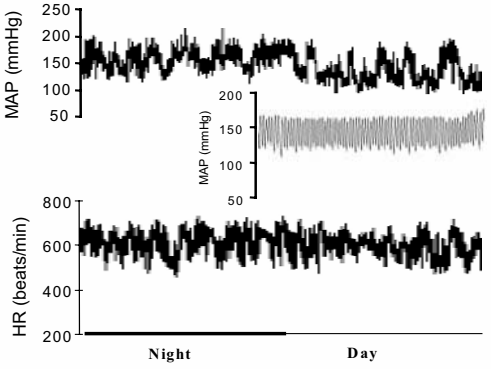

Figure 1. Representative 24-h plot of mean arterial pressure (MAP) and heart rate (HR) in a KCC-3 -/- mouse. The plot shows 10-min means of MAP and HR data. The inset shows 10 seconds of actual arterial pressure tracing. Pulse pressure was 30-40 mmHg which is typical when using the telemetric recording system.

For measurement of cardiovascular parameters, we chose telemetry since this method provides for accurate and long-term recordings in mice.[31, 32] Arterial pressure was measured continuously for 24 h with evaluation of the day/night pattern. Figure 1 shows an example of a 24 h recording of MAP and HR in a KCC3 -/- mouse. Blood pressure was high throughout the 24 h period, with peak levels of 185 mmHg. HR was within normal range for mice. The inset provides an expanded view of the telemetric pressure recording. The pulse pressure averaged 30-40 mmHg with MAP ranging from 110 to 185 mmHg. Quantitative analysis showed that KCC3 -/- mice were characterized by a marked hypertension during both the day and night periods (134±26 and 148±19 mmHg, day and night MAP, respectively [Figure 2]). MAP increased in KCC3 -/- mice by more than 30 mmHg above controls (Figure 2). There was also a day/night rhythm in HR (575.6 ± 21.0 vs. 626.8 ± 10.8 beats/min) but no effect of genotype (575.6 ± 21.0 vs. 555.6 ± 10.5 beats/min during the day period and 626.8 ± 10.8 vs. 612.1 ± 29.8 beats/min during the night, KCC3 -/- vs. KCC3 +/+).

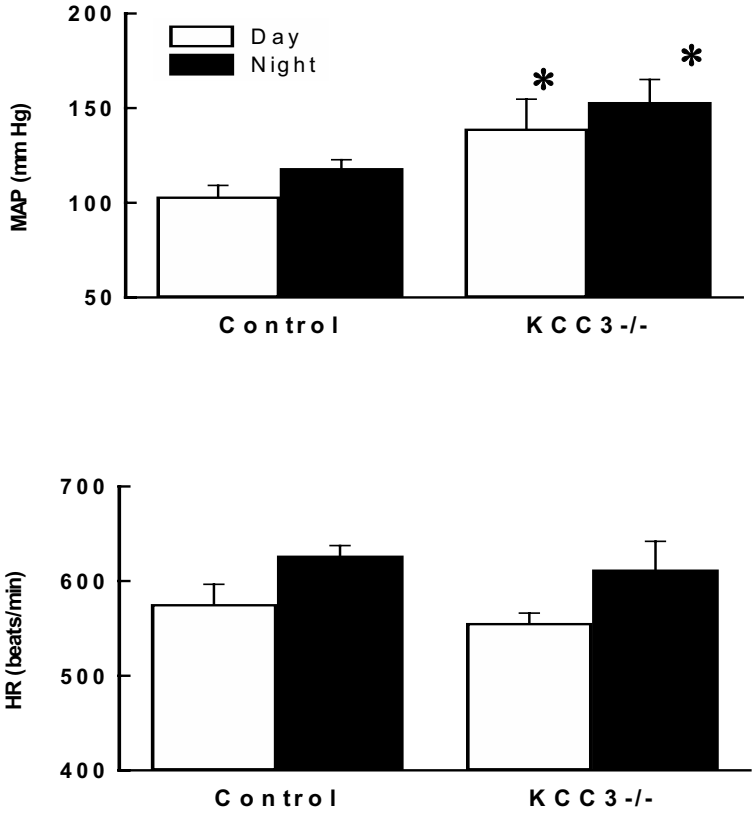

Figure 2. MAP and HR in KCC3 -/- and control +/+ mice during the day and night periods. Mean values were calculated from continuously recorded data (500 Hz). MAP, $F(1,7) = 6.57$, $p < 0.05$ for group and $F(1,7) = 29.05$, $p < 0.002$, for day/night. Light control vs light KCC3 -/-, $p < 0.01$. Dark control vs dark KCC3 -/-, $p < 0.01$. HR, $F(1,7) = 0.03$, NS for group and $F(1,7) = 8.08$, $p < 0.03$ for day/night. * = $p < 0.01$. Values are mean ± SEM, n = 4/group.

4. DISCUSSION

Essential hypertension is a polygenic and multifactorial disease.[15, 34, 35] Two of the more recent theories propose a role for abnormalities in monovalent ion transport.[12-17, 36,] Abnormalities in Na/Li countertransport, Na-K-Cl cotransport, Na/K pump, Na/H exchanger and some ion channels have been associated with hypertension in human and animal models.[12-15, 36] Here, we present evidence for a new piece in the complex puzzle of blood pressure control the K-Cl cotransporter and specifically, the KCC3 gene.

To test the hypothesis that alterations in KCC cotransport are involved in blood pressure regulation, we conducted studies in KCC3 knockout mice. Results show there was a chronic elevation in MAP with no change in HR. Since HR was unchanged in the face of higher MAP, there also appears to be alterations in baroreflex function, perhaps

mediated by central neural changes. There were no changes in hematocrit or plasma osmolality suggesting that volume overload was not a causative factor in the hypertension. Since the KCC3 protein is lacking in all tissues, it is not possible to determine the localization of the cellular mediator. It is likely that changes in vascular ion transport play a role, especially in view of our previous findings in VSMC.[25-29] In this respect, it is possible that up-regulation of alternative compensatory mechanisms elicited by the presence of KCC1 may have dampened the impact of KCC3 knockout. Furthermore, experiments are needed to rule out the possibilities that the high blood pressure is due to a primary defect in hypothalamus (increased NaCl intake) or kidney (decreased pressure natriuresis). In abstract form, Wang et al., have reported renal abnormalities in the same mice, but the abnormality affects HCO_3 handling and the authors have not reported a change in blood pressure.[37]

In addition to the hypertension, KCC3 knockout mice also showed a polydipsia. There was a significant increase in water intake which was not associated with volume or osmolar changes. The lack of change in hematocrit or plasma osmolality suggests there was a balance between intake and excretion. More importantly, the data suggest there was no defect in the ability to excrete a water load, i.e., the vasopressin system was functioning normally. The change in water intake is not likely related to hypertension which was shown to inhibit thirst.[38] The renin angiotensin system may also play a role via its activation of NO and reactive oxygen signaling[8]. There are associations between angiotensin, hypertension and water intake[8, 39]

The important question arising from our studies relates to the mechanism by which the KCC3 transporter regulates blood pressure. K-Cl COT activity and mRNA expression are enhanced by NO donors[24-29] and a decrease in NO production has been proposed as a cause of blood pressure increases.[6, 8, 11] We show that deletion of at least one of the KCC isoforms causes severe hypertension in mice. Therefore, a decrease in NO production should correlate with a decrease in K-Cl cotransport function. Non-functional mutations in KCC3 have been reported in individuals showing a severe peripheral neuropathy.[23] Four distinct protein-truncating mutations were identified in Canadian, Turkish and Italian families. The peripheral neuropathy matches the severe locomotor phenotype observed in KCC3 knockout mice. It is of interest to determine whether individuals carrying KCC3 mutations show changes in NO production and blood pressure control.

The mechanism underlying the high blood pressure observed in KCC3 knockout mice may be related (and opposite[40]) to the effect of NKCC1 deletion, which produces hypotension and decreased vascular smooth muscle tone.[41] Furthermore, these mechanisms likely differ from those underlying the blood pressure increase due to trafficking and/or regulation of renal Na-Cl cotransporters.[42, 43]

In conclusion, results show that disruption of the KCC3 gene in mice produces an animal model of hypertension and polydipsia. These results provide evidence for a role of the K-Cl cotransporter-3 in the regulation of blood pressure and water balance.

5. ACKNOWLEDGMENTS

Supported by NAHA 0050451N, Wright State University Pruett Seed Grant Program, Wright State University Research Challenge Grant Program to NCA, NIH NS36758 to ED and HL69319 to MM.

6. REFERENCES

1. R.W. Alexander, Theodore Cooper Memorial Lecture. Hypertension and the pathogenesis of atherosclerosis. Oxidative stress and the mediation of arterial inflammatory response: a new perspective, *Hypertension* **25**, 155-161 (1995).
2. R.W. Alexander, Atherosclerosis as disease of redox-sensitive genes, *Trans Am Clin Climatol Assoc* **109**, 129-145 (1998).
3. A. Aviv, Chronology versus biology: telomeres, essential hypertension, and vascular aging, *Hypertension* **40**, 229-232 (2002).
4. C .Berry, M.J. Brosnan, J. Fennell, C.A. Hamilton and A.F. Dominiczak, Oxidative stress and vascular damage in hypertension, *Curr Opin Nephrol Hypertens* **10**, 247-255(2001).
5. B. Leclercq, E.A. Jaimes and L. Raij, Nitric oxide synthase and hypertension, *Curr Opin Nephrol Hypertens* **11**, 185-189 (2002).
6. S.R. Maxwell, Coronary artery disease-free radical damage, antioxidant protection and the role of homocysteine, *Basic Res Cardiol* **95**, I65-71 (2000).
7. M. Morris, M. Marcelo, H. Hassain and P. Goldschmitt, Hypertension in transgenic mice expressing the Rac protein in vascular smooth muscle. *Hypertension* **36**, 686, 2000.
8. J.F. Reckelhoff and J.C. Romero, Role of oxidative stress in angiotensin-induced hypertension. *Am J Physiol Regul Integr Comp Physiol* **284**, R893-912., 2003.
9. R.M. Touyz, Oxidative stress and vascular damage in hypertension. *Curr Hypertens Rep* **2**, 98-105., 2000.
10. C.S. Wilcox, Reactive oxygen species: roles in blood pressure and kidney function. *Curr Hypertens Rep* **4**: 160-166., 2002.
11. C.S. Wilcox and W.J. Welch, Oxidative stress: cause or consequence of hypertension. *Exp Biol Med (Maywood)* **226**, 619-620., 2001.
12. N.C. Adragna, M.L. Canessa, H. Solomon, E. Slater and D.C. Tosteson, Red cell lithium-sodium countertransport and sodium-potassium cotransport in patients with essential hypertension, *Hypertension* **4**, 795-804 (1982).
13. M. Canessa, N. Adragna, H.S. Solomon, T.M. Connolly and D..C Tosteson, Increased sodium-lithium countertransport in red cells of patients with essential hypertension, *N Engl J Med* **302**, 772-776 (1980).
14. R. Garay, C. Rosati and P. Meyer, Na+ transport in primary hypertension, *Ann N Y Acad Sci* **488**, 187-195 (1986).
15. S.N. Orlov, N.C. Adragna, V.A. Adarichev and P. Hamet, Genetic and biochemical determinants of abnormal monovalent ion transport in primary hypertension. *Am J Physiol* **276**, C511-536., 1999.
16. K. Van Norren, T. Thien, J.H. Berden, L.D. Elving and J.J. De Pont, Relevance of erythrocyte Na+/Li+ countertransport measurement in essential hypertension, hyperlipidaemia and diabetic nephropathy: a critical review. *Eur J Clin Invest* **28**, 339-352., 1998.
17. L. Yap, A. Arrazola, F. Soria and J. Diez, Is there increased cardiovascular risk in essential hypertensive patients with abnormal kinetics of red blood cell sodium-lithium countertransport? *J Hypertens* **7**, 667-673 (1989).
18. P.K. Lauf, J. Bauer, N.C. Adragna, H. Fujise, A.M. Zade-Oppen, K.H. Ryu and R. Delpire, Erythrocyte K-Cl cotransport: properties and regulation, *Am J Physiol* **263**, C917-932 (1992).
19. P.K. Lauf and N.C. Adragna, K-Cl Cotransport: Properties and Molecular Mechanism, *Cell Physiol Biochem* **10**, 341-354 (2000).
20. E. Delpire, Cation-chloride cotransporters in neuronal communications, *News Physiol Sci* **15**, 309-312 (2000).
21. E. Delpire and D.B. Mount, Human and murine phenotypes associated with defects in cation-chloride cotransport, *Annu Rev Physiol* **64**, 803-843 (2002).
22. N.S. Woo, J. Lu, R. England, R. McClellan, S. Dufour, D.B. Mount, A.Y. Deutch, D.M. Lovinger and E. Delpire, Hyperexcitability and epilepsy associated with disruption of the mouse neuronal-specific K-Cl cotransporter gene. *Hippocampus* **12**, 258-268, 2002.
23. H.C. Howard, D.B. Mount, D. Rochefort, N. Byun, N. Dupre, J. Lu, X. Fan, L. Song, J.B. Riviere, C. Prevost, J. Horst, A. Simonati, B. Lemcke, R. Welch, R. England, F.Q. Zhan, A. Mercado, W.B. Siesser, A.L. George, Jr., M.P. McDonald, J.P. Bouchard, J. Mathieu, E. Delpire and G.A. Rouleau, The K-Cl cotransporter KCC3 is mutant in a severe peripheral neuropathy associated with agenesis of the corpus callosum, *Nat Genet* **32**, 384-392 (2002).
24. N.C. Adragna and P.K. Lauf, Role of nitrite, a nitric oxide derivative, in K-Cl cotransport activation of low-potassium sheep red blood cells, *J Membr Biol* **166**, 157-167 (1998).
25. N.C. Adragna, R.E. White, S.N. Orlov and P.K Lauf, K-Cl cotransport in vascular smooth muscle and erythrocytes, possible implication in vasodilation, *Am J Physiol Cell Physiol* **278**, C381-390 (2000).

26. N.C Adragna, J. Zhang, M. Di Fulvio, T.M. Lincoln and P.K. Lauf, KCl cotransport regulation and protein kinase G in cultured vascular smooth muscle cells, *J Membr Biol* **187**, 157-165 (2002).
27. M. Di Fulvio, P.K. Lauf and N.C. Adragna, Nitric oxide signaling pathway regulates potassium chloride cotransporter-1 mRNA expression in vascular smooth muscle cells, *J Biol Chem* **276**, 44534-44540 (2001).
28. M. Di Fulvio, T.M. Lincoln, P.K. Lauf and N.C. Adragna, Protein kinase G regulates potassium chloride cotransporter-3 expression in primary cultures of rat vascular smooth muscle cells, *J Biol Chem* **276**, 21046-21052 (2001).
29. M. Di Fulvio, P.K. Lauf, S. Shah and N.C. Adragna, NONOates regulate KCl cotransporter-1 and -3 mRNA expression in vascular smooth muscle cells, *Am J Physiol Heart Circ Physiol* **284**, H1686-1692 (2003).
30. Y. Chen, M. Morris, E. Delpire, P.K. Lauf and N.C. Adragna, Hypertension in K-Cl cotransporter-3 knockout mice, *FASEB J* **17**, A 858 (2003).
31. G.M. Butz and R.L. Davisson, Long-term telemetric measurement of cardiovascular parameters in wake mice: a physiological genomics tool, *Physiol Genomics* **5**, 89-97 (2001).
32. L.F. Joaquim, Y. Chen, R Fazan, D..S Dias, H.C. Salgado and M. Morris, Radiotelemetry and spectral analysis in angiotensin AT1aKnockOut (AT1KO) mice, *Pharmacologist* **44**, A 93 (2002).
33. R. Puryear, K.V. Rigatto, J.A. Amico and M. Morris, Enhanced salt intake in oxytocin deficient mice. *Exp Neurol* **171**, 323-328., 2001.
34. F. Navarro-Lopez, Genes and coronary heart disease. *Rev Esp Cardiol* **55**, 413-431., 2002.
35. R.M. Souyz, Molecular and cellular mechanisms regulating vascular function and structure--implications in the pathogenesis of hypertension. *Can J Cardiol* **16**, 1137-1146., 2000.
36. M. Canessa, Erythrocyte sodium-lithium countertransport: another link between essential hypertension and diabetes, *Curr Opin Nephrol Hypertens* **3**, 511-517 (1994).
37. T. Wang, E. Delpire, G. Giebisch, S. Hebert and D.B. Mount, Impaired fluid and bicarbonate absorption in proximal tubules (PT) of KCC3 knockout mice. *FASEB J.* **17**, A464, 2003.
38. E.M. Stricker and A.F. Sved, Controls of vasopressin secretion and thirst: similarities and dissimilarities in signals. *Physiol Behav* **77**, 731-736, 2002.
39. S. Morimoto, M.D. Cassell and C.D. Sigmund, Glia- and neuron-specific expression of the renin-angiotensin system in brain alters blood pressure, water intake, and salt preference, *J Biol Chem* **277**, 33235-33241 (2002).
40. F. Akar, E. Skinner, J.D. Klein, M. Jena, R.J. Paul and W.C. O'Neill, Vasoconstrictors and nitrovasodilators reciprocally regulate the Na+-K+- 2Cl- cotransporter in rat aorta, *Am J Physiol* **276**, C1383-1390 (1999).
41. J.W. Meyer, M. Flagella, R..L Sutliff, J.N. Lorenz, M.L. Nieman, C.S. Weber, R.J. Paul and G.E. Shull, Decreased blood pressure and vascular smooth muscle tone in mice lacking basolateral Na(+)-K(+)-2Cl(-) cotransporter, *Am J Physiol Heart Circ Physiol* **283**, H1846-1855 (2002).
42. F.H. Wilson, K.T. Kahle, E. Sabath, M.D. Lalioti, A.K. Rapson, R.S. Hoover, S.C. Hebert, G. Gamba and R.P. Lifton, Molecular pathogenesis of inherited hypertension with hyperkalemia: the Na-Cl cotransporter is inhibited by wild-type but not mutant WNK4. *Proc Natl Acad Sci USA* **100**, 680-684., 2003.
43. C.L. Yang, J. Angell, R. Mitchell and D.H. Ellison, WNK kinases regulate thiazide-sensitive Na-Cl cotransport. *J Clin Invest* **111**, 1039-1045., 2003.

36

PHYSIOLOGY AND PATHOPHYSIOLOGY OF THE ERYTHROCYTE GARDOS CHANNEL IN HEMATOLOGICAL DISEASES

Carlo Brugnara, Lucia De Franceschi, and Alicia Rivera*

1. ABSTRACT

The erythrocyte intermediate conductance Ca-activated K channel (IK1), first described by Gardos, has been shown to play an important role in the pathological dehydration of human and mouse sickle erythrocytes. Studies by various groups have demonstrated K loss mediated by the activation of this pathway when sickle erythrocytes are subjected to deoxygenation. Transient, localized increases in cytoplasmic Ca induced by sickling are a possible mechanism for this activation. In addition, it has been shown that the Gardos channel of sickle and normal erythrocytes can be activated in oxygenated conditions by PGE_2, endothelin-1, and chemokines. Since many of these biological mediators are increased systemically and locally in sickle cell disease, it is possible sickle cells may also dehydrate in the absence of deoxygenation. Studies on the Gardos channel of sickle erythrocytes have led to testing of specific inhibitors *in vivo*: the imidazole antimy-cotic clotrimazole (CLT) showed promising cellular effects *in vivo* which led to the development of a novel compound (ICA-17043) currently in phase II clinical trials.[1] *In vivo* studies with clotrimazole in normal human subjects and control mice showed no significant changes in erythrocyte volume and K content, supporting the idea that the Gardos channel does not play a role in regulating ion content of normal cells. However, the Gardos channel seems to play a role in controlling cell volume in other hematological conditions: Halperin et al.[2] have shown that complement-induced hemolysis is modulated and reduced by K loss via the Gardos pathway. A role of the Gardos channel in hereditary spherocytosis (HS) has been advocated for a long time but with little experimental evidence. We have studied the ion transport properties and the effects of *in vivo* Gardos channel blockade in a mouse model with complete deficiency of all 4.1 proteins isoforms.[3] 4.1-/- erythrocytes exhibit cell dehydration, with reduced cell K content and markedly increased Na content and permeability to Na, mostly mediated by Na/H exchange. The Na/H exchange of 4.1-/- cells is markedly activated by exposure to hypertonic conditions and exhibits an abnormal dependence on osmolarity and internal pH. In 4.1 -/- erythrocytes, the V_{max} of the Gardos channel is significantly higher than in controls (from 9.75 ± 1.06 vs. 6.08 ± mmol/L cell x min, $p<0.04$). In addition, 4.1 -/- erythrocytes showed a significantly lower affinity constant for internal Ca^{2+} (from 1.47 to 1.01 μM, $p<0.03$). When 4.1 -/- mice were treated with oral CLT, a Gardos channel blocker, worsening of anemia, increased mortality and increased cell dehydration/ fragmentation were noted. Essentially similar but less severe changes in red cell features were obtained *in vivo* with a CLT analog devoid of the imidazole moiety in 4.1 -/- mice, and with CLT

in 4.2-/-, and band 3 -/+ mice. The present data indicate that K and water loss via the Gardos channel may play a crucial role in compensating for the reduced surface membrane area of murine HS erythrocytes and protecting erythrocytes from lysis.

2. REFERENCES

1. (Stocker et al., Blood 2003; 101:2412)
2. Halperin et al. (J. Clin. Invest 1989; 83:1466)
3. Shi TS et al., J. Clin. Invest. 1999; 103:331)

* *Carlo Brugnara, Lucia De Franceschi, and Alicia Rivera, Children's Hospital Boston and Harvard Medical School, Boston, MA, USA; Department of Clinical and Experimental Medicine, Section of Internal Medicine, University of Verona, Verona, Italy*

37

SWELLING-ACTIVATED CALCIUM-DEPENDENT POTASSIUM CHANNELS IN AIRWAY EPITHELIAL CELLS

José M. Fernández-Fernández, Esther Vázquez, Maite Arniges, Muriel Nobles, Aoife Currid and Miguel A. Valverde*

1. ABSTRACT

Airway epithelial cells are exposed to changes in the osmolality of their environment under physiological and pathological conditions. The cell regulatory volume decrease (RVD) response triggered by hypotonic stress requires the coordinated activity of Cl^- and K^+ channels. We have investigated the molecular nature of K^+ channels mediating RVD response in human tracheal and bronchial epithelial cells. Our molecular, electrophysiological and pharmacological studies demonstrate the functional expression of calcium-dependent K^+ channels in human airways and their contribution to the RVD response. While the main swelling-activated K^+ channel in tracheal cells is an intermediate conductance potassium channel (IK, KCNN4),[1] in bronchial cells, a big conductance K^+ channel (BK, KCNMA1) is the key player.[2] Early work in murine small intestine have established a link between the cystic fibrosis transmembrane conductance regulator (CFTR) and volume regulation, suggesting the defective RVD response observed in murine intestinal crypts of cystic fibrosis (CF) mice is caused by the dysfunction of a calcium-dependent K^+ channel.[3, 4] Likewise, we have found that RVD response is impaired in both human CF tracheal[1] and bronchial epithelial cells. Furthermore, we have shown that this defect in volume regulation is due to the lack of swelling-induced activation of the calcium-dependent potassium channel mediating RVD response.[1] Our results suggest that, at least in bronchial epithelial cells, the increase in intracellular Ca^{2+} necessary for potassium channel activation in response to hypotonicity, is achieved by an increased Ca^{2+} entry

trough a swelling-activated cation channel. The molecular identity of this Ca^{2+} entry pathway might be related to TRPV4,[2] a TRP channel that has been described as responsive to changes in extracellular osmolarity.[5-7] Our more recent data also suggest the altered modulation of B (big conductance) K channels in response to cell swelling might be linked to alterations in regulation of the Ca^{2+} entry pathway in CF bronchial cells.

[Funded by the Spanish Ministry of Science and Technology - grant number SAF2000-0085.]

2. REFERENCES

1. E. Vázquez et al., *Proc Natl Acad Sci USA* **98**, 5329-5334 (2001).
2. J.M. Fernández-Fernández et al., *Am J Physiol Cell Physiol* **283,** C1705-C1714 (2002).
3. M.A. Valverde et al., *Proc Natl Acad Sci USA* **92,** 9038-9041 (1995).
4. M.A. Valverde et al., *Cell Physiol Biochem* **10**, 321-328 (2000).
5. W. Liedtke et al., *Cell* **103**, 525-535 (2002). _
6. R. Strotmann et al., *Nat Cell Biol* **2**, 695-702 (2000).
7. H. Watanabe et al., *J Biol Chem* **277**, 13569-13577 (2002).

***** *José M. Fernández-Fernández, Esther Vázquez, Maite Arniges, Muriel Nobles, Aoife Currid and Miguel A. Valverde***,** *Unitat de Senyalització Cellular, Departament de Ciències Experimentals i de la Salut, Universitat Pompeu Fabra, C/ Dr. Aiguader 80, 08003 Barcelona, Spain*

38

KCNQ CHANNELS ARE SENSORS OF CELL VOLUME

Morten Grunnet, Thomas Jespersen, Nanna K. Jørgensen, Nanna MacAulay, Nicole Schmitt, Olaf Pongs, Henrik S. Jensen, Søren-Peter Olesen and Dan A. Klaerke*

1. ABSTRACT[1]

Many important physiological processes involve changes in cell volume, e.g., the transport of salt and water in epithelial cells and the contraction of muscle cells. These cells respond to swelling with a so-called regulatory volume decrease which involves the activation of K^+ channels. However, the molecular identity of the involved K^+ channels has not been clear, and in particular, the mechanism for activation has been obscure.

To examine the effect of cell volume changes on cloned K^+ channels, voltage-regulated K^+ channels of the KCNQ type (KCNQ1-5) were co-expressed with aquaporin 1 water-channels (AQP1) in *Xenopus* oocytes to ensure adequate cell volume changes in response to altered extracellular osmolarity. The KCNQ1, KCNQ4 and KCNQ5 current amplitudes immediately responded to changes in cell volume; during cell swelling the currents increased by approximately 70% and decreased to approximately 50% of control during cell shrinkage. In fact, the currents through these channels precisely reflected the cell volume of the oocytes during small volume changes, whereas some saturation of the

responses was seen after volume changes above 5-10%. In all cases, the effects of changes in cell volume were readily reversible. In contrast, the related KCNQ2 and KCNQ3 channels, which are prominently expressed in neurons, were insensitive to cell volume changes. Incubation of the oocytes with cytochalasin D and experiments with truncated KCNQ1 channels suggested these channels sense cell volume changes through interactions between the cytoskeleton and the N-terminus of the channel protein. However, chimeras between the volume-sensitive KCNQ1 channels and the volume-insensitive KCNQ2 channels showed that the N-terminal of the KCNQ1 channels is necessary but not sufficient for the volume-sensitivity of the KCNQ channels.

In conclusion, we suggest certain KCNQ1 channels such as KCNQ1, KCNQ4 and KCNQ5 are strictly regulated by small changes in cell volume whereas others, e.g.. KCNQ2/3 are not. Regulation of K^+ channels by cell volume is most likely mediated through interactions between the cytoskeleton and certain parts of the K^+ channel proteins. This regulatory mechanism may explain how voltage-regulated ion channels are regulated during salt and water transport in epithelial cells where membrane potential is relatively constant.

2. REFERENCES

1. M. Grunnet, T. Jespersen, N. MacAulay, N.K. Jorgensen, N. Schmitt, O. Pongs, S.P. Olesen and D.A. Klaerke, KCNQ1 channels sense small changes in cell volume**,** *J. Physiol*., 2003, published online.

* *M. Grunnet, T. Jespersen, N.K.* Jørgensen, N. MacAulay, *Henrik S. Jensen, Søren-Peter Olesen and Dan A. Klaerke, Dept. of Medical Physiology, The Panum Institute, University of Copenhagen, Denmark, N. Schmitt and O. Pongs, Institut für Neuronale Signalverarbeitung, ZMNH, University of Hamburg, Germany*

39

MEMBRANE LOCALIZATION OF THE NEURONAL K-CL COTRANSPORTER (K-Cl COT, KCC2) IN RAT CEREBELLUM

Kenneth B.E. Gagnon, Peter K. Lauf, and Robert E.W. Fyffe*

1. INTRODUCTION

Chloride (Cl) together with bicarbonate is the most abundant free anion in living animal cells and is not distributed in thermodynamic equilibrium across the plasma membrane.[1] Upregulation of KCC2 (neuronal K-Cl COT isoform) by the second postnatal week implicates it as one of the main Cl extruders responsible for the neuronal GABA-receptor-mediated switch from depolarizing and excitatory to hyperpolarizing and inhibitory.[2]

Previous immunohistochemical studies with a polyconal rabbit antibody to an extracellular epitope of rat KCC2 (rb anti-rtKCC2 ECL) revealed wide-spread distribution of the neuronal K-Cl COT in brainstem, cerebrum, cerebellum and spinal cord.[3] In this study,

immunofluorescent secondary antibodies were used to determine the membrane distribution of KCC2 by co-localizing rb anti-rtKCC2 ECL immunolabeling with other primary antibodies to calbindin (a calcium binding protein) and glutamic acid decarboxylase (enzyme with converts glutamic acid to γ–amino butyric acid).

Basket cells, one of the principal interneurons in the molecular layer of the cerebellum, exhibited extensive dendritic and somatic labeling suggesting that, as an inhibitory neuron, Cl regulation is vital. Double immunofluorescent labeling with rb anti-rtKCC2 ECL and mouse anti-calbindin suggests KCC@ is also prominently distributed in the soma and proximal dendritic branching of Purkinje cells. Also, glutamic acid decarboxylase (GAD) is a marker for pre-synaptic boutons, thus the lack of co-localization between rb anti-rtKCC2 ECL and ms anti-GAD suggests KCC2 is post-synaptically distributed.

In summary: (i) KCC2 is distributed in the neuronal soma and dendritic processes of Purkinje and interneurons of rat cerebellum; and (ii) KCC2 appears to be post-synaptic.

1. F.J. Alvarez-Leefmans, S.M. Gamino, F. Giraldez and I. Nogueron, Intracellular chloride regulation in amphibian dorsal root ganglion neurones studied with ion-selective microelctrodes, *J Physiol,* **406,** 225-246 (1988).
2. G.H. Clayton, G.C. Owens, J.S. Wolff and R.L. Smith, Ontogeny of cation-Cl-cotransporter expression in rat neocortex, *Brain Res Dev Brain Res,* **109**, 281-92 (1998).
3. K.B.E. Gagnon, R.E.W. Fyffe, B Robertson and P.K. Lauf, Immunohistochemical staining of mature rat brain neurons by polyclonal antisera against two epitopes with KCC2, a neuronal isoform of K-Cl cotransport, In: *Soc. Neurosci.* New Orleans, LA, **A330**, 12 (2000).

* Kenneth B.E. Gagnon and Peter K. Lauf, Pathology Dept., Robert E.W. Fyffe, Anatomy & Physiology Dept., Wright State University, Dayton, OH 45435

40

K-Cl COTRANSPORT (K-Cl COT, KCC) ACTIVATION BY *N*-ETHYLMALEIMIDE IN C6 GLIOMA CELLS

Kenneth B.E. Gagnon, Norma C. Adragna, Robert E.W. Fyffe, and Peter K. Lauf*

1. ABSTRACT

Astrocytes make up greater than 50% of the cell population of the mammalian central nervous system and provide both structural and functional support to the neuronal population. Reverse transcriptase polymerase chain reaction[1], protein immunoblotting,[2] and immunohistochemical evidence[3] indicate the presence of both Na-K-2Cl cotransporter (COT) and K-Cl COT in astrocytes. Of the four known isoforms of the K-Cl COT, only KCC1 is present in C6 glioma cells.[4]

Rubidium (Rb) influx was measured in isotonic salt solution with/without 1 mM *N*-ethylmalemide (NEM), an established agonist of K-Cl COT and antagonist of Na-K-2Cl

COT.[5] Addition of pharmacological inhibitors allowed the total Rb influx to be separated into: the Na/K pump (1 mM ouabain), Na-K-2Cl COT (5 μM bumetanide), K-Cl COT (2mM furosemide), and ground permeability (furosemide-insensitive component). K-Cl COT was determined as the furosemide-sensitive Rb influx or the bumetanide-insensitive Cl-dependent Rb influx (flux in chloride minus flux in sulfamate).

Pre-treatment with NEM for 10 min stimulated the Na/K pump, K-Cl COT, and ground permeability by 200%, 600%, and 425%, respectively. In contrast, 10 min pre-treatment with NEM had no significant effect on Na-K-2Cl COT activity. A longer NEM pre-treatment (20 min) resulted in a loss of K-Cl COT stimulation consistent with findings in HEK293 and vascular smooth muscle cells.[6] Additionally, the Na-K-2Cl COT and ground permeability were inhibited by 100 and 600%, respectively. Bumetanide (20 μM) inhibited the NEM stimulation of bumetanide-insensitive Rb influx (K-Cl COT) by 80%. Intracellular K content remained constant regardless of pre-treatment with ouabain, bumetanide, and furosemide, but was reduced by 51-65% upon NEM pre-treatment, consistent with earlier findings in HEK293 cells.[7] Addition of furosemide completely prevented the NEM-induced intracellular K loss.

In summary: (i) NEM stimulated K-Cl COT in C6 glioma cells by 600%; (ii) stimulation of K-Cl COT after 10 min NEM pre-treatment (with no effect on Na-K-2Cl COT activity) suggests a difference in the activation coefficient between the two cotransporters in C6 glioma cells; (iii) loss of NEM stimulation of K-Cl COT (and nearly complete inhibition of Na-K-2Cl COT activity) as a function of NEM pre-treatment time suggests an additional component in the regulation of both Na-K-2Cl COT and K-Cl COT activity; and (iv) the furosemide-sensitive NEM-induced intracellular K loss may be due in part to K-Cl efflux through KCC1.

1. J.A. Payne, T.J. Stevenson, L.F. Donaldson, Molecular characterization of a putative K-Cl cotransporter in rat brain. A neuronal-specific isoform, *J Biol Chem*, **271**, 16245-52 (1996).
2. C.M. Gillen, S. Brill, J.A. Payne, B. Forbush, III, Molecular cloning and functional expression of the K-Cl cotransporter from rabbit, rat, and human. A new member of the cation-chloride cotransporter family, *J Biol Chem*, **271**, 16237-44 (1996).
3. T.Q. Vu, J.A. Payne, D.R. Copenhagen, Localization and developmental expression patterns of the neuronal K-Cl cotransporter (KCC2) in the rat retina, *J Neurosci*., **20**, 1414-23 (2000).
4. K.B.E. Gagnon, R.E.W. Fyffe, M. Di Fulvio, N.C. Adragna, P.K. Lauf, Properties of K-Cl cotransport (COT) in C6 Glioma cells, *FASEB J,* **16** A640 (2002).
5. P.K. Lauf, N.C. Adragna, K-Cl cotransport: properties and molecular mechanism, *Cell Physiol Biochem*, **10**, 341-54 (2000).
6. P.K. Lauf, J. Zhang, J. Zhang, N.C. Adragna, Transient nature of the stimulatory 'NEM effect' on K-Cl cotransport in KCC1-transfected HEK293 and primary rat aortic smooth muscle cells, *J Gen Physiol*, **116**, 20A (2000).
7. P.K. Lauf, J. Zhang, K.B. Gagnon, E. Delpire, R.E. Fyffe, N.C. Adragna, K-Cl cotransport: immunohistochemical and ion flux studies in human embryonic kidney (HEK293) cells transfected with full-length and C-terminal-domain-truncated KCC1 cDNAs, *Cell Physiol Biochem,***11**, 143-60 (2001).

* Kenneth B.E. Gagnon and Peter K. Lauf, Pathology Dept., Norma C. Adragna, Pharmacology & Toxicology Dept., Robert E.W. Fyffe, Anatomy & Physiology Dept., Wright State University, Dayton, OH 45435.

41

EXPRESSION OF PLASMA MEMBRANE CA^{2+} ATPASE IN CRAYFISH DURING MOLTING

Y.P. Gao, M. Nade and M.G. Wheatly*

1. INTRODUCTION

Plasma membrane calcium ATPases (*PMCAs*) are ubiquitously expressed proteins that couple the extrusion of calcium across the plasma membrane with the hydrolysis of ATP.[1] Together with Na^+/Ca^{2+} exchangers (NCX), they are the major plasma membrane transport system responsible for the longterm regulation of resting intracellular Ca^{2+} concentration.[2] Mammalian *PMCAs* are encoded by four separate genes, and additional isoform variants are generated via alternative RNA splicing of the primary gene transcripts. Expression of different *PMCA* isoforms and splice variants in mammals is regulated in a developmental, tissue- and cell type-specific manner, suggesting these pumps are functionally adapted to the physiological needs of particular cells and tissues.[3-6]

A few *PMCA* genes have been cloned from non-mammalian species including the invertebrates, *C. elegans*[7] and crayfish (GenBank accession No. AY455931) and some lower vertebrates including tilapia (GenBank accession No. P58165) and bullfrog (GenBank accession No. AF337955 and AF337956). However, tissue specific PMCA expression has not been studied in invertebrates. The natural molting cycle of crayfish, *Procambarus clarkii*, is an ideal model for the study of discontinuous Ca^{2+} homeostasis.[8] Our previous work has indicated that the sarco/endoplasmic reticulum Ca^{2+} ATPase (SERCA) is expressed in a wide range of tissues and that expression in both tail and heart muscle is downregulated during periods of elevated Ca^{2+} flux (pre/postmolt[9-10]) compared with intermolt (zero net flux). This study focuses on the tissue distribution and differential expression of crayfish kidney *PMCA3* as a function of the molting cycle.

2. EXPERIMENTAL

Total RNA was isolated from gill, kidney, heart and tail muscle utilizing the TriZol reagent (Invitrogen). Northern blot analysis was performed to determine levels of *PMCA3* expression using a 1000 bp fragment corresponding to the crayfish *PMCA3* as a probe. Membrane protein from the same tissues was extracted and resolved in 7.5% SDS-PAGE. A polyclonal antibody against crayfish PMCA3 protein generated in our lab was used as probe. ECL chemiluminescent protein detection system was used to detect the proteins. For the *in-situ* hybridization study, crayfish kidneys at different molting phases

were fixed with 4% paraformaldehyde and 20% sucrose and sectioned. The sections were then mounted on slides and hybridized with a TdT labeled 42 bp *PMCA3* probe. The slides were loaded in a Fuji cassette and scanned after three days on the Fuji imaging system and the data were visualized with Visual Imaging software.

3. RESULTS AND DISCUSSION

The tissue distribution of crayfish *PMCA3* gene was examined using a Northern blot of total RNA from crayfish gill, kidney, heart and tail muscle tissues probed with the 1000 bp fragment initially isolated. A 7.5 kb band was expressed in all four tissues tested (Figure 1).

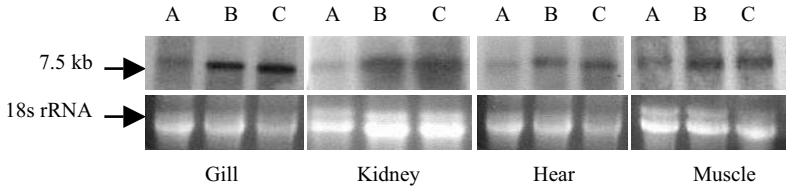

Figure 1. Expression of *PMCA3* mRNA in different tissues of crayfish during molting. 18s rRNA band serves as the control. A: intermolt, B: premolt and C: postmolt

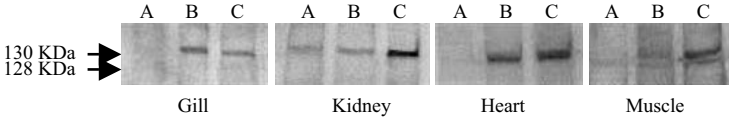

Figure 2. Expression of PMCA3 protein in different tissues of crayfish during molting. A: Intermolt, B: premolt and C: postmolt.

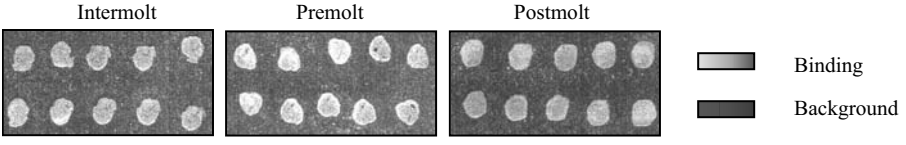

Figure 3. In situ hybridization of PMCA3 in kidney of crayfish during molting.

The expression level of *PMCA3* mRNA in all four tissues examined was upregulated during pre- and postmolt compared with intermolt (Figure 1). Similar to the expression of mRNA, a 130 kDa major protein band was expressed in kidney, gill, heart and tail muscle. The expression level was very low in the intermolt stage, and increased markedly during pre/post molt (Figure 2). *In situ* hybridization in kidney confirmed that PMCA expression was upregulated in pre- and postmolt and that distribution was concentrated on the margins of the kidney (location of the kidney tubule Figure 3).

4. CONCLUSIONS

Northern blot analysis indicated that the level of *PMCA3* mRNA expression in all tissues increased significantly in pre/postmolt stages as compared to a very low level in the intermolt stage. Similar expression patterns were confirmed at the protein level by Western blotting. *In situ* hybridization confirmed that PMCA3 expression is increased in pre- and postmolt in kidney. Collectively these results indicate that the crayfish *PMCA3* plays a crucial role in maintaining Ca^{2+} homeostasis during the fluctuations in Ca^{2+} flux associated with the crayfish molting cycle.

5. ACKNOWLEDGMENTS

This research was supported by NSF grant IBN 0076035 to MGW.

1. E.E. Strehler and D.A. Zacharias, Role of alternative splicing in generating isoform diversity among plasma membrane calcium pumps. *Physiol. Rev*. **81**, 21-50 (2001).
2. E.E. Strehler, In: Principles of Medical Biology, edited by E. E. Bittar and N. Bittar (Greenwich, 1996), pp. 125-150.
3. Zacharias and C. Kappen, Developmental expression of the four plasma membrane calcium ATPase (*PMCA*) genes in the mouse*. Biophys. Acta*. **1428**, 397-405 (1999).
4. E. Guerini, A. Garcia-Martin, A. Gerber, C. Volbracht, M. Leist, C. Gutierrez Merino and E. E. Carafoli, The expression of plasma membrane Ca^{2+} pump isoforms in cerebellar granule neurons is modulated by Ca^{2+}. *J. Biol. Chem.* **274**, 1667-1676 (1999).
5. S. Carafoli and T. Stauffer, The plasma membrane calcium pump: functional domains, regulation of the activity, and tissue specificity of isoform expression. *J. Neurobiol.* **25**, 312-324 (1994).
6. J. Lehotsky, Distribution of plasma membrane Ca^{2+} pump (PMCA) isoforms in the gerbil brain: effect of ischemia-reperfusion injury. *Mol. Chem. Neuropathol*. **25**, 175-187 (1999).
7. N. Kraev and E.E. Carafoli, Identification and functional expression of the plasma membrane calcium ATPase gene family from *Caenorhabditis elegans. J. Biol. Chem.* **274**, 4254-8 (1999).
8. M.G. Wheatly, Calcium homeostasis in Crustacea: the evolving role of branchial, renal, digestive and hypodermal epithelia. *J. Exp. Zool.* **283**, 277-284 (1999).
9. Z. Zhang, D. Chen and M.G. Wheatly, Cloning and characterization of sarco/endoplasmic reticulum Ca^{2+}-ATPase (SERCA) from crayfish axial muscle. *J. Exp. Biol.***203,** 3411-3423 (2000).
10. D. Chen, Z. Zhang, M.G. Wheatly and Y. Gao, Cloning and characterization of the heart muscle isoform of sarco/endoplasmic reticulum Ca^{2+} ATPase (SERCA) from crayfish. *J. Exp. Biol.* **205**, 2677-2686 (2002).

* Y.P. Gao, M. Nade and M.G. Wheatly, Department of Biological Sciences, Wright State University, Dayton, OH 45435 USA

42

SALINITY AFFECTS CRAYFISH PMCA AND NCX EXPRESSION

Y. P. Gao and M. G. Wheatly*

1. INTRODUCTION

Crayfish, native to freshwater, maintain body fluid concentrations above ambient by active uptake of ions at the gills and reabsorption from primary filtrate resulting in urinary dilution.[1] They also have epithelial membranes that are relatively impermeable to passive ion loss. The cellular model for epithelial Ca^{2+} uptake (influx) involves two stages: Ca^{2+} initially enters passively through epithelial Ca^{2+} channels (ECaC) in the apical membrane, then exits the basolateral membrane actively through the combined actions of the plasma membrane Ca^{2+}-ATPase (PMCA) and a Na^{+}/Ca^{2+} exchanger (NCX).[2] These two energy-dependent transmembrane proteins are responsible for routine regulation of intracellular Ca^{2+} concentration as well as mediating mass vectorial flux. We recently cloned a full-length *PMCA3* and a partial *NCX* from crayfish kidney and explored expression patterns as a function of the molting cycle. We have shown that expression of both proteins increases when Ca^{2+} influx is elevated in pre/postmolt (compared with intermolt). As molting is hormonally controlled, we chose to explore salinity stress (70% salt water, SW) as a convenient way to alter the electrochemical gradient for Ca^{2+} across the apical membrane in intermolt crayfish and in so doing, elevate intracellular Ca^{2+} artificially. Others have conducted similar studies in fish.[2-6]

2. EXPERIMENTAL

Crayfish *Procambarus clarkii* were obtained from Carolina Biological Supply and maintained in 40 L aquaria with filtered aerated water. After crayfish were transferred to 70% salt water at room temperature, gill, liver and kidney tissues were removed from three animals at 1 day, 3 days, 5 days and 7 days. Total RNA was isolated from gill, kidney and liver utilizing the TriZol reagent (Invitrogen).

Northern blot analysis was performed to determine the expression of *PMCA3* and *NCX* in gill, liver and kidney tissues using a 1000 bp fragment corresponding to the crayfish *PMCA3* and a 840bp fragment corresponding to the crayfish *NCX* as probes.

3. RESULTS AND DISCUSSION

The expression of *PMCA3* and *NCX* in gill increased significantly after 1 day when crayfish were transferred from fresh water to 70% salt water and remained high for one week salinity exposure (Figure 1). Similarly, expression of *PMCA3* and *NCX* in kidney increased significantly after 1 day when crayfish were transferred from fresh water to 70% salt water and remained high for an entire week (Figure 2). Expression of *PMCA3* and *NCX* in liver was unaffected by transfer to salt water (Figure 3). Flik et al.[2] reported that the NCX exchanger and PMCA activities increased almost fivefold and eightfold, respectively, after freshwater trout were acclimated to 70% sea water. However, no significant difference was found in killifish.[5]

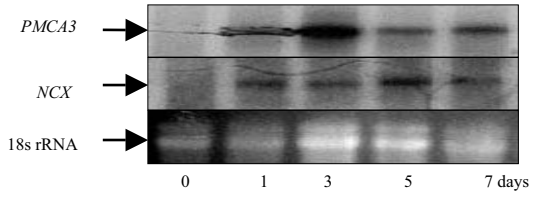

Figure 1. Expression of *NCX* and *PMCA3* in gill with days after transfer to 70% salt water. 18s rRNA band serves as the control.

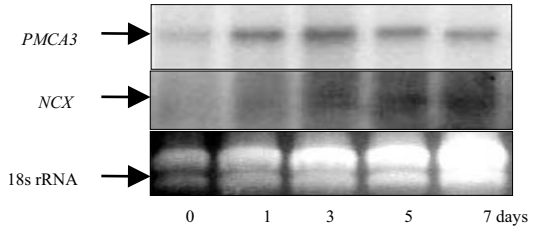

Figure 2. Expression of *NCX* and *PMCA3* in kidney with days after transfer to 70% salt water. 18s rRNA band serves as the control.

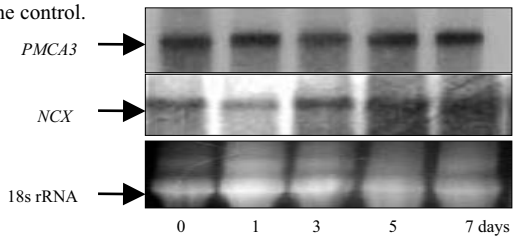

Figure 3. Expression of *NCX* and *PMCA3* in liver with days after transfer to 70% salt water. 18s rRNA band serves as the control.

4. CONCLUSION

Exposure to elevated external Ca^{2+} resulted in upregulation of *PMCA3* and *NCX* in both gill and kidney; however, expression in liver remained unchanged. Gill and kidney appear to respond to elevated apical Ca^{2+} entry with increased basolateral efflux. The

liver may be pre-adapted to handle Ca^{2+} load in the diet and, as such, does not need to increased expression of basolateral export mechanisms when environmental levels are elevated. We will further explore these trends through protein analysis.

5. ACKNOWLEDGMENTS

This research was supported by NSF grant IBN 0076035 to MGW.

1. M.G. Wheatly, Calcium homeostasis in crustacea: the evolving role of branchial, renal, digestive and hypodermal epithelia. *J. Exp. Zool.* **283,** 277-284 (1999).
2. G. Flik, T. Kaneno, A. M. Greeo, J. Li and J. C. Fenwick, *Fish Physiol. Biochem.* **17,** 385-396 (1997).
3. S.F. Perry, A. Shahsavarani, T. Georgalis, M. Bayaa, M. Furimsky and S.L.Y. Thomas, Integrated responses of Na^+/HCO_3^- cotransporters and V-type H^+-ATPases in the fish gill and kidney during respiratory acidosis. *J. Exp. Zool.* **300**, 53-63 (2003).
4. G. Flik and C. Haond, Na^+ and Ca^{2+} pumps in the gills, epipodites and branchiostegites of the european lobster Homarus gammarus: effects of dilute sea water. *J. Exp. Biol.* **203**, 213-220 (2000).
5. P.M. Verbost, S.E. Bryson, S.E.W. Bonga and W.S. Marshall, Na^+-dependent Ca^{2+} uptake in isolated opercular epithelium of Fundulus heteroclitus. *J. Comp. Physiol. B* **167**, 205-212 (1997).
6. W.S. Marshall, Na^+, Cl^-, Ca^{2+} and Zn^{2+} transport by fish gills: retrospective review and prospective synthesis. *J. Exp. Zool.* **293**, 264-283 (2002).

* Y. P. Gao and M. G. Wheatly, Department of Biological Sciences, Wright State University, Dayton, OH 45435 USA

43

CRAYFISH EPITHELIAL CA^{2+} CHANNEL-LIKE GENE (*ECAC*)

Y.P. Gao and M.G. Wheatly*

1. INTRODUCTION

The crustacean molting cycle has become a model for studying Ca^{2+} transporting proteins in epithelia (gills, liver, kidney) of lobsters,[1] crabs[2-3] and crayfish.[4-7] Crustaceans alternate between periods of Ca balance (intermolt), Ca loss (premolt) and impressive Ca uptake (postmolt cuticular mineralization). Physiological approaches have focused on the energy-dependent processes involved in Ca^{2+} influx primarily at the basolateral membrane (plasma membrane calcium ATPase, PMCA and sodium/calcium exchanger, NCX) and to a lesser extent at the apical membrane (NHE/CaHE and NCX). Implicit in the accepted model for epithelial Ca^{2+} uptake is that entry across the apical membrane is primarily passive and mediated via Ca channels.

The epithelial Ca^{2+} channel (ECaC) was first discovered in rat kidney in 1999[8] and then cloned from rabbit,[9] human,[9] and mouse kidney[10, 11] as well as gill of puffer fish (accession No. AY232821) and rainbow trout (accession No. AY256348). The ECaC is an

apical channel involved in Ca^{2+} entry that serves as a gatekeeper in transcellular Ca^{2+} (re)absorption and in so doing plays a critical role in the maintenance of intracellular Ca^{2+} homeostasis. To better understand Ca^{2+} (re)absorption during crayfish molting, this study attempted to clone and functionally characterize *ECaC* from freshwater crayfish (*Procambarus clarkii*) tissues.

2. EXPERIMENTAL

Based on published *ECaC* sequences, two primers were designed to target a fragment of approximately 1032 bp. RT-PCR was conducted using first strand cDNA from postmolt crayfish kidney. 3' and 5' RACE systems for rapid amplification of cDNA ends were performed. Distribution of crayfish *ECaC* in different tissues and expression in kidney throughout the molting cycle were evaluated by quantitative PCR.

3. RESULTS AND DISCUSSION

A full-length cDNA of *ECaC* was obtained from crayfish kidney. It consisted of 2,687 bp with an open reading frame of 2,169 bp encoding a protein of 722 amino acids with a predicted molecular mass of 87 kDa. A GenBank search revealed that the crayfish *ECaC* showed high homology (60-80%) to published *ECaCs* from distant subgroups including puffer fish *ECaC*, rainbow trout *ECaC*, human *ECaC*, rabbit *ECaC* and rat *CaT1* (Figure 1).

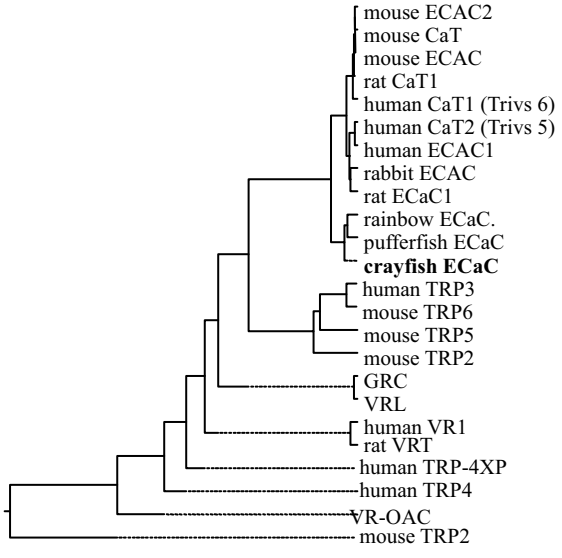

Figure 1. Phylogram based on full-length sequence of ECaCs and other ion channels.

A search in the protein database also revealed a significant but low homology (20%) to previously published ion channels. With primers specific to the crayfish *ECaC*, a 1032

bp product corresponding to the expected size was intensely amplified in kidney and gill (both Ca transporting epithelia), but no signals were detected from other tissues including unfertilized egg, axial muscle, cardiac muscle and liver (Figure 2A). Compared with intermolt, expression of crayfish *ECaC* increased in kidney in the premolt and the postmolt phases of the molting cycle (Figure 2B) associated with elevated transepithelial Ca flux.

Figure 2A

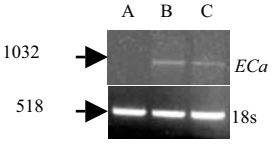

Figure 2B

Figure 2A. Distribution of crayfish *ECaC* in a panel of crayfish tissue cDNA. Expected length of the PCR fragments (bp) is indicated with an arrow. The amplified 18s fragment demonstrates the integrity of the cDNA samples. E; egg, T; tail muscle, H; heart, L; liver, G; gill and K; kidney. **Figure 2B.** Expression of ECaC in kidney during moulting. The amplified 18s fragment demonstrates the integrity of the cDNA samples. A; intermolt, B; premolt and C; postmolt.

4. CONCLUSIONS

ECaC is upregulated in pre- and postmolt stage (compared with intermolt) associated with elevated renal Ca^{2+} (re)absorption. Basolateral *PMCA3* expression exhibited a similar profile in other studies. Collectively these results indicate that the expression of genes controlling Ca entry (apical, *ECaC*) and exit (basolateral, *PMCA*) from epithelial cells are closely coordinated. *ECaC* was more abundant in epithelial tissues that effect Ca^{2+} translocation (gill, kidney) than in non-epithelial tissues.

5. ACKNOWLEDGMENTS

This research was supported by NSF grant IBN 0076035 to MGW.

1. G.A. Ahearn, and Z. Zhuang, Cellular mechanisms of calcium transport in crustaceans. *Physiol. Zool*. **69**, 383-402 (1996).
2. C. Lucu and G. Flik, Na+-K+-ATPase and Na+/Ca2+ exchange activities in gills of hyperregulating Carcinus maenas. *Am. J. Physiol*. **276**, 490-9 (1999).
3. G. Flik , P.M. Verbost, W. Atsma and C. Lucu, calcium transport in gill plasma membrane of crab *Carcinus maenas*; evidence for carriers driven by ATP and Na^+ gradient. *J. Exp. Biol*. **195**, 109-22 (1994).
4. M.G. Wheatly, Z. Zhang , J. Weil, J. Rogers, L. Stiner , Localization and molecular characterization of the crayfish NCX. *J Exp. Biol*. **204**, 959-66 (2001).
5. M.G. Wheatly, R.C, Pence, J.R. Weil, ATP-dependent calcium uptake into basolateral vesicles from transporting epithelia of intermolt crayfish .*Am. J. Physiol*. **276**, 566-74 (1999).
6. M.G. Wheatly, Crustacean models for study calcium transport: the journey from whole organisms to molecular mechanisms. *J. Mar. Biol*. **77**, 107-125 (1997).
7. M.G. Wheatly, and T. Toop, physiological responses of the crayfish *Pacifastacus leniusculus* (Dana0) to environmental hyperoxia. II. The role of the antennal gland. *J. Exp. Biol*. **143**, 53-70 (1989).

8. J.B. Peng, X.Z.Chen, U.V. Berger, P.M, Vassilev, H. Tsukaguchi, E.M, Brown and M.A. Hedige, Molecular cloning and characterization of a channel-like transporter mediating intestinal calcium absorption. *J. Biol. Chem.* **274**, 22739-46(1999).
9. D. Müller, J.G.J., Hoenderop, IC, Meij, LPJ. van den Heuvel, MVAM. Knoers, AI. den Hollander, P. Eggert, V. García-Nieto, F. Claverie-Martín and RJM Bindels, Molecular cloning, tissue distribution, and chromosomal mapping of the human epithelial Ca2+ channel (ECAC1). *Genomics* **67**, 48-53 (2000).
10. K. Weber, R.G. Erben, A. Rump, J. Adamski, Gene structure and regulation of the murine epithelial calcium channels ECaC1 and 2. *Biochem Biophys Res Commun.* **289**, 1287-94 (2000).
11. M. Suzuki, K. Ishibashi, G. Ooki, S. Tsuruoka, M. Imai, Electrophysiologic characteristics of the Ca-permeable channels, ECaC and CaT, in the kidney. *Biochem Biophys Res Commun*. **274**, 344-9(2002).

* Y.P. Gao and M.G. Wheatly, Department of Biological Science, Wright State University, Dayton, OH 45435, USA

44

MODULATION OF KCNQ4 CHANNELS BY CHANGES IN CELL VOLUME

Charlotte Hougaard, Dan A. Klaerke, Søren-Peter Olesen, Else K. Hoffmann, and Nanna K. Jorgensen*

1. INTRODUCTION AND RESULTS

Most cell types respond to cell swelling by undergoing a regulatory volume decrease (RVD) response often mediated by KCl loss through separate K^+ and Cl^- channels. We have investigated the sensitivity of KCNQ4 channels toward changes in cell volume as well as cellular signalling pathways involved in channel regulation. KCNQ4 channels were expressed in HEK-293 cells and studied using the whole-cell patch-clamp technique.

Exposing KCNQ4-expressing HEK-293 cells to a hyposmotic (200 mOsm) solution resulted in a rapid increase in the K^+ current amplitude whereas a hyperosmotic (400 mOsm) cell shrinkage completely abolished the current (Figure 1A). In untransfected HEK-293 cells virtually no K^+ current was observed under iso- or hyposmotic condi-tions. The KCNQ channel inhibitors linopirdine and bepridil completely blocked the iso- and swelling-induced K^+ current in KCNQ4-expresssing cells corroborating that the swelling-induced K^+ current was KCNQ4 mediated.[1]

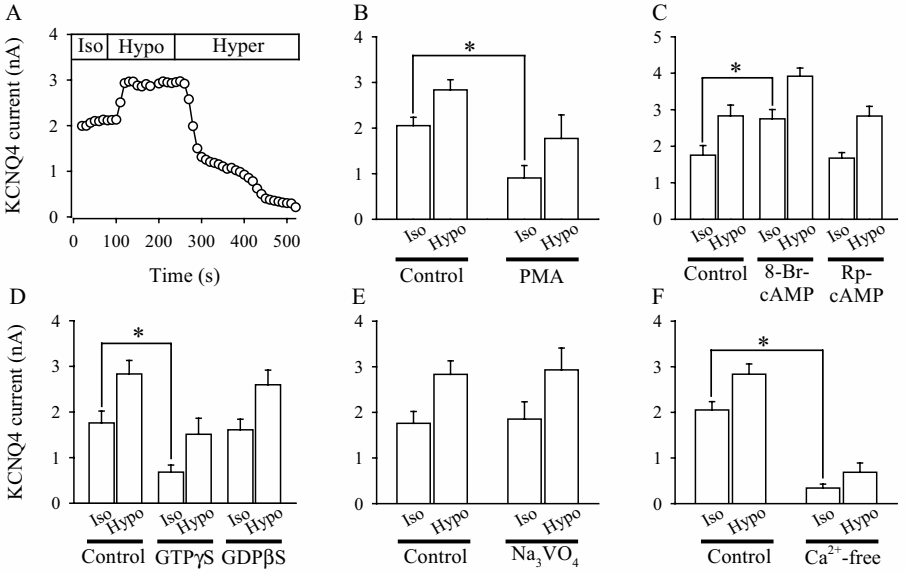

Figure 1. Modulation of KCNQ4 current by osmotic changes and cellular signalling pathways. HEK-293 cell stably expressing KCNQ4 channels used for experiments. Standard whole-cell patch-clamp experiments conducted as described in.[1] **A.** Effect of osmotic changes on KCNQ4 current. KCNQ4 current measured at equilibrium potential for Cl^-. Extracellular osmolarity changed by omission/addition of D-mannitol (n=16). **B.** PKC as modulator of KCNQ4 activity. PKC activated by addition of 100 nM PMA to the extracellular solution (n=6 for PMA, n=16 for control). **C.** PKA as modulator of KCNQ4 channels. PKA activated or inhibited by addition of 8-Br-cAMP (1 mM, n=9) or Rp-cAMP (1 mM, n=5), respectively, to pipette solution, n=10 for control. **D.** Role of G proteins in modulation of KCNQ4 channels. G proteins activated or inhibited by addition of GTPγS (40 μM, n=7) or GDPβS (1 mM, n=6), respectively, n=10 for control. **E.** Role of tyrosine phosphatases in modulation of KCNQ4 activity. Na_3VO_4 (400 μM, n=5) added to the pipette solution, n=10 for control. **F.** Role of Ca^{2+} in modulation of KCNQ4 activity. Experiments conducted at permissive Ca^{2+} level (0.1 mM EGTA; n=16, Control) or in absence of Ca^{2+} (10 mM EGTA, n=7). * indicates $p<0.05$, student's *t*-test for unpaired observations. NOTE: KCNQ4 current after swelling in all experiments significantly higher than under isosmotic conditions and swelling-induced increase in current was not significantly different in treated and untreated cells except in F. Data previously reported in.[1]

The observation that channels are activated by cell swelling in patch-clamp experiments does not *per se* demonstrate that they are involved in RVD in intact cells. However, linopirdine significantly inhibited the RVD process in KCNQ4-expressing HEK-293 cells verifying that KCNQ4 channels are activated by cell swelling in intact cells and contribute to volume regulation following osmotic cell swelling.[1]

Modulation of KCNQ4 channel activity by cellular signalling pathways is essentially un-described. We investigated the possible role of classical pathways such as PKC, PKA, tyrosine phosphorylation, G proteins and Ca^{2+} as modulators of KCNQ4 activity both under iso- and hyposmotic conditions.[1] Interference with these pathways has prominent effects on swelling-induced osmolyte loss and RVD in numerous cell types.[2] Under isosmotic conditions the KCNQ4 current amplitude was increased following stimulation of PKA (8-Br-cAMP, Figure 1C), but reduced after activation of PKC (PMA, Figure 1B) or stimulation of G proteins (GTPγS, Figure 1D). Although stimulation of PKA and G proteins modulated the KCNQ4 current, their activation is not required for normal

channel activity as witnessed by the lack of effect of PKA and G protein inhibitors (Rp-cAMP, Figure 1C and GDP S, Figure 1D, respectively) on the KCNQ4 current under isosmotic conditions. Stimulation of either PKA, PKC or G proteins failed to affect the potentiation of the KCNQ4 current by cell swelling, suggesting that they are not involved in a signalling pathway leading to increased KCNQ4 activity following cell swelling (Figure 1B-D). Both the isosmotic and the swelling-activated KCNQ4 current were unaffected by the protein tyrosine phosphatase inhibitor Na_3VO_4 (Figure 1E) and the *src* kinase inhibitor PP2, arguing against an important role of tyrosine phosphorylation events in the regulation of KCNQ4 channels. Removal of intra- and extracellular Ca^{2+} suppressed the KCNQ4 current under both iso- and hyposmotic conditions (Figure 1F). However, in the absence of Ca^{2+}, cell swelling still produced a significant increase in the KCNQ4 current amplitude, demonstrating that Ca^{2+} is not the primary messenger responsible for activation of KCNQ4 channels after cell swelling.

1. C. Hougaard, D.A. Klaerke, E.K. Hoffmann, S-P Olesen, and N.K. Jorgensen, Modulation of KCNQ4 channel activity by changes in cell volume, In press: *Biochim. Biophys. Acta* (2003).
2. F. Lang, G.L. Busch, M. Ritter, H. Volkl, S. Waldegger, E. Gulbins, and D. Häussinger, Functional significance of cell volume regulatory mechanisms, *Physiol. Rev.* **78,** 247-306 (1998).

* Charlotte Hougaard and Else K. Hoffmann, Biochemical Department, August Krogh Institute, Universitetsparken 13, DK-2100 Copenhagen O, Denmark. Dan A. Klaerke, Søren-Peter Olesen and Nanna K. Jorgensen, Department of Medical Physiology, The Panum Institute, Blegdamsvej 3, DK-2200 Copenhagen N, Denmark

45

PKA PHOSPHORYLATION OF SGK MODULATES ADH-STIMULATED Na^+ TRANSPORT IN A6 MODEL RENAL CELLS

Nathan Kast, Nicola Perrotti and Bonnie L. Blazer-Yost

1. ABSTRACT

The A6 cell line, derived from the kidney of *Xenopus laevis*, is a well-characterized cell culture model of the principal cells of the mammalian distal nephron. In this high resistance cell line, serosal application of insulin, ADH (anti-diuretic hormone) or aldosterone results in a stimulation of transcellular Na^+ transport.

Previous work from our laboratories[1, 2] has shown that activation of a kinase involved in the phosphoinositide pathway, sgk (serum glucocorticoid-induced kinase), is required for basal as well as hormone stimulated transport. Expression of a dominant negative, kinase dead, mutant of sgk abrogates the activity of the endogenous enzyme and results in a decrease of basal transport as well as inhibition of hormone stimulated transport. Conversely, over-expression of wt sgk potentiates basal and ADH-stimulated

Na^+ transport with no effect on insulin- or aldosterone-stimulated transport, suggesting that activation of sgk is a rate-limiting step in the ADH-stimulated pathway but not the pathways stimulated in response to the other two hormones. PKA (cAMP-dependent protein kinase A) is activated in response to ADH stimulation and could potentially phosphorylate sgk. Therefore, we produced A6 cell lines stably expressing sgk-T369A, a form of the enzyme containing a mutation in a PKA phosphorylation site.

The resulting cell lines exhibited normal insulin-stimulated transport (data not shown). However, as shown in Figure 1, the basal transport rate as well as the natriferic (salt retaining) response to ADH was diminished in the cells stably expressing sgk-T369A. These data show that expression of the mutant enzyme negatively affects ADH-stimulated Na^+ transport. The most likely explanation is that the mutant form of sgk competes with the wt endogenous isoform. These results, together with our previous findings, indicate that sgk phosphorylation by PKA is an integral and likely rate-limiting step in the Na^+ transport response elicited by ADH.

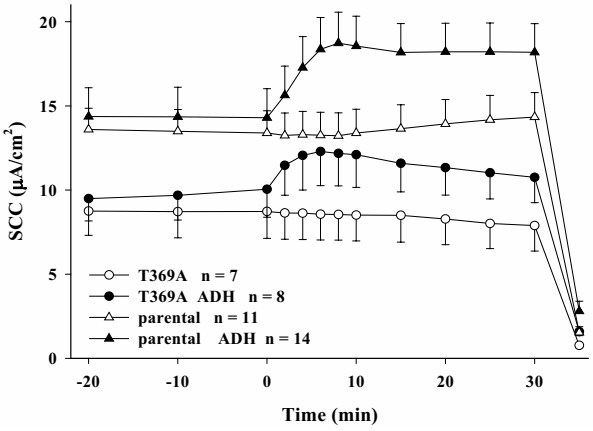

Figure 1. ADH stimulated ion transport in the A6 cell line. SCC = short circuit current, a measure of net ion transport in high resistance epithelial monolayers.[3] Parental cell lines are indicated by the triangular shapes; cell lines stably expressing the sgk mutant, T369A, are indicated by circular shapes. ADH (100 mU/ml) was added at T=0 to the cultures indicated by the filled symbols. Amiloride (10^{-5}M) was added to all experiments at t=30 minutes to indicate the proportion of the transport due to net Na^+ transport. Symbols are $\pm$ S.E.M. The basal currents of the T369A cells were significantly lower than the parental line at each time point measured ($P<0.05$). The ADH-stimulated increase in current at maximum (8 min) was significantly higher in the parental cells than in the mutant line ($P<0.005$).

2. ACKNOWLEDGMENTS

These studies were supported by an Indiana University – Purdue University Undergraduate Research Opportunities Program and a COFIN/FIRB 2002 grant from the Italian Department of Education.

1. C.J. Faletti, N. Perrotti, S.I. Taylor and B.L. Blazer-Yost, sgk: An essential convergence point for peptide and steroid hormone regulation of ENaC-mediated Na^+ transport, *Am. J. Physiol. Cell Physiol.*

282, C494-C500 (2002).
2. N. Perrotti, R.A. He, S.A. Phillips, C.R. Haft and S.I. Taylor, Activation of serum- and glucocorticoid-induced protein kinase (sgk) by cyclic AMP and insulin, *J. Biol. Chem.* **276**, 9406-9412 (2001).
3. H.H. Ussing and K. Zerahn, Active transport of sodium as the source of electric current in the short-circuited isolate frog skin, *Acta. Physiol. Scand.* **23**, 110-127 (1951).

* Nathan Kast and Bonnie L. Blazer-Yost, Biology Department, Indiana University–Purdue University at Indianapolis, IN 46202. Nicola Perrotti, Dipartimento di Medicina Sperimentale e Clinica, Universita Magna Graecia, Catanzaro, Italy

46

CELL VOLUME MODIFIES AN ATP-SENSITIVE ANION CONDUCTANCE IN CULTURED HIPPOCAMPAL ASTROCYTES

Guangze Li and James E. Olson*

1. INTRODUCTION

Maintenance and regulation of cell volume are fundamental physiological processes. Previous data showed that swelling of cultured rat astrocytes in 220 mOsm medium activates an outwardly rectifying anion current.[1] This current is considered to be mediated by a chloride channel that also conducts the amino acid taurine. The mechanism by which cell swelling activates chloride conductance is not clear; however, recent studies support an important role for extracellular ATP in swelling-induced amino acid efflux[2] and anion current activation.[3] Herein, we will examine the interaction between volume and ATP in cultured rat hippocampal astrocytes.

2. EXPERIMENTAL

Hippocampal astrocytes were prepared using methods previously described for cerebral cortical astrocytes.[4] Electrophysiological studies were performed after 2-4 weeks *in vitro*. Whole cell patch clamp recordings were made from cells maintained at 35±0.5°C. The components of isosmotic CsCl electrode and perfusion solutions were prepared as previously described.[5] Hyposmotic perfusion solution (250 mOsm) was identical to isosmotic perfusion solution but contained less sucrose. Non-selective cation currents were eliminated by adding 1 mM TEA and 300 μM $NiCl_2$ to the perfusion solution. Under these conditions, Cl^- is the predominant charge carrier through the astrocyte cell membrane.[1] Membrane currents were measured in voltage-clamp mode every 30 sec during 90 msec voltage steps to final values ranging between -120 mV and

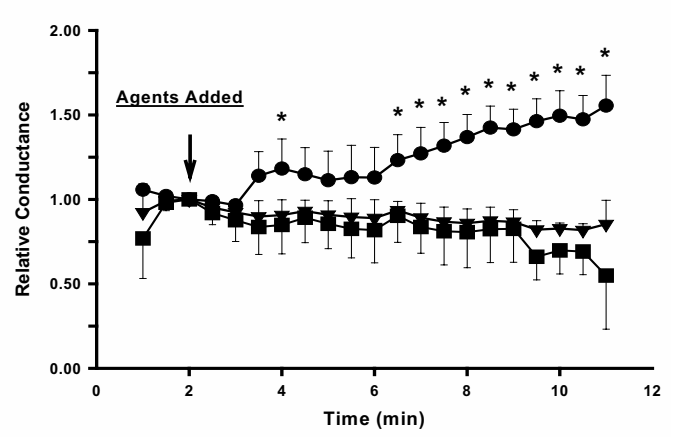

Figure 1. Time course of ATP- and hyposmotic-activated anion conductance in cultured hippocampal astrocytes. Data are shown for cells exposed to hyposmotic perfusion solution (triangles), 100 μM ATP in isosmotic perfusion solution (squares), or 100 μM ATP in hyposmotic perfusion solution (circles). Values are the mean±SEM for 4 independent determinations. * indicates values significantly different from 1.0. ($p<0.05$).

+120 mV from a holding potential of 0 mV. Membrane conductance at each time point was calculated by linear regression between -70 mV and +70mV and expressed relative to the initial conductance measured in isosmotic conditions.

3. RESULTS AND DISCUSSION

Exposure to hyposmotic CsCl perfusion solution caused no change in astrocyte membrane anion conductance (Figure 1). Similarly, adding 100 μM ATP to isosmotic CsCl perfusion did not alter membrane conductance. However, when cells were exposed to 100 μM ATP in hyposmotic perfusion solution, a 48% increase in membrane conductance was observed within 8 min. In contrast, adding 100 μM ADP to cells in hyposmotic perfusion solution produced no change in membrane anion conductance (data not shown). Thus, extracellular ATP and hyposmotic swelling act synergistically to increase anion conductance of cultured hippocampal astrocytes. The lack of response with ADP exposure suggests P2Y receptors are not involved at the moderate degree of osmotic swelling shown here.

1. J.E. Olson and G.Z. Li, Increased potassium, chloride, and taurine conductances in astrocytes during hyposmotic swelling. *Glia*, **20**(Jul) 254-61 (1997).
2. A.A. Mongin, and H.K. Kimelberg, ATP potently modulates anion channel-mediated excitatory amino acid release from cultured astrocytes, *Am J Physiol Cell Physiol*, **283**(2) C569-578 (2002).
3. M. Darby, et al., ATP released from astrocytes during swelling activates chloride channels. *J Neurophysiol,* **89**(4) 1870-7 (2003).
4. J.E. Olson, and D. Holtzman, Respiration in rat cerebral astrocytes from primary culture. *J Neurosci Res,* **5**(6) 497-506 (1980).
5. G. Li, Y. Liu, and J.E. Olson, Calcium/calmodulin-modulated chloride and taurine conductances in cultured rat astrocytes, *Brain Res*, **925** (Jan)1-8 (2002).

* Guangze Li and James E. Olson, James E. Olson, Departments of Emergency Medicine and Anatomy & Physiology, Wright State University, Dayton, Ohio 45435

47

ADH-STIMULATED Na^+ TRANSPORT: INTERACTION BETWEEN THE cAMP/PKA AND PHOSPHOINOSITIDE SIGNALING PATHWAYS

Charity Nofziger and Bonnie L. Blazer-Yost*

The biochemical pathways stimulated in response to hormones such as aldosterone, anti-diuretic hormone (ADH), and insulin in principle cells found in the renal distal nephron remain unresolved. These hormones maintain salt and water homeostasis and may, therefore, play a predominant role in metabolic diseases such as essential hypertension. Due to this role, it is vital that the hormone-stimulated signaling pathways be elucidated to the fullest extent.

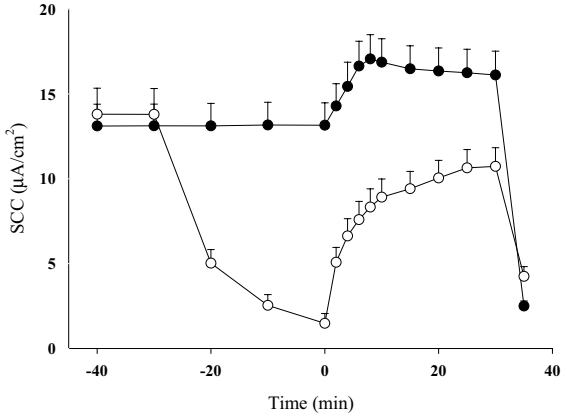

Figure 1. Effect of LY294002 on basal and ADH-stimulated Na^+ retention. Short-circuit current (SCC) is a measure of net ion flux. 100 mU/ml ADH was added at t=0 and 10^{-5} M amiloride was added at t=30. Filled circles indicate ADH alone; n=20. Open circles indicate LY294002 (50 μM) addition 30 min. prior to ADH; n=12. Symbols are shown as means ± S. E.

The A6 cell line from Xenopus *laevis* kidney, serves as a model for the principle cells by maintaining a high transepithelial resistance (>1000 Ω/cm^2), and by displaying amiloride-sensitive ion transport. Changes in net transepithelial ion flux can be accurately measured in such lines using the short-circuit current electrophysiological technique.[1] The A6 cell line displays a basal transepithelial current and responds to both steroid (aldosterone) and peptide (ADH and insulin) stimulation with an increase in transcellular Na^+ flux. This

flux is mediated via the apical membrane epithelial Na^+ channel (ENaC), a multimeric protein channel specifically inhibited by low concentrations (10^{-5} M) of amiloride. It is known that ADH increases Na^+ reabsorption via the cAMP/protein kinase-A (PKA) pathway, whereas aldosterone and insulin initiate their effects on ENaC via the phosphoinositide (PI) pathway. In addition, the salt-retaining actions of the various hormones have additive effects on Na^+ transport, suggesting that ADH and insulin are independently causing increases in Na^+ retention. However, recent studies indicate that there may be cross-talk between the two pathways.

Previous data from our laboratory have shown that a specific inhibitor of phosphoinositide-3-kinase (PI3-kinase), LY294002, blocks basal, aldosterone, and insulin-stimulated Na^+ transport.[2, 3] Figure 1 shows that addition of ADH to LY294002-pretreated tissue leads to either a potentiation of ADH-mediated Na^+ reabsorption or to the restitution of the inhibited basal current.

Whereas the ADH-stimulated transport in control A6 cells is virtually all Na^+ flux, the ADH response in LY294002-treated A6 cells is not exclusively amiloride sensitive, thus, implying that the inhibition of PI3-kinase may activate additional ion transport systems. We hypothesize that this LY294002-mediated potentiation in the ADH response may be caused by Cl^- secretion—most likely through the apical cystic fibrosis transmembrane regulator (CFTR). Therefore, we utilized an inhibitor of CFTR—5-nitro-2-(3-phenylpropylamino)-benzoic acid (NPPB). Cells pretreated with both amiloride and LY294002 responded to ADH with an NPPB-sensitive and amiloride-insensitive transport (data not shown).

These data suggest a complex interaction between the signaling pathways controlling transepithelial Na^+ reabsorption. We propose both the PI and PKA pathways may converge at some point before ENaC, perhaps as early as cAMP or PI3-kinase, or as late as serum, glucocorticoid-induced kinase (sgk).[4] In either case, further studies are needed to unveil the route(s) the three hormones use to control salt and water homeostasis via ENaC.

1. H. H. Ussing and K. Zerahn, Active transport of sodium as the source of electric current in the short-circuited isolate frog skin, *Acta. Physiol. Scand*. **23**, 110-127 (1951).
2. R. D. Record, L.L. Froelich, C.J. Vlahos and B.L. Blazer-Yost, Phosphatidylinositol 3-kinase activation is required for insulin-stimulated sodium transport in A6 cells, *Am. J. Physiol. Endocrinol. Metab*. **274**, E611-E617 (1998).
3. B. L. Blazer-Yost, T.G. Paunescu, S.I. Helman, K.D. Lee and C.J. Vlahos, Phosphoinositide 3-kinase is required for aldosterone regulated sodium reabsorption., *Am. J. Physiol. Cell Physiol*. **277**, C531-C536 (1999).
4. B. L. Blazer-Yost and C. Nofziger, The role of the phosphoinositide pathway in hormonal regulation of the epithelial sodium channel, Abstract, *International Cell Symposium*, Dayton, OH (Sep 20-25, 2003).

* Charity Nofziger and Bonnie L. Blazer-Yost, Biology Department., Indiana University-Purdue University at Indianapolis, Indianapolis, Indiana 46202

48

EFFECT OF ALDOSTERONE ON Na^+ TRANSPORT IN A MODEL RENAL EPITHELIAL CELL LINE

A proteomic approach

Puneet Souda, Frank Witzmann and Bonnie L. Blazer-Yost*

1. ABSTRACT

Aldosterone, a principle hormone controlling salt and water balance in vertebrates, acts by altering the expression of defined proteins in transporting epithelial cells. While several aldosterone-induced proteins have been identified, the mechanism of hormone action as well as the key, rate-limiting steps involved in the pathway remain unknown.

A proteomics approach was used to identify the differential expression of proteins in epithelial cells treated with aldosterone (2.7×10^{-6} M) for 12 hours. The A6 cell line derived from the kidney of *Xenopus laevis,* serves as a model renal epithelial cell line for studying transport phenomenon and was used in the experiments. Two series of experiments consisted of a matchset containing 10 control and 7 aldosterone-treated samples and a second matchset with 6 control and 6 aldosterone-treated samples. The solubilizing conditions were optimized to produce a fraction consisting mainly of membrane and cytoskeletal proteins.[1, 2] The separatory component of the analysis involved Immobilized pH Gradient (IPG) strips as the first dimension and sodium dodecyl sulfate polyacrylamide gel electroporesis (11-19% non-linear gradient gels) in the second dimension. Running conditions for the first dimension were optimized using 24 hours passive rehydration of 24 cm IPG strips followed by 120,000 volt-hours for isoelectric focusing. The second dimension was conducted on 20cm x 25cm large format gels with the ability to resolve >5000 proteins which were scanned using a transmission densitometer and analyzed using PDQuest image analysis software. The protein spots were digested using trypsin and spotted on a mass spectrometer plate for identification.

Results showed consistent repression of a protein with an iso-electric point (pI) of 9 and molecular weight of 34 kDa in both matchsets. This protein was identified as the tail domain of moesin, using Matrix Assisted Laser Desorption Ionization-Time of Flight (MALDI-TOF) mass spectrometer with more than 99% accuracy.

In the first matchset, the average optical densities (OD) of the protein spots were 5970.8 and 427.9, respectively, a 13.95 fold decrease in the presence of aldosterone. In the second matchset, the average ODs for the same spot were 1479.2 (control) and 56.6 (aldosterone), a 26.13 fold decrease.

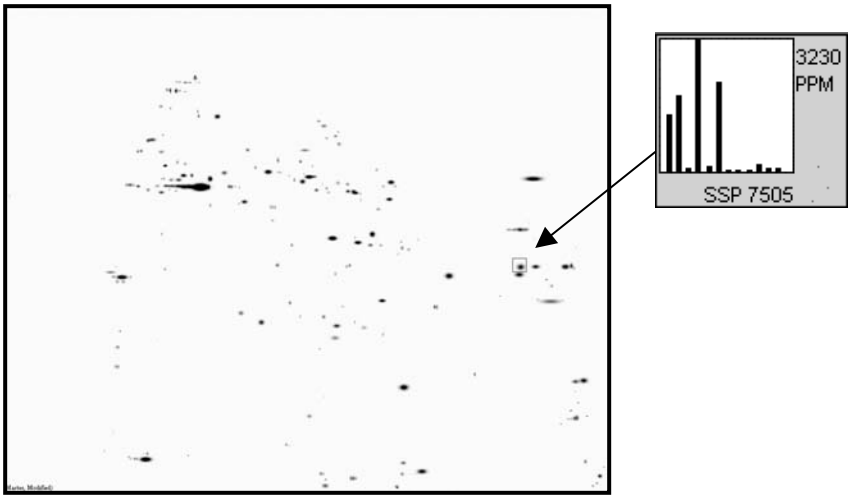

Figure 1. A representative image of matchset showing downregulation of spot 7505 identified as FERM tail domain of moesin. Graph: first 6 vertical bars represent spot intensity for spot 7505 in 6 control cells; next 6 vertical bars represent spot intensity in 6 aldosterone-treated cells. The spot is represented inside the small square indicated by arrow.

The protein consistently repressed is actually a partial protein consisting of the FERM (band four-point-one, ezrin, radixin, moesin group) tail domain of moesin. The N-terminal FERM domain of moesin binds to the membrane and a C-terminal F-actin binding segment of moesin binds to the cytoskeleton.[3, 4] The down-regulation of moesin FERM tail domain suggests that under control conditions, a specific proteolytic degradation of the moesin protein occurs and aldosterone inhibits this cleavage reaction. To our knowledge, this is the first description of such a protoeolytic cleavage occurring *in vivo*. Although these data are preliminary, they suggest a mechanism whereby aldosterone may inhibit protein turnover.

2. REFERENCES

1. M. P. Molloy, B. R. Herbert, B. J. Walsh, M. J. Tyler, M. Traini, J. Sanchez, D. F. Hochstrasser, K. L. Williams and A. A. Gooley, Extraction of membrane proteins by differential solubilization for separation using two-dimensional gel electrophoresis, *Electrophoresis,* **19**, 837-844 (1998).
2. F. A. Witzmann, J.W. Clack, K. Geiss, S. Hussain, M. J. Juhl, C. M. Rice and C. Wang, Proteomic evaluation of cell preparation methods in primary hepatocyte cell culture, *Electrophoresis,* **23**, 2223-2232 (2002).
3. M. A. Pearson, D. Reczek, A. Bretscher and P. A. Karplus, Structure of the ERM protein moesin reveals the FERM domain fold masked by an extended actin binding tail domain, *Cell*, **101**, 259-270 (2000).
4. A. Bretscher, Regulation of cortical structure by the ezrin-radixin-moesin protein family, *Curr Opin in Cell Biol,* **11**, 109-116 (1999).

* Puneet Souda, Frank Witzmann and Bonnie L. Blazer-Yost, Biology Department., Indiana University-Purdue University at Indianapolis, Indianapolis, Indiana 46202

49

UPREGULATION OF NCX PROTEIN IN HEPATOPANCREAS AND ANTENNAL GLAND OF FRESHWATER CRAYFISH ASSOCIATED WITH ELEVATED CA^{2+} FLUX

La'Tonia M. Stiner, Yongping Gao and Michele Wheatly*

1. INTRODUCTION

The molting cycle of the freshwater crayfish *Procambarus clarkii* has emerged as an ideal model to study cellular/molecular mechanisms of Ca^{2+} homeostasis because of its ability to maximally absorb Ca^{2+} from a Ca^{2+} deficient environment.[1] Freshwater contains only 1 mM Ca^{2+} as opposed to the 10 mM Ca^{2+} afforded by marine environments. The model is based on a negligible net transepithelial Ca^{2+} flux during intermolt that changes to vectorial Ca^{2+} flux around ecdysis. During premolt, 20% of cuticular Ca^{2+} is reabsorbed for deposition into $CaCO_3$ disks and the remainder is excreted. Postmolt is characterized by net environmental Ca^{2+} uptake rates of 2-10 mmol/kg/h and remobilization of stored Ca^{2+}. Both sources are subsequently used for the calcification of a new exoskeleton. The Ca^{2+} transporting epithelia are the gills, antennal gland (kidney), hepatopancreas (liver) and cuticular hypodermis. Arthropod molting is coordinated by the steroid ecdysone and unknown environmental cues. Previous studies have shown a marked increase in basolateral Ca^{2+} pump expression during postmolt, suggesting that Ca^{2+} transporting proteins are upregulated during periods of elevated transepithelial Ca^{2+} uptake. Kinetic studies suggest that the NCX is the primary extrusion mechanism for basolateral Ca^{2+} efflux. Therefore, we propose that the NCX may be upregulated during premolt and postmolt compared with intermolt in hepatopancreas and antennal gland.

2. EXPERIMENTAL

2.1. Western Blotting

Frozen tissue was ground to a powder and combined with extraction buffer. The sample was homogenized with a Dounce homogenizer and 18, 21, and 23 gauge needles. Homogenates were centrifuged for 1 hr at 13,000 x g at 4°C. The supernatant was retained and the pellet was stored at –80°C. The supernatant was further cleared by centrifugation at 13,000 x g for 30 min at 4°C. Cleared samples were stored at –80°C. Proteins were separated on an 8% SDS-PAGE gel and transferred to polyvinyl-lidene fluoride (PVDF) membranes. Membranes were blocked for 1 hr in a nonfat dry milk/TTBS (Tris buffered saline/Tween-20) and incubated overnight with our homologous NCX antibody (1:1000) in milk/TTBS soln. Membranes were rinsed twice and

washed for 15 min in a milk/TTBS soln at RT. An HRP-conjugated 2^{o} Ab was incubated for 1 hr in a milk/TTBS soln at RT. Blots were rinsed twice and washed for 15 min with milk/TTBS, followed by the application of the chemilumi-nescence reagent (ECL Amersham Pharmacia). Blots were photographed via Fuji LAS-3000.

3. RESULTS

3.1 Western Blotting

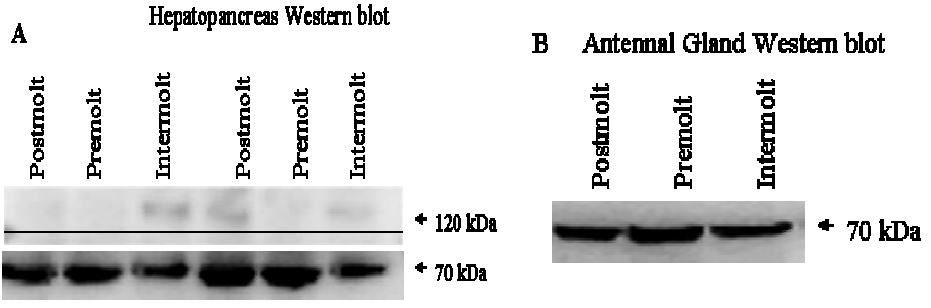

Figure 1. Western blots of calcium transporting epithelia during intermolt, premolt and postmolt: (A) hepatopancreas; (B) antennal gland. In both tissues, NCX expression is greater in premolt and postmolt compared to intermolt.

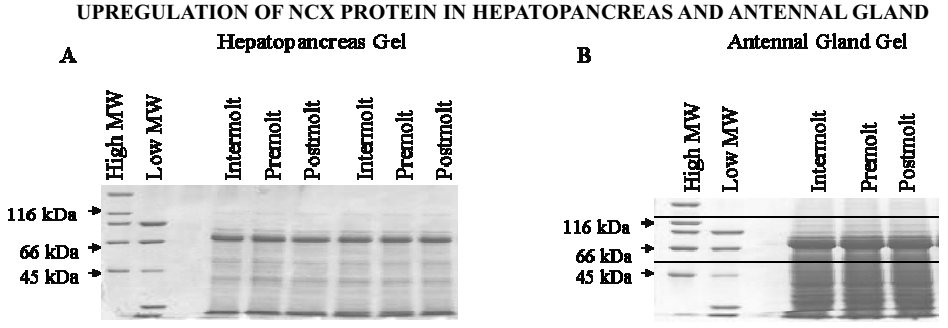

Figure 2. Coomassie stained gels as an equal loading control: (A) hepatopancreas; (B) antennal gland.

4. DISCUSSION

Our Western analysis (Figure 1) shows an increase in NCX protein levels in premolt and postmolt compared to intermolt in both the hepatopancreas and antennal gland. In hepatopancreas, both the 120 and 70 kDa bands were visible. However, the 120 kDa band was less intense, mostly likely due to degradation by proteases. Hepatopancreatic NCX expression appears greater in postmolt than premolt which could be due to the greater role the digestive system plays in ingestion of dietary Ca^{2+} immediately after ecdysis. Antennal gland analysis has revealed only a 70 kDa band, which is in direct agreement with

the primary literature. The 120 kDa band was undetectable and shown not to contain the active portion of the protein. In this case, NCX expression appears to be greater in premolt than postmolt.

Coomassie stained gels were used as an equal loading control since commercially available internal control antibodies did not react with crayfish proteins (Figure 2).

5. ACKNOWLEDGMENTS

We thank the National Science Foundation for our funding. We also thank Dr. J. Turchi, Dr. B. Hull and Kambiz Tahmeseb for their technical support.

6. REFERENCES

1. M.G. Wheatly, R.C. Pence and J.R. Weil, ATP-dependent calcium uptake into basolateral vesicles from transporting epithelia of intermolt crayfish, *American J.Physiol*. **276,** R566-574 (1999).

* La'Tonia M. Stiner, Yongping Gao and Michele Wheatly, Department of Biological Science, Wright State University, Dayton, OH 45435, USA

SARABANDA

for Peter Lauf, M.D.

Hector Rasgado-Flores
Cello Part Edited by Adrian Lauf

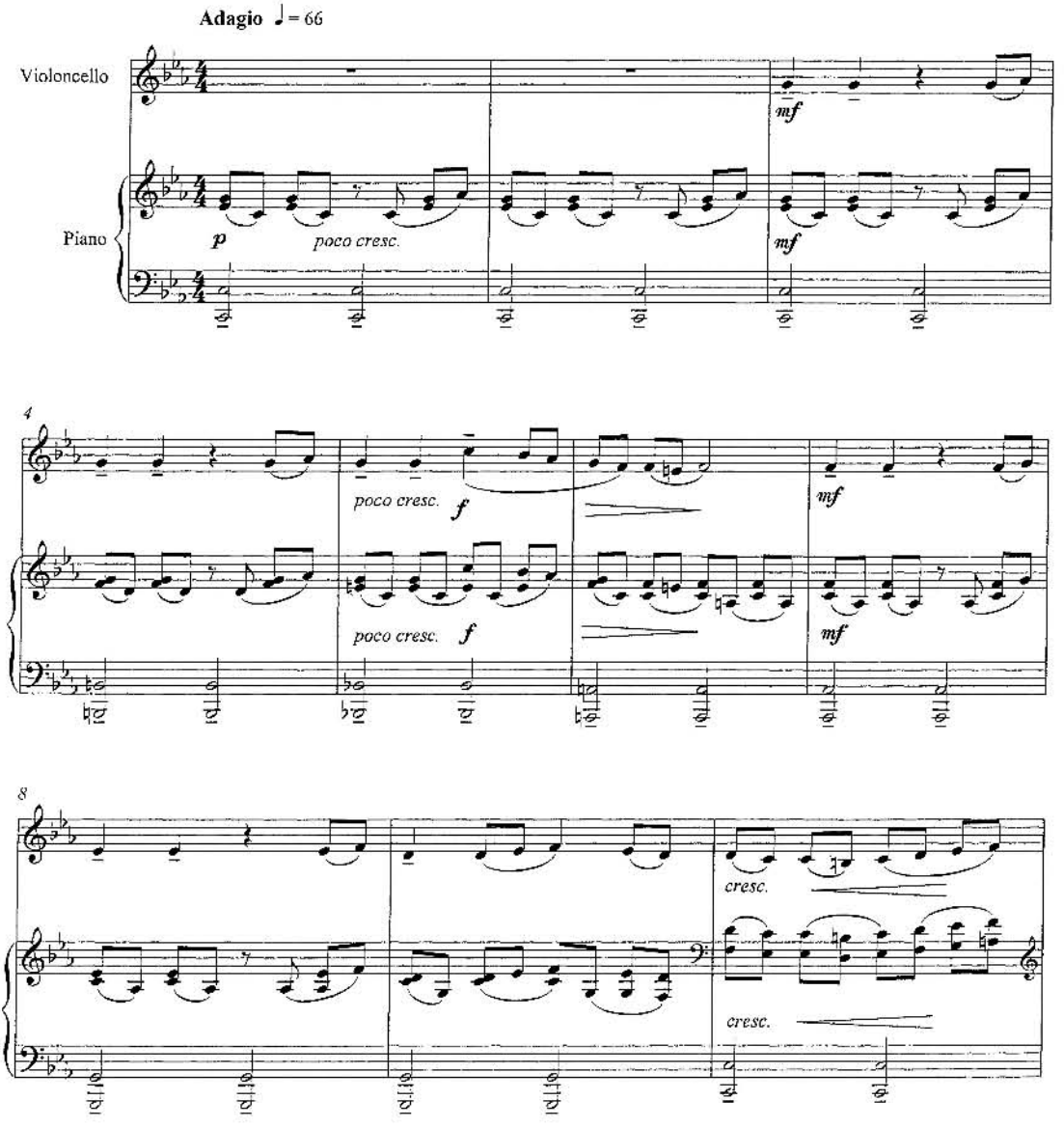

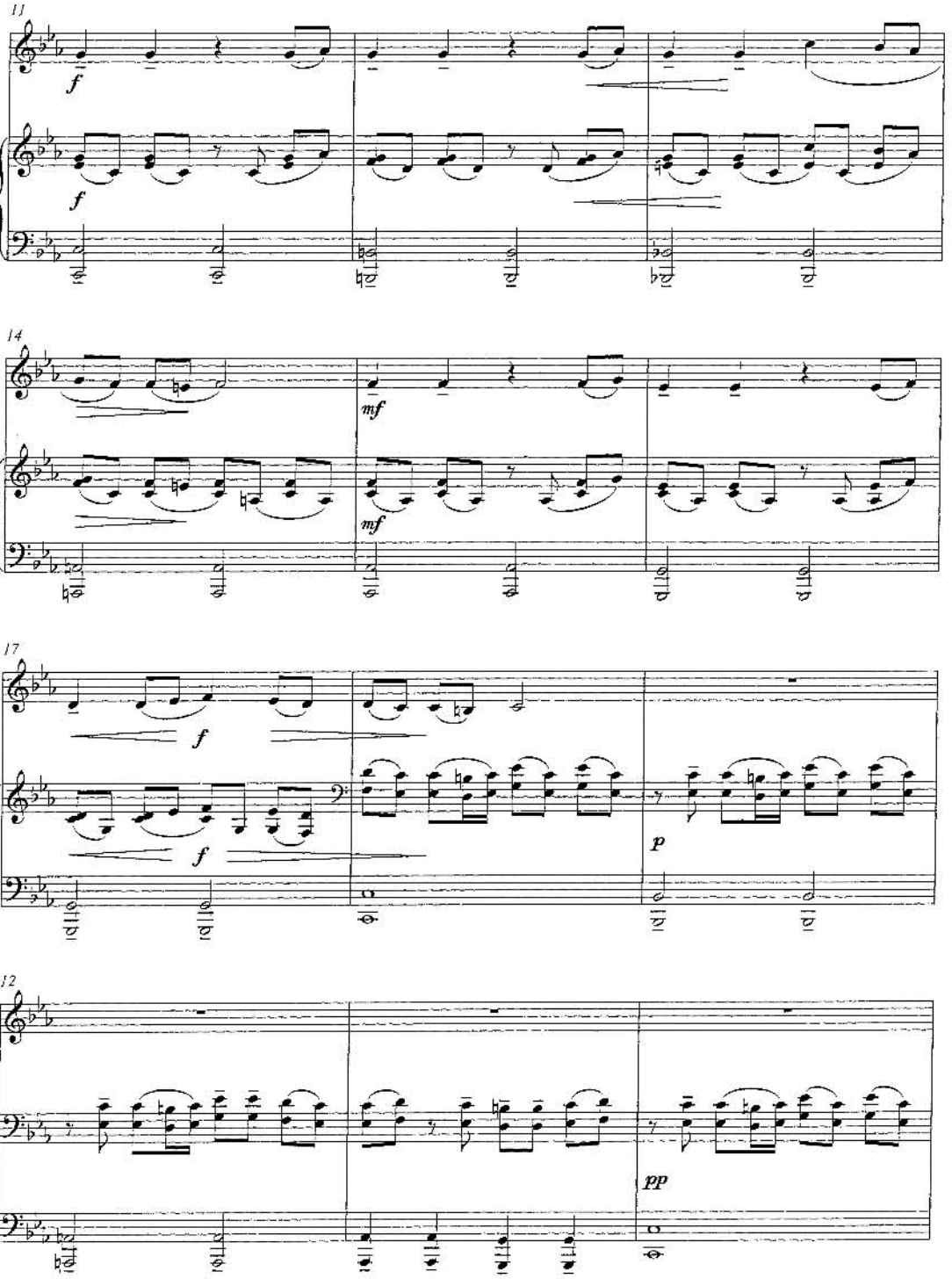
11
f
f
14
mf
mf
17
f
f
p
12
pp

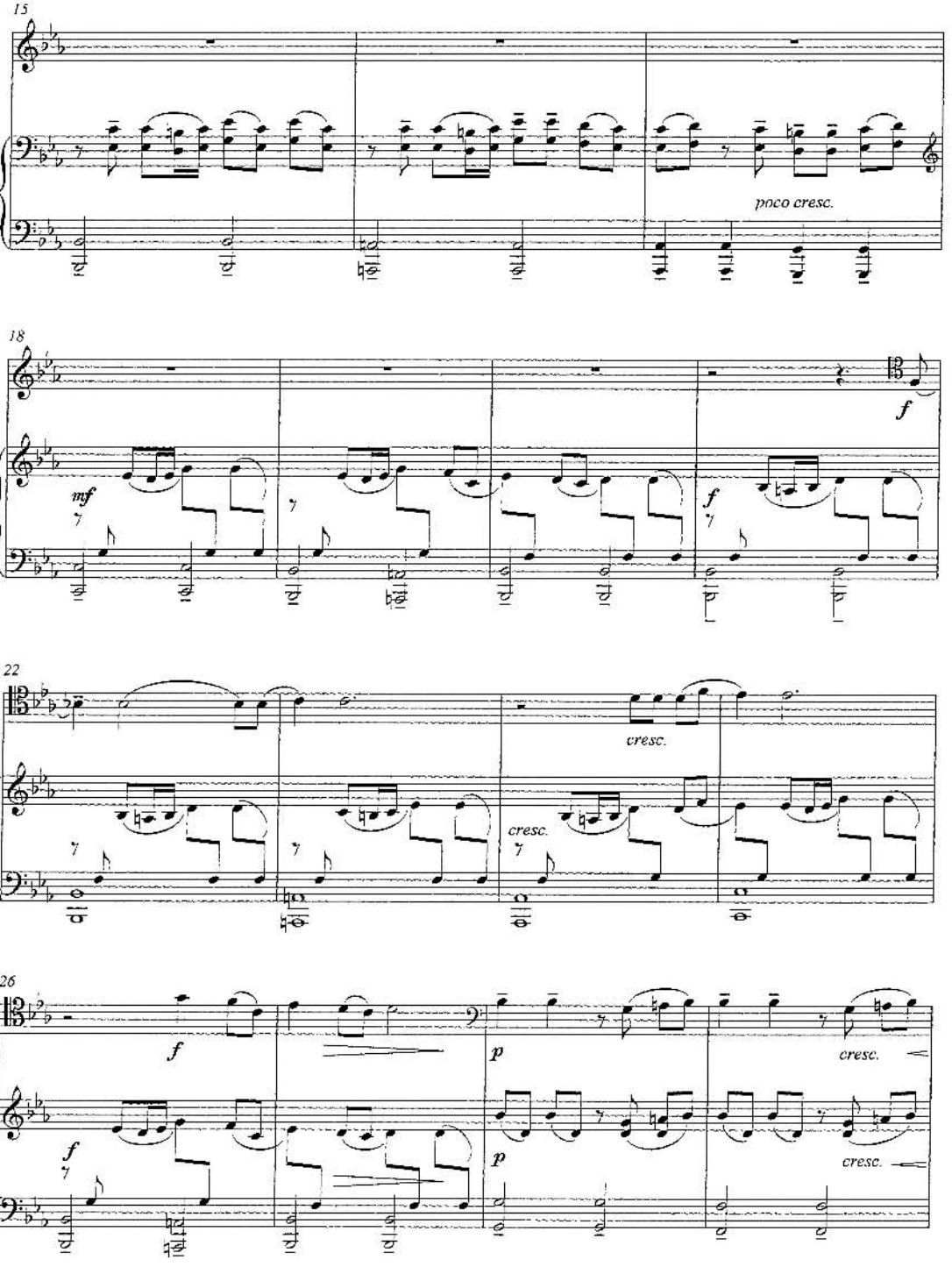
15
poco cresc.
18
mf
f
f
22
cresc.
cresc.
26
f
p
cresc.
f
p
cresc.

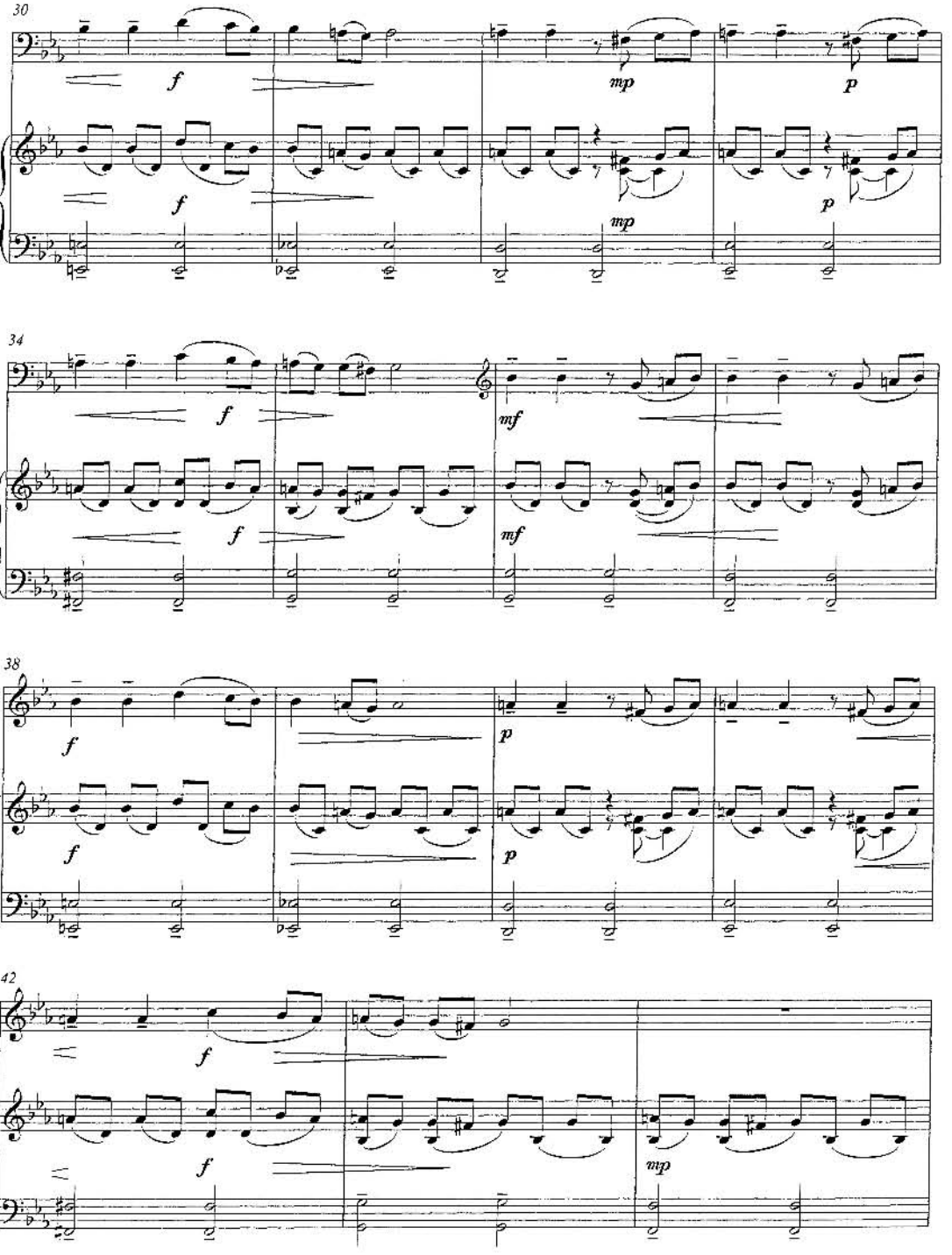
30
f
f
mp
mp
p
p
34
f
f
mf
mf
38
f
f
p
p
42
f
f
mp

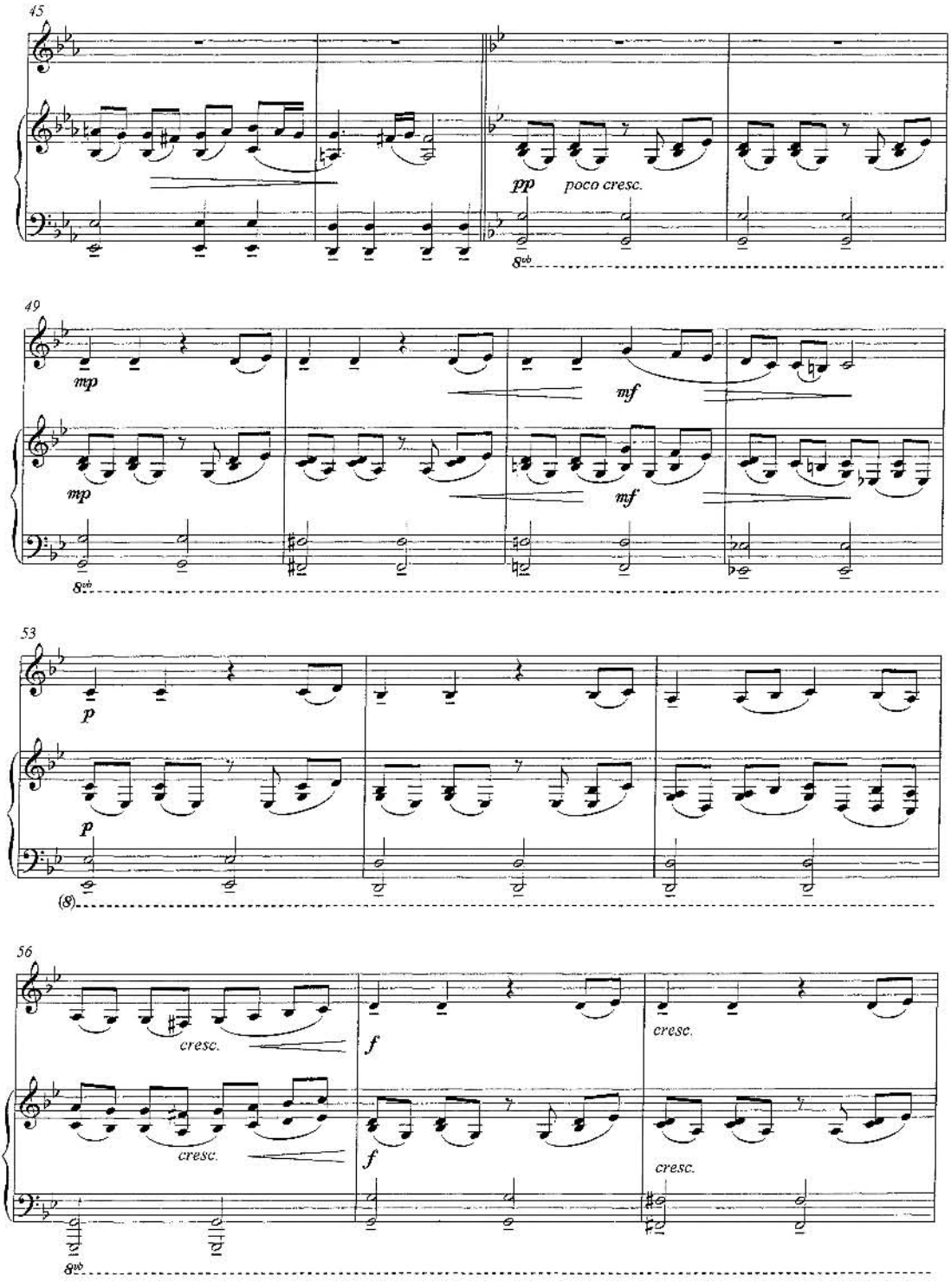
45
pp
poco cresc.
8vb
49
mp
mp
mf
mf
8vb
53
p
p
(8)
56
cresc.
f
cresc.
cresc.
f
cresc.
8vb

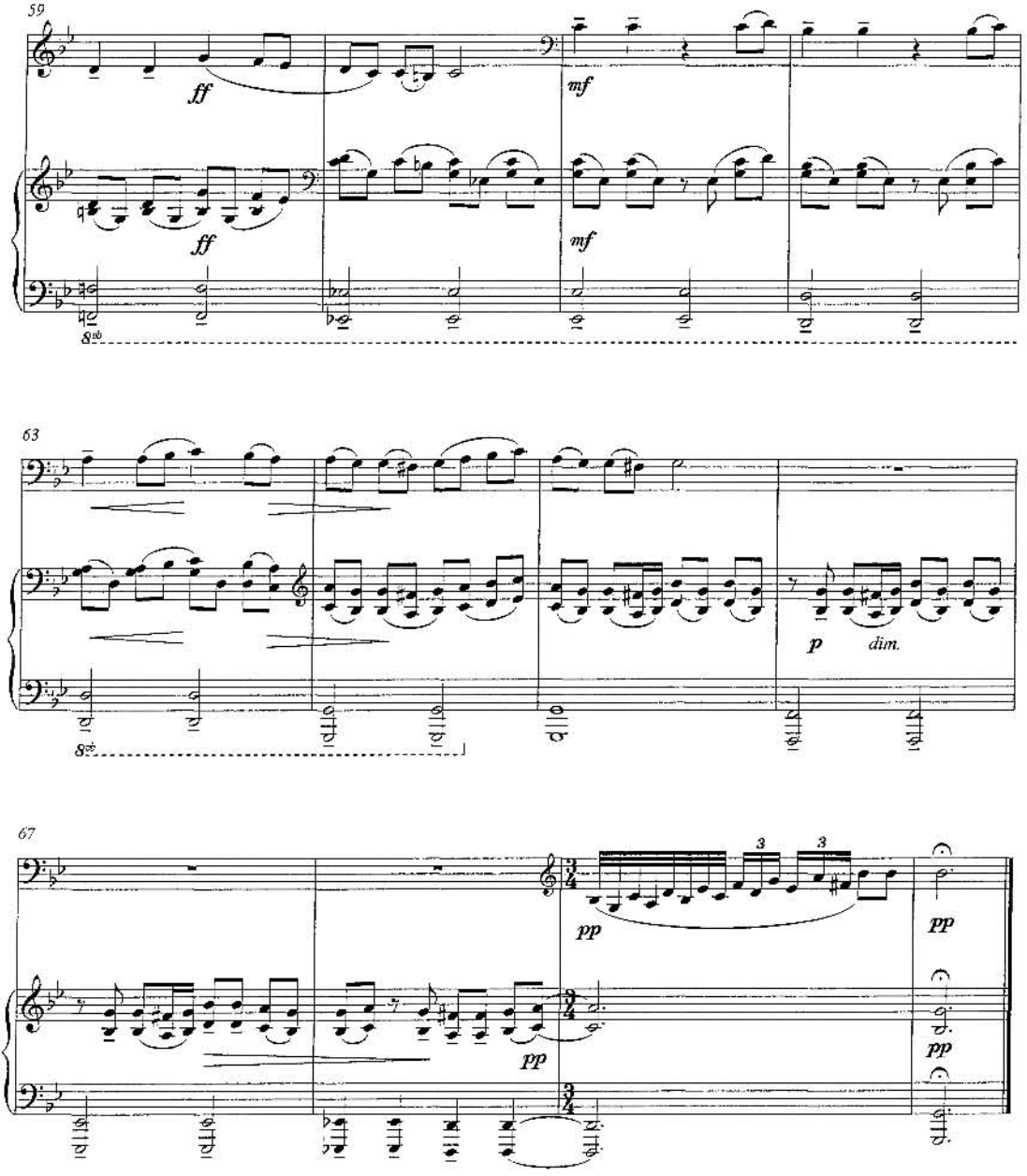
59
ff
ff
mf
mf
8vb
63
p
dim.
8vb
67
pp
pp
pp
pp
3
3

Index

A
Abstracts, 387–392
Acidosis, lactic, effect on necrotic cell anion channels, 207–208
ACPN (peripheral neuropathy with or without agenesis of the corpus callosum) syndrome, 34–35
Acquired immunodeficiency syndrome (AIDS), "excessive" apoptosis in, 190
Actinomycin D
  apoptosis-inducing activity of, 192
  caspase activator-inducing activity of, 294, 295
  effect on ouabain's antiapoptotic activity, 221
Adenosine monophosphate, cyclic (cAMP)
  in cystic fibrosis transmembrane regulator (CFTR) activation, 349
Adenosine triphosphatase (ATPase), in sodium cell volume regulation, 7
Adenosine triphosphate (ATP)
  in astrocyte anion conductance, 405–406
  in intestinal epithelial regulatory volume decrease (RVD), 342–344
  in neuronal-glial signaling, 315
β-Adrenergic agonists, paNHE1-activating effect of, 93, 94, 96
Airway epithelial cells, calcium-dependent potassium channels in, 388–389
Akt, 363
Alanine, in regulatory volume decrease, 369
β-Alanine, in regulatory volume decrease, 369
Aldosterone
  action mechanism of, 409
  definition of, 409
  in protein turnover, 409–410
  in renal epithelial sodium channel regulation, 359–360, 361, 362, 365
  in renal sodium transport, 403–404, 409–410
α-Actinin, as human syncytiotrophoblast component, 235–236, 239, 240, 241
Amiloride sensitivity
  of erythrocyte cell membrane, 213
  of paNHE1 protein, 92
  of sodium channels, 254, 255, 259–260
Amino acid efflux pathways, protein tyrosine kinase-mediated, 302
Amino acids, as osmolytes, 369
4-Amino-5-(4-methylphenyl)-7-(t-butyl)pyrazolol[3,4-d]pyrimidine, 80, 81, 82, 83, 85
4-Aminopyridine, effect on potassium channels during apoptosis, 196
Ammonium, in basolateral membrane, 131–132
  chloride secretion-inhibiting effects of, 132–133, 137
  colonic secretory cell ion channel effects of, 131–139
  concentration of, 131–132
  pH effects of, 132, 136
  potassium channel effects of, 133, 137
  sodium-potassium-ATPase interactions with, 133, 137
  sodium-potassium-chloride cotransporter interactions with, 132–133, 137
  transepithelial resistance effect of, 133–134
Amyloid β peptide, effect on astroglial glutamate uptake, 317
Anion channels, in apoptosis volume decrease (AVD), 227
  activation of, 206–207
Anion conductance, ATP-sensitive, in hippocampal astrocytes, 405–406
Anion conductance channels, in IMCD-K2 cell line, 109–118
Antidiuretic hormone
  in renal epithelial sodium channel regulation, 359, 360, 363
  in renal transcellular sodium transport, 403–405
Anti-Fas antibody, effect on apoptosis, 195, 197
Antisense oligodeoxynucleotides, 245
Apoptosis, 179, 189–203
  actinomycin D-induced, 192
  caspases in
    activation of, 293, 294
    inhibition of, 206–207, 293–300
  cell shrinkage associated with, 189, 190, 219, 226

as cell shrinkage-mediated necrosis, 220
chloride channels in, 198
in C7-MDCK cells
effect of mannitol on, 224–225
in hyperosmotically-shrunken cells, 224–225
DNA cleavage during, 190
during embryonic development, 190
in erythrocytes, 211–217
calcium-sensitive Gardos potassium channels in, 213, 214
ceramide release in, 215
characteristics of, 212
energy deletion-induced, 211, 214
erythropoietin-related inhibition of, 213–214
in glucose-6-phosphate dehydrogenase deficiency, 211–212, 214
ionomycin-induced, 212
non-selective cation channels in, 212–214, 215
osmotic shock-induced, 211, 213
oxidase stress-induced, 211, 213, 214
phosphatidylserine in, 211, 212, 213, 214, 215
in *Plasmodium falciparum* infections, 212, 214
in sickle cell disease, 211–212, 214
sphringomyelinase activation in, 215
in thalassemia, 211–212, 214
excessive, 190
in HeLa cells
in hyperosmotically-shrunken cells, 224
potassium transmembrane gradient-related suppression of, 228
in hyperosmotically-shrunken cells, 224–226
in immune system cells, 220
inhibition of, 219–223
bumetanide-related, 175
caspase inhibitor-related, 206–207, 293–300
erythropoietin-related, 213–214
gene expression-related, 221–222
Na^+i-dependent Ca^{2+}i-insensitive mechanism-related, 223
$[Na^+]_i/[K^+]_i$ ratio inversion-related, 220–222
Na^+i-mediated Ca^{2+}i-independent coupling in, 222–223
insufficient, 190
ion channels during, 196–198
sodium movement in, 199–200
ion-mediated activation of, 195–196, 201
in Jurkat cells
anti-Fas-induced, 199–200
cell shrinkage associated with, 226
in hyperosmotically-shrunken cells, 224, 225
ion-mediated, 195, 197
n-type voltage-gated potassium channels in, 227
potassium transmembrane gradient-related suppression of, 228
morphological changes during, 190, 192
n-type voltage-gated potassium channels in, 227
signaling cascades in, 190–192
in vascular smooth muscle cells
gene expression-mediated, 221–222
in hyperosmotically-shrunken cells, 224–225
inhibition of, 219–223
in isosmotic *versus* hyposmotic conditions, 227–228
Na^+i-dependent Ca^{2+}i-insensitive mechanism-mediated, 223
$[Na^+]_i/[K^+]_i$ ratio inversion-mediated, 220–222
Na^+i-mediated Ca^{2+}i-independent coupling in, 222–223
in serum-deprived conditions, 227–228
Apoptosis inducing factor, 192
Apoptosis-protease-activating factor-1 (APAF-1), 192
Apoptosome formation, caspase-9 in, 195
Apoptotic bodies, 190
definition of, 205
phagocytosis of, 205, 206
Apoptotic cells, cell shrinkage phases in, 205
Apoptotic factors, 192
Apoptotic signaling cascade, 195–196
caspase-3 in, 197
chloride in, 198
Apoptotic volume decrease (AVD), 179–188
anion channels in, 227
activation of, 206–207
aquaporins in, 179–187, 195
definition of, 193, 205
ion loss during, 195
isosmotic, 226
potassium inhibition in, 179
potassium ion efflux in, 180, 181, 185, 187
relationship with regulatory volume decrease (RVD), 193–195, 196–197
in serum-deprived *versus* hyperosmotic conditions, 226
transporters in, 226–227
volume-sensitive outwardly rectifying chloride channels (VSOR) in, 206–207

Aquaporins, 192
in apoptotic volume decrease (AVD), 180–187, 195
regulation of, 180
structure of, 180
Arachidonic acid, effect on astroglial glutamate uptake, 317
Arsenite, 81, 82, 83–84
A6 cell lines, antidiuretic hormone-mediated sodium transport and reabsorption in, 403–405, 407–408
Aspartate, release from swollen astrocytes, 316
Astrocyte-neuronal signaling, 313–323
adenosine triphosphate-mediated, 313
astroglial glutamate uptake impairment-related alteration of, 316–320
cell volume regulation in, 316
as cognitive impairment (mental fatigue) cause, 316–320
treatment for, 320
volume transmission in, 316
glutamate aspartate transporter (GLSAT) in, 314, 316–317
inhibition of, 317
glutamate transporter (GLT-1) in, 314, 316–317
inhibition of, 317
in glutaminergic synaptic region, 315
Astrocytes
in blood-brain-barrier formation, 313
characteristics and properties of, 313–314
glutamate-monitoring function of, 314
hippocampal, ATPase-sensitive anion conductance in, 405–406
potassium-chloride cotransport in, 391–392
purine receptors on, 315
receptors on, 313
sodium-potassium-2 chloride cotransport in, 391–392
synaptic relationships of, 313

B
Balanus nubilis muscle cells. *See* Barnacle muscle cells
Barnacle muscle cells, hypotonicity-induced cell volume regulation in, 263–293
effect of calcium ions on, 266–290
osmotic properties and, 266–268
regulatory volume decrease effects of, 270–272
sarcolemmal hydraulic water permeability and, 268–270, 289–290
time-course of, 270–272
verapamil-sensitive sodium-dependent membrane depolarization in, 270–272
intracellular cAMP in, 265
intracellular cGAMP in, 265
intracellular ionic strength modification in, 265–266
membrane tension in, 266
regulatory volume decrease (RVD) in, 270–290
arginine in, 274, 275
aspartate in, 274, 275
calcium ions in, 274–275, 276–281
cAMP in, 277–281, 288–290
cGMP in, 278, 279, 280–281
chloride ions in, 274, 275, 276
cyclic nucleotides in, 277–281, 288–290
extracellular pH changes during, 276–277
extracellular space in, 272–274
free amino acids in, 274, 275, 276
glycine in, 274, 275, 276, 288–289
in hypotonic conditions, 274–276
intracellular ionic strength in, 282–286
intracellular ionic strength volume sensors in, 282–286
intracellular macromolecular crowding volume sensors in, 286–288, 289
in isosmotic and hypotonic conditions, 274–276
in isotonic conditions, 274–276
mechanical membrane deformation volume sensors in, 281–282
osmolytes in, 272–276
potassium ions in, 274, 275, 276, 288–289
sarcolemmal hydraulic water permeability in, 267, 268–270
sodium ions in, 274, 275, 288–289
taurine in, 274, 275–276
time course of, 270–272
volume sensors in, 281–288
Bartter disease, 57
Basket cells, 391
Basolateral membrane
ammonium in, 131–132
chloride secretion effects of, 132–133, 137
concentration of, 131–132
pH effects of, 132, 136
potassium channel effects of, 133, 137
sodium-potassium-ATPase interactions, 133, 137
sodium-potassium-chloride cotransporter interactions, 132–133, 137

transepithelial resistance effect of, 133–134
chloride channels in, 119
activation of, 119
β-adrenergic receptor-mediated, 120, 122
calcium-dependent signaling in, 120
cAMP-dependent signaling in, 120
as CLC3 channel variant, 123
comparison with cystic fibrosis transmembrane regulator channel, 126
epinephrine-related activation of, 124–125
forskolin-related activation of, 124–125
prostaglandin E_2-related activation of, 124
prostanoid EP2-mediated, 120, 121
relationship with electrogenic potassium secretion, 120, 126–127
vasoactive intestinal peptide-mediated, 120
in crayfish, epithelial calcium efflux in, 397–398
potassium channels in, 119
activation of, 119, 121–123
β-adrenergic receptors in, 120, 122
cAMP-dependent signaling in, 120, 121, 122
effect of forskolin-stimulation chloride secretion in, 121, 122, 123
electrogenic potassium secretion in, 120, 126–127
IK (KCNN4) channels, 121
KvLQY channels, 121
prostanoid EP2 receptors in, 120, 122
sodium-potassium-2 chloride cotransporter-dependence of, 119, 121, 126
Bcl-2 family, 192
Bendroflumethiazide, 57
Bepridil, 401
Betaine
in osmotic cell swelling, 339
in regulatory volume decrease (RVD), 369
Blood-brain barrier
astrocytes in, 313
functions of, 67
sodium-potassium-2 chloride cotransporter in, during cerebral ischemia, 67–75
bumetanide inhibition of, 71–73
cellular location of, 70–71, 74
edema formation and, 71–73, 74
peptide-sensitive regulation of, 68–70
Boc-D-fmk caspase inhibitor, 293–294, 295, 298, 299
Brain, interstitial fluid in, 67
Brain-derived neurotrophic factor, 32–33
Bronchial epithelial cells, calcium-dependent potassium channels in, 388–389
Bumetanide, 57
apoptosis-inhibiting activity of, 175
cerebral edema-attenuating activity of, 71–73
erythrocyte potassium-chloride cotransport-inhibiting activity of, 14–15
sodium-potassium-2 chloride cotransporter-inhibiting activity of, 78
Bumetanide-sensitive sodium-chloride symporters, 55
Bumetanide-sensitive sodium-chloride transporter (BSC/NKCC), 55, 56–57, 59–63
Bumetanide-sensitive sodium-potassium-2 chloride cotransporter, renal apical isoforms of, 59–63

C
Caenorhabiditis elegans
ICln protein splice variants in, 245–250
putatively generic leak channels in, 7
Calcium
in arthropod molting, 411–413
in Ehrlich ascites tumor cells, 171
osmosensitive fluxes of, 309, 310
Calcium-calmodulin kinase II, 310
Calcium cation channels, in airway epithelial cell potassium channel activation, 388–389
Calmodulin
in Ehrlich ascites tumor cells, 171
NHE1 binding to, 90
Calu-3 cells, protein-protein interaction-mediated electrolyte transporter regulation in, 349–358
protein kinase-δ–F-actin binding, 352–353, 356
protein kinase-ε–RACK1 binding, 352, 353–355, 356
Calyculin A, 79, 80, 81, 82, 83, 93–95, 172
Carbonic anhydrase II, 90
Caspase(s)
in apoptosis induction, 190–191
in apoptosis inhibition, 206–207
in apoptotic volume decrease (AVD), 195
potassium-mediated activation of, 195
Caspase 1, potassium-mediated activation of, 195
Caspase 3, 296
in apoptotic signaling cascade, 197
dATP/cytochrome c-dependent activation of, 195
inhibition of, 297
in vascular smooth muscle cell apoptosis, 220
Caspase 6, activation of, 293

Caspase 8/10
activation of, 293
inhibition of, 297, 298
Caspase 9, inhibition of, 297, 298
Caspase 12
activation of, 293
inhibition of, 298
Caspase inhibitors, 293–300
cytotoxicity of, 293–294
Cation-chloride cotransporter (CCC) superfamily, 77
Cation-chloride cotransporters (CCC)
homological similarity with potassium-chloride transporters, 30–31
Ste20 protein kinase regulation of, 43–47
Caveolin-1, 344
Cdc-42/Rac/Rho protein family, 308–309
Cell death. *See also* Apoptosis; Necrosis; Oncosis
function of, 189
of single cells, 220
Cell growth, cell volume regulation in, 169
Cell membrane
fragility of, 1, 2
potassium permeability of, 3–4, 6
Cell proliferation
cell volume regulation in, 169
membrane transport protein inhibition and, 175
Cell shrinkage
as apoptosis consequence, 226
sodium-potassium-2 chloride cotransporter-stimulating activity of, 79
Cell swelling, as potassium-chloride cotransport activator, 30
Cell volume regulation
in cellular function, 169
history of (1978 to the present), 1–9
Double Donnan concept, 3–4
fragile membrane concept, 1, 2
isotonicity of cytoplasm concept, 2–3
"orphaned questions" in, 6–8
pump-leak hypothesis, 4–6, 7–8
as signaling changes, 169
Ceramide, in erythrocyte apoptosis, 215
Cerebellum, KCC2 membrane localization in, 390–391
c-Fos gene, 222–223
cGMP. *See* Guanosine monophosphate, cyclic (cGMP)
Charybdotoxin, 213
Chelerythrine, 172
Chloride
ammonium-mediated secretion of, in basolateral membrane, 132–133, 137
in apoptotic signaling cascade, 198
colonic epithelial secretion of, 119
protein tyrosine kinase-mediated hyposmotic efflux of, 302
volume-regulated current, in HCL cells, 141–145
Chloride channels
in apoptosis, 198
basolateral, in colonic crypt cells, 119
activation of, 119
-adrenergic receptor-mediated, 120, 122
calcium-dependent signaling in, 120
cAMP-dependent signaling in, 120
as CLC3 channel variant, 123
comparison with cystic fibrosis transmembrane regulator channel, 126
epinephrine-related activation of, 124–125
forskolin-related activation of, 124–125
prostaglandin E_2-related activation of, 124
prostanoid EP2-mediated, 120, 121
relationship with electrogenic potassium secretion, 120, 126–127
vasoactive intestinal peptide-mediated, 120
inhibitors of, effect on apoptotic cell death, 198
outwardly rectifying, 198
volume-sensitive, 307
volume-sensitive outwardly rectifying (VSOR), 207–208
Chloride-coupled cotransporters (CCC). *See also specific* chloride-coupled cotransporters
definition of, 55
structure of, 56
Chloride deficiency, sodium-potassium-2 chloride cotransporter-stimulating activity of, 79
Chloride transporters, protein kinase C isotype binding to, 351–352
Chlorthalidone, 57
c-Jun gene, 222
C-Jun kinase, sodium-potassium-2 chloride cotransporter-regulating activity of, 79
Cl. *See* Chloride
Clotrimazole, 213, 387–388
c-Myc gene, 222
Cognitive impairment, altered glial-neuronal signaling-related, 316–321
treatment for, 320
Colonic crypt cells, basolateral
chloride channels in, 119, 123–126
activation of, 119
-adrenergic receptor-mediated, 120, 122

calcium-dependent signaling in, 120
cAMP-dependent signaling in, 120
as CLC3 channel variant, 123
comparison with cystic fibrosis transmembrane regulator channel, 126
epinephrine-related activation of, 124–125
forskolin-related activation of, 124–125
prostaglandin E_2-related activation of, 124
prostanoid EP2-mediated, 120, 121
relationship with electrogenic K secretion, 120, 126–127
vasoactive intestinal peptide-mediated, 120
electrogenic potassium secretion in, 126–127
potassium channels in, 119
activation of, 121–123
c-AMP-dependent signaling in, 120
forskolin-mediated, 120–121
Colonic secretory cells, ion channels in, effect of ammonium on, 131–139
Concanavalin A, 305–306
Contractile vacuoles, 7
isosmolarity of, 2
Cortactin, 240
Cotransporter kinase, 79
in ferret erythrocytes, 80–85
Cotransporter phosphatase, 80–85
Crayfish. *See Procambarus clarkii*
C7-MDCK cells, apoptosis in
effect of mannitol on, 224–225
in hyperosmotically-shrunken cells, 224–225
c-Src protein tyrosine kinase, in volume-sensitive taurine release, 373–374, 376
Cyclohexamide, effect on ouabain's antiapoptotic activity, 221
Cysteine scanning, of the ICln protein channel pore, 102–106
Cystic fibrosis transmembrane regulator (CFTR), 109, 110, 111, 113–114, 115–117, 388
cAMP-mediated activation of, 349
effect on antidiuretic-mediated sodium transport, 408
E3KARP protein interactions with, 354
fluid secretion-mediating function of, 349
NHERF2 protein interactions with, 354, 355
protein kinase A-mediated activation of, 349
Cystic fibrosis transmembrane regulator (CFTR) anion channels, epithelial apoptosis-inhibiting activity of, 227
Cystic fibrosis transmembrane regulator (CFTR) chloride channel, 126
Cytochalasin B, 174
Cytochalasin D, effect on polycystin-2, 236, 237, 238, 241
Cytokines, effect on astroglial glutamate uptake, 317
Cytoplasm, isotonicity of, 1, 2–3
Cytoskeleton, in Ehrlich ascites tumor cells, 174

D
Death-inducing-signaling-complex (Disc), 190–191
Dexamethasone, 226–227
DIOA-sensitive potassium-chloride cotransporters, 55
Diuretics
loop
sodium-chloride cotransporter affinity of, 57
sodium-potassium-2 chloride cotransporter-inhibiting activity of, 78
sodium-chloride cotransporter affinity of, 57
thiazide-type
sodium-chloride cotransporter affinity of, 57
thiazide-sensitive sodium-chloride cotransporter affinity of, 57–58
DNase, caspase-activated, 196, 198
Dopamine, astrocyte receptor-coupled, 313
Double Donnan equilibrium, 3–4
Double Donnan system, 4
Dystrophin, 239

E
EAAC1 glutamate transporter, 317
ECaC. *See* Epithelial calcium channels (ECaC)
Ecdysone, 411
Edema, cerebral, blood-brain barrier sodium-potassium-2 chloride cotransporter in, 71–73, 74
Ehrlich ascites tumor cells (EATC), effects of cell shrinkage in, 169–178
membrane transport protein activation, 169
non-selective cation channels in, 170, 171
signaling events, 169, 171–174
sodium/hydrogen exchanger (NHE1) in, 169, 170, 171, 172–173, 174, 175
sodium-potassium-2 chloride cotransporter in, 170, 171, 172, 173, 174, 175
Ehrlich Lettré tumor cells, 169
E3KARP, 354
Encephalopathy, hyperammonemia associated with, 132
Endocytosis, in intestinal epithelial volume-regulated anion conductance, 343–344

Endothelial cells, of the blood-brain barrier, sodium-potassium-2 chloride cotransport in, 68–74
Endothelins, effect on astroglial glutamate uptake, 317
Epidermal growth factor (EGF), effect on hyposmolarity-mediated taurine efflux, 305, 306
Epidermal growth factor receptors (EGFRs)
  activation of
    hyperosmolarity-related, 302, 303–304, 305–307
    lectins-related, 305–306
    taurine osmosensitive fluxes in, 307–310
  effect on regulatory volume decrease (RVD), 304–306
  in volume-sensitive taurine release, 373
Epilepsy, KCC2 protein in, 33–34, 36
Epithelial calcium channel-like *(ECaC)* gene, in crayfish, 398–401
Epithelial calcium channels (ECaC), in crayfish
  salinity-mediated transmembrane protein expression in, 396–398
  transmembrane calcium regulatory function of, 398–399
Epithelial cells, nitric oxide in, 147, 148
Epithelial electrolyte transporters, protein-protein interaction-based regulation of, 349–358
Epithelial sodium channels (ENaCs), renal
  amiloride-sensitive, 359–360
  hormonal regulation of
    aldosterone-related, 359–360, 361, 362, 365
    antidiuretic hormone-related, 359, 360, 363
    cAMP/PKA pathway in, 364–365
    insulin-like growth factor-1-related, 359
    insulin-related, 359, 360, 361–362, 364, 365
    phosphatidylinositide 3-kinase pathway in, 359–368
    sgk in, 363–365
ERK (extracellular signaling-regulated protein kinase), 307
ERK-1/2 (extracellular signaling-regulated protein kinase-1/2), 95
  ATP-induced activation of, 342, 344, 345
Erythrocytes
  apoptosis in, 211–217
    calcium-sensitive Gardos potassium channels in, 213, 214
    ceramide release in, 215
    characteristics of, 212
    energy deletion-induced, 211, 214
    erythropoietin-related inhibition of, 213–214
    in glucose-6-phosphate dehydrogenase deficiency, 211–212, 214
    ionomycin-induced, 212
    non-selective cation channels in, 212–214, 215
    osmotic shock-induced, 211, 213
    oxidase stress-induced, 211, 213, 214
    phosphatidylserine in, 211, 212, 213, 214, 215
    in *Plasmodium falciparum* infections, 212, 214
    in sickle cell disease, 211–212, 214
    sphringomyelinase activation in, 215
    in thalassemia, 211–212, 214
  Gardos K channels in, 387–388
  potassium-chloride cotransporter in
    bumetanide-related inhibition of, 14–15
    effect of *N*-ethylmaleimide on, 11–24
    effect of thiol modification on, 11–15, 24
    furosemide-related inhibition of, 14–15
    L^1 antigen in, 15
    L_p antigen in, 15
    membrane and regulatory models of, 15–18
    post-stimulatory inactivation of, 19
    redox-dependence of, 12–13, 25
  potassium-chloride cotransport in, 29–30
  sodium-potassium-2 chloride cotransporter in, 77–88
    cotransport rate in, 78, 83, 84
    equilibrium quotient of, 77–78
    in ferret red blood cells, 78, 80–82
    multiple kinase/phosphatase model of, 82–85
    multiple-site phosphorylation of, 79–85
    properties of, 77–78
    regulation of, 79
  sodium-potassium pump studies in, 5–6
Erythropoietin, in erythrocyte apoptosis, 213–214
Ethylisopropylamiloride, 213
N-Ethylmaleimide (NEM), potassium-choride cotransport effects of, 391–392
  membrane and regulatory models of, 15–18
  post-stimulatory inactivation, 19–25
  thiol modification and, 11–15, 19, 24
European eels, NHE1 in, 91
Exocytosis
  cell swelling-induced, 325–330
  in intestinal epithelial volume regulated anion conductance, 343–344
  signal transduction pathway in, 328–329
Extracellular signaling-regulated protein kinase (ERK), 307

Extracellular signaling-regulated protein kinase-1/2 (ERK-1/2)
ATP-induced activation of, 342, 344, 345
Ezrin/radixin/moesin (FERM) proteins, 90

F
F-actin, 173, 174
NHE1 binding to, 90
FAK, 307
Fas ligand, apoptosis-inducing activity of, 190, 191, 206
FERM tail, of moesin protein, 410
Ferret erythrocytes, sodium-potassium-2 chloride cotransporter in, 78, 80–82
Fgr Src tyrosine kinase, 30
Filamins, 239
Fish, erythrocyte NHE1 in, 89–98
Fluid secretion, across epithelia, 119
Fodrin, 194
Forskolin, basolateral membrane potassium channel-activating effects of, 120, 121, 122, 123
Free oxygen radicals, effect on astroglial glutamate uptake, 317
Furosemide, 14–15, 57, 72
Furosemide-sensitive sodium-chloride cotransporters, 60

G
Gab-1 protein, 308
Gamma-aminobutyric acid (GABA), 31–32
astrocyte receptor-coupled, 313
de novo synthesis of, 314
GCK (germinal center kinase), 43
Gelsolin, 50, 193, 239
Gene expression, as mediator of $[Na^+]_i/[K^+]_i$ antiapoptotic activity, 221
Genistein, 80, 81, 82, 83, 85
Germinal center kinase (GCK), 43
Gibbs-Donnan equilibrium, 223
Gitelman disease, 57, 59
Glial cells. *See also* Astrocytes
major groups of, 313
Glial-neuronal signaling. *See* Astrocyte-neuronal signaling
Glucocorticoids, effect on astroglial glutamate uptake, 317, 319
Glucose-6-phosphate dehydrogenase deficiency, 211–212, 214
Glutamate
astrocyte receptor-coupled, 313
de novo synthesis of, 314
Glutamate, in regulatory volume decrease, 369
Glutamate aspartate transporter (GLAST), interaction with astrocytes, 314
Glutamate receptors, astroglial, 315
Glutamate transporter (GLT-1), interaction with astrocytes, 314
Glutaminergic neurotransmission, astrocytic-neuronal signaling in, 313–323
Glutaminergic synaptic region, astrocyte-neuronal signaling in, 315
Glycine, in regulatory volume decrease (RVD), 369
G proteins
astrocyte receptor-coupled, 313
as KCNQ4 channel modulator, 402–403
in volume regulated anion conductance, 341
Grb-2 protein, 308
Growth factors. *See also specific* growth factors
sodium-potassium-2 chloride cotransporter-stimulating activity of, 79
GSH, in potassium-chloride cotransport, 12–13, 22, 23
Guanosine monophosphate, cyclic (cGMP)
in nitric oxide-mediated sodium/hydrogen exchanger regulation, 152–154
in nitric oxide-mediated sodium/potassium-2 chloride cotransport, 149–150, 151
Guanosine triphosphatases, small, hyposmolarity-related activation of, 307

H
α-Haemolysin, 100
Hax-1, 240
Hck Src tyrosine kinase, 30
Heat shock protein 105, 49
HEK (human embryonic kidney) 293 cells, potassium-chloride cotransport inactivation in, 19–24
HeLa cells, apoptosis in
in hyperosmotically-shrunken cells, 224
potassium transmembrane gradient-related suppression of, 228
Hematological diseases, erythrocyte potassium Gardos channels in, 387–388
Hemosiderin, effect on astroglial glutamate uptake, 317
Herbimycin, 302
HER-293 cells, KCNQ4 channel modulation in, 401–403
by cellular signaling pathways, 401, 402–403
by cell volume-related changes, 401–402, 403
Hippocampus, taurine-mediated volume regulation of, 331–338
Histamine, astrocyte receptor-coupled, 313
HSPCO38, 249
HTC cells, volume-activated chloride currents in, 141–145
Hydrochlorothiazide, 57

Hyperammonemia, encephalopathy associated with, 132
Hyperosmotically-shrunken cells, apoptosis in, 224–226
Hypertension, 57
  KCC3 gene in, 379–385
  KCC proteins in, 35
  potassium-chloride cotransporter in, 379–385
Hypertonicity, in tissue cells, 2–3
Hypotension, KCC proteins in, 35
Hypotonicity
  of contractile vacuole contents, 7
  effect on barnacle muscle cell regulatory volume decrease
    arginine in, 274, 275
    aspartate in, 274, 275
    calcium ions in, 266–268, 271, 274–275, 276–281
    cAMP in, 277–281, 288–290
    cGMP in, 278, 279, 280–281
    chloride ions in, 274, 275, 276
    cyclic nucleotides in, 277–281, 288–290
    extracellular pH changes during, 276–277
    extracellular space determination in, 272–274
    free amino acids in, 274, 275, 276
    glycine in, 274, 275, 276, 288–289
    intracellular ionic strength in, 282–286
    intracellular macromolecular crowding volume sensors in, 286–288
    in isosmotic and hypotonic conditions, 274–276
    mechanical membrane deformation volume sensors in, 281–282
    osmolytes in, 271, 272–276, 288–290
    potassium ions in, 274, 275, 276, 288–289
    sarcolemmal hydraulic water permeability and, 267, 268–270
    sodium ions in, 274, 275, 288–289
    taurine in, 274, 275–276
    time course of, 270–2272
    verapamil-sensitive calcium channels in, 270–272, 285–286, 288
    volume sensors in, 281–288
  volume-activated chloride current effects, 143
Hypoxia, sodium-potassium-2 chloride cotransporter-stimulating activity of, 79

I
ICA-17043, 387
ICln protein, human, interaction with HSPCO38 protein, 249
ICln protein, reconstituted in lipid bilayers
  amino acid hydrophobicity pattern of, 100
  cell swelling-induced translocation of, 99
  definition of, 245
  in regulatory volume decrease-related anion current activation, 245
  in RNA splicing, 245
  transmembrane topology of, 100, 103
  wild-type, cysteine scanning of, 102–106
ICln protein channel pore, cysteine scanning of, 102–106
  effect of cadmium on, 100, 102–106
ICln 1 protein, 245, 246, 247
IClnN2 protein, reconstituted in lipid bilayers, 245-251
  amino acid sequences of
    alignment of, 245-246
    antibody recognition of, 249, 250
  inactivation behavior of, 247-251
    amino acid-directed antibodies in, 249, 250-251
    single-channel currents in, 248-249
IMCD-K2 cell line, anion conductance channels in, 109–118
Inositol-1,4,5-triphosphate (IP_3), 315
Insulin
  in renal epithelial sodium channel regulation, 359, 360, 361–362, 364, 365
  in renal sodium transport, 403–404
  sodium transport-stimulating activity of, 408
Insulin-like growth factor-1, 359, 360, 361–362, 364, 365
Interleukin-1b, purine receptors on, 315
Intestine 407 epithelial cells
  adenosine triphosphate release in, 342–344
  chloride-selective ion channels in, 340
  organic osmolyte release in, 342
  potassium-selective ion channels in, 340
  regulatory volume decrease (RVD) in, 339–347
  vesicle cycling activation in, 342–344
  volume regulated anion channel (VRAC) in, 340–341
    lipid raft-mediated regulation of, 344–345
Invitrogen, 393
Ion channel inhibitors, as apoptosis modulators, 196–198
Ionomycin, in erythrocyte apoptosis, 212
Ischemia, cerebral, sodium-potassium-2 chloride cotransporter in, 67–75
  bumetanide inhibition of, 71–73
  cellular location of, 70–71, 74
  edema formation and, 71–73, 74
  peptide-sensitive regulation of, 68–70
Isoproterenol, paNHE1-activating effect of, 93, 94, 95, 96

Isosmolarity, 1, 2–3
Isotonicity, of cytoplasm, 1, 2–3

J
Jasplakinolide, NKCC1-activating effect of, 352, 353, 355
JNK, 307, 308
Jurkat cells
  apoptosis in
    anti-Fas-induced, 199–200
    cell shrinkage associated with, 226
    in hyperosmotically-shrunken cells, 224, 225
    ion-mediated, 195, 197
    n-type voltage-gated potassium channels in, 227
    potassium transmembrane gradient-related suppression of, 228
  Fas-ligand-mediated taurine release from, 227
  outwardly rectifying chloride channels in, 198

K
K. *See* Potassium
KCC
  cysteine residue modification in, 36
  homological similarity to cation-chloride cotransporters, 30–31
  temperature-dependent inhibition of, 30
KCC1, 18, 31
  localization in cerebellar membrane, 390–391
  molecular physiology of, 31
  renal, 31
  structure of, 31
KCC2, 18, 31–34, 36
  molecular physiology of, 31–34, 36
  tyrosine kinase-mediated phosphorylation of, 33
KCC3, 34–35, 279–285
  interaction with SPAK subfamily of STE20 kinase, 43–44
  molecular physiology of, 34–35
KCC3a, 18–19, 34, 44
  molecular physiology of, 34
KCC3b, 18–19
KCC4, 18–19, 35–36
  molecular physiology of, 35–36
KCNQ4 channels
  cellular signaling pathway-related modulation of, 401, 402–403
  cell volume change-related modulation of, 401–402, 403
KCNQ channels, as cell volume sensors, 389–390
Kidney
  aquaporin regulation in, 180
  epithelial sodium channels in. *See* Epithelial sodium channels (EnaCs), renal
  nitric oxide production in, 147–148
  sodium-chloride cotransporters in
    bumetanide-sensitive sodium-chloride symporters, 55
    bumetanide-sensitive transporter (BSC/NKCC), 55, 56–57, 59–63
    sodium-chloride DIOA-sensitive cotransporters, 55
    thiazide-sensitive sodium-chloride cotransporters (TSC), 55, 56, 57–59
Kinases. *See also specific* kinases
  phosphoinositide-dependent substrates of, 363
Knockout mice, hypertensive, 379–385

L
Lactic acid, effect on astroglial glutamate uptake, 317
Lactoacidosis, effect on necrotic cell anion channels, 207–208
L_1 antigen, erythrocyte in potassium-chloride cotransport, 15
Laplace equation, 266
Lavendustin, 302
Leak channels, 7
Learning, glial-neuronal signaling in, 314–315
Lectins, epidermal growth factor receptor-activating effects of, 305–306
Lettré cells, microvilli in, 6
Leukocidin, 100
Leukotrienes, effect on astroglial glutamate uptake, 317
Linopirdine, 401, 402
Lipid mediators, in Ehrlich ascites tumor cell signaling events, 173–174
Lipid rafts, 344–345
L_p antigen, in erythrocyte potassium-chloride cotransport, 15
L644,711, 161, 162, 164, 165
LY294002, 307, 407, 408

M
Macromolecular crowding, 281–282
  membrane transporter-mediated control of, 219–220
  sodium-potassium pump-mediated control of, 219–220
  as volume detector, 301–302
Macula densa cells, sodium-potassium-2 chloride cotransport in, 151
Magnesium, intracellular removal of, 83, 890–82
Mannitol, apoptosis-inducing activity of, 224–226

Mean arterial pressure, 381, 382–383
Membrane model, of erythrocyte sodium-chloride cotransport, 17–18
Membrane tyrosine receptors, in osmotransduction, 301–312
Memory, glial-neuronal signaling in, 314–315
Metabotropic glutamate receptors, astroglial, 315
N-Methyl-D-asparate glutamate receptors, 317
Methylmethanethiolsulfonate (MMTS), 12
Metolazone, 57, 58
Microglial cells
  astrocyte-mediated differentiation and deactivation of, 315
  in neuronal-glial signaling, 320–321
Middle cerebral artery occlusion model, of stroke, 71–73, 74
mIMCD3 renal epithelial cells, hyperosmotically-shrunken, apoptosis in, 224
Mitochondria, in apoptotic signaling pathway, 192
ML-7, 172
Moesin, 410
Molting cycle, in crayfish, 411–413
  calcium ion homeostasis in, 411–413
  epithelial calcium channel (ECaC) in, 396–398
  epithelial calcium channel-like *(ECaC)* gene expression in, 398–401
  PMCA (plasma membrane Ca^{2+}-ATPase) gene in, 393–395, 396–398, 401
  salinity effects on, 396–398
    on *PMCA* (plasma membrane Ca^{2+}-ATPase) gene expression, 396–398
    on sodium-calcium exchanger (NXC) expression, 396–398
Mortalin, 221–222
Mucus, 119
Muscle cells
  in barnacles. *See* Barnacle muscle cells
  skeletal. *See* Skeletal muscle cells
Myosin II, 173, 174
Myosin light chain kinase, 79, 172

N
Na. *See* Sodium
NAD(P)H oxidase, in volume-mediated taurine release, 372–373
Natriferic hormones, effects on renal epithelial sodium channels, 359–368
NCX protein, in crayfish, 411–413
Necrosis
  characteristics of, 189–190
  ion balance in, 190
  necrotic volume increase (NVI) during, 179
  as pathological cell death, 189
Necrotic volume decrease (NVD)
  anion channel inhibition in, 207–208
  volume-sensitive outwardly rectifying chloride channels (VSOR) in, 207–208
Necrotic volume increase (NVI), 179, 205
Nedd4-2, 363
Nephrons, nitric oxide in, 1471–48
Neurodegenerative diseases, "excessive" apoptosis-related, 190
Neuromodulators, astroglial membrane receptors for, 313, 314
Neuronal cells, apoptosis in, 228
Neuronal maturation, KCC2 protein in, 31–33
Neuropathic pain, KCC2 protein in, 34, 36
Neuropathy, peripheral, KCC3 gene mutation-related, 383
Neurotransmitters, astroglial membrane receptors for, 313, 314
NHE protein, renal, nitric oxide regulation of, 152–153
NHE1 protein, 169. *See also* paNHE1 protein
  in Ehrlich ascites tumor cells, 170, 171, 172–173, 174, 175
  in hypoxia/ischemia-induced cell damage, 89–90
  as multi-protein complex component, 90
  physiological functions of, 89–90
  protein phosphorylation-mediated regulation of, 90
NHE3 protein, renal, nitric oxide regulation of, 152, 153–154
NHERF2, 354, 355
Nicotinamide adenine dinucleotide phosphate (NADPH) oxidase, in volume-sensitive taurine release, 372–373
NIH3T3 cells, volume-sensitive taurine release in, 369–378
Nitric oxide (NO)
  in astroglial glutamate uptake, 317
  in blood pressure regulation, 379
  as endothelium-derived relaxing factor, 147
  functions of, 147
  in hypertension, 383
  potassium-chloride cotransporter effects of, 379, 383
  renal chloride-dependent transporter-regulatory activity of, 152
  renal production of, 147–148
  renal sodium-potassium-2 chloride cotransport-regulatory activity of, 147, 148–151
    cGMP-dependent mechanism of, 149–150, 151

cGMP-dependent phosphodiesterase in, 149, 150
in macula densa cells, 151
NKCC2 in, 149, 150, 151
in thick ascending limb, 148–150
tubulo-glomerular feedback mechanism and, 151
renal sodium-potassium-hydrogen exchanger-regulatory activity of, 152–154
cGMP-dependent mechanism of, 152–154
in proximal tubule, 152
in thick ascending limb, 152–154
Nitric oxide synthase
endothelial, 147, 148, 150
inducible, 147, 148, 150
neuronal, 147, 148, 150, 151
5-Nitro-2-(3-phenylpropylamino-)-benzoic acid (NPPB), 408
NKC, homological similarity with KCC proteins, 30–31
NKCC1, 44, 45–46, 169
activation of, 30
protein kinase C-mediated, 349
in Ehrlich ascites tumor cells, 170
fluid secretion-mediating function of, 349
homological similarity with KCC proteins, 30–31
protein kinase C-mediated activation of, 351–354, 355
F-actin cytoskeleton/protein kinase C isotype interaction in, 352–353, 355–356
RACK1/protein kinase C isotype interaction in, 353–356
NKCC2, 149, 150, 151
homological similarity with KCC proteins, 30–31
Noradrenaline
astroctyte receptor-coupled, 313
sodium-potassium-2 chloride cotransporter-stimulating activity of, 79
Nucleases, potassium-related inhibition of, 196
NXC (Na^+-Ca^{2+} exchanger), expression in crayfish, 396–398
Nx protein, 249, 250

O
Oncosis
cell shrinkage during, 219
definition of, 220
in ouabain-treated C7-MDCK cells, 223–224
Osmolytes, organic
in cellular osmotic pressure regulation, 369
in regulatory volume decrease (RVD), 301, 342, 345
in regulatory volume increase (RVI), 192–193
sodium-coupled symport of, 219–220
Osmotic shock, erythrocyte apoptosis-inducing effects of, 211, 213
Osmotic stress, causes of, 339–340
Osmotransduction, membrane tyrosine receptors in, 301–312
OSR1 (oxidative stress-related kinase), 79
OSR1 (oxidative stress-related kinase) STE20 kinase subfamily, 43, 45, 46, 47–48
interactions of, 47–48
Otoferlin, 49–50
Ouabain
antiapoptotic activity of, 220–221
gene expression-induced activity of, 221–222
oncosis-inducing activity of, 223–224
as sodium-potassium pump inhibitor, 5, 6
Oxytocin, 326, 328

P
paNHE1 protein, 89–98
activation pathways in, 93–95
amiloride insensitivity of, 92
chloride/bicarbonate exchanger-mediated regulatory volume increase in, 92, 93
5'-*N*-ethylisopropyl/amiloride insensitivity of, 92
as HNE1 homologue, 90–91
HOE 694 insensitivity of, 92
regulation of, working model for, 95–97
sequence of, 90–91, 92
Parkinson's Law, 4
PBFI (potassium chelator), 226–227
Peptide hormones, cell swelling-induced secretion of, 325–330
Peripheral neuropathy with or without agenesis of the corpus callosum (ACPN) syndrome, 34–35
Peroxynitrite, effect on astroglial glutamate uptake, 317
$pFAK^{125}$, in volume-sensitive taurine release, 374–375, 376
pH, basolateral, effect of ammonia and ammonium on, 132, 136
Phagocytosis, of apoptotic bodies, 205, 206
Phloretin, 206
Phosphatidylinositol (4,5) bisphosphate
in Ehrlich ascites tumor cell signaling events, 173–174
NHE1 binding to, 90
Phosphatidylinositol 3-kinase
hyposmolarity-related activation of, 308

in renal epithelial sodium channel regulation, 359–368
in transepithelial sodium reabsorption, 408
in volume-regulated anion conductance, 342, 345
Phosphatidylserine, in erythrocyte apoptosis, 211, 212, 213, 214, 215
Phosphodiesterases, cGMP-dependent, 149, 150
Phosphoinositide, in epithelial sodium channel regulation, 359–368
Phospholipase(s), in osmotic fluxes, 309
Phospholipase A_2, in volume-sensitive taurine release, 370, 375
Phospholipase C, in volume-activated chloride currents, 141, 142, 143, 145
Phosphorylation
multiple-site, in red blood cells, 79–85
potassium tyrosine-mediated, 341
of sodium-potassium-2 chloride cotransporter, 79, 80–85
tyrosine
KCNQ4 channel modulation in, 402, 403
of n-type potassium channels, 197
Pimozide, 171
PKD2 gene, polycystin-2 as product of, 235, 236, 2420
Plasma membrane
necrosis-related rupture of, 189–190
in regulatory volume decrease (RVD), 193
in regulatory volume increase (RVI), 192
water movement through, 180
Plasma membrane Ca^{2+}-ATPase *(PMCA)* gene, 393–395, 396–398, 401
Plasmodium falciparum infections, erythrocyte apoptosis in, 212, 214
PMCA (plasma membrane Ca^{2+}-ATPase) gene, 393–395, 396–398, 401
Polycystin-2, syncytial, 235–244
effect of α-actinin on, 239, 240, 241
effect of cytochalasin D on, 236, 237, 238, 241
Polydipsia, animal model of, 380–381, 383
Polythiazide, 57–58
Portal vein, ammonium concentration in, 131–132
Potassium
in apoptosis, 199
in serum-deprived cells, 228
in caspase activation, 195
colonic epithelial secretion of, 119
in neuronal-glial signaling, 315
nuclease-inhibiting activity of, 196
Potassium channels
in airway epithelial cells, 388–389
in apoptosis, 196–199
in apoptotic volume decrease (AVD), 226–227
in basolateral membrane
activation of, 119, 121–123
-adrenergic receptors in, 120, 122
cAMP-dependent signaling in, 120, 121, 122
effect of ammonium on, 133, 137
effect of forskolin-stimulated chloride secretion in, 121, 122, 123
electrogenic potassium secretion in, 120, 126–127
forskolin-mediated, 120–121, 122, 123
IK (KCNN4) channels, 121
KvLQY channels, 121
prostanoid EP2 receptors in, 120, 122
sodium-potassium-2 chloride cotransporter-dependence of, 119, 121, 126
calcium-gated, in apoptosis, 227
Gardos
in erythrocyte apoptosis, 213, 214
in hematological diseases, 387–388
in sickle cell anemia, 157
KCNQ-type, 389–390
KCNQ4-type
cellular signaling pathway-related modulation of, 401, 402–403
cell volume change-related modulation of, 401–402, 403
Kv1.3-type, in apoptosis, 227
n-type
in apoptosis, 227
tyrosine phosphorylation of, 197
Potassium-chloride cotransport
in astrocytes, 391–392
membrane and regulatory models of, 15–18
post-stimulatory inactivation of, 19–25
thiol modification-related activation of, 11–15, 19, 24
Potassium-chloride cotransporter
definition of, 379
DIOA-sensitive, 55
in erythrocytes, 29–30
bumetanide-related inhibition of, 14–15
effect of *N*-ethylmaleimide on, 11–24
effect of furosemide on, 14–15
effect of thiol modification on, 11–15, 24
L_1 antigen in, 15
L_p antigen in, 15
membrane and regulatory models of, 15–18
post-stimulatory inactivation of, 19
redox-dependence of, 12–13, 25

N-ethylmaleimide-related activation of
in C6 glioma cells, 391–392
in erythrocytes, 11–24
homological similarity with cation-chloride transporters, 30–31
in hypertension, *KCC3* gene in, 379–385
KCC2 isoform, 18, 31–34, 36
KCC3 isoform, 279–285
KCC3a isoform, 18–19
KCC3b isoform, 18–19
KCC4 isoform, 18–19, 35–36
localization in cerebellum, 390–391
molecular physiology of, 29–41
KCC1, 31
KCC2, 31–34, 36
KCC3, 34–35
KCC3a, 34
KCC4, 35–36
in nephrons, nitric oxide regulation of, 152
Potassium flux, in apoptosis signaling cascade, 195–196
Potassium permeability, of the cell membrane, 3–4, 6
Potassium tyrosine phosphorylation, in volume-regulated anion conductance, 341
PPI. *See* 4-Amino-5-(4-methylphenyl)-7-(t-butyl)pyrazolol[3,4-d]pyrimidine
Procambarus clarkii, molting cycle in
calcium ion homeostasis in, 411–413
epithelial calcium channel-like *(ECaC)* gene expression in, 398–401
PMCA (plasma membrane Ca^{2+}-ATPase) gene in, 393–395, 396–398, 401
salinity effects on, 396–398
on plasma membrane calcium ATPase (PMCA) expression, 396–398
on sodium-calcium exchanger (NXC) expression, 396–398
Programmed cell death. *See also* Apoptosis; Necrosis; Oncosis
cell shrinkage associated with, 174
cell volume regulation in, 169
NGE1-mediated, 89
NHE1 inhibition-related, 174–175
Prolactin, 326, 327
Proline, in regulatory volume decrease, 369
Protein(s)
in regulatory volume decrease (RVD), 369
(R/K)FX(V/I)XXXX motif of, STE 20 kinase binding with, 44, 47–51
Protein kinase(s)
in Ehrlich ascites tumor cells, 171–172
in release of organic osmolytes, 345
Protein kinase A, 363
in aquaporin phosphorylation, 180
in cystic fibrosis transmembrane regulator activation, 349
as KCNQ4 channel modulator, 402–403
in NKCC1 activation, 351–354, 355
in sgk phosphorylation, 403–404
Protein kinase B, 363
Protein kinase C
in Ehrlich ascites tumor cell signaling events, 173
as KCNQ4 channel modulator, 402, 403
in NKCC1 activation, 349
F-actin cytoskeleton/protein kinase C isotype interaction in, 352–353, 355–356
RACK1/protein kinase C isotype interaction in, 353–356
Protein kinase C-δ, as F-actin binding partner, 352–353, 356
Protein kinase C-ε, as RACK1 binding partner, 352, 353–355, 356
Protein kinase G, in sodium-potassium-2 chloride cotransport, 149–150
Protein phosphastase-1, 30
Protein phosphastase-2A, 30
Protein phosphatase
Ser/Thr, 173
sodium-potassium-2 chloride cotransporter-regulating activity of, 79
Protein phosphatase-1, in sodium-potassium-2 chloride cotransporter phosphorylation, 79, 80, 82–83
Protein phosphatase inhibitors, Ser/Thr, paNHE1-activating effect of, 93–95, 96
Protein tyrosine kinases, in volume-sensitive taurine release, 370–371, 373–375
Proteomics, 409–410
Proximal tubules
basolateral potassium-chloride cotransport in, 35
KCC protein-mediated solute transport in, 35–36
nitric oxide-regulated sodium/hydrogen exchanger in, 152
Pseudohypoaldosteronism type II (PHAII), 57
Pseudopleuronectes americanus. See Winter flounder
p38 kinase, 307, 308
in Ehrlich ascites tumor cells, 171–172, 174
p38 MARK, 50
p21 Rho protein, 309
in volume-regulated anion conductance, 342, 345
Pump-leak hypothesis, 4–6, 7–8

Q
Q-VD-OPh caspase inhibitor, 293–300

R
RACK1 (receptor for activated C-kinase), as protein kinase C-ε binding partner, 352, 353, 355, 356
Ras family, 307
Ras/MAPK (mitogen-activated protein kinase) pathway, 308
Rat hepatocytes, hypertonicity-induced sodium channels in, 253–261
  activation mechanisms of, 257–258
  amiloride sensitivity of, 254, 255, 259–260
  comparison with other cation channels, 259
  molecular correlates of, 255–256
  in regulatory volume increase, 254, 259–260
Reactive oxygen species
  apoptosis-inducing activity of, 192
  tyrosine kinase receptor-activating effects of, 304
  as volume-sensitive taurine release mediators, 369–378
    effects of hypotonic exposure on, 371–373, 375–376
    epidermal growth factor receptors in, 373
    MAP kinase p38 in, 374–375
    NAD(P)H oxidase in, 372–373
    $pFAK^{125}$ in, 374–375, 376
    phosphatases in, 370–371
    phospholipase A_2 in, 370, 375
    protein tyrosine kinase c-Scr in, 373–374, 376
    protein tyrosine kinases in, 370–371, 373–375
    protein tyrosine phosphatase in, 375–376
    tyrophostines in, 373
Red blood cells. *See* Erythrocytes
Regulatory volume decrease (RVD)
  in airway epithelial cells, 388–389
  in barnacle muscle cells
    arginine in, 274, 275
    aspartate in, 274, 275
    calcium ions in, 266–268, 274–275, 276–281
    cAMP in, 277–281, 288–290
    cGMP in, 278, 279, 280–281
    chloride ions in, 274, 275, 276
    cyclic nucleotides in, 277–281, 288–290
    extracellular pH changes during, 276–277
    extracellular space in, 272–274
    free amino acids in, 274, 275, 276
    glycine in, 274, 275, 276, 288–289
    in hypotonic conditions, 274–276
    intracellular ionic strength in, 282–286
    intracellular ionic strength volume sensors in, 282–286
    intracellular macromolecular crowding volume sensors in, 286–288
    in isosmotic and hypotonic conditions, 274–276
    in isotonic conditions, 274–276
    mechanical membrane deformation volume sensors in, 281–282
    osmolytes in, 272–276
    potassium ions in, 274, 275, 276, 288–289
    sarcolemmal hydraulic water permeability and, 267, 268–270
    sodium ions in, 274, 275, 288–289
    taurine in, 274, 275–276
    time course of, 270–2272
    volume sensors in, 281–288
  definition of, 141, 192, 193, 301, 339, 369
  ICln protein-mediated anion currents in, 245
  in intestinal epithelial cells, 339–347
  macromolecular crowding in, 219–220, 281–282
  mechanisms of, 192–193, 339
  NHE1 in, 89
  relationship with apoptotic volume decrease (AVD), 193–195, 196–197
  as signal transducer, 89
  steps in, 301
Regulatory volume increase (RVI)
  definition of, 339
  macromolecular crowding in, 219–220
  mechanisms of, 339
Renal epithelial cells, aldosterone-mediated expression in, 409–410
Renal inner medullary collecting duct, anion conductance channels in, 109–118
  calcium ion-activated chloride conductance (CaCC), 109, 111–117
  chloride channels, 111–113
  cystic fibrosis transmembrane regulator (CFTR), 109, 110, 111, 113–114, 115–117
  vitelliform macular dystrophy protein bestrophin anion channel, 113
  volume-regulated anion conductance (VRAC), 109, 112, 113, 114–117
Rheumatoid arthritis, “excessive” apoptosis-related, 190

S
Salamanders, NHE1 in, 90, 91
Salinity stress, effect on crayfish transmembrane protein expression, 396–398
SBFI (sodium chelator), 227

Serotonin, astroctyte receptor-coupled, 313
Serum and glucocorticoid induced protein kinase (sgk), 363–365
  protein kinase A-mediated phosphorylation of, 403–404
  sodium-potassium-2 chloride cotransporter-regulating activity of, 79
  in transepithelial sodium reabsorption, 408
sgk. *See* Serum and glucocorticoid induced protein kinase (sgk)
Shc protein, 308
Sickle cell anemia/disease
  erythrocyte apoptosis in, 211–212, 214
  Gardos potassium channels in, 157, 387
Signaling
  apoptotic, 195–196
    caspase 3 in, 197
    chloride in, 198
  astrocyte-neuronal, 313–323
    adenosine triphosphate-mediated, 313
    astroglial glutamate uptake impairment-related alteration of, 316–320
    glutamate aspartate transporter (GLSAT) in, 314, 316–317
    glutamate transporter (GLT-1) in, 314, 316–317
    in glutaminergic synaptic region, 315
  in Ehrlich ascites tumor cells, 169, 171–174
Skeletal muscle cells
  cell volume-cell contraction interactions in, 263–292
  free amino acids content of, 263
  glycine content of, 263
  intracellular osmolality increase in, 263
  magnesium ion content of, 263
  potassium ion content of, 263
  taurine content of, 263
  water content of, 263
SLC12A gene mutations, 57
SLC12A3 gene mutations, 57, 59
Smac/DIABLO, 192
Sodium, in apoptosis, 199–200
Sodium-calcium exchanger
  in canine erythrocytes, 5–6
Sodium channels, hypertonicity-induced, in hepatocytes, 253–261
Sodium-chloride cotransporters
  furosemide-sensitive, 60
  renal, molecular physiology of, 55–65
    bumetanide-sensitive sodium-chloride symporters, 55
    bumetanide-sensitive transporter (BSC/NKCC), 55, 56–57, 59–63
    sodium-chloride DIOA-sensitive cotransporters, 55
    thiazide-sensitive sodium-chloride cotransporters (TSC), 55, 56, 57–59
  structure-function relationship in, 58–59
  thiazide-sensitive (TSC), 55, 56, 57–59, 152
    affinity for thiazide-type diuretics, 57–58
    mammalian/teleost comparison of, 57–58
Sodium-chloride symporters, bumetanide-sensitive, 55
Sodium-coupled symport, of organic osmolytes, 219–220
Sodium/hydrogen (Na^+/H^+) exchanger, in macromolecular crowding, 219–220
Sodium ion conductance, in Ehrlich ascites tumor cells, 170, 171
Sodium ion/hydrogen ion exchanger system. *See also* NHE1 protein
  in Ehrlich ascites tumor cells, 170, 171
Sodium-potassium adenosine triphosphatase (Na-K ATPase)
  anti-Fas-induced apoptosis-enhancing effects of, 199–200
  in basolateral membrane, effect of ammonium on, 133, 137
  in sodium cell volume regulation, 7
Sodium-potassium-2 chloride cotransport
  in astrocytes, 391–392
  renal, nitric oxide inhibition of, 47, 148–151
Sodium-potassium-chloride cotransport, in macromolecular crowding, 219–220
Sodium-potassium-2 chloride cotransporter
  in basolateral membrane, 119
    effect of ammonium on, 132–133, 137
  in blood-brain barrier, during ischemia, 67–75
    bumetanide inhibition of, 71–73
    cellular location of, 70–71, 74
    edema formation and, 71–73, 74
    peptide-sensitive regulation of, 68–70
  bumetanide-sensitive, 71–73
    renal apical isoforms of, 59–63
  in Ehrlich cells, 170
  in erythrocytes, 77–88
    cotransport rate in, 78, 83, 84
    equilibrium quotient of, 77–78
    in ferret red blood cells, 78, 80–82
    multiple kinase/phosphatase model of, 82–85
    multiple-site phosphorylation of, 79–85
    properties of, 77–78
    regulation of, 79
  phosphorylation of, 79, 80–85
  renal, molecular physiology of, 55–65

Sodium-potassium pump, 4–6
inhibition of
early-response genes in, 222
in oncosis, 223–224
in macromolecular crowding control, 219–220
sodium-mediated ATPase stimulation of, 7
Sodium transport
antidiuretic hormone-mediated
cAMP/PKA signaling pathway in, 407–408
phosphoinositide signaling pathway in, 408
renal
effect of aldosterone on, 403–404
effect of antidiuretic hormone on, 403–405
effect of insulin on, 403–404
Solute-carrier family 12 genes (SLC12), 55, 56
Solute cotransporter superfamily (SLC), 19
SPAK STE20 kinase subfamily, 43–51
binding regulation of, 46–47
binding site analysis of, 44–45
cation-chloride cotransporters of, 43–47
interaction with KCC3, 43–44
interactors of, 43–44, 47–48
Spherocytosis, hereditary, Gardos potassium channels in, 387–388
Sphringomyelinase, in erythrocyte apoptosis, 215
Spongiome, 7
Src 307
Staurosporine, 30, 80, 81, 82, 83, 85
apoptosis-inducing activity of, 192, 206–207
Steady-state volume, cellular, 169
STE20 kinase/protein, 43–53
definition of, 43
as MAP kinase upstream activator, 43
OSR1 subfamily of, 43, 45, 46, 47–48
protein (R/K)FX(V/I)XXXX motif binding by, 44, 47–51
SPAK subfamily of, 43–51
binding regulation of, 46–47
binding site analysis of, 44–45
interaction with cation-chloride cotransporters, 43–51
interaction with KCC3, 43–44
interactors of, 43–44, 47–48
subfamilies of, 43
Stroke, middle cerebral artery occlusion model of, 71–73, 74
Syncytiotrophoblast
anatomy of, 235
polycystin-2 non-selective cation channel of, 235–244
α-actinin content of, 235–236
cytoskeletal regulation of, 235–244
EBP50-related protein content of, 236
microvillus actin cytoskeleton in, 235–236
as *PKD2* gene product, 235, 236, 2420

T
Tamoxifen, neuroprotective effects of, 164–165
Taurine
in barnacle muscle cell volume regulation, 274, 275–276
Fas-ligand-mediated release of, 227
in hippocampal volume regulation, 331–338
hyposmolarity-mediated activation/efflux of, 304–305, 306, 310
in intestinal epithelial regulatory volume decrease (RVD), 342
intracellular concentration of, 369
as osmoregulatory molecule, 227, 316, 339
reactive oxygen species-mediated volume release of, 369–378
effects of hypotonic exposure on, 371–373, 375–376
epidermal growth factor receptors in, 373
5-lipoxygenase in, 370, 375–376
NAD(P)H oxidase in, 372–373
phosphatases in, 370–371
phospholipase A_2 in, 370, 375
protein tyrosine kinases in, 370–371, 373–375
tyrophostines in, 373
reactive oxygen species-mediated volume-sensitive release of, 369–378
volume-activated, 302
Temperature change, cellular response to, 7–8
Thalassemia, erythrocyte apoptosis in, 211–212, 214
Thick ascending limb of Henle (TALH), bumetanide-sensitive sodium-potassium-2 chloride cotransporter isoforms in, 59–63
functional properties of, 59–61
regulatory properties of, 61–63
vasopressin-induced activation of, 63
Thiol modification, in potassium-chloride cotransporter activation, 11–15, 19, 24
Thymocytes, apoptotic, aquaporins in, 183–187
Thyrotropin-releasing hormone, 326, 327, 328
T lymphocytes, CTLL, $K_v1.3$-deficient, 197
Torasemide, 72
Tracheal epithelial cells, calcium-dependent potassium channels in, 388–389
Transepithelial resistance, ammonium-mediated, 133–134
Transport systems, passive, 7

Traumatic brain injury, volume regulated anion channels (VRACs) in, 158–165
excitatory amino acid release in, 160–165
perivascular astrocyte swelling in, 159–165
Tricholomethizide, 57, 58
Tropomyosin-1, 240, 241
Troponin-I, 240, 241
Trout, NHE1 in, 89, 91
TSC. *See* Sodium-chloride cotransoprter, thiazide-sensitive
Tumor necrosis factor, 227
Tumor necrosis factor-α
apoptosis-inducing activity of, 206
potassium current-inhibiting activity of, 196
purine receptors on, 315
Tumor necrosis factor-α, effect on astroglial glutamate uptake, 319
Tumor necrosis factor family, in apoptosis induction, 190
Tyrophostines, in taurine volume-mediated release, 373
Tyrosine kinase receptors (TKRs)
reactive oxygen species-mediated activation of, 304
regulatory volume decrease-mediated activation of, 302–304
in volume sensing/transduction cascade, 302
Tyrosine kinases
effect on potassium-chloride cotransport, 30
neuronal KCC2 phosphorylating activity of, 33
in volume regulated anion conductance, 345
Tyrosine phosphorylation
KCNQ4 channel modulation in, 402, 403
of n-type potassium channels, 197
Tyrphostins, 302

U
Ultraviolet radiation, apoptosis-inducing activity of, 192
Urea, as potassium-chloride cotransport activator, 30

V
Vascular endothelial cells, hyperosmotically-shrunken, apoptosis in, 224
Vascular physiology, KCC proteins in, 35
Vascular smooth muscle cells, apoptosis in
in hyperosmotically-shrunken cells, 224–225
inhibition of, 219–223
gene expression mediation of, 221–222
Na^+i-dependent Ca^{2+}i-insensitive mechanism-mediated, 223
$[Na^+]_i/[K^+]_i$ ratio inversion-related, 220–222
Na^+i-mediated Ca^{2+}i-independent coupling in, 222–223
in isosmotic *versus* hyposmotic conditions, 227–228
in serum-deprived conditions, 227–228
Vasopressin
aquaporin-regulating activity of, 180
sodium-potassium-2 chloride cotransporter-stimulating activity of, 79
Vesicles, subcellular, as membrane reserves, 6
Vesicular exocytoplasmic space, in cell volume regulation, 7
Virchow, Rudolf, 220
Vitelliform macular dystrophy protein bestrophin anion channel, 113
Volume regulated anion channels (VRACs), 157–167
activation of, 157–158
in intestine 407 epithelial cells, 340–341
lipid raft-mediated regulation of, 344–345
in traumatic brain injury, 158–165
excitatory amino acid release in, 160–165
perivascular astrocyte swelling in, 159–165
Volume-regulated anion channel (VRAC)
activation of, 341–342
properties of, 341–342
in renal inner medullary collecting duct, 109, 112, 113, 114–117
Volume sensing, mechanisms of, 301–302
Volume-sensitive outwardly rectifying chloride channels (VSOR), 207–208
Volume transmission, astrocytes in, 316
VSMC. *See* Vascular smooth muscle cells

W
Water balance, K-Cl cotransporter-3 in, 380–381, 383
Winter flounder, red blood cell paHNE1 protein in, 89–95
WNK1 protein kinase, mutations in, 57
WNK4 protein kinase, 48–49
mutations in, 57

Z
ZVAD-fmk, 219, 220, 226, 293–294, 295, 298, 299